

**ÉCOLE DOCTORALE DES SCIENCES DE LA VIE ET DE LA SANTÉ (ED414)**  
**Laboratoire d'Innovation Thérapeutique (UMR 7200)**

# THÈSE

présentée par : **Wanyin CHEN**

soutenue le : **24 Mai 2017**

Pour obtenir le grade de : **Docteur de l'Université de Strasbourg**

Discipline/ Spécialité : Sciences du Vivant,

Aspects moléculaires et cellulaires de la biologie

**Reprofilage d'une petite molécule chimique à  
activité thérapeutique et cellules souches  
cancéreuses. Etude et compréhension du  
mécanisme d'action du bisacodyl sur les cellules  
souches cancéreuses isolées de glioblastome**

**THÈSE dirigée par :**

**Dr ZENIOU MEYER Maria**

Maître de conférences, Université de Strasbourg

**RAPPORTEURS :**

**Pr GAUDUCHON Pascal**

Professeur émérite, Université de Caen Normandie

**Dr MOREAU Marc**

Directeur de recherches émérite CNRS, Centre de Biologie du  
Développement, UMR 55470 Université Paul Sabatier, Toulouse

**AUTRES MEMBRES DU JURY :**

**Dr DANTZER Françoise**

Directeur de recherches CNRS, Institut de recherche de l'Ecole  
de biotechnologie de Strasbourg (IREBS), UMR 7242



## **Reprofilage d'une petite molécule chimique à activité thérapeutique et cellules souches cancéreuses.**

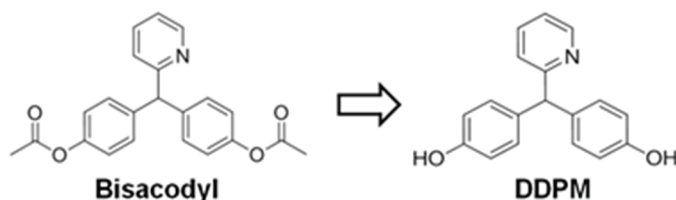
### **Etude et compréhension du mécanisme d'action du bisacodyl sur les cellules souches cancéreuses isolées de glioblastome**

#### **I. Introduction**

Les glioblastomes (GBM) sont les formes les plus sévères et les plus agressives de tumeurs gliales. Les traitements actuels de ces tumeurs associent la chirurgie à de la radiothérapie et de la chimiothérapie avec un agent alkylant de l'ADN, le Témозolomide (TMZ). Malgré cette combinaison de traitements, la survie médiane des patients n'excède pas 15 mois [1]. Ce mauvais pronostic est dû, entre autres, à l'hétérogénéité des glioblastomes avec, notamment, la présence de cellules souches cancéreuses (CSCs) quiescentes, particulièrement résistantes aux traitements conventionnels [2][3][4]. Cibler les CSCs (en prolifération et surtout quiescentes) fait donc partie des thérapies d'avenir pour le traitement de ce type de tumeurs.

Un criblage effectué au sein de notre équipe et une étude de relations structure/activité a conduit à l'identification d'une molécule optimisée possédant une action cytotoxique envers les CSCs de glioblastome (GSCs) en prolifération et en quiescence uniquement dans des conditions de faible acidité correspondant à celles retrouvées au sein des tumeurs [5]. Il s'agit du bisacodyl, commercialisé comme laxatif, et de son métabolite actif, le DDPM (désacétyl-bisacodyl) (Figure 1).

**Figure 1. Structure du bisacodyl et de son métabolite actif, le DDPM.**



Grâce à leur profil d'activité, ces molécules sont prometteuses en tant que nouveaux agents anticancéreux. Les objectifs de ma thèse étaient : i) de comprendre le mécanisme moléculaire impliqué dans l'activité cytotoxique du bisacodyl/DDPM sur les GSCs et ii) d'identifier sa/ses cible(s) protéiques directe(s).

## II. Résultats

### **Caractérisation phénotypique et fonctionnelle des GSCs quiescentes**

Au laboratoire, nous travaillons sur plusieurs types de GSCs en prolifération (TG1, TG1 C1 (OB1)), qui ont été caractérisés phénotypiquement (expression de marqueurs de surface) et fonctionnellement (clonalité, différenciation, initiation tumorale) par l'équipe du Dr Chneiweiss (Institut de Biologie Paris Seine). Le modèle cellulaire des GSCs, qui se maintiennent et se développent en culture en formant des neurosphères, a été transposé avec succès dans notre laboratoire. Afin de se rapprocher de l'état dormant des CSGs retrouvé *in vivo*, nous avons mis au point des conditions expérimentales *in vitro* permettant d'étudier ces cellules à l'état quiescent. Les GSCs quiescentes sont obtenues en absence de renouvellement du milieu de culture pendant 9 jours et ont été caractérisées par l'absence d'incorporation d'EdU dans leur ADN et par une très faible expression du marqueur de prolifération Ki-67. L'état quiescent obtenu dans ces conditions est réversible. Nous avons également montré que les GSCs quiescentes maintiennent les caractéristiques phénotypiques et fonctionnelles observées dans les cellules en prolifération (expression des mêmes marqueurs de surface, clonalité, capacité de différenciation *in vitro* et d'initiation de tumeurs *in vivo*). J'ai participé à cette caractérisation en étudiant les propriétés clonales et la capacité de différenciation de ces cellules après leur réintroduction dans un milieu favorisant leur prolifération.

### **Mise en évidence et validation des mécanismes moléculaires impliqués dans la cytotoxicité du bisacodyl/DDPM sur les GSCs**

Nos précédents travaux avaient permis de montrer que le bisacodyl et le DDPM induisent la mort nécrotique des GSCs avec une plus grande efficacité envers ces cellules à l'état quiescent et uniquement dans un microenvironnement légèrement acide. De plus, ce composé est actif sur de grandes tumorsphères issues d'une multiplication clonale des GSCs et présentant plusieurs des caractéristiques des glioblastomes *in vivo* (cellules en prolifération et en quiescence, centre nécrotique, gradient croissant d'hypoxie en allant vers le centre de la sphère) [6]. Néanmoins, au début de ma thèse, les mécanismes moléculaires sous-jacents à cette activité étaient totalement inconnus.



L'utilisation de puces phosphoprotéiques (R&D systems), nous a, dans un premier temps, permis d'identifier, dans les GSCs TG1 C1 (OB1) quiescentes, plusieurs protéines dont l'état de phosphorylation varie après action du composé. Nous nous sommes focalisés sur la protéine kinase WNK1 (With No Lysine Kinase 1) dont la phosphorylation sur son résidu Thréonine 60 (T60) est diminuée par le bisacodyl/DDPM. WNK1 fait partie d'une famille de 4 serine/thréonine kinases régulant plusieurs canaux et transporteurs dans le rein et les autres tissus. Un rôle de ces kinases et/ou de leurs substrats a été décrit dans différentes tumeurs dont les gliomes. Les WNKs ont été par ailleurs impliquées dans l'adaptation et la survie des cellules cancéreuses à leur environnement, notamment en cas de stress métabolique. Les fonctions des kinases WNK impliquent leur activité catalytique et/ou des interactions avec leurs partenaires régulées par le niveau de phosphorylation de la T60 dans WNK1. Ces deux activités peuvent exister de manière indépendante ou être associées pour le bon fonctionnement de l'enzyme [7].

L'effet du bisacodyl/DDPM sur le niveau de phosphorylation de la T60 de WNK1 en fonction du temps de traitement avec le composé, a été confirmé par immunoblot dans deux types de GSCs (TG1 et TG1 C1 (OB1)) à l'état quiescent alors que le niveau d'expression de WNK1 reste inchangé dans toutes les conditions testées (GSCs en prolifération à pH physiologique ou GSCs quiescentes à pH acide). Cet effet n'a pas été observé avec un dérivé inactif du bisacodyl/DDPM ou dans les GSCs en prolifération à pH physiologique, condition dans laquelle le composé ne présente pas d'activité. Il est intéressant de noter qu'en l'absence de traitement, le niveau de phosphorylation de la T60 de WNK1 est beaucoup plus élevé dans les GSCs quiescentes par rapport à ces mêmes cellules en prolifération suggérant un rôle de cette modification dans la physiopathologie des cellules à l'état quiescent.

Contrairement aux modifications activité-dépendantes du niveau de phosphorylation de la T60 de WNK1, l'activité catalytique de l'enzyme, mesurée grâce à l'étude du niveau de phosphorylation de deux substrats connus de WNK1, les kinases SPAK (STE20/SPS1 related proline/alanine-rich protein kinase) et OSR1 (Oxidative Stress-Responsive kinase 1), est modifiée de manière transitoire par le bisacodyl/DDPM également dans des conditions dans lesquelles le composé n'est pas actif (GSCs en prolifération à pH physiologique). Néanmoins, le niveau de

phosphorylation des substrats de WNK1 est plus élevé dans les cellules quiescentes en absence de traitement. Le rôle de l'activité catalytique de WNK1 dans l'action du bisacodyl/DDPM ne peut donc pas être déterminée avec certitude sur la base de ces résultats.

Nous avons ensuite étudié le niveau d'expression et le niveau de phosphorylation de la kinase Akt pour laquelle la T60 de WNK1 pourrait être un substrat, ainsi que de la protéine kinase SGK1 (Serum and Glucocorticoid regulated Kinase 1) qui a été impliquée dans la signalisation de WNK1 dans d'autres systèmes. Nos résultats montrent qu'alors que le niveau d'expression d'Akt reste inchangé dans les différentes conditions testées, le niveau de phosphorylation de ce partenaire potentiel de WNK1 est également diminué de manière activité-dépendante par le bisacodyl/DDPM. Contrairement à WNK1 et Akt, le niveau d'expression de SGK1 augmente dans les GSCs quiescentes traitées avec le composé. Malgré cette augmentation, le niveau de phosphorylation de cette enzyme est également diminué au cours du temps de traitement et ceci de manière activité-dépendante. Par ailleurs, l'activité de co-transporteurs  $\text{Na}^+/\text{HCO}_3^-$  NBC (NBCe1 et/ou NBCn1), qui font partie des cibles connues de WNK1 et dont la fonction peut être modulée par le pH, est nécessaire à l'action du bisacodyl/DDPM sur les GSCs TG1 et TG1 C1 (OB1). En effet, le prétraitement ou le co-traitement des cellules avec un inhibiteur de ces co-transporteurs préserve les GSCs quiescentes de l'activité cytotoxique du composé. Cet effet protecteur de l'inhibition de NBC a été observé aussi bien sur des neurosphères de GSCs dissociées que sur les grandes tumoresphères clonales dérivées de ces cellules. Il est intéressant de noter que des expériences de RT-PCR quantitative et/ou d'immunoblot sur des extraits membranaires de GSCs nous ont permis de mettre en évidence un niveau d'expression plus élevé de NBCe1 et de NBCn1 dans les cellules TG1 C1 (OB1) comparé à celui des cellules TG1. Ce niveau d'expression plus élevé des co-transporteurs est associé à une plus grande sensibilité des cellules TG1 C1 (OB1) au bisacodyl/DDPM et à un effet protecteur moindre de l'inhibition de NBC.

En l'absence de petites molécules modulant directement l'activité de WNK1 (notamment son activité liée à la phosphorylation de son résidu T60), nous avons ensuite mesuré l'effet du bisacodyl/DDPM en présence d'activateurs et d'inhibiteurs connus d'Akt (SC-79 et VIII, respectivement), ou d'un inhibiteur de SGK1 (GSK 650394) étant donné que ces deux kinases agiraient en amont de WNK1 dans la

voie. Nous avons montré que l'inhibition d'Akt et/ou de SGK1 potentialise l'effet cytotoxique du bisacodyl/DDPM sur les GSCs quiescentes. En revanche, le prétraitement des cellules avec SC-79, l'activateur d'Akt, protège légèrement les cellules de l'action cytotoxique du composé. Par ailleurs, l'inhibiteur VIII d'Akt réduit significativement l'effet protecteur de l'inhibition de NBC. Les effets de ces modulateurs de la voie de WNK1 sont plus importants dans les cellules TG1 par rapport aux cellules TG1 C1 (OB1).

L'activité du bisacodyl/DDPM a été également évaluée i) en présence d'une expression diminuée de WNK1 par ARN interférence et ii) en présence d'une surexpression de la kinase. Afin de diminuer l'expression de WNK1, nous avons cloné 3 séquences oligonucléotidiques ciblant le messenger de WNK1 et une séquence mutée dans le vecteur pEGFP-N2-RNAi (don du Dr. N. Vitale, INCI, Strasbourg, France) sous le contrôle d'un promoteur H1 reconnu par l'ARN polymérase III et permettant l'expression des shRNAs. Les constructions ainsi obtenues ont été introduites par transfection avec le système Amaxa (LONZA) dans les GSCs en prolifération et quiescentes. La diminution de l'expression de WNK1 a été confirmée 48h et 72h après transfection par immunoblot. Une des trois séquences oligonucléotidiques ciblant WNK1 s'est avérée être plus efficace. Une faible augmentation de la mortalité des GSCs quiescentes exprimant les shRNAs (comptage au bleu de Trypan après 48h et 72h de transfection) a été observée. Néanmoins, des expériences de cytométrie en flux n'ont pas permis de confirmer ces résultats. A cause d'une grande variabilité des résultats obtenus à ce jour, il est difficile de conclure sur l'effet de la diminution de l'expression de WNK1 dans les GSCs en prolifération. Enfin, une surexpression de 48h des shRNAs contre WNK1 dans les GSCs quiescentes n'affecte pas de manière significative l'effet du bisacodyl/DDPM dans ces cellules suggérant que la diminution de la phosphorylation de la T60 de WNK1 induite par le composé agit de manière similaire à la réduction de l'expression de WNK1 provoquée par l'ARN interférant.

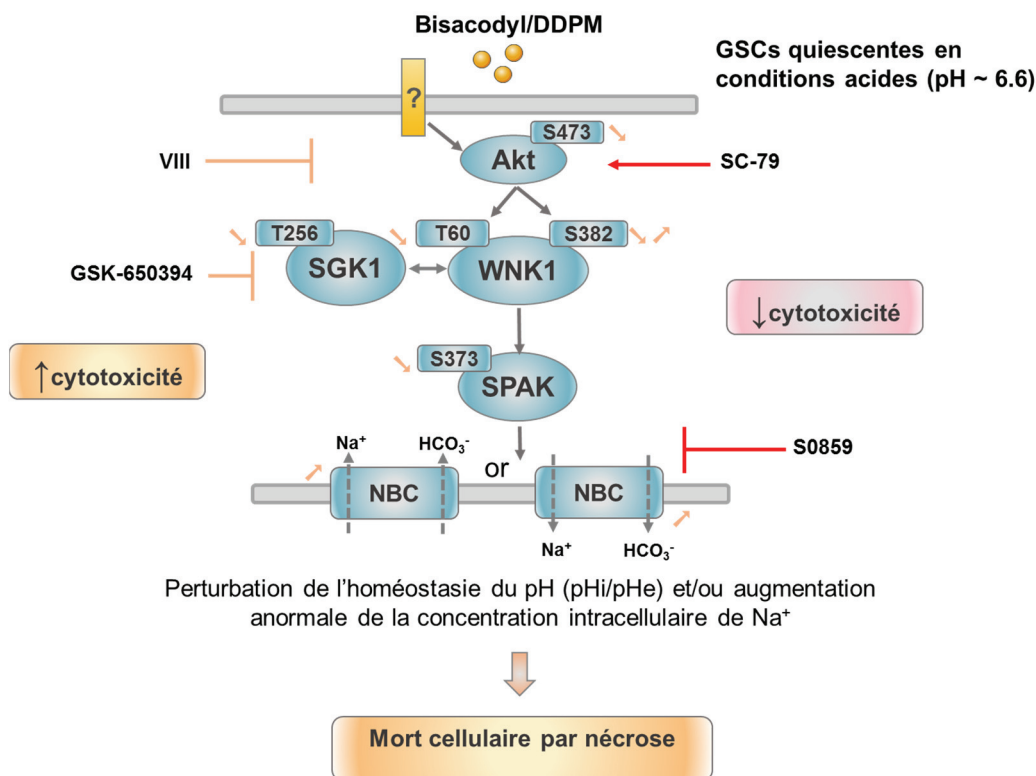
Concernant la surexpression de WNK1, l'ADNc codant Flag-WNK1 a été cloné dans le vecteur pEGFP-N2-RNAi. Néanmoins, il n'a pas été possible de transfecter les GSCs avec ce plasmide qui a une taille beaucoup plus grande (~12 Kpb) que celle des plasmides utilisés précédemment (~5 Kpb). De plus, dans une expérience de transfection contrôle dans les cellules HEK293 la protéine d'intérêt

n'était pas surexprimée à partir de cette construction. La raison de cet échec n'est pas connue. Pour pallier à ces problèmes nous avons :

i) modifié le système d'expression en clonant l'ADNc de WNK1 dans les vecteurs destinateurs du système Gateway (don du Dr. E. Real, Faculté de Pharmacie, Strasbourg, France). Nous avons ainsi obtenu 3 constructions, pEGFP C1, pmCherry C1 et pCIneo 3Flag-WNK1 WT permettant d'exprimer WNK1 en fusion avec EGFP, mCherry ou 3 étiquettes Flag, respectivement, sous le contrôle d'un promoteur CMV.

ii) essayé de mettre au point des conditions de transfection pour améliorer l'introduction de plasmides de grande taille dans les GSCs en testant l'effet de la quantité de plasmide, du nombre de passages après décongélation et du protocole Amaxa sur l'efficacité de transfection des cellules en prolifération et quiescentes. Nous avons ainsi identifié des conditions permettant de transfecter avec une efficacité suffisante (taux de transfection ~ 50%) les GSCs en prolifération. Les taux de transfection obtenus pour les cellules quiescentes n'étaient pas satisfaisants. Pour pouvoir tester l'effet d'une surexpression de WNK1 sur les GSCs quiescentes, nous avons établi des lignées TG1 stables permettant de surexprimer la forme sauvage de WNK1 en fusion avec 3 étiquettes Flag et mis ces cellules en quiescence en absence de renouvellement du milieu de culture pendant 9 jours. La surexpression de WNK1 protège les GSCs de l'action du bisacodyl/DDPM, probablement en contrecarrant l'effet négatif du composé sur la phosphorylation de la T60. Cet effet protecteur de la surexpression de WNK1 a été aussi observé de manière plus significative sur des macro-tumorsphères dérivées de GSCs surexprimant de manière stable la forme sauvage de WNK1. L'ensemble de ces résultats suggère un rôle de la signalisation *via* WNK1 et ses partenaires dans la cytotoxicité du bisacodyl sur les GSCs quiescentes. Un modèle du mode d'action du bisacodyl/DDPM sur les cellules souches de glioblastome quiescentes dans des conditions de faible acidité est représenté sur la Figure 2.

**Figure 2. Modèle du mode d'action du bisacodyl/DDPM sur les cellules souches cancéreuses de glioblastome (GSCs).**



Dans les GSCs (cellules souches de glioblastome) quiescentes dans un microenvironnement acide, le bisacodyl/DDPM conduit à une diminution activité-dépendante de la phosphorylation du résidu Thréonine 60 (T60) de WNK1 (With No Lysine Kinase 1). Le niveau de phosphorylation (et donc probablement le niveau d'activité catalytique) des kinases Akt et SGK1 (Serum and Glucocorticoid regulated Kinase 1), impliquées dans la phosphorylation de la T60 de WNK1 dans d'autres systèmes, est également diminué par le composé de manière activité-dépendante. L'activité catalytique de WNK1 nécessitant la phosphorylation de son résidu Sérine 382 (S382) est également diminuée de manière transitoire par le composé. Ces événements conduiraient à une activité diminuée de la kinase SPAK (STE20/SPS1 related proline/alanine-rich protein kinase) qui à son tour résulterait en une augmentation anormale du niveau d'expression et donc du niveau d'activité des co-transporteurs Na<sup>+</sup>/HCO<sub>3</sub><sup>-</sup> NBC (dont NBCe1 et/ou NBCn1) à la surface des cellules. NBCe1 et NBCn1 régulent le pH intracellulaire (pHi) en transportant du bicarbonate (HCO<sub>3</sub><sup>-</sup>) dans les cellules. En fonction de la stœchiométrie du transport du Na<sup>+</sup> et du HCO<sub>3</sub><sup>-</sup> ou grâce à une réversion du gradient du transport qui peut avoir lieu même dans des conditions de faible acidité, NBCe1 peut également exporter du HCO<sub>3</sub><sup>-</sup> avec des effets opposés sur la régulation du pHi et du pH extracellulaire (pHe). La direction du cotransport par les co-transporteurs NBC est montrée alors que la stœchiométrie du transport n'est pas précisée sur la figure. La dérégulation du pHi/pHe peut être à l'origine de la cytotoxicité du bisacodyl/DDPM sur les GSCs (nécrose). Alternativement, la mort des GSCs pourrait être due à une augmentation anormale de la concentration cytosolique de Na<sup>+</sup> (co-transporté avec le HCO<sub>3</sub><sup>-</sup>) qui conduirait à une forte augmentation de la concentration calcique intracellulaire et à des dommages au niveau des mitochondries induisant la nécrose. En accord avec ce modèle, les inhibiteurs d'Akt (VIII) et de SGK1 (GSK-650394) renforcent l'effet du bisacodyl/DDPM sur les GSCs alors que l'activation d'Akt (par SC-79) ou l'inhibition des co-transporteurs NBC protègent ces cellules de l'effet du composé. ? : la/les cible(s) protéique(s) directe(s) du bisacodyl/DDPM ne sont pas connues.

Afin d'identifier les fonctions de WNK1 impliquées dans l'action du bisacodyl/DDPM et dans la physiopathologie des CSGs, des constructions permettant de surexprimer des mutants non phosphorylables ou phosphomimétiques de la T60 (T60A, T60D/E, respectivement) impliquée dans les interactions de la kinase avec ses partenaires, et aussi un mutant dépourvu d'activité catalytique (K233M), ont été obtenus et clonés, comme la séquence sauvage, dans les vecteurs d'expression. La localisation de la protéine surexprimée sauvage ou mutée a été évaluée par immunocytochimie dans les cellules en prolifération et quiescentes. La localisation observée coïncide avec la localisation décrite pour la WNK1 dans d'autres systèmes. De plus, l'état de quiescence ou la présence des mutations ne semble pas affecter la localisation de la protéine. Des lignées stables TG1 surexprimant ces différents mutants ont été également générées.

Des macro-tumorsphères ont été ensuite obtenues à partir des cellules TG1 surexprimant la forme sauvage ou les formes mutées de WNK1 (T60A/D/E et K233M) et traitées avec le bisacodyl/DDPM. L'effet du composé sur ces cellules a été comparé à l'effet obtenu sur des GSCs contrôle transfectées de manière stable avec un vecteur vide. La surexpression de la protéine sauvage ou des mutants phosphomimétiques de la T60 (T60D ou T60E) a montré un effet protecteur sur les cellules ce qui n'était pas le cas de la surexpression du mutant non-phosphorylable T60A ou du mutant catalytiquement inactif (K233M) de WNK1. Ces données suggèrent que la diminution du niveau de phosphorylation de la T60 de WNK1 ainsi que la modification (diminution transitoire) de son activité catalytique provoquées par le bisacodyl/DDPM sont indispensables à l'action cytotoxique du composé sur les GSCs.

Les GSCs surexprimant de manière stable la forme sauvage ou les formes mutées de WNK1 ont aussi été utilisées pour rechercher un éventuel rôle de WNK1 dans la physiopathologie de ces cellules. Ainsi, nous avons montré que la surexpression de certaines formes mutées de WNK1 (T60A et T60E) conduisait à une plus grande mortalité des GSCs à l'état quiescent. De plus, les propriétés clonales de ces cellules et les taux de croissance des sphères étaient aussi affectées en présence de certaines des mutations. Enfin, la surexpression de la forme sauvage de WNK1 ou des formes mutées de la T60 (T60A, D ou E) provoque des modifications de la morphologie des macro-tumorsphères dérivées de ces

cellules. L'ensemble de ces résultats suggère un rôle jusqu'alors inconnu de la kinase WNK1 dans la physiopathologie des GSCs.

### **Identification de la/des cible(s) directe(s) du bisacodyl/DDPM dans les GSCs**

Un autre de mes objectifs était d'identifier la/les cible(s) protéique(s) directe(s) du bisacodyl/DDPM par chromatographie d'affinité. Pour cela, des billes greffées avec un dérivé actif du bisacodyl/DDPM par les chimistes du laboratoire ont été mises en contact avec des extraits protéiques de GSCs. Les résultats obtenus à ce jour (bandes d'intérêt en quantité trop faible) n'ont pas permis d'identification des protéines présentes dans ces bandes par spectrométrie de masse.

## **III. Conclusion**

Les résultats obtenus au laboratoire démontrant un effet anti-tumoral du bisacodyl *in vivo* renforcent son intérêt en tant que nouvel potentiel agent anti-cancéreux. Néanmoins, la connaissance des mécanismes d'action du composé dans les GSCs est un prérequis avant tout futur développement de ce composé. Un des objectifs majeurs de ma thèse était de mettre en évidence et de valider les mécanismes moléculaires impliqués dans la cytotoxicité du bisacodyl/DDPM. Les résultats obtenus ont permis d'impliquer la kinase WNK1 et ses partenaires Akt, SGK1 et NBC dans ce processus (Figure 2). Par ailleurs, nos données suggèrent un rôle de WNK1 dans la physiopathologie des GSCs (augmentation de leur mortalité en conditions de quiescence, modification de leurs propriétés clonales, altération du taux de croissance des sphères et modification de l'aspect morphologique de grandes tumoresphères dérivées de ces cellules surexprimant la forme sauvage et/ou des formes mutées de WNK1). Il est intéressant de noter qu'à notre connaissance, aucun rôle de WNK1 dans les cellules souches cancéreuses n'a été décrit dans la littérature scientifique auparavant. L'ensemble de ce travail a donc permis d'élucider un des mécanismes d'action du bisacodyl/DDPM dans les GSCs et ce faisant d'identifier de nouvelles cibles thérapeutiques potentiellement intéressantes pour traiter les glioblastomes.

## **Bibliographie**

1. Alifieris C, Trafalis DT. Glioblastoma multiforme: Pathogenesis and treatment. *Pharmacol Ther.* 2015;152: 63–82. doi:10.1016/j.pharmthera.2015.05.005

2. Meacham CE, Morrison SJ. Tumour heterogeneity and cancer cell plasticity. *Nature*. 2013;501: 328–337. doi:10.1038/nature12624
3. SENGUPTA A, CANCELAS JA. Cancer Stem Cells: A Stride Towards Cancer Cure? *J Cell Physiol*. 2010;225: 7–14. doi:10.1002/jcp.22213
4. Moore N, Houghton J, Lyle S. Slow-Cycling Therapy-Resistant Cancer Cells. *Stem Cells Dev*. 2012;21: 1822–1830. doi:10.1089/scd.2011.0477
5. Zeniou M, Fève M, Mameri S, Dong J, Salomé C, Chen W, et al. Chemical Library Screening and Structure-Function Relationship Studies Identify Bisacodyl as a Potent and Selective Cytotoxic Agent Towards Quiescent Human Glioblastoma Tumor Stem-Like Cells. *PLOS ONE*. 2015;10: e0134793. doi:10.1371/journal.pone.0134793
6. Dong J, Aulestia FJ, Assad Kahn S, Zeniou M, Dubois LG, El-Habr EA, et al. Bisacodyl and its cytotoxic activity on human glioblastoma stem-like cells. Implication of inositol 1,4,5-triphosphate receptor dependent calcium signaling. *Biochim Biophys Acta BBA - Mol Cell Res*. doi:10.1016/j.bbamcr.2017.01.010
7. McCormick JA, Ellison DH. The WNKs: Atypical Protein Kinases With Pleiotropic Actions. *Physiol Rev*. 2011;91: 177–219. doi:10.1152/physrev.00017.2010



## Acknowledgement

First and foremost, I offer my sincerest gratitude to my advisor Dr. Maria ZENIOU, who has supported me throughout my master and Ph.D. pursuit with her tremendous patience and immense knowledge whilst allowing me the room to work in my own way. I would like to thank you for encouraging my research and for allowing me to grow as a research scientist. One simply could not wish for a better or friendlier advisor like you.

For this dissertation I would also like to thank my reading committee members, professor Pascal GAUDUCHON, Dr. Marc MOREAU, and other members of my oral defense committee, Dr. Françoise DANTZER and professor Marie-Claude KILHOFFER, for your precious time, interest, and help. I would also like to thank Professor Jacques HAIECH for all the kindness and support although my master and Ph.D. studies.

I thank my fellow labmates who are or were in our team, Dr Jihu DONG who gave me guidance at the beginning of my thesis and shared some of his expertise with me. Other former group members, Leonel NGUEKEU ZEBAZE, Laëtitia CHEZEAU, Vanessa NEVES CARVALHO SANTOS and Aude DELEAU for the stimulating discussions, for the hard days we were working together, and for all the fun we've had in the last years. In particular, my dear co-worker and great friend Farah HAJJAR, and her lovely young children. I have had pleasure to work with or alongside of you.

Thanks laboratory director, Professor Marcel HIBERT for his kindness for providing me all the support without hesitation, and other members of Dr. Frédéric BIHEL group, and former group member Dr. Songlin NIU for their agreeable collaboration.

I would also like to acknowledge our collaborators in Paris, Dr. Hervé CHNEIWEISS and Dr. Marie-Pierre JUNIER, for their generosity for providing us the cells.

My sincere thanks also go to Dr. Pascal VILLA, Christel VALENCIA, and Sophie GIORIA, Adeline OBRECHT at PICBIS (Platform of Integrative Chemical Biology of Strasbourg, Illkirch), who provided me an opportunity to join their platform, and gave me access to the laboratory and research facilities. Without their precious support, it would not be possible to conduct this research. It was delightful to have the opportunity to work majority of my research with you.

I also thank Claudine EBEL and colleagues for their technical assistance in regard of all the flow cytometry experiments at IGBMC (Institut de génétique et de biologie moléculaire et cellulaire, Illkirch).

A very special gratitude goes out to all down at Ligue Contre Le Cancer for providing the funding for my first 3 years' Ph.D work and our research project. My work was also supported by the LABEX ANR-10-LABX-0034\_Medalis, and the Agence Nationale de la Recherche (ANR) (JH), Université de Strasbourg and Centre National de la Recherche Scientifique (CNRS).

All my sincere apologies to those who I have not mentioned, but a great pleasure and honor to have known and worked with you.

I would also like to thank all of my friends, especially Qian ZHAO, who works in Professor Laurent DESAUBRY's team in our lab, supported me in writing, and incited me to strive towards my goal, and pass through all the hard moments along the way. And the inspiring and fun talks with their labmates made me a lot of fun and courage to continue all along the time.

Lastly, a special thanks to my family. Words cannot express how grateful I am to my grandmothers, my parents who raised me with unconditional love and supported me in all my pursuits. My sister and my brother-in-law, and their adorable daughter for all of the joy you've gave to me. All the sacrifices and supports that you've made on my behalf, your concerns and love for me were what sustained me this far. Thank you.

Wanyin CHEN  
University of Strasbourg  
April 2017

# Abbreviations

ABC: ATP-binding cassette transporter

ABCB5: ATP-binding cassette subfamily B member 5

ABCG5: ATP-binding cassette subfamily G member 5

AID: autoinhibitory domain

$\alpha$ -KG:  $\alpha$ -ketoglutarate

ALDH1: aldehyde dehydrogenase 1

AML: acute myeloid leukemia

$\alpha$ SMA: alpha smooth muscle actin

AR: amphiregulin

ATM: ataxia-telangiectasia mutated

ATP: adenosine triphosphate

ATRX:  $\alpha$ -thalassemia/mental retardation syndrome X-linked

bFGF: basic fibroblast growth factor

BSA: bovine serum albumin

BER: base excision repair

BT: brachytherapy

BTC:  $\beta$ -cellulin

CA: carbonic anhydrase

CAFs: cancer-associated fibroblastic cells

CaMKII: calcium/calmodulin-dependent protein kinase type II

CART: chimeric antigen receptors-modified T cells

CCD: coiled -coil domain

CCLE: cancer cell line encyclopedia

CD: cluster of differentiation

CDK: cyclin-dependent kinase

CDKN2A/B: cyclin dependent kinase inhibitor 2A/B

CFU: colony-forming unit

CFTR: cystic fibrosis transmembrane conductance regulator

CGAR: The Cancer Genome Atlas Research

CHI3L1: chitinase 3-like 1

Chk 2: checkpoint kinase 2

CML: chronic myelogenous leukemia

CNS: central nervous system

CNV: copy number variation

CUL3: cullin 3

CSCs: cancer stem-like cells

CSFs: colony-stimulating factors

CT: Computed tomography

CTL: cytotoxic T lymphocytes

CTL-4: cytotoxic T-lymphocyte antigen 4

CXCL8/12: C-X-C motif chemokine 8/12

CXCR: C-X-C motif chemokine receptor

DAPI: 4', 6-diamidino-2-phenylindole

DCs: dendritic cells

DDPM: 4, 4'-dihydrodiphenyl-2-pyridyl-methane

DDR1: discoidin domain receptor

DMSO: dimethyl sulfoxide

DMEM: Dulbecco's modified eagle medium

ECM: extracellular matrix

EC50: half maximal effective concentration

EdU: 5-ethynyl-2'-deoxyuridine

EDTA: ethylenediaminetetraacetic acid

EGF: epidermal growth factor

EGFR: epidermal growth factor receptor

ENaC: epithelial sodium channel

EpCAM: epithelial cell adhesion molecule, also known as ESA (epithelial specific antigen) or TROP1

ERKs: extracellular signal-regulated kinases

EMEM: eagle's minimum essential medium

ENL: erythema nodosum leprosy

FACS: fluorescence-activated cell sorting

FBS: fetal bovine serum

FDA: Food and Drug Administration

FGF2: fibroblast growth factor 2

FGFR: fibroblast growth factor receptor

FoxM1: forkhead box M1

FSRT: fractionated stereotactic radiotherapy

FTI: farnesyltransferase inhibitor

GABRA1: gamma-aminobutyric acid type A receptor alpha 1 subunit

G-CSF: granulocyte colony-stimulating factor

GSC: glioblastoma stem-like cell

GBM: glioblastoma

G-CIMP: glioma-CpG island methylator phenotype

GFAP: glioma fibrillary acidic protein

GLUT1/3: glucose transporter type 1/3

G6PDH: glucose 6-phosphate dehydrogenase

GSH: reduced glutathione

GSIs: gamma-secretase inhibitors

GTP: guanosine triphosphate

hAFP: human alpha-feto protein

HDAC: histone deacetylase

H/E: hematoxylin/eosin

HFSRT: hypofractionated stereotactic radiotherapy

2-HG: 2-hydroxygutarate

HGF: hepatocyte growth factor

Hh: hedgehog

HIF: hypoxia-inducible factor

HREs: hypoxia-responsive elements

HRP: horseradish peroxidase

HSPs: heat shock proteins

hTERT: human telomerase reverse transcriptase

HTS: high-throughput screening

IDH1/2: isocitrate dehydrogenase 1/2

IGF-1: insulin-like growth factor 1

IL-6: interleukin-6

IP3R1/3: inositol 1,4,5-trisphosphate receptor 1/3

IR: ionizing radiation

IRBIT: inositol 1,4,5-trisphosphate (IP3) receptor-binding protein released with IP3

JNK: c-Jun N-terminal kinase

KLHL3: kelch-like family member 3

LAK: lymphocyte-activated killer cells

L1CAM: L1-cell adhesion molecule

LDHA: lactate dehydrogenase A

LOH: loss of heterozygosity

MAPK: mitogen-activated protein kinase

MCTs: monocarboxylate transporters

MDM2/4: mouse double-minute 2/4

MDSCs: myeloid-derived suppressor cells

MEK: MAPK kinase

MEKK: MAPK kinase kinase

MERTK: myeloid-epithelial-reproductive tyrosine kinase

MET: mesenchymal-epithelial transition

MGMT: O-6-methylguanine-DNA methyltransferase

MRI: magnetic resonance imaging

MRS: magnetic resonance spectroscopy

MMPs: matrix metalloproteinases

MMR: mismatch repair

mTOR: mammalian target of rapamycin

mTORC1/2: mammalian target of rapamycin complex 1/2

NADP<sup>+</sup>: nicotinamide adenine dinucleotide phosphate

NAPDH: reduced nicotinamide adenine dinucleotide phosphate

NBC: Na<sup>+</sup>/HCO<sub>3</sub><sup>-</sup> cotransporter

NCC: Na<sup>+</sup>/Cl<sup>-</sup> cotransporter

NCGC: National institute of health's Chemical Genomics Center

NDCBE: Na<sup>+</sup>-driven Cl<sup>-</sup>/HCO<sub>3</sub><sup>-</sup> exchanger

NEFL: neurofilament light polypeptide

NF-1: neurofibromin 1

NF- κB: nuclear factor kappa-light-chain-enhancer of activated B cells

NHE: Na<sup>+</sup>/ H<sup>+</sup> exchanger| sodium hydrogen exchanger

NKCC: Na<sup>+</sup>/K<sup>+</sup>/2Cl<sup>-</sup> cotransporter

NOD/SCID: non-obese diabetic/severe combined immunodeficiency

NSCLC: non-small cell lung cancer

OCT-3/4: octamer-binding transcription factor 3/4

OS: overall survival

OSR1: oxidative stress-responsive kinase 1

PARPs: poly ADP-ribose polymerases

PBS: phosphate buffered saline

PCNA: proliferating cell nuclear antigen

PD-1: programmed cell death protein 1

PDGF: platelet-derived growth factor

PDGFRA: platelet derived growth factor receptor alpha

PK1: phosphoinositide-dependent kinase 1

PET: positron emission tomography

PFA: paraformaldehyde

PFS: progression-free survival

PIP2: phosphatidylinositol- 4,5 -bisphosphate

PIP3: phosphatidylinositol- 3,4,5 -triphosphate

PI3K: phosphoinositide 3-kinase

PKC: protein kinase C

PP1: protein phosphatase 1

PPAR $\gamma$ : peroxisome proliferator-activated receptor  $\gamma$

PRDs: proline-rich domains

PTEN: phosphatase and tensin homolog

RB1: retinoblastoma 1

RIN: RNA integrity number

RIP1: receptor interacting protein 1

ROMK1: renal outer medullar potassium 1

ROS: reactive oxygen species

RSK: ribosomal s6 kinase

RTKs: receptor tyrosine kinases



RTL: relative telomere length

sAC: soluble adenylyl cyclase

SAR: structure-activity relationship

SGK1: serum and glucocorticoid regulated kinase 1

SH3: Src homology domain 3

SHH: sonic hedgehog

SLC: solute carrier family

SOX2: sex determining region Y-box 2

SP: side population

SPAK: STE20/SPS1 related proline/alanine-rich protein kinase

SSEA-1: stage-specific embryonic antigen

STAT3: signal transducer and activator of transcription 3

SYT1: synaptotagmin 1

TAMs: tumor-associated macrophages

TBS: tris-buffered saline

TCA: tricarboxylic acid

TCGA: The Cancer Genome Atlas

TCR: T cell receptor

TEMs: TIE-2 expressing monocytes

TERT: telomerase reverse transcriptase

TGF- $\beta$ : Transforming growth factor-beta

TME: tumor microenvironment

TMZ: Temozolomide

TNF: Tumor necrosis factor

TP53: Tumor protein 53

TSC1/2: tuberous sclerosis proteins 1/2, also known as hamartin/tuberin

TTF: tumor treating field

uPA: urokinase-type plasminogen activators

VEGF: vascular endothelial growth factor

WHO: World Health Organization

WNK1: with no lysine (K) kinase 1

ZEB1: zinc finger E-box binding homeobox

# Contents

<b>Scope of my thesis</b>	<b>1</b>
<b>I. Introduction</b>	<b>2</b>
<b>1.1 Glioma and glioblastoma</b>	<b>2</b>
1.1.1 Glioma and histological classification	2
1.1.2 Glioblastoma	3
1.1.2.1 Primary glioblastoma	5
1.1.2.2 Secondary glioblastoma	5
1.1.2.3 Causes and risk factors	6
1.1.2.4 Symptoms and diagnosis	7
1.1.2.4.1 Symptoms	7
1.1.2.4.2 Diagnosis	7
1.1.3 Molecular characterization of glioblastoma	7
1.1.3.1 Genetic profiling of GBM	7
1.1.3.1.1 IDH mutation	8
1.1.3.1.2 G-CIMP	9
1.1.3.1.3 MGMT promoter methylation	10
1.1.3.1.4 EGFR amplification	10
1.1.3.1.5 TP53 mutations	12
1.1.3.1.6 ATRX mutation	12
1.1.3.1.7 TERT promoter mutation	12
1.1.3.1.8 Chromosome losses	13
1.1.4 Classification of GBM subtypes based on genomic alterations	14
1.1.4.1 Classical	15
1.1.4.2 Proneural	15
1.1.4.3 Neural	16
1.1.4.4 Mesenchymal	16
1.1.5 CNS WHO2016 Classification	16
1.1.5.1 IDH-wild-type GBM	17
1.1.5.2 IDH-mutated GBM	17
1.1.5.3 GBM NOS	17
1.1.6 Signaling pathways in GBMs	18
1.1.6.1 RTK/PI3K/Akt pathway	19
1.1.6.2 RAS/RAF/MAPK pathway	19
1.1.6.3 The TP53 pathway	20
1.1.6.4 Retinoblastoma (RB) tumor suppressor protein signaling pathway	21
1.1.6.5 Other signaling pathways	21
1.1.7 Tumor microenvironment in glioblastoma	22
1.1.7.1 Tumor microenvironment (TME)	23
1.1.7.1.1 Tumor vasculature	23
1.1.7.1.2 The stromal cell types and immune cell types of the TME	24
1.1.7.1.2.1 The angiogenic vascular cells	24
1.1.7.1.2.2 Cancer-associated fibroblastic cells	25
1.1.7.1.2.3 Immune cells	25
1.1.7.1.3 The extracellular matrix (ECM)	26

1.1.7.2	TME in glioblastoma	28
1.1.7.2.1	Angiogenesis in GBM	28
1.1.7.2.2	Hypoxia in GBM	28
1.1.7.2.3	Acidity and GBM	29
1.1.7.2.4	Glioblastoma microenvironment and therapy resistance	30
1.1.8	Treatments for glioblastoma	31
1.1.8.1	First-line treatments for new diagnosed glioblastoma	31
1.1.8.2	Treatments for recurrent glioblastoma	33
1.1.8.2.1	Repeat surgical resection	33
1.1.8.2.2	Repeat irradiation	33
1.1.8.2.3	Systemic therapy	35
1.1.8.3	Immunotherapy and other emerging therapies	35
1.1.8.3.1	Immunotherapy	35
1.1.8.3.2	Emerging advances in radiotherapy	37
1.1.8.3.3	Inhibitors of growth factors and their receptors	37
1.1.8.3.4	Inhibitors of intracellular signaling pathways	38
1.1.8.3.5	Inhibition of angiogenesis	39
<b>1.2</b>	<b>Glioblastoma and Cancer stem-like cells</b>	<b>40</b>
1.2.1	Tumor heterogeneity	40
1.2.2	Discovery of cancer stem-like cells	42
1.2.3	Cancer stem-like cell properties	44
1.2.3.1	Expression of cell surface and functional markers	44
1.2.3.2	Self-renewal and long-term proliferation ability	47
1.2.3.3	Differentiation potential	47
1.2.3.4	Increased pro-survival signaling	48
1.2.3.5	Resistance to DNA damage	48
1.2.3.6	Increased efflux capacity of the Hoechst dye	48
1.2.3.7	In vivo tumor initiation capacity	49
1.2.3.8	Dormancy (Quiescence)	49
1.2.3.9	Plasticity	51
1.2.3.10	Increased stemness and aggressivity in hypoxic/acidic tumor microenvironment	52
1.2.3.11	Metastatic potential	52
1.2.3.12	Therapy resistance	53
1.2.4	CSCs and evolution of models of tumor initiation and heterogeneity	55
1.2.4.1	The clonal evolution (stochastic) model	55
1.2.4.2	The hierarchical model based on CSCs	56
<b>1.3</b>	<b>WNK kinases</b>	<b>59</b>
1.3.1	The WNK family of protein kinases	59
1.3.1.1	Organization and expression of human WNK genes	59
1.3.1.2	Protein structure of WNK kinases	60
1.3.1.3	Tissue expression pattern of WNK kinases	62
1.3.1.4	Subcellular localization of WNK proteins	63
1.3.1.5	Stimuli and mechanisms of WNK activation	63
1.3.2	WNK functions	65
1.3.2.1	Fluid and electrolyte homeostasis	65
1.3.2.2	Cell proliferation, migration and survival	67

1.3.2.3	Vesicular trafficking	69
1.3.2.4	Other WNK functions	69
1.3.3	WNK kinases in cancer - Focus on WNK1	71
1.3.3.1	WNK kinases in glioma	72
<b>II.</b>	<b>Results</b>	<b>74</b>
<b>Part I.</b>	Phenotypic and functional characterization of proliferating and quiescent glioblastoma stem-like cells and identification of bisacodyl	<b>74</b>
<b>Part II.</b>	Study of bisacodyl signaling pathways in GSCs: involvement of WNK1 and its signaling partners	<b>118</b>
<b>III.</b>	<b>Discussion and conclusion</b>	<b>201</b>
<b>3.1.</b>	<b>Glioblastoma: development of new therapeutic strategies in the presence of GSCs and of a complex tumor microenvironment</b>	<b>201</b>
<b>3.2</b>	<b>Experimental models for brain tumor studies</b>	<b>202</b>
3.2.1	<i>In vitro</i> and <i>in vivo</i> experimental models	202
3.2.2	The spheroid model in brain tumors	205
3.2.3	Spheroid formation ability and cancer stem cells	205
3.2.4	GSC in vitro models used in our study	207
<b>3.3</b>	<b>Bisacodyl in GSCs</b>	<b>208</b>
3.3.1	Bisacodyl	208
3.3.2	Bisacodyl/DDPM cytotoxicity profile in GSCs	209
3.3.3	Mechanisms and signaling pathways of bisacodyl in GSCs	210
3.3.4	Direct protein targets of bisacodyl in GSCs	213
3.3.5	Therapeutic interests of bisacodyl	215
<b>3.4</b>	<b>Interests of WNK1 in GBM pathology and potential as a therapeutic target</b>	<b>216</b>
3.4.1	WNK1 in GSCs	216
3.4.2	Interests for WNK1 as a new protein kinase target	217
<b>3.5</b>	<b>Drug repositioning</b>	<b>219</b>
<b>IV.</b>	<b>APPENDIX 1</b>	<b>252</b>

# List of Figures

FIGURE 1. BRAIN ANATOMY AND DISTRIBUTION OF GLIOBLASTOMAS BY SITE .....	4
FIGURE 2. PRIMARY AND SECONDARY GLIOBLASTOMA AND ASSOCIATED GENETIC ALTERATIONS.....	6
FIGURE 3. CLASSIFICATION OF GLIOBLASTOMAS BASED ON GENOMIC ALTERATIONS AND GENE EXPRESSION PROFILES .....	15
FIGURE 4. CRITICAL SIGNALING PATHWAYS ALTERED IN GLIOBLASTOMA.....	22
FIGURE 5. TUMOR MICROENVIRONMENT AND MAJOR CELL TYPES INVOLVED .....	27
FIGURE 6. CANCER STEM-LIKE CELL PROPERTIES. ....	42
FIGURE 7. CANCER STEM-LIKE CELL MECHANISMS OF THERAPY RESISTANCE .....	53
FIGURE 8. NOVEL PARADIGMS FOR CANCER TREATMENT.....	55
FIGURE 9. MODELS FOR TUMOR INITIATION AND TUMOR HETEROGENEITY.....	58
FIGURE 10. PROTEIN STRUCTURE OF WNKS.....	62
FIGURE 11. ROLES OF WNKS AND CORE SIGNALING PATHWAYS INVOLVED .....	70
FIGURE 12. ISOLATION AND IN VITRO CULTURE OF PROLIFERATING AND QUIESCENT GLIOBLASTOMA STEM-LIKE CELLS FROM PATIENTS .....	75
FIGURE 13. CHARACTERIZATION OF QUIESCENT GLIOBLASTOMA STEM-LIKE CELLS .....	76
FIGURE 14. CHEMICAL STRUCTURES OF BISACODYL AND DDPM AND ACTIVITY PROFILES TOWARDS PROLIFERATING AND QUIESCENT GLIOBLASTOMA STEM-LIKE CELLS.....	77
FIGURE 15. CLONAL 3D GLIOBLASTOMA STEM-LIKE CELL-DERIVED MACRO-TUMOROSPHERES SHARE MANY ASPECTS OF GLIOBLASTOMA TUMORS.....	119
FIGURE 16. EFFECT OF DDPM ON CLONAL MACRO-TUMOROSPHERES OBTAINED FROM GLIOBLASTOMA STEM-LIKE CELLS .....	120
FIGURE 17. EVALUATION OF BISACODYL'S ACTIVITY IN AN ORTHOTOPIC XENOGRAFT MODEL OF GLIOBLASTOMA OBTAINED WITH GLIOBLASTOMA STEM-LIKE CELLS .....	121
FIGURE 18. HISTOPATHOLOGICAL FEATURES OF GLIOBLASTOMA.....	202
FIGURE 19. SPHEROID FORMATION METHODS AND THEIR APPLICATIONS .....	204
FIGURE 20. AFFINITY CHROMATOGRAPHY FOR IDENTIFYING DIRECT PROTEIN TARGET(S) OF BISACODYL.....	215
FIGURE 21. COMPARISON OF TRADITIONAL DE NOVO DRUG DEVELOPMENT VERSUS DRUG REPOSITIONING.....	220

# List of Tables

TABLE 1. WHO CLASSIFICATION OF DIFFUSE GLIOMAS BASED ON HISTOLOGICAL AND GENETIC FEATURES .....	3
TABLE 2. WHO 2016 CLASSIFICATION OF GLIOBLASTOMAS ACCORDING TO IDH STATUS.....	18
TABLE 3. CELL SURFACE MARKERS USED FOR THE IDENTIFICATION/ISOLATION OF CANCER STEM-LIKE CELLS FROM VARIOUS TUMOR TYPES. ....	45
TABLE 4. WNK1 MUTATIONS IDENTIFIED IN TUMORS .....	71

## Scope of my thesis

Glioblastoma is an extremely aggressive and fatal brain cancer with very poor prognosis and short-term median survival for patients. Cancer cells with stem-like properties that have been isolated from glioblastomas and many other tumors have emerged as major players in therapy failure, namely because they are able to enter into a quiescent state and escape from most conventional antiproliferation therapies. Moreover, cancer stem-like cells were shown to acquire a more aggressive and stem-like phenotype in hypoxic/acidic tumor microenvironments which are a frequent feature in glioblastoma. Thus, treatments targeting glioblastoma stem-like cells are promising novel therapeutic strategies against glioblastoma.

With the aim of finding compounds targeting proliferating and quiescent glioblastoma stem-like cells, *in vitro* models for proliferating and quiescent glioblastoma stem-like cells derived from patient samples were developed and characterized in our lab. Bisacodyl and its active metabolite DDPM were subsequently identified in a high-throughput screen of the Prestwick chemical library mainly composed of FDA (Food and Drug Administration)-approved drugs. Bisacodyl/DDPM promote necrosis in quiescent glioblastoma stem-like cells and their proliferating counterparts only in acidic conditions. Moreover, bisacodyl was shown to target inner layer quiescent cells within 3D clonal macro-tumorspheres derived from glioblastoma stem-like cells and to induce tumor shrinkage in a mouse model of glioblastoma.

In this context, my thesis work was focused in studying the molecular mechanisms of the cytotoxicity of bisacodyl in glioblastoma stem-like cells under quiescent/acidic culture conditions. Based on our data, the serine/threonine kinase WNK1 and several of its protein partners were involved in the cytotoxic/necrotic effect of the compound.

Thus, the introduction of my thesis will consist of three parts to describe literature on glioblastoma and on cancer stem-like cells and glioblastoma stem-like cells. The last part will concern the WNK1 protein and its functions in other systems.



# **I. Introduction**

## **1.1 Glioma and glioblastoma**

### **1.1.1 Glioma and histological classification**

Gliomas are one of the most common types of brain cancer. These tumors, arising from glial cells, represent over 27% of all brain tumors and 80% of all brain and central nervous system malignancies. Based on the cell type from which they originate, there are three main types of gliomas: astrocytomas, oligodendrogliomas, and ependymomas. Tumors that display a mixture of these different cells are called mixed gliomas [1].

About 2-3% of brain tumors are ependymomas arising from ependymal cells that line the ventricles of the brain and the center of the spinal cord and whose normal function is to repair damaged nerve tissue. Ependymomas are relatively more diagnosed in children or young adults and about 30% of pediatric ependymomas are diagnosed in children younger than 3 years old. According to the Central Nervous System (CNS) World Health Organization (WHO) classification based on histological features (including cellularity, the presence of mitosis, vasculature, and necrosis), from low grade to high grade, there are four major types of ependymomas: subependymomas (grade I) and myxopapillary ependymomas (grade I) are typically slow-growing ependymomas, ependymomas (grade II or III) are the most common type of these tumors, and anaplastic ependymomas (grade III) which correspond to fast-growing malignancies [2].

Oligodendrogliomas originate from oligodendrocytes, a type of cells that support and insulate the axons by forming myelin sheaths in the central nervous system (CNS). They can be grade II- oligodendrogliomas or grade III corresponding to anaplastic oligodendrogliomas. They represent about 10% of gliomas and most of them are found in adults (50-60 years old) and are more frequent in men than in women.

Astrocytomas, represent approximately 75% of all gliomas. They are tumors arising from astrocytes, a type of star-shaped cells involved in synaptic functions, blood brain barrier maintenance and water and ion homeostasis in the brain [3].

According to the WHO classification, the grade of astrocytomas varies from I to IV based on histological and genetical abnormalities of the cells. Pilocytic astrocytoma and subependymal giant astrocytoma are grade I astrocytomas who are typically localized tumors. Diffuse astrocytomas, also called low-grade astrocytomas, are grade II astrocytomas. Anaplastic astrocytoma is a grade III tumor. Grade IV astrocytomas, also called glioblastomas, are the most aggressive and the most common form of astrocytomas (Table 1) [2].

Type	Grade	Genetic features	Histological features	Median survival (years)
Diffuse astrocytoma	II	IDH mutant ATRX loss and p53 mutations	Found diffusely infiltrating into surrounding neural tissue, increased cellularity, no mitosis	6-8
Anaplastic astrocytoma	III	IDH mutant ATRX loss and p53 mutations	Highly infiltrating tumors with increased mitotic activity, no necrosis or vascular proliferation	3
Glioblastoma	IV	IDH mutant IDH wild-type	Infiltrating glial neoplasm with necrosis and micro-vascular proliferation, high rate of mitosis	1-2
Oligo-dendroglioma	II	IDH mutant and 1p/19q co-deleted	Occur in the white matter and cortex of the cerebral hemispheres, low mitotic activity, no necrosis	3-10
Anaplastic oligo-dendroglioma	III	IDH mutant and 1p/19q co-deleted	High cellular density, increased mitotic features, endothelial hyperplasia, no necrosis	3

**Table 1. WHO classification of diffuse gliomas based on histological and genetic features, adapted from [2][4].** IDH: isocitrate dehydrogenase; ATRX:  $\alpha$ -thalassemia/mental retardation syndrome X-linked.

### 1.1.2 Glioblastoma

Glioblastoma (GBM) multiform (WHO grade IV astrocytoma) is the most frequent and aggressive type of brain and CNS malignancy. It represents 15.1% of all primary brain tumors and over 55% of all gliomas. GBMs are primarily diagnosed at older ages with a median age at diagnosis of 64 years old compared to a median

age of 59 for all other primary brain and CNS tumors. Among primary brain and CNS tumors diagnosed in the United States between 2008 and 2012, GBMs showed an incidence of about 3 cases in a 100,000 population. The incidence rate of GBM in males is 1.6 times higher than in females [1].

GBMs are more commonly located in the supratentorial region (mostly in frontal, temporal and parietal lobes and less frequently in occipital lobes (Figure 1), are rarely seen in the cerebellum and are very rare in the spinal cord [5]. They are histologically distinct from other astrocytomas because of the presence of necrotic zones and increased abnormal vasculogenesis.

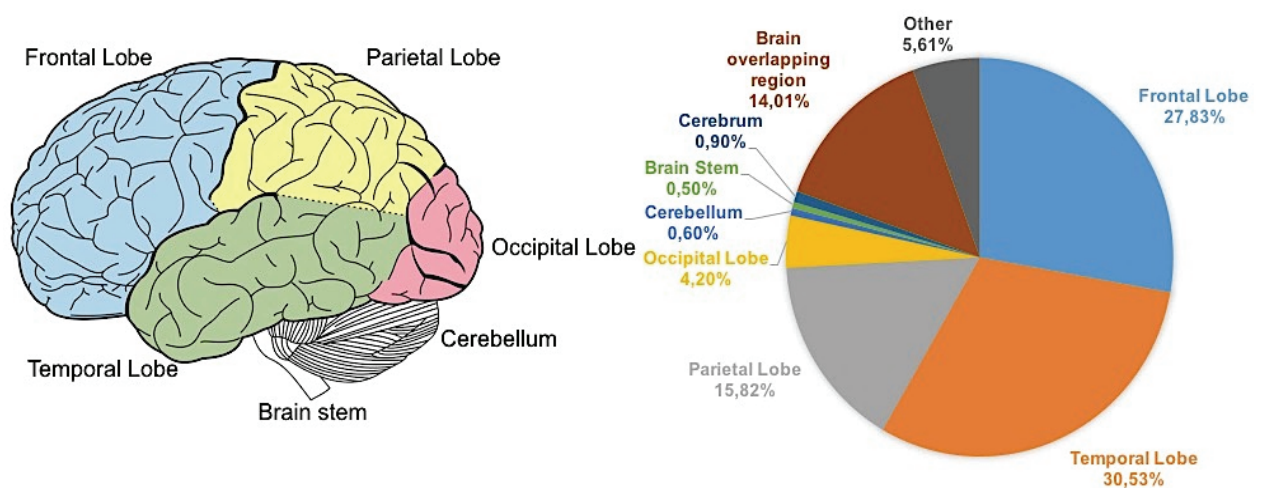


**Figure 1 Brain anatomy and distribution of glioblastomas by site, data from Cedars-Sinai, 1998-2013.** Glioblastomas are mainly located in the frontal, temporal or parietal lobes of the brain. The occipital lobe, cerebellum and spinal cord are much less frequent sites for glioblastoma development.

Traditionally, GBMs have been classified as primary or secondary on the basis of their clinical presentation. Primary GBMs arise in the brain “*de novo*” whereas secondary GBMs evolve from lower-grade astrocytomas. Primary and secondary GBMs evolve through different genetic pathways, carry distinct genetic alterations, affect patients at different ages and have different outcomes (Figure 2).

### **1.1.2.1 Primary glioblastoma**

Primary glioblastomas account for more than 90% of GBMs. They are very aggressive and can rapidly spread into other parts of the brain. Primary GBMs occur predominantly in the temporal lobe and are mainly diagnosed in patients over 62 years of age with a higher incidence in males. These high-grade (WHO grade IV) tumors have no detectable precursor lesions and display the worst prognosis (median survival <15 months).

Typical genetic alterations in these tumors include EGFR (epidermal growth factor receptor) gene amplification, PTEN (phosphatase and tensin homolog) mutations accompanied by chromosome 10q loss of heterozygosity ((LOH) 10q), p16 gene deletions and a high frequency of telomerase reverse transcriptase (hTERT) promoter mutations. Primary GBMs also show a low frequency of TP53 (tumor protein) and IDH1 (isocitrate dehydrogenase 1) mutations and MDM2 (Mouse Double-Minute 2) gene amplification exclusively in the absence of TP53 mutations (Figure 2) [6][7].

### **1.1.2.2 Secondary glioblastoma**

Secondary GBMs develop from low-grade diffuse astrocytomas (WHO grade II) or anaplastic astrocytomas (WHO grade III) through additional malignant transformation. They occur less frequently than primary GBMs (about 5-10% of GBMs are secondary GBMs). Conversely to primary GBMs, secondary GBMs are present at higher rates in younger patients (under 45 years old) and in women. The hallmark of secondary GBMs is the presence of IDH1 mutations, accompanied with TP53 and ATRX ( $\alpha$ -thalassemia/mental retardation syndrome X-linked) mutations and LOH 10q. They often lack EGFR amplification and have a low frequency of PTEN mutations (Figure 2) [8].

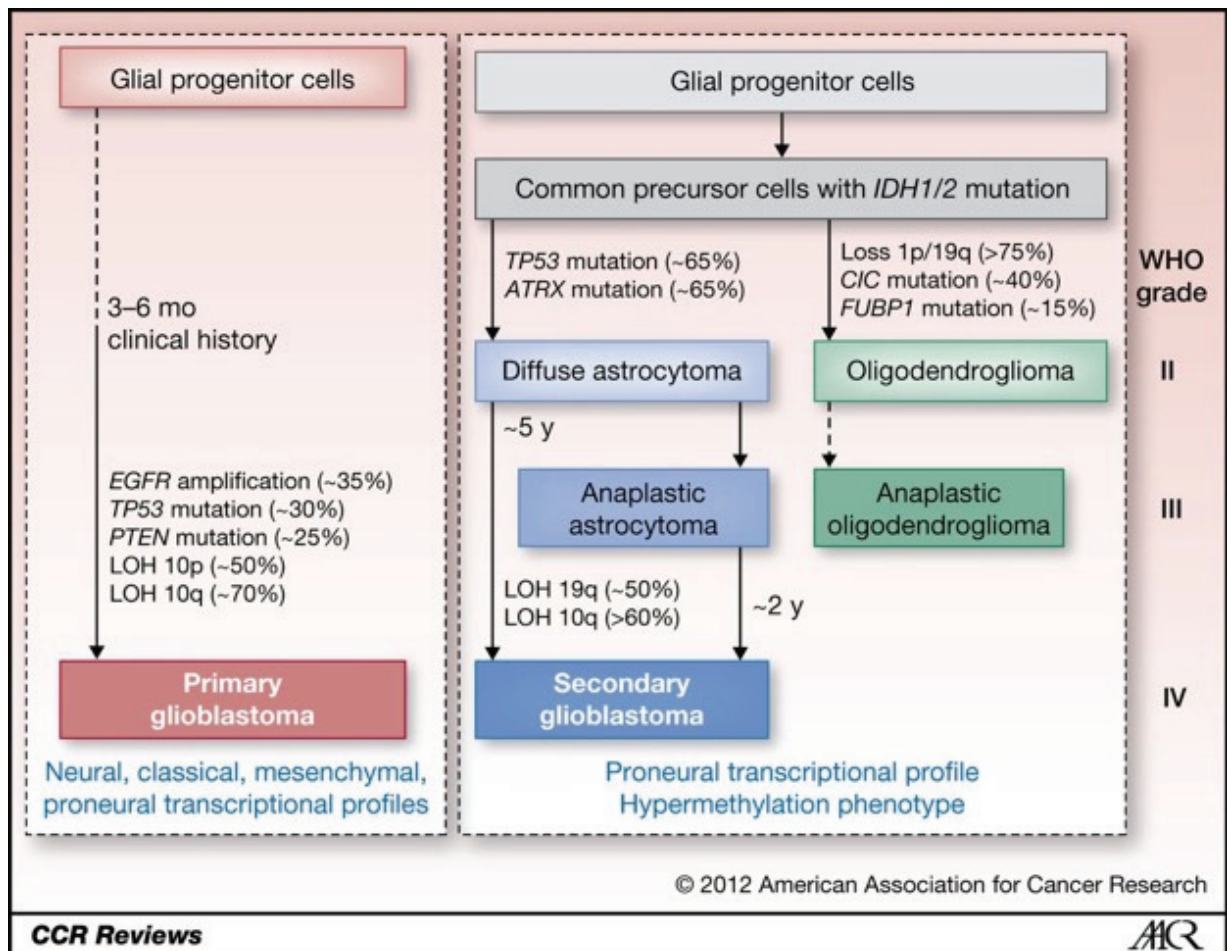


**Figure 2. Primary and secondary glioblastoma and associated genetic alterations, from [9].** Primary glioblastomas (WHO grade IV astrocytomas) have no detectable precursor lesions and represent more than 90% of all glioblastomas. Secondary glioblastomas develop from lower grade (WHO grade II or III) diffuse gliomas. Primary and secondary glioblastomas differ with respect to the genetic alterations present in cancer cells. IDH: isocitrate dehydrogenase; ATRX:  $\alpha$ -thalassemia/mental retardation syndrome X-linked; EGFR: epidermal growth factor receptor; PTEN: phosphatase and tensin homolog; LOH: loss of heterozygosity; CIC: capicua transcriptional repressor; FUBP1: far upstream element binding protein 1.

### 1.1.2.3 Causes and risk factors

The cause of brain tumors including glioblastoma is poorly understood despite a great deal of studies aiming to identify possible environmental, occupational, familial and genetic risk factors.

There is no conclusive evidence of GBM being connected to life-style characteristics such as physical activity levels, smoking history, alcohol

consumption, use of drug of any kind or dietary exposure to N-nitroso compounds (cured or smoked meat or fish) [10]. The only proven environmental risk factor for gliomas is exposure to ionizing radiation.

Most brain cancers are not hereditary, though some studies showed a positive family history of increased glioma risk across all races/ethnicities. However, no specific genetic alterations have been established as risk factors. In very few cases, GBMs can be associated to genetic syndromes such as Li-Fraumeni syndrome, Von Hippel-Lindau syndrome, Neurofibromatosis (I and II), Turcot syndrome and Tuberous Sclerosis [11].

#### **1.1.2.4 Symptoms and diagnosis**

##### **1.1.2.4.1 Symptoms**

The first and most common symptoms for patients with GBM are headaches, seizures, memory loss and personality/behavioral changes. Since tumor growth interferes with the normal function of the brain, additional symptoms may be present depending on the location of the tumor.

##### **1.1.2.4.2 Diagnosis**

The diagnosis often begins with a neurological examination followed by an imaging test. Magnetic resonance imaging (MRI), computed tomography (CT) and/or positron emission tomography (PET) scans may be used to identify the size, border and location of the tumor. These approaches are sometimes accompanied by a magnetic resonance spectroscopy (MRS) scan to measure the chemical and mineral composition within the abnormal brain tissue. However, the only way to confirm a brain tumor is a GBM, is the examination of the tumor tissue under a microscope and molecular/genetic analysis is required to make an exact diagnosis. The relative survival estimates for GBM are quite low; less than 10% of patients survive five years post diagnosis [12].

#### **1.1.3 Molecular characterization of glioblastoma**

##### **1.1.3.1 Genetic profiling of GBM**

All GBMs are WHO grade IV astrocytomas but exhibit significant genetic heterogeneity underlying differences in prognosis and response to treatment.

Various prognostic markers have been identified in GBM, including the methylation status of the O6-methylguanine-DNA methyltransferase (MGMT) gene promoter, the presence of isocitrate dehydrogenase enzyme 1/2 (IDH1/2) gene mutations, overexpression of EGFR, PTEN gene mutations, presence of glioma-CpG island methylator phenotype (G-CIMP), TP53 gene mutations and genetic losses of chromosomes.

### **1.1.3.2 IDH mutation**

Isocitrate dehydrogenase (IDH) is a tricarboxylic acid cycle enzyme that has 3 isoforms catalyzing the oxidative decarboxylation of isocitrate to  $\alpha$ -ketoglutarate ( $\alpha$ -KG). IDH1 and 2 are NADP<sup>+</sup> (nicotinamide adenine dinucleotide phosphate)-dependent enzymes, with cytosolic/peroxisomal and mitochondrial localizations, respectively. IDH1 is thought to be involved in lipid metabolism and glucose sensing whereas IDH2 regulates oxidative respiration. IDH3 is a mitochondrial, NAD<sup>+</sup>-dependent isoform that plays an essential role in aerobic energy production in the tricarboxylic acid (TCA) cycle [13].

Reduced nicotinamide adenine dinucleotide phosphate (NADPH) is mainly produced by glucose 6-phosphate dehydrogenase (G6PDH), malate dehydrogenase, and IDH. NADP<sup>+</sup>-dependent isoforms IDH1/2 form homodimers and generate NADPH from NADP<sup>+</sup> by catalyzing the oxidative decarboxylation of isocitrate to  $\alpha$ -KG outside of the KREB cycle (TCA cycle). NADPH is a major reducing compound in cells required by both glutathione reductase and thioredoxin reductase for the generation of reduced glutathione (GSH) and reduced thioredoxin, which are the basis of two crucial cellular antioxidant systems.

Mutations in IDH1 were first reported by Parsons and colleagues in 2008 [8] and recently emerged as important diagnostic and prognostic markers in GBM. Mutations of IDH1 are rare in primary GBM (10%), but have been associated with a large majority (80%) of grade II-III gliomas and secondary GBMs that develop from these lower grade precursor lesions. The most common IDH mutation is a heterozygous point mutation with a change of guanine to adenine at position 395 (G395A) leading to the replacement of arginine at position 132 by histidine (R132H, IDH1-R132H, or mIDH1) [14]. This arginine residue is located in the active site of the enzyme and is critical for isocitrate binding. Mutant IDH1 catalyzes the

conversion of  $\alpha$ -KG to the “oncometabolite” 2-hydroxyglutarate (2-HG) and during this process it converts NADPH to NADP<sup>+</sup>, conversely to the reaction occurring in the presence of wildtype IDH1. Therefore, the R132H mutation results in a reduction of the levels of  $\alpha$ -KG and NADPH, which are necessary to maintain normal levels of GSH involved in cell defense mechanisms against ROS (reactive oxygen species). As a consequence, upon exposure to free radicals and ROS, cells with low levels of IDH activity in the presence of the R132H mutation, become more sensitive to oxidative damage [13][15]. Thus, negative IDH-R132H mutation status in diffuse glioma of older adults is a poor prognostic factor associated with an extremely fast progression of the disease.

It has been reported that IDH1 mutation is more frequently associated with TP53 mutations and 1p/19q loss of heterozygosity (LOH) in secondary GBMs [16]. However, mutated IDH1 has been reported to be associated with longer progression-free survival despite of histology, 1p/19q deletion status or MGMT promoter methylation status [14].

### **1.1.3.3 G-CIMP**

A CpG island methylator phenotype (CIMP) was first reported and characterized in human colorectal cancer in 1999 [17]. In 2010, the Cancer Genome Atlas (TCGA) research network identified a CIMP phenotype as a distinct clinical and molecular feature allowing to define various subtypes of gliomas. Glioma-CpG island methylator phenotype (G-CIMP) is characterized by glioma-specific CpG island hypermethylation of a subset of loci [18].

G-CIMP has been associated with transcriptional inactivation of several tumor-suppressor genes including the retinoblastoma gene (RB1). In some studies, G-CIMP resulted in up-regulation of genes functionally related to cellular metabolic processes and positive regulation of macromolecules. These findings may be related to a metabolic adjustment of tumor cells allowing them to maintain their proliferating state and may explain the tumorigenic processes in G-CIMP positive tumors. However, the G-CIMP phenotype was also associated to decreased expression of several genes whose high expression levels were previously related to bad outcome as well as of genes involved in mesenchymal cellular phenotypes and tumor invasion. In this regard, the G-CIMP positive GBMs often carry the IDH



mutated status and the G-CIMP positive phenotype is significantly more frequent in secondary compared to primary forms of the disease and in younger patients [19]. The IDH-mutation/G-CIMP positive status is reported to be a good prognostic factor in GBM patients [20].

#### **1.1.3.4 MGMT promoter methylation**

The O6-methylguanine-DNA methyltransferase (MGMT) gene is located on chromosome 10q26 and encodes a DNA-repair protein that transfers alkyl groups from the O6 position of guanine, an important site of DNA alkylation, to an internal cysteine residue. This irreversible reaction is followed by the ubiquitination and degradation of the MGMT protein [21].

MGMT plays an important role in direct DNA repair. In the case of GBM patients, treated by ionizing radiation (IR) and the DNA alkylating agent temozolomide (TMZ), MGMT is an important component of DNA repair pathways involved in the removal of IR- and TMZ-induced lesions leading rapidly to occurrence of resistance and tumor relapse. Indeed, the major lesions induced by TMZ are N7-methylguanine (N7-meG) and N3-methyladenine (N3-meA), which are primarily repaired by base excision repair (BER), and O6-methylguanine (O6-meG), a highly cytotoxic lesion which can be removed by MGMT. In the absence of MGMT, unrepaired O6-meG can form an O6-meG/T mismatch that is recognized by the mismatch repair (MMR) machinery [22].

Epigenetic silencing of the MGMT gene expression by promoter CpG methylation is commonly observed in GBM patients (45%) and is associated with increased sensitivity to TMZ and increased survival (median survival > 6 months) [21]. Therefore, nowadays, it is widely accepted that MGMT promoter methylation in GBMs is a predictor of response to alkylating chemotherapy.

#### **1.1.3.5 EGFR amplification**

The epidermal growth factor receptor (EGFR) is a transmembrane tyrosine kinase receptor which consists of two cysteine-rich extracellular domains and an intracellular tyrosine kinase domain. Epidermal growth factor (EGF), transforming

growth factor- $\alpha$  (TGF- $\alpha$ ),  $\beta$ -cellulin (BTC) and amphiregulin (AR) are specific ligands for EGFR [23]. EGFR belongs to the ErbB family of receptor tyrosine kinases (RTKs) which is a highly-conserved group of structurally homologous type 1 tyrosine kinases (kinase transmembrane glycoproteins), that transduce extracellular stimuli to the cell nucleus to promote cell differentiation, proliferation, and migration.

EGFR gene amplification, mutations and rearrangements are observed in more than 60% of GBMs with a high frequency ( >40%) in primary GBM. These genetic defects enhance tumor growth, survival, progression, invasion and resistance to therapy through activation of several signaling networks and metabolic reprogramming [24]. The most common EGFR variant in GBMs, EGFRvIII, is characterized by a an in-frame deletion of exons 2-7 which leads to a loss of 267 amino acids in the extracellular domain resulting in dimerization and ligand-independent constitutive activity of the receptor [25][26]. In addition, heterogeneity of EGFR mutations was observed in individual cells of the same sample, with most of the cells expressing only wild-type EGFR, EGFRvIII or EGFR with an exon 4 deletion (EGFR del4) and a small number of GBM cells expressing both wild-type and mutant forms of the receptor. Some studies have been conducted in order to find out how this cellular heterogeneity contributes to tumor progression and maintenance of intra-tumoral heterogeneity in GBM [24]. The authors showed that in the wild type EGFR/ EGFRvIII co-expressing cells, the binding of EGF to wild type EGFR leads to activation of downstream kinase pathways including the RAS/RAF/MEK/MAPK (mitogen-activated protein kinases) and the PI3K/Akt (phosphatidylinositol-3-kinase/Akt) pathways. The EGFRvIII isoform can form heterodimers with wild-type EGFR and induce signal transduction in the absence of EGF. Moreover, activated wild-type EGFR subsequently phosphorylates EGFRvIII, triggering nuclear transport of EGFRvIII, enhancing phosphorylation of STAT3 (signal transducer and activator of transcription 3) and increased cellular transformation [25][27]. Another mechanism of EGFRvIII tumorigenicity has been described in which EGFRvIII glioma cells secrete micro-vesicles expressing EGFRvIII into surrounding EGFRvIII negative cells, thus mediating signaling and enhancing tumorigenicity without expression of EGFRvIII in neighboring cells. Inda and colleagues also observed that expression of EGFRvIII induces secretion of interleukin-6 (IL-6) and leukemia inhibitory factor (LIF) cytokines which activate

gp130 leading to wild-type EGFR activation in neighboring cells and generating a paracrine loop to enhance the rate of tumor growth [28].

#### **1.1.3.6 TP53 mutations**

Alteration or loss of function of the tumor suppressor p53 (TP53) is a common event in many tumors. Mutations of the TP53 gene have been found in 60% to 70% of secondary GBMs and 25% to 30% of primary GBMs and occur more commonly in younger patients [5]. Mutations of TP53 in GBM are most commonly found in the DNA-binding domain, namely within six mutation sites (corresponding to codons 175, 245, 248, 249, 273, and 282). These alterations result in the loss or gain of function of mutated TP53 as well as to dominant negative effects on the endogenous wild-type TP53 protein [29]. However, the use of TP53 mutations as molecular markers of GBMs remains controversial due to lack of clear association to GBM prognosis.

#### **1.1.3.7 ATRX mutation**

Originally, ATRX was named after a complex human genetic disease, X-linked alpha thalassemia mental retardation (ATR-X) syndrome, which is caused by a dysfunction of the ATRX protein [30]. ATRX is a critical member of a multiprotein complex playing an important role in regulating chromatin remodeling, nucleosome assembly and telomere maintenance [31]. Subsequently, ATRX mutations have been identified in many tumors, including GBM, and associated with increased telomere length, suggesting a role of this protein in telomere length maintenance [32]. ATRX mutations are more common in secondary GBMs (80%) compared to primary ones (7%) and are highly associated to IDH and TP53 mutations. ATRX alterations were found more frequently in younger patients, in agreement with what was seen for IDH mutations in GBM [31].

#### **1.1.3.8 TERT promoter mutation**

Telomeres are long stretches of 5'-TTAGGG-3' DNA repeats, capped on the end of chromosomes to protect them from degradation, end-to-end fusion and recombination. One of the hallmarks of pluripotent or totipotent embryonic stem cells, is their ability to maintain their telomeres' length *via* high telomerase activity.

Telomerase reverse transcriptase (TERT) is the catalytic subunit of telomerase and its expression level is a rate-limiting factor of telomerase expression/activity [33].

More than 85-90% of cancer cells are reported to have an upregulation of telomerase activity, a major mechanism to overcome replicative telomere shortening and to confer unrestricted growth of cancer cells. The gain-of-function mutations most reported in gliomas are C288T and C250T in the TERT promoter. These mutations located upstream of the ATG start site confer enhanced TERT promoter activity. In a study conducted by Nonoguchi et al. in 2013, TERT promoter mutations were identified in 55% of GBM patients, of which, 73% had a C228T mutation and 27% had the C250T mutation [34]. In 2015, Mosrati et al. identified TERT promoter mutations in 85.9% of primary GBMs studied, 74.7% of which had the C228T mutation and 25.3% presented the C250T mutation [35]. In another study reported by Hou and colleagues in 2015, TERT promoter mutations and relative telomere length (RTL) were investigated in a large cohort of patients with well-characterized gliomas including GBMs. They showed that 67.3% of all GBMs were TERT wild-type, 21.2% had the C228T mutation whereas 11.5% presented the C250T mutation. Interestingly, patients with TERT promoter mutations namely the C228T change were resistant to radiotherapy. However, the RTL was significantly shorter even in TERT wild-type tumors indicating that other molecular mechanisms may be involved in the regulation of telomere length. For example, a strong correlation was observed between ATRX mutations and TERT status since 92.9% of TERT wild-type gliomas had an ATRX inactivation. These findings suggest that RTL may also be regulated by ATRX inactivation [36]. In addition, many studies suggested a strong correlation between TERT promoter mutations and wild-type IDH- status, chromosome 7 gain and chromosome 10 loss [32]. Overall, enhanced TERT expression is more frequent in primary (82%) compared to secondary GBMs (35%). Importantly, primary GBM patients without TERT mutations survived considerably longer than patients with these mutations (median survival of 27 vs. 14 months) [37].

### **1.1.3.9 Chromosome losses**

A lot of chromosomal alterations have been described in GBM. Particularly common regions of loss include areas on 1p, 6q, 9p, 10p, 10q, 13q, 14q, 15q, 17q,

18q, 19q, 22q, and Y [7][8]. Many of these genetic losses result in alterations in the function of specific tumor suppressor genes with direct effects on gliomagenesis. Loss of heterozygosity (LOH) on chromosome 10, resulting in the loss of the tumor suppressor PTEN, is a hallmark of GBM, occurring in 60-80 % of cases. Gain of gene expression due to genomic alterations in the form of chromosome duplications and specific allele extrachromosomal amplification are much less frequent events [7]. The most common gains of gene expression events are amplification of the EGFR gene on chromosome 7, of the CDK4 (cyclin-dependent kinase 4) and MMD2 (murine double-minute 2, also known as E3 ubiquitin-protein ligase) genes on chromosome 12 and of the PDGFRA (platelet derived growth factor receptor alpha) gene on chromosome 4 [38]. Amplification of chromosome 19 was also reported in GBM based on copy number variation (CNV) and gene expression analyses of GBM tumors [8]. The 1p/19q deletions (loss of the short arm of chromosome 1 and of the long arm of chromosome 19) are a prognostic factor to predict response to chemotherapy for oligodendroglioma [5]. However, 1p/19q co-deletion didn't show an impact on survival in GBM patients [39].

#### **1.1.4 Classification of GBM subtypes based on genomic alterations**

In 2010, Verhaak et al. classified GBMs into 4 subtypes based on the TCGA data describing recurrent genomic abnormalities in these tumors. Genetic aberrations and gene expression signatures define the four subtypes of GBM as Classical, Proneural, Neural and Mesenchymal. Individual gene expression subtypes were each associated with specific genetic and epigenetic alterations (Figure 3). Following this first molecular classification of GBMs, additional research was devoted to identify novel alterations through broad genomic, epigenomic, transcriptomic and proteomic analyses. The aim of these studies is to provide a profound comprehension of GBM molecular characteristics which will eventually lead to more efficient targeted therapies for patients with different subtypes of GBM.

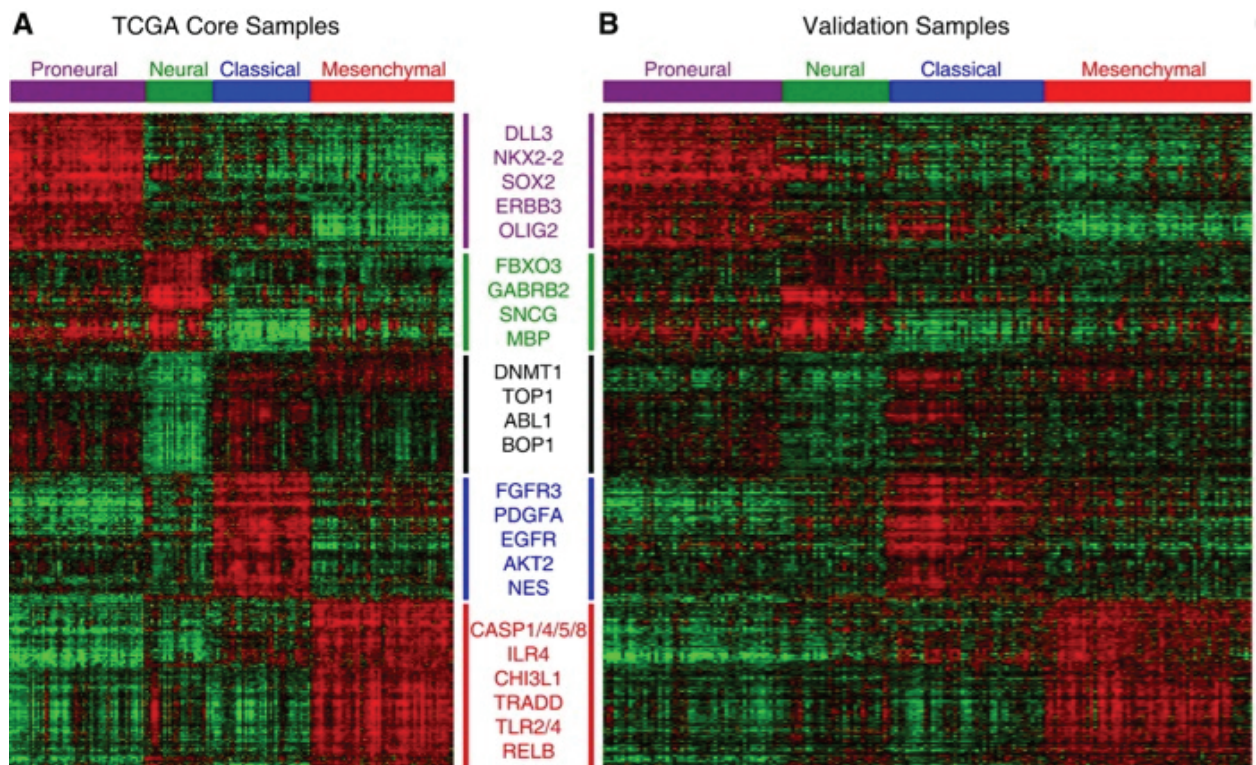


**Figure 3. Classification of glioblastomas based on genomic alterations and gene expression profiles, from [40].** **A.** Gene expression profile of 173 TCGA glioblastoma samples. **B.** Gene expression profiles in glioblastomas based on previously published data sets. Based on these data, glioblastomas were classified as proneural, neural, classical and mesenchymal defining four distinct gene expression profiles.

#### 1.1.4.1 Classical

Chromosome 7 amplification accompanied to loss of chromosome 10 was seen in 100% of classical subtypes of GBM. High-level EGFR amplification was observed in 97% of the cases, co-occurring with the 9p21.3 homozygous deletions of CDKN2A (encoding for both p16INK4A and p14<sup>ARF</sup>). Other alterations of the RB pathway were almost never associated to EGFR gene amplification and deletion of 9p21.3 [40]. The classical subtype of GBM also shows a lack of TP53 and IDH1 mutations.

#### 1.1.4.2 Proneural

The proneural group was identified by high expression of oligodendrocytic development genes such as PDGFRA, NKX2-2 and OLIG2 and several proneural development genes such as SOX2, DCX, DLL3, ASCL1 and TCF4. This subtype

was associated with younger age patients, PDGFRA abnormalities and IDH1 and TP53 mutations, all of which have previously been involved mainly in secondary GBMs [40]. G-CIMP (Glioma-CpG island methylator phenotype) is another molecular biomarker of the proneural subgroup which is highly dependent on the presence of IDH mutations. G-CIMP tumors represent 30% of all proneural GBM tumors [18][41]. This signature allows subdivision of proneural GBMs into two distinct subgroups, IDH mutant highly enriched in G-CIMP and IDH wild-type and absence of G-CIMP [18][20].

#### **1.1.4.3 Neural**

The neural subtype shows association with oligodendrocytic and astrocytic differentiation and it is characterized by the expression of neuronal markers such as NEFL (neurofilament light polypeptide), GABRA1 (gamma-aminobutyric acid (GABA) type A receptor alpha 1 subunit), SYT1 (synaptotagmin 1) and SLC12A5 (solute carrier family 12 potassium/chloride transporter member 5) [40].

#### **1.1.4.4 Mesenchymal**

The mesenchymal subtype exhibits expression of mesenchymal markers such as CHI3L1 (chitinase 3-like 1) and MET (mesenchymal-epithelial transition) and high activity of mesenchymal marker CD44 (cluster of differentiation 44) combined with astrocytic markers MERTK (myeloid-epithelial-reproductive tyrosine kinase) suggesting an epithelial-to-mesenchymal transition. Mesenchymal subtype GBMs also show an elevated expression of genes whose products are involved in the TNF (tumor necrosis factor) and NF- $\kappa$ B (nuclear factor kappa-light-chain-enhancer of activated B cells) pathways. This is consistent with high overall necrosis and inflammatory infiltration observed in this subtype. NF-1 hemizygous deletion/mutations were observed in 53% of mesenchymal subtype samples and were frequently associated to PTEN deficiency [40].

### **1.1.5 CNS WHO2016 Classification**

In 2016, the WHO incorporated molecular parameters to refine the classification of CNS tumors initially mainly based on histological characteristics.

Namely, IDH status has been integrated in the classification of GBMs. With these new diagnostic criteria, GBMs have been divided into three major types: IDH-wildtype, IDH-mutant and NOS GBM (Table 2).

#### **1.1.5.1 IDH-wildtype GBM**

Many clinical studies showed that GBM with wildtype IDH1 is the most common form, accounting for about 90% of these tumors. This corresponds to the clinically defined primary GBM and is predominantly found in patients over 55 years of age [2]. IDH-wild-type GBMs are prevalent in the temporal and frontal lobes [6].

#### **1.1.5.2 IDH-mutated GBM**

GBM with mutated IDH1 accounts for about 10% of all GBMs. IDH mutations are very frequent in secondary GBMs (> 80% of the cases) but rare in primary GBMs (< 5%) [2][9]. All IDH mutations observed in this subtype are heterozygous and affect R132 as mentioned above [14]. IDH-mutated GBMs are mainly distributed in the frontal lobe [6]. Patients with IDH-mutated GBM are significantly younger, with a median age of  $41 \pm 5.06$  years compared to patients with wild-type IDH ( $57 \pm 2.29$  years old at age of diagnosis). The mean survival time of IDH-mutated patients is also significantly longer than the one of patients with IDH-wild-type GBM [14].

#### **1.1.5.3 GBM NOS**

In the CNS WHO2016 classification, a GBM tumor lacking a diagnostic mutation is given a NOS designation. This implies that there is insufficient information on this tumor to assign a more specific code. In most cases, the NOS subtype is attributed to GBMs that have not been fully tested for relevant genetic alterations. In rare instances, this subtype may also include tumors that have been tested but do not show the genetic alterations studied [2].



	IDH-wildtype glioblastoma	IDH-mutant glioblastoma
Synonym	Primary glioblastoma, IDH-wildtype	Secondary glioblastoma, IDH-mutant
Precursor lesion	Not identifiable; develops de novo	Diffuse astrocytoma Anaplastic astrocytoma
Proportion of glioblastomas	~90%	~10%
Median age at diagnosis	~62 years	~44 years
Male-to-female ratio	1.42:1	1.05:1
Mean length of clinical history	4 months	15 months
Median overall survival		
Surgery + radiotherapy	9.9 months	24 months
Surgery + radiotherapy + chemotherapy	15 months	31 months
Location	Supratentorial	Preferentially frontal
Necrosis	Extensive	Limited
<i>TERT</i> promoter mutations	72%	26%
<i>TP53</i> mutations	27%	81%
<i>ATRX</i> mutations	Exceptional	71%
<i>EGFR</i> amplification	35%	Exceptional
<i>PTEN</i> mutations	24%	Exceptional

**Table 2. WHO 2016 classification of glioblastomas according to IDH status, adapted from [2].** The 2016 WHO classification defines two distinct classes of glioblastoma: IDH (isocitrate dehydrogenase) wildtype and IDH mutant lesions. Proportion, median age at diagnosis, male to female ratio, prognosis, location and histological and molecular characteristics of each subtype are indicated. Glioblastomas lacking a diagnostic mutation are designated as NOS glioblastomas. *ATRX*:  $\alpha$ -thalassemia/mental retardation syndrome X-linked; *EGFR*: epidermal growth factor receptor; *PTEN*: phosphatase and tensin homolog; *TERT*: telomerase reverse transcriptase.

### 1.1.6 Signaling pathways in GBMs

Enormous progress has been made during the past two decades in revealing important genetic events resulting in modifications in cellular signaling pathways involved in GBM development and progression. The most important genetic and epigenetic aberrations were found in the following cellular signaling pathways: dysregulation of growth factor signaling *via* amplification and mutational activation

of receptor tyrosine kinase (RTK) genes; activation of the PI3K (phosphatidylinositol-3 kinase) pathway and inactivation of the TP53 and retinoblastoma tumor suppressor pathways (Figure 4) [42].

#### **1.1.6.1 RTK/PI3K/Akt pathway**

The RTK/PI3K/Akt pathway involved in 88% of GBMs, plays an important role in tumor cell proliferation and invasion. This pathway involves RTK transmembrane glycoproteins such as EGFR, ErbB2 (HER2), PDGFR, c-met, DDR1 (discoidin domain receptor 1) as well as tumor suppressor protein phosphatase PTEN and protein kinases PI3K, Akt and mTOR (mammalian target of rapamycin). The binding of growth factors on RTKs results in activation of PI3K, which subsequently catalyzes phosphorylation of PIP2 (phosphatidylinositol 4,5-bisphosphate) into PIP3 (phosphatidylinositol 3,4,5-triphosphate). Conversely, PTEN inversely turns PIP3 into PIP2. PIP3 then activates phosphoinositide-dependent kinase-1 (PDK1) which phosphorylates Akt at Thr308. mTOR kinase within the mTORC2 complex (mammalian target of rapamycin complex) also phosphorylates Akt at Ser473. These two phosphorylation events lead to Akt activation. Activated Akt in turn activates mTORC1 by inactivating the TSC1/TSC2 (tuberous sclerosis protein 1/2, also known as hamartin/tuberin) suppressor complex. This signaling pathway affects cell survival, proliferation, and motility [43][44].

RTKs are often highly expressed in GBM. The most frequent alterations (mutations/ amplifications) are observed for EGFR (45% of GBMs), followed by amplifications of the PDGFR gene (13%). In addition, PI3K mutations are observed in 15% of cases. Decreased PTEN activity is another important way to activate the RTK/PI3K/Akt pathway. Homozygous deletion/mutation of PTEN was found in 36-40% of GBMs [42].

#### **1.1.6.2 RAS/RAF/MAPK pathway**

RAS proteins belong to the class of small GTPases. These proteins can be activated by RTKs whereas they are negatively regulated by NF-1 (neurofibromin 1). Activated RAS (RAS-GTP) then activates serine/threonine kinase RAF which subsequently activates MEK (also called MAPKK for mitogen-activated protein

kinase kinase), which in turn activates MAPK (Mitogen-Activated Protein Kinase). Activated MAPK translocates into the nucleus, resulting in activation of various transcription factors such as Elk1, c-myc, Ets and PPAR $\gamma$  (peroxisome proliferator-activated receptor  $\gamma$ ), thus promoting cell proliferation, differentiation and survival [44]. Although RAS mutations are rare in human GBM (2%), deregulation of the RAS/RAF/MAPK signaling pathway in these tumors is attributed to the activation of its upstream positive regulators including EGFR and PDGFR, and to the inactivating mutations/ homozygous deletions of its negative regulator NF-1 (18% of GBM) [42].

#### **1.1.6.3 The TP53 pathway**

The TP53 gene encodes a transcription factor regulating target genes involved in cell cycle arrest (G1-S transition control), cell death, cell differentiation, senescence, DNA repair and neovascularization in response to diverse cellular stresses. In normal cells, TP53 activity is negatively regulated by MDM2 and MDM4 *via* the ubiquitination and proteasomal degradation of the protein. Conversely, the p14<sup>ARF</sup> gene, part of the complex CDKN2A (cyclin dependent kinase inhibitor 2A) locus on chromosome 9p21, encodes a protein that directly binds to MDM2 and inhibits MDM2-mediated TP53 inhibition and degradation. 87% of GBMs were reported to have an altered TP53 signaling pathway. Besides the homozygous deletion/mutation of TP53 (in 35% of GBMs), homozygous deletions/mutations in p14<sup>ARF</sup> were also frequently found in GBM (49%) and amplifications of MDM2 and MDM4 were also observed (14% and 7%, respectively) [42][44].

In addition to the p14<sup>ARF</sup>/MDM2/TP53 pathway, DNA damage caused by radiotherapy in tumor cells was shown to activate the sensor kinase ATM (ataxia-telangiectasia mutated), which in turn leads to activation of the checkpoint kinase 2 (Chk2). Activated Chk2 is able to regulate TP53-dependent apoptosis. The Chk2 gene is located on chromosome 22q12.1. 22% of GBMs were reported to have a single-copy loss of a chromosomal area containing this gene [42][44].

#### **1.1.6.4 Retinoblastoma (RB) tumor suppressor protein signaling pathway**

The RB pathway suppresses cell cycle entry and progression by controlling the transition from G1 to the S phase of the cell cycle. The CDKN2A p16INK4a protein binds to CDK4 and inhibits the CDK4/cyclin D1 complex, thus inhibiting cell cycle transition. The most common alteration in the RB pathway in patients with GBM is a deletion of the CDKN2A/CDKN2B locus in chromosome 9p21 encoding the p16INK4a and p14<sup>ARF</sup> proteins (~50%) followed by amplification of the CDK4 locus (14%) and homozygous deletion/mutation of the RB1 gene (11%) [42].

#### **1.1.6.5 Other signaling pathways**

According to the study of The Cancer Genome Atlas Research (CGAR) Network, genetic alterations in GBMs concern mainly (74%) the signaling pathways described in previous sections suggesting that deregulation of these pathways is a core requirement for glioblastoma pathogenesis [42]. However, other signaling pathways have been reported as being altered in GBM. For example, the NF- $\kappa$ B pathway was shown to be constitutively activated or upregulated, mainly in response to cytokines, in GBM cells. These modifications were associated to poor prognosis in GBM [45]. A study showed a key role of NF- $\kappa$ B activation by RIP1 (receptor interacting protein 1), overexpressed in 30% of GBM, which also mediated regulation of MDM2 and TP53 downregulation in GBM [46]. NF- $\kappa$ B may also play an important role in DNA damage repair and cell cycle progression by inducing mesenchymal differentiation and may thus affect the response of GBM tumors to radiotherapy [47].

The Wnt/ $\beta$ -catenin pathway is another pathway which plays a significant role in the proliferation and survival of tumor cells and which is emerging as an important target for glioblastoma therapy. In addition, the Notch signaling pathway was proved to enhance glioma stem cell phenotype and accelerate tumor initiation and progression in mouse models [48]. All these signaling pathways are functioning as a delicate network in GBM pathology making this tumor a very complicated ecosystem, in which the tumor cells and the stromal cells can cooperate together and impact GBM therapies.

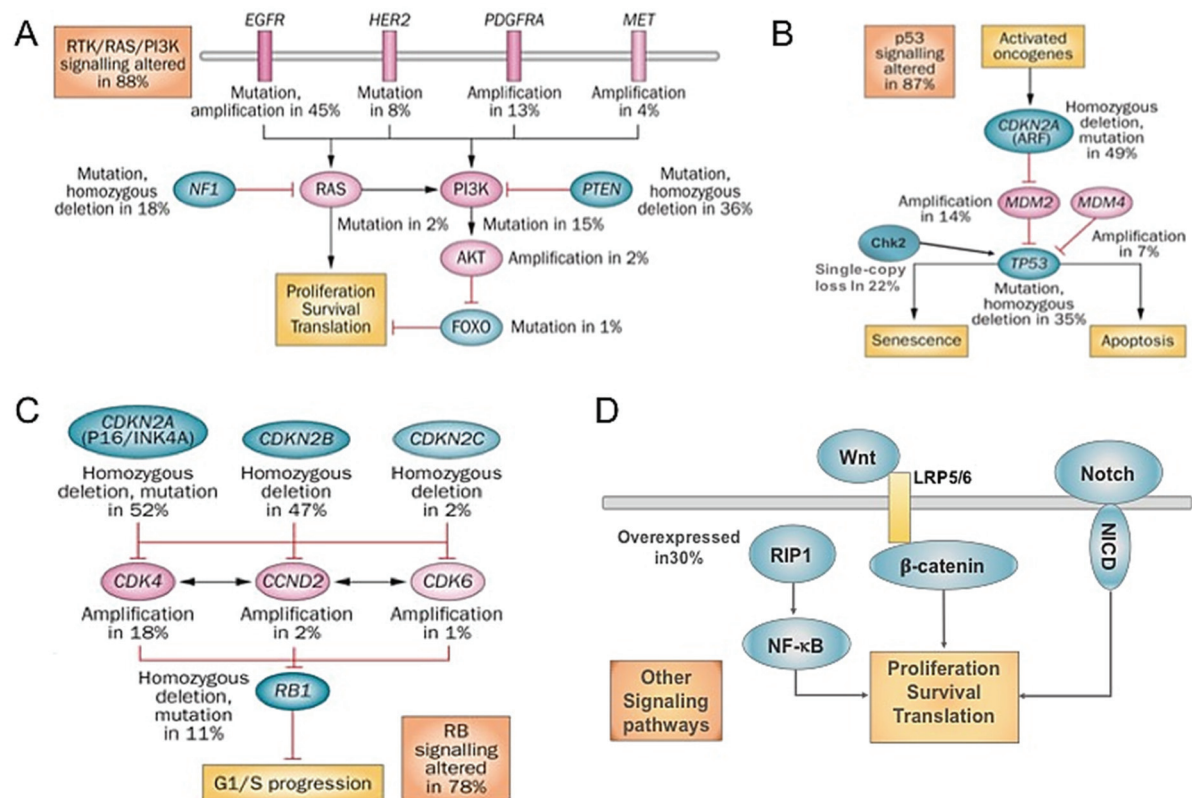


**Figure 4. Critical signaling pathways altered in glioblastoma, adapted from [49].** **A.** RTK/RAS/PI3K pathways. The binding of growth factors to receptor tyrosine kinases (RTKs), activates signaling pathways including the RAS/RAF/MAPK and/or PI3K/Akt/mTOR cascades. Activation of these pathways promotes cell proliferation, survival and motility. **B.** TP53 pathway and **C.** RB signaling pathway are important tumor suppressor pathways functioning by promoting senescence and apoptosis and by suppressing cell cycle entry. Loss-of-function mutations in the TP53 and RB genes are frequently observed in GBM. **D.** Other signaling pathways including NF-κB, Wnt/β-catenin, and Notch pathways are also contributing to cell proliferating and survival and are activated in GBM. Akt: also known as protein kinase B; CCND2: G1/S-specific cyclin-D2; CDK: cyclin-dependent kinase; CDKN2: cyclin-dependent kinase inhibitor family; Chk2: check-point kinase 2; EGFR: epidermal growth factor receptor; FOXO: forkhead box O3 transcription factors; HER2: receptor tyrosine-protein kinase ErbB2; LPR: low-density lipoprotein receptor-related protein 5/6; MDM2/4: mouse double minute 2/4; MET: receptor tyrosine kinase with high affinity for hepatocyte growth factor; NF1: neurofibromin 1; NICD: Notch intracellular domains; PDGFRA: platelet-derived growth factor receptor alpha; PI3K: phosphatidylinositol 3-kinase; PTEN: phosphatase and tensin homolog; RB: retinoblastoma; RIP1: receptor-interacting protein kinase 1.

### 1.1.7 Tumor microenvironment in glioblastoma

In recent years, advances have been made in the comprehension of gene expression and cellular signaling pathways in tumors and many anti-tumor agents and therapeutic approaches were developed. As a consequence, overall survival of

cancer patients has been significantly prolonged. According to the most recent report of cancer statistics published on CA in 2017, a Cancer Journal for Clinicians, from 1991 to 2014, the overall death rate due to cancer dropped by 25%. That means that in the United States, during the last two decades, there were approximately 2,143,200 less deaths due to cancer. Nevertheless, over the past decade, the overall cancer incidence rate (2004-2013) was stable and the cancer death rate declined by only 1.5% per year [50]. Moreover, tumor relapse is almost always encountered in all types of tumors and drug resistances are frequently observed. Thus, besides the genetic alternations *per se*, the maintenance and expansion of tumors may be additionally strongly influenced by external signals from the tumor microenvironment.

#### **1.1.7.1 Tumor microenvironment (TME)**

Since 1863 when Rudolf Virchow first proposed the link between chronic inflammation and cancer following the observation that infiltrating leukocytes are a hallmark of tumors, a lot of studies were conducted to understand the inflammatory microenvironment in malignant tissues and the origin of cancer lesions [51]. Nowadays, the concept of tumor microenvironment (TME) is profoundly understood and the pivotal role of TME during tumor initiation, progression and invasion, but also in drug resistance, is well accepted.

The TME is the cellular environment in which the tumor exists. It comprises various non-malignant cells (endothelial cells, fibroblasts, immune cells, etc.), their extracellular components (cytokines, growth factors, hormones, extracellular matrix (ECM), etc.) and a tumor surrounding vascular network (Figure 5) [52]. In the next sections, we are going to discuss these major components of the tumor microenvironment.

##### **1.1.7.1.1 Tumor vasculature**

Compared with normal blood vessels, the tumor vasculature exhibits aberrant structural and functional properties and results in areas of hypoxia and limited nutrient supply and distance from vascular beds was shown to be crucial for the distribution of drugs within tumors [52]. Several methods for blood vessel formation were discovered in normal tissues. These include sprouting angiogenesis,

recruitment of bone-marrow-derived cells and/or endothelial progenitor cells that differentiate into endothelial cells at the vascular wall and intussusception which corresponds to vessel splitting. In addition to these three vessel formation processes, tumor cells can use pre-existing vessels and line tumor vessels. Finally, tumor cells with stem cell properties may differentiate to endothelial cells with genetic aberrations to generate new vessels [53]. Vessel formation is followed by maturation and entry of endothelial cells in quiescence and their covering by pericytes. Unlike normal vessels, tumor vessels are highly heterogeneous, tortuous, branch chaotically and have a cragged vessel lumen. Additionally, pericytes and the basement membrane are also abnormal within the tumor vasculature. As a result, blood supply is heterogeneous and oxygen, nutrients, immune cells and drugs are eventually distributed unevenly. These particularities of tumor vasculatures create a hostile environment characterized by hypoxia, low pH, low nutrient content and high fluid pressure. These conditions are more selective for more malignant cancer cells. Moreover, leaky tumor vessels facilitate the migration of cancer cells as well as their escape from drugs [53].

#### **1.1.7.1.2 The stromal cell types and immune cell types of the TME**

Multiple cell types of TME are classified into three categories along with their key functional contributions: angiogenic vascular cells; cancer-associated fibroblastic cells and infiltrating immune cells [54].

##### **1.1.7.1.2.1 The angiogenic vascular cells**

The angiogenic vascular cells, mainly endothelial cells which include endothelial tip cells, stalk cells and tube cells, are essential for vessel formation. Endothelial cells are covered by pericytes to maintain the maturity and stability of vessels. They are major contributors for angiogenesis to support blood supply of oxygen and nutrients in tumors. Endothelial cells can also modulate cancer cell dissemination and seeding, and limit cytotoxic T lymphocyte and natural killer T cell inflammation [54].



#### **1.1.7.1.2.2 Cancer-associated fibroblastic cells**

Cancer-associated fibroblastic cells (CAFs), namely activated fibroblasts, constitute a large proportion of stromal cells within the TME and include activated fibroblasts, alpha smooth muscle actin ( $\alpha$ SMA)-positive myofibroblasts and activated adipocytes [54]. The majority of CAFs is derived from fibroblasts residing in connective tissue close to a tumor. These cells are recruited and activated in response to many growth factors and cytokines such as TGF- $\beta$  (transforming growth factor beta), FGF2 (fibroblast growth factor 2) and PDGF (platelet-derived growth factor) that are abundant in the TME but they can also derive from pericytes and smooth muscle cells from the vasculature [55]. CAFs modulate the stroma in a paracrine manner by increasing the secretion of urokinase-type plasminogen activators (uPA), matrix metalloproteinases (MMPs) and ECM components which increase proliferation of tumor cells, tumor growth, invasion and angiogenesis [55]. They are also a source of growth factors such as hepatocyte growth factor (HGF), VEGF and PDGF [52] and chemokines IL-8/CXCL8 (the ligand of CXCR1 and CXCR2) and CXCL12 (C-X-C motif chemokine 12), also known as the stromal cell-derived factor 1 (SDF1), the ligand for CXCR4 (chemokine receptor 4). Secretion of such factors promotes angiogenic responses thus driving tumor growth [55] as well as the migration of other cells into the TME [54]. CAFs have also been shown to play a role in metabolic reprogramming in cancer cells, in which they can optimize metabolic efficiency by alternatively using glucose and lactate and other energy-rich molecules [54]. Recently, data have also revealed that activated adipocytes can provide free fatty acids to cancer cells and generate ATP *via* mitochondrial oxidation, thereby promoting tumor progression [56].

#### **1.1.7.1.2.3 Immune cells**

Both the innate and adaptive immune systems have been implicated in promoting and preventing tumor growth. Two groups of infiltrating immune cells have been involved in the TME during tumorigenesis and tumor progression: the myeloid lineage cells and lymphoid lineage cells, which have distinct functions during tumorigenesis. Myeloid lineage cells include TAMs (tumor-associated macrophages), TEMs (TIE-2 expressing monocytes), mast cells and MDSCs (myeloid-derived suppressor cells). Lymphoid lineage cells essentially comprise NK



cells (natural killer cells), CTL (CD8 T cells), Th cells (helper T cells), T<sub>reg</sub> cells (regulatory T cells) and B cells. Immune cells are playing a crucial role in immune suppression during tumor progression and metastasis [57][58].

TAMs have a clear role at the leading edge of tumors, by driving invasive cellular phenotypes [57]. For example, in GBM, these cells were shown to facilitate tumor migration and invasion through EGF secretion [59]. Angiogenesis is also induced by TAMs thus facilitating metastatic cell escape [60]. TEMs are another subpopulation of tumor-infiltrating myeloid cells. They are present along the vessels at the periphery of tumors whereas barely detectable in central necrotic zones. These cells were reported to promote tumor invasion by increasing the levels of circulating MMP9 (matrix metalloproteinase 9) and other tumor-remodeling molecules that contribute to the invasiveness of glioma cells [61].

MDSCs are immunosuppressive precursors of dendritic cells, macrophages and granulocytes. T<sub>reg</sub> cells are an immune suppressive T cell population that regulates the expansion and activation of T and B cells and can suppress antitumor immune responses. As tumor grows, immune-suppressor cells, including MDSCs and T<sub>reg</sub> cells, are mobilized into the circulation in response to chemokine pathways involving for example CXCL12 -CXCR4 and CXCL5-CXCR2, that are produced in many types of tumors. The mechanism that MDSCs and T<sub>reg</sub> cells use to suppress the antitumor immune response is thought to involve their ability to infiltrate the growing tumor and to disrupt immune surveillance by interfering with antigen factors such as TGF- $\beta$ , FGF or PDGF, by blocking T and B cell proliferation and activation and by inhibiting NK cell cytotoxicity [60]. Major cell types of the TME and their contributions to tumor progression are shown in Figure 5.

#### **1.1.7.1.3 The extracellular matrix (ECM)**

In addition to tumor vasculature and specific cell types, the ECM is another major component of the TME. The ECM is a complex network of a large collection of physically and biochemically distinct components, including proteins, glycoproteins, proteoglycans and polysaccharides. Functions of the ECM include bridging between cells, binding to cell-surface adhesion receptors which contributes to spatial arrangements and orientation of cells and tissue organization and support of cell survival and differentiation [62]. In addition to core ECM components

(fibronectins, collagens, laminins etc.), the ECM also contains growth factors, cytokines and ECM-remodeling enzymes that collaborate with ECM proteins in cell signaling. Both tumor cells and stromal cells are sources of distinct ECM components. Interestingly, the composition of the ECM influences the metastatic potential of tumor cells [63]. Therefore, the ECM composition within the TME may help to predict clinical outcome.

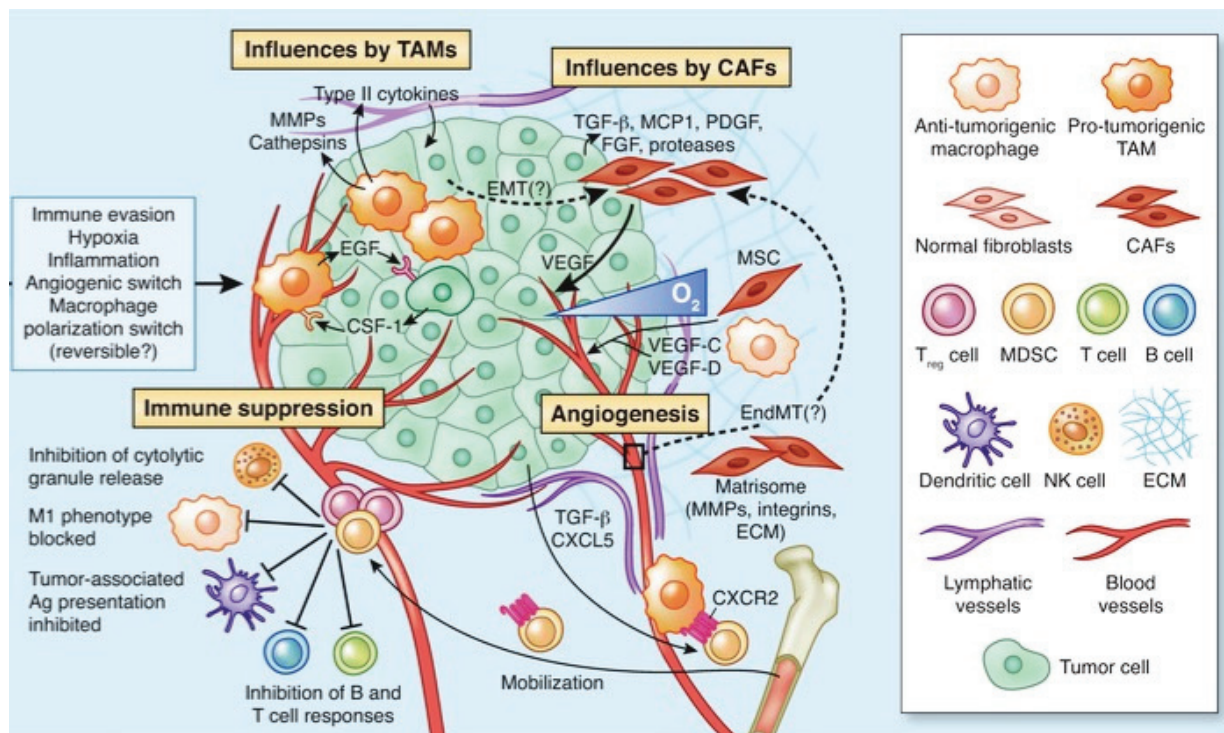


**Figure 5. Tumor microenvironment and major cell types involved, from [57].** Multiple stromal cell types support tumorigenic process. TAMs (tumor-associated macrophages) support tumor growth, angiogenesis and invasion by secreting cytokines and growth factors such as EGF (epidermal growth factor). MDSCs (myeloid-derived suppressor cells) and  $T_{reg}$  (regulatory T cells) cells mobilized by cytokines and chemokines, such as TGF- $\beta$  and CXCL5-CXCR2, disrupt immune surveillance through inhibition of antigen presentation by DCs (dendritic cells), inhibition of T cells, B cells and NK (natural killer) cells. CAFs (cancer associated fibroblasts) which become activated in response to tumor-derived factors such as TGF- $\beta$  (transforming growth factor- $\beta$ ), FGF (fibroblast growth factor) and PDGF (platelet derived growth factor), secrete ECM (extracellular matrix) proteins and promote proliferation of tumor cells, tumor growth, invasion, angiogenesis and metabolic reprogramming of tumor cells.

### **1.1.7.2 TME in glioblastoma**

GBMs are distinguished from low-grade gliomas by the presence of high vascularization and focal necrosis. These GBM features were associated to some characteristics of the tumor microenvironment which are angiogenesis, hypoxia and acidification. These crucial GBM microenvironmental factors and their involvement in tumor development and progression as well as in therapeutic resistance have been the subject of extensive studies in the past years.

#### **1.1.7.2.1 Angiogenesis in GBM**

One of the most important features of GBM is high microvascular proliferation surrounding pseudopalisading necrotic areas. Extensive angiogenesis in GBM is often a response to low oxygen levels within the tumor, which in turn increases the expression of angiogenic factors and their downstream signaling pathways [64]. As we discussed before, the main differences between tumor angiogenesis and normal vasculature, is the presence, in the first case, of structural and functional abnormalities such as dilatations, incomplete or absent basement membranes, high permeability as well as irregular architecture of vessels. All these alterations lead to irregular blood flow and thus to insufficient supply of oxygen and nutrients throughout the tumor.

#### **1.1.7.2.2 Hypoxia in GBM**

Conversely to normal brain tissue presenting physiological oxygen concentrations ranging between 12.5 and 2.5% ( $pO_2 = 200$  to  $100$  mmHg) and because of the irregularities of GBM vascular networks, most of these tumors present mild to moderate/severe hypoxia, with oxygen concentrations ranging between 2.5 and 0.5% ( $pO_2 = 20$  to  $4$  mmHg) for mild hypoxia and between 0.5 and 0.1% ( $pO_2 = 4$  to  $0.75$  mmHg) for moderate/severe hypoxia [65][66]. Necrotic areas within GBMs are commonly characterized by severe hypoxia. Nevertheless, tumor cells are able to survive in the vicinity of these areas due to the development of several adapting molecular/genetic mechanisms. For example, hypoxia promotes the recruitment of pro-angiogenic bone-marrow derived cells including myeloid cells such as TEMs (TIE-2-expressing monocytes) and TAMs (tumor-associated macrophages), neutrophils, mast cells and  $CD11b^+GR-1^+$  (myeloid lineage marker

and granulocytic marker) myeloid-derived suppressor cells, which release angiogenic signals such as VEGF, BV8 (also known as PROK2) and MMPs (matrix metalloproteinases) to promote cell proliferation and survival [53]. Hypoxia was also shown to increase telomerase activity *via* MAPK signaling in solid tumors [67]. Most importantly, such levels of hypoxia are sufficient to increase HIF-1 $\alpha$  (hypoxia inducible factor 1 $\alpha$ ) protein levels. HIF-1 $\alpha$  is a crucial transcription factor which in response to hypoxia, regulates expression of its target genes including the ones encoding VEGF, several glycolytic enzymes, glucose transporters GLUT1 and GLUT3, CA9 (carbonic anhydrase 9), erythropoietin and insulin-like growth factor binding proteins [66][68]. These proteins play a pivotal role in GBM survival, resistance and invasion.

The hypoxic intratumoral environment in GBM and other solid tumors constitutes a serious problem for the treatment of these tumors with chemotherapeutic drugs and radiotherapy. Indeed, some drugs as well as radiation therapy require oxygen to be maximally cytotoxic. In addition, hypoxic conditions promote altered cell metabolism that reduces the cytotoxicity of drugs or leads to drug efflux pump upregulation (for example, the P-gp, P-glycoprotein that belongs to a family of ATP-binding cassette (ABC) transporters) thus decreasing drug concentrations in tumor cells. Moreover, following radiotherapy, a high expression level of HIF-1 was observed in tumor cells indicating an important role of this transcription factor in therapy resistance [69].

### **1.1.7.2.3      Acidity and GBM**

One of the hallmarks of cancer cells is their ability to switch their metabolism from oxidative phosphorylation to glycolysis for energy production. This metabolic switch is performed even in normal oxygen levels and is known as the Warburg effect [70]. Hypoxic conditions also favor the induction of glycolytic pathways, which provide metabolic intermediates to be used for the biosynthesis of amino acids, nucleotides and lipids, thus conferring a selective advantage to proliferating tumor cells [71].

Persistence of glycolytic pathways in cancer cells results in high acid (*i.e.* lactic acid, protons) production and export in the TME. As a consequence, pH in

human tumors, including GBMs, may be as low as 5.9 with a mean of around 6.8, whereas normal brain tissue has a pH of 7.1 [65]. In these acidic conditions, intracellular pH (pHi) has to be maintained at slightly alkaline values (pH 7.2-7.4) in order to preserve cell proliferation and tumor survival. Tumor cells have thus developed various mechanisms to maintain an alkaline pHi and a slightly acidic extracellular pH (pHe). For example, these cells have increased ability to export acidic catabolites (such as carbon dioxide, carbonic acid or lactic acid) and import weak bases (such as  $\text{HCO}_3^-$  ions) by the intermediate of transporters. In addition,  $\text{H}^+$  ions are directly extruded by exchange for other cations or by vacuolar ATPase (V-ATPase) [71]. The main players involved in the regulation of tumor pH include carbonic anhydrases (CA2, CA9 and/or CA12) which regulate the pH by catalyzing the hydration of carbon dioxide to protons and bicarbonate ions, the plasma membrane-bound proton vacuolar (V-ATPase) and  $\text{Na}^+/\text{H}^+$  exchanger 1 (NHE1 also known as SLC9A1), that contribute to  $\text{H}^+$  extrusion, sodium/bicarbonate co-transporters (NBCs) and  $\text{Cl}^-/\text{HCO}_3^-$  exchanger (NDCBE also known as SLC4A8), that favor  $\text{HCO}_3^-$  influx, thus leading to cytoplasmic alkalization, and the monocarboxylate transporters MCT1, MCT2, MCT3 and MCT4, which transport glycolytic metabolites such as lactic acid and other monocarboxylates [71][72]. Glucose transporters, namely GLUT1, have been shown to have high expression levels in brain tumors including in GBM cells.

#### **1.1.7.2.4 Glioblastoma microenvironment and therapy resistance**

In a GBM tumor, the periphery of the tumor mass is highly vascularized and cells within this area containing enough oxygen and nutrients express high levels of VEGF and low levels of HIF-1 $\alpha$ . Due to lower oxygen, pH and nutrient content, inner layers of GBM tumors contain cells with high levels of HIF-1 $\alpha$  which is stabilized under such conditions as well as increased expression of GLUT1 and CA9. The inner core of the tumor is almost anoxic and may be the area where the stem cells are situated, together with the hypoxic layer. Cells within this necrotic zone show strong expression of MGMT and high levels of GLUT1 and CA9 [65]. In the external vascular zone, cells provide growth factors such as VEGF, IGF, EGF, chemokines such as CXCL8 and CXCL12 and interleukins to promote tumor progression, invasion and migration.

In hypoxic areas, the radiation dose needed to kill the cells is three times higher than the one required in normoxic areas. In addition, DNA damage induced by formation of free oxygen radicals is reduced and can be repaired more easily [66]. There is also evidence demonstrating that HIF1 plays a major role in drug resistance induced by hypoxia and its high expression level (due to stabilization of the protein) has been associated with tumor progression and poor prognosis in patients with GBM [73]. The acidic conditions of the TME also increase the resistance of GBM cells to multiple drugs by influencing their diffusion or active transport across the membrane [65]. Thus, targeting the TME may be a promising strategy for the treatment of GBM.

### **1.1.8 Treatments for glioblastoma**

Unfortunately, there is to date no curative treatment for GBM and median survival of patients without therapeutic intervention does not exceed 3 months. Initial treatments consist of maximal safe surgical resection followed by radiotherapy together with alkylating chemotherapy. With this combined therapy, the median survival is still of less than 15 months [74].

#### **1.1.8.1 First-line treatments for new diagnosed glioblastoma**

The standard care for patients with newly diagnosed GBM includes surgical tumor resection followed by a 6-week course of radiotherapy with concomitant administration of the DNA alkylating agent temozolomide (TMZ), followed by adjuvant temozolomide treatment for a minimum of 6 months [75]. The aim of surgery is to remove as much of the tumor tissue as possible. However, due to the location of tumors, mostly in frontal and temporal lobes in the case of GBMs, it is often difficult to completely remove the tumor mass. In addition, some tumor locations such as in the eloquent cortex, in basal ganglia or in brain stem, are not amenable to surgical intervention [76]. In most cases of surgery, the tumor is partially removed to reduce the symptoms by performing a craniotomy and opening of the skull to reach the tumor site with the help of computer-assisted image-guidance. When necessary, intra-operative mapping techniques are used to determine the locations of the motor, sensory and speech/language cortex and thus help the surgeon decide which part of the tumor it is safe to remove.

After recovery from surgery, a concurrent radiotherapy can begin. It is planned with dedicated computed tomography (CT) and three-dimensional planning systems. A standard focal radiotherapy consists in fractionated focal irradiation for a total dose of 60 Gy [75]. The goal of radiation therapy is to selectively kill the remaining tumor cells at the primary site as well as tumor cells that have infiltrated the surrounding normal brain tissue.

Concomitant chemotherapy consists in TMZ administration at a dose of 75 mg per square meter of body-surface area per day, given from the first day of radiotherapy until the last day of radiotherapy. After a 4-week break, patients receive 6 28-day cycles and sometimes up to 12 28-day cycles of a 5-day schedule adjuvant TMZ administration during 6 months (150-200 mg per square meter of body-surface area) [75].

The addition of concurrent TMZ chemotherapy with radiotherapy and 6 months of follow-up after the completion of radiotherapy, was proven to be beneficial to the median survival of patients with newly diagnosed GBM. Nevertheless, the challenge remains to improve the regimen of radiotherapy plus TMZ.

It is well known now that the response to alkylating therapy is significantly influenced by the levels of MGMT (O6-Methyl Guanine Methyl Transferase) expression in tumor tissue of patients. Thus, patients with a normal MGMT status (no reduction of MGMT expression by promoter methylation) are less susceptible to respond to TMZ-based therapy. Despite these findings, almost all patients with newly diagnosed GBM receive irradiation with concomitant and adjuvant TMZ because testing the MGMT status is not yet generalized upon diagnosis [77].

Chemotherapy approaches present additional limitations. For example, many chemotherapeutics other than TMZ are not able to cross the blood-brain barrier. This significantly impairs the drug's delivery to the brain parenchyma and to the tumor itself.

Besides the standard of care for newly diagnosed GBM, represented by the Stupp protocol described in the previous section, several clinical trials evaluating angiogenesis inhibitors are worth to be noticed. Bevacizumab (Avastin), a monoclonal antibody that binds and neutralizes vascular endothelial growth factor

(VEGF), was granted an approval by the USA Food and Drug Administration (FDA) in May 2009 for the treatment of recurrent GBM due to a clinical response or tumor shrinkage of up to 50%, in combination with irinotecan, a topoisomerase 1 inhibitor [78][79]. Subsequently, studies were designed to use this agent of interest as first-line treatment combined with radiotherapy and TMZ in patients with newly diagnosed GBM. The median progression-free survival (PFS) was longer and the quality of life was improved compared to conventional radiotherapy/TMZ administration. However, no significant benefit on overall survival was observed in patients with newly diagnosed GBM [80][81].

Additional compounds that are being tested with encouraging clinical results in newly diagnosed GBM include cilengitide, an integrin inhibitor, combined with radiotherapy and TMZ [82], and cediranib, an oral pan-VEGFR inhibitor. Evaluation of other tyrosine kinase inhibitors or PI3K and mTOR inhibitors was not conclusive.

#### **1.1.8.2 Treatments for recurrent glioblastoma**

Despite these combinations of treatments, almost all GBM patients experience tumor recurrence at or near the primary tumor bed. After initial therapy fails, therapeutic options are very limited and generally not effective. There is no standard of care for recurrent GBM. In general, salvage treatment options may involve re-resection, focal irradiation, and systemic therapy [12].

##### **1.1.8.2.1 Repeat surgical resection**

Repeat resection is typically offered at the time of initial presentation of progression, if it is feasible when considering some important prognostic factors such as age, performance status and presumed extent of maximal safe resection. A second surgical resection may prolong life in some patients but randomized trials to evaluate the role of repeat resection are still lacking. However, a second surgery in GBM can be helpful for accurate diagnosis, especially in cases where pseudoprogression or radiation necrosis is suspected [76].

##### **1.1.8.2.2 Repeat irradiation**

Repeat irradiation poses serious risks and results in necrosis of healthy brain tissue because most patients have already undergone a previous full course of



radiotherapy. Therefore, historically, re-irradiation is usually only proposed to a relatively small number of patients with recurrent tumors which are well localized and who present a good performance status [83]. Nowadays, thanks to the advances in radiosurgery techniques, re-irradiation is more frequently applied in patients with recurrent GBM. Several radiation techniques, including interstitial brachytherapy, single-dose radiosurgery and fractionated stereotactic re-irradiation were applied in a subset of patients with recurrent GBM in the past decades.

The principle of interstitial brachytherapy (BT) is the use of radioactive isotopes to deliver ionizing radiation directly into the tumor site while sparing normal surrounding brain tissue. Isotopes, such as iodine-125 (I-125) and iridium-129 (192-Ir), with unstable nuclei, break down to more stable forms and high-energy gamma rays are released into the surrounding tumor tissue resulting in the production of electrons which ultimately disrupt atomic bonds and eventually destroy tumor tissue [84]. This is an aggressive salvage treatment option that may only be used in a very small number of patients with recurrent GBM because of its high toxicity including increased seizure occurrence, worsening of neurological deficits, infections, hemorrhages, pulmonary embolus and radiation therapy necrosis [85]. The longest median overall survival after BT by 2015 was of 15.9 months [84].

Single-dose radiosurgery is a stereotactic radiosurgery that uses specialized radiation delivery systems to deliver a high dose of radiation at the site of the tumor with subsequent less treatment-associated morbidity. Some results showed a benefit for patients with recurrent malignant gliomas. However, the potential morbidity becomes a concern when the tumor volume is larger or if the tumor is at or close to eloquent structures. For this reason, a protocol using fractionated stereotactic radiotherapy was developed in 1993 [86].

Fractionated stereotactic radiotherapy (FSRT) consists of normofractionated stereotactic and hypofractionated stereotactic radiotherapy (HFSRT). HFSRT decreases overall treatment time for patients and consequently potential toxicity. Applied either alone or in combination with chemotherapy, HFSRT was beneficial to patients with recurrent GBM in some clinical trials. The longest survival time observed was of 38.8 months suggesting that HFSRT may be extremely beneficial to some patients. Other data also suggest that efficacy and toxicity of HFSRT are

favorable compared to single-dose radiosurgery and the invasive modality of interstitial brachytherapy [87].

### **1.1.8.2.3 Systemic therapy**

Most ongoing clinical trials in patients with recurrent GBM are investigating systemic therapeutic protocols. Nitrosoureas are DNA alkylating agents characterized by high lipophilicity that permits blood-brain barrier penetration and which were initially used as first-line treatments of GBM. Following the approval of TMZ in 1999 and in 2005, TMZ became the treatment of choice for newly diagnosed GBM whereas nitrosoureas were moved into a second-line treatment option in monotherapy and in combination regimens for recurrent GBM [88].

Several trials have evaluated the efficacy and safety of TMZ as a monotherapy for recurrent or progressive GBMs. A standard TMZ regimen of a 5-day schedule and a variety of metronomic schedules of administration were employed but no significant improvement on median overall survival (OS) was observed [12].

Bevacizumab was approved for the treatment of recurrent GBM in 2009 by the FDA as we have mentioned before. However, this therapeutic approach is not available for use in the European union because of the absence of a randomized trial with a bevacizumab-free control arm. In addition, the clinical benefit of bevacizumab is questionable given the relatively short duration of response and the possibility that much of the response seen with imaging techniques could be a function of tumor-associated vascular stabilization rather than a true antitumor effect.

### **1.1.8.3 Immunotherapy and other emerging therapies**

#### **1.1.8.3.1 Immunotherapy**

Given the contribution of GBM cells to the generation and maintenance of an immunosuppressive microenvironment, immunotherapy research is rapidly expanding over the past decade in GBM [89]. Current immunotherapeutic approaches being evaluated in GBM clinical trials can be divided into two categories: active or passive immunotherapy. Active immunotherapy refers to the use of foreign antigens to activate the innate tumor-specific immune system, such as cancer vaccination, immune stimulatory gene therapy and immunomodulatory checkpoint

blockade. Passive immunotherapy refers to the introduction of exogenous immune substances against tumors directly into the body and which do not require the activation of the patient's own immune system. Passive immunotherapy includes approaches such as adoptive cell therapies, oncolytic virotherapy and antibody administration [90].

Rindopepimut, a peptide-based vaccine targeting EGFRvIII tumor-specific surface antigens was evaluated in patients with newly diagnosed GBM with promising results and was thus further examined in a subsequent phase II clinical trial in combination with standard radiotherapy and TMZ. DC (dendritic cell) vaccines are other approaches using autologous tumor lysates or common tumor antigens to induce an immune response against cancer. A phase III clinical trial based on the use of DC vaccines is ongoing with encouraging results [91]. Tumor-derived heat shock proteins (HSPs) may also be used as tumor antigen carriers alone or in combination with DCs to activate CD4<sup>+</sup> and CD8<sup>+</sup> T cell response [90][92]. Several phase II clinical trials using autologous tumor-derived heat-shock protein peptide complex-96 (HPSC-96) were conducted in patients with newly diagnosed or recurrent GBM [90][93].

Immunomodulatory checkpoint inhibitors are another promising immunotherapeutic approach. Such compounds are able to induce antitumor activity by blocking inhibitory molecules and their receptors on effector immune cells, leading to a robust T cell response against tumor cells [91]. Currently, three FDA approved immune checkpoint inhibitors, including ipilimumab, a fully humanized IgG1 monoclonal antibody targeting cytotoxic T-lymphocyte antigen 4 (CTL-4), and nivolumab and pembrolizumab targeting programmed cell death protein1 (PD-1), are evaluated in patients with recurrent GBM in several clinical trials [91][94]. The first large phase III trial of nivolumab in patients with GBM was initiated in 2014 [95].

Adoptive cell immunotherapy is a treatment based on the administration to patients of *ex-vivo* stimulated immune cells, either by systemic injection or directly into the tumor. Both lymphocyte-activated killer cells (LAK) and cytotoxic T lymphocytes (CTL) have been studied in patients with recurrent GBMs [92]. Other studies reported responses to intratumoral or systemic administration of autologous tumor-specific T lymphocytes [96]. The tumor antigen-specific TCR (T cell receptor)-

transgenic cells and chimeric antigen receptors-modified T cells (CART) did not reach clinical trials for the moment [90].

Although preliminary results for some of these immunotherapeutic approaches, namely immunomodulatory checkpoint inhibitors, are promising and generally encouraging with some phase III clinical trials, further investigations are needed to improve effectiveness and at the same time prevent serious adverse effects which may be caused by activated immune responses.

#### **1.1.8.3.2 Emerging advances in radiotherapy**

Tumor treating field (TTF) therapy uses alternating electric fields to target rapidly dividing tumor cells. TTFs are generated by a battery-powered alternating current generator, operating at 200 kHz, with maximum voltage alternating from +50 to -50 V. TTF-exposed cells exhibit violent membrane blebbing at the onset of anaphase, resulting in aberrant mitotic exit. After aberrant mitotic exit, cells exhibited abnormal nuclei and signs of cellular stress and of immunogenic cell death suggesting that TTF treatment may induce an antitumor immune response. TTF has been approved by the USA FDA in 2011 for recurrent GBM. It is also being investigated in newly diagnosed GBM during the sequential TMZ phase after the whole course of radiotherapy. The analysis showed both improved progression-free survival and overall survival in the TTF/TMZ combined arm compared with TMZ alone (PFS 7.1 versus 4.0 months, OS 20.5 versus 15.6 months) [97].

#### **1.1.8.3.3 Inhibitors of growth factors and their receptors**

Molecular studies in GBMs show that several cell surface receptors are frequently overexpressed or mutated, including EGFR and PDGFR (platelet derived growth factor receptor) [8]. Thus, these aberrantly over activated receptors are considered as potential therapeutic targets and inhibitors of these receptor tyrosine kinases are under investigation.

One of the approved drugs directed against EGFR is the small-molecule kinase inhibitor gefitinib, an oral low-molecular weight adenosine triphosphate mimetic of the anilinoquinazoline family that reversibly inhibits the tyrosine kinase activity associated to this receptor. In a phase II clinical study, the expression of wild

type EGFR or mutant EGFR forms in patients was not associated with the sensitivity to the drug and no objective tumor responses were recorded in patients included in this study [98]. Subsequent studies with gefitinib as monotherapy or in combinations for GBM treatment failed to show significant benefit for patients compared to standard treatment [91]. Other EGFR inhibitors have also been investigated in GBM including erlotinib, lapatinib, afatinib and a chimeric monoclonal antibody against EGFR- cetuximab. However, the efficacy of EGFR inhibitors in the treatment of GBM is generally very limited [91].

PDGFR is another cell surface receptor commonly overexpressed and activated in GBM, especially in the proneural subtype [40]. Multiple kinase inhibitors of PDGFR such as imatinib, dasatinib and nintedanib and anti-angiogenic multi-kinase inhibitors affecting PDGFR, like sunitinib, sorafenib and vandetanib, were investigated in patients with GBM in different clinical trials. However, no evidence of significant OS benefit has been observed [91].

#### **1.1.8.3.4      Inhibitors of intracellular signaling pathways**

Aberrant signaling components in intracellular signaling pathways have been observed in almost all types of tumors. Many important intracellular effectors such as RAS, PI3K and PLC (phospholipase C) are recruited to the cell membrane after growth factor receptor activation and initiate various signal transduction pathways to regulate apoptosis, cell proliferation and differentiation [99]. Inhibition of components involved in these aberrant signal transduction pathways seems to be a promising targeted therapeutic approach for the treatment of GBM.

The RAS protein is involved in deregulated signaling pathways through growth factor receptors and requires a post-translational modification by farnesyltransferase for its translocation to the cell membrane. Tipifarnib, a potent and selective non-peptidomimetic farnesyltransferase inhibitor (FTI), was tested in a phase II trial in recurrent GBM patients with a good tolerance and modest activity [100]. Another oral farnesyltransferase inhibitor, lonafarnib, is under investigation in a phase I dose-finding study in combination with TMZ for patients with recurrent GBM [101].

mTOR, can also be activated by RAS. Sirolimus (rapamycin) and its synthesized analogs, everolimus and temsirolimus, have been evaluated in clinical trials for patients with malignant gliomas [99]. Temsirolimus associated to radiotherapy demonstrated modest efficacy in a phase II study in recurrent GBM patients [102].

PKC (protein kinase C) is also a serine/threonine kinase that regulates cell proliferation, invasion and angiogenesis. Tamoxifen, an anti-estrogen drug which also inhibits PKC, has been tested in clinical trials but failed to show clinical benefit [99]. Enzastaurin, a competitive small molecule inhibitor of PKC- $\beta$ , demonstrated a modest anti-glioma activity in recurrent GBM patients treated by radiotherapy [103].

Other inhibitors directed against these pathways such as inhibitors of histone deacetylase (HDAC)- vorinostat (Zolinza; Merck), depsipeptide (FK228) and valproic acid, and Src inhibitor dasatinib (Sprycel), have also been evaluated in cells and the clinical trials are ongoing [99].

Many other targeted therapeutics affecting different aberrantly activated intracellular signaling pathways are being examined in GBM, including inhibitors of poly ADP-ribose polymerases (PARPs) targeting the DNA repair pathway or inhibitors of STAT3 [91]. A specific PARP inhibitor, veliparib (ABT-888) is currently examined for the treatment of GBM in ongoing clinical trial [104].

#### **1.1.8.3.5 Inhibition of angiogenesis**

GBMs are excessively vascularized tumors characterized by aberrant blood vessels. This high vascularization was attributed to the high expression levels of vascular endothelial growth factor (VEGF). Therefore, inhibitors of VEGF and its receptors seem to have high therapeutic potential for the treatment of GBM [105].

The most widely used inhibitor of anti-VEGF by now is bevacizumab, as mentioned before. However, a meta-analysis of three well-designed clinical trials recently showed that bevacizumab failed to increase OS and had a higher rate of serious adverse events compared to the placebo arm [81].

Cediranib, another oral pan-VEGF receptor tyrosine kinase inhibitor, failed to show an OS benefit in patients with recurrent GBM in two phase III trials, either in

combination with lomustine chemotherapy or with an inhibitor of PKC- $\beta$  whose activation can lead to VEGF expression [106]. Administration of this molecule during a phase II study, led to normalization of tumor vessels and reduction of brain edema in GBM patients. However, increased tumor infiltration was observed after the treatment with cediranib in a mouse model, suggesting that blocking angiogenesis may promote tumor cell growth along blood vessels in order to maintain nutrient and oxygen supply [107]. Another oral pan-VEGFR inhibitor, aflibercept, an antiangiogenic drug, is under investigation in clinical trials. Other trials using combinations of antiangiogenic agents or antiangiogenic strategies associated with chemotherapy also failed to demonstrate an anti-tumor activity in clinical trials [108].

Despite all the research efforts and clinical trials conducted, unfortunately, anti-VEGF/VEGFR agents, inhibitors of signaling pathways or other antiangiogenic strategies, alone or in combination with chemo-radiotherapy, all failed to show a significant OS benefit for GBM patients by now. This may indicate that the great molecular/genetic heterogeneity in GBM prevents the observation of a beneficial effect in unselected subsets (non-stratified populations) of GBM patients.

## **1.2 Glioblastoma and Cancer stem-like cells**

### **1.2.1 Tumor heterogeneity**

It is now well accepted that tumor masses are complex, highly heterogeneous ecosystems including not only tumor cells but also several types of stromal cells. As discussed in previous sections, tumor cells and microenvironmental factors form a complex system contributing to tumor initiation, progression, invasion and therapy resistance. In recent years, deeper sequencing and improved bioinformatic methods further suggest that individual tumors are often composed of a dominant genetic clone plus one or more genetically distinct subclones and different gene-expression signatures can be detected in different regions of the same tumor. In addition to genetic heterogeneity, epigenetic modifications were also shown to contribute to functional heterogeneity between cells of a single tumor [109]. Multiple tumor cell subpopulations within single cancers have been described for melanoma, sarcoma, colon cancer [109] and other solid

tumors including GBM [110]. Moreover, it was proposed that not all cells within tumors have equal capacity of tumorigenesis and that only a small population of non-differentiated tumor cells, expressing specific molecular markers, is able to initiate the formation of heterogeneous tumors following transplantation into immune-compromised mice [111]. Thus, tumorigenic cells seem to be intrinsically different from other non-tumorigenic cancer cells. Such tumorigenic cells within a tumor were proposed to correspond to cancer stem or stem-like cells. Alternatively, CSCs were designated as the tumor initiating and or propagating cancer cell subpopulation. In this manuscript, we will refer to them as cancer stem-like cells (CSCs).

CSCs are thus a subpopulation of cancer cells with clonal long-term repopulation and self-renewing capacity as well as multilineage differentiation potential, thus endowed with the ability to initiate propagate and maintain tumors (Figure 6) [112][113].



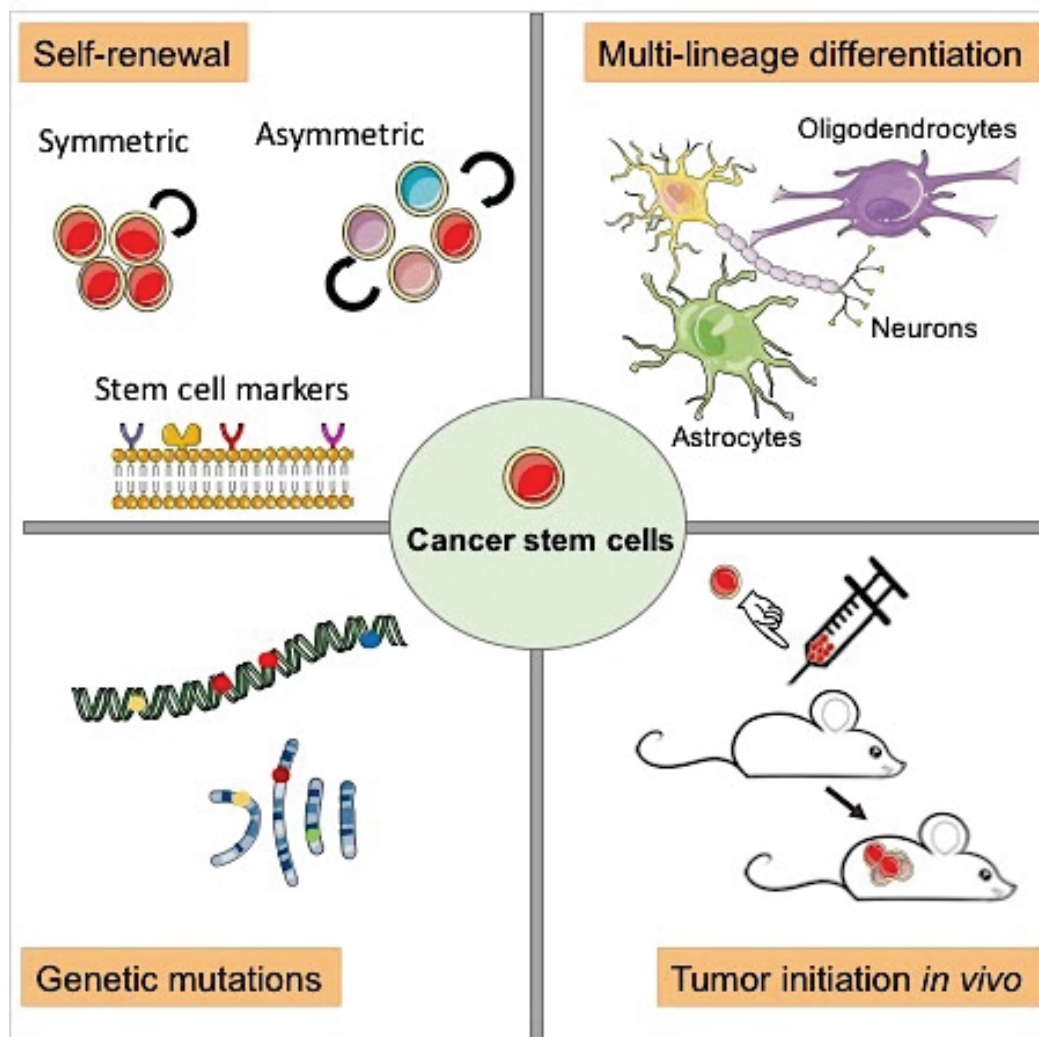


**Figure 6. Cancer stem-like cell properties.** Cancer stem-like cells express stem-cell markers and have long-term self-renewal capacity and can divide in symmetric or asymmetric modes. These cells are also endowed with multi-lineage differentiation ability under specific culture conditions and display genetic alterations that confer malignancy. A hallmark of cancer stem-like cells is their ability to initiate and propagate tumors *in vivo* after serial transplantation of low numbers of cells in immunocompromised animal models. Tumors developing *in vivo*, from these cells, are similar to the tumors in patients from which the cancer stem-like cells were derived.

### 1.2.2 Discovery of cancer stem-like cells

The first evidence for the existence of stem-like cells was reported in the late-90s by Bonnet and Dick. These authors identified a subpopulation of CD (Cluster of Differentiation)  $34^+/\text{CD}38^-$  leukemic cells with tumorigenic ability in immune-compromised mice. These cells possess several hematopoietic stem cell characteristics (cell surface marker expression, proliferation and self-renewal

abilities), and the capacity to reconstitute the full spectrum of leukemic cells from patients with acute myeloid leukemia (AML) [114], suggesting that they may originate from normal stem cells rather than from more committed progenitors. Following this first report in hematopoietic malignancies, Al-Hajj and colleagues brought the first evidence of the presence of CSCs in solid tumors, namely in breast cancer, by discovering a subpopulation of CD44<sup>+</sup>/CD24<sup>-/low</sup> breast cancer-initiating cells although this surface marker expression profile was later demonstrated not to be a universal tumorigenic marker [109][113]. Brain tumor stem cells that can produce tumors in serial transplantation settings in NOD/SCID (non-obese diabetic/severe combined immunodeficiency) mice have also been isolated from human medulloblastomas and GBM. The first evidence for GBM stem cells was provided by Singh and colleagues then followed by Galli and co-workers in 2003-2004. Singh et al., revealed the existence of CD133<sup>+</sup> (a cell surface antigen, prominin 1) cell population from human adult brain tumors that exhibits stem cell properties *in vitro*, and proposed a xenograft assay to demonstrate the *in vivo* tumor initiating potential of these cells. They showed that by injecting as few as 100 CD133<sup>+</sup> GBM cells in NOD/SCID mice, it was possible to generate tumors by serial transplantation. In addition, the tumors obtained were phenotypically similar to the ones present in patients and from which the CD133<sup>+</sup> cells were isolated [115][116]. Galli then showed that transformed, stem-like neural progenitors that are able to establish tumors with all of the classical features of GBM upon serial transplantation, could be isolated from adult GBM patients' biopsies. These cells also showed multipotency *in vitro* since they were able to differentiate into neurons, astrocytes and oligodendrocytes under certain conditions. This property was maintained even after long-term culture *in vitro* [110]. Subsequently, Yuan et al. and Hemmati et al. identified CSCs from adult and pediatric GBMs, respectively [117][118]. More recently, Patru and colleagues published the identification and phenotypic and functional characterization of CSCs from a series of GBM tissues of adult patients [119].

To date, based on various experimental settings, CSCs have been identified in many other solid tumors including but not limited to pancreatic, colon, head and neck, hepatic, lung, prostate, bladder and ovarian malignancies, as well as melanoma and musculoskeletal sarcomas [112].

### **1.2.3 Cancer stem-like cell properties**

#### **1.2.3.1 Expression of cell surface and functional markers**

Due to the advent of the fluorescence-activated cell sorting (FACS) technology, it is possible to sort phenotypically distinct subpopulations of tumor cells to subsequently investigate their functional potential. Using this approach, a number of markers have been associated to CSCs in multiple types of tumors [120]. For example, cell surface antigen expression profiles have been widely explored for identification and isolation of CSCs, originally in human leukemia and subsequently in solid tumors. Acute myeloid leukemia CSCs were identified as cells expressing CD34 and lacking CD38 expression. The CD44 adhesion molecule has been associated to CSC phenotypes in breast cancer as well as in colon, prostate, pancreatic, head and neck, ovarian, lung and liver malignancies. CD133 expression was described and used for isolation of CSCs from various solid tumors including GBM, prostate, colon, lung, pancreatic and ovarian cancers as well as melanoma.

Other cell surface markers used to characterize cancer stem cells in multiple types of solid tumors include ABCG5 (ATP-binding cassette subfamily G member 5), CD90 (Thy-1) and EpCAM (epithelial cell adhesion molecule) also known as ESA (epithelial specific antigen) or TROP1 [121][122]. Some examples of CSC surface markers are shown on Table 3.

**Table 3 Cell surface markers in cancer stem cells**

Tumor type	CSCs surface markers
Acute myeloid leukemia	CD34 <sup>+</sup> CD38 <sup>-</sup>
Acute lymphoid leukemia	CD34 <sup>+</sup> CD19 <sup>-</sup> , CD34 <sup>+</sup> CD38 <sup>-</sup>
Breast cancer	CD44 <sup>+</sup> CD24 <sup>-</sup> , CD55 <sup>+</sup> , CD61 <sup>+</sup>
Brain cancer	CD133 <sup>+</sup> , CD133 <sup>+</sup> EGFRvIII <sup>+</sup> , SSEA-1 <sup>+</sup> , integrin $\alpha 6^{hi}$
Colon cancer	CD133 <sup>+</sup> , EpCAM <sup>hi</sup> CD44 <sup>+</sup> , CD66c <sup>bright</sup>
Colorectal cancer	EpCAM <sup>+</sup> ESA <sup>+</sup>
Prostate cancer	CD44 <sup>+</sup> $\alpha 2\beta 1^{hi}$ CD133 <sup>+</sup>
Pancreatic cancer	CD44 <sup>+</sup> CD24 <sup>+</sup> ESA <sup>+</sup> , CD133 <sup>+</sup> CXCR4 <sup>+</sup> , FoxM1 <sup>hi</sup>
Head and neck cancer	CD44 <sup>+</sup>
Ovarian cancer	CD44 <sup>+</sup> CD117 <sup>+</sup> , CD133 <sup>+</sup>
Lung cancer	CD133 <sup>+</sup> , CD44 <sup>+</sup> , CD166 <sup>+</sup>
Liver cancer	CD133 <sup>+</sup> , CD90 <sup>+</sup>
Gastric cancer	CD44 <sup>+</sup>
Melanoma	ABCB5 <sup>+</sup> , CD133 <sup>+</sup>

**Table 3. Cell surface markers used for the identification/isolation of cancer stem-like cells from various tumor types, adapted from [120].** CD: cluster of differentiation; SSEA-1: stage-specific embryonic antigen, CD15 or Lewis X; EpCAM: epithelial cell adhesion molecule; ESA: epithelial-specific antigen; CXCR4: chemokine receptor specific for stromal-derived-factor-1 (SDF-1 also called CXCL12); FoxM1: a proliferation-associated transcription factor Forkhead box M1; ABCB5: ATP-binding cassette subfamily B member 5.

In addition to cell surface markers, functional markers, most of which are associated to the intrinsic properties of CSCs, have been used for the isolation/characterization of this tumor cell subpopulation. For example, breast, bladder, lung, colon, esophageal and head and neck squamous cell tumor CSCs were shown to have increased ALDH1 (aldehyde dehydrogenase 1) expression [123]. Expression of OCT-4 (octamer-binding transcription factor 4), SOX2 (sex determining region Y-box 2) and Nanog transcription factors as well as of

components of the Wnt/ $\beta$ -catenin, Notch and Hedgehog (Hh) signaling pathways were also associated to the stem-like phenotype of CSCs [124][125].

Markers described in GBM CSCs include cell surface proteins such as CD133 and L1CAM (L1-cell adhesion molecule, CD171), the intermediate filament protein nestin, GFAP, transcription factors SOX2, Nanog and OCT-3/4, the RNA-binding protein musashi, the poly-comb transcriptional repressors Bmi1 and Ezh2 and proteins of the Notch and STAT3 signaling pathways as well as cytoplasmic enzyme ALDH1 [126][127].

Markers such as SSEA-1 (stage-specific embryonic antigen, CD15 or Lewis X), A2B5 and integrin  $\alpha$ 6, have also been explored in GBM CSCs. Despite a high proportion of CD133<sup>-</sup> cells, SSEA-1-based selection enriched for CSCs by 100-fold in almost every GBM evaluated in a study conducted by Son and colleagues. They have shown that in their tumor samples, most CD133<sup>+</sup> tumor cells are SSEA-1<sup>+</sup>, and that the SSEA-1<sup>+</sup> subpopulation cells are highly tumorigenic *in vivo* and have self-renewal and multi-lineage differentiation potentials *in vitro* [128]. Another study conducted by Ogden and colleagues revealed a subpopulation of GBM CSCs characterized by the expression of a glial progenitor surface marker, A2B5. The A2B5<sup>+</sup> population presented high tumorigenic potential [129]. In another study, Rich and colleagues examined the GBM CSC perivascular microenvironment in patient specimens and identified integrin  $\alpha$ 6 as a protein co-expressed with conventional CSC markers. Furthermore, data obtained by these authors suggested that integrin  $\alpha$ 6 can be used as a GBM CSCs' enrichment marker in tumors that express little or no detectable levels of CD133 [130].

In addition to their utility for the identification/isolation of CSC populations, cancer stem cell markers have been also widely used to predict therapy response in patients. Several studies showed that EGFR inhibitor-resistant NSCLC (non-small cell lung cancer) cells exhibited high expression of ALDH1 and OCT-4. CD44 upregulation in metastatic clear cell renal cell carcinoma patients was associated with poor response to sunitinib which failed to kill CD44 positive cells. Another study showed that the CD44<sup>+</sup>/CD24<sup>-</sup> phenotype could be used as a predictive factor for poor response to trastuzumab in HER2-positive breast cancer patients [131]. These studies revealed the possibility to predict therapy response by assessing the

expression of CSC signatures and provided possible strategies for overcoming therapy resistance by targeting CSCs.

It is however important to notice that none of the markers used to isolate cancer stem cells is expressed exclusively by these cells. For example, CD133, expressed in CSCs from various solid tumors including GBM, is also present in normal brain stem cells and non-tumorigenic cells in various tumors and tissues. The same is true for other commonly used CSC markers such as CD44, Sca1, and CD 90 (Thy-1) [113][132]. In addition, CD133<sup>+</sup> cells were also shown to be able to initiate brain tumor formation in recipient animals [113]. Moreover, surface marker expression profiles may vary during tumor growth *in vivo* and as a function of experimental conditions *in vitro* and heterogeneity in marker expression was described between patients and even within the same tumor [133]. Combining different phenotypic and functional markers was proposed to improve CSC characterization but is still not sufficient [113]. It is now widely accepted that marker expression must be associated to functional validation to definitely define a cancer cell as a CSC.

### **1.2.3.2 Self-renewal and long-term proliferation ability**

Cancer stem-like cells share important properties with normal tissue stem cells, including self-renewal (by symmetric and asymmetric division) and long-term proliferation ability both *in vitro* and *in vivo* (Figure 6). Preferential activation of the Wnt/ $\beta$ -catenin, Notch, Hedgehog (Hh) and Bmi1 (polycomb ring finger oncogene) signaling pathways, involved in embryonic development and known for their implication in stem cell self-renewal, was extensively reported in CSCs [134]. Evaluation of these properties is performed *in vitro* through sphere assays and serial colony-forming unit (CFU) assays (replating assays). Such assays measure the ability of CSCs plated at limiting dilutions to form spheres in *in vitro* experimental settings.

### **1.2.3.3 Differentiation potential**

CSCs, like normal stem cells are also endowed with differentiation ability (Figure 6). Abundant evidence has revealed that CSCs have the potential to differentiate into several types of cancer cells as well as to transdifferentiate into

several stromal cells [135]. In several studies in GBMs, evidences showed that cancer stem-like cells isolated from malignant tissue of GBM patients have the ability to generate tumor cells and tumor-derived endothelium [136][137]. Patru and colleagues also isolated a subpopulation of stem-cell like cells from human adult GBM and showed that these cells exhibit capacity to neuronal- and glial-lineage differentiation [119].

*In vitro*, differentiation potential of CSCs is demonstrated by loss of sphere forming ability and cell attachment upon exposure to serum and by modifications in expression levels of stem-cell and differentiation markers [138]. Moreover, tumorigenic properties of CSCs are lost in the differentiated state.

#### **1.2.3.4 Increased pro-survival signaling**

Many studies suggested that many anti-apoptotic molecules are overexpressed in CSCs. For example, CSCs from high grade astrocytomas overexpress the apoptosis regulators BCL2 and BCL-XL proteins, which negatively regulate mitochondrial membrane permeabilization and cytochrome C release and block apoptosis [139]. Moreover, higher levels of survivin and lower levels of caspase 8 were described in CSCs derived from other types of brain tumors [140][141]. As a consequence, CSCs show higher resistance to pro-apoptotic signals compared to other cells of the tumor mass.

#### **1.2.3.5 Resistance to DNA damage**

CSCs from various tumors were shown to be more resistant to DNA damage. This may be achieved through preferential activation of checkpoint cell cycle arrest, enhanced DNA damage responses and lower levels of ROS in these cells [22].

#### **1.2.3.6 Increased efflux capacity of the Hoechst dye**

One of the characteristic properties of CSCs is their high capacity to exclude the Hoechst dye. This property defines CSCs as the side population (SP) cells and is commonly applied for their isolation from tumors [142]. This CSC property is due to increased expression of proteins belonging to the ATP-binding (ABC) cassette transporter family in these cells. Overexpression of ABC transporters, including P-glycoprotein (also known as multi drug resistance protein 1 (MDR1) or ABCB1),

multi-drug resistance associated proteins 1 and 2 (MRP1/2 or ABCC1/2) and breast cancer resistance protein (BCRP or ABCG2), was described in malignancies such as GBM, lung, prostate and ovarian cancer and nasopharyngeal carcinoma [143].

#### **1.2.3.7 In vivo tumor initiation capacity**

As previously mentioned, one of the major features of the CSC subpopulation of cancer cells is their tumor initiating ability. Thus, the gold standard assay for CSC validation measures the *in vivo* ability of limiting dilutions of these cells to recapitulate the heterogeneity and complexity of the initial tumor following serial orthotopic or ectopic transplantation in appropriate animal models (Figure 6). In the study conducted by Patru et al., small numbers of CSCs (200-1000 living cells) isolated from GBM samples were able to initiate tumors after orthotopic xenografting in Nude mice [119]. Numerous other studies also showed the capacity of CSCs to regenerate tumors in immune-deficient mice [129][136].

#### **1.2.3.8 Dormancy (Quiescence)**

Transient and long-term quiescence, the latter also termed dormancy, are generally believed to be fundamental attributes of adult stem cells. These cells, are present in recipient tissues predominantly in a quiescent, non-dividing G0 state but are also able to exit quiescence and rapidly expand and differentiate in response to stress. This process is strictly controlled by both intrinsic regulatory mechanisms and extrinsic signals. Intrinsic positive regulators of cell quiescence include TP53 signaling, ROS level regulation by transcription factors of the FoxO family or ATM checkpoint regulator and HIF-1 $\alpha$  transcription factor stabilization and regulation of downstream genes. Conversely, mTOR signaling acts as a negative regulator of stem cell quiescence. Extrinsic factors provided by the stem cell niche include Tie-2/angiopoietin-1, TGF- $\beta$  and bone morphogenic proteins signaling, thrombopoietin, N-cadherin and integrins, Osteopontin and Wnt/ $\beta$ -catenin signaling in the microenvironment of stem cells [144].

Tumor dormancy in clinical observation was originally reported by Willis in the late 1940s and then redefined by Hadfield in the early 1950s as a temporary mitotic arrest and a tumor growth arrest during which the tumor mass is kept constant. Cellular dormancy was also observed in tumors. During this phenomenon,



intrinsic and/or extrinsic mechanisms drive a small group of cancer cells to enter quiescence, a stable, non-proliferative state which can be determined by the lack of proliferation markers in these cells and which is reversible [145].

CSCs, just like their normal counterparts, can enter the quiescent state which appears to be necessary for preserving the CSC pool within tumors. Indeed, in several cancers, including breast and colon malignancies, relapse can occur after long lag periods. This late recurrence can be explained by the survival and long-term persistence of quiescent CSCs after treatment [144]. Evidences for the presence of quiescent CSCs were also reported in a NOD/SCID/IL2 $\gamma$  null mouse model of human AML. Following treatment with granulocyte colony-stimulating factors (G-CSFs), these quiescent AML CSCs were able to re-enter into the cell cycle [146]. In melanoma, a subpopulation of slow-cycling cells was identified by using the H3K4 histone demethylase JARID1B as a biomarker. This subpopulation is required for continuous tumor growth [147]. In human liver cancer, CD13 was demonstrated as a marker of potentially dormant CSCs in cell lines and clinical samples [148]. A dormant CSC population with hAFP<sup>+</sup> (human alpha-feto protein)/CD13<sup>+</sup>/PCNA<sup>-</sup> (proliferating cell nuclear antigen) phenotype has been revealed in an hepatocellular carcinoma mouse model [149]. Quiescent CSCs were also isolated from ovarian cancer, a colon adenocarcinoma cell line and GBMs [150].

Quiescent label-retaining GBM CSCs (GSCs) endowed with tumor initiation/propagation properties were first described by Deleyrolle et al. [151]. Chen and al. then identified glioblastoma CSCs expressing a transgene that labels quiescent adult neural stem cells of the subventricular zone and staining negative for proliferation marker Ki-67 expression, in a genetically engineered mouse model of glioma. Following treatment with TMZ, this cancer cell subpopulation could drive tumor regrowth through the production of highly dividing cells [152]. Furthermore, RNA seq-based single cell transcriptomic analysis was used to demonstrate that GBMs are highly heterogeneous tumors with variable proportions of cells expressing markers that have previously been associated with quiescence. These cells are also characterized by the presence of a stemness signature which is attributed to glioblastoma CSCs [153]. Finally, HIF1 $\alpha$ -positive quiescent GBM cells with stem properties were localized by immunocytochemical-based methods in perinecrotic niches in patient specimens [154].

### 1.2.3.9 Plasticity

Initially, CSCs were believed to originate from the stem cells of the original tissue through acquisition of gene mutations that contribute to tumorigenicity. Later, it was shown that these cells may also arise from committed progenitor cells or differentiated cells through multiple mutagenic events conferring them CSC-like characteristics. For example, in blast crisis chronic myeloid leukemia (CML), committed granulocyte-macrophage progenitors were shown to acquire long-term self-renewal capacity due to the accumulation of serial genetic mutations [113]. In addition to accumulation of genetic alterations, acquisition or loss of stem-like properties may be induced by epigenetic modifications, microenvironmental/niche cues and conditions and/or as a result of treatment. For example, a recent study conducted by Suvà et al. in 2014, showed that differentiated GBM cells can be fully reprogrammed into tumor stem-like cells by induction of a core set of neurodevelopmental transcription factors (POU3F2, SOX2, SALL2, and OLIG2) [155]. In experimental models of melanoma, tumor cells could acquire stem-like properties depending on cues from their niche. In addition, the acquired CSC-like state was reversible [156]. Moreover, increased expression of JARID1B, a histone demethylase functioning as a regulator of tumorigenicity in melanoma cell lines, was observed in hypoxic conditions. This change in the expression level of JARID1B was accompanied by a high *in vitro* self-renewal potential for these cells [147]. Additional microenvironmental signals that can regulate cancer stem-cell fate and metastatic potential include reorganizations of the extracellular matrix, autocrine factors and endothelial or immune-cell secreted molecules, as well as low nutrient supply. A more detailed description of CSC plasticity inducing factors and its implications in therapy resistance may be found in Chen et al., 2016 (Appendix 1) [150].

CSCs were initially considered as a static well defined subpopulation of cancer cells with invariable functional characteristics distinguishing them from cells of the tumor mass. In view of the above data, it is now clear that the CSC phenotype represents a dynamic state that any cell may acquire depending on signals provided by its microenvironment and/or by treatment conditions. Epigenetic modifications are a major source of this kind of cell plasticity although genomic alterations and selection of mutant cells may also participate to this phenomenon.

#### **1.2.3.10 Increased stemness and aggressivity in hypoxic/acidic tumor microenvironment**

As previously mentioned, hypoxia is one of the hallmarks of solid tumors including GBM and transcription factors of the HIF family play pivotal roles in cellular responses under these conditions. Hypoxic conditions were shown to lead to an increase in stem-cell marker expression in numerous cancer cell lines (Figure 7) [157] and HIF2 $\alpha$  function was linked to the stem-cell properties and tumorigenic potential of GBM CSCs [158][159]. Dedifferentiated phenotype promotion in hypoxic conditions was described in various malignancies including breast carcinomas, neuroblastoma and medulloblastoma [160][161][162][163]. In melanoma cells, hypoxic conditions were shown to lead to HIF-dependent Snail1 overexpression, decreased E-cadherin levels and acquisition of melanoma CSC features [164].

Acidic microenvironments were also shown to promote CSC-like phenotypes. For example, an increase in the expression of CSC markers including OLIG2, OCT4 and NANOG was observed when GBM CSCs or CSC-depleted cultures of glioblastoma cells were exposed to low pH. In addition, cells under these conditions acquired greater neurosphere formation capacity *in vitro* as well as increased tumorigenicity *in vivo* [165].

#### **1.2.3.11 Metastatic potential**

Because of their properties, CSCs are attractive candidates as tumor cells participating in the metastatic process. CSCs have been linked to EMT (epithelial to mesenchymal transition), a process during which differentiated polarized epithelial cells acquire a mesenchymal phenotype and an invasive potential [166][167], and subsets of circulating tumor cells with metastatic initiation ability were shown to express high levels of stem cell markers [168][169][170]. In addition, metastases development was related to loss of differentiation-inducing factors or acquisition of stem cell signaling [171]. Finally, through regulation of components of their niche, CSCs were shown to participate to metastatic colonization at secondary target organs [172].

### 1.2.3.12 Therapy resistance

Because of their specificities, including high expression of drug efflux pumps, more efficient DNA repair, enhanced anti-apoptotic systems [120], maintenance in a dormant state within tumors *in vivo*, ability to survive and increased stemness and tumorigenicity in hypoxic/acidic tumor microenvironments and their plastic phenotype, CSCs are believed to be more resistant to therapy compared to other cells of the tumor mass (Figure 7) [173].

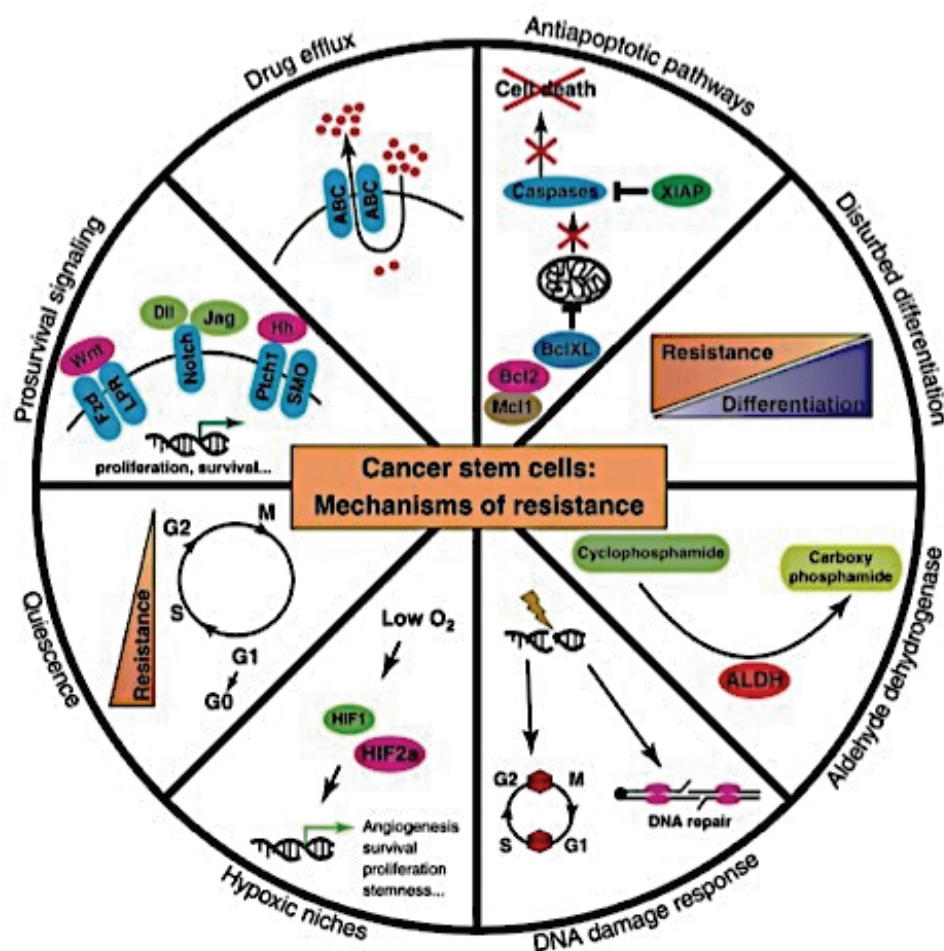


**Figure 7. Cancer stem-like cell mechanisms of therapy resistance, adapted from [173].** Cancer stem-like cells have developed several mechanisms to escape conventional treatment. These include increased pro-survival and antiapoptotic signaling, more efficient DNA damage response and drug efflux mechanisms and metabolic changes conferring to these cells a selective advantage. Their ability to be maintained within tumor masses *in vivo* in a quiescent slow-growing state preserves these cells from antiproliferative chemotherapy. Finally, hypoxic and acidic conditions of the tumor microenvironment were shown to increase aggressive and stem-like phenotypes of these cells.

Indeed, it was shown in several experimental models that the radiation dose required for eradication of a tumor inversely correlates with the logarithm of the number of CSCs present within the tumor mass [174]. The resistance of GBM CSCs towards radiotherapy and chemotherapy has been extensively studied in the last decade. Resistance mechanisms to TMZ, the current standard of care for GBM, were particularly investigated. Although some experimental data demonstrated that TMZ was able to preferentially deplete GBM CSCs in a dose- and time-dependent way *in vitro* [175] and that primary GBM response to therapy occurs in a patient-specific fashion and is independent of the CSC phenotype [176], most studies pointed to a chemo-resistant phenotype of GBM CSCs towards alkylating agents [126].

The resistance of GBM CSCs towards radiotherapy and chemotherapy involves several mechanisms. CSCs isolated from GBM were shown to express higher levels of MGMT, a DNA repair enzyme able to remove methyl groups added to DNA by alkylating agents such as TMZ [126]. TMZ resistance of GBM CSCs *via* regulation of MGMT expression is promoted by the JNK (c-Jun N-terminal kinase) and MEK-ERK-MDM2-TP53 signaling pathways [177][178]. In addition to MGMT, the DNA repair protein ALKBH2 (AlkB homolog2), was identified as a mediator of TMZ resistance in human GBM [179]. Moreover, Bao and colleagues showed that CD133<sup>+</sup> glioma cell subpopulations with CSC properties are able to resist to radiation *in vitro* and *in vivo* through increased expression of proteins involved in checkpoint cell cycle arrest such as ATM, Rad17 and Chk1 and Chk2 (checkpoint kinases 1 and 2) [180].

In addition to more efficient DNA repair, glioma CSCs have also enhanced efflux capacity of chemotherapeutic agents through overexpression of ATP-binding cassette transporters (ABCTs) such as ABCG2 on their cell surface. This resistance mechanism was linked to the PTEN/PI3K/Akt pathway [181]. Moreover, the quiescent state of GBM CSCs within their hypoxic/acidic tumor microenvironment, was related, as previously mentioned, to enhanced tumorigenic capacity and chemo-resistance [119][154][182]. Mechanisms of treatment resistance in CSCs are summarized in Figure 7.

CSC resistance to therapy led in recent years to a new paradigm suggesting that relapse of tumors may be attributed to the survival of these cells under currently used therapeutic approaches. Thus, it was proposed that more efficient cancer treatment requires therapeutic strategies targeting all the types of cancer cells including CSCs (Figure 8). As a consequence, several approaches aiming to target CSCs have been explored or are currently under investigation. Several examples of CSC targeting attempts are given in Chen et al., 2016 (Appendix 1) [150].

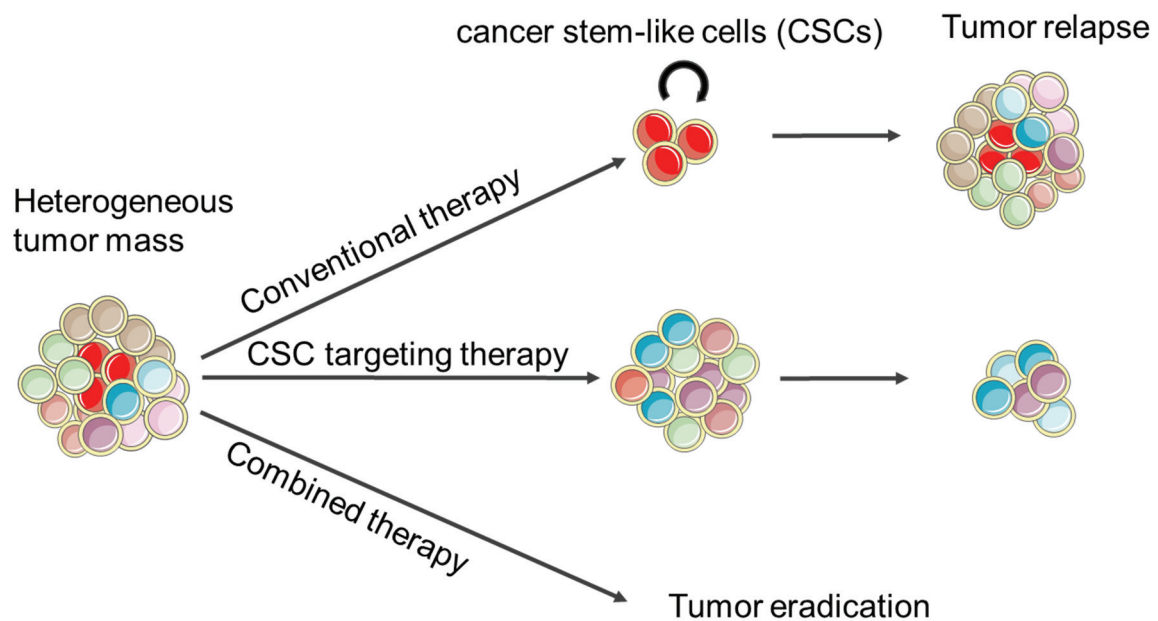


**Figure 8. Novel paradigms for cancer treatment.** Conventional therapy targets tumor mass cells and preserves or even favors the selection of cancer stem-like cells (CSCs). Because of their specific properties, intact CSCs may then lead to tumor relapse. It was thus proposed, that to be efficient, novel treatments should combine CSC targeting and conventional therapeutic approaches.

## 1.2.4 CSCs and evolution of models of tumor initiation and heterogeneity

### 1.2.4.1 The clonal evolution (stochastic) model

Initially, the clonal evolution (stochastic) model was proposed to explain the heterogeneity observed in most if not all tumors (Figure 9A). A guiding principle of this model proposed by Nowell, is that tumor initiation and progression result from

random and sequential acquisition of genetic variations that contribute to subsequent clonal expansions of cells with a selective growth advantage. Thus, this model suggests tumor initiation and progression as a result of genetic instability and sequential selection by an evolutionary process. In this case, heterogeneity results from the random accumulation of mutations in distinct sub-clones of the tumor mass [183].

The first genetic evidence of the clonal progression of cancer in patients was provided in 1963 by Levan and colleagues through studies of a case of CML (chronic myeloid leukemia). These authors observed, in the same patient, the coexistence of Ph (Philadelphia) chromosome-positive cells that differed in their sex chromosome complement, one set being 46Ph;XY and the other being 47Ph;XXY. The karyotype of normal cells in this patient was 46;XY. These observations suggested the formation of a sub-clone of leukemic cells characterized by a duplication of the X chromosome [184]. Furthermore, concurrent evidence of multistep genetic model of tumorigenesis was described by Vogelstein and colleagues in colorectal tumors. They showed for the first time that human colorectal tumors are clonally derived and that 75% of the tumors are characterized by a loss of chromosome 17p [184]. These studies allow the establishment of a cancer development model that follows the rules of Darwinian evolution, where a cell acquiring a mutation (or mutations) conferring an advantage over other cells that lack of this/these mutation(s), will flourish and produce a clonal population that dominates the site where it originated.

#### **1.2.4.2 The hierarchical model based on CSCs**

Conversely to the clonal evolution (stochastic) model, the hierarchical or CSC model postulates that, because of their ability to self-renew and proliferate in the long-term and their multi-lineage differentiation capacity, only a small subpopulation of cancer cells, the CSCs, may be the driving force of tumorigenesis and tumor heterogeneity. Thus, according to this model, tumors are hierarchically organized with CSCs found at the apex of this hierarchy. In this case, tumor heterogeneity results from CSC symmetric and asymmetric divisions and differentiation which progressively generates more restricted progenitor cells ultimately yielding mature cell types who lose tumor initiation ability (Figure 9B). As

mentioned in previous sections, CSCs with unique tumorigenic potential among cancer cells have been isolated from a number of hematopoietic and solid tumors including GBM. In all cases, only CSCs were able to generate tumors similar to the ones observed in patients in *in vivo* experimental models, supporting the hierarchical organization of tumors proposed by the CSC model. It is important to underlie that the CSC model does not imply that CSCs arise from oncogenic transformation of normal stem cells since any cell in the hierarchy with proliferative ability could be at the origin of CSCs and thus of tumors [185][186].

The validity of the CSC model is still debated, due to concerns with the functional assay (xenotransplantation) used to validate the CSC phenotype. In this assay, serial dilutions of isolated cells are transplanted into immune-compromised mice to evaluate the tumorigenic capacity of subpopulations of cancer cells designated as CSCs. Thus, transplantation assays evaluate the potential of cancer cells to form tumors under certain conditions rather than their actual fate in the native tumor. Lineage tracing or fate mapping assays would be more useful for defining the actual fate of tumor cells in the native tumor environment. Another important question is whether many or few cells with tumorigenic potential contribute to tumor growth. High-coverage sequencing of human tumors may bring insights as to genetic heterogeneity within tumors and to the types and proportions of cells that are responsible for relapse after therapy [187]. It is conceivable that some tumors may contain a steep developmental hierarchy, where only few self-renewal competent CSCs exist among other non-tumorigenic cancer cells. Other tumors may contain an intermediate hierarchy in which the number of CSCs or tumor initiating cells is relatively high. Finally, some tumors may be composed of numerous cells with genetic alterations or epigenetic modifications conferring them high self-renewal and tumorigenic potential. In this case, most tumor cells are tumorigenic and hierarchical organization is lost [109].

Based on these observations and on experimental data demonstrating that non-CSC populations may acquire CSC functionalities depending on the cell environmental context, more complex models in which the clonal evolution and CSC hierarchy models may co-exist have been proposed. Therefore, the resulting fluid CSC model postulates that CSCs within tumors are not a static entity but an



evolving/fluid one. Genetic and epigenetic changes may accumulate in cancer cells and influence their CSC state over time (Figure 9C).

The fluid CSC model is supported by data identifying genetically diverse CSC populations in several hematological cancers. Moreover, during metastasis, a large number of additional genetic mutations was identified in cells alongside of founder mutations within the parental clones. Dimitros and colleagues uncovered a dynamic equilibrium of CSCs and non-CSCs in breast cancer mediated by IL-6 signaling. Furthermore, non-CSCs in basal breast cancer were shown to switch to a CSC-like state, depending on ZEB1 (zinc finger E-box binding homeobox1) function. ZEB1 is a protein associated with EMT activation and stemness maintenance of tumor cells such as pancreatic cancer cells [188]. In addition, Dick and colleagues showed that Bcr-Abl1 lymphoblastic leukemia stem cells are subject to clonal evolution [112].

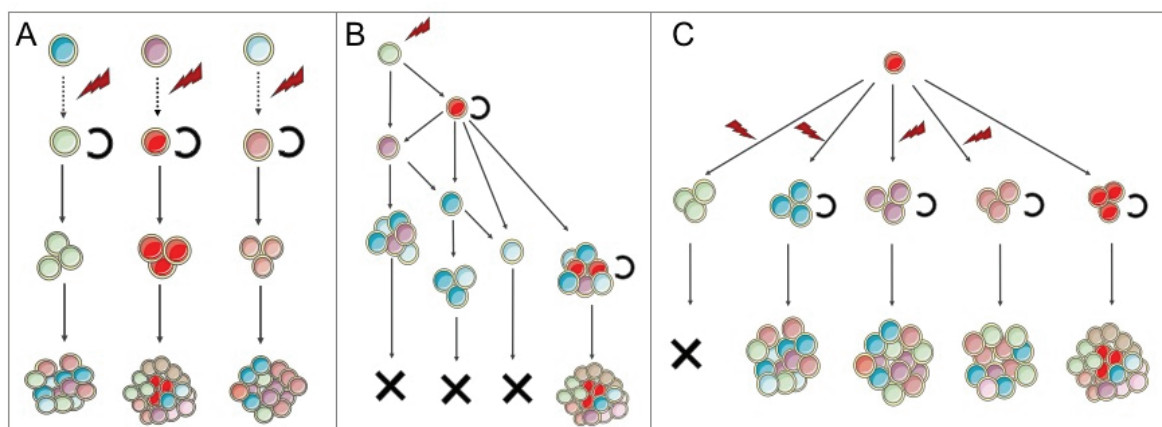


**Figure 9. Models for tumor initiation and tumor heterogeneity. A.** The clonal evolution model: in this model, random and sequential acquisition of genetic variations in any cancer cell may confer tumor initiation ability. Clonal expansion of individual sub-clones would lead to the formation of a heterogeneous tumor mass. **B.** The CSC (cancer stem-like cell) hierarchical model: only a subpopulation of cancer cells with stem-like properties has self-renewal and multi-lineage differentiation ability and is thus able to generate a heterogeneous tumor mass. **C.** The fluid evolutionary model: genetic/epigenetic changes and environmental cues may modulate the tumor initiation/propagation ability and stem-like properties of any cell which would then be able to initiate and propagate heterogeneous tumors.

## 1.3 WNK kinases

### 1.3.1 The WNK family of protein kinases

WNKs (With-No-lysine (K) Kinases) are a family of serine-threonine protein kinases that have particular protein kinase domains due to the position of their catalytic lysine. This makes WNKs structurally distinct from all other members of the protein kinase superfamily. The first member of the WNK family, WNK1, was cloned by Cobb and colleagues in 2000 from a rat brain cDNA library during a search aiming to identify novel members of the MAP/extracellular signal-regulated protein kinase (ERK) family [189]. Subsequently, four human WNK family members have been identified by Verissimo and Jordan in 2001 [190]. Soon after the identification of the four isoforms in this family, mutations in two of them, WNK1 and WNK4, have been linked to a hereditary form of human hypertension (Familial Human Hypertension: FHHT), known as pseudohypoaldosteronism type II (PHAII) or Gordon's syndrome. PHAII is an autosomal dominant disorder in which patients present hypertension, hyperkalemia (high serum potassium levels) and hyperchloremia [170]. Mutations in the *WNK1* gene that cause PHAII are large deletions in the first intron leading to increased expression of the wild-type protein whereas missense mutations in the *WNK4* gene are the cause of this disease. More recently, a mutation in *WNK1* was identified in an autosomal recessive neuropathy due to a loss of peripheral sensory nerves and characterized by a loss of perception to pain, touch and heat [192].

#### 1.3.1.1 Organization and expression of human WNK genes

In humans, WNK family members are encoded by 4 distinct genes. The human *WNK1* gene located on chromosome 12p13.33 spans 160 kb and was initially proposed to contain 28 exons (GenBank accession number: AJ296290). More recent studies identified four additional exons bringing the total number of exons in the human *WNK1* gene to 32. These are exons 8b and HSN2, mainly present in the nervous system, and exons 26a and 26b. 8 out of these 32 exons (8b, HSN2, 9, 11, 12, 26, 26a and 26b) are alternatively spliced in a tissue-specific manner, giving rise to a big number of WNK1 isoforms. That may explain the multiplicity of WNK1 functions in different tissues. Moreover, alternative promoter

usage gives rise to an ubiquitous full-length WNK1 isoform and a shorter kidney-specific isoform, KS-WNK1 [193].

The *WNK2* gene localizes on chromosome 9q22.31, spans 136 kb and contains 30 exons. The *WNK3* gene is located on chromosome Xp11.22, spans 165 kb and contains 24 exons. The *WNK4* gene is smaller compared to the other *WNK* genes. It is located on chromosome 17q21.31, spans 16 kb and contains 19 exons [192].

### **1.3.1.2 Protein structure of WNK kinases**

WNKs are big proteins of 2382 amino-acids (251 KDa), 2217 amino-acids (243 KDa), 1743 amino-acids (192 KDa) and 1243 amino-acids (135 KDa) for WNK1, 2, 3 and 4, respectively (Figure 10) [194]. They are unique among protein kinases because the lysine required for ATP-binding lies in the phosphate anchor ribbon (kinase subdomain I) instead of in  $\beta$  strand 3 (kinase subdomain II), its position in all other members of the protein kinase superfamily. All four WNK proteins contain a kinase domain, an autoinhibitory domain (AID), autophosphorylation sites, coiled-coil domains (CCDs) and proline-rich domains (PRDs) (Figure 10) [192]. More specifically, WNK1 contains, in addition to the N-terminal kinase domain and the adjacent auto-inhibitory domain, three potential coiled-coil domains and four proline-rich regions with PXXP motifs, a glutamine-rich region (residues 571-812), two serine-rich regions (residues 1404-1562, 2027-2065) as well as a potential bipartite nuclear localization signal located between residues 567 and 584 that overlaps the second coiled-coil region [190].

The four WNK proteins share high homology within their kinase domains (> 85% homology) and the adjacent auto-inhibitory domain (> 46%) but present low similarity in other regions. WNKs' activation requires phosphorylation of at least one serine residue within the WNK kinase domain. This serine has been identified as S382, S356, S308, and S322 of WNK1, WNK2, WNK3 and WNK4, respectively. Phosphorylation of WNK1 S378, also localized in the catalytic domain, is dispensable to enhance activity [189]. WNK catalytic activity is also regulated by the conserved auto-inhibitory domain [192]. The activation loop sequences of WNK1 and WNK4 are identical [195]. Coiled-coil domains play a major role in protein-protein interactions. Proline-rich domains (PRDs) provide putative binding sites for

proteins. Protein domains that bind PRDs are mostly involved in the modulation of cell signaling. Typically, SH3 (Src homology domain 3) domains, present in more than 300 human proteins, bind canonical PRDs, including PXXP motifs in target proteins. All WNK family members contain putative SH3-binding motifs [192].

Another important residue in WNK1 is Threonine 60 (T60) at the N-terminus of the protein. T60 lies in an Arg-Arg-Arg-Arg-His-Thr-Met sequence which is a potential AGC kinase phosphorylation motif. This sequence is conserved in all characterized mammalian WNK1 isoforms. However, among human WNK isoforms, only WNK4 has a serine residue (S47) in its N-terminus lying in an AGC kinase (including protein kinase PKA, PKC and PKG) putative phosphorylation site [196]. An additional serine residue lying in an AGC kinase consensus motif (S1169), corresponding to serine 1261 (S1261) in WNK1, is present in WNK4 (Figure 10) [192][197].

Other serine and/or threonine WNK1 residues (S15, S167, S1261, T1848, S2372) were shown to be phosphorylated following stimulation and 3 constitutively C-terminal WNK1 phosphorylated residues (S2012, S2019, S2032) were described [192].

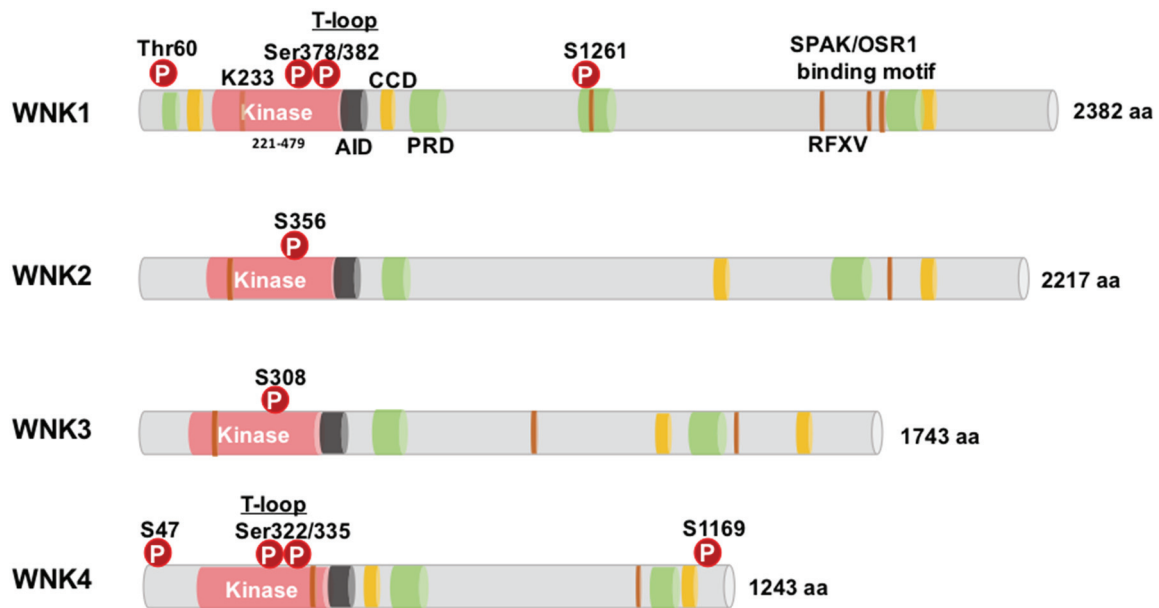


**Figure 10. Protein structure of WNKs.** The human WNK protein family is composed of 4 proteins encoded by distinct genes: WNK1 (2382 amino-acids (aa)), WNK2 (2217 aa), WNK3 (1743 aa) and WNK4 (1243 aa). Human WNK serine/threonine kinases share a N-terminal catalytic domain and an adjacent autoinhibitory domain (AID). The catalytic activity of WNKs is conditioned by phosphorylation of serine residues within the kinase domain (S382 in WNK1) and the presence of a catalytic lysine (WNK1 K233). Phosphorylation of WNK1 S378 enhances the catalytic activity of WNK1. Phosphorylation of threonine 60 (T60) lying in an AGC kinase phosphorylation motif in the N-terminus of WNK1 was proposed to modulate interactions of WNK1 with other protein partners and may be independent from the catalytic activity of the enzyme. An equivalent N-terminal serine residue lying in an AGC kinase phosphorylation motif is only present in WNK4. WNK1 S1261 and WNK4 S1169 also lie in phosphorylation motifs for AGC-family kinases. WNK proteins also contain several putative coiled-coil domains (CCDs) as well as proline rich motifs (PRDs) involved in protein-protein interactions. Protein kinases SPAK and OSR1 are downstream targets of WNK proteins in many cell systems. RFXV motifs corresponding to SPAK/OSR1 binding sites are also indicated.

### 1.3.1.3 Tissue expression pattern of WNK kinases

The full-length isoform of WNK1 is ubiquitously expressed, with particularly high levels in the testis, heart, kidney and skeletal muscle. WNK1 is also expressed in the brain, the spinal cord, the cerebellum, in dorsal root ganglia, the aorta and the lung and very weak levels are present in the liver. Conversely, expression of the shorter KS-WNK1 isoform is restricted to the kidney [193]. The highest expression for WNK2 is observed in heart, brain and colon whereas only low levels of WNK3 are present in brain. WNK3 is also expressed in lung, kidney, liver, and pancreas and in fetal tissues including placenta, fetal brain, lung and kidney. WNK4 is

enriched in several tissues including kidney, pancreas, bile duct, colon, brain (blood-brain barrier), epididymis and skin [192].

#### **1.3.1.4 Subcellular localization of WNK proteins**

The subcellular localization of overexpressed WNK1 was first studied by Xu and colleagues in HEK 293 cells. In their study they showed that the majority of WNK1 is excluded from the nucleus and that it is a cytoplasmic protein not restricted to the plasma membrane [189]. Subsequent studies in other systems revealed the presence of endogenous WNK1 in the cell cytoplasm in most cases. For example, punctate cytoplasmic staining was observed for endogenous WNK1 in HeLa cells and in breast and colon cancer cell lines. Additional nuclear punctate staining was also observed in these cells. In the INS-1 pancreatic cell line, WNK1 was rather associated to vesicular as well as lateral membranes. In HEK 293 cells subjected to hypertonic stress, WNK1 relocalized from the cytoplasm to vesicles budding from the Golgi. Finally, available data suggest that the localization of WNK1 does not depend on its phosphorylation status [192][198]. WNK2 protein was shown to localize both in the cytoplasmic and membrane compartments whereas WNK3 has a diffuse distribution in HeLa cells and moved to the nucleus upon cell apoptotic death. Finally, WNK4 may localize in lateral membranes and cytoplasm and is redistributed from the cytoplasm to membrane compartments upon hypertonic stress [192].

#### **1.3.1.5 Stimuli and mechanisms of WNK activation**

Kinase activity is required for numerous function of WNKs. There are two major mechanisms by which WNK kinase activity is regulated. One of them is through autophosphorylation of residues in the activation loop of their catalytic domain, namely, S382 and S378 for WNK1 or equivalent residues in other WNK family members (Figure 10). In addition to autophosphorylation, these serine residues may also be the substrates of other WNK family members [195]. As already mentioned in one of the previous sections, phosphorylation of S382 is required for catalytic activity whereas phosphorylation of S378 only facilitates activation. The other mechanism regulating WNK protein catalytic activity is by the presence of the auto-inhibitory domain that lies immediately after the C-terminal part of the catalytic domain. This domain suppresses kinase activity until an activating signal displaces

it from its inhibitory site. The activating signal(s) that release this autoinhibition are currently unknown [199]. In addition to autoinhibition, WNK kinases can inhibit the kinase activity of other members in this family. For example, *in vitro* studies demonstrated that WNK1 autoinhibitory domain is able to inhibit the catalytic activity of WNK2 and 4, suggesting interactions between these proteins [195]. Such interactions were shown to involve the coiled-coil domains of WNKs [192].

Despite the high homology between WNK protein catalytic domains, substrate specificities have been described. These are thought to involve two residues within a substrate binding groove in the catalytic domain of these kinases. In WNK1, these residues correspond to V318 and A448 [192].

A major physiological regulator of WNK proteins' catalytic activity is tonicity. Hypertonic and hypotonic stress increase WNK1 phosphorylation on S382 and catalytic activity in HEK 293 cells and in colon and breast cancer cell lines [195]. Like WNK1 and WNK4, WNK2 exhibited enhanced autophosphorylation and protein kinase activity in cells exposed to hypertonic conditions [200].

The catalytic activity of WNKs may be associated to other WNK protein functions. Alternatively, some WNK functions are independent from substrate phosphorylation by these proteins. Through their proline-rich domains, their coiled-coil domains or other protein binding sites, WNKs function as scaffolds for protein complex formation by multiple intra- and/or intermolecular interactions [201][202]. Such interactions were observed between WNKs and proteins involved in exocytosis or endocytosis such as synaptotagmins, intersectin or Munc18c, in transcriptional regulation such as Smad2 or in ion channel activity such as protein kinases SPAK (STE20/SPS1-related proline alanine rich kinase), OSR1 (oxidative stress response kinase-1) and SGK1 (serum and glucocorticoid-regulated protein kinase 1) [203]. For example, RFXV/I (Arg-Phe-Xaa-Val/Ile) motifs in WNKs, namely WNK1, 3 and 4, interact with a unique 92 amino acid conserved C-terminal domain in SPAK/OSR1. This leads to regulation of SPAK-OSR1 activity through WNK kinase-dependent or independent mechanisms [204].

Kinase activity-independent functions, namely of WNK1, were also associated to the phosphorylation status of its T60 residue in the N-terminal part of this protein. Sequence analysis revealed that this residue lies in a putative Akt1/SGK

phosphorylation site. Insulin and insulin-like growth factor 1 (IGF-1) were shown to regulate WNK1 T60 phosphorylation through the activation of PI3K, which subsequently phosphorylates PIP2 to generate PIP3. The latter then acts as an activator for PDK1 (phosphoinositide-dependent kinase 1), which activates members of the AGC family of kinases, including Akt1 and SGK1 [192]. *In vitro* studies in HEK 293 cells showed that Akt strongly phosphorylates WNK1 at T60. This phosphorylation event is inhibited by PI3K inhibitors. SGK1 was also shown to be able to modify the phosphorylation status of T60 in WNK1 [205][206]. The WNK4 S1169 (in a consensus Akt/SGK1 phosphorylation motif) and S1196 residues, are also substrates of SGK1 [192][197].

Finally, CUL3 (cullin 3) and KLHL3 (kelch-like family member 3) proteins were identified as upstream regulators of WNKs. These proteins target WNKs for degradation by the proteasome. KLHL3, an adaptor protein, brings the WNKs to CUL3 which is part of an E3 ubiquitin ligase and thus promotes the ubiquitination of WNKs [207].

### **1.3.2 WNK functions**

#### **1.3.2.1 Fluid and electrolyte homeostasis**

The most prominent and best understood role of WNK proteins is the regulation of Na<sup>+</sup>, K<sup>+</sup>, Cl<sup>-</sup>, HCO<sub>3</sub><sup>-</sup> and Ca<sup>2+</sup> trafficking and transporting in epithelia. WNKs regulate ion transporters or ion channels either by modulating their expression at the plasma membrane and/or their activity. For example, WNK1, WNK3 and WNK4 modulate the levels of the inward Na<sup>+</sup>/Cl<sup>-</sup> cotransporter NCC at the plasma membrane. WNK4 reduces surface expression of NCC, in a kinase-activity dependent manner, through promoting its accumulation in the lysosomes and inhibition of its trafficking to the plasma membrane. WNK4 inhibition of NCC expression involves the ERK1/2 signaling pathway [202][208]. WNK3 and WNK4 showed an opposite effect on NCC activity requiring the catalytic activity as well as the amino-terminal domain of WNK3 [209]. WNK1 is able to suppress the inhibitory effect of WNK4 on NCC expression independently of its catalytic activity but rather through interaction between the two proteins [210]. Activated WNK1 was also shown to interact with and phosphorylate serine and/or threonine residues in two



WNK1 substrates which are themselves protein kinases, SPAK and OSR1 (SPAK Thr233 and Ser373 and OSR1 Thr185 and Ser325). These phosphorylation events lead to SPAK/OSR1 kinase activity stimulation, NCC phosphorylation and increase in co-transporter activity. Thus, WNK1 is also able to regulate directly NCC activity without affecting its expression levels in a kinase-activity dependent manner [192]. Given the effects of WNK4 and WNK1 on NCC function (inhibition and stimulation, respectively), it was proposed that hypertension observed in PHAII patients caused either by WNK4 inactivating mutations or by WNK1 overexpression, might be attributed, at least in part, to increased function of this cotransporter.

Increased function of the epithelial sodium channel ENaC was also proposed to be one of the factors underlying hypertension in PHAII patients. Wild-type WNK4 was shown to inhibit the activity of this channel whereas WNK1 was reported to increase ENaC activity *via* a mechanism involving PI3K, SGK1 and increased surface expression of this protein. This WNK1 function required the N-terminal domain of WNK1 but not its catalytic action. WNK4 acted on ENaC activity through a similar mechanism [211][212].

Another feature of PHAII is hyperkalemia. Renal outer medullar potassium 1 (ROMK1) channel expression is inhibited by both WNK1 and WNK4 through stimulation of its intersectin-dependent endocytosis [213][214]. In HEK 293 cells, insulin and IGF1 stimulation resulted in Akt and SGK1 activation, subsequent phosphorylation of WNK1 T60 by both kinases, and ROMK1 endocytosis. Conversely to the kinase activity of WNK1, phosphorylation of T60 was required for the effect on ROMK1 function [206].

Na<sup>+</sup>/K<sup>+</sup>/2Cl<sup>-</sup> cotransporters NKCC1/2 and K<sup>+</sup>/Cl<sup>-</sup> cotransporters of the KCC family may also be regulated by WNK proteins through phosphorylation of SPAK/OSR1 which does not influence the surface expression of these cotransporters [192][202][215]. Intracellular concentrations of chloride anions, modulated by the activity of NKCC and KCC cotransporters are necessary for cell volume control and transport across epithelia.

Another group of transporters regulated by the WNKs are the Cl<sup>-</sup> and/or HCO<sub>3</sub><sup>-</sup> transporters NBCe1-B [216], SLC26A3, SLC26A6, SLC26A9 and chloride channel CFTR (cystic fibrosis transmembrane conductance regulator). The WNKs

inhibit surface expression of NBCe1-B, SLC26A9 and CFTR and activity of all these transporters in a kinase activity-independent manner [202].

There are five  $\text{Na}^+$ -coupled  $\text{HCO}_3^-$  transporters (NBCs) (NBCe1, NBCe2, NBCn1, NBCn2 ( $\text{Na}^+/\text{HCO}_3^-$  cotransporters) and NDCBE ( $\text{Na}^+$ -driven  $\text{Cl}^-/\text{HCO}_3^-$  exchanger)) in the SLC4 protein family. NBCe1 and NBCe2 are  $\text{Na}^+$ -coupled electrogenic transporters while NBCn1, NBCn2 and NDCBE are electroneutral. NBCe1 moves one  $\text{Na}^+$  and two  $\text{HCO}_3^-$  ions into the cell, causing the increase in intracellular  $\text{Na}^+$  and pH ( $\text{pHi}$ ) [217]. Shift to a  $\text{Na}^+:\text{HCO}_3^-$  stoichiometry of 1:3 or acidic extracellular pH is able to reverse the gradient of transport resulting in  $\text{HCO}_3^-$  export with opposite effects on intracellular and extracellular pH ( $\text{pHe}$ ) regulation [218][219]. NBCs play important roles in acid-base homeostasis as well as in the regulation of cell volume and intracellular pH.

As we mentioned, NBCe1 function is inhibited by WNK1 acting as a scaffold to recruit SPAK to the N-terminus of NBCe1. SPAK subsequently phosphorylates NBCe1, thus reducing its cell surface expression and activity. This inhibitory WNK/SPAK pathway-mediated effect on NBCe1 can be reversed by IRBIT (inositol 1,4,5-triphosphate (IP3) receptor-binding protein released with IP3). IRBIT inhibits WNK/SPAK by recruiting PP1 (protein phosphatase 1) to the SPAK/NBCe1 complex thus leading to NBCe1 dephosphorylation and increased cell surface expression and activity [216][220].

### **1.3.2.2 Cell proliferation, migration and survival**

It is well known that MAPK pathways are evolutionarily conserved kinase modules, comprising several cascades such as the ERK, JNK and p38 pathways, that control fundamental cellular processes including cell growth, proliferation, differentiation, migration and apoptosis. Among mammalian MAPK pathways, the ERK pathway is well studied for its role in cell proliferation, and deregulation of this pathway is of particular relevance to cancer [221]. WNK proteins were involved in cell proliferation regulation in part through regulation of MAPK signaling pathways. In HEK 293, HeLa cells and neural progenitors, WNK1 was shown to positively regulate cell proliferation following EGF stimulation of ERK5 *via* MEKK2/3 without

affecting the activation of ERK1/2, JNK or p38 MAPK kinases. In neural progenitors, inhibition of WNK1 resulted in reduction of both EGF-related proliferation and migration of these cells [222][223]. WNK4 has been reported to have a positive effect on ERK1/2 and p38 phosphorylation in response to EGF stimulation of HEK 293 cells [224]. Conversely to WNK1 which stimulates cell proliferation in an ERK5-dependent manner, WNK2 has been shown to negatively modulate growth factor-induced cell growth through inhibition of the MEK1/ERK1/2 pathway [225]. In agreement with this observation, downregulation of WNK2 expression, through aberrant methylation over the entire CpG island region of the *WNK2* gene, was observed in human gliomas including GBM [200].

As mentioned before, in various systems, WNK1 regulates and/or is regulated by protein kinases such as Akt, SPAK/OSR1 and SGK1, which are mostly investigated for their roles in cell volume sensing and osmotic homeostasis which may be linked to cell cycle progression. SPAK is also a known activator of the p38 and JNK cascades and OSR1 acts upstream of CaMKII (calcium/calmodulin-dependent protein kinase type II) and p38. However, the molecular details of how the phosphorylation of SPAK/OSR1 by WNK1 relates to cell proliferation have not yet been investigated [194].

Conversely to its positive role on cell proliferation by activating ERK5, WNK1 was shown to negatively regulate this process in insulin treated 3T3-L1 adipocytes. This WNK1 function involves T60 phosphorylation of WNK1 by Akt [226].

Additionally, *via* their N-terminus, WNKs, interact with and regulate SGK1 in a kinase activity-independent manner [227][228]. WNK1 was proposed to regulate cell cycle progression through SGK1. SGK1 is known to regulate degradation of the cyclin-dependent kinase inhibitor protein P27, which acts in G0 and early G1 to inhibit E-Cdk2 and impairs TGF- $\beta$ -mediated cell cycle arrest [229]. Moreover, TGF- $\beta$  initiates growth arrest by assembling receptor complexes that activate Smad transcription factors [194]. WNK1 is able to interact with, phosphorylate and inhibit Smad2, suggesting it imposes an inhibitory effect on TGF- $\beta$  signaling.

Moreover, in HeLa cells, WNK1 was shown to re-localize to mitotic spindles where it colocalized with tubulin during cell division. Depletion of WNK1 resulted in

defects in mitotic spindles, chromosome segregation and abscission, suggesting a role of this kinase in several steps of the mitotic process [198].

In addition to cell proliferation, WNK proteins were also involved in cell survival and evasion from apoptosis. WNK3 was shown to promote cell survival by recruiting Hsp70 (Heat-shock protein 70) to procaspase-3 and inhibiting its activation [230]. Depletion of WNK1 and WNK3 was reported to increase apoptosis in HeLa cells and a protective role of *C. elegans* WNK was proposed in cells challenged by hyperosmotic stress. Finally, WNKs were linked to proteins, including Rho GTPases, which are well known actors of actin cytoskeleton dynamics control and cell migration [194].

#### **1.3.2.3 Vesicular trafficking**

In insulin-secreting pancreatic INS-1 cells, WNK1 was shown to colocalize on secretory vesicles with synaptotagmin 2, a calcium binding protein well known for its function in calcium-regulated exocytosis. Moreover, WNK1 was able to phosphorylate synaptotagmin 2 and modify its calcium sensing properties and subsequent interactions [231]. In addition, WNK1 was shown to interact with Munc-18, in a catalytic activity independent manner, and regulate SNARE complex assembly and exocytosis of insulin containing vesicles in pancreatic cells [232]. Finally, WNK1 and WNK4 were shown to stimulate clathrin-dependent endocytosis of the ROMK1 potassium channel through interactions with the endocytic scaffold protein intersectin [213].

#### **1.3.2.4 Other WNK functions**

Recently, WNK kinases were reported to play a role in canonical Wnt-signaling [233]. WNK1 was also reported to be essential for embryonic development since WNK1-knockout embryos fail to develop [234]. Moreover, WNK1 was newly identified as a regulator of PLC- $\beta$  signaling in cells by promoting the synthesis of PIP2 *via* stimulation of phosphatidylinositol 4-kinase III $\alpha$ . WNK1 kinase activity is not required. IGFs potentiate this process *via* PI3K activation, which recruits and activates Akt that phosphorylates WNK1 at Thr60 [235]. Thus, in this way, WNK1 coordinates signaling between G protein coupled receptors and Akt kinase pathways [235]. Finally, autophagy, a catabolic process involving lysosomal-

mediated degradation and recycling of damaged proteins and organelles, is inhibited by WNK1 [236]. WNK1 protein functions are summarized in Figure 11.

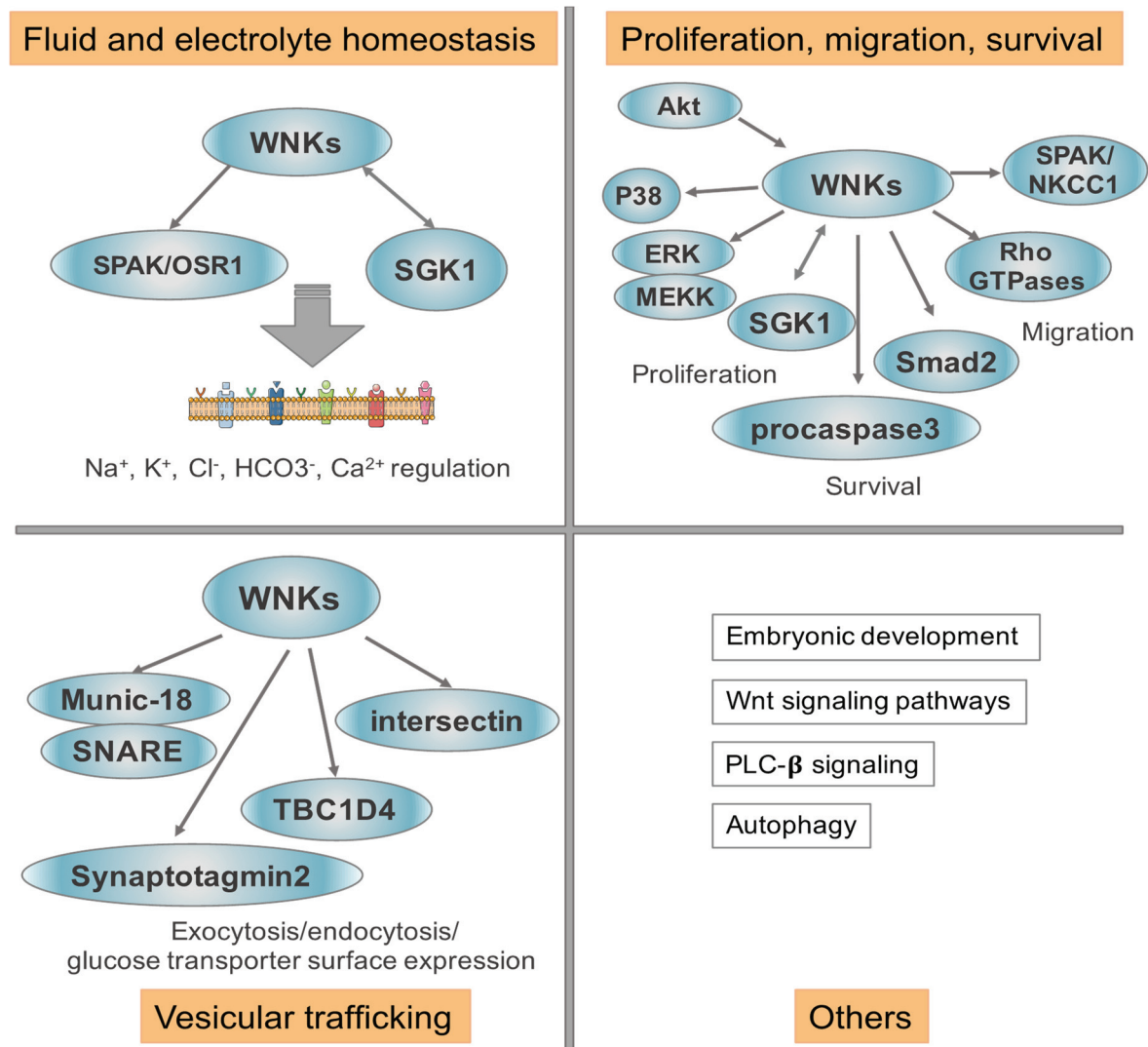


**Figure 11. Roles of WNKs and core signaling pathways involved.** Through their ability to regulate ion channel and co-transporter function, either directly or via SPAK/OSR1 or SGK1 kinases, WNK proteins are major players in fluid and electrolyte homeostasis. WNKs were also shown to positively or negatively regulate cell proliferation by participating in Akt, ERK/MAPK, p38, SGK1 and Smad2-related pathways. A role of WNKs in cell migration through SPAK/NKCC1 co-transporter or small GTPase protein regulation was also described. Several WNK proteins were involved in cell survival namely in cell stress conditions. A role of WNKs in vesicular trafficking (exocytosis, endocytosis, glucose transporter-containing vesicle traffic to the plasma membrane) was also proposed based on the ability of these proteins to interact with and regulate the function of many proteins involved in these processes including synaptotagmin 2, Munc-18 regulating the assembly of the SNARE complex and the Rab GTPase activating protein TBC1D4. Additional WNK functions include a role in embryonic development, in Wnt and PLC-β signaling and a recently described implication in autophagy.

### 1.3.3 WNK kinases in cancer - Focus on WNK1

In the last few years, the advances of sequencing technologies provided the possibility to systematically sequence cancer genomes. Several point mutations in the *WNK1* gene were identified in breast, ovary, colon, lung, and brain cancer (Table 4). For now, there is no evidence showing a functional impact of these mutations in tumors and these somatic mutations in the *WNK1* gene were not considered as tumor-initiating mutations. However, they may have other effects during tumor growth and survival, in view of the multiple functions of WNK1 [194]. Indeed, as mentioned in previous sections, WNK1 was involved in cell proliferation and survival as well as in cell migration and inhibition of TGF- $\beta$ /Smad signaling involved in EMT. Deregulation of these processes may underlie the effects of WNK1 mutations in cancer. Moreover, electrolyte homeostasis is also important for cells to maintain their proliferation and survival. As we have discussed before, WNK1 exhibits critical functions in the regulation of Na<sup>+</sup>, K<sup>+</sup>, H<sup>+</sup>, Cl<sup>-</sup>, HCO<sub>3</sub><sup>-</sup> and Ca<sup>2+</sup> concentrations in many cell systems.

**Table 4 WNK1 mutations identified in tumors**

Tissue	Histology/type	zygosity	cDNA	mutation
Breast	Pleomorphic lobular carcinoma (PLC)	heterozygote	c.1255G>C	Missense
Breast	Invasive ductal carcinoma (IDC)	heterozygote	c.5395C>G	Missense
Breast	PLC	heterozygote	c.6569C>G	Missense
Ovary	Serous carcinoma	heterozygote	c.2829C>T	silent
Colon	Colorectal	heterozygote	c.3596A>G	Missense
Brain	Glioblastoma	heterozygote	c.5293G>A	Missense
Lung	Adenocarcinoma	heterozygote	c.7086C>A	Missense

**Table 4. WNK1 mutations identified in tumors, adapted from [194].**

Through its functions, WNK1 may also be involved in the adaptation of cancer cells to the conditions of their microenvironment and/or to their specific requirements linked to high proliferative activity. One of the characteristics of cancer cells is upregulated glycolysis even in aerobic conditions, for which elevated expression of GLUTs (glucose transporters) has been described in many types of tumors, including in GBM. WNK1 was shown to promote GLUT1 surface expression in HEK 293 cells [237]. In addition, a role in GLUT4 translocation by recruiting the syntaxin 4-inhibitory protein Munc18c was proposed for WNK1 in other systems [232]. The direct interaction of WNK1 with synaptotagmin 2, which is a substrate of WNK1 implicated in vesicle fusion in neuronal cells, provides alternative putative mechanisms to explain how WNK1 might regulate glucose transporter availability at the plasma membrane [231].

Increased production of glycolytic metabolites such as lactic acid and protons in cancer cells creates a low intracellular pH which is not a favorable environment to cells. To cope with this, cancer cells increase, among others, the expression of the  $\text{Na}^+/\text{H}^+$  exchanger NHE1, driving the extrusion of protons into the extracellular compartment. To avoid excessive acidification of extracellular compartments, an important supporting activity in pH regulation by NHE can be provided by the chloride/bicarbonate ( $\text{Cl}^-/\text{HCO}_3^-$ ) anion exchangers of the SLC26A family which are able to export  $\text{HCO}_3^-$  from intracellular compartments. The combined activities of NHE and SLC26A lead to electroneutral NaCl absorption with net  $\text{H}^+$  secretion, resulting in a slightly alkaline intracellular pH and a slightly acidic extracellular pH [194].  $\text{Na}^+/\text{HCO}_3^-$  transporters may also participate to intracellular pH alcalinization by driving bicarbonate entry into the cells [217]. It was shown that WNKs regulate the expression of SLC26A family members such as SLC26A3, SLC26A6, SLC26A9, as well as of the  $\text{Na}^+/\text{HCO}_3^-$  co-transporter NBCe1 [202].

#### **1.3.3.1 WNK kinases in glioma**

Conversely to WNK2 which acts as a tumor suppressor in glioma, WNK1 and 3 were shown to be favorable factors to progression of these tumors. In GBM cell lines and cells derived from patients proposed to possess stem-like properties, WNK3 was involved in cell migration and invasion through modulation of the activity

of the NKCC1 protein involved both in cell volume regulation and interactions of plasma membrane components to the cytoskeleton [238][239][240]. Two studies link WNK1 to glioblastoma. The first one is on the effect of TMZ on apoptotic death of primary GBM cells and GBM cells with stem-like properties. In these cells, NKCC1 was shown to play an essential role in the maintenance of K<sup>+</sup> and Cl<sup>-</sup> levels and volume homeostasis to restrain the TMZ-induced loss of these ions and cell volume reduction. This resulted in a resistant phenotype to TMZ-induced apoptosis. Blocking NKCC1 activity sensitized glioma cells to TMZ. NKCC1 activity in primary GBM cells was associated to its phosphorylation which is mediated by WNK1 [241]. The second study reported results indicating that WNK1-OSR1 mediate phosphorylation and activation of the NKCC1 ion cotransporter to facilitate glioma cell migration. Surprisingly, TMZ treatment was shown to activate the WNK1/OSR1/NKCC1 signaling pathway and to enhance glioma cell migration. Inhibiting NKCC1 or siRNA knockdown of WNK1 or OSR1, significantly decreased this effect of TMZ on GBM cells [242].



## II. Results

### Part I. Phenotypic and functional characterization of proliferating and quiescent glioblastoma stem-like cells and identification of bisacodyl

As mentioned in the introduction section, cancer stem-like cells including the ones isolated from human glioblastoma (GSCs) are believed to be major players of therapy resistance, namely because of their ability to reside within tumors *in vivo* in a quiescent slow-growing state preserving them from anti-proliferating cell-targeting chemotherapies.

Our project is based on a collaboration with the team of Dr. Hervé Chneiweiss in Paris (Neuroscience Paris Seine - IBPS, CNRS UMR 8246/ Inserm U1130/ UPMC UMCR18) who has isolated GSCs from biopsy tissues from different glioblastoma patients (Sainte Anne Hospital, Paris, France). Malignant tissue samples were dissociated and cells were selected and cultured in serum-free medium (containing bFGF and EGF). Under such conditions, GSCs expand as neurospheres (Figure 12). Proliferating GSCs were phenotypically and functionally characterized for stem-cell marker expression, clonality, multilineage differentiation and *in vivo* tumor initiation/propagation ability [119]. The *in vitro* proliferating GSC cell model and generation of master and working cell banks, was successfully transposed in our lab with respect to the standardized cell culture conditions and phenotypic and functional characterization of the cells.

Given the importance of the quiescent state in therapeutic resistance, we set up *in vitro* culture conditions to obtain quiescent slow-growing GSCs. Such cells are obtained from proliferating GSCs after 9-16 days without medium renewal (Figure 12).

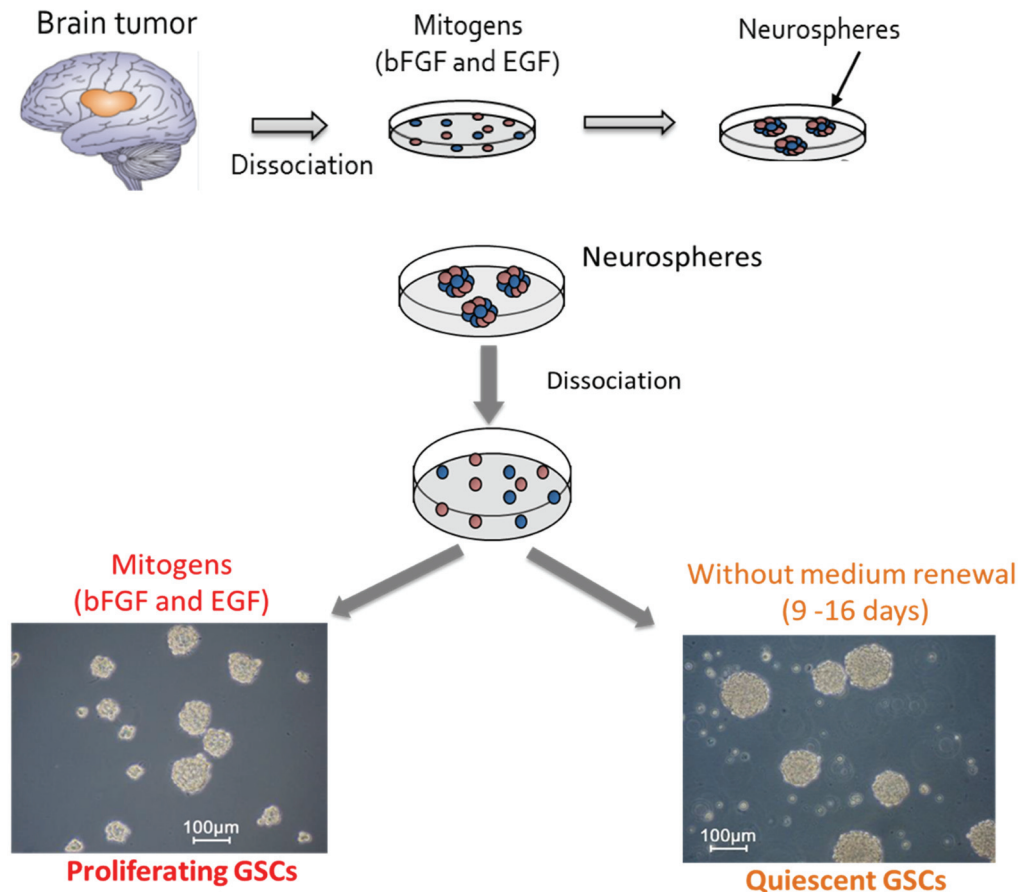


**Figure 12. Isolation and *in vitro* culture of proliferating and quiescent glioblastoma stem-like cells (GSCs) from patients.** Cells from glioblastoma tumors are dissociated and put in culture in serum-free medium containing EGF (epidermal growth factor) and bFGF (basic fibroblast growth factor). Under these conditions, only cancer cells with stem-like properties including long-term proliferation and self-renewal ability are able to survive in the long term and expand as neurospheres. Quiescent slow-growing GSCs are obtained from their proliferating counterparts in the absence of medium renewal for 9-16 days.

Quiescent slow-growing GSCs obtained in these conditions do no longer incorporate EdU (5-Ethyl-2'-deoxyuridine) and express very low levels of the Ki67 proliferation marker. Moreover, the quiescent state may be reversed by addition of proliferating cell culture medium. We also showed that growth factor deprivation does not result in an increase in the expression of pro-apoptotic markers and does not induce a senescent state (absence of  $\beta$ -galactosidase activity). Finally, quiescent GSCs maintained cancer stem-like cell properties of their proliferating counterparts: stem cell marker expression, cell surface marker expression, clonality and ability to differentiate when re-introduced in proliferating cell culture conditions

as well as engraftment capacity *in vivo* (Figure 13). I participated to this characterization by performing some of the clonality tests and by studying stem cell/cell surface marker expression as well as the differentiation ability of these cells. The entire characterization of quiescent GSCs is described in a publication that I co-authored and which is included in the manuscript (Publication 1) [138].

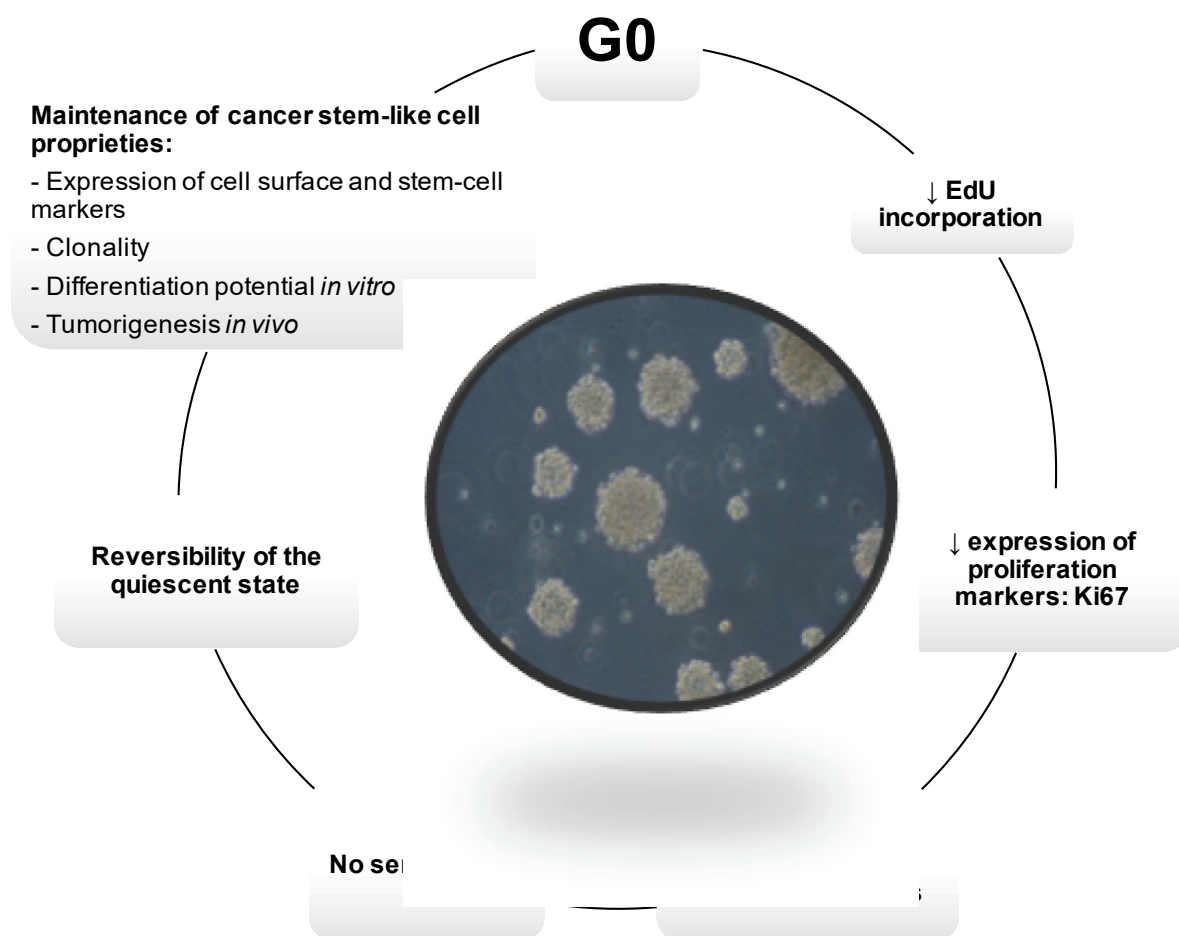


**Figure 13. Characterization of quiescent glioblastoma stem-like cells (GSCs).** Quiescent GSCs obtained in the absence of medium renewal for 9 days do not incorporate EdU (5-ethyl-2'-deoxyuridine). These cells express very low levels of proliferation markers such as Ki67. Growth factor deprivation does not underlie high expression of pro-apoptotic markers nor a senescent state. Moreover, the quiescent state obtained under these conditions is reversible. Finally, cancer stem-like phenotypic and functional properties are maintained in quiescent GSCs.

With the aim to find small molecules targeting GSCs, a high-throughput differential screening of the Prestwick chemical library, which consists of more than

1200 small molecules most of which are FDA-approved drugs, was performed on proliferating and quiescent GSCs from patients. The laxative drug bisacodyl (4,4'-diacetoxydiphenyl-2-pyridyl-methane) and its active metabolite DDPM (4,4'-dihydroxydiphenyl-2-pyridyl-methane) were identified as compounds exhibiting a selective cytotoxic effect towards quiescent GSCs with an EC<sub>50</sub> (half maximum effective concentration) of ~ 1 μM (Figure 14) and not showing cytotoxicity towards control cells including human primary astrocytes (HA cells) and non-cancerous human fetal neural stem cells (f-NSCs). A structure to function relationship (SAR) study on bisacodyl/DDPM allowed the identification of the minimal pharmacophoric pattern of the compound. Corresponding data are presented in Zeniou et al., 2015 (Publication 1) [138].

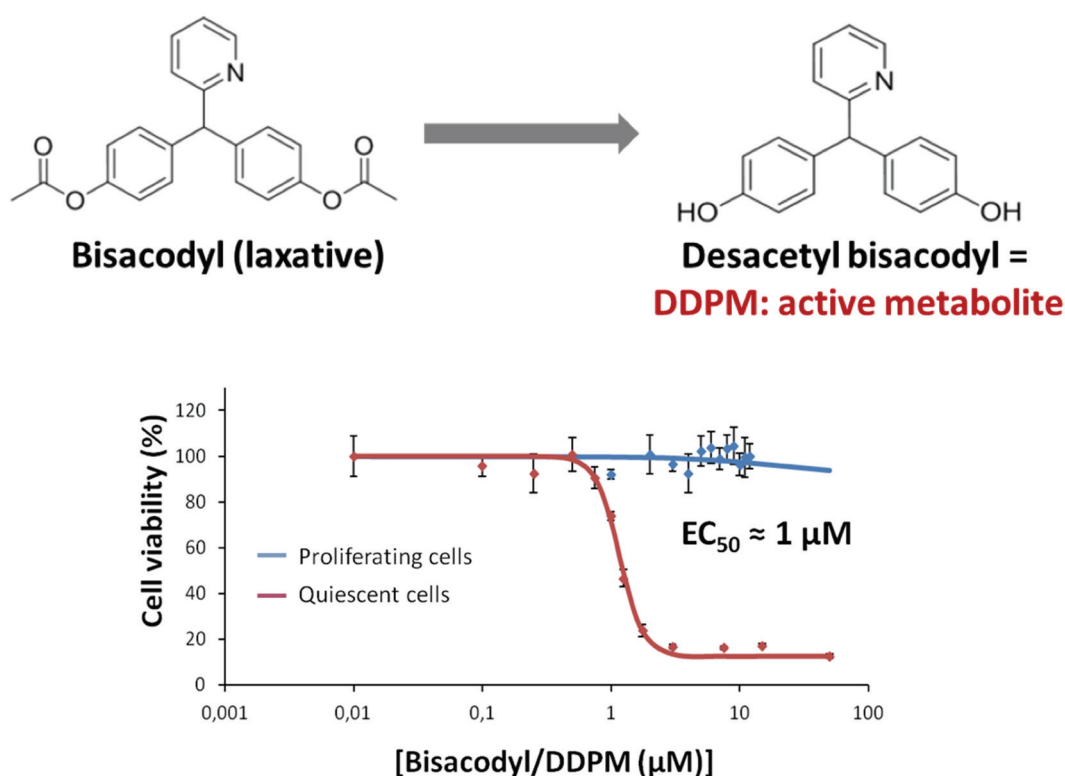


**Figure 14. Chemical structures of bisacodyl and DDPM and activity profiles towards proliferating and quiescent glioblastoma stem-like cells (GSCs).** Chemical structures of bisacodyl and DDPM and activity profiles towards proliferating and quiescent GSCs. The chemical structures of bisacodyl (4,4'-diacetoxydiphenyl-2-pyridyl-methane) and its active metabolite DDPM (4,4'-dihydroxydiphenyl-2-pyridyl-methane) are shown. Under the screening conditions, these compounds are cytotoxic to quiescent GSCs (EC<sub>50</sub> ~ 1 μM) but do not affect the viability of GSCs maintained in proliferating culture conditions. Cell viability was measured with the ATP-Glo cell viability assay from Promega evaluating ATP levels in wells containing cells that were treated with bisacodyl/DDPM for 24 hours.

## **Publication 1**

### **Chemical Library Screening and Structure-Function Relationship Studies Identify Bisacodyl as a Potent and Selective Cytotoxic Agent Towards Quiescent Human Glioblastoma Tumor Stem-Like Cells**

Zeniou M, Fève M, Mameri S, Dong J, Salomé C, Chen W, et al. (2015)

PLoS ONE 10(8): e0134793. doi:10.1371/journal.pone.0134793

RESEARCH ARTICLE

# Chemical Library Screening and Structure-Function Relationship Studies Identify Bisacodyl as a Potent and Selective Cytotoxic Agent Towards Quiescent Human Glioblastoma Tumor Stem-Like Cells



Maria Zeniou<sup>1</sup>\*, Marie Fève<sup>1</sup>, Samir Mameri<sup>1</sup><sup>¶</sup>, Jihu Dong<sup>1</sup>, Christophe Salomé<sup>1</sup>, Wanyin Chen<sup>1</sup>, Elias A. El-Habr<sup>2</sup>, Fanny Bousson<sup>1</sup>, Mohamadou Sy<sup>1</sup>, Julie Obszynski<sup>1</sup>, Alexandre Boh<sup>1</sup>, Pascal Villa<sup>3</sup>, Suzana Assad Kahn<sup>2</sup><sup>¶</sup>, Bruno Didier<sup>1,3</sup>, Dominique Bagnard<sup>4</sup>, Marie-Pierre Junier<sup>2</sup>, Hervé Chneiweiss<sup>2</sup>, Jacques Haiech<sup>1</sup>, Marcel Hibert<sup>1</sup><sup>‡</sup>, Marie-Claude Kilhoffer<sup>1</sup><sup>‡</sup>

**1** Laboratoire d'Innovation Thérapeutique, Université de Strasbourg / CNRS UMR7200, Laboratoire d'Excellence Medalis, Faculté de Pharmacie, 74 route du Rhin, 67401 Illkirch, France, **2** Neurosciences Paris Seine-IBPS, CNRS UMR 8246/ Inserm U1130/ UPMC UMCR18, 7 quai Saint Bernard, 75005 Paris, France, **3** Plateforme de Chimie Biologie Intégrative (PCBIS), Université de Strasbourg / CNRS UMS 3286, Laboratoire d'Excellence Medalis, ESBS Pôle API-Bld Sébastien Brant, 67401 Illkirch, France, **4** U682, Inserm, Université de Strasbourg, 3, Avenue Molière, 67200 Strasbourg, France

## OPEN ACCESS

**Citation:** Zeniou M, Fève M, Mameri S, Dong J, Salomé C, Chen W, et al. (2015) Chemical Library Screening and Structure-Function Relationship Studies Identify Bisacodyl as a Potent and Selective Cytotoxic Agent Towards Quiescent Human Glioblastoma Tumor Stem-Like Cells. PLoS ONE 10(8): e0134793. doi:10.1371/journal.pone.0134793

**Editor:** Christopher Heeschen, Spanish National Cancer Centre (CNIO), SPAIN

**Received:** September 30, 2014

**Accepted:** July 14, 2015

**Published:** August 13, 2015

**Copyright:** © 2015 Zeniou et al. This is an open access article distributed under the terms of the [Creative Commons Attribution License](https://creativecommons.org/licenses/by/4.0/), which permits unrestricted use, distribution, and reproduction in any medium, provided the original author and source are credited.

**Data Availability Statement:** All relevant data are within the paper and its Supporting Information files.

**Funding:** This work was supported by the drug research center Labex (Laboratory of Excellence) Medalis, "La Ligue contre le Cancer", the "Agence Nationale pour la Recherche (ANR)", SATT Conectus Alsace (Technology Transfer Office of the University of Strasbourg), University of Strasbourg, CNRS, the French "Ministère de l'Enseignement Supérieur et de la Recherche" and by "Région Ile de France-Cancéropôle" (EAEH fellowships). Marie Fève is

¶ These authors contributed equally to this work.

¶a Current address: Institut de Chimie, Université de Strasbourg / CNRS UMR 7177, 4 rue Blaise Pascal, 67000 Strasbourg, France

¶b Current address: Institute for Stem Cell Biology and Regenerative Medicine, Stanford University, Stanford, California, United States of America

‡ These authors also contributed equally to this work.

\* [zeniou@unistra.fr](mailto:zeniou@unistra.fr)

## Abstract

Cancer stem-like cells reside in hypoxic and slightly acidic tumor niches. Such microenvironments favor more aggressive undifferentiated phenotypes and a slow growing "quiescent state" which preserves them from chemotherapeutic agents that essentially target proliferating cells. Our objective was to identify compounds active on glioblastoma stem-like cells, including under conditions that mimic those found *in vivo* within this most severe and incurable form of brain malignancy. We screened the Prestwick Library to identify cytotoxic compounds towards glioblastoma stem-like cells, either in a proliferating state or in more slow-growing "quiescent" phenotype resulting from non-renewal of the culture medium *in vitro*. Compound effects were assessed by ATP-level determination using a cell-based assay. Twenty active molecules belonging to different pharmacological classes have thus been identified. Among those, the stimulant laxative drug bisacodyl was the sole to inhibit in a potent and specific manner the survival of quiescent glioblastoma stem-like cells. Subsequent structure-function relationship studies led to identification of 4,4'-dihydroxydiphenyl-2-pyridyl-methane (DDPM), the deacetylated form of bisacodyl, as the pharmacophore. To our knowledge, bisacodyl is currently the only known compound targeting glioblastoma

indebted to French "Ministère de l'Enseignement Supérieur et de la Recherche" for doctoral fellowship. Wanyin Chen received PhD funding from "La Ligue contre le Cancer".

**Competing Interests:** The authors have declared that no competing interests exist.

cancer stem-like cells in their quiescent, more resistant state. Due to its known non-toxicity in humans, bisacodyl appears as a new potential anti-tumor agent that may, in association with classical chemotherapeutic compounds, participate in tumor eradication.

## Introduction

Because of their location, invasiveness and resistance to standard therapies, treating malignant brain tumors is challenging. This is especially true for glioblastoma (GBM), the most common and high grade form of glioma [1, 2]. Current glioblastoma treatments combine surgery, radiotherapy and chemotherapy with temozolomide, a DNA-alkylating agent [3]. Despite multiple therapeutic approaches, median survival of glioblastoma patients rarely exceeds 2 years [4].

Glioblastomas are histopathologically heterogeneous with cells characterized by various degrees of proliferative ability, differentiation and/or invasiveness. In the past years, the cancer stem cell model was proposed to explain tumor heterogeneity [5–7]. A subpopulation of malignant cancer stem-like cells, with tumor-propagating, self-renewal and differentiation capacities, was first isolated and characterized from hematopoietic malignancies [8] and subsequently from solid tumors of the brain and other organs [6]. In addition, numerous studies support the participation of cancer stem-like cells in tumor recurrences after treatment. Glioblastoma stem-like cells (GSCs) are more resistant to radiation-induced apoptosis and survive chemotherapy through increased expression of drug transporters. Finally, impaired functioning of apoptotic pathways has been described in these cells [9].

Thus, to be effective, cancer treatments should also target cancer stem-like cells, either by killing them or by forcing them to acquire a differentiated state more sensitive to conventional treatments [5, 10]. In this context, different strategies have been used to target such cells [11–13]. So far, however, most published data aim at finding molecules targeting proliferating tumor stem-like cells despite increasing evidence arguing in favor of the existence of relatively quiescent cancer stem-like cells within the tumor bulk *in vivo* [14]. Slowly proliferating cells with stem cell properties and tumor-initiation ability were identified in several solid tumors including ovarian, liver, breast cancer and melanoma [15–18]. In addition, a slow-cycling stem cell subpopulation from pancreatic adenocarcinoma has been shown to be endowed with increased tumorigenic and invasive potential as compared with faster-cycling cells from the same tumors [19]. More importantly, the quiescent state may contribute to the resistance of cancer stem-like cells to current chemotherapeutic agents. It was shown that leukemic stem cells survive in the dormant G0 phase of the cell cycle after chemotherapy and that relapses and metastases of breast cancer often occur after long intervals, suggesting an involvement of cells in a deep dormant phase [20–22]. Moreover, several studies have reported the resistance to conventional treatments of relatively quiescent cells from ovarian, breast and pancreatic tumors [14]. Thus, there is a great need to find new drugs that target both proliferating and quiescent tumor stem-like cells.

With the aim of tracking chemical compounds with the aforementioned properties, we screened the Prestwick Library, using patient derived human GSCs. The activity of the compounds was evaluated on both proliferating cells and on cells grown under conditions favoring their quiescence. Most hit compounds were active under both conditions and showed cytotoxicity towards control cell types including human primary astrocytes (HA cells) and non-cancer human fetal neural stem cells (f-NSCs). Interestingly, one drug, bisacodyl, showed high specificity towards quiescent GSCs. Subsequent structure-function relationship studies identified



4,4'-dihydroxydiphenyl-2-pyridyl-methane (DDPM), the metabolite of bisacodyl as the minimal pharmacophore carrying activity. Because of its specific activity profile, bisacodyl appears as a potential chemotherapeutic agent, able to target the particularly resistant quiescent cancer stem-like cells present within human tumors, that may be used as adjuvant in a multi-therapy approach.

## Materials and Methods

### Materials

Bisacodyl (4,4'-diacetoxydiphenyl-2-pyridyl-methane; CAS number: 603-50-9) and DDPM (4,4'-dihydroxydiphenyl-2-pyridyl-methane; CAS number: 603-41-8) also called BHPM (bis-(p-hydroxyphenyl)-pyridyl-2-methane) were purchased from Sigma-Aldrich.

### Ethics statement

The biomedical research was conducted according to the declaration of Helsinki, to the French laws and was approved by the institutional review board of Sainte Anne Hospital, Paris, France. Patients have given written informed consent. Isolation and characterization of neural stem cells from human fetal brain at embryonic day 50–55 (Carnegie stage 19–22) were performed under ethical approval from the University Paris-Descartes internal review board using tissue donated with written informed consent after elective termination of pregnancy.

### Cell culture

Glioblastoma (WHO grade IV glioma) stem-like cells (TG1, TG16 and OB1 GSCs) were derived from tumor samples of 3 patients (Sainte Anne Hospital, Paris, France), as previously described [23], and expanded as neurosphere cultures. In proliferating cultures, neurospheres were mechanically dissociated in single-cell suspensions twice a week. Quiescent cells were obtained by non-renewal of the medium for 9–16 days following cell seeding. Experimental procedures used to phenotypically and functionally characterize proliferating and quiescent GSCs are described in the phenotypic and functional characterization section of Materials and Methods.

Primary human astrocytes (HA cells) were expanded in AM Medium (from ScienCell Research Laboratories, Carlsbad California) according to the manufacturer's instructions.

Human embryonic kidney 293 cells (HEK 293 cells) were expanded in minimum essential medium with 2 mM L-glutamine, 100 IU/mL–100 µg/mL penicillin-streptomycin and 10% FBS.

Human fetal neural stem cells (f-NSCs) were isolated and cultured as previously described [24].

Human brain tumor cells U-87 MG (American Type Culture Collection, ATCC) were expanded in ATCC complete growth medium according to the manufacturer's instructions.

Master and working cell banks were established for all cell types. Cells were used at defined ranges of cell passages. Additional information concerning cell source, handling and resource sharing information is provided in [S1 Table](#).

### Phenotypic and functional characterization of GSCs

**Measurements of cell cycle, cell proliferative activity and cell viability.** DNA synthesis activity of TG1 and OB1 GSCs at different conditions (1–16 days without medium renewal, 9 days without medium renewal followed by medium change at day 9 and day 13) was assessed with the Click-iT EdU (5-ethynyl-2'-deoxyuridine) Flow Cytometry Assay Kit from Invitrogen. Cell viability was measured using 7-AAD included in this kit.



For Ki-67 expression studies and cell cycle analysis using propidium iodide staining, cells were permeabilized and fixed in 70% ethanol at -20°C for 2h. They were then incubated with FITC-conjugated Ki-67 mouse anti-human antibody (Life technologies, MHI6701) or FITC-conjugated mouse IgG1 isotype control (Life technologies, MG101) at room temperature for 30 min. After a treatment with 10 µg/mL RNase A and 20 µg/mL of propidium iodide for 30 min at room temperature, cells were analyzed on a FACSCalibur flow cytometer (BD Biosciences).

**Expression of apoptosis and cell cycle related genes.** Total RNA was isolated from 5–10 x 10<sup>6</sup> TG1 or OB1 GSCs using the TRI Reagent (Euromedex, France) according to the manufacturer's instructions. RNeasy mini kit columns (QIAGEN) were used for further purification of the RNA samples. Cells were used in the following conditions: proliferating, quiescent (9 days without medium renewal) and proliferating after quiescence corresponding to quiescent cells (9 days without medium renewal) reintroduced into a proliferating medium for 1–4 days. NanoDrop ND-1000 (Labtech) was used for absorption spectra analysis and RNA purity assessment. Absorption ratios A260/A280 and A260/A230 were comprised between 1.8 and 2.1. RNA concentration was determined using the Qubit fluorometer and the Quant-it RNA Assay Kit from Invitrogen. RNA integrity was further evaluated with an Agilent 2100 Bioanalyzer and the RNA 6000 LabChip kit. Only RNA with a RNA Integrity Number (RIN) higher than 9 was processed (2100 expert software, Agilent Technologies). 1 µg of total RNA was reverse transcribed to single-stranded cDNA using the High Capacity cDNA Reverse Transcription kit (Applied Biosystems, Life Technologies). Real-time PCR analysis was performed with individual TaqMan gene expression assays in an ABI Prism 7000HT apparatus (Applied Biosystems, Life Technologies) using standard experimental conditions designed by the manufacturer. Individual assay IDs are as follows: p53: Hs 01034249-m1; BAX: Hs00180269-m1; p21: Hs 00355782-m1. Results were normalized to the 18S rRNA expression levels determined in all conditions. Results are shown as mean ± SD of two independent experiments.

**Senescence evaluation.** Senescence-associated β-galactosidase (SA-β-gal) activity was examined with Cellular Senescence Assay Kit (Merck Millipore, KAA002) according to the manufacturer's protocol. Briefly, cells were fixed with paraformaldehyde-based Fixing Solution for 10 min at room temperature and then incubated with SA-β-gal Detection Solution at 37°C overnight before microscopy examination. U-87 MG cells treated with 100 µM TMZ for 5 days were used as a positive control.

**Expression of stemness, pluripotency and differentiation markers.** TaqMan QPCR Assays (Applied Biosystems, Life Technologies) were used for determination of stemness and differentiation marker mRNA expression levels as indicated in [S1 Methods](#). Validation of gene expression levels for some genes (IFITM1: Hs00705137-s1, GBX2: Hs00230965-m1, NANOG: Hs04399610-g1) with individual gene expression assays (Applied Biosystems, Life Technologies) was performed as described in the expression of apoptosis and cell cycle related genes section of Materials and Methods. The percentage of proliferating and quiescent cells expressing the Nanog protein (antibody from R&D) was determined by FACS analysis ([S1 Methods](#)).

**Expression of surface markers, clonal, *in vitro* differentiation and *in vivo* engraftment properties.** Surface marker expression, clonal properties of both proliferating and quiescent cells, as well as their *in vitro* differentiation ability and their *in vivo* engraftment properties, were assessed according to [S2](#), [S3](#), [S4](#) and [S5](#) Methods, respectively.

## Primary and secondary chemical screens

The Prestwick Library (commercialized by Prestwick Chemical) used in this screen is composed of 1120 off-patent drugs (mostly FDA-approved) and some natural substances.

Proliferating or quiescent TG1 GSCs were seeded (30 000 and 40 000 viable cells/well, respectively) into 96-well opaque bottom plates (Greiner) with the Biomek FX robot (Beckman Coulter). Each compound from the Prestwick Library was then added (final concentration: 50  $\mu$ M; 1% DMSO). Each molecule was tested once. Negative control wells (12/96 per assay plate) contained cells treated with 1% DMSO (final concentration) and positive control wells (4/96 per assay plate) contained cells treated with the fungal toxin ophiobolin A (Sigma Aldrich) at 50  $\mu$ M with 1% DMSO. Ophiobolin A is cytotoxic both to proliferating and quiescent GSCs. Relative ATP levels were measured 24 hours later using the CellTiter-Glo reagent (Promega) according to the manufacturer's instructions. Luminescence in each well was measured with the Victor3 plate reader (PerkinElmer).

Relative ATP levels in each well were determined by calculating the percentage of luminescent signal in the well with respect to the average signal measured in negative control wells. Compounds were considered as hits if relative ATP levels in the respective wells were less than 5% and/or if the corresponding luminescent signal was lower than the mean signal of negative control wells minus 5 times the standard deviation from this value.

Primary screen hits were further tested in duplicate, at two concentrations (50 and 5  $\mu$ M) on proliferating and quiescent TG1 GSCs. Cell plating and treatment with compounds were as for the primary screen. Hit selection/confirmation criteria for quiescent cells were as described above. Due to a higher variability on proliferating cells' assay plates, compounds were considered as hits if the corresponding luminescent signal was lower than the mean signal of negative control wells minus only 3 times the standard deviation from this value.

Screen reliability was evaluated by the Z' factor [25] for each assay plate. The median Z' factors were 0.615 and 0.68 for the primary and secondary screens, respectively. Results were taken into account only if Z' > 0.5.

## Dose-response curves and EC<sub>50</sub> determination

Hits were validated by performing dose-response curves on the viability of proliferating and quiescent TG1 cells under conditions similar (cell density, time of treatment) to those used for the primary and secondary screens (n = 3).

The EC<sub>50</sub> value was determined for each compound by fitting the data points according to the following equation:

$$y = \frac{S_{max} + S_{min} * \left(x * \frac{1}{EC_{50}}\right)^n}{1 + \left(x * \frac{1}{EC_{50}}\right)^n}$$

where y represents the expected response, x is the chemical compound concentration, S<sub>max</sub> and S<sub>min</sub> are the maximum and minimum responses recorded, respectively and n is the Hill coefficient. Curve fitting was performed using Microsoft Excel Solver component.

Similar dose response curves were performed using GSCs isolated from GBM of two other patients (TG16 and OB1 GSCs) grown under proliferating and quiescent conditions. Dose response curves were also performed using f-NSCs (100 000 cells/well), HEK 293 and HA cells (50 000 cells/well).

## Cell viability measurements

Proliferating and quiescent TG1 cells and HA cells were treated with bisacodyl (10  $\mu$ M, 1% DMSO for TG1 cells; 50  $\mu$ M, 1% DMSO for HA cells) for 24 hours. Cell mortality was evaluated by trypan blue staining (0.1% (v/v)). Control cells were incubated for 24 hours in their medium in the absence or presence of 1% DMSO.

## Evaluation of bisacodyl stability in cells' medium

Bisacodyl was dissolved in freshly prepared TG1 culture medium or quiescent TG1 conditioned culture medium at a final concentration of 10  $\mu$ M in 1% DMSO. The solution was kept at room temperature. At given times (2 min, 2h, 4h, 6h and 24h), aliquots of 150  $\mu$ L were taken and mixed with 150  $\mu$ L of acetonitrile in order to precipitate proteins. After vortexing, the mixture was centrifuged at 15 000g for 10 min. Supernatants were analyzed by HPLC using a kintex 2.6 $\mu$  C18 100A (50x4.6 mm) column. Areas under the compound elution peaks were used for quantification. Reference solutions of bisacodyl or derivatives were used for calibration. Bisacodyl, its monoester derivative and the bi-phenolic form (DDPM) were eluted at 1.78 min, 1.56 min and 1.35 min, respectively.

## Synthesis of bisacodyl and bisacodyl derivatives

Commercially available bisacodyl and DDPM could also be synthesized according to our reported procedures ([S6 Methods](#)). General methods for bisacodyl and bisacodyl derivative synthesis and reaction schemes are given as supporting information ([S6 Methods](#)). HPLC-MS chromatograms of all the compounds with the exception of commercial ones are presented in [S7 Methods](#).

## Dose-response curves and EC50 calculations for SAR studies

All chemical compounds synthesized were dissolved in DMSO to obtain 10 mM stock solutions.

Proliferating or quiescent TG1 cells were seeded in 50  $\mu$ L of their respective media (30 000 and 40 000 viable cells/well, respectively) into 96-well opaque bottom plates (Greiner, Courtaboeuf, France). Compound treatment was performed by adding 50  $\mu$ L of compound solutions (in the presence of 2% DMSO in culture medium). Negative control wells contained cells treated with 1% DMSO and positive control wells contained cells treated with the antihistaminic drug Terfenadine (50  $\mu$ M) (BIO-TREND) which was identified during the screening process and shown to be cytotoxic to all the cell types used in this study. ATP levels were measured 24h later and EC<sub>50</sub> values were determined as described above. All compounds were tested in triplicate in each experiment. Independent experiments were performed at least twice for almost all of the compounds.

## Results

### Quiescence of glioblastoma stem-like cells *in vitro*

Proliferating TG1 GSCs ([Fig 1A](#), left panel) were previously selected and expanded in culture through the neurosphere assay. These cells were extensively characterized and showed long-term self-renewal, clonal properties and ability to initiate tumor formation *in vivo* thus fulfilling the criteria of tumor stem-like cells [23]. To achieve quiescence of TG1 GSCs *in vitro*, proliferating cells were seeded (day 0) and left without medium renewal. EdU incorporation and 7-AAD staining were used to assess cell proliferation and viability. GSCs maintained in culture up to 16 days without medium renewal were morphologically similar to their proliferating counterparts. They form neurospheres ([Fig 1A](#)) which at day 9 were similar to those formed under proliferating conditions and slightly looser at day 16. At day 0, just after cell passaging, 50–60% of the cells incorporated EdU ([Fig 1B](#)). The percentage of cells going through the S phase increased significantly at days 1 and 2 and then returned to initial levels by day 4. A marked decrease was observed between days 4 and 8. The low level of DNA synthesis activity measured at day 8 remained almost similar between days 8 and 16. TG1 GSC viability

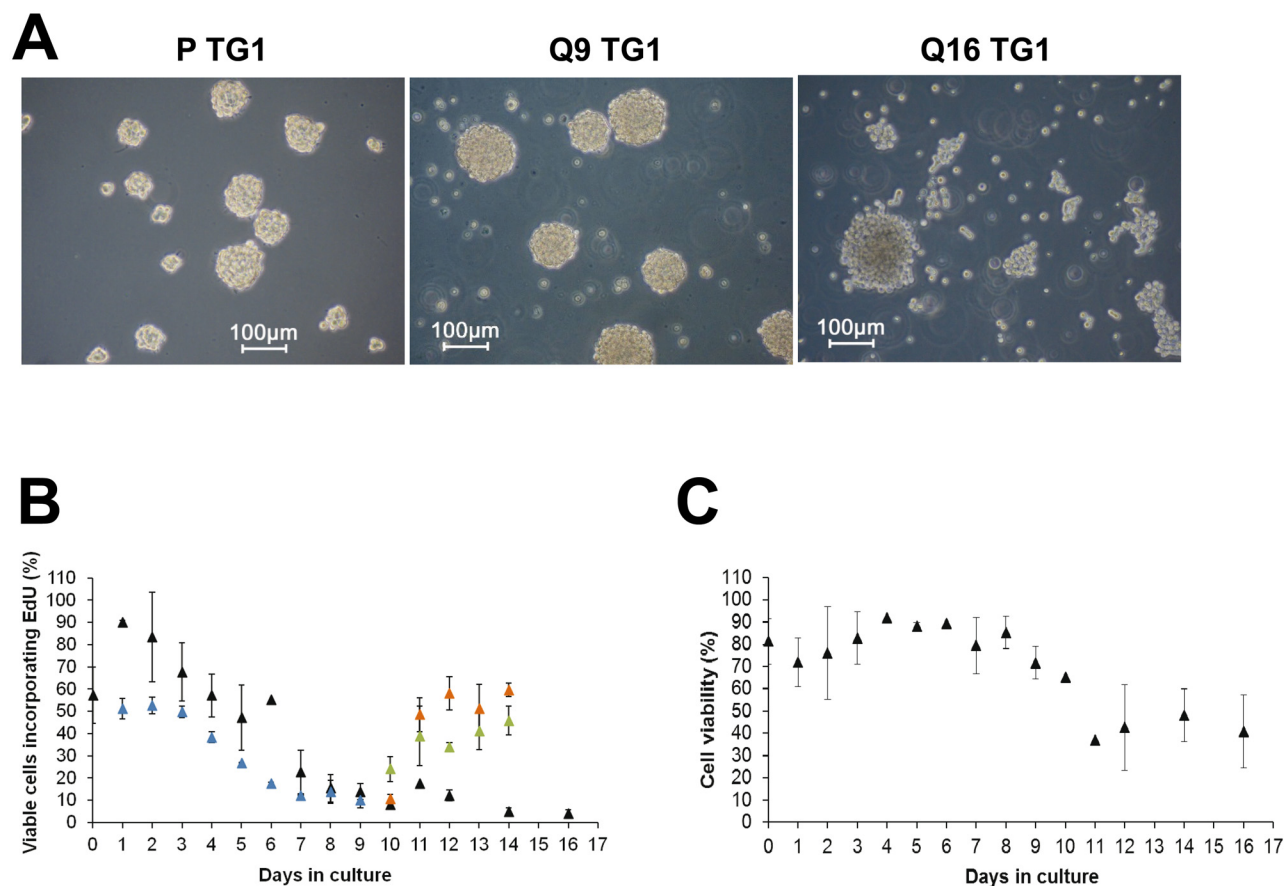


**Fig 1. EdU incorporation and cell viability measurements on proliferating and quiescent TG1 and OB1 GSCs maintained *in vitro*.** (A) In the absence of serum (NS34 culture medium), proliferating TG1 GSCs (P TG1) grow as neurospheres (left panel). Non-proliferating quiescent TG1 GSCs are generated *in vitro* by leaving cells without medium change for 9–16 days (middle panel: Q9 quiescent TG1 cells; right panel: Q16 quiescent TG1 cells). Scale bars, 100 µm. (B) EdU incorporation into TG1 (black triangles) and OB1 GSCs' DNA (blue triangles) grown without medium renewal for 1–16 days or into cells grown without medium renewal for 9 days and then subjected to freshly prepared culture medium at days 9 and 13 (TG1 cells: orange triangles; OB1 cells: green triangles). Results are from at least two independent experiments. (C) Survival of TG1 cells grown in culture for 1–16 days without medium renewal. Survival was assessed using 7-AAD. Mean  $\pm$  SD ( $n = 3$ ).

doi:10.1371/journal.pone.0134793.g001

measured at the same time points was not significantly decreased until day 9, whereas the number of cells incorporating EdU was already markedly affected at this time point (Fig 1B and 1C). At later time points, the number of viable cells decreased and then remained stable between days 11 and 16 (Fig 1C). Similar EdU incorporation profiles were obtained for OB1 and TG16 GSCs although the percentage of OB1 cells incorporating EdU was generally lower than the one observed for TG1 cells (Fig 1B for OB1 cells). To evaluate if quiescence was reversible, TG1 and OB1 cells left for 9 days without medium renewal (and called thereafter Q9 cells) were reintroduced into freshly prepared NS34 culture medium. Medium change was preformed twice, at day 9 and at day 13. As indicated in Fig 1B, medium renewal led to an increase of the percentage of TG1 and OB1 GSCs incorporating EdU suggesting that cells are able to re-enter the S phase, *i.e.* that the non-dividing state obtained by the absence of medium renewal is reversible. Cell cycle exit and reentrance of TG1 and OB1 GSCs was confirmed by cell cycle analysis using propidium iodide staining coupled to the study of modifications of Ki-67 protein levels, known to be high in dividing cells and low in non-cycling cells. As shown in Fig 2A, 2B and 2D, absence of medium renewal led to a significant increase in the number of TG1 and

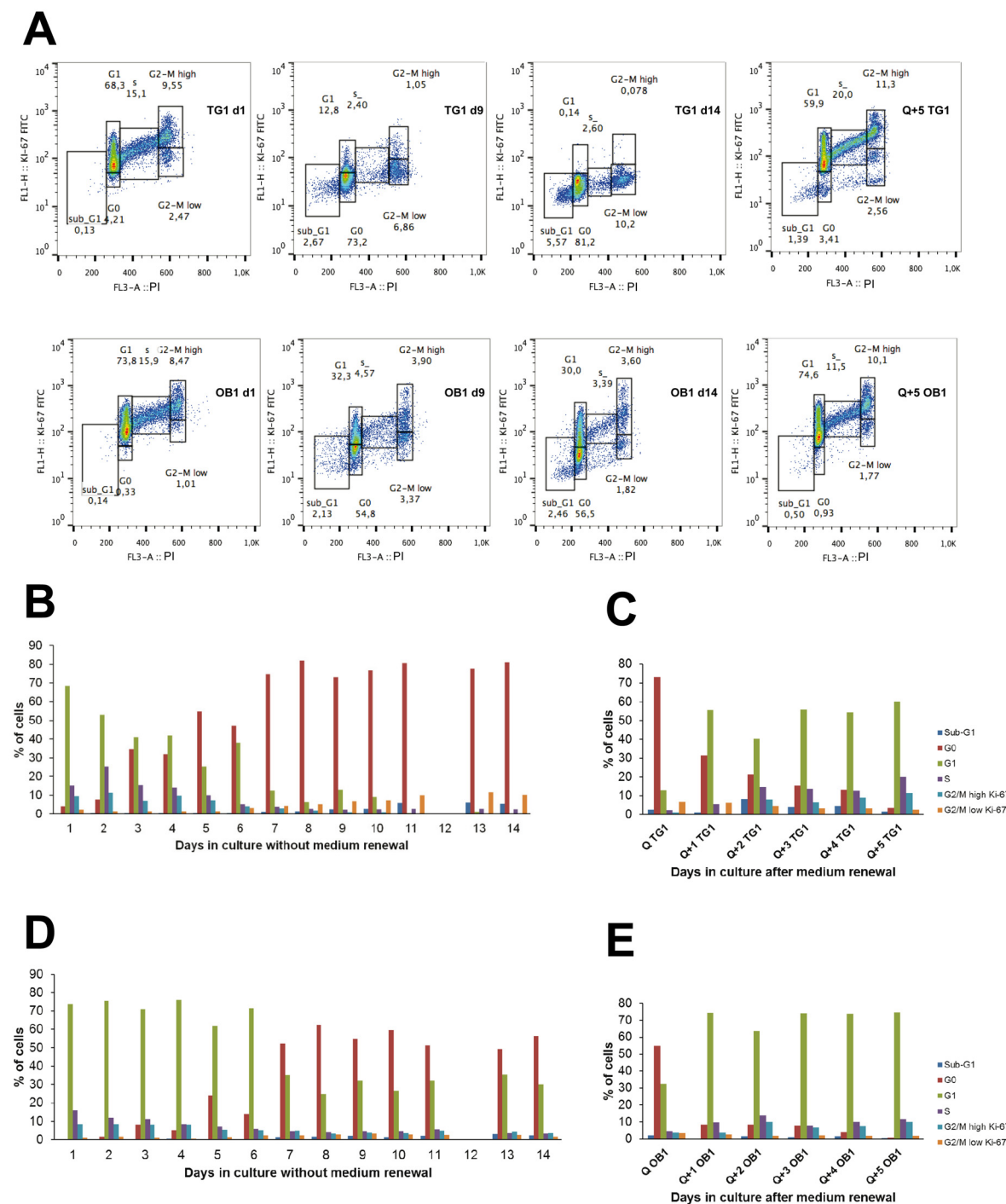


**Fig 2. Cell cycle analysis and Ki-67 expression in TG1 and OB1 GSCs under different *in vitro* culture conditions.** (A) TG1 (upper panel) and OB1 (lower panel) GSCs maintained in culture for 1, 9 and 14 days without medium renewal (d1, d9, d14, respectively) or cells obtained after 9 days without medium renewal and subjected to freshly prepared culture medium for 5 days (Q+5) were permeabilized and stained with anti-Ki-67 antibodies conjugated to FITC and propidium iodide (PI). (B-E) Histograms represent the percentage of TG1 (B, C) and OB1 (D, E) cells present in the G1, S, G2/M phases of the cell cycle as well as the percentage of quiescent cells in G0 and of cells showing DNA fragmentation (sub-G1). Cells in the G2/M phase were further distinguished as a function of the Ki-67 proliferation marker expression levels (G2/M high Ki-67 and G2/M low Ki-67). Analysis was performed on cells maintained for 1–14 days without medium renewal (B, D for TG1 and OB1 cells, respectively) or on cells left without medium renewal for 9 days (Q) and re-introduced into freshly prepared culture medium for 1 (Q+1), 2 (Q+2), 3 (Q+3), 4 (Q+4) or 5 (Q+5) days (C, E for TG1 and OB1 cells, respectively).

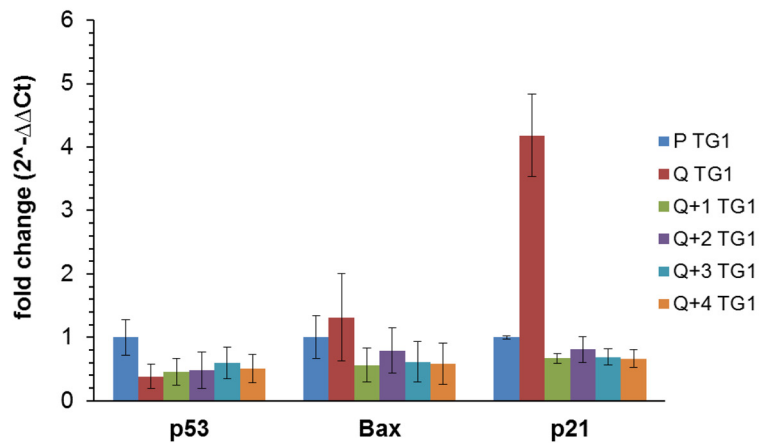
doi:10.1371/journal.pone.0134793.g002



OB1 cells in the G0 phase with a maximum obtained after 8 days in non-renewed medium. From days 8 to 14, the percentage of cells in the G0 phase did not vary significantly (Fig 2B and 2D). Concomitant with the increase of the percentage of cells in the G0 phase, there is a decrease in the number of dividing cells (cells expressing Ki-67 in the G1, S and G2/M phases of the cell cycle) (Fig 2A upper and lower panels and Fig 2B and 2D). When Q9 quiescent cells were submitted to fresh medium, both TG1 and OB1 GSCs were able to re-enter the cell cycle as shown by the increase of the percentage of cells in G1, S, G2/M and the decrease of the number of cells in phase G0 (Fig 2A upper and lower panels and Fig 2C and 2E). Interestingly, the mRNA levels of p21, a cyclin-dependent kinase inhibitor, reported to control both entry into quiescence and maintenance of the quiescent state [26] and whose expression may be controlled by p53, were significantly higher (4 fold) in quiescent TG1 GSCs after 9 days without medium renewal compared to their proliferating counterparts. The expression of this gene decreased when cells were placed back in proliferating conditions (Fig 3A). No significant changes in the expression level of this gene were observed between proliferating and quiescent OB1 GSCs (Fig 3B) pointing to differences between these two GSC types. Of note, the percentage of cells showing DNA fragmentation (cells in sub-G1) did not significantly vary from day 1 to day 14 without medium change in TG1 and OB1 GSCs (Fig 2A upper and lower panels and Fig 2B and 2D). mRNA expression levels of p53, a known apoptosis regulator, showed a slight decrease (c.a. 50%) in Q9 quiescent TG1 GSCs which remained unchanged when these cells were reintroduced in proliferating conditions for 1–4 days (Fig 3A). No significant variations were observed in p53 expression levels in OB1 GSCs under similar conditions (Fig 3B). The mRNA levels of Bax, a mediator of mitochondrial apoptosis whose expression is controlled by p53, were also similar in proliferating *versus* Q9 quiescent TG1 and OB1 GSCs (Fig 3A and 3B). These data reinforce the previous results and suggest that cells maintained *in vitro* without medium renewal for several days did not undergo massive apoptosis. In addition, the absence of  $\beta$ -galactosidase positive TG1 or OB1 GSCs after 9 days without medium renewal suggested that the cells obtained under these conditions were not senescent (Fig 3D and 3E). Altogether, these data strongly support the conclusion that quiescent and viable non-dividing GSCs may be obtained *in vitro* after several days without medium renewal.

To determine whether quiescent culture conditions modify the stem-like phenotype of GSCs by inducing cell differentiation, expression of 90 well-defined genes validated as pluripotency or differentiation markers was analyzed in TG1 and OB1 GSCs grown under proliferating or quiescent conditions using TaqMan Human Stem Cell Pluripotency Arrays. Each array contains 7 genes expressed in undifferentiated cells or involved in maintenance of pluripotency, 31 genes correlated with stemness and 52 differentiation markers (see list in S2 Table). 18S rRNA, which did not show any expression change under the experimental conditions tested, was used as housekeeping gene. Only genes with  $\Delta$ Ct (gene cycle threshold (Ct) minus 18S rRNA cycle threshold) values  $\leq 21$  in at least one of the conditions tested were considered. Genes with  $\Delta$ Ct values  $> 21$  corresponded to genes with low expression and poor signal to noise ratios. 23 genes were considered to be significantly expressed. As shown in Fig 4A and 4B, most of these genes (but GBX2, IFITM1 and LAMC1 (only in OB1 cells)) did not show a major change in their expression between proliferating and quiescent states. Namely, no significant changes in gene expression were observed for the pluripotency markers Sox2 and Nanog (confirmed in individual TaqMan assays for Nanog, see Fig 4C and 4D). Nanog expression was also evaluated at the protein level using FACS. More than 85% of the cells expressed this marker. This percentage remained similar between proliferating and quiescent cells (85% *vs* 89%, respectively, for TG1 GSCs; 88% *vs* 86% respectively, for OB1 GSCs). In addition, nuclear localization of Nanog was confirmed by immunocytochemistry (data not shown). Nanog expression also remained stable when quiescent cells re-enter the cell cycle (Fig 4C and 4D).

A



B

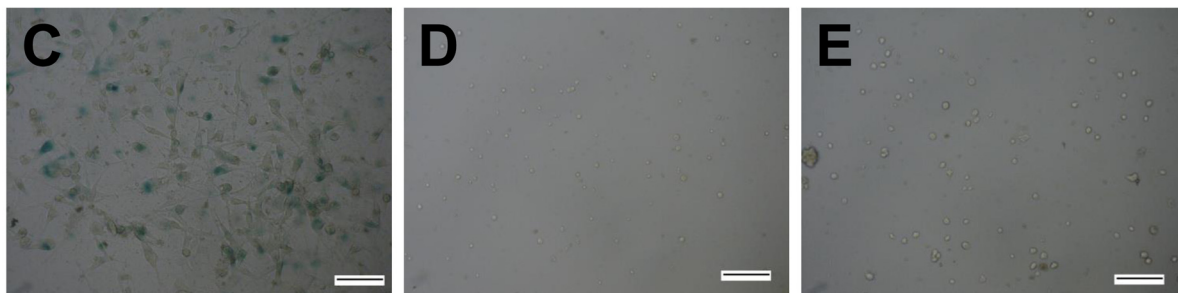
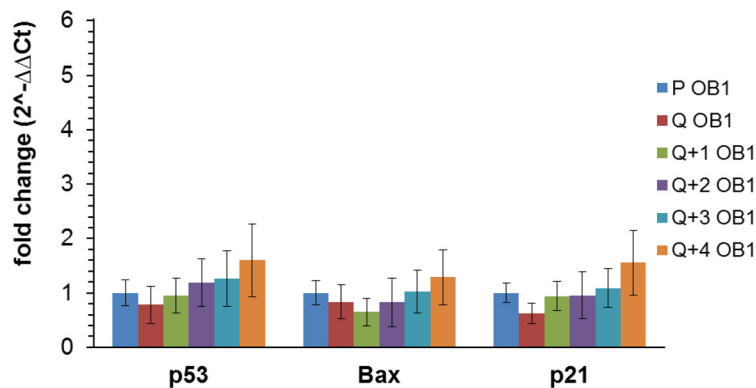
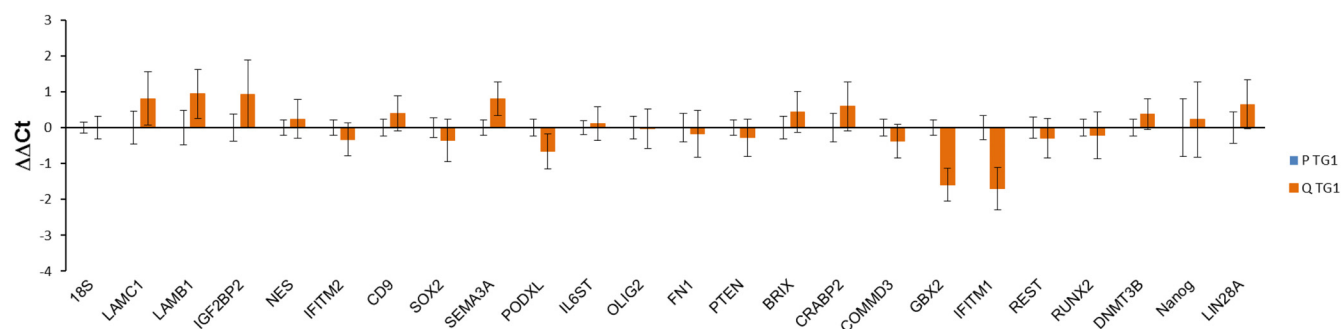


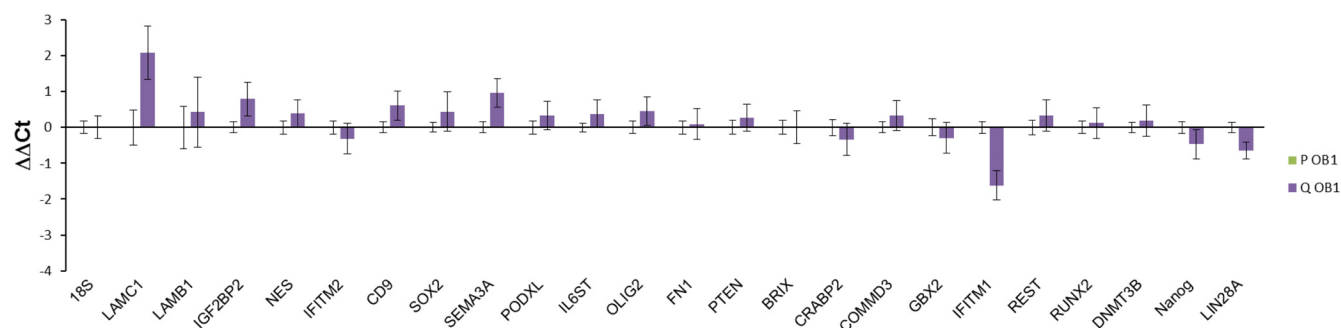
**Fig 3. Expression of apoptosis and cell cycle related genes and absence of senescence related activity in TG1 and OB1 cells under different *in vitro* culture conditions.** (A-B) Histograms representing mRNA expression levels of p53, Bax and p21 genes in proliferating (P) and quiescent (Q) TG1 (A) and OB1 (B) GSCs obtained after 9 days without medium renewal or quiescent cells after 9 days without medium renewal reintroduced in proliferating culture medium for 1–4 days (Q+1–Q+ 4). Results were expressed as fold change ( $2^{-\Delta\Delta C_t}$ ) taking proliferating TG1 (A) or OB1 (B) cells as calibrator. 18S rRNA was used as housekeeping gene. Data were from two independent experiments, each performed in duplicate. (C-E) Senescence-related  $\beta$ -galactosidase activity measurements in U-87 MG cells treated with TMZ (100  $\mu$ M) for 5 days (C; positive control) and in quiescent TG1 and OB1 GSCs obtained after 9 days without medium renewal (D, E, respectively). Scale bars: 100  $\mu$ m.

doi:10.1371/journal.pone.0134793.g003

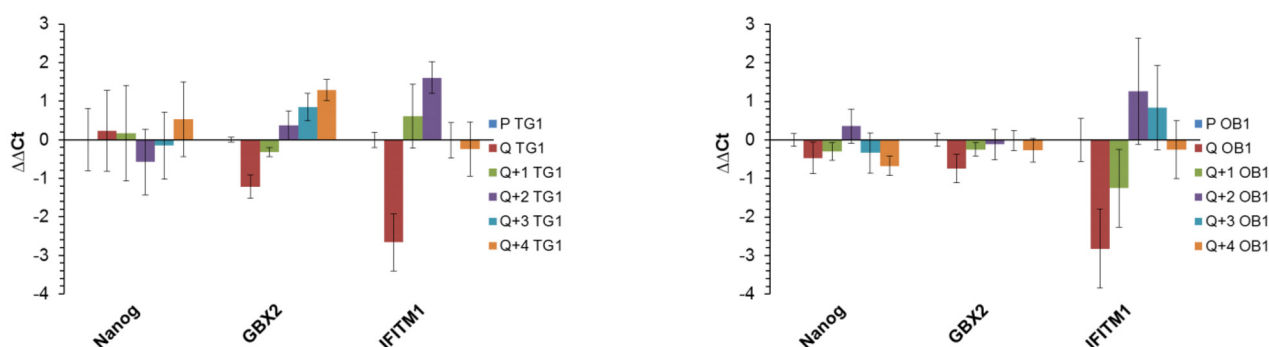
A



B



C



D

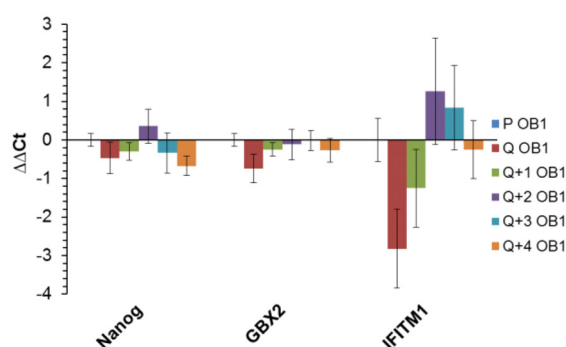


**Fig 4. Expression of stemness, pluripotency or differentiation related genes in TG1 and OB1 cells under different *in vitro* culture conditions.** (A-B) Histograms representing mRNA expression levels of stemness, pluripotency or differentiation associated genes included in the TaqMan Human Stem Cell Pluripotency Array from Life Technologies in proliferating (P) and quiescent (Q) (9 days without medium renewal) TG1 (A) and OB1 (B) GSCs. Results were normalized to the 18S rRNA levels and expressed as  $\Delta\Delta C_t$  taking proliferating TG1 (A) and OB1 (B) GSCs as calibrator samples. Data are from three independent experiments, each performed in duplicate. (C-D) Histograms representing mRNA expression levels of Nanog, GBX2 and IFTM1 genes in proliferating (P) and quiescent (Q) TG1 (C) and OB1 (D) GSCs obtained after 9 days without medium renewal or quiescent cells after 9 days without medium renewal reintroduced in proliferating culture medium for 1–4 days (Q+1–Q+4). Results are expressed as in A–B. Data are from two independent experiments, each performed in duplicate.

doi:10.1371/journal.pone.0134793.g004



The expression of GBX2 and IFITM1, two other stemness markers which presented some variation between proliferative and quiescent states on the arrays, was further analyzed in individual TaqMan assays. As shown in [Fig 4C and 4D](#), quiescence induced a slight increase in GBX2 mRNA levels in TG1 GSCs ( $\Delta\Delta\text{Ct}$ :  $-1.22 \pm 0.3$ ; fold change:  $2.32 \pm 0.48$ ) and OB1 cells ( $\Delta\Delta\text{Ct}$ :  $-0.75 \pm 0.37$ ; fold change:  $1.68 \pm 0.43$ ). These variations were reversed when quiescent cells re-entered the cell cycle ([Fig 4C and 4D](#)). The GBX2 gene product has previously been shown to promote reprogramming and maintenance of the pluripotent state of mouse embryonic stem-cells downstream of a LIF/Stat3-dependent pathway [27]. A greater change in expression was observed for IFITM1 when TG1 and OB1 cells became quiescent ( $\Delta\Delta\text{Ct}$ :  $-2.66 \pm 0.75$ ; fold change:  $6.32 \pm 3.26$  and  $\Delta\Delta\text{Ct}$ :  $-2.82 \pm 1.02$ ; fold change:  $7.06 \pm 4.99$ , respectively) ([Fig 4C and 4D](#)). When cells were reintroduced into proliferating conditions (following medium renewal), IFITM1 expression decreased rapidly to reach levels similar to those observed in proliferating GSCs ([Fig 4C and 4D](#)). IFITM1 was previously shown to regulate proliferation either negatively or positively depending on the cell model [28, 29]. Our data are in favor of an anti-proliferative effect of IFITM1 since its expression increases in quiescent cells. Finally, a slight decrease in the expression of LAMC1, an early differentiation marker, was detected but only in quiescent OB1 cells. On the overall, quiescence did not appear to cause major changes in the stemness of GSCs.

To further characterize quiescent TG1 and OB1 GSCs, we examined various properties previously described for these cells in proliferating conditions, namely the expression of cell surface markers, their clonal and differentiation properties as well as their engraftment ability after orthotopic injection in mouse brain. Concerning cell surface markers, quiescent GSCs expressed CXCR4 and CD56 and were CD133 negative, similarly to their proliferating counterparts ([S1A–S1C Fig](#)) [23, 30, 31]. In addition, quiescence did not alter TG1 and OB1 GSCs' clonal properties since isolated quiescent cells, when placed back into fresh culture medium, formed new neurospheres ([S2A and S2B Fig](#)). Moreover, as their proliferating counterparts [23], quiescent cells kept their ability to differentiate when exposed to serum containing medium. Results for differentiation of both proliferating and quiescent TG1 and OB1 GSCs are presented in [S3 Fig](#). Serum addition led to cell adherence and morphological changes reflected by flattening and acquisition of a fusiform shape. These morphological changes were accompanied by a decrease in the expression of the stemness-related gene Sonic Hedgehog (SHH) in proliferating and quiescent TG1 GSCs and in proliferating OB1 cells ([S3B and S3D Fig](#)). Concomitantly, a marked increase in the expression of the astrocytic marker glial fibrillary acid protein (GFAP) was observed in proliferating TG1 and OB1 cells and in quiescent TG1 GSCs ([S3C and S3E Fig](#)). A significant change in the expression of the neuronal marker  $\beta$ 3 tubulin (TUBB3) was only observed when quiescent cells (TG1 or OB1) were subjected to differentiation ([S3B and S3D Fig](#)). Altogether these data suggest that quiescent GSCs obtained *in vitro* maintain their differentiation ability when subjected to serum supplemented medium and point to a preferential differentiation (under the conditions used) towards an astrocytic phenotype.

The last point investigated in this study concerned GSCs' *in vivo* engraftment ability. This property was reported previously for TG1 and OB1 GSCs [23, 30]. Results presented in [S4 Fig](#) suggest that intracerebral engraftment was not altered when quiescent GSCs were injected into immune-deficient animal brains. Indeed, eight weeks after orthotopic injection, human cells were present in mouse brains, with no differences in cellularity whether injected cells were proliferating or quiescent ([S4A and S4B Fig](#)). In addition, in both cases, Ki-67 positive cells were detected, suggesting that the quiescent phenotype may be reversed *in vivo* ([S4C and S4D Fig](#)).

Altogether, the results presented suggest that i) quiescence can be obtained *in vitro* for GSCs, ii) quiescent GSCs retain the stem, clonal, differentiation and *in vivo* engraftment

properties of their proliferative counterparts. GSCs were thus designated as quiescent after 9 to 16 days in culture without medium renewal.

## Prestwick Library screening of proliferating and quiescent GSCs

The Prestwick Library was screened in order to find molecules with cytotoxic activity on proliferating and/or quiescent GSCs (Fig 5A). In the primary screen (Fig 5B), about 5% of the compounds tested significantly reduced the relative ATP level of proliferating or quiescent TG1 cells. Of the 1120 compounds, 57 were active on proliferating cells and 69 on quiescent GSCs, with 40 compounds exhibiting similar effects on both cell types. Seventeen compounds triggered an increase in ATP levels.

To confirm hits from the primary screen, a secondary screen was performed on 86 compounds that reduced relative ATP levels and 16 molecules that increased them. The secondary screen confirmed the activity of approximately 50% of the compounds that lowered ATP levels (29/57 compounds for proliferating TG1 GSCs and 33/69 for cells grown under quiescent conditions) (Fig 5C). Twenty-three of the confirmed hits were active on both proliferating and quiescent TG1 GSCs. None of the 16 compounds tested for their potential to increase cell ATP levels was confirmed. Results of primary and secondary screens are summarized in S3 Table.

Dose-response curves were generated using both proliferating and quiescent TG1 GSCs for 20 out of 39 active compounds selected in the secondary screen (list in Table 1). Compounds excluded were antibacterial, antifungal, anti-parasitic agents or molecules endowed with known detergent activity. All those excluded compounds showed activity on both proliferating and quiescent cells. Preliminary experiments were performed on the 20 selected compounds to verify that measured luminescence changes were related to an effect of the tested molecule on cell ATP levels and not to an interference with the readout setup. Analysis of the different dose-response curves allowed classifying the compounds into three groups, according to their EC<sub>50</sub> values for TG1 GSCs in either their proliferative or quiescent state (Table 1). Structures and smile codes of the twenty hit compounds are represented in S4 Table.

Representative results of the activity profiles of each group are shown in Fig 6A. Suloctidil, a vasodilator, is representative of a group of compounds (group 1) with cytotoxic activity towards both proliferating and quiescent TG1 GSCs (Fig 6A, left panel). For this group, compound EC<sub>50</sub> on proliferating GSCs was less than two-fold higher or lower compared to the value observed on their quiescent counterparts. Twelve compounds belong to this family (Table 1). The antipsychotic zuclopenthixol hydrochloride (Fig 6A, middle panel) is representative of a group of 4 molecules which exhibited higher activity towards proliferative cells (group 2). In this group, compound EC<sub>50</sub> was more than two fold lower for proliferative TG1 GSCs compared to quiescent cells. Group 3, represented by the laxative bisacodyl (Fig 6A, right panel) unveils molecules with selectivity for quiescent TG1 GSCs. In this group, EC<sub>50</sub> of a given compound was at least two fold lower for quiescent TG1 GSCs compared to proliferative cells. Bisacodyl was the molecule with the lowest EC<sub>50</sub> and which appeared with outstanding specificity for quiescent TG1 GSCs (Fig 6A right panel and Table 1).

The activity of the 20 molecules was further tested on stem-like cells derived from two other distinct human glioblastomas (TG16 and OB1 GSCs). As for TG1 GSCs, dose response curves were performed on cells grown under proliferating and quiescent conditions. Activity profiles and EC<sub>50</sub> values obtained were similar to those observed for TG1 GSCs (Table 1 and Fig 7).

To determine the specificity of the selected compound towards GSCs, dose-response curves were performed on the non-cancerous neural cells f-NSCs, and HA cells as well as on the non-neural cell line HEK 293. Most of the 20 compounds, namely those belonging to groups 1 and 2 (Table 1), showed cytotoxicity, after the 24 hours of the test, towards all the cell types

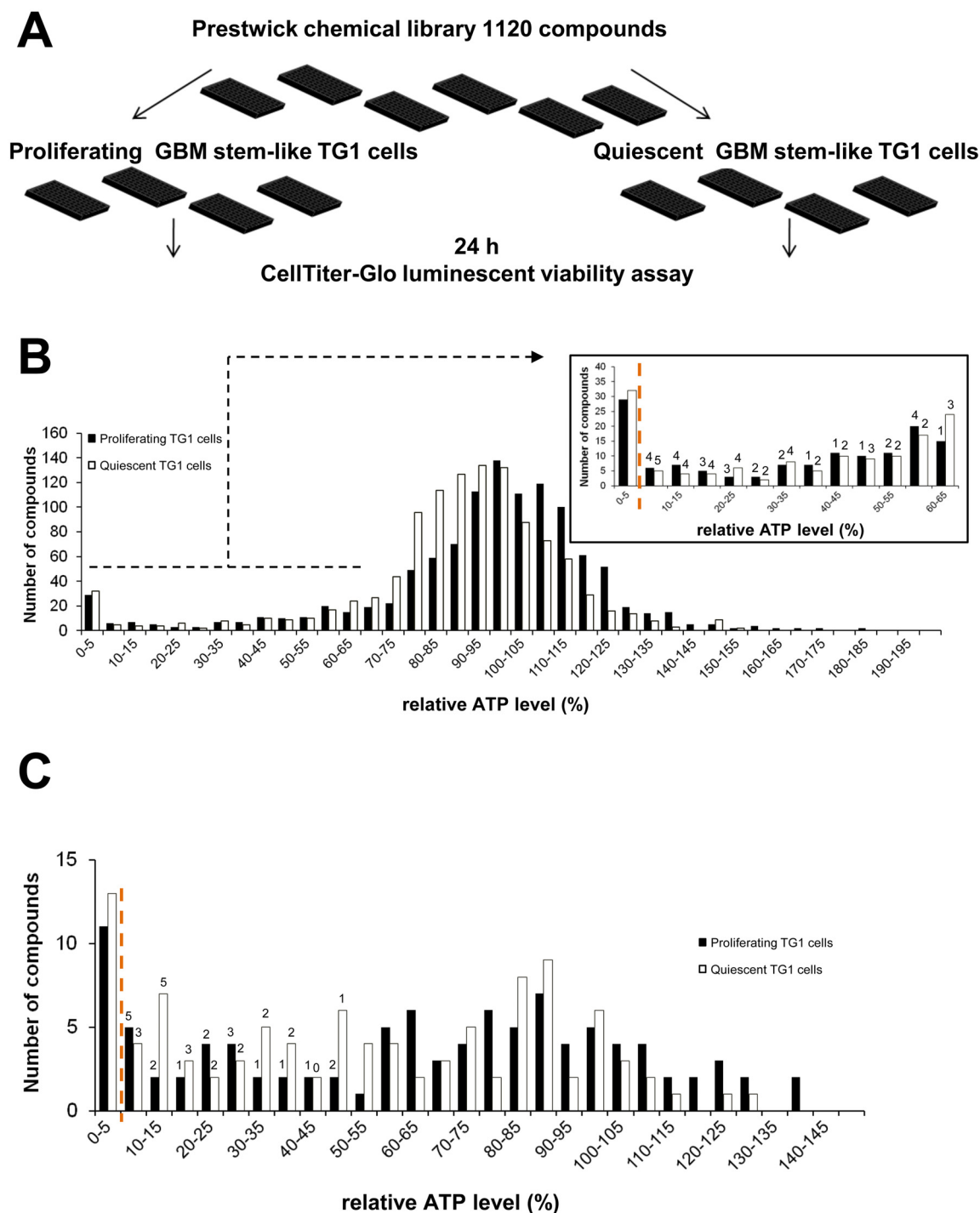


**Fig 5. Prestwick Library screen on GSCs using the ATP-Glo cell based assay.** (A) Schematic representation of the assay design and protocol. GBM: glioblastoma. (B) Results of the primary screen are represented as histograms of the relative ATP signal levels obtained for each compound screened against proliferating (black bars) and quiescent (open bars) TG1 cells. Molecules producing ATP levels that exceeded 200% of the control levels are not shown. Zoom in of results for compounds with an ATP level below 65% of the control levels is provided. A compound was considered as a hit either if it reduced relative ATP levels to less than 5% of control levels (compounds on the left of the orange dotted line) or if the corresponding luminescent signal was lower than the mean signal of negative control wells minus 5 times the standard deviation from this value (number of molecules indicated on the top of each bar). (C) 86 compounds reducing relative ATP levels and 16 molecules increasing relative ATP levels were tested in a secondary screen at concentrations of 5 and 50  $\mu$ M. Results of the secondary screen performed at 50  $\mu$ M are shown following the same representation as in (B).

doi:10.1371/journal.pone.0134793.g005

**Table 1. EC50 values of Prestwick Library hit compounds on the different cell types tested.**

ATC classification	Compound name	Therapeutic/ pharmacological class	P TG1 GSCs EC <sub>50</sub> (μM)	Q TG1 GSCs EC <sub>50</sub> (μM)	P TG16 GSCs EC <sub>50</sub> (μM)	Q TG16 GSCs EC <sub>50</sub> (μM)	P OB1 GSCs EC <sub>50</sub> (μM)	Q OB1 GSCs EC <sub>50</sub> (μM)	Astrocytes (HA cells) EC <sub>50</sub> (μM)	f-NSC EC <sub>50</sub> (μM)	HEK 293 EC <sub>50</sub> (μM)
<b>Group 1</b>											
C01BD01	Amiodarone hydrochloride	Cardiovascular system/ Antiarrhythmic/Adrenergic blocker	10±3	10±3	11±1	14±5	12±1	19±1	22±7	10	28±4
C01DX02	Prenylamine lactate	Vasodilator	22±3	27±3	32±2	42±8	30±7	49±4	30±2	9±2	25±6
C04AX19	Sulotidil	Vasodilator peripheral/ Hypolipidemic	11±1	13±1	13.5 ±0.1	14±6	15±2	20±4	11±1	5±1	10±1
C08CA02	Felodipine	Cardiovascular system/ Antihypertensive/Calcium channel blocker	38±1	30±3	39±4	33±3	43±5	41±6	36±6	59±12	55±2
C08EA01	Fendiline hydrochloride	Cardiovascular system/ Antiarrhythmic/Antianginal/L- calcium channel blocker	22±1	32±1	42±1	45±16	40±13	48±9	42±8	11±1	34±9
C08EX02	Perhexilin maleate	Cardiovascular/Vasodilator	10±1	14±3	11±1	21±4	12±1	22±4	12±2	3±1	12±1
G03DC03	Lynestrenol	Progestogen	36±2	43±8	32±2	28±6	26±5	56±10	20±1	23±5	57±8
KEGG Brite C09154	Ellipticine	Anticancer	13±1	19±5	13±1	56±10	8±1	30±9	5±1	7±2	13±2
L02BA01	Tamoxifen citrate	Anticancer	14±2	20±1	20±1	20±3	28±3	29±3	15±4	14±9	30±10
N06AB06	Sertraline	Antidepressant/Psychoanaleptic	19±1	39±1	31±1	44±9	32±11	45±2	24±1	10±2	23±1
P02CF01	Ivermectin	Antiparasitic/Anthelmintic/Acaricid	3±1	4±1	1.5 ±0.2	6±2	3±1	7±2	3±1	4±1	13±1
KEGG C08921	Beta-Escin	Peripheral vascular disorders/ Antioedematous/ Antiinflammatory/Glucocorticoid like?	17±3	12±3	6±1	8±1	12±1	6±1	7±1	nd	31±1
<b>Group 2</b>											
N05AF05	Zuclopenthixol hydrochloride	Antipsychotic	20±3	52±3	29±5	48±18	27±9	> 100	12±1	13±1	29±1
R06AX11	Astemizole	Antihistaminic	12±2	28±3	17±2	58±9	13±3	43±16	19±4	6.3 ±0.2	21±9
R06AX12	Terfenadine	Antihistaminic	8±1	17±1	9±1	24±6	10±2	22±4	9±2	4±1	8±1
KEGG Brite CPD:C07609	Parthenolide	Antiinflammatory/Antisecretory/ Spasmolytic	15±2	48±6	10±2	nd	18±4	35±11	59±4	8.4 ±0.2	13±5
<b>Group 3</b>											
A06AB02	Bisacodyl	Cathartic laxative	> 100	1.07 ±0.04	> 100	1.3 ±0.1	> 100	0.5 ±0.1	0.6+/-0.3*	> 100	> 100
C03CC01	Ethacrynic acid	Diuretic	81±11	41±11	> 100	12±2	60±20	24±3	> 100	21±11	> 100
KEGG c01514	Luteolin	Expectorant	> 100	20±2	> 100	34±4	> 100	18±4	> 100	70±36	> 100
G03DA04	Progesterone	Progestogen	> 100	25±11	75±6	25±9	89±29	23±11	> 100	> 100	36±10

Screening of the Prestwick Library on TG1 human glioblastoma stem-like cells (GSCs) unveiled 20 molecules decreasing the relative ATP level in these cells. Dose response curves were performed with the 20 molecules using ATP Glo assay as readout. Molecules were tested on 3 different types of proliferating (P) and quiescent (Q) GSCs (TG1, TG16, OB1), non-cancer neural cells including human fetal neural stem cells (f-NSC) and primary astrocytes (HA cells) as well as HEK 293 cells, a non-cancer and non-neural cell line. Hits are classified into 3 groups according to their differential activity or not on proliferative and quiescent TG1 GSCs. In each group, molecules were clustered according to their ATC (Anatomical, Therapeutic, Clinical) classification. nd: not determined.

\*: the maximum effect observed for this compound on HA cells was a reduction of only 30% of ATP levels which was not due to cell death.

doi:10.1371/journal.pone.0134793.t001

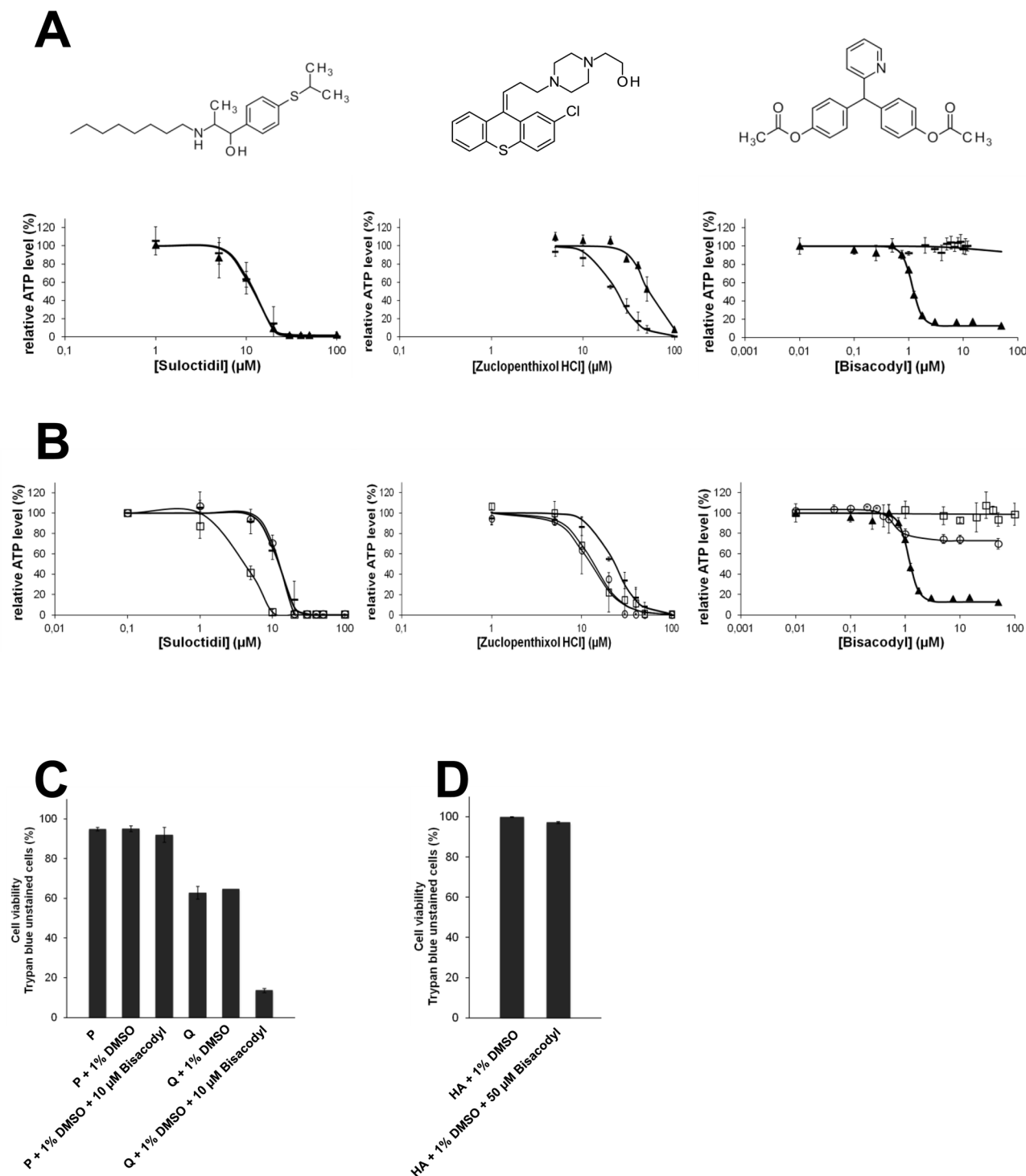


**Fig 6. Dose-response curves for compounds exhibiting the strongest cytotoxic effect on GSCs.** (A) Chemical structures of selected compounds and dose-response curves of suloctidil (left), zuclopenthixol HCl (middle) and bisacodyl (right) with representative activity profiles on proliferating (—) and quiescent (▲) TG1 GSCs. The fitted sigmoidal logistic curve to ATP-Glo cell survival assay readouts is shown on each plot ( $n = 3$ ). (B) Dose-response curves of suloctidil (left), zuclopenthixol HCl (middle) and bisacodyl (right) on proliferating TG1 cells (—), quiescent TG1 cells (▲), human primary astrocytes (○) and human fetal neural stem cells (□). Curves were fitted as in A ( $n = 3$ ). (C-D) Cell viability measurements (trypan blue staining) on proliferating (P) or quiescent (Q) TG1 cells (C) and HA cells (D) treated with bisacodyl (compound 1 in Fig 9).

doi:10.1371/journal.pone.0134793.g006

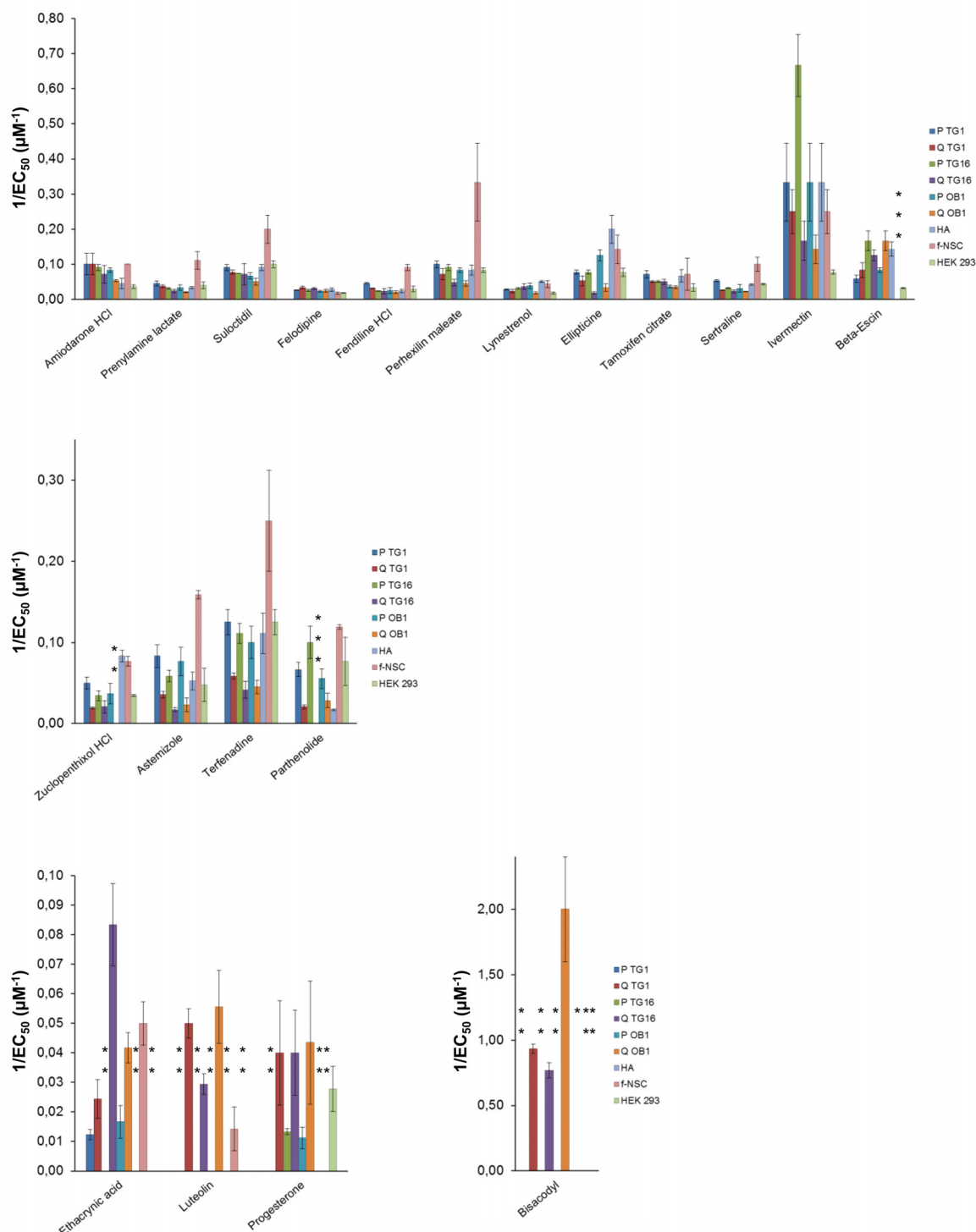


**Fig 7. Activity of Prestwick Library hit compounds on GSCs and control cell types.** Graphical presentation of the activity of the high-throughput screen hit compounds (expressed as  $1/EC_{50}$ ) on proliferating (P) and quiescent (Q) GSCs derived from three patients (TG1, TG16 and OB1), human primary astrocytes (HA cells), human fetal neural stem cells (f-NSC) and a human embryonic kidney cell line (HEK 293). Upper, middle and low panels: group 1, group 2 and group 3 molecules as defined in Table 1, respectively.  $EC_{50}$  values correspond to mean values calculated from fitted dose-response curves to ATP-Glo assay readings of three independent experiments ( $n = 3$ ). \*: Given that the maximum effect of bisacodyl on HA cells is a 30% reduction of ATP levels which is not due to cell death (see Fig 6D), the corresponding  $EC_{50}$  value was not taken into account. \*\*:  $EC_{50}$  values observed  $>100 \mu M$ . \*\*\*:  $EC_{50}$  values not determined.

doi:10.1371/journal.pone.0134793.g007



tested, whether they were neural or not, cancerous or not (Table 1 and Fig 7). Compounds of group 3 which showed higher activity on quiescent GSCs compared to proliferative ones were mostly inactive or showed reduced activity on the other cell types. One molecule, bisacodyl, stood out from the rest by showing a specific activity on GSCs grown under quiescent conditions, with a low  $EC_{50} \sim 1 \mu M$  (Figs 6A and 7; Table 1). For quiescent TG1 GSCs, trypan blue and 7-AAD staining indicated that the ATP level decrease induced by bisacodyl resulted from cell death (Fig 6C). In addition, bisacodyl showed no activity on f-NSCs and HEK 293 cells (Table 1, Figs 6B and 7). A decrease in the relative ATP level could be observed for HA cells (primary astrocytes) (Fig 6B). However, using trypan blue exclusion, we showed that bisacodyl did not alter HA viability (Fig 6D), suggesting that this compound might induce metabolic changes in these cells.

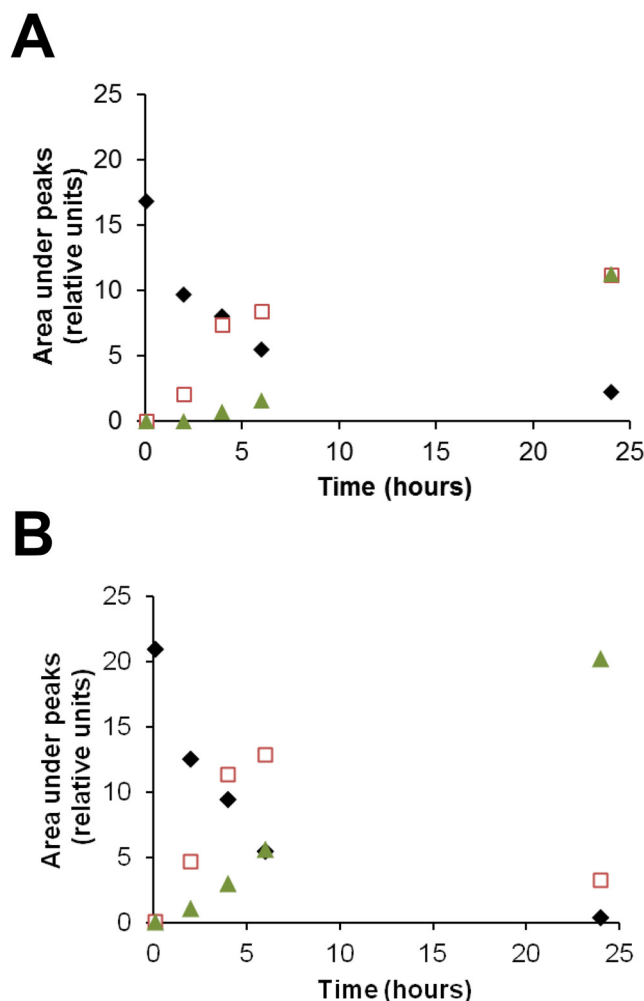
Altogether, these data, pointed to bisacodyl as a highly potent and selective inhibitor of quiescent GSC survival. This property drew our attention and triggered further investigation of the molecule.

### Bisacodyl acts on GSCs via DDPM, its active metabolite

Bisacodyl (Fig 6A upper-right panel) is a marketed laxative compound corresponding to a pro-drug. Following oral administration, it is rapidly converted to its active metabolite 4,4'-dihydroxydiphenyl-2-pyridyl-methane (DDPM) also known as BHPM, through hydrolysis of its two acetyl groups [32]. To get deeper insight into the active compound under our experimental conditions, stability of bisacodyl in GSCs' culture medium as well as activity of DDPM on TG1 GSCs were investigated. Stability of bisacodyl in the culture media (freshly prepared medium for proliferating conditions, conditioned medium in contact with quiescent cells for 9 days for quiescent conditions) was followed as a function of time using HPLC as indicated under Materials and Methods. Bisacodyl eluted from the column as a peak at 1.78 min. In proliferating condition medium, this peak disappeared with a half-life of 4 hours whereas a half-life of 2 hours was observed in quiescent cell conditioned medium (Fig 8A and 8B). Concomitantly, in both proliferating condition culture medium and quiescent cell conditioned medium, two other peaks appeared on the chromatogram. One of them, with a 1.56 min retention time, was transient and corresponds to the monoester derivative of bisacodyl (compound 3 in Fig 9). The second, with a 1.35 min retention time, corresponds to DDPM (compound 2 in Fig 9). As shown in Fig 8B, DDPM was the only derivative present in the quiescent TG1 GSCs' conditioned medium after 24h. Evolution of the areas under the three peaks as a function of time (Fig 8A and 8B) is in favor of the hydrolysis of bisacodyl (Fig 6A upper-right panel and compound 1, Fig 9) in the culture medium and formation of DDPM (compound 2, Fig 9). As ATP level readouts were performed after a 24h of GSCs' incubation with bisacodyl, one might suggest that the effect observed was due to DDPM. The effect of DDPM (obtained commercially or synthesized in-house) on the relative ATP level of TG1 GSCs was therefore evaluated. Experimental results were totally superimposable to those obtained using bisacodyl (data not shown) with the same specificity towards TG1 GSCs grown under quiescent conditions, suggesting that bisacodyl (Fig 6A upper-right panel and compound 1, Fig 9) is hydrolyzed to its active DDPM derivative (compound 2, Fig 9) in the cell culture media of both proliferative and quiescent TG1 GSCs. A similar activity profile was obtained with compound 3 (Fig 9), the monoester derivative of bisacodyl.

### Bisacodyl pharmacophore identification

With the aim at identifying the pharmacophore elements present on DDPM (compound 2, Fig 9), additional derivatives were synthesized (Fig 9). The importance of the two hydroxyl groups

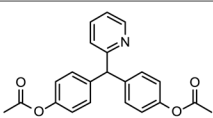
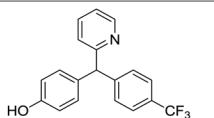
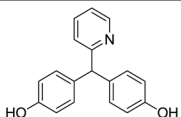
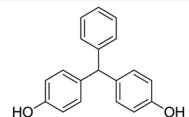
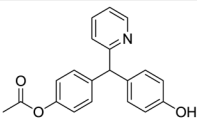
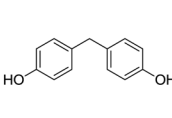
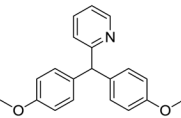
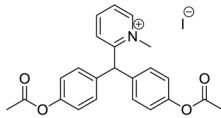
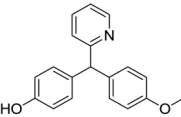
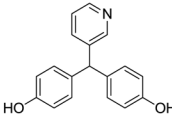
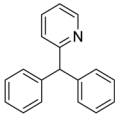
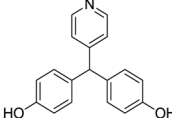
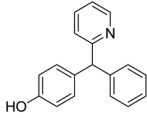
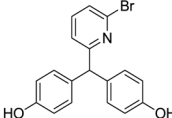
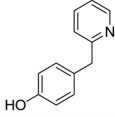
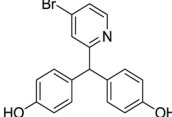
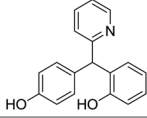
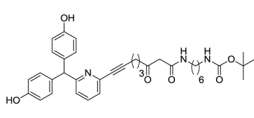
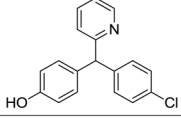


**Fig 8. Bisacodyl stability in GSCs' culture media.** Bisacodyl was dissolved in freshly prepared culture medium used for the culture of proliferating cells (A) or in conditioned culture medium of quiescent TG1 GSCs (B) at a final concentration of 10  $\mu$ M in 1% DMSO. The presence of bisacodyl (diamonds) and its deacetylated derivatives (mono- (squares) and di- (triangles) deacetylated forms), was followed as a function of time. Ordinate represents area under the HPLC elution peaks of the different molecular species present.

doi:10.1371/journal.pone.0134793.g008

was investigated through synthesis of non-hydrolysable methoxy- derivatives (compounds 4 and 5, Fig 9). Compound 4 with two methoxyphenyl rings was inactive on both proliferative and quiescent TG1 GSCs, whereas compound 5 with one free phenol group and one methoxyphenyl ring was, similarly to DDPM, active on quiescent TG1 GSCs only, albeit with a 8 fold higher  $EC_{50}$ . Compound 6 in which the hydroxyl groups of DDPM (compound 2) were removed can be considered as inactive, similarly to compound 4. On the other hand, compound 7 where only one of the two hydroxyl groups of DDPM was removed behaved similarly to compound 5 and exhibited selective activity on quiescent TG1 GSCs with an  $EC_{50}$  of  $17.1 \pm 6.3 \mu$ M. Solubility measurements indicated that the lack of activity of compound 6 was not due to reduced solubility (data not shown). The activity of the molecule thus appeared to require at least one phenol group in the structure. The second phenyl ring is however important since a total loss in activity was observed for compound 8 where one of the phenol groups was replaced by hydrogen and compound 9 where one of the two hydroxyl groups was moved



Compound number	Structure	n (number of experiments)	Proliferating TG1 GSCs EC <sub>50</sub> (μM)	Quiescent TG1 GSCs EC <sub>50</sub> (μM)	Compound number	Structure	n (number of experiments)	Proliferating TG1 GSCs EC <sub>50</sub> (μM)	Quiescent TG1 GSCs EC <sub>50</sub> (μM)
1		3	>100	1.07 ± 0.04	11		2	> 100	12.4 ± 6.9
2		3	>100	1.0 ± 0.5	12		4	60.8 ± 10.4	14.2 ± 8.8
3		3	>100	1.0 ± 0.5	13		3	No activity	No activity
4		4	No activity	No activity	14		1	>100	>100
5		3	>100	8.0 ± 6.0	15		3	>100	8.0 ± 3.0
6		2	>100	84.8 ± 4.1	16		3	>100	39.0 ± 2.0
7		2	>100	17.1 ± 6.3	17		2	No activity	2.04 ± 0.3
8		2	No activity	No activity	18		2	No activity	0.36 ± 0.06
9		2	No activity	57.6 ± 0.7	19		1	No activity	3.84
10		2	>100	4.0 ± 1.4					

**Fig 9. Structure-activity data.** Tables representing structure-activity data of bisacodyl (compound 1) and bisacodyl derivatives (compounds 2–19) on proliferating and quiescent TG1 glioblastoma stem-like cells (GSCs). The ATP-Glo cell survival assay was used to measure compound activity. Compound structures are shown. Compounds were tested in triplicate in each experiment.

doi:10.1371/journal.pone.0134793.g009

to the ortho position. Interestingly, the *p*-chloro- and *p*-trifluoromethyl-phenyl monophenols **10** and **11** retained activity ( $EC_{50} = 4.0 \pm 1.4 \mu M$  and  $12.4 \pm 6.9 \mu M$ , respectively) with an excellent selectivity versus proliferating TG1 GSCs, suggesting that pharmacomodulation is possible at this position.

In a second step, the importance of the pyridyl ring and the position of the nitrogen atom on the ring were investigated. Phenyl replacement of the pyridyl ring (compound **12**) resulted

in an at least 10 fold activity decrease of DDPM (compound 2) towards quiescent GSCs. Furthermore, the compound presented activity on cells grown under proliferative conditions, although high concentrations were needed for activity. Removing the pyridyl group (compound 13) or forming a methyl pyridinium (compound 14) resulted in a total loss of activity towards TG1 GSCs. The importance of the nitrogen atom position on the pyridyl ring was also investigated. Compounds 15 and 16 with nitrogen in positions *meta* and *para*, respectively, kept their total specificity towards quiescent GSCs. However, their efficacy was decreased compared to DDPM (compound 2), with a ~8-fold increase in EC<sub>50</sub> for compound 15 and ~40-fold for compound 16. Those data suggested a role of the pyridyl ring in the activity of DDPM (compound 2) towards GSCs and its specificity towards cells grown under quiescent conditions. Optimal activity was obtained with the nitrogen atom at the ortho position of the ring.

We further checked the incidence of pyridyl ring substitutions. As shown in Fig 9, mono bromide substituted derivatives appeared promising. Bromide at position 6 of the pyridyl ring (compound 17) did not alter activity and specificity. Furthermore, compound 18, with the bromide at position 4, showed increased activity towards quiescent GSCs compared to compound 1. DDPM (compound 2), thus appears amenable for further structure activity relationship (SAR) studies aiming at increasing its activity.

The position 6 was also explored for the production of derivatives that could be used for other purposes and namely target identification. Addition of a linker at this position led to compound 19, which retained activity and selectivity as DDPM (compound 2). This result opens the possibility to synthesize substituted resins or to develop derivatives for pull down assays. A target identification program based on related compounds is currently under investigation.

In conclusion, our results indicate that bisacodyl (compound 1, Fig 9) acts through its deacetylated metabolite, DDPM (compound 2, Fig 9), and the minimal pharmacophoric pattern consists in a p-hydroxyphenyl-aryl-pyridyl-2-methane. Minor modifications lead to changes in potency and/or specificity though pharmacomodulation appears feasible both on the aryl and pyridinyl nuclei, as currently studied. The SAR study is currently on-going and will be disclosed later.

## Discussion

Scientific literature of the past several years points to the presence of quiescent, slow-cycling cancer stem-like cells in a number of tumor types [14]. Namely, a restricted cell population of Ki-67 negative and nestin positive cells was identified in a murine glioblastoma model and stem-like cells with molecular signatures applying to slow-rate dividing cells were evidenced by a single-cell RNA-seq approach [33, 34]. Tumor cell quiescence including the dormant phenotype observed for cancer stem-like cells *in vivo*, represents a major mechanism underlying treatment resistance or tumor recurrence and/or metastasis several years following initial therapeutic intervention [33, 35, 36]. Cellular quiescence is defined as an actively maintained state of proliferation arrest with cells being able to re-enter the cell cycle in response to proliferating stimuli. Quiescent cells are characterized by the lack of expression of proliferation and apoptotic markers, low rate of BrdU incorporation and label retention properties indicating a low turnover [36]. In this study, we have identified culture conditions that induce *in vitro* quiescence of GSCs. Quiescence of these cells was demonstrated by reduction of EdU incorporation, lowering of Ki-67 expression with concomitant absence of significant variations in the expression of apoptosis-related genes. In addition, increased expression of the cell cycle negative regulatory protein p21 was observed in quiescent TG1 GSCs. Interestingly, our data point out the reversibility of the quiescent state following re-exposure to proliferating culture conditions. In addition, we show that quiescent GSCs obtained *in vitro* retain all the characteristics of their

proliferating counterparts including cell surface and stem-cell marker expression, clonal and differentiation properties as well as *in vivo* engraftment ability. Quiescent GSCs as well as their proliferating counterparts were subsequently used in a screening assay aiming at identifying compounds with activity on these cells.

Screening the Prestwick Library using the ATP-Glo cell assay, disclosed 20 molecules that decreased cells' ATP levels in a dose-dependent manner. Changes in ATP levels may reflect alteration in either energy metabolism and/or cell survival. The complete drop in cell ATP level observed in the presence of most of the active molecules we identified, points to a cytotoxic effect.

The Prestwick Library is mainly composed of FDA-approved drugs plus some natural substances. Most hit molecules can thus be clustered according to the ATC (Anatomic, Therapeutic and Clinic) classification ([Table 1](#)). Seven out of the twenty hit molecules belong to anatomic group C of molecules acting on the cardiovascular system, although with different therapeutic indications and pharmacological modes of action. Nine more molecules belong to six other anatomical groups and four molecules are natural products. Among those twenty molecules, only tamoxifen and ellipticine are considered as anti-cancer drugs. The Prestwick Library contains 60 other molecules labeled as anticancer drugs. Most of them are antiproliferative agents. However the experimental screening conditions used in the present study, with short time exposure of cells to chemical compounds (24h compared to 48h or 72h classically), did not uncover those anticancer molecules. Tamoxifen, an estrogen receptor (ER) modulator derived from triphenylethylene, is used for ER-positive breast cancer treatment and prevention of breast cancer in high-risk women [37]. At doses in the micromolar range, the compound also exerts ER independent cytotoxic activity on different cell types [38–40]. Cytotoxicity towards human and rat glioma cell lines was reported to occur *via* PKC, PI3K/AKT, JNK and ERK signaling pathways [41, 42]. Tamoxifen has also been evaluated, in association with temozolomide, as a second line therapeutic strategy for the treatment of recurrent glioblastoma [43]. Recently, apoptotic cell death induced by tamoxifen (with EC<sub>50</sub> values of approximately 30  $\mu$ M) has been reported in the tumorigenic human neural glial cell line HNGC-2 which forms neurospheres and presents neural stem cell markers [44]. This is in agreement with the cytotoxic effect on human GSCs observed in the present study. However, our data also point to the lack of specificity of the molecule at those doses, as it presents the same efficacy towards non-cancerous cells such as human astrocytes and neural stem cells. In addition, the activity of the molecule does not seem to be related to the proliferative state of the cells, as similar efficacy was observed for proliferative and quiescent GSCs.

The second molecule, ellipticine, is a planar alkaloid isolated from *Apocyanaceae* plants. A methyl-hydroxy derivative (Celiptium) was developed by Sanofi for treating metastatic breast malignancies, but the drug showed numerous adverse effects. Besides its intercalating properties and inhibition of topoisomerase II, ellipticine and derivatives act on a variety of targets [45–49]. Ellipticine presents cytotoxicity towards various cancer cell lines including U-87 MG glioblastoma cells [50–53]. Recently, the molecule has been shown to reduce proliferation and self-renewal ability of aldehyde dehydrogenase 1 class A1-positive breast cancer stem cells [54]. On GSCs treated for 24h, the cytotoxic activity of ellipticine is uncovered at concentrations > 10  $\mu$ M. A difference in sensitivity between GSCs can be observed as OB1 and TG16 GSCs appear more sensitive to the molecule when grown under proliferative conditions, whereas TG1 cells exhibit the same sensitivity, whether proliferating or quiescent. However, the cytotoxic activity of ellipticine is not specific to cancer cells and the molecule acts, even with higher efficacy, on non-cancer cells (HA cells and f-NSCs in the present study).

Among the hit molecules retained in our screening setting and used in other non-cancer indications, some were already reported to reduce cancer cell viability. Among the molecules in

group 1 ([Table 1](#)), the vasodilator drug prenylamine has been shown to induce an intracellular calcium increase and cell death in human ovarian tumor cells at a concentration of 100  $\mu\text{M}$  [55]. However, this molecule shows high risks of cardiac arrhythmias and its antiproliferative activities were not further investigated. Fendiline, known as a L-type calcium channel blocker was shown to inhibit, in a calcium independent manner, the survival of human oral cancer cells (OC2) at concentrations between 5–25  $\mu\text{M}$  [56]. In the same concentration range, fendiline inhibits K-Ras signaling in a variety of cancer cells (pancreatic, colon, lung and endometrial) that express oncogenic K-Ras and, as a result, their proliferation [57]. The calcium antagonist vasodilator perhexiline was also reported to decrease proliferation of the human colon cancer cell line HT29 with an  $\text{EC}_{50}$  of ca 10  $\mu\text{M}$  [58], and in the micromolar concentration range, to stimulate phagocytosis and induce mTORC1 inhibition in MCF7 cells [59]. These latter two activities were shared, at concentrations  $> 10\mu\text{M}$ , with amiodarone, a highly prescribed antiarrhythmic agent which acts on diverse ion channels, namely the  $(\text{Na}^{+})/\text{Ca}^{(2+)}$  exchanger (NCX), L-type  $\text{Ca}^{(2+)}$  channels and  $\text{Na}^{(+)}$  channels. Antiproliferative activities of the molecule on prostate cancer cells through potassium channel inhibition was reported earlier [60].

The serotonin reuptake inhibitor sertraline was shown to induce apoptosis of PC-3 cells [61] and human MG63 osteosarcoma cells [62] at concentrations of ca 30  $\mu\text{M}$ . The drug also exerted a cytotoxic activity on the U-87 human GBM cell line with an  $\text{EC}_{50}$  of 8  $\mu\text{M}$  and acted in synergy with imatinib to decrease U-87 cell proliferation *via* a drastic decrease in Akt phosphorylation and in an additive manner with temozolomide [63]. An antiproliferative phospho-Akt dependent activity of the drug has also been reported for melanoma cells [64]. Clinical trials using sertraline in combination with standard treatments have been performed for glioblastoma and colon cancer [65, 66]. The molecule also appeared in the list of nine repurposed drugs that could be used as adjuvants in new innovative GBM care [67]. In the present study, we show that sertraline also exhibits cytotoxicity towards GSCs at concentrations of ca 20  $\mu\text{M}$ . However it shows the same potency towards the non-cancerous human astrocytes.

Cancer cell growth inhibitory effects and chemosensitization have also been reported for the anthelmintic drug ivermectin on human ovarian cancer cells [68, 69] and leukemia cells [70]. The molecule acted in the 5–20  $\mu\text{M}$  range through mechanisms such as inhibition of the oncogenic protein kinase PAK1 [68, 69], inhibition of importin/HE4 (human epididymis protein 4) [71] or increase in ROS production [70]. Antiproliferative activities and chemosensitization are also properties of beta escin, a natural mixture of triterpenoid saponins which acts on leukemia cells [72], hepatocellular carcinoma [73, 74], cholangiocarcinoma [75], human lung carcinoma A549 cells [76], human acute leukemia Jurkat T cells [77], human colon carcinoma cell lines [78] and pancreatic cancer cells [79]. Several mechanisms appear to sustain the activity of the molecule, namely apoptosis [75], downregulation of JAK/STAT pathways [74, 76] and inhibition of nuclear kappa B factor [80, 81]. The involvement of the antihypertensor and antianginal felodipine in cancer cell death is not very well documented although one report involved this compound in cholangiocarcinoma [82].

Thus, most molecules of group 1, showed activity on other (non stem-like) cancer cell types (even if information is sometimes limited) at concentrations in the same range as those reported in [Table 1](#) for their cytotoxicity on proliferating or quiescent GSCs. However, at these concentrations, the molecules were also cytotoxic towards non cancer cells and namely astrocytes, HEK 293 cells and neural stem cells.

Concerning molecules of group 2, the histamine H1 receptor antagonist astemizole, currently used as antimalarial and antihistaminic drug, has been proposed as a potential chemotherapeutic agent [83–85]. Its anti-proliferative activity occurs through different mechanisms, namely by targeting proteins involved in cancer progression including human ether a-go-go 1

(hEag1) and Eag-related gene (hErg) potassium channels [83, 85–89] and by modulating autophagy [84]. Terfenadine, a second histamine H1 receptor antagonist has previously been reported for its apoptosis-inducing properties against a variety of cancer cells [90–92], including human melanoma cells [93, 94] and more recently prostate cancer cells [95]. The molecule appears to act through a variety of mechanisms, some implying changes in calcium homeostasis or ROS production. So far, there are no reports of terfenadine effects on human glioblastoma. In the present study we show that terfenadine and astemizole show cytotoxic activity on GSCs with higher efficacy on proliferating cells ( $EC_{50}$  of ca 10  $\mu$ M; comparable to the one measured for other cancer cells). The molecules remain active on quiescent cells, but  $EC_{50}$  values are increased by about two fold. As for the other molecules already discussed, there is no specificity for cancer cells compared to non-cancer cells. In addition, their activity on ether a-go-go  $K^+$  channels ( $IC_{50}$  in the nanomolar range) also sustains the cardiotoxic effect of these molecules with QT interval prolongation and torsades de pointe [96–99].

Cytotoxic activity of the sesquiterpene lactone parthenolide has been reported several decades ago [100, 101]. Since, the molecule was shown to act on various cancer cell types including GBM cells [102–104] in which it induced apoptosis *via* an AKT/NF- $\kappa$ B dependent pathway [104]. However, as for other cancer cells, more pathways may be activated [105–107].  $EC_{50}$  values between 13 and 29  $\mu$ M were determined for different GBM cells (U373, U-87, C6 and U138 MG), similar to those reported here for proliferative GSCs (Table 1). Astrocytes appeared less sensitive to parthenolide with an  $EC_{50}$  value of  $186 \pm 10$   $\mu$ M in the literature [104] and  $59 \pm 4$   $\mu$ M in our study. Recently, structurally related molecules with activity towards a variety of cancer cells in the nanomolar and low micromolar range were obtained [108]. As far as the neuroleptic zuclopenthixol is concerned, only one publication relates its possible involvement in apoptosis of mouse lymphoma cells. [109]. Zuclopenthixol is the cis-isomer of clopenthixol, a mixed antagonist of dopaminergic G-protein coupled receptors D1 and D2 [110]. A comparative GPCR receptor expression study in TG1, OB1, HA and f-NSC cells performed in our laboratory [31] pointed to DR2 receptor expression in these cells. However, the high concentrations of zuclopenthixol required to induce cytotoxicity do not suggest the involvement of this receptor in GSC cell death induced by this compound.

Molecules in group 3 correspond to compounds with selectivity towards quiescent GSCs. Interestingly, two compounds of this group, ethacrynic acid (EA) and luteolin, are known in the literature as chemoadjuvants or for their anticancer properties towards a variety of cancer cell types. EA, a loop diuretic which inhibits the  $Na^{(+)}-K^{(+)}-2Cl^{(-)}$  kidney symport, presents additional effects and namely inhibitory activity towards glutathione S-transferase [111] which was used to overcome chemotherapeutic drug resistance [112–115], including in GBM [116]. Besides, EA was also shown as an inhibitor of multiple myeloma [117–119], renal cancer, as well as of chronic lymphocytic leukemia cell survival [120] by interfering with the Wnt/beta-catenin signaling pathway [121]. Depending on the cell type, concentrations between ca 40 and 230  $\mu$ M were required to induce cell death. At those high concentrations, cytotoxicity of the molecule can be observed for TG1 and OB1 GSCs in the proliferative and quiescent state (Table 1). As we did not test our molecules at concentrations above 100  $\mu$ M, no information can be given for an effect of EA at high concentrations on proliferative TG16. Among the non-cancer cells tested here, f-NSCs appear the most sensitive to EA with an  $EC_{50}$  of  $21 \pm 11$   $\mu$ M. This difference in activity of EA depending on the cell type or physiological state of the cell may be further explored.

Luteolin, the second molecule of group 3 with known potential anticancer activity is a bioflavonoid (3',4',5,7-tetrahydroxy-flavone) found in various plants, including dietary food vegetables. The molecule shows antimicrobial, anti-inflammatory, antioxidant and anticancer activities [122–124]. The efficacy of the molecule relies on a variety of mechanisms as reviewed



in [122, 125–127]. More recently, apoptosis and inhibition of the JAK/STAT3 pathway in cholangiocarcinoma [128], upregulation of miR34a in gastric cancer cells [129], apoptosis and upregulation of Fas signaling in Hep-2 cells [130], apoptosis and interference with PI3K/Akt/mTOR signaling in non-small cell lung cancer [131], cell cycle arrest and apoptosis of liver cancer cell lines [132], ROS generation and intracellular copper mobilization in different cancer cell types [133] and inhibition of cyclin G-associated kinase in PC-3 prostate cancer cells [134] were reported for luteolin. Effective concentrations vary, depending on the cell type and the time of exposure, between 8 and 50  $\mu$ M. Concerning neural cancers, it was shown that under non cytotoxic doses (15–30  $\mu$ M), luteolin interferes with GBM cell migration [135]. Only one publication deals with luteolin effects on glioma stem-like cells and shows that treatment of U251 glioma stem-like cells with 10  $\mu$ M luteolin significantly inhibits their sphere forming abilities [136]. In the present study, cytotoxicity of luteolin at concentrations below 100  $\mu$ M was only observed for GSCs in the quiescent state, pointing to differences in signaling pathways between the two states. The present study also discloses a higher resistance of proliferating GSCs towards luteolin compared to other cells tested in the literature (which, with one exception, were non stem-like cells). Interestingly, under the concentrations tested, luteolin did not show any effect on astrocytes and HEK 293 cells and high concentrations are required to affect f-NSCs. Thus, through its pleiotropic targets, luteolin appears as a potential therapeutic agent, but a poor pharmacological tool which does not allow better knowledge of GSCs' pathophysiology.

No cytotoxicity or antiproliferative activity towards cancer cells was attributed so far to the remaining compounds identified in our screening, *i.e.* suloctidil and lynestrenol in group 1 and bisacodyl and progesterone in group 3. Suloctidil is a vasodilator and anti-platelet agent that has recently been found in a repurposing screen at 50  $\mu$ M to have fungicidal activity on *Cryptococcus neoformans* (a property shared with several other molecules found in the present screen, namely perhexiline, tamoxifen, amiodarone and sertraline [137]). However, as opposed to the other molecules, no antitumor activity has been reported for this compound. Its activity profile on GSCs and non-cancer cell lines is similar to the one observed for perhexiline, amiodarone or sertraline, which were documented as affecting cancer cell survival. Thus, at concentrations in the low micromolar range, suloctidil might be considered as a cytotoxic agent, with no specificity towards cancer cells.

The stimulant laxative bisacodyl appeared in this study as a molecule with highly selective cytotoxicity towards GSCs in their quiescent state and no adverse effect towards non-cancer neural cells. Furthermore, the molecule exerts its unique cytotoxic activity with the highest efficacy ( $EC_{50}$  value in the micromolar range) compared to the other molecules tested and this activity was observed for temozolomide-resistant GSCs [23] originating from GBM of three different patients and presenting different molecular signatures (*i.e.* p53 mutation is observed in TG16 but not in TG1 or OB1 cells). We showed that in the culture medium, bisacodyl is transformed into DDPM, its known *in vivo* active metabolite. Similar results on cell viability were obtained using either bisacodyl or DDPM. The key structural elements necessary to retain activity and/or specificity have been characterized. They consist in the p-phenolarylpyridinyl-methane scaffold with some limited pharmacomodulation freedom on the aryl and pyridine moieties that remain to be further explored. DDPM and its mono bromide substituted derivative corresponding to compound 18 presented in this study remain the most potent and specific compounds identified so far.

The molecular mechanisms underlying the cytotoxic effect of bisacodyl/DDPM on GSCs as well as the direct molecular target(s) of the active metabolite are under investigation. The laxative effect of bisacodyl is thought to occur *via* a mechanism involving ion channel ( $Na^+/K^+$ ) perturbation at the intestinal level. However, few mechanistic studies are available for this old

drug marketed in the sixties. The present finding appeals further studies to unveil both the specific activity of bisacodyl/DDPM on quiescent GSCs and some aspects of GSC functioning. Finding a molecule with selective cytotoxic activity on quiescent GSCs is very attractive as cancer stem-like cells are known to be particularly chemo- and radio-resistant. Their ability to enter quiescence *in vivo* reinforces their propensity to escape chemotherapies [14]. To our knowledge, bisacodyl/DDPM is the first small molecule endowed with cytotoxic activity towards slow-growing cancer stem-like cells. None of the chemical screens described in the literature investigated cancer stem-like cells under dormant conditions, whatever the cancer type considered [12, 13, 138, 139]. The present finding opens new avenues for an old molecule with an original mode of action towards cells designated as central culprits in cancer maintenance and relapse after therapy.

## Supporting Information

**S1 Fig. Expression of surface markers in proliferating and quiescent GSCs.** (A-B) Immunohistochemical staining of proliferating and quiescent TG1 and OB1 GSCs with CXCR4 (A) and CD56 (B) antibodies. Nuclei are stained with DAPI. Image magnification: 40x. Scale bars, 20  $\mu$ m. (C) Expression of the CD133 surface marker was evaluated in proliferating (P) and quiescent (Q) TG1 and OB1 GSCs using flow cytometry (lower panels). Controls using FITC-conjugated antibody isotypes are shown (upper panels). The percentage of CD133 positive cells is indicated. (TIF)

**S2 Fig. Evaluation of clonal properties of proliferating and quiescent GSCs.** (A) Evaluation of the clonal properties of proliferating (—) and quiescent (▲) TG1 cells. The graph represents the mean number of spheres obtained after 3 weeks in culture as a function of the initial number of cells in a well. (B) Evaluation of the clonal properties of proliferating (—) and quiescent (▲) OB1 cells. Results are represented as in (A). Images of clonal neurospheres obtained from TG1 and OB1 GSCs after 3 weeks are shown as inserts in (A) and (B), respectively. (TIF)

**S3 Fig. Differentiation ability of proliferating and quiescent TG1 and OB1 GSCs.** (A) Phase contrast images of proliferating (P) and quiescent (Q) GSCs dissociated and incubated in culture medium supplemented with 10% fetal calf serum (FCS) for 0 (d0) to 14 days (d14). Scale bars: 100  $\mu$ m. (B-E) Histograms representing mRNA expression levels of the sonic hedgehog (SHH),  $\beta$ 3-tubulin (TUBB3) and glial fibrillary acid protein (GFAP) genes in proliferating (P) and quiescent (Q) TG1 (B, C) and OB1 (D, E) GSCs cultured in differentiation inducing medium containing 10% FCS for 0 (d0) to 14 days (d14). Results, related to the cycle threshold (Ct) value obtained for each gene, were normalized to the 18S rRNA expression levels in each condition and are shown as fold change ( $2^{\Delta\Delta Ct}$ ) observed in proliferating or quiescent TG1 or OB1 cells after 14 days in the presence of serum compared to the expression observed in the same cells at day 0. Data are from two independent experiments. (TIF)

**S4 Fig. *In vivo* engraftment properties of proliferating and quiescent GSCs.** (A-B) Proliferating (A) or quiescent (B) GSCs were grafted in the left striatum of nude mice. Mice were sacrificed 8 weeks later and brain sections were immunostained with an antibody recognizing specifically human vimentin. Brown vimentin staining thus allows identifying human cells. Scale bar in insert images of the whole brain indicating the region containing human GSCs: 500  $\mu$ m. Scale bars in enlarged images: 100  $\mu$ m. (C-D) Immunohistochemical labeling of brain sections obtained as in (A-B) with an anti-Ki-67 antibody. (TIF)

**S1 Methods. Expression of stemness, pluripotency and differentiation markers in proliferating and quiescent GSCs.** The expression levels (mRNA) of 90 genes enclosing stemness, pluripotency and differentiation markers and 6 endogenous controls (see [S2 Table](#)) were studied in both proliferating and quiescent TG1 and OB1 GSCs using the real-time PCR based TaqMan Human Stem Cell Pluripotency Array (Applied Biosystems, Life Technologies). Briefly, total RNA was extracted using TriReagent (Invitrogen). cDNA synthesis was performed with 10 µg of total RNA at 37°C for 2 hours using the High Capacity cDNA Archive kit (Applied Biosystems, Life Technologies). Quantitative PCR was performed using the ABI Prism 7900HT Sequence Detection System (Applied Biosystems). Cycle threshold (Ct) values were measured. Ribosomal RNA18s was used as housekeeping gene. Expression levels of Nanog, GBX2 and IFITM1 were also verified using individual TaqMan gene expression assays from Applied Biosystems, Life Technologies as described in the Materials and Methods section. FACS analysis was used to study Nanog protein expression in proliferating and quiescent TG1 and OB1 GSCs. Neurospheres were dissociated and cells were resuspended in PBS. Fixable viability Dye eFluor 450 labeling (eBioscience) was performed to irreversibly label dead cells. Following washing with PBS, cells were fixed with 2% paraformaldehyde in PBS (10 min at room temperature). Permeabilization (5 min at room temperature) was performed in the presence of 0.1% of saponin and cells were then washed once in HBSS buffer containing saponin (0.1%). Non-specific sites were blocked in PBS solution containing 3% BSA and 2.5% of fetal bovine serum for 30 min at room temperature. Primary antibody labeling (anti-Nanog rabbit polyclonal; Abcam; 1/200) was performed overnight at 4°C. Secondary antibody incubation (1 hour at room temperature) was followed by FACS analysis. Cells labeled with the secondary antibody in the absence of the primary antibody were used as negative controls.

(DOCX)

**S2 Methods. Expression of surface markers. Detection of CXCR4 and CD56 expression using immunocytochemistry.** Cells were mechanically dissociated and centrifuged onto slides with a Cytospin centrifuge. Cellular auto-fluorescence was blocked by incubating cells with 0.06% KMnO<sub>4</sub> at room temperature for 10 min. After a blockade with 1% BSA in PBS, cells were incubated with CXCR4 antibodies (Merck Millipore, AB1847, 1:50) or CD56 antibodies (BioLegend, 304601, 1:25) at 4°C overnight. Cells were then washed and incubated with Alexa 488-conjugated secondary antibodies (Jackson Immuno Research, 1:250) for 20 min in the dark at room temperature. DAPI was used for counterstaining before fluorescence microscopy observation. **Evaluation of CD133 expression by flow cytometry.** Following mechanical dissociation and washing in PBS, 1x10<sup>6</sup> proliferating and quiescent TG1 and OB1 cells were resuspended in 100 µL PBS with 0.5% BSA. Cells were then incubated with 10 µL of FITC-conjugated CD133 antibody (Miltenyi Biotec, 130-105-226) or 10 µL of FITC-conjugated isotype control (Miltenyi Biotec, 130-104-562) for 10 min in the dark in a refrigerator. Cells were washed in 2mL PBS with 0.5% BSA and then analyzed with a FACSCalibur flow cytometer (BD Biosciences). Propidium iodide was used to exclude dead cells.

(DOCX)

**S3 Methods. Clonality tests.** Clonality of proliferating and quiescent TG1 and OB1 GSCs was evaluated in 96-well plates seeded at various cell densities (1, 2, 5, 10, 20 and 50 cells/well) in 0.2 ml of freshly prepared NS34 medium (16 wells/cell density condition). The number of wells containing at least one secondary sphere as well as the number of spheres in each well were evaluated after 3 weeks in culture.

(DOCX)



**S4 Methods. Evaluation of *in vitro* differentiation properties of GSCs.** Proliferating and quiescent (9 days without medium renewal) TG1 and OB1 GSCs were dissociated and seeded in freshly prepared NS34 medium supplemented with 10% FBS (Day 0). Cells were then maintained in this differentiation-inducing culture medium for 14 days. At day 0 and day 14,  $2.5\text{--}5 \times 10^6$  cells in each condition were collected and total RNA was extracted, purified, characterized and reverse transcribed as described in the Materials and Methods section. Expression at the mRNA level of stem cell and differentiation markers (Sonic Hedgehog (SHH): Hs 00179843-m1,  $\beta$ 3 tubulin (TUBB3): Hs 00801390-S1 and glial fibrillary acid protein (GFAP): Hs00909233-m1) was determined using individual TaqMan gene expression assays (Applied Biosystems, Life Technologies) and quantitative PCR analysis as described in previous sections. (DOCX)

**S5 Methods. Evaluation of *in vivo* engraftment properties of GSCs.** Mice (NMRI Nude, Janvier) were anesthetized by inhalation of isoflurane.  $10^5$  glioblastoma OB1 cells (proliferating and quiescent) were injected into the left striatum of mice (4 mice per experimental setting), using a stereotaxic set-up with a 10  $\mu$ L Hamilton syringe. The needle was kept in place for 5 min after injection and then slowly removed. 8 weeks after injection, mice were anesthetized with xylazine, then perfused with 4% formaldehyde. Mouse brains were fixed in 4% formaldehyde, embedded in paraffin and cut into serial 10  $\mu$ m-thick sections. Human cells were identified with immunohistochemical staining with an antibody against vimentin (clone V9, Dako). Ki-67 positive cells were identified with immunohistochemical staining with corresponding antibodies from Dako (clone MIB-1). (DOCX)

**S6 Methods. Experimental section for the synthesis of the chemical compounds.** (DOCX)

**S7 Methods. LC/MS analytical data.** (DOCX)

**S1 Table. Cell source, cell handling and resource sharing information.** P: proliferating; Q: quiescent. (DOCX)

**S2 Table. Assay ID numbers, IDs and names of genes included in the TaqMan Human Stem Cell Pluripotency Arrays from Applied Biosystems, Life Technologies.** List of the 90 stem cell or differentiation associated genes and 6 housekeeping genes (ACTB, RAF1, CTNNB1, GAPDH, EEF1A1, 18S) included in the Human Stem Cell Pluripotency Array from Life Technologies. (DOCX)

**S3 Table. Primary and secondary screen hit compounds.** GSCs: glioblastoma stem-like cells. Hit compounds selected both in the primary and secondary screens for their activity in at least one of the conditions tested are highlighted in yellow. (DOCX)

**S4 Table. Hit compound structures.** Molecules were disclosed from the Prestwick Library for their activity on GSCs. (XLSX)

## Acknowledgments

We thank "La Ligue contre le Cancer" for PhD funding of Wanyin Chen. Marie Fève was supported by a French Ministry of Higher Education and Research scholarship and the University of Strasbourg. We thank Dr René Frydman (Antoine Bécclère hospital, Clamart, France) and Dr Hervé Coffiny for providing fetal brain tissues and the Sainte Anne neurosurgery team for providing glioblastoma tissues, Patrick Gizzi (PCBIS-TechMed, Illkirch France) for physicochemical analyses and Justine Viéville and Patrick Wehrung (Plateforme d'Analyse Chimique de Strasbourg Illkirch (PACSI), France), for LC-MS analyses. We also thank Ryan Djemili, Louis Dorin, Florence Konalian, Gomady Vetrivel, Florine Schmidlin, Sarah Vollmer and Gauthier Denninger, students of the IUT Robert Schuman, and Mérouane Belkou for the re-synthesis of some compounds.

## Author Contributions

Conceived and designed the experiments: MZ SM CS HC MPJ JH MH MCK. Performed the experiments: MZ MF SM JD CS WC EAEH FB MS JO AB. Analyzed the data: MZ MF SM JD CS WC EAEH FB DB JH MH MCK. Contributed reagents/materials/analysis tools: SAK PV BD DB MPJ HC. Wrote the paper: JD MZ CS SM JD MPJ JH MH MCK.

## References

1. Dunn GP, Rinne ML, Wykosky J, Genovese G, Quayle SN, Dunn IF, et al. Emerging insights into the molecular and cellular basis of glioblastoma. *Genes Dev.* 2012; 26(8):756–84. doi: [10.1101/gad.187922.112](https://doi.org/10.1101/gad.187922.112) PMID: [22508724](https://pubmed.ncbi.nlm.nih.gov/22508724/)
2. Furnari FB, Fenton T, Bachoo RM, Mukasa A, Stommel JM, Stegh A, et al. Malignant astrocytic glioma: genetics, biology, and paths to treatment. *Genes Dev.* 2007; 21(21):2683–710. PMID: [17974913](https://pubmed.ncbi.nlm.nih.gov/17974913/)
3. Stupp R, Mason WP, van den Bent MJ, Weller M, Fisher B, Taphoorn MJ, et al. Radiotherapy plus concomitant and adjuvant temozolomide for glioblastoma. *N Engl J Med.* 2005; 352(10):987–96. PMID: [15758009](https://pubmed.ncbi.nlm.nih.gov/15758009/)
4. Alifieris C, Trafalis DT. Glioblastoma multiforme: Pathogenesis and treatment. *Pharmacology & therapeutics.* 2015.
5. Cruz MH, Siden A, Calaf GM, Delwar ZM, Yakisich JS. The stemness phenotype model. *ISRN oncology.* 2012; 2012:392647. doi: [10.5402/2012/392647](https://doi.org/10.5402/2012/392647) PMID: [22928120](https://pubmed.ncbi.nlm.nih.gov/22928120/)
6. Frank NY, Schatton T, Frank MH. The therapeutic promise of the cancer stem cell concept. *J Clin Invest.* 2011; 120(1):41–50.
7. Sengupta A, Cancelas JA. Cancer stem cells: a stride towards cancer cure? *J Cell Physiol.* 2010; 225(1):7–14. doi: [10.1002/jcp.22213](https://doi.org/10.1002/jcp.22213) PMID: [20458736](https://pubmed.ncbi.nlm.nih.gov/20458736/)
8. Bonnet D, Dick JE. Human acute myeloid leukemia is organized as a hierarchy that originates from a primitive hematopoietic cell. *Nat Med.* 1997; 3(7):730–7. PMID: [9212098](https://pubmed.ncbi.nlm.nih.gov/9212098/)
9. Frosina G. Frontiers in targeting glioma stem cells. *Eur J Cancer.* 2011; 47(4):496–507. doi: [10.1016/j.ejca.2010.11.017](https://doi.org/10.1016/j.ejca.2010.11.017) PMID: [21185169](https://pubmed.ncbi.nlm.nih.gov/21185169/)
10. Reya T, Morrison SJ, Clarke MF, Weissman IL. Stem cells, cancer, and cancer stem cells. *Nature.* 2001; 414(6859):105–11. PMID: [11689955](https://pubmed.ncbi.nlm.nih.gov/11689955/)
11. Hothi P, Martins TJ, Chen L, Deleyrolle L, Yoon JG, Reynolds B, et al. High-throughput chemical screens identify disulfiram as an inhibitor of human glioblastoma stem cells. *Oncotarget.* 2012; 3(10):1124–36. PMID: [23165409](https://pubmed.ncbi.nlm.nih.gov/23165409/)
12. Pollard SM, Yoshikawa K, Clarke ID, Danovi D, Stricker S, Russell R, et al. Glioma stem cell lines expanded in adherent culture have tumor-specific phenotypes and are suitable for chemical and genetic screens. *Cell Stem Cell.* 2009; 4(6):568–80. doi: [10.1016/j.stem.2009.03.014](https://doi.org/10.1016/j.stem.2009.03.014) PMID: [19497285](https://pubmed.ncbi.nlm.nih.gov/19497285/)
13. Visnyei K, Onodera H, Damoiseaux R, Saigusa K, Petrosyan S, De Vries D, et al. A molecular screening approach to identify and characterize inhibitors of glioblastoma stem cells. *Mol Cancer Ther.* 2011; 10(10):1818–28. doi: [10.1158/1535-7163.MCT-11-0268](https://doi.org/10.1158/1535-7163.MCT-11-0268) PMID: [21859839](https://pubmed.ncbi.nlm.nih.gov/21859839/)
14. Moore N, Lyle S. Quiescent, slow-cycling stem cell populations in cancer: a review of the evidence and discussion of significance. *J Oncol.* 2011.

15. Gao MQ, Choi YP, Kang S, Youn JH, Cho NH. CD24+ cells from hierarchically organized ovarian cancer are enriched in cancer stem cells. *Oncogene*. 2010; 29(18):2672–80. doi: [10.1038/onc.2010.35](https://doi.org/10.1038/onc.2010.35) PMID: [20190812](https://pubmed.ncbi.nlm.nih.gov/20190812/)
16. Haraguchi N, Ishii H, Mimori K, Tanaka F, Ohkuma M, Kim HM, et al. CD13 is a therapeutic target in human liver cancer stem cells. *J Clin Invest*. 2010; 120(9):3326–39. doi: [10.1172/JCI42550](https://doi.org/10.1172/JCI42550) PMID: [20697159](https://pubmed.ncbi.nlm.nih.gov/20697159/)
17. Pece S, Tosoni D, Confalonieri S, Mazzarol G, Vecchi M, Ronzoni S, et al. Biological and molecular heterogeneity of breast cancers correlates with their cancer stem cell content. *Cell*. 2010; 140(1): 62–73. doi: [10.1016/j.cell.2009.12.007](https://doi.org/10.1016/j.cell.2009.12.007) PMID: [20074520](https://pubmed.ncbi.nlm.nih.gov/20074520/)
18. Roesch A, Fukunaga-Kalabis M, Schmidt EC, Zabierowski SE, Brafford PA, Vultur A, et al. A temporally distinct subpopulation of slow-cycling melanoma cells is required for continuous tumor growth. *Cell*. 2010; 141(4):583–94. doi: [10.1016/j.cell.2010.04.020](https://doi.org/10.1016/j.cell.2010.04.020) PMID: [20478252](https://pubmed.ncbi.nlm.nih.gov/20478252/)
19. Dembinski JL, Krauss S. Characterization and functional analysis of a slow cycling stem cell-like subpopulation in pancreas adenocarcinoma. *Clin Exp Metastasis*. 2009; 26(7):611–23. doi: [10.1007/s10585-009-9260-0](https://doi.org/10.1007/s10585-009-9260-0) PMID: [19421880](https://pubmed.ncbi.nlm.nih.gov/19421880/)
20. Guan Y, Gerhard B, Hogge DE. Detection, isolation, and stimulation of quiescent primitive leukemic progenitor cells from patients with acute myeloid leukemia (AML). *Blood*. 2003; 101(8):3142–9. PMID: [12468427](https://pubmed.ncbi.nlm.nih.gov/12468427/)
21. Holyoake T, Jiang X, Eaves C, Eaves A. Isolation of a highly quiescent subpopulation of primitive leukemic cells in chronic myeloid leukemia. *Blood*. 1999; 94(6):2056–64. PMID: [10477735](https://pubmed.ncbi.nlm.nih.gov/10477735/)
22. Meng S, Tripathy D, Frenkel EP, Shete S, Naftalis EZ, Huth JF, et al. Circulating tumor cells in patients with breast cancer dormancy. *Clin Cancer Res*. 2004; 10(24):8152–62. PMID: [15623589](https://pubmed.ncbi.nlm.nih.gov/15623589/)
23. Patru C, Romao L, Varlet P, Coulombel L, Raponi E, Cadusseau J, et al. CD133, CD15/SSEA-1, CD34 or side populations do not resume tumor-initiating properties of long-term cultured cancer stem cells from human malignant glioma-neuronal tumors. *BMC Cancer*. 2010; 10:66. doi: [10.1186/1471-2407-10-66](https://doi.org/10.1186/1471-2407-10-66) PMID: [20181261](https://pubmed.ncbi.nlm.nih.gov/20181261/)
24. Thirant C, Bessette B, Varlet P, Puget S, Cadusseau J, Tavares Sdos R, et al. Clinical relevance of tumor cells with stem-like properties in pediatric brain tumors. *PLoS One*. 2011; 6(1):e16375. doi: [10.1371/journal.pone.0016375](https://doi.org/10.1371/journal.pone.0016375) PMID: [21297991](https://pubmed.ncbi.nlm.nih.gov/21297991/)
25. Zhang JH, Chung TD, Oldenburg KR. A Simple Statistical Parameter for Use in Evaluation and Validation of High Throughput Screening Assays. *J Biomol Screen*. 1999; 4(2):67–73. PMID: [10838414](https://pubmed.ncbi.nlm.nih.gov/10838414/)
26. Perucca P, Cazzalini O, Madine M, Savio M, Laskey RA, Vannini V, et al. Loss of p21 CDKN1A impairs entry to quiescence and activates a DNA damage response in normal fibroblasts induced to quiescence. *Cell Cycle*. 2009; 8(1):105–14. PMID: [19106607](https://pubmed.ncbi.nlm.nih.gov/19106607/)
27. Tai CI, Ying QL. Gbx2, a LIF/Stat3 target, promotes reprogramming to and retention of the pluripotent ground state. *J Cell Sci*. 2013; 126(Pt 5):1093–8. doi: [10.1242/jcs.118273](https://doi.org/10.1242/jcs.118273) PMID: [23345404](https://pubmed.ncbi.nlm.nih.gov/23345404/)
28. Yang G, Xu Y, Chen X, Hu G. IFITM1 plays an essential role in the antiproliferative action of interferon-gamma. *Oncogene*. 2007; 26(4):594–603. PMID: [16847454](https://pubmed.ncbi.nlm.nih.gov/16847454/)
29. Yu F, Ng SS, Chow BK, Sze J, Lu G, Poon WS, et al. Knockdown of interferon-induced transmembrane protein 1 (IFITM1) inhibits proliferation, migration, and invasion of glioma cells. *J Neurooncol*. 2011; 103(2):187–95. doi: [10.1007/s11060-010-0377-4](https://doi.org/10.1007/s11060-010-0377-4) PMID: [20838853](https://pubmed.ncbi.nlm.nih.gov/20838853/)
30. Fareh M, Turchi L, Virolle V, Debruyne D, Almairac F, de-la-Forest Divonne S, et al. The miR 302–367 cluster drastically affects self-renewal and infiltration properties of glioma-initiating cells through CXCR4 repression and consequent disruption of the SHH-GLI-NANOG network. *Cell Death Differ*. 2012.
31. Feve M, Saliou JM, Zeniou M, Lennon S, Carapito C, Dong J, et al. Comparative Expression Study of the Endo-G Protein Coupled Receptor (GPCR) Repertoire in Human Glioblastoma Cancer Stem-like Cells, U87-MG Cells and Non Malignant Cells of Neural Origin Unveils New Potential Therapeutic Targets. *PLoS One*. 2014; 9(3):e91519. doi: [10.1371/journal.pone.0091519](https://doi.org/10.1371/journal.pone.0091519) PMID: [24662753](https://pubmed.ncbi.nlm.nih.gov/24662753/)
32. Jauch R, Hankwitz R, Beschke K, Pelzer H. Bis-(p-hydroxyphenyl)-pyridyl-2-methane: The common laxative principle of Bisacodyl and sodium picosulfate. *Arzneimittelforschung*. 1975; 25(11):1796–800. PMID: [1243088](https://pubmed.ncbi.nlm.nih.gov/1243088/)
33. Chen J, Li Y, Yu TS, McKay RM, Burns DK, Kernie SG, et al. A restricted cell population propagates glioblastoma growth after chemotherapy. *Nature*. 2012; 488(7412):522–6. doi: [10.1038/nature11287](https://doi.org/10.1038/nature11287) PMID: [22854781](https://pubmed.ncbi.nlm.nih.gov/22854781/)
34. Patel AP, Tirosh I, Trombetta JJ, Shalek AK, Gillespie SM, Wakimoto H, et al. Single-cell RNA-seq highlights intratumoral heterogeneity in primary glioblastoma. *Science*. 2014; 344(6190):1396–401. doi: [10.1126/science.1254257](https://doi.org/10.1126/science.1254257) PMID: [24925914](https://pubmed.ncbi.nlm.nih.gov/24925914/)
35. Sosa MS, Bragado P, Aguirre-Ghiso JA. Mechanisms of disseminated cancer cell dormancy: an awakening field. *Nat Rev Cancer*. 2014; 14(9):611–22. doi: [10.1038/nrc3793](https://doi.org/10.1038/nrc3793) PMID: [25118602](https://pubmed.ncbi.nlm.nih.gov/25118602/)

36. Wang SH, Lin SY. Tumor dormancy: potential therapeutic target in tumor recurrence and metastasis prevention. *Experimental hematology & oncology*. 2013; 2(1):29.
37. Komm BS, Mirkin S. An overview of current and emerging SERMs. *The Journal of steroid biochemistry and molecular biology*. 2014.
38. Obrero M, Yu DV, Shapiro DJ. Estrogen receptor-dependent and estrogen receptor-independent pathways for tamoxifen and 4-hydroxytamoxifen-induced programmed cell death. *J Biol Chem*. 2002; 277(47):45695–703. PMID: [12244117](#)
39. Li C, Zhou C, Wang S, Feng Y, Lin W, Lin S, et al. Sensitization of glioma cells to tamoxifen-induced apoptosis by PI3-kinase inhibitor through the GSK-3beta/beta-catenin signaling pathway. *PLoS One*. 2011; 6(10):e27053. doi: [10.1371/journal.pone.0027053](#) PMID: [22046442](#)
40. Guo WZ, Shiina I, Wang Y, Umeda E, Watanabe C, Uetake S, et al. Ridaifen-SB8, a novel tamoxifen derivative, induces apoptosis via reactive oxygen species-dependent signaling pathway. *Biochem Pharmacol*. 2013; 86(9):1272–84. doi: [10.1016/j.bcp.2013.08.020](#) PMID: [23973528](#)
41. Couldwell WT, Hinton DR, He S, Chen TC, Sebat I, Weiss MH, et al. Protein kinase C inhibitors induce apoptosis in human malignant glioma cell lines. *FEBS Lett*. 1994; 345(1):43–6. PMID: [8194597](#)
42. Feng Y, Huang J, Ding Y, Xie F, Shen X. Tamoxifen-induced apoptosis of rat C6 glioma cells via PI3K/Akt, JNK and ERK activation. *Oncology reports*. 2010; 24(6):1561–7. PMID: [21042752](#)
43. DIC A, Carrabba G, Lanfranchi G, Menghetti C, Rampini P, Caroli M. Continuous tamoxifen and dose-dense temozolomide in recurrent glioblastoma. *Anticancer research*. 2013; 33(8):3383–9. PMID: [23898108](#)
44. Jagtap JC, Dawood P, Shah RD, Chandrika G, Natesh K, Shiras A, et al. Expression and regulation of prostate apoptosis response-4 (Par-4) in human glioma stem cells in drug-induced apoptosis. *PLoS One*. 2014; 9(2):e88505. doi: [10.1371/journal.pone.0088505](#) PMID: [24523904](#)
45. Andrews WJ, Panova T, Normand C, Gadal O, Tikhonova IG, Panov KI. Old drug, new target: ellipticines selectively inhibit RNA polymerase I transcription. *J Biol Chem*. 2013; 288(7):4567–82. doi: [10.1074/jbc.M112.411611](#) PMID: [23293027](#)
46. Garbett NC, Graves DE. Extending nature's leads: the anticancer agent ellipticine. *Curr Med Chem Anticancer Agents*. 2004; 4(2):149–72. PMID: [15032720](#)
47. Ohashi M, Sugikawa E, Nakanishi N. Inhibition of p53 protein phosphorylation by 9-hydroxyellipticine: a possible anticancer mechanism. *Jpn J Cancer Res*. 1995; 86(9):819–27. PMID: [7591958](#)
48. Prudent R, Moucadel V, Nguyen CH, Barette C, Schmidt F, Florent JC, et al. Antitumor activity of pyridocarbazole and benzopyrindole derivatives that inhibit protein kinase CK2. *Cancer Res*. 2010; 70(23):9865–74. doi: [10.1158/0008-5472.CAN-10-0917](#) PMID: [21118972](#)
49. Stiborova M, Breuer A, Aimova D, Stiborova-Rupertova M, Wiessler M, Frei E. DNA adduct formation by the anticancer drug ellipticine in rats determined by 32P postlabeling. *Int J Cancer*. 2003; 107(6):885–90. PMID: [14601046](#)
50. Martinkova E, Dontenwill M, Frei E, Stiborova M. Cytotoxicity of and DNA adduct formation by ellipticine in human U87MG glioblastoma cancer cells. *Neuro endocrinology letters*. 2009; 30 Suppl 1:60–6. PMID: [20027146](#)
51. Martinkova E, Maglott A, Leger DY, Bonnet D, Stiborova M, Takeda K, et al. alpha5beta1 integrin antagonists reduce chemotherapy-induced premature senescence and facilitate apoptosis in human glioblastoma cells. *Int J Cancer*. 2010; 127(5):1240–8. doi: [10.1002/ijc.25187](#) PMID: [20099278](#)
52. Stiborova M, Poljakova J, Martinkova E, Borek-Dohalska L, Eckschlager T, Kizek R, et al. Ellipticine cytotoxicity to cancer cell lines—a comparative study. *Interdisciplinary toxicology*. 2011; 4(2):98–105. doi: [10.2478/v10102-011-0017-7](#) PMID: [21753906](#)
53. Stiborova M, Frei E. Ellipticines as DNA-targeted chemotherapeutics. *Curr Med Chem*. 2014; 21(5):575–91. PMID: [24059226](#)
54. Pandrangi SL, Chikati R, Chauhan PS, Kumar CS, Banarji A, Saxena S. Effects of ellipticine on ALDH1A1-expressing breast cancer stem cells—an in vitro and in silico study. *Tumour biology: the journal of the International Society for Oncodevelopmental Biology and Medicine*. 2014; 35(1):723–37.
55. Popper LD, Batra SC. Release of intracellular calcium by prenylamine in human ovarian tumour cells. *Cancer letters*. 1993; 71(1–3):5–10. PMID: [8364898](#)
56. Huang C, Huang C, Cheng J, Liu S, Chen I, Tsai J, et al. Fendiline-evoked [Ca<sup>2+</sup>]<sub>i</sub> rises and non-Ca<sup>2+</sup>-triggered cell death in human oral cancer cells. *Human & experimental toxicology*. 2009; 28(1):41–8.
57. van der Hoeven D, Cho KJ, Ma X, Chigurupati S, Parton RG, Hancock JF. Fendiline inhibits K-Ras plasma membrane localization and blocks K-Ras signal transmission. *Mol Cell Biol*. 2013; 33(2):237–51. doi: [10.1128/MCB.00884-12](#) PMID: [23129805](#)

58. Batra S, Alenfall J. Effect of diverse categories of drugs on human colon tumour cell proliferation. *Anti-cancer research*. 1991; 11(3):1221–4. PMID: [1888153](#)
59. Balgi AD, Fonseca BD, Donohue E, Tsang TC, Lajoie P, Proud CG, et al. Screen for chemical modulators of autophagy reveals novel therapeutic inhibitors of mTORC1 signaling. *PLoS One*. 2009; 4(9): e7124. doi: [10.1371/journal.pone.0007124](#) PMID: [19771169](#)
60. Abdul M, Hoosein N. Expression and activity of potassium ion channels in human prostate cancer. *Cancer letters*. 2002; 186(1):99–105. PMID: [12183081](#)
61. Huang JK, Chang HT, Chou CT, Shu SS, Kuo CC, Tsai JY, et al. The mechanism of sertraline-induced  $[Ca^{2+}]_i$  rise in human PC3 prostate cancer cells. *Basic & clinical pharmacology & toxicology*. 2011; 109(2):103–10.
62. Lin KL, Chi CC, Lu T, Tseng LL, Wang JL, Lu YC, et al. Effect of sertraline on  $[Ca^{2+}]_i$  and viability of human MG63 osteosarcoma cells. *Drug Chem Toxicol*. 2013; 36(2):231–40. doi: [10.3109/01480545.2012.710625](#) PMID: [22931138](#)
63. Tzadok S, Beery E, Israeli M, Uziel O, Lahav M, Fenig E, et al. In vitro novel combinations of psychotropics and anti-cancer modalities in U87 human glioblastoma cells. *International journal of oncology*. 2010; 37(4):1043–51. PMID: [20811727](#)
64. Reddy KK, Lefkove B, Chen LB, Govindarajan B, Carracedo A, Velasco G, et al. The antidepressant sertraline downregulates Akt and has activity against melanoma cells. *Pigment Cell Melanoma Res*. 2008; 21(4):451–6. doi: [10.1111/j.1755-148X.2008.00481.x](#) PMID: [18710373](#)
65. Caudill JS, Brown PD, Cerhan JH, Rummans TA. Selective serotonin reuptake inhibitors, glioblastoma multiforme, and impact on toxicities and overall survival: the mayo clinic experience. *Am J Clin Oncol*. 2011; 34(4):385–7. PMID: [20859197](#)
66. Walker AJ, Grainge M, Bates TE, Card TR. Survival of glioma and colorectal cancer patients using tricyclic antidepressants post-diagnosis. *Cancer Causes Control*. 2012; 23(12):1959–64. doi: [10.1007/s10552-012-0073-0](#) PMID: [23065071](#)
67. Kast RE, Boockvar JA, Bruning A, Cappello F, Chang WW, Cvek B, et al. A conceptually new treatment approach for relapsed glioblastoma: coordinated undermining of survival paths with nine repurposed drugs (CUSP9) by the International Initiative for Accelerated Improvement of Glioblastoma Care. *Oncotarget*. 2013; 4(4):502–30. PMID: [23594434](#)
68. Hashimoto H, Messerli SM, Sudo T, Maruta H. Ivermectin inactivates the kinase PAK1 and blocks the PAK1-dependent growth of human ovarian cancer and NF2 tumor cell lines. *Drug Discov Ther*. 2009; 3(6):243–6. PMID: [22495656](#)
69. Hashimoto H, Sudo T, Maruta H, Nishimura R. The direct PAK1 inhibitor, TAT-PAK18, blocks preferentially the growth of human ovarian cancer cell lines in which PAK1 is abnormally activated by autophosphorylation at Thr 423. *Drug Discov Ther*. 2010; 4(1):1–4. PMID: [22491145](#)
70. Sharmeen S, Skrtic M, Sukhai MA, Hurren R, Gronda M, Wang X, et al. The antiparasitic agent ivermectin induces chloride-dependent membrane hyperpolarization and cell death in leukemia cells. *Blood*. 2010; 116(18):3593–603. doi: [10.1182/blood-2010-01-262675](#) PMID: [20644115](#)
71. Lokich E, Singh RK, Han A, Romano N, Yano N, Kim K, et al. HE4 expression is associated with hormonal elements and mediated by importin-dependent nuclear translocation. *Sci Rep*. 2014; 4:5500. doi: [10.1038/srep05500](#) PMID: [24975515](#)
72. Niu YP, Li LD, Wu LM. Beta-aescin: a potent natural inhibitor of proliferation and inducer of apoptosis in human chronic myeloid leukemia K562 cells in vitro. *Leuk Lymphoma*. 2008; 49(7):1384–91. doi: [10.1080/10428190802090151](#) PMID: [18452082](#)
73. Zhou XY, Fu FH, Li Z, Dong QJ, He J, Wang CH. Escin, a natural mixture of triterpene saponins, exhibits antitumor activity against hepatocellular carcinoma. *Planta Med*. 2009; 75(15):1580–5. doi: [10.1055/s-0029-1185838](#) PMID: [19579181](#)
74. Tan SM, Li F, Rajendran P, Kumar AP, Hui KM, Sethi G. Identification of beta-escin as a novel inhibitor of signal transducer and activator of transcription 3/Janus-activated kinase 2 signaling pathway that suppresses proliferation and induces apoptosis in human hepatocellular carcinoma cells. *J Pharmacol Exp Ther*. 2010; 334(1):285–93. doi: [10.1124/jpet.110.165498](#) PMID: [20378717](#)
75. Shen DY, Kang JH, Song W, Zhang WQ, Li WG, Zhao Y, et al. Apoptosis of human cholangiocarcinoma cell lines induced by beta-escin through mitochondrial caspase-dependent pathway. *Phytotherapy research: PTR*. 2011; 25(10):1519–26. doi: [10.1002/ptr.3435](#) PMID: [21394804](#)
76. Ji DB, Xu B, Liu JT, Ran FX, Cui JR. beta-Escin sodium inhibits inducible nitric oxide synthase expression via downregulation of the JAK/STAT pathway in A549 cells. *Mol Carcinog*. 2011; 50(12):945–60. doi: [10.1002/mc.20762](#) PMID: [21400616](#)



77. Zhang Z, Gao J, Cai X, Zhao Y, Wang Y, Lu W, et al. Escin sodium induces apoptosis of human acute leukemia Jurkat T cells. *Phytotherapy research: PTR*. 2011; 25(12):1747–55. doi: [10.1002/ptr.3457](https://doi.org/10.1002/ptr.3457) PMID: [21452372](https://pubmed.ncbi.nlm.nih.gov/21452372/)
78. Seweryn E, Glensk M, Sroda-Pomianek K, Ceremuga I, Włodarczyk M, Gamian A. Cytotoxic effects of four aescin types on human colon adenocarcinoma cell lines. *Nat Prod Commun*. 2014; 9(3): 387–90. PMID: [24689224](https://pubmed.ncbi.nlm.nih.gov/24689224/)
79. Rimmon A, Vexler A, Berkovich L, Earon G, Ron I, Lev-Ari S. Escin Chemosensitizes Human Pancreatic Cancer Cells and Inhibits the Nuclear Factor-kappaB Signaling Pathway. *Biochemistry research international*. 2013; 2013:251752. doi: [10.1155/2013/251752](https://doi.org/10.1155/2013/251752) PMID: [24282639](https://pubmed.ncbi.nlm.nih.gov/24282639/)
80. Harikumar KB, Sung B, Pandey MK, Guha S, Krishnan S, Aggarwal BB. Escin, a pentacyclic triterpene, chemosensitizes human tumor cells through inhibition of nuclear factor-kappaB signaling pathway. *Mol Pharmacol*. 2010; 77(5):818–27. doi: [10.1124/mol.109.062760](https://doi.org/10.1124/mol.109.062760) PMID: [20103608](https://pubmed.ncbi.nlm.nih.gov/20103608/)
81. Gupta SC, Tyagi AK, Deshmukh-Taskar P, Hinojosa M, Prasad S, Aggarwal BB. Downregulation of tumor necrosis factor and other proinflammatory biomarkers by polyphenols. *Arch Biochem Biophys*. 2014.
82. Braconi C, Swenson E, Kogure T, Huang N, Patel T. Targeting the IL-6 dependent phenotype can identify novel therapies for cholangiocarcinoma. *PLoS One*. 2010; 5(12):e15195. doi: [10.1371/journal.pone.0015195](https://doi.org/10.1371/journal.pone.0015195) PMID: [21179572](https://pubmed.ncbi.nlm.nih.gov/21179572/)
83. Garcia-Quiroz J, Camacho J. Astemizole: an old anti-histamine as a new promising anti-cancer drug. *Anti-cancer agents in medicinal chemistry*. 2011; 11(3):307–14. PMID: [21443504](https://pubmed.ncbi.nlm.nih.gov/21443504/)
84. Nelson MP, Shacka JJ. Autophagy Modulation in Disease Therapy: Where Do We Stand? *Curr Pathobiol Rep*. 2013; 1(4):239–45. PMID: [24470989](https://pubmed.ncbi.nlm.nih.gov/24470989/)
85. de Guadalupe Chavez-Lopez M, Hernandez-Gallegos E, Vazquez-Sanchez AY, Gariglio P, Camacho J. Antiproliferative and proapoptotic effects of astemizole on cervical cancer cells. *Int J Gynecol Cancer*. 2014; 24(5):824–8. PMID: [24819656](https://pubmed.ncbi.nlm.nih.gov/24819656/)
86. Hemmerlein B, Weseloh RM, Mello de Queiroz F, Knotgen H, Sanchez A, Rubio ME, et al. Overexpression of Eag1 potassium channels in clinical tumours. *Mol Cancer*. 2006; 5:41. PMID: [17022810](https://pubmed.ncbi.nlm.nih.gov/17022810/)
87. Pardo LA, Suhmer W. Eag1 as a cancer target. *Expert Opin Ther Targets*. 2008; 12(7):837–43. doi: [10.1517/14728222.12.7.837](https://doi.org/10.1517/14728222.12.7.837) PMID: [18554152](https://pubmed.ncbi.nlm.nih.gov/18554152/)
88. Asher V, Sowter H, Shaw R, Bali A, Khan R. Eag and HERG potassium channels as novel therapeutic targets in cancer. *World J Surg Oncol*. 2010; 8:113. doi: [10.1186/1477-7819-8-113](https://doi.org/10.1186/1477-7819-8-113) PMID: [21190577](https://pubmed.ncbi.nlm.nih.gov/21190577/)
89. Roy J, Vantol B, Cowley EA, Blay J, Linsdell P. Pharmacological separation of hEAG and hERG K<sup>+</sup> channel function in the human mammary carcinoma cell line MCF-7. *Oncology reports*. 2008; 19(6): 1511–6. PMID: [18497958](https://pubmed.ncbi.nlm.nih.gov/18497958/)
90. Liu JD, Wang YJ, Chen CH, Yu CF, Chen LC, Lin JK, et al. Molecular mechanisms of G0/G1 cell-cycle arrest and apoptosis induced by terfenadine in human cancer cells. *Mol Carcinog*. 2003; 37(1): 39–50. PMID: [12720299](https://pubmed.ncbi.nlm.nih.gov/12720299/)
91. Blaya B, Nicolau-Galmes F, Jangi SM, Ortega-Martinez I, Alonso-Tejerina E, Burgos-Bretones J, et al. Histamine and histamine receptor antagonists in cancer biology. *Inflamm Allergy Drug Targets*. 2010; 9(3):146–57. PMID: [20632959](https://pubmed.ncbi.nlm.nih.gov/20632959/)
92. Hadzijusufovic E, Peter B, Gleixner KV, Schuch K, Pickl WF, Thaiwong T, et al. H1-receptor antagonists terfenadine and loratadine inhibit spontaneous growth of neoplastic mast cells. *Exp Hematol*. 2010; 38(10):896–907. doi: [10.1016/j.exphem.2010.05.008](https://doi.org/10.1016/j.exphem.2010.05.008) PMID: [20570632](https://pubmed.ncbi.nlm.nih.gov/20570632/)
93. Jangi SM, Ruiz-Larrea MB, Nicolau-Galmes F, Andollo N, Arroyo-Berdugo Y, Ortega-Martinez I, et al. Terfenadine-induced apoptosis in human melanoma cells is mediated through Ca<sup>2+</sup> homeostasis modulation and tyrosine kinase activity, independently of H1 histamine receptors. *Carcinogenesis*. 2008; 29(3):500–9. doi: [10.1093/carcin/bgm292](https://doi.org/10.1093/carcin/bgm292) PMID: [18174239](https://pubmed.ncbi.nlm.nih.gov/18174239/)
94. Nicolau-Galmes F, Asumendi A, Alonso-Tejerina E, Perez-Yarza G, Jangi SM, Gardeazabal J, et al. Terfenadine induces apoptosis and autophagy in melanoma cells through ROS-dependant and -independent mechanisms. *Apoptosis*. 2011; 16(12):1253–67. doi: [10.1007/s10495-011-0640-y](https://doi.org/10.1007/s10495-011-0640-y) PMID: [21861192](https://pubmed.ncbi.nlm.nih.gov/21861192/)
95. Wang WT, Chen YH, Hsu JL, Leu WJ, Yu CC, Chan SH, et al. Terfenadine induces anti-proliferative and apoptotic activities in human hormone-refractory prostate cancer through histamine receptor-independent Mcl-1 cleavage and Bak up-regulation. *Naunyn-Schmiedeberg's archives of pharmacology*. 2014; 387(1):33–45. doi: [10.1007/s00210-013-0912-x](https://doi.org/10.1007/s00210-013-0912-x) PMID: [24048439](https://pubmed.ncbi.nlm.nih.gov/24048439/)
96. Hey JA, del Prado M, Sherwood J, Kreutner W, Egan RW. Comparative analysis of the cardiotoxicity proclivities of second generation antihistamines in an experimental model predictive of adverse clinical ECG effects. *Arzneimittelforschung*. 1996; 46(2):153–8. PMID: [8720304](https://pubmed.ncbi.nlm.nih.gov/8720304/)

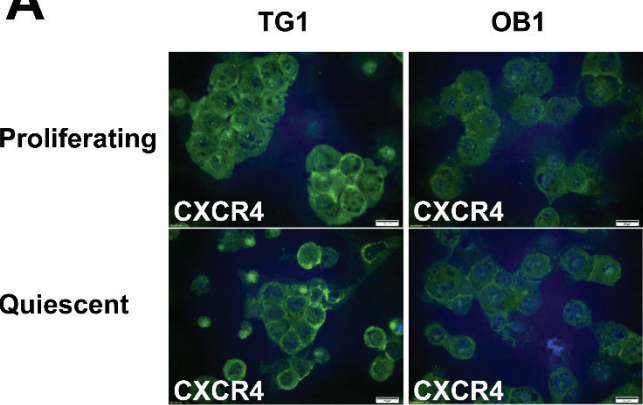
97. Roberts DJ. Cardiotoxicity of second-generation antihistamines. *Drugs*. 1999; 57(6):1033–4. PMID: [10400411](#)
98. Paakkari I. Cardiotoxicity of new antihistamines and cisapride. *Toxicol Lett*. 2002; 127(1–3):279–84. PMID: [12052668](#)
99. Qian JY, Guo L. Altered cytosolic Ca<sup>2+</sup> dynamics in cultured Guinea pig cardiomyocytes as an in vitro model to identify potential cardiotoxicants. *Toxicol In Vitro*. 2010; 24(3):960–72. doi: [10.1016/j.tiv.2009.12.027](#) PMID: [20064605](#)
100. Wiedhopf RM, Young M, Bianchi E, Cole JR. Tumor inhibitory agent from *Magnolia grandiflora* (Magnoliaceae). I. Parthenolide. *J Pharm Sci*. 1973; 62(2):345.
101. Hoffmann JJ, Torrance SJ, Wiedhopf RM, Cole JR. Cytotoxic agents from *Michelia champaca* and *Talauma ovata*: parthenolide and costunolide. *J Pharm Sci*. 1977; 66(6):883–4. PMID: [889597](#)
102. Anderson KN, Bejcek BE. Parthenolide induces apoptosis in glioblastomas without affecting NF-kappaB. *J Pharmacol Sci*. 2008; 106(2):318–20. PMID: [18277052](#)
103. Zanutto-Filho A, Braganhol E, Schroder R, de Souza LH, Dalmolin RJ, Pasquali MA, et al. NFkappaB inhibitors induce cell death in glioblastomas. *Biochem Pharmacol*. 2011; 81(3):412–24. doi: [10.1016/j.bcp.2010.10.014](#) PMID: [21040711](#)
104. Nakabayashi H, Shimizu K. Involvement of Akt/NF-kappaB pathway in antitumor effects of parthenolide on glioblastoma cells in vitro and in vivo. *BMC Cancer*. 2012; 12:453. doi: [10.1186/1471-2407-12-453](#) PMID: [23039130](#)
105. Zhao X, Liu X, Su L. Parthenolide induces apoptosis via TNFRSF10B and PMAIP1 pathways in human lung cancer cells. *J Exp Clin Cancer Res*. 2014; 33:3. doi: [10.1186/1756-9966-33-3](#) PMID: [24387758](#)
106. Carlisi D, D'Anneo A, Martinez R, Emanuele S, Buttitta G, Di Fiore R, et al. The oxygen radicals involved in the toxicity induced by parthenolide in MDA-MB-231 cells. *Oncology reports*. 2014; 32(1):167–72. doi: [10.3892/or.2014.3212](#) PMID: [24859613](#)
107. Sun J, Zhang C, Bao YL, Wu Y, Chen ZL, Yu CL, et al. Parthenolide-Induced Apoptosis, Autophagy and Suppression of Proliferation in HepG2 Cells. *Asian Pac J Cancer Prev*. 2014; 15(12):4897–902. PMID: [24998560](#)
108. Janganani V, Penthala NR, Madadi NR, Chen Z, Crooks PA. Anti-cancer activity of carbamate derivatives of melampomagnolide B. *Bioorganic & medicinal chemistry letters*. 2014; 24(15):3499–502.
109. Varga A, Sabat R, Mucsi I, Flores VC, Kaiser HE, Molnar J. Effects of butaclamol, clopenthixol, mepromazine and cannabinal stereoisomers on apoptosis induction. *Anticancer research*. 2001; 21(4A):2709–12. PMID: [11724344](#)
110. Hyttel J, Christensen AV. Biochemical and pharmacological differentiation of neuroleptic effect on dopamine D-1 and D-2 receptors. *J Neural Transm Suppl*. 1983; 18:157–64. PMID: [6135740](#)
111. Somberg JC, Molnar J. The pleiotropic effects of ethacrynic acid. *Am J Ther*. 2009; 16(1):102–4. PMID: [19142157](#)
112. Byun SS, Kim SW, Choi H, Lee C, Lee E. Augmentation of cisplatin sensitivity in cisplatin-resistant human bladder cancer cells by modulating glutathione concentrations and glutathione-related enzyme activities. *BJU Int*. 2005; 95(7):1086–90. PMID: [15839938](#)
113. Depeille P, Cuq P, Passagne I, Evrard A, Vian L. Combined effects of GSTP1 and MRP1 in melanoma drug resistance. *Br J Cancer*. 2005; 93(2):216–23. PMID: [15999103](#)
114. Wang R, Liu C, Xia L, Zhao G, Gabrilove J, Waxman S, et al. Ethacrynic acid and a derivative enhance apoptosis in arsenic trioxide-treated myeloid leukemia and lymphoma cells: the role of glutathione S-transferase p1-1. *Clin Cancer Res*. 2012; 18(24):6690–701. doi: [10.1158/1078-0432.CCR-12-0770](#) PMID: [23082001](#)
115. Musdal Y, Hegazy UM, Aksoy Y, Mannervik B. FDA-approved drugs and other compounds tested as inhibitors of human glutathione transferase P1-1. *Chemico-biological interactions*. 2013; 205(1):53–62. doi: [10.1016/j.cbi.2013.06.003](#) PMID: [23769903](#)
116. Juillerat-Jeanneret L, Bernasconi CC, Bricod C, Gros S, Trepey S, Benhattar J, et al. Heterogeneity of human glioblastoma: glutathione-S-transferase and methylguanine-methyltransferase. *Cancer Invest*. 2008; 26(6):597–609. doi: [10.1080/07357900802072913](#) PMID: [18584351](#)
117. Schmeel LC, Schmeel FC, Kim Y, Endo T, Lu D, Schmidt-Wolf IG. Targeting the Wnt/beta-catenin pathway in multiple myeloma. *Anticancer research*. 2013; 33(11):4719–26. PMID: [24222106](#)
118. Kim Y, Gast SM, Endo T, Lu D, Carson D, Schmidt-Wolf IG. In vivo efficacy of the diuretic agent ethacrynic acid against multiple myeloma. *Leuk Res*. 2012; 36(5):598–600. doi: [10.1016/j.leukres.2012.01.025](#) PMID: [22386728](#)

119. Schmidt M, Sievers E, Endo T, Lu D, Carson D, Schmidt-Wolf IG. Targeting Wnt pathway in lymphoma and myeloma cells. *Br J Haematol*. 2009; 144(5):796–8. doi: [10.1111/j.1365-2141.2008.07503.x](https://doi.org/10.1111/j.1365-2141.2008.07503.x) PMID: [19036118](https://pubmed.ncbi.nlm.nih.gov/19036118/)
120. Lu D, Liu JX, Endo T, Zhou H, Yao S, Willert K, et al. Ethacrynic acid exhibits selective toxicity to chronic lymphocytic leukemia cells by inhibition of the Wnt/beta-catenin pathway. *PLoS One*. 2009; 4(12):e8294. doi: [10.1371/journal.pone.0008294](https://doi.org/10.1371/journal.pone.0008294) PMID: [20011538](https://pubmed.ncbi.nlm.nih.gov/20011538/)
121. Koller CM, Kim Y, Schmidt-Wolf IG. Targeting renal cancer with a combination of WNT inhibitors and a bi-functional peptide. *Anticancer research*. 2013; 33(6):2435–40. PMID: [23749892](https://pubmed.ncbi.nlm.nih.gov/23749892/)
122. Lopez-Lazaro M. Distribution and biological activities of the flavonoid luteolin. *Mini Rev Med Chem*. 2009; 9(1):31–59. PMID: [19149659](https://pubmed.ncbi.nlm.nih.gov/19149659/)
123. Seelinger G, Merfort I, Schempp CM. Anti-oxidant, anti-inflammatory and anti-allergic activities of luteolin. *Planta Med*. 2008; 74(14):1667–77. doi: [10.1055/s-0028-1088314](https://doi.org/10.1055/s-0028-1088314) PMID: [18937165](https://pubmed.ncbi.nlm.nih.gov/18937165/)
124. Gabor M. Anti-inflammatory and anti-allergic properties of flavonoids. *Prog Clin Biol Res*. 1986; 213:471–80. PMID: [2872680](https://pubmed.ncbi.nlm.nih.gov/2872680/)
125. Weng CJ, Yen GC. Flavonoids, a ubiquitous dietary phenolic subclass, exert extensive in vitro anti-invasive and in vivo anti-metastatic activities. *Cancer Metastasis Rev*. 2012; 31(1–2):323–51. doi: [10.1007/s10555-012-9347-y](https://doi.org/10.1007/s10555-012-9347-y) PMID: [22314287](https://pubmed.ncbi.nlm.nih.gov/22314287/)
126. Lin Y, Shi R, Wang X, Shen HM. Luteolin, a flavonoid with potential for cancer prevention and therapy. *Curr Cancer Drug Targets*. 2008; 8(7):634–46. PMID: [18991571](https://pubmed.ncbi.nlm.nih.gov/18991571/)
127. Kandaswami C, Lee LT, Lee PP, Hwang JJ, Ke FC, Huang YT, et al. The antitumor activities of flavonoids. *In Vivo*. 2005; 19(5):895–909. PMID: [16097445](https://pubmed.ncbi.nlm.nih.gov/16097445/)
128. Aneknan P, Kukongviriyapan V, Prawan A, Kongpetch S, Sripan B, Senggunprai L. Luteolin Arrests Cell Cycling, Induces Apoptosis and Inhibits the JAK/STAT3 Pathway in Human Cholangiocarcinoma Cells. *Asian Pac J Cancer Prev*. 2014; 15(12):5071–6. PMID: [24998588](https://pubmed.ncbi.nlm.nih.gov/24998588/)
129. Wu H, Huang M, Liu Y, Shu Y, Liu P. Luteolin Induces Apoptosis by Up-regulating miR-34a in Human Gastric Cancer Cells. *Technol Cancer Res Treat*. 2014.
130. Zhang H, Li X, Zhang Y, Luan X. Luteolin induces apoptosis by activating Fas signaling pathway at the receptor level in laryngeal squamous cell line Hep-2 cells. *Eur Arch Otorhinolaryngol*. 2014; 271(6):1653–9. doi: [10.1007/s00405-014-2903-z](https://doi.org/10.1007/s00405-014-2903-z) PMID: [24477342](https://pubmed.ncbi.nlm.nih.gov/24477342/)
131. Hong Z, Cao X, Li N, Zhang Y, Lan L, Zhou Y, et al. Luteolin is effective in the non-small cell lung cancer model with L858R/T790M EGF receptor mutation and erlotinib resistance. *Br J Pharmacol*. 2014; 171(11):2842–53. doi: [10.1111/bph.12610](https://doi.org/10.1111/bph.12610) PMID: [24471765](https://pubmed.ncbi.nlm.nih.gov/24471765/)
132. Ding S, Hu A, Hu Y, Ma J, Weng P, Dai J. Anti-hepatoma cells function of luteolin through inducing apoptosis and cell cycle arrest. *Tumour biology: the journal of the International Society for Oncodevelopmental Biology and Medicine*. 2014; 35(4):3053–60.
133. Khan HY, Zubair H, Faisal M, Ullah MF, Farhan M, Sarkar FH, et al. Plant polyphenol induced cell death in human cancer cells involves mobilization of intracellular copper ions and reactive oxygen species generation: a mechanism for cancer chemopreventive action. *Mol Nutr Food Res*. 2014; 58(3):437–46. doi: [10.1002/mnfr.201300417](https://doi.org/10.1002/mnfr.201300417) PMID: [24123728](https://pubmed.ncbi.nlm.nih.gov/24123728/)
134. Sakurai MA, Ozaki Y, Okuzaki D, Naito Y, Sasakura T, Okamoto A, et al. Gefitinib and Luteolin Cause Growth Arrest of Human Prostate Cancer PC-3 Cells via Inhibition of Cyclin G-Associated Kinase and Induction of miR-630. *PLoS One*. 2014; 9(6):e100124. doi: [10.1371/journal.pone.0100124](https://doi.org/10.1371/journal.pone.0100124) PMID: [24971999](https://pubmed.ncbi.nlm.nih.gov/24971999/)
135. Cheng WY, Chiao MT, Liang YJ, Yang YC, Shen CC, Yang CY. Luteolin inhibits migration of human glioblastoma U-87 MG and T98G cells through downregulation of Cdc42 expression and PI3K/AKT activity. *Mol Biol Rep*. 2013; 40(9):5315–26. doi: [10.1007/s11033-013-2632-1](https://doi.org/10.1007/s11033-013-2632-1) PMID: [23677714](https://pubmed.ncbi.nlm.nih.gov/23677714/)
136. Feng X, Zhou Q, Liu C, Tao ML. Drug screening study using glioma stem-like cells. *Mol Med Rep*. 2012; 6(5):1117–20. doi: [10.3892/mmr.2012.1040](https://doi.org/10.3892/mmr.2012.1040) PMID: [22923060](https://pubmed.ncbi.nlm.nih.gov/22923060/)
137. Butts A, DiDone L, Koselny K, Baxter BK, Chabrier-Rosello Y, Wellington M, et al. A repurposing approach identifies off-patent drugs with fungicidal cryptococcal activity, a common structural chemotype, and pharmacological properties relevant to the treatment of cryptococcosis. *Eukaryot Cell*. 2013; 12(2):278–87. doi: [10.1128/EC.00314-12](https://doi.org/10.1128/EC.00314-12) PMID: [23243064](https://pubmed.ncbi.nlm.nih.gov/23243064/)
138. Germain AR, Carmody LC, Morgan B, Fernandez C, Forbeck E, Lewis TA, et al. Identification of a selective small molecule inhibitor of breast cancer stem cells. *Bioorganic & medicinal chemistry letters*. 2012; 22(10):3571–4.
139. Gupta PB, Onder TT, Jiang G, Tao K, Kuperwasser C, Weinberg RA, et al. Identification of selective inhibitors of cancer stem cells by high-throughput screening. *Cell*. 2009; 138(4):645–59. doi: [10.1016/j.cell.2009.06.034](https://doi.org/10.1016/j.cell.2009.06.034) PMID: [19682730](https://pubmed.ncbi.nlm.nih.gov/19682730/)

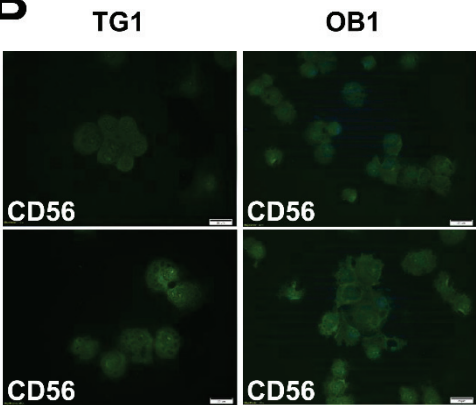


# S1 Figure

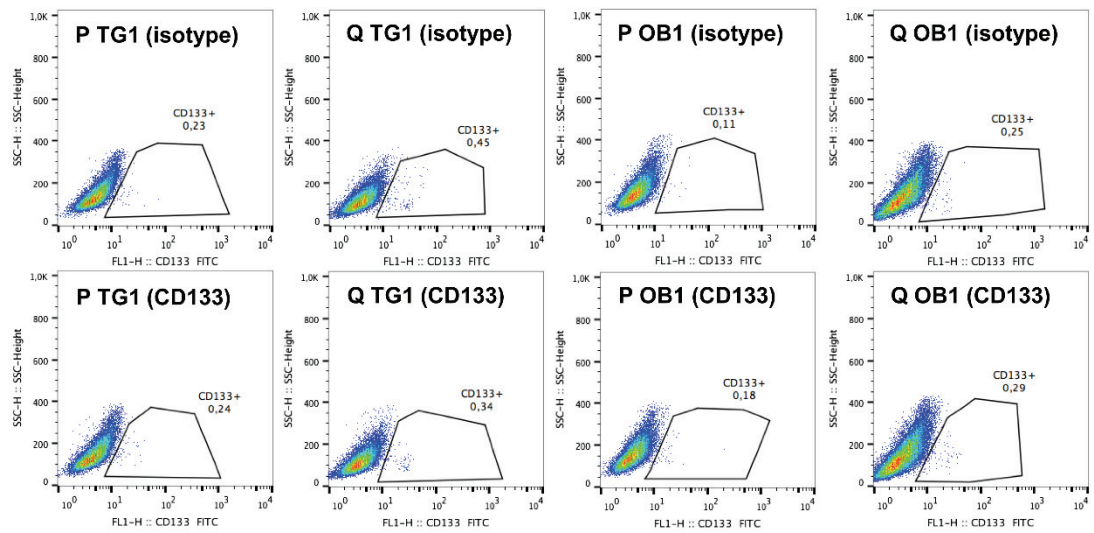
**A**



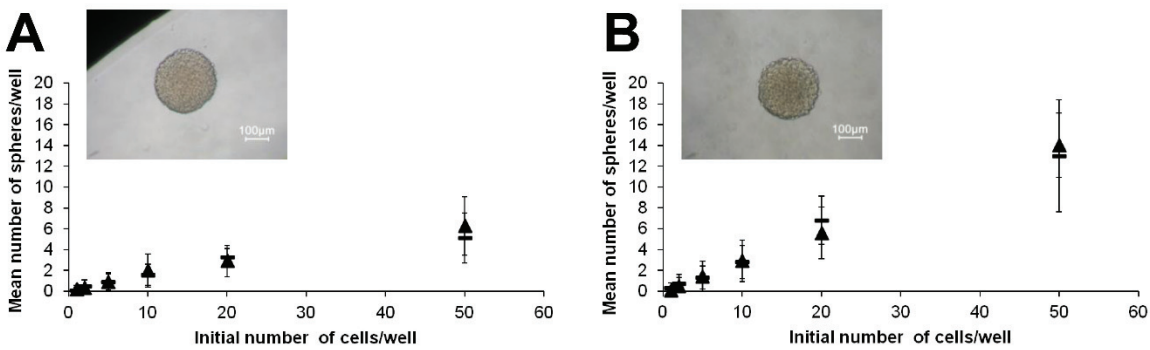
**B**



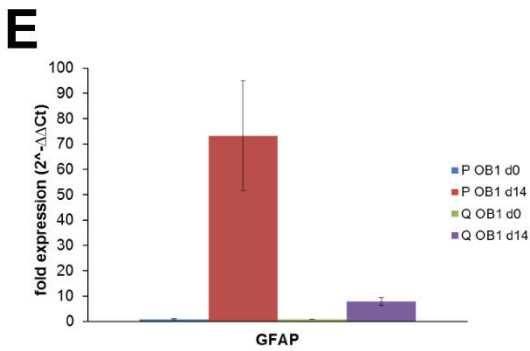
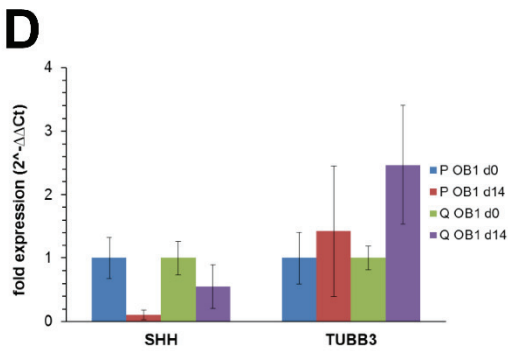
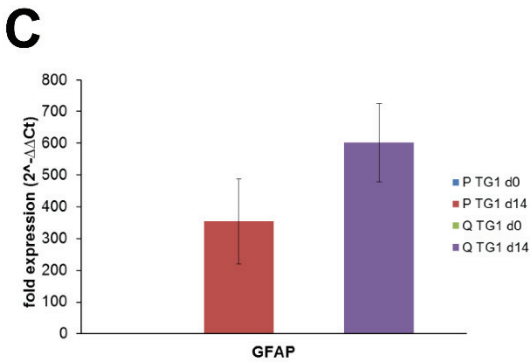
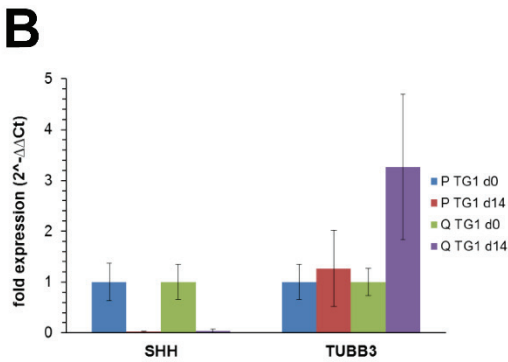
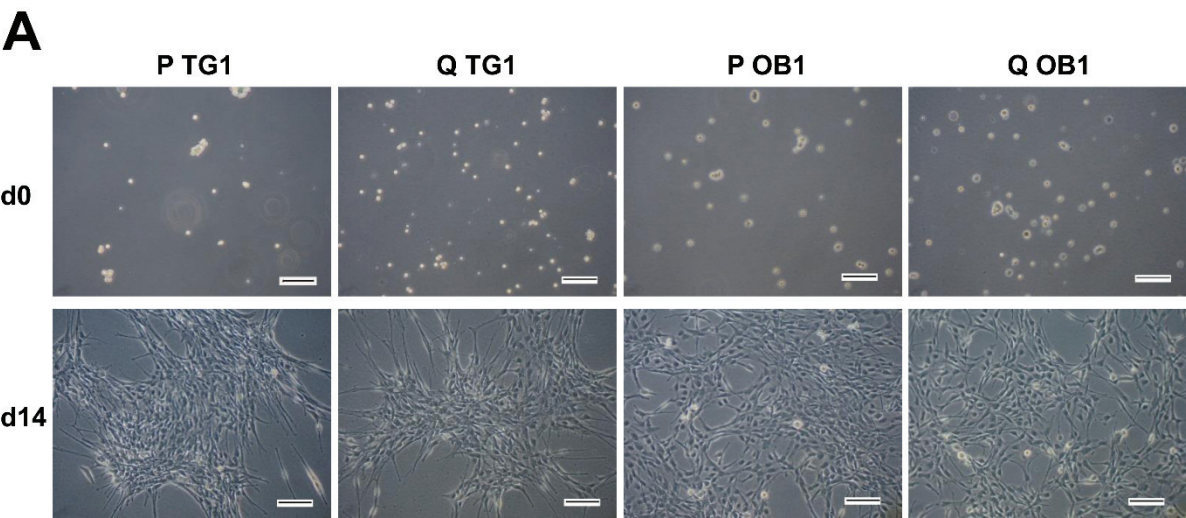
**C**



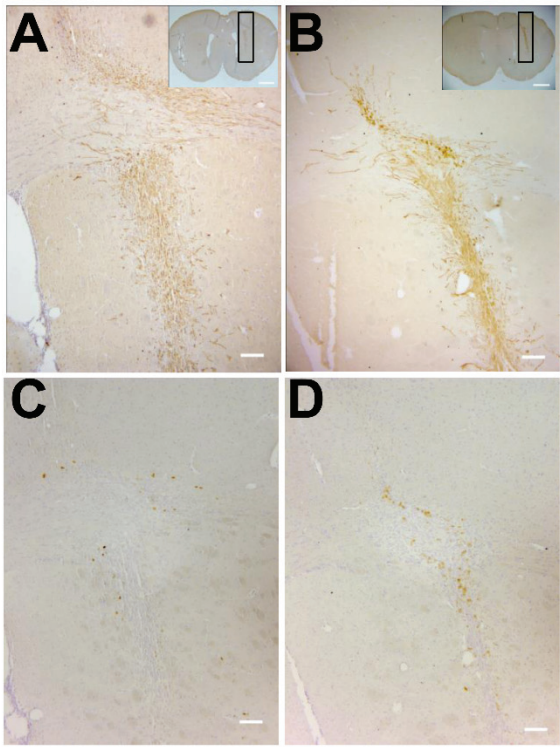
# S2 Figure



# S3 Figure



**S4 Figure**



## **Part II. Study of bisacodyl signaling pathways in GSCs: involvement of WNK1 and its signaling partners**

Under the high throughput screening conditions, bisacodyl/DDPM had a cytotoxic activity only towards quiescent GSCs obtained in the absence of medium renewal for several days. It was subsequently shown in the lab that bisacodyl/DDPM are also active on proliferating GSCs upon acidification of their culture medium. Moreover, GSCs induced *in vitro* to quiescence, resulting in an acidification of their extracellular medium, were protected from bisacodyl/DDPM action when medium pH was adjusted to physiological pH values. Interestingly, bisacodyl/DDPM were also active on clonal GSC-derived macro-neurospheres, a 3D culture model developed and characterized in our lab. Such macro-tumorspheres partly mimic the complexity of intratumoral microenvironments in glioblastoma (Figure 15 and Figure 16). Indeed, hematoxylin/eosin (H/E) staining revealed that the external part of GSC-derived macro-tumorspheres is composed of living cells whereas the center is necrotic. Ki67 immunostaining showed that peripheral living cells express this proliferation marker at different levels. Only the cells at the outer edge of the sphere rim were showing a high proliferation activity. Quiescent cells lacking expression of Ki67 are present in the inner layers of the sphere close to the necrotic center. Additionally, the oxygen distribution within spheres was measured using a hypoxyprobe. As expected, a hypoxic zone was present near the necrotic center. Cells within this region also preferentially express glucose transporters GLUT1/3. GLUT-1 expression is a marker of hypoxia which favors glycolytic mechanisms and acidification of the extracellular microenvironment of cells in these conditions (Figure 15). Bisacodyl/DDPM treatment of clonal GSC-derived tumorspheres induced a disruption of spheres and cell death which was confirmed using a cell viability assay (Figure 16). Interestingly, H/E staining demonstrated that the bisacodyl/DDPM-induced cell death occurred in cells located in the inner layers of the sphere rim which correspond to quiescent slow-growing cells maintained in hypoxic/acidic conditions (Figure 16). In the same study, bisacodyl/DDPM anti-tumor activity was demonstrated in an orthotopic mouse model of glioblastoma (Figure 17). Finally, bisacodyl/DDPM was shown to interfere with inositol 1,4,5-triphosphate receptor (IP3R1)-mediated intracellular calcium release induced by acetylcholine and carbachol in quiescent GSCs and higher levels of IP3R1



expression were observed under quiescent culture conditions. More details concerning these data can be found in Dong et al. 2017 [243].

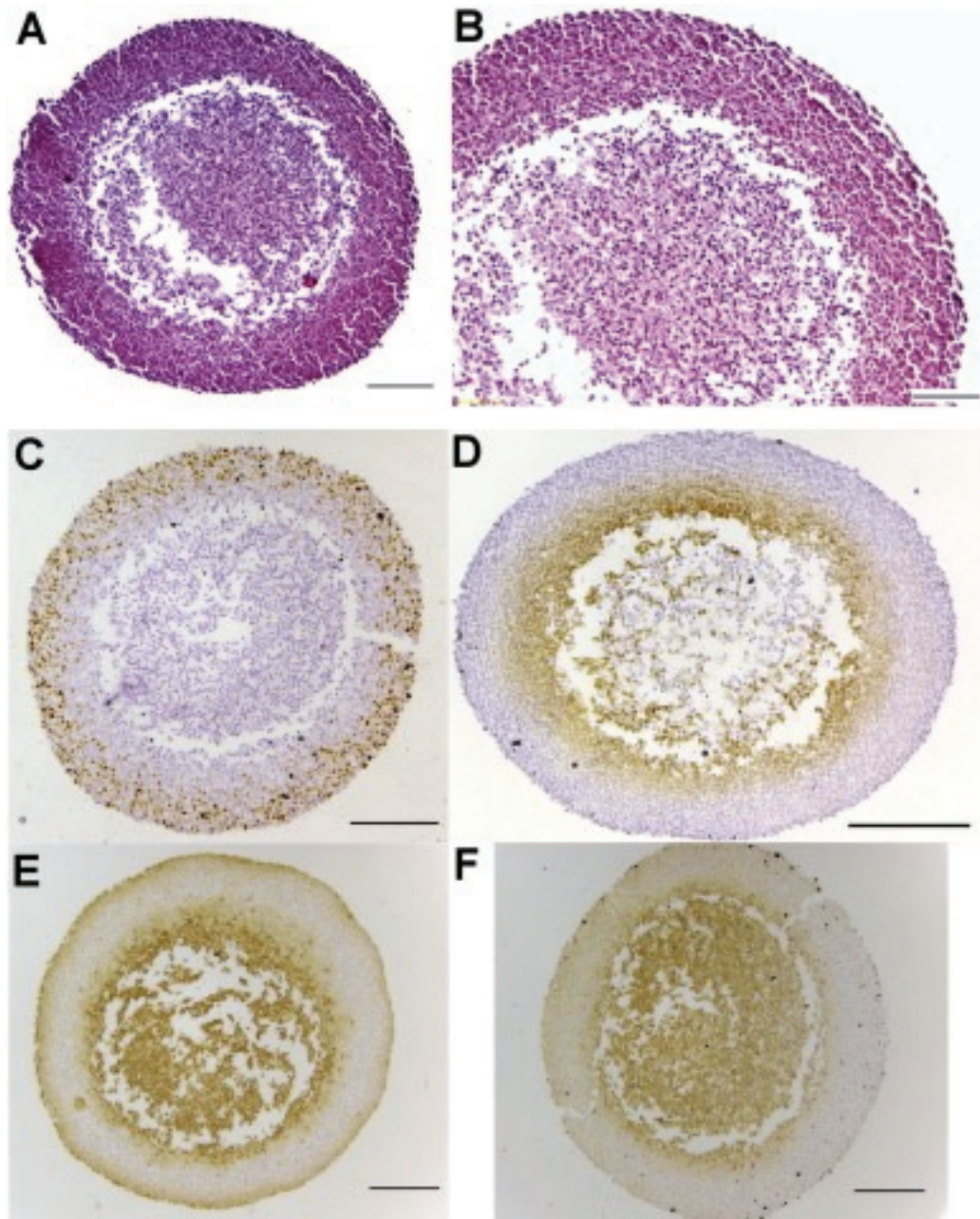


**Figure 15. Clonal 3D glioblastoma stem-like cell-derived macro-tumorspheres share many aspects of glioblastoma tumors, from [242].** **A/B.** Hematoxylin/eosin staining of sphere sections. Clonal macro-tumorspheres present a necrotic center and outer layer high cellularity regions. **C.** Ki67 proliferation marker immunostaining. Proliferating cells are located at the sphere periphery whereas inner layer cells do not express this proliferation marker. **D.** Detection of hypoxic zones by using the Hypoxyprobe™-1 kit. **E/F.** GLUT1 (E) and GLUT3 (F) sphere section immunostaining. Hypoxic regions are found near the necrotic center. Scale bar: 200  $\mu\text{m}$  for all except B (100  $\mu\text{m}$ ).

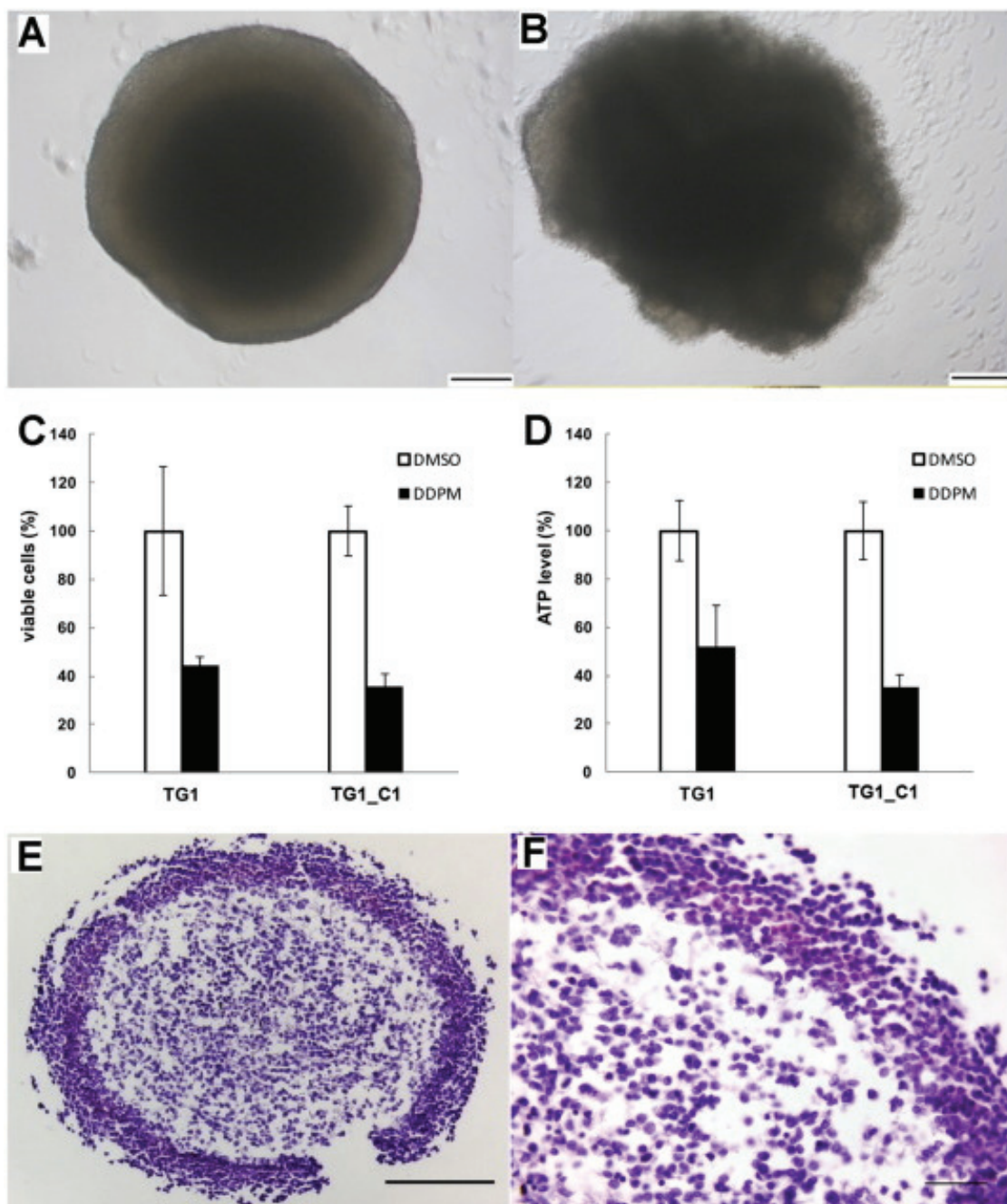


**Figure 16. Effect of DDPM on clonal macro-tumorspheres obtained from glioblastoma stem-like cells (GSCs), from [243].** A/B. Phase-contrast image of TG1 GSC-derived clonal tumorspheres treated with 1% DMSO (A) or 10  $\mu$ M DDPM (B) for 72 h. C/D. Determination of the number of viable cells (C) and cellular ATP levels (D) in TG1 and TG1 C1 GSC-derived tumorspheres after DDPM treatment.  $p < 0.001$ . E/F. Hematoxylin/eosin staining of sections of a TG1 GSC clonal macro-tumorsphere treated with 10  $\mu$ M DDPM for 10 h. Scale bars: 200  $\mu$ m in A, B and E; 50  $\mu$ m in F.

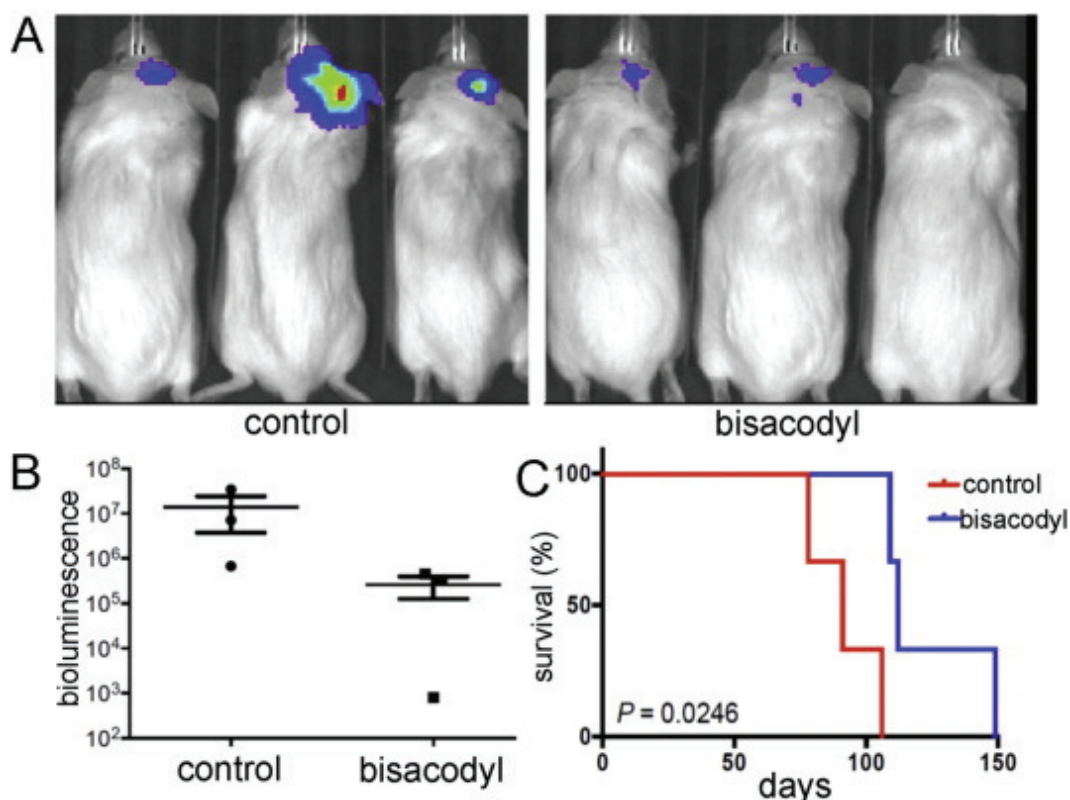


**Figure 17. Evaluation of bisacodyl's activity in an orthotopic xenograft model of glioblastoma obtained with glioblastoma stem-like cells, from [243].** **A.** Bioluminescence images of mice treated with vehicle or bisacodyl for 45 days. **B.** Quantification of bioluminescence signals. **C.** Kaplan-Meier survival analysis of mice treated with vehicle or bisacodyl.  $p < 0.05$ .

Based on the above data, bisacodyl appears as an interesting new chemotherapeutic agent that would be able to target quiescent GSCs in the context of acidic and hypoxic tumor microenvironments without affecting normal cells present at physiological pH conditions. The main aim of my thesis project was to identify the signaling pathways underlying the cytotoxicity of bisacodyl in GSCs.

By using a human phospho-array kit from R&D systems, we observed that bisacodyl/DDPM significantly decreased the phosphorylation status of several proteins including the serine/threonine kinase WNK1 on Thr60, in quiescent GSCs. We decided to focus on WNK1 for several reasons. As we discussed before, first of all, WNK1 is a well-known regulator of numerous ion channels and co-transporters such as ROMK, ENaC, NKCC, NCC, KCC, NBCe1 and CFTR. Moreover, WNK1 is also an important player in vesicular traffic, pH regulation and metabolic adaptation for cell proliferation and survival. Finally, WNK1 is a newly emerged protein kinase



in cancer and no studies linked this protein to the physiopathology of glioblastoma stem-like cells. On the other hand, bisacodyl is a laxative drug functioning through regulation of intestinal motility, water secretion or absorption and electrolyte homeostasis through inhibition of  $\text{Na}^+/\text{K}^+$  ATPase, PKC-dependent stimulation of prostaglandin E2 release resulting in decreased aquaporin-3 expression in the colon, and inducible nitric oxide (NO) synthase stimulation and NO production in intestinal epithelia [244][245][246][247][248]. In addition, the compound is active on quiescent cells which represent a particular metabolic state and this activity is only observed in acidic conditions. All these pieces of information impel us to investigate the link between the cytotoxicity of bisacodyl/DDPM and the decreased phosphorylation status of WNK1 Thr60 observed in quiescent GSCs treated with the compound. Our results suggest that several WNK1 signaling partners in other systems, including protein kinases Akt and SGK1 and NBC  $\text{Na}^+/\text{HCO}_3^-$  co-transporters are involved in bisacodyl signaling in GSCs. The corresponding data are presented in the manuscript under the form of a publication to be submitted (Publication 2).

## Publication 2

**Bisacodyl signaling pathway study uncovers WNK1 kinase and protein partners Akt, SGK1 and NBC-family Na<sup>+</sup>/HCO<sub>3</sub><sup>-</sup> co-transporters as novel therapeutic targets in cancer stem-like cells from human glioblastoma**

Wanyin Chen, Leonel Nguekeu Zebaze, Jihu Dong, Laëtitia Chézeau, Songlin Niu, Frédéric Bihel, Emmanuel Boutant, Eléonore Réal, Pascal Villa, Marie-Pierre Junier, Hervé Chneiweiss, Marcel Hibert, Jacques Haiech, Marie-Claude Kilhoffer, Maria Zeniou

In preparation

## **Title page**

# **Bisacodyl signaling pathway study uncovers WNK1 kinase and protein partners Akt, SGK1 and NBC-family Na<sup>+</sup>/HCO<sub>3</sub><sup>-</sup> co-transporters as novel therapeutic targets in cancer stem-like cells from human glioblastoma**

**Wanyin Chen<sup>1</sup>, Leonel Nguekeu Zebaze<sup>1</sup>, Jihu Dong<sup>1</sup>, Laëtitia Chézeau<sup>1</sup>, Songlin Niu<sup>1</sup>, Frédéric Bihel<sup>1</sup>, Emmanuel Boutant<sup>2</sup>, Eléonore Réal<sup>2</sup>, Pascal Villa<sup>3</sup>, Marie-Pierre Junier<sup>4</sup>, Hervé Chneiweiss<sup>4</sup>, Marcel Hibert<sup>1</sup>, Jacques Haiech<sup>1</sup>, Marie-Claude Kilhoffer<sup>1</sup>, Maria Zeniou<sup>1</sup>**

**1** Laboratoire d'Innovation Thérapeutique, Centre National de la Recherche Scientifique/Université de Strasbourg, UMR7200, Laboratoire d'Excellence Medalis, Faculté de Pharmacie, 74 route du Rhin, 67401 Illkirch, France ;

**2** Laboratoire de Biophotonique et Pharmacologie, UMR7213, Centre National de la Recherche Scientifique/Université de Strasbourg, Faculté de Pharmacie, 74 route du Rhin, 67401 Illkirch, France ;

**3** Plateforme de Chimie Biologie Intégrative (PCBIS), Université de Strasbourg / CNRS UMS 3286, Laboratoire d'Excellence Medalis, ESBS Pôle API - Bld Sébastien Brant, 67401 Illkirch, France;

**4** Neurosciences Paris Seine - IBPS, CNRS UMR 8246/ Inserm U1130/ UPMC UMC18, 7 quai Saint Bernard, 75005 Paris, France ;

**Correspondence to:** Maria Zeniou

**email:** [zeniou@unistra.fr](mailto:zeniou@unistra.fr)

**Keywords :** bisacodyl, glioblastoma cancer stem-like cells, WNK1, Akt/SGK1, NBC Na<sup>+</sup>/HCO<sub>3</sub><sup>-</sup> co-transporters

## Abstract

Glioblastomas, the most aggressive brain malignancies, are highly heterogeneous tumors for which, the presence of cancer cells with stem-like and tumor initiation/propagation properties, is largely responsible for poor prognosis. Glioblastoma cancer stem-like cells (GSCs) reside in hypoxic and acidic niches favoring cell quiescence and drug resistance. Thus, new approaches targeting this specific cancer cell subpopulation within its niche, are promising strategies for treating glioblastoma.

In a high throughput screen, we identified the laxative bisacodyl as a compound with selective cytotoxicity towards quiescent GSCs only in acidic microenvironments similar to those found within tumors. Bisacodyl was further shown to induce tumor shrinking and to increase survival in *in vivo* glioblastoma models. In the present study, based on phosphokinase protein arrays and pharmacological and genetic modulation of signaling pathways, we report data involving the WNK1 serine/threonine protein kinase in bisacodyl activity in dissociated quiescent GSCs previously grown as neurospheres. Involvement of WNK1 was further supported by data obtained in GSC-derived 3D macro-tumorspheres containing inner-layer quiescent cells in hypoxic/acidic conditions and which mimic many aspects of glioblastoma tumors *in vivo*. WNK1 partners including the Akt and SGK1 protein kinases and NBC-family  $\text{Na}^+/\text{HCO}_3^-$  co-transporters were also shown to modulate the compound's effect on GSCs. Interestingly, our findings also highlighted a previously unknown role of WNK1 functions in GSC physiopathology thus uncovering novel potentially interesting therapeutic targets in glioblastoma which is to date an incurable disease.

## Introduction

Glioblastoma (GBM) is the most common form of malignant brain tumor with an incidence reported between 3-4 cases per 100,000 population and a gender preference for male adults [1]. The median survival of GBM patients without treatment is of 3 months. With the standard of care, which consists in surgery, radiotherapy and concurrent temozolomide (TMZ) chemotherapy, the average survival of patients ranges from 9 to 19 months and less than 4.7% of them survive 5 years after diagnosis [1][2].

In many if not most cancers, including GBM, progress in investigating the molecular biology of tumors and more precise characterization of tumor cell subpopulations has led to the identification of cells that are more susceptible to initiate propagate and maintain tumors [3][4][5]. Such cells have been designated as tumor initiating/propagating or cancer stem or stem-like cells.

The hallmark of glioblastoma stem-like cells (GSCs), and of stem-like cells from other tumors, is their ability to recapitulate the heterogeneity and complexity of tumors from which they derive following serial orthotopic or ectopic transplantation *in vivo* [6] [7][8][9]. This GSC property is supported by the long-term self-renewal ability of these cells, their capacity to divide symmetrically or asymmetrically giving rise to GSCs or to GSCs as well as to more committed progenitors, respectively, and finally by their multilineage differentiation ability producing differentiated low tumorigenic cancer cells [10]. In addition to their aforementioned properties, a slow-growing quiescent state within tumor masses *in vivo* was reported for cancer stem-like cells, including the ones from GBM [5][11]. Label retaining GSCs with *in vivo* tumorigenic potential were initially described by Deleyrolle et al. [12]. GSCs lacking Ki-67 proliferation marker expression were subsequently described in a genetically engineered mouse model of glioma [5] and a RNA-seq-based approach highlighted the presence of cells expressing both stem-cell and quiescent cell markers in glioblastoma samples from patients [13]. Finally, quiescent glioblastoma cells were localized in perinecrotic niches in patient specimens [14].

Initially believed to correspond to a static cell subpopulation within tumors with invariable properties, cancer stem-like cells are nowadays believed to correspond to a transient state that any tumor cell may acquire. Genetic and epigenetic determinants as well as signaling cues emanating from the tumor

microenvironment or the cancer stem-like cell niche, were shown to drive acquisition or loss of cancer stem-like cell properties. Therapeutic intervention was also involved in the plastic properties of cells within tumors [15][16][17]. For example, hypoxic conditions, frequently observed in GBM, were shown to facilitate GSCs' self-renewal and affect spheroid formation, a characteristic of brain-derived cells with stem cell-like properties in the absence of serum [18]. Further studies showed the important role of hypoxia-inducible factors, namely HIF2 $\alpha$ , stabilized by hypoxic conditions in cancer, in GSC growth, survival, stemness and tumorigenic potential [19][20]. Additional microenvironmental signals that can regulate cancer stem cell fate and metastatic potential include reorganizations of the extracellular matrix, autocrine and paracrine factors, low nutrient supply, signals derived from immune cells and acidic stress [3]. Interestingly, low oxygen conditions were also shown to favor the quiescent phenotype of GSCs within tumors [14].

In addition to their increased self-renewal and proliferation abilities, the cancer stem cell-like phenotype was also associated to modifications in signaling cascades favoring cell survival, increased resistance to DNA damage and drug efflux [21][22]. Thus, in recent years, cancer stem-like cells have emerged as clinically relevant targets for the treatment of cancer. Namely, the quiescent state, which may be reversed in the presence of appropriate environmental cues, is believed to be one of the major determinants of treatment resistant phenotypes in these cells and tumor recurrence. For example, it was shown, in glioblastoma animal models, that following treatment with TMZ, the quiescent GSC subpopulation was able to survive and drive tumor regrowth through the production of highly dividing cells. Interestingly, ablation of these cells hindered tumor development [5]. Thus, novel therapeutic approaches targeting GSC-like cells in their proliferating and namely their quiescent state, within the tumor microenvironmental conditions (low oxygen and low pH), are promising approaches for GBM treatment.

We have previously developed and extensively characterized *in vitro* experimental models of TMZ-resistant proliferating and quiescent GSCs derived from GBM patients. Reversible GSC cell quiescence was induced *in vitro* in the absence of medium renewal for 9 days and resulted in extracellular medium acidification with pH reaching a value of ~ 6.6 compared to a medium pH value of ~ 7.4 measured in proliferating GSC cell-culture conditions [9][23]. Screening of the Prestwick Chemical library, mainly composed of FDA-approved drugs, on

proliferating and quiescent GSCs, identified the stimulant laxative bisacodyl (4,4'-diacetoxydiphenyl-2-pyridyl-methane) and its active metabolite DDPM (4,4'-dihydroxydiphenyl-2-pyridyl-methane), as compounds exhibiting a selective cytotoxic activity on dissociated quiescent GSCs previously grown in neurosphere cultures. Cells treated with the compound presented morphological changes linked to necrotic cell death [23]. Further studies uncovered that acidity can induce the quiescent state in proliferating GSCs and sensitize these cells to DDPM. Bisacodyl/DDPM was also active on inner-layer quiescent cells within big GSC-derived 3D clonal macro-tumorspheres recapitulating many aspects of GBM tumors *in vivo*. Moreover, the *in vivo* antitumor activity of the compound was demonstrated in orthotopic xenograft mouse models of GBM and inositol 1,4,5-triphosphate receptor-dependent calcium signaling was proposed as a putative mechanism underlying bisacodyl/DDPM cytotoxicity. To our knowledge, bisacodyl/DDPM is the only reported compound with anti-cancer stem-like cell activity under such conditions [24].

Further characterization of bisacodyl/DDPM signaling partners in quiescent GSCs and cells within GSC-derived macro-tumorspheres, uncovered a major contribution of the serine/threonine protein kinase WNK1 (With no-lysine(K) kinase 1) in the physiopathology of GSCs and in the compound's effect on this particularly resistant cancer stem-like cell population. In humans, WNK1 is member of a protein family composed of three additional proteins, WNK2, WNK3 and WNK4. WNK protein functions have been associated to a variety of cell processes including fluid and electrolyte homeostasis, cell proliferation, migration and survival as well as vesicular trafficking and autophagy. Mutations in *WNK1* and *WNK4* genes have been associated to inherited forms of hypertension. WNK functions may be dependent or independent from the enzymes' catalytic activity. Namely, catalytic activity independent functions, involving scaffolding with other protein partners, underlined by the phosphorylation status of the Thr60 residue within the N-terminus of WNK1, have been described [25][26][27][28].

Our data also implicate other known WNK1 partners, namely protein kinases Akt and SGK1 (Serum and glucocorticoid-stimulated protein Kinase-1) as well as NBC  $\text{Na}^+/\text{HCO}_3^-$  co-transporters in bisacodyl/DDPM cytotoxicity in GSCs. The WNK1 protein was previously shown to promote cell volume regulation, resistance to TMZ and cell migration in cell lines from GBM through its ability to modulate the

activity of ion cotransporters of the NKCC family [29][30]. We report here, for the first time a role of WNK1 and several WNK1 partners in the physiopathology of GSCs uncovering novel potentially interesting therapeutic targets for the treatment of GBM which is to date an incurable disease.



## Results

### **DDPM modifies the phosphorylation status of WNK1 Thr60 in quiescent GSCs maintained in acidic pH culture conditions**

We have previously shown that bisacodyl and its active derivative DDPM are cytotoxic towards GSCs from patients (including the TG1 and TG1 C1 cell types) induced to quiescence *in vitro* only when these cells are maintained in slightly acidic pH culture conditions and provided data suggesting that calcium signaling depending on inositol 1,4,5-triphosphate receptor function might be involved in this action. Conversely, at physiological pH values, these compounds do not affect the viability of *in vitro* proliferating GSCs [23][24]. Chemical structures of bisacodyl and DDPM and representative dose-response curves on proliferating and quiescent TG1 GSCs are given on Supplementary Figure S1. However, the signaling pathways involved in bisacodyl/DDPM cytotoxicity and selectivity toward quiescent cells in acidic conditions are still not completely explored.

With the aim to identify proteins whose phosphorylation at selected residues is modified by bisacodyl/DDPM, protein extracts from quiescent GSCs were treated either with DMSO alone or in the presence of bisacodyl's active derivative DDPM (10  $\mu$ M) and put in contact with human phospho-kinase array kit membranes (R&D system). These membranes allow to explore the phosphorylation status of more than 40 selected kinase phosphorylation sites. Treatment of quiescent GSCs with DDPM resulted in the modification of the phosphorylation status of several kinases and kinase substrates (Figure 1A). Among them, the phosphorylation of WNK1 at Thr60 is strongly reduced in DDPM-treated quiescent GSCs compared to control cells (Figure 1A, black arrow). WNK1 protein levels and Thr60 phosphorylation status were subsequently determined by western blotting in proliferating and quiescent TG1 and TG1 C1 GSCs (Figure 1B). Our results indicate that whereas overall WNK1 protein levels are equivalent between proliferating and quiescent TG1 and TG1 C1 GSCs, respectively, as well as between TG1 and TG1 C1 GSCs (Figure 1B, middle panel), p-Thr60-WNK1 levels are significantly higher in quiescent TG1 and TG1 C1 GSCs compared to their proliferating counterparts (Figure 1B, right panel). Moreover, the phosphorylation of WNK1-Thr60 was decreased in a time-dependent manner by DDPM treatment in quiescent TG1 GSCs maintained in their culture medium which is slightly acidic, *i.e.* in conditions in which

bisacodyl/DDPM is cytotoxic (Figure 1C, middle panels). Conversely, p-Thr60-WNK1 levels were not modified in proliferating TG1 GSCs treated with the compound (Figure 1C, left panel). A slight decrease in p-Thr60 levels was observed in quiescent TG1 GSCs treated with an inactive derivative of the compound (structure and activity profile of the bisacodyl/DDPM inactive derivative are presented in Supplementary Figure 1S) for 10 min but longer treatment in these conditions had no effect on the phosphorylation status of WNK1 on this residue (Figure 1C, right panel). Overall levels of non-phosphorylated WNK1 on Thr60 were not significantly modified by the compound (Figure 1C, western blot quantification blots). The same conclusions can be drawn from results obtained in TG1 C1 GSCs treated in similar conditions (Supplementary Figure S2A). Altogether, these results suggest a functional role of WNK1 Thr60 phosphorylation status in quiescent GSC physiopathology and DDPM activity in these cells.

### **DDPM modifies the phosphorylation status of WNK1 partners in GSCs**

WNK1 Thr60 lies within an AGC kinase consensus phosphorylation motif [31]. Moreover, AGC protein kinases Akt and SGK1 were shown to phosphorylate this WNK1 residue in several systems [31][32][33].

We thus investigated the possibility that bisacodyl/DDPM might also modify the phosphorylation status and subsequently the activity of these two protein kinases. Akt full activation requires phosphorylation of two residues, Thr308 located in the catalytic domain which is phosphorylated by PDK1 (Phosphoinositide-dependent-protein Kinase 1), and a more C-terminal serine residue (Ser473) which is phosphorylated by the mTORC2 complex [34]. Overall Akt and p-Ser473-Akt levels were investigated in proliferating and quiescent TG1 GSCs. Like for WNK1, the levels of the Akt protein were similar between proliferating and quiescent cells whereas p-Ser473-Akt was present in significantly higher proportion in quiescent *versus* proliferating TG1 GSCs (Figure 2A, upper left panel). Similar observations were made in proliferating and quiescent TG1 C1 GSCs even if the variability in western blotting quantifications from independent experiments did not allow to attain statistical significance in this case (Supplementary Figure S2B). Treatment of proliferating and quiescent TG1 and TG1 C1 GSCs with DDPM, resulted in a time-dependent decrease in the phosphorylation status of Akt Ser473 only in quiescent culture conditions (Figure 2A and Supplementary Figure S2B). A slight decrease

(less than two times) in the levels of p-Ser473-Akt was observed in quiescent TG1 GSCs following a 10 min or a 30-min treatment with an inactive derivative of DDPM (Figure 2A, lower right panel). However, this slight decrease was not comparable to the effect of DDPM on quiescent TG1 cells (decrease of almost 10 times in the phosphorylation levels of Akt Ser 473). Interestingly, the reduction in the phosphorylation status of Ser473 as well as of Akt Thr308 was also observed on the phosphokinase array test presented in Figure 1A.

SGK1 is also able to phosphorylate Thr60 in WNK1. SGK1 full catalytic activation is achieved through phosphorylation of Thr256 within the activation loop of the enzyme by PDK1 combined to Ser422 phosphorylation within a C-terminal hydrophobic motif by mTORC2 [35][36]. Conversely to WNK1 and Akt, both overall SGK1 and p-Thr256-SGK1 levels were significantly lower in quiescent TG1 GSCs compared to their proliferating counterparts (Figure 2B, upper left panel). This was also the case in quiescent *versus* proliferating TG1 C1 GSCs although statistical significance was not attained in this case (Supplementary Figure S2C, upper panel). Upon treatment of proliferating TG1 GSCs with DDPM, a slight decrease in SGK1 levels was observed after 120 min of contact with the compound whereas levels of p-Thr256 significantly increased (Figure 2B, lower left panel). Opposite effects (increase in overall SGK1 levels and decrease in Thr256 phosphorylation) were observed in quiescent TG1 GSCs treated with the compound (Figure 2B, middle lower panel). A slight increase in p-Thr256-SGK1 levels was also observed in quiescent TG1 GSCs treated with the inactive derivative of bisacodyl/DDPM (Figure 2B, lower right panel). In TG1 C1 GSCs, treatment of quiescent cells with DDPM also resulted in a slight but statistically significant decrease in the phosphorylation status of Thr256 of SGK1 whereas no statistically significant modifications were observed in other conditions (Supplementary Figure S2C). These data suggest that like for WNK1, Akt and SGK1 protein kinases may be involved in bisacodyl/DDPM signaling in quiescent GSCs. In proliferating conditions, higher levels of SGK1 and p-SGK1 in the absence of treatment as well as modifications observed when GSCs were challenged with DDPM, suggested a role of this kinase also in the physiopathology of proliferating GSCs.

### **DDPM modifies the catalytic activity of WNK1 and affects the phosphorylation status of WNK1 targets SPAK and OSR1 in proliferating and quiescent GSCs**

WNK1 is a serine/threonine kinase of the WNK (With no lysine (K)) family, named after the unique placement of the lysine involved in ATP-binding and catalyzing phosphoryl transfer in subdomain I, rather than subdomain II, where it is located in all other serine/threonine kinases. WNK1 functions through its catalytic activity which requires the auto-phosphorylation of at least one serine residue (Ser382 in human WNK1) within its activation loop. The catalytic lysine K233 is also required for phosphotransferase activity towards WNK1 substrates. Some WNK1 functions rather involve scaffolding to protein partners mediated by the phosphorylation of WNK1 at Thr60 located at the N-terminal part of the protein and whose phosphorylation status is modified by bisacodyl/DDPM. WNK1 activities (scaffolding and catalytic activation) may be associated or function independently [25].

In order to determine whether the catalytic activity of WNK1 is also affected by bisacodyl/DDPM, the kinase activity of the enzyme was measured indirectly by determining the phosphorylation status of two known WNK1 substrates, *i.e.* SPAK (STE20/SPS1-related proline/alanine-rich kinase) and OSR1 (Oxidative stress-responsive kinase 1) in proliferating and/or quiescent TG1 and TG1 C1 GSCs as well as in the same cell types treated for variable durations with DDPM or with the bisacodyl/DDPM derivative lacking activity (Figure 3 and Supplementary Figure S2D) [37].

Our results showed that the phosphorylation levels of SPAK/OSR1 (p-Ser373/p-Ser325) were significantly higher in quiescent TG1 GSCs compared to proliferating TG1 cells, suggesting a higher kinase activity of WNK1 in quiescent GSCs. Overall SPAK and OSR1 levels were similar between proliferating and quiescent TG1 cells (Figure 3, upper left panel). Similar tendencies were observed in quiescent *versus* proliferating TG1 C1 GSCs (Supplementary Figure S2D). Additionally, the phosphorylation of SPAK/OSR1 on selected residues was transiently decreased by DDPM treatment both in quiescent and proliferating TG1 and TG1 C1 GSCs whereas overall expression levels of SPAK and OSR1 did not vary significantly under these conditions (Figure 3 and Supplementary Figure S2D). Conversely, pSer373-SPAK/p-Ser325-OSR1 phosphorylation status was not modified in quiescent TG1 and TG1 C1 GSCs treated with the inactive derivative of

the compound (Figure 3 and Supplementary Figure S2D). Altogether these results suggested that WNK1 basal catalytic activity, as measured by the status of phosphorylation of SPAK and OSR1 on selected residues, is higher in quiescent GSCs compared to their proliferating counterparts indicating a putative role of the enzyme in the maintenance of a viable quiescent state. DDPM treatment resulted in a transient decrease in SPAK/OSR1 phosphorylation and thus WNK1 catalytic activity which was observed both in conditions in which the compound is active (quiescent GSCs maintained in slightly acidic culture conditions) and in conditions in which the molecule is not cytotoxic to GSCs (proliferating cells at physiological pH).

### **Inhibition of NBC $\text{Na}^+/\text{HCO}_3^-$ co-transporters including NBCe1, a downstream target of the WNK1 signaling pathway, protects dissociated quiescent GSCs and GSC-derived macro-neurospheres from DDPM action**

Previous studies showed that WNK1 is able to limit surface expression and thus activity of NBCe1, an electrogenic  $\text{Na}^+/\text{HCO}_3^-$  cotransporter involved in ion content and pH regulation in several systems [38]. WNK1 exerts this inhibitory effect on NBCe1 expression/activity by recruiting SPAK to the co-transporter and this WNK1 function requires its N-terminal domain (WNK1<sup>1-119</sup>). Depletion of either WNK1 or SPAK significantly increases NBCe1 levels at the plasma membrane. In this WNK1/SPAK pathway, the kinase activity of WNK1 is not required whereas the catalytic function of its downstream effector SPAK is necessary [39]. Our hypothesis was that in quiescent GSCs, DDPM, by reducing the phosphorylation levels of WNK1 Thr60 might lead to an abnormal increase in NBCe1 plasma membrane expression and activity in these cells leading to the cytotoxic effect of the compound under quiescent culture conditions.

To test this hypothesis, quiescent TG1 and TG1 C1 GSCs were pretreated with various concentrations of S0859, a compound described as an NBC  $\text{Na}^+/\text{HCO}_3^-$  inhibitor with activity on both electrogenic and electroneutral NBC-family co-transporters including NBCe1 [40]. Pretreatment was maintained for 24 hours before DDPM was added for an additional time lapse of 24 hours. We show that S0859 partially reversed the cytotoxic effect of the compound in quiescent TG1 and TG1 C1 GSCs. In TG1 cells, this protective effect was observed for 20-100  $\mu\text{M}$  of S0859 with statistical significance attained for  $\geq 50 \mu\text{M}$  of the compound. Higher

concentrations ( $\geq 80 \mu\text{M}$ ) of the inhibitor were required to observe statistically significant differences in quiescent TG1 C1 cells (Figure 4A, left panel for TG1 GSCs and right panel for TG1 C1 GSCs). Dose-response curves of DDPM in the presence of increasing concentrations of S0859 on quiescent TG1 and TG1 C1 GSCs indicated that IC<sub>50</sub> values of DDPM increase in the presence of S0859 whereas maximal effect of the compound is reduced (Supplementary Figure S3A and S3B). These data suggested that DDPM and S0859 are probably not competing for the same binding sites on target proteins.

The protective effect of S0859 was further assessed on TG1 GSC-derived macro-neurospheres, an *in vitro* 3D model developed in our laboratory. We had previously reported that TG1 and TG1 C1 GSC-derived large size neurospheres (diameter of  $\geq 600 \text{ nm}$  (and up to  $1 \text{ mm}$ )), termed macro-neurospheres or macro-tumorspheres, recapitulate some of the characteristics of tumors *in vivo*. These include a necrotic center, the presence of cells lacking expression of proliferation markers in the inner part of the sphere and hypoxic/acidic gradients from the outer to the inner part of the structure. Moreover our data indicated that DDPM was able to target the inner layer of quiescent cells under the 3D big neurosphere culture conditions [24]. Pretreatment of such neurospheres with S0859 ( $100 \mu\text{M}$ ) was again able to preserve, at least in part, TG1 GSCs within the structure from DDPM cytotoxicity (Figure 4B, left and right panels). Thus, NBC-mediated  $\text{Na}^+/\text{HCO}_3^-$  co-transporter activity seems to be important for bisacodyl/DDPM cytotoxicity on quiescent glioblastoma GSCs.

As mentioned above, higher concentrations of S0859 are required to observe a significant protective effect of the compound in DDPM-treated TG1 C1 GSCs compared to TG1 cells. We thus decided to investigate the NBCe1 mRNA levels as well as the membrane-bound NBCe1 protein levels by RT-qPCR and western blot on membrane protein extracts in proliferating and quiescent TG1 and TG1 C1 GSCs (Figure 4C and 4D, respectively). NBCe1 overall mRNA levels were higher in TG1 C1 cells compared to TG1 GSCs whereas no significant differences were observed in quiescent TG1 or TG1 C1 GSCs compared to their proliferating counterparts (Figure 4C). Membrane-bound NBCe1 protein levels were also significantly higher in TG1 C1 compared to TG1 GSCs but no differences were observed between quiescent and proliferating GSCs of these two cell types suggesting that NBCe1 levels might explain the differences observed in the protective effect of S0859 on

DDPM activity in TG1 *versus* TG1 C1 GSCs (Figure 4D). In addition to NBCe1, S0859 can inhibit the activity of other  $\text{Na}^+/\text{HCO}_3^-$  co-transporters [40][41]. Among them, the NBCn1 protein, whose function has been associated to cancer, could be a downstream target of the WNK1/SPAK pathway [38][42]. NBCn1 levels were also higher in proliferating and quiescent TG1 C1 GSCs as compared to TG1 cells (Supplementary Figure S4A). In order to distinguish between NBCe1 and NBCn1 contributions in the protective effect of S0859 on quiescent GSCs, we used DIDS (4,4'-Diisothiocyanatostilbene-2,2'-disulfonate), a stilbene derivative acting as a non-selective inhibitor of anion transport and that is able to inhibit NBCe1 and all other  $\text{Na}^+$ -coupled  $\text{HCO}_3^-$  co-transporters but not NBCn1. Indeed, blockade of NBCn1 is poor even at concentrations of 500  $\mu\text{M}$  of DIDs [38]. The effect of DIDS was assessed on quiescent GSCs treated with DDPM. As shown on Supplementary Figure S4B, TG1 GSCs were highly sensitive to DIDS even in the absence of DDPM. TG1 C1 cells were less sensitive to the compound since higher concentrations of DIDS were required to induce cell death (compare graphs in left and right panel in Supplementary Figure S4B). This observation is in agreement with the higher expression levels of at least NBCe1 in these cells compared to TG1 GSCs (Figure 4D). In the presence of DDPM, DIDS was not able to reverse even partly the effect of the compound (Supplementary Figure S4B left and right panels). Thus, either NBCn1 is not involved in DDPM cytotoxicity on GSCs or the cytotoxicity of DIDs alone, namely on quiescent TG1 GSCs, prevents observation of such an effect.

### **Modulation of WNK1 signaling partners Akt, SGK1 and NBC $\text{Na}^+/\text{HCO}_3^-$ co-transporters NBCe1/NBCn1 impacts DDPM cytotoxic activity in dissociated quiescent GSCs previously grown as neurospheres**

We showed in previous sections that DDPM treatment results in a time-dependent inhibition of the phosphorylation status of WNK1 Thr60 and two potential WNK1 Thr60 phosphorylating proteins, the Akt and SGK1 protein kinases, on residues that are involved in the catalytic activity of these enzymes. We thus decided to investigate the effect of DDPM in quiescent TG1 and TG1 C1 GSCs in the presence of increasing concentrations of the Akt and SGK1 inhibitors VIII and GSK 650394, respectively, or with combinations of both compounds (Figure 5A, 5B and 5C, respectively). WNK1-reported inhibitor-WNK463 was not used since it is a pan-

WNK kinase inhibitor targeting the catalytic activity of WNK1 and whose effect on WNK1 Thr60 phosphorylation and/or associated functions is unknown [43].

As shown in Figures 5A and 5B, combination of DDPM to the Akt inhibitor VIII or to the SGK1 inhibitor GSK 650394, significantly increased the cytotoxicity of the compound in quiescent TG1 GSCs even at concentrations at which these inhibitors do not show cytotoxicity in the absence of DDPM. Combination of both compounds reinforced DDPM activity on quiescent TG1 GSCs compared to DDPM with either inhibitor alone (Fig 5C). In quiescent TG1 C1 GSCs, the VIII Akt inhibitor was also able to increase DDPM cytotoxicity at VIII concentrations which do not affect the viability of cells (Supplementary Figure S5A) whereas, SGK1 inhibition, only affected DDPM activity at high concentrations (80  $\mu$ M) (Supplementary Figure S5B). Moreover, a concentration of 30  $\mu$ M of the SGK1 inhibitor was not able to potentiate the activity of the VIII Akt inhibitor on DDPM action in quiescent TG1 C1 GSCs (Supplementary Figure S5C). In both cell types (TG1 and TG1 C1 GSCs), Akt inhibition by VII was able to partially abolish the protective effect of the S0859 NBC inhibitor on quiescent cells treated with DDPM, suggesting a link between Akt and NBC  $\text{Na}^+/\text{HCO}_3^-$  co-transporter function and DDPM activity in these cells (Figure 5D and Supplementary Figure S5D). Finally, conversely to VIII, pre-treatment of TG1 and TG1 C1 GSCs with the Akt activator SC-79 partially protected quiescent TG1 and TG1 C1 GSCs from DDPM activity (Figure 5E and Supplementary Figure S5E). However, as for other modulators of the Akt-SGK1-WNK1 signaling pathway, SC-79 had a fainter protective effect on TG1 C1 compared to TG1 GSCs (compare effects on Figure 5 and Supplementary Figure S5).

Altogether these data establish a link between proteins of the Akt/SBK1/WNK1/NBC signaling module and bisacodyl cytotoxicity in quiescent GSCs isolated from glioblastoma patients even though some differences in response to inhibitors are observed between TG1 and TG1 C1 cell types.

### **Modulation of WNK1 levels and/or activity impacts GSC cell survival, aspect of GSC-derived macro-neurospheres and GSC clonal properties and growth**

To assess directly the role of the WNK1 protein in bisacodyl/DDPM activity on glioblastoma GSCs, we first generated GSCs in which WNK1 expression was transiently reduced by an shRNA based-approach. A significant reduction in the



expression of endogenous WNK1 was observed in TG1 and TG1 C1 GSCs transfected with the vector encoding WNK1 targeting shRNAs whereas no effect was observed in cells transfected with control vectors (empty shRNA vector or vector encoding scramble shRNAs) (Supplementary Figure S6A). Under these conditions, neither quiescent GSC viability nor DDPM effect were significantly modified as determined by FACS analysis (Supplementary Figure S6B and S6C). The absence of effect of WNK1 knockdown might be explained by insufficient inhibition of the function of the protein in transfected cells or by insufficient transfection rates for quiescent TG1 and TG1 C1 GSCs. Alternatively, a potential compensation system may retain the function of the WNK/SPAK pathway on NBC co-transporters since WNK4 was reported to interact with SPAK and OSR1 and to phosphorylate and activate these kinases through its N-terminal. Moreover, a phosphorylation site equal to Thr60 in WNK1 and lying in an AGC kinase phosphorylation motif is present in WNK4 and this kinase was also involved in the regulation of the NBCe1 co-transporter [27][44].

To overcome these limitations, modulation of WNK1 activity was obtained through overexpression of the wild-type (WT) protein (associated to FLAG tags) in GSCs. To obtain more information as to the WNK1 functions (scaffolding involving phosphorylation of Thr60 and/or catalytic activity) associated to the compound's effect, FLAG-tagged non-phosphorylatable and phosphomimetic mutants of Thr60 (T60A, T60D/E, respectively) as well as a catalytically inactive mutant obtained by the mutation of the catalytic lysine (K233M) were also overexpressed in both proliferating and quiescent GSCs. In agreement with localization patterns observed for overexpressed or endogenous WNK1 in other cell systems [25][45][46], in proliferating TG1 and TG1 C1 GSCs, the FLAG-tagged WT WNK1 was generally localized in the cytoplasm where a punctate staining was often observed. A punctate staining was also observed in the nucleus of several cells (Supplementary Figure S7 and data not shown). Introduction of the T60A, T60D/E and K233 mutations did not alter the subcellular localization of the corresponding proteins (Supplementary Figure S7 and data not shown). In quiescent GSCs, the expression of the WT and mutant forms of WNK1 was similar to the one observed in proliferating GSCs (Supplementary Figure S7). However, in general, the levels of expression of the WT and mutant WNK1 proteins was lower in quiescent cells.

To further study the impact of WNK1 modulation, we established TG1-derived cell lines stably overexpressing WT and mutant forms of the kinase. TG1 cells stably transfected with an empty vector were used as a control (Supplementary Figure S8).

The viability of WT and mutant WNK1 overexpressing cells was evaluated by Trypan blue dye exclusion in proliferating and quiescent (7 days and 9 days without medium renewal) culture conditions. As shown in Figure 6A, no differences between cell types were observed in proliferating cell cultures. Conditions favoring quiescence increased the overall levels of cell mortality in control as well as in WT and mutant WNK1 overexpressing cells. Moreover, overexpression of the T60A and T60E mutants resulted in a significant increase in cell mortality compared to control TG1 cells (and WT WNK1 overexpressing cells for the T60E mutant), suggesting involvement of the Thr60 phosphorylation status in the survival of GSCs which is only revealed when cells are challenged by the quiescent culture conditions (growth factor deprivation and extracellular medium acidification). Overexpression of the catalytically inactive mutant of WNK1 (K233M) did not affect cell survival in either proliferating or quiescent culture conditions (Figure 6A). Interestingly, macro-neurospheres derived from WT and T60A and T60D/E mutant WNK1-overexpressing cells were different with respect to their overall aspect compared to control empty vector spheres and K233 WNK1 overexpressing TG1 cells (Figure 6B). Surrounding isolated cells of these cell types were observed and secondary spheres seemed to originate from the primary neurosphere present in the well (Figure 6B). Similar phenotypes were not observed in smaller neurospheres derived from these cells (data not shown). Thus, positive or negative regulation of the Thr60 phosphorylation status may influence cell behavior within macro-neurospheres. Alternatively, as both WT and non-phosphorylatable and phosphomimetic mutants of Thr60 produce similar effects, one could assume that increased WNK1 catalytic activity due to the overexpression of a functional catalytic domain within the protein, might be responsible for these events.

Additional characterization of WT and mutant WNK1 overexpressing TG1 cells was performed through evaluation of their clonal properties by determining the total number of neurospheres present in a well and plotting it as a function of the initial number of seeded cells ranging from 1-50 cells/well. Sphere counting was done two weeks following cell seeding. Results obtained at all initial cell number

conditions are represented on Supplementary Figure S9A. As illustrated on Figure 6C, in which only two initial cell number/well conditions are represented (20 cells and 50 cells/well), Thr60 mutations did not influence clonal properties of TG1 GSCs. Conversely, WT WNK1 or catalytically inactive WNK1 mutant (K233M) overexpression resulted in a reduction in clonal amplification abilities of corresponding TG1 cells (Figure 6C).

Finally, the growth rate of individually replated neurospheres from stable TG1 cell lines was assessed by determining neurosphere volume at different time points with the ImageJ software. Growth curves obtained from control (empty vector transfected TG1 cells) and WT and mutant WNK1 overexpressing TG1 GSCs are shown on Supplementary Figure S9B. Statistically different results at the 34-day time point are represented for more clarity on Figure 6D. A significant reduction in growth rate was observed with Thr60 phosphomimetic mutants and the K233M catalytically inactive mutant of WNK1 (Figure 6D) whereas no differences were observed between the T60A and control or WT WNK1 overexpressing neurospheres (Figure 6D).

Altogether, these data suggest a novel role of the WNK1 protein functions in several aspects of GSC physiopathology.

### **Modulation of WNK1 levels, T60 phosphorylation and catalytic activity impacts DDPM action GSC-derived macro-neurospheres**

To definitely validate the involvement of WNK1 in the activity of bisacodyl/DDPM in GSCs, macro-neurospheres derived from TG1 cells stably overexpressing WT and mutant forms of the protein were treated with the compound (3  $\mu$ M) for 24 hours. Subsequently, cell viability was evaluated by measuring ATP levels present in treated wells. Results were normalized to the cell viability of neurospheres from the same cell type treated with DMSO (viability of 100 %). Macro-neurospheres from empty vector control stably transfected cells were treated in similar conditions and compared to their corresponding control treated (1% DMSO) cells. As illustrated in Figures 7A and 7B, DDPM treatment resulted, as expected, in a decrease in the number of viable cells both in empty vector control TG1 GSCs and WT WNK1 overexpressing cells (Figures 7A and 7B). Interestingly, overexpression of WT WNK1 resulted in a decreased cytotoxic effect of DDPM on GSCs from glioblastoma patients compared to the effect observed in empty vector

control cells (Figures 7A and 7B). Similar results were observed when control and WT WNK1 overexpressing cells were treated with combinations of DDPM with the Akt or the SGK1 inhibitors (Figures 7B) suggesting that WNK1 is probably acting downstream of these kinases to underlie cytotoxicity of bisacodyl/DDPM in GSCs. Conversely, WNK1 overexpression did not modify the protective effect of the NBCe1 inhibitor S0859 on neurospheres from TG1 cells (Figure 7B). This result would be in favor of a downstream role of NBC co-transporters with respect to WNK1 in the signaling pathway of bisacodyl/DDPM in GSCs.

Finally, DDPM activity was evaluated at 24, 48 and 72 hours of treatment of macro-tumorspheres derived from TG1 cells stably overexpressing WT and mutant (T60A, T60D/E and K233M) forms of WNK1 and compared to the activity of the compound at the same time-points in empty vector stably transfected cells assembled in macro-tumorspheres (Figure 7C). 3 macro-spheres of each cell type were used for each condition (2  $\mu$ M DDPM in 1% DMSO or 1% DMSO alone). Overexpression of the WT and Thr60 phosphomimetic mutants significantly protected cells from DDPM activity compared to empty vector transfected control cells. The protective effect was observed at all time-points for WT and T60E forms of WNK1 and was more pronounced for the T60E compared to the T60D mutant (Figure 7C). Although not statistically significant, some protection was observed when the T60A mutant of WNK1 was overexpressed in TG1 cells compared to control cells namely after 72 hours of treatment. Altogether these data suggested that the decrease in Thr60 phosphorylation levels is required for DDPM activity on GSCs since an increase in the levels of Thr60-phosphorylated WNK1 protected the cells from bisacodyl/DDPM action. However, other WNK1 functions must be involved since the T60A mutant did not increase but rather weakly decreased the compound's cytotoxic effect on GSCs. Finally, no protection was observed when the K233M mutant was overexpressed in TG1 cells. The absence of protective effect of the WNK1 K233M mutant argues in favor of an involvement of modifications (transient reduction) in WNK1 catalytic activity in DDPM cytotoxicity in GSCs and further suggests that the increase in potentially phosphorylatable Thr60 levels is not enough to preserve these cells from bisacodyl/DDPM action.

## Discussion

Based on recent advances in cancer biology, tumors are nowadays considered as complex and highly heterogeneous entities composed of a variety of cancer cell types with distinct genetic, epigenetic and metabolic characteristics. Non-malignant cancer-associated fibroblasts and immune cells, their extracellular components including extracellular matrix and secreted cytokines and growth factors as well as tumor surrounding vascular networks, constitute specific tumor microenvironments and contribute to cancer cell function and malignancy [47][48][49].

Irregularities in tumor vascular networks, distance from vessels and metabolic specificities of cancer cells favoring glycolytic processes over oxidative phosphorylation for energy production even in normoxic conditions, create low nutrient (and xenobiotic), oxygen and pH conditions for cells positioned in inner layers of tumors [50][51]. These hostile extra-cellular microenvironmental conditions also condition aggressiveness and tumorigenic potential of cancer cells [52][53].

Based on intrinsic properties and cues from surrounding cancer cells and tumor microenvironmental conditions, any cell within a tumor mass may acquire tumor initiating/propagating potential and cancer stem-like cell properties [10][15]. Moreover, as previously mentioned, cancer cells with stem cell-like characteristics are induced to a quiescent slow-growing state in hypoxic, acidic and low nutrient conditions described in glioblastoma and other human malignancies [52][54].

In view of tumor complexity and tumor cell specific characteristics and because compounds which retain activity and specificity within tumor microenvironments are lacking, an unmet medical need is still a reality for many if not most human malignancies including glioblastoma. The stimulant laxative bisacodyl and its active derivative DDPM were identified by our team in a differential screening approach on proliferating and quiescent cancer-stem-like cells isolated from glioblastoma patients as compounds inducing necrotic cell death only in dissociated quiescent GSCs previously cultured *in vitro* as neurospheres [23]. Subsequent analysis of bisacodyl/DDPM activity profiles revealed that the compounds were also active on proliferating GSCs upon extracellular medium acidification. Moreover, GSCs induced *in vitro* to quiescence, resulting in an acidification of their extracellular medium, were protected from bisacodyl/DDPM

action when medium pH was adjusted to physiological pH values [24]. Interestingly, bisacodyl/DDPM was also active on clonal 3D GSC-derived macro-neurospheres which partly mimic the complexity of intratumoral microenvironments in glioblastoma and could prolong survival in an orthotopic mouse model of the disease [24]. Thus, bisacodyl/DDPM possesses a unique and particularly interesting activity profile which is of relevance to the development of novel more effective cancer treatments. In clinic, bisacodyl is currently used as a stimulant laxative to treat constipation and for bowel cleansing prior to colonoscopy. The laxative effect of the compound was attributed to effects on intestinal motility, water secretion or absorption and electrolyte homeostasis through inhibition of  $\text{Na}^+/\text{K}^+$  ATPase, PKC-dependent stimulation of prostaglandin E2 release resulting in decreased aquaporin-3 expression in the colon, and inducible nitric oxide (NO) synthase stimulation and NO production in intestinal epithelia [55][56][57][58][59]. In quiescent GSCs, we have previously described interference of bisacodyl with calcium signaling [24].

In this report, we studied in detail phosphorylation cascades modulated by bisacodyl/DDPM in two types of GSCs, TG1 and TG1 C1 cells. Bisacodyl/DDPM signaling was explored *in vitro* in two conditions in which the compound is active: i) dissociated quiescent GSCs obtained from neurospheres maintained in slightly acidic extracellular medium and ii) GSC-derived macro-neurospheres containing inner layer quiescent cells in a hypoxic/acidic surrounding microenvironment. Dissociated GSCs from neurospheres present in proliferating cell culture medium (pH ~ 7.4) which are not sensitive to the compound, dissociated quiescent GSCs treated with an inactive derivative of bisacodyl/DDPM and GSC-derived macro-neurospheres incubated with vehicle (DMSO) were used as controls.

In dissociated quiescent TG1 and TG1 C1 GSCs, bisacodyl was shown to decrease the phosphorylation levels of Thr60 in the WNK1 serine/threonine protein kinase. This modification was not observed in control conditions indicating that it is probably relevant to the compound's activity on GSCs under quiescent conditions. Interestingly, basal p-Thr60 levels were significantly higher in quiescent compared to proliferating TG1 and TG1 C1 GSC culture conditions further supporting the involvement of WNK1 Thr60 phosphorylation levels in the maintenance of a viable quiescent GSC state.

WNK1 Thr60 located in the N-terminal part of the protein lies in a consensus phosphorylation site for kinases of the AGC family [25]. Moreover, in other cell

systems, AGC kinases Akt and SGK1 were linked to WNK1 functions through the modulation of p-Thr60 levels [32][33][31]. Based on these observations, we explored the levels of expression and phosphorylation status on selected residues involved in catalytic activation of Akt and SGK1 enzymes. Whereas the overall levels of Akt did not differ between proliferating and quiescent GSCs, higher levels of the phosphorylated and presumably active form of the enzyme were detected in quiescent cells in agreement with what was previously observed for WNK1. Moreover, bisacodyl/DDPM treatment resulted in a significant activity-dependent reduction in the phosphorylation/activation status of the protein. Conversely to WNK1 and Akt, overall expression levels and phosphorylation of SGK1 Thr256 were lower in quiescent cells compared to their proliferating counterparts. SGK1 Thr256 phosphorylation was however negatively affected by bisacodyl/DDPM treatment, with similar kinetics as the ones observed for phosphorylated forms of WNK1 and Akt, despite an increase in the overall levels of the protein upon treatment. In other cell types, SGK1 mRNA and protein expression levels as well as subcellular localization, were shown to be subject to stringent stimulus-dependent regulation and disappearance or appearance of SGK1 mRNAs were shown to occur at very short intervals (less than 20 min) [35]. In quiescent TG1 GSCs, SGK1 protein levels were significantly higher after a 2-hour treatment with the compound whereas overall levels of active forms of the enzyme were reduced in the presence of bisacodyl/DDPM. Interestingly, opposite effects on SGK1 overall expression levels and T256 phosphorylation status were observed in proliferating TG1 GSCs challenged with the compound without apparent cytotoxicity. Taken together, these data suggested that bisacodyl/DDPM may target quiescent GSCs through an Akt and/or SGK1-dependent reduction of the phosphorylation status of Thr60 in WNK1 since high levels of phosphorylated WNK1 on this position seem to be linked to GSC survival in quiescent culture conditions.

Like Thr60 phosphorylation levels, catalytic activity of the WNK1 protein was higher in quiescent compared to proliferating GSCs in basal conditions. Treatment with bisacodyl/DDPM resulted in a transient catalytic activity decrease in quiescent GSCs but a similar activity profile was observed in non-responding cells maintained in proliferating culture conditions. Based solely on this observation, it was not possible to conclude as to the role of WNK1 catalytic function in bisacodyl/DDPM cytotoxicity.

In other systems, the N-terminal domain of WNK1 was shown to act as a scaffold to recruit SPAK protein kinase to the N-terminal domain of the Na<sup>+</sup>/HCO<sub>3</sub><sup>-</sup> co-transporter NBCe1. This WNK1 function, which was independent from the catalytic activity of the enzyme, resulted in the phosphorylation of the N-terminal domain of NBCe1 by SPAK and had an inhibitory effect on the co-transporter by reducing its cell surface expression. WNK1/SPAK-mediated NBC co-transporter surface expression/activity negative regulation is antagonized by IRBIT (inositol receptor binding protein released with inositol 1, 4, 5 triphosphate), an enzyme regulating both inositol 1, 4, 5 triphosphate receptors and ion co-transporters including NBCe1 [39][42]. At the resting state or when inositol 1, 4, 5 triphosphate (IP3) concentrations are low near IP3 receptors, IRBIT is bound to IP3 receptors and suppresses their activation. Increased levels of IP3 displace IRBIT and activate IP3R-mediated Ca<sup>2+</sup> release from intracellular stores. Released IRBIT is able to bind to NBC co-transporters and enhance their activity both by increasing their cell surface levels and by directly modulating their activation status. Interestingly, higher expression of IP3R1 was observed in quiescent GSCs in acidic conditions. Thus, in these cells, binding of IRBIT to IP3 receptors combined with high levels of WNK1 Thr60 phosphorylation may cooperate to maintain NBC co-transporter activity to levels allowing cell survival in these particular conditions. Other co-transporters, including NBCn1, share similar N-terminal domains with NBCe1 and could thus be regulated by similar mechanisms [39][42]. It is thus conceivable, that, reduction of p-Thr60 levels in the N-terminus of WNK1 induced by bisacodyl/DDPM, might relieve the regulatory effect of WNK1 on NBCe1 and/or other related co-transporter cell surface expression level and function, and that excessive activation of these proteins would be involved in necrotic death evoked by the compound. Combinations of bisacodyl/DDPM with S0859, an inhibitor of NBC Na<sup>+</sup>/HCO<sub>3</sub><sup>-</sup> co-transporters including NBCe1 and NBCn1, significantly reduced the cytotoxic effect of the compound both on dissociated TG1 and TG1 C1 GSCs and TG1 GSC-derived macro-neurospheres. These results argue in favor of an effect of the compound on Na<sup>+</sup>/CO<sub>3</sub><sup>-</sup> co-transporter function which would be required for the xenobiotics' toxic effect. Interestingly, NBCe1 mRNA levels and NBCe1 and NBCn1 membrane protein expression are higher in TG1 C1 GSCs compared to TG1 cells. These higher expression levels might explain a higher sensitivity of TG1 C1 cells to bisacodyl/DDPM [23] and a less effective protection of TG1 C1 cells by the



Na<sup>+</sup>/HCO<sub>3</sub><sup>-</sup> co-transporter inhibitor S0859. Concomitant treatment of GSCs with bisacodyl/DDPM and DIDS, a compound inhibiting several co-transporters including NBCe1 but not NBCn1, did not allow to determine the respective contribution of these co-transporters in bisacodyl/DDPM cytotoxicity, probably because of DIDS' own high cytotoxicity on treated cells.

Involvement of Akt and SGK1 kinases in bisacodyl/DDPM activity in GSCs, presumably through the regulation of the phosphorylation status of WNK1 Thr60, was further supported by the fact that modulation of these kinases using targeting inhibitors (for Akt and/or SGK1) or activators (for Akt) was influencing the effect of the compound both on dissociated GSCs and GSC-derived macro-neurospheres. A functional link in the response to the compound was established at least for Akt and Na<sup>+</sup>/HCO<sub>3</sub><sup>-</sup> co-transporters of the NBC family potentially regulated by WNK1/SPAK, since Akt inhibition, which is expected to result, based on our hypothesis, in increased Na<sup>+</sup>/HCO<sub>3</sub><sup>-</sup> co-transporter activity leading to cell death, could partially reverse the protective effect of the S0859 Na<sup>+</sup>/HCO<sub>3</sub><sup>-</sup> co-transporter inhibitor. Differences in Na<sup>+</sup>/HCO<sub>3</sub><sup>-</sup> co-transporter expression levels may underlie less pronounced effects of these modulators on TG1 C1 compared to TG1 GSCs.

Direct involvement of WNK1 protein function in bisacodyl/DDPM activity on GSCs was suggested by the observation that the compound's cytotoxicity was reduced in macro-tumorspheres derived from GSCs stably overexpressing the wild-type human WNK1 isoform which would be expected to reduce Na<sup>+</sup>/HCO<sub>3</sub><sup>-</sup> co-transporter membrane levels and activity in treated cells. Partial but significant reversal of bisacodyl/DDPM's cytotoxicity in GSCs overexpressing phosphomimetic (T60D/E) but not non-phosphorylatable (T60A) mutants of WNK1 on Thr60 definitely involved the phosphorylation status of this residue in the compound's signaling in GSCs. However, failure of the T60A mutant to reinforce bisacodyl/DDPM effect on GSCs associated to a weak protective effect suggested that other WNK1 functions were involved. Overexpression of a kinase-dead mutant of the protein did not preserve GSCs from bisacodyl/DDPM activity suggesting that inhibition of the protein's catalytic activity observed in quiescent GSCs treated with bisacodyl/DDPM would be required for the compound's effect. If this is the case, catalytically constitutively active mutants of WNK1, reversing the effect of the compound on WNK1 enzymatic activity, would be expected to show a protective effect on treated GSCs.

Based on our experimental data, we propose that bisacodyl/DDPM acts on quiescent GSCs under extracellular acidic conditions or on GSC-derived macro-tumorspheres in which inner-layer slow-growing cells are exposed to hypoxic/acidic microenvironments, through negative regulation of Akt-SGK1-WNK1 signaling which would lead to a non-physiological increase of plasma membrane  $\text{Na}^+/\text{HCO}_3^-$  co-transporter levels and function and GSC necrotic cell death (Figure 8). It is of note, that no difference in NBCe1/Nbcn1  $\text{Na}^+/\text{HCO}_3^-$  cotransporter expression levels was observed between bisacodyl/DDPM-sensitive quiescent GSCs compared to non-responding proliferating GSCs maintained in physiological pH conditions. Thus, preferential targeting of quiescent GSCs by bisacodyl/DDPM is probably linked to a stronger dependency for proper co-transporter function in these cells compared to proliferating cells that are not challenged by growth factor deprivation and acidic stress. Alternatively, differences in surface membrane bound NBC levels may exist but have not been revealed in membrane extracts not distinguishing between plasma membrane and intracellular vesicular membrane bound proteins. Alternative methods are thus required to test this hypothesis.

To avoid cell death in acidic extracellular conditions, intracellular pH ( $\text{pH}_i$ ) has to be maintained at slightly alkaline values ( $\text{pH}$  7.2-7.4). Tumor cells have thus developed various mechanisms to maintain an alkaline  $\text{pH}_i$  and a slightly acidic extracellular pH ( $\text{pH}_e$ ). For example, these cells have increased ability to export acidic catabolites (such as carbon dioxide, carbonic acid or lactic acid) and import weak bases (such as  $\text{HCO}_3^-$  ions) by the intermediate of transporters. In addition,  $\text{H}^+$  ions are directly extruded by exchange for other cations or by vacuolar ATPase (V-ATPase) [60]. NBCe1 and NBCn1  $\text{Na}^+/\text{HCO}_3^-$  co-transporters catalyze  $\text{HCO}_3^-$  influx which would subsequently lead to  $\text{pH}_i$  alcalinization and extracellular pH ( $\text{pH}_e$ ) acidification. Depending on  $\text{Na}^+:\text{HCO}_3^-$  stoichiometry (2 or 3  $\text{HCO}_3^-$  for 1  $\text{Na}^+$ ), or gradient reversal even in slightly acidic conditions, the electrogenic NBCe1 co-transporter can also operate net efflux of  $\text{HCO}_3^-$  with opposite effects on  $\text{pH}_i/\text{pH}_e$  regulation [38][61]. Thus, deregulation of  $\text{Na}^+/\text{HCO}_3^-$  co-transporters operated by bisacodyl/DDPM may disrupt intra-cellular and/or extra-cellular pH homeostasis outside of ranges required for cell survival and lead to cell death. Alternatively, necrotic cell death in GSCs treated with bisacodyl/DDPM may result from an abnormal modification of intracellular  $\text{Na}^+$  which is concomitantly transported by NBCe1/NBCn1 proteins. Elevated intracellular  $\text{Na}^+$  was shown to result in

intracellular  $\text{Ca}^{2+}$  overload leading to mitochondrial damage and necrotic cell death. Moreover, NBC cotransporters were involved in intracellular  $\text{Na}^+$  concentration modifications in several systems [62][63][64]. Altogether, our data strongly support the idea that deregulation of an Akt/SGK1/NBC co-transporter-related pathway is involved in bisacodyl's cytotoxicity in GSCs although direct protein targets of the compound in these cells remain unknown.

In a previous report, we have shown that pre-treatment with bisacodyl inhibits  $\text{Ca}^{2+}$  mobilization from intracellular stores mediated by acetylcholine or carbachol IP3 (inositol 1,4,5-triphosphate) production and activation of IP3 receptors including IP3R1 [24]. Interestingly, Akt-mediated phosphorylation of WNK1 Thr60 was shown to promote PIP2 (phosphatidylinositol 4,5-bisphosphate) synthesis through phosphatidylinositol 4-kinase IIIa activation, thus sustaining PLC- $\beta$  signaling, IP3 production and IP3 receptor activation mediated by Gq-coupled GPCRs (G protein coupled receptors) [65]. Inhibition of WNK1 Thr60 phosphorylation elicited by bisacodyl may thus underlie the negative effect of the compound on  $\text{Ca}^{2+}$  signaling in quiescent GSCs [24].

In addition to its involvement in bisacodyl/DDPM signaling, our data highlight a yet unknown contribution of WNK1 in cancer stem-like cell physiopathology since overexpression of the native protein or of WNK1 isoforms with modifications of the phosphorylation status of WNK1 Thr60 influence GSC cell viability in quiescent culture conditions and modify the aspect of GSC-derived macro-neurospheres. Moreover, clonal properties of GSCs are sensitive to WT and kinase-dead WNK1 overexpression whereas the growth rate of neurospheres derived from cells overexpressing Thr60 phosphomimetic mutants and catalytically-deficient WNK1 is reduced. To date, several WNK1 mutations have been associated to cancer although the contribution of these modifications in tumor initiation is unknown [66]. In other systems, WNK1 functions have been associated to cell proliferation, migration and survival. Cell stress conditions and namely metabolic stress, were proposed to reveal WNK protein functions in the maintenance of a viable state [67]. This is in agreement with our observations suggesting that WNK1 function and downstream transporter regulation is a critical event for the maintenance of a viable quiescent state in which cells are challenged by particular microenvironmental conditions since disruption of this pathway by bisacodyl/DDPM leads to cell death. Conversely, the WNK1 pathway does not seem to influence viability of GSCs

maintained in proliferating conditions. Through its ability to regulate water, electrolyte and pH homeostasis as well as receptor trafficking (including glucose transporters) at the cell surface, WNK1 may also play a role in metabolic adaptation of cancer cells to their microenvironment [44][68][69]. Deregulation of these processes may underlie the effects of WNK1 mutations in cancer. In glioblastoma, WNK1 was involved in resistance to TMZ-induced apoptosis and glioblastoma cell migration through regulation of the NKCC1 co-transporter [29][30]. However, none of these studies was performed in cancer cells with stem-like properties. To our knowledge, this is the first study directly implicating the WNK1 protein and signaling partners in the maintenance of viable cancer stem-like cells isolated from glioblastoma, thus uncovering novel potentially interesting therapeutic targets for the treatment of the disease.

## **Materials and methods**

### **Materials**

Bisacodyl (4,4'-diacetoxydiphenyl-2-pyridyl-methane; CAS number: 603-50-9) was purchased from Sigma-Aldrich. DDPM (4,4'-dihydroxydiphenyl-2-pyridyl-methane), the active derivative of bisacodyl was synthesized in-house based on previously described methods [23]. Methods for the synthesis of the inactive derivative of bisacodyl/DDPM are provided in supplementary Materials and Methods. Chemical structures of bisacodyl, DDPM and inactive derivative as well as characteristic activity profiles of these compounds on proliferating and quiescent TG1 GSCs are shown in Supplementary Figure S1.

S0859 NBC co-transporter inhibitor (CAS 1019331-10-2), DIDS (4,4'-Diisothiocyanatostilbene-2,2'-disulfonate), a stilbene derivative that is able to inhibit NBCe1 and all other Na<sup>+</sup>-coupled HCO<sub>3</sub><sup>-</sup> transporters but not NBCn1 (CAS 207233-90-7), Akt activator SC79 (CAS 305834-79-1) and SGK1 inhibitor GSK 650394 (CAS 890842-28-1) were purchased from Sigma-Aldrich. The Akt inhibitor VIII (CAS 612847-09-3) was from Calbiochem (Merck Millipore).

### **Ethics statement**

The biomedical research was conducted according to the declaration of Helsinki, to the French laws and was approved by the institutional review board of Sainte Anne Hospital, Paris, France. Patients have given written informed consent.

### **Primary glioblastoma stem cell culture**

TG1 and TG1 C1 (OB1) glioblastoma (WHO grade IV glioma) stem-like cells (GSCs) were derived from tumor samples of patients (Sainte Anne Hospital, Paris, France) as previously described [9][23] and expanded as neurosphere cultures in NS34 medium. In proliferating cultures, neurospheres were mechanically dissociated in single-cell suspensions twice a week. Quiescent cells were obtained by non-renewal of the medium for 9 days following cell seeding. The quiescent slow-growing state of cells obtained in these conditions as well as its reversibility were verified [23]. Both proliferating and quiescent GSCs were also phenotypically and functionally characterized as to the expression of stemness and pluripotency

markers as well as to their clonal, *in vitro* differentiation and *in vivo* engraftment properties [9][23]. Master and working cell banks were established for all cell types. Cells were used at defined ranges of cell passages.

### ***In vitro* formation of clonal and non-clonal macro-neurospheres (macro-tumorspheres) from GSCs**

For clonal-macro-neurosphere formation, GSCs were dissociated into single cells and seeded into 96-well plates at a density of 1 cell/well in 200  $\mu$ L of NS34 medium. 50  $\mu$ L of medium were added into each well every week and individual spheres were transferred into 24-well plates in 1 mL of NS34 medium at week 2. One single sphere was kept in each well to avoid sphere aggregation. The medium was changed once a week. For non-clonal macrospheres, GSCs were dissociated and seeded into 96-well round bottom plates at a density of 5000 cells/well in 200  $\mu$ L of NS34 medium. The plates then were centrifuged at a speed of 1000 rpm for 5 min to precipitate the cells at the bottom of well. The medium was changed once a week during the first 2 weeks and every 2 days afterwards. Individual spheres were used when they reached a size of 800  $\mu$ m to 1 mm of diameter for treatments with vehicle (DMSO), DDPM or DDPM combined to NBC, Akt and or SGK1 inhibitors as indicated.

### **Construction of plasmids for WT and mutant WNK1 overexpression**

Full length synthetic gene for human WNK1 (GenBank accession No. NM\_018979.3) assembled from oligonucleotides and/or PCR products and cloned into a pMA plasmid was purchased from GeneArt. WNK1 coding sequence was PCR amplified with primers including attB1 and attB2 sites for Gateway cloning (Thermo Fisher Scientific). AttB1-WNK1-attB2 amplified fragments were gel-purified (Macherey-Nagel NucleoSpin Gel and PCR clean-up kit). The WT WNK1 coding sequence was then introduced *via* a BP recombination reaction in the pDONR 207 vector. Point mutations to obtain T60A, T60/D, E and K233M mutants were generated in WNK1 coding sequences in the pDONR 207 vector with the QuickChange II XL Site-Directed Mutagenesis kit following the instructions of the manufacturer (Agilent Technologies). All constructs were verified by sequencing of the entire open reading frames and surrounding sequences. A LR recombination

reaction was then performed based on standard Gateway cloning protocols to obtain pCIneo 3-FLAG gateway system mammalian expression vectors for overexpression of WT and mutant isoforms of WNK1 in GSCs. Sequences of the entire cloned fragments and surrounding vector were also verified. A pCIneo 3-FLAG control vector with several STOP codons immediately downstream of the 3-FLAG tag coding sequences (Empty vector) was used as a control. Gateway system materials and vectors were kindly provided by Dr Réal (Faculty of Pharmacy, Strasbourg, France). Primer sequences used for PCR amplification and cloning, mutagenesis and sequencing are available in Supplementary Table S1.

### **Procedure for establishing TG1 GSCs overexpressing WT and mutant forms of WNK1**

TG1 GSCs were transfected with the pCIneo-3FLAG STOP control vector (empty vector) or with pCIneo-3FLAG vectors encoding WT and mutant (T60A, T60D, T60E and K233M) WNK1 with Primary Cell Nucleofector™ Solution P3 and the Amaxa 4D-Nucleofector™ System (Lonza) according to the manufacturer's instructions. Non-transfected TG1 GSCs were used as controls. 48 hours post-transfection, antibiotic-containing fresh medium was used for the selection which was performed with geneticin G418 (Sigma Aldrich) at a concentration of 400 µg/mL for a week until the negative control cells were all dead. Antibiotic concentrations were then reduced to 200 µg/mL for two more weeks. At the end of the selection procedure, TG1 cells stably expressing WT and mutant forms of WNK1 and TG1 cells stably transfected with the pCIneo-3FLAG STOP vector (empty vector) were maintained in medium with G418 (100 µg/mL) for subsequent experiments.

### **Cell viability measurements**

Following dissociation, cells were plated in 96-well micro-well plates (opaque bottom) (Greiner) in 100 µl of NS34 medium, at a density ranging from 30,000 to 50,000 cells/well and treated for 24 hours with DDPM and/or Akt and/or SGK1 inhibitors at indicated concentrations. For combinations of DDPM with NBC co-transporter inhibitor S0859, Akt activator SC-79 or DIDS, GSCs were pre-treated with these compounds for 24 hours prior to addition of DDPM. Inhibitor and DDPM concentrations in each experiment are given in Figure legends. Negative control

wells contained cells treated with DMSO (1%; vehicle). At the end of treatments, CellTiter-Glo® luminescent cell viability assay was used according to the instructions of the manufacturer (Promega). Luminescence was measured in a multilabel reader, including a luminometer (EnVision™, PerkinElmer). Each condition was tested in triplicates.

In some experiments, cell viability of dissociated cells was evaluated with the Trypan blue exclusion test by using a Trypan Blue solution, 0.4% (ThermoFisher).

For large spheres, cell viability assays were performed with CellTiter-Glo®3D cell viability assay (Promega). Spheres (one sphere per well), were plated in 100 µL of medium (1% DMSO) containing or not DDPM and/or inhibitors of Akt and SGK1. Pre-treatment with S0859 was performed as indicated in the corresponding figure legend. At the end of treatment (24 hours or longer as indicated), reagent of cell viability assay was added (100 µL) and after 30 minutes of incubation, 100 µL of mixed cell-reagent solution was taken from each well and measured with a luminometer as described above.

### **Limiting dilution assay for measurements of GSC's clonal properties**

Limiting dilution assay was performed as following: new passaged proliferating GSCs were dissociated and plated in 96-well micro-well plates in 200 µL of NS34 medium. Final cell dilutions ranged from 1-50 cells/well. 16 wells were tested for each condition. 50 µL of NS34 medium were added in each well every week until 2 weeks, when the mean number of spheres obtained for each cell density and each cell type (TG1 cells stably overexpressing WT and mutant forms of WNK1 (T60A, T60D, T60E, K233M or control TG1 cells stably transfected with empty vector pCineo-3FLAG stop) was calculated and plotted against the initial number of cells per well.

### **Measurements of GSC-derived sphere growth rates**

Cells were prepared and seeded as described for limiting dilution assays (final cell dilution of 1 cell/well in 200 µL of NS34 medium). Subsequently, 50 µL of NS34 medium were added in each well every week. Two weeks later (day 14), small spheres were formed and 12 spheres per cell type were chosen and transferred into 24-well plates in 1 mL of NS34 medium (1 sphere/well). From then, half of the culture



medium in each well was replaced by freshly prepared medium at days 21, 24, 27, 30 and 34. Photos of each sphere were taken at the same time-points. Volume ( $\mu\text{m}^3$ ) of GSC-derived spheres from control (empty vector) and WT and mutant WNK1 (T60A, T60D, T60E, K233M) expressing GSCs was evaluated at 21, 24, 27, 30 and 34 days following cell seeding with the ImageJ software.

### **Human Phospho-kinase Array**

A human phospho-kinase array purchased from R&D Systems was used for profiling the relative site-specific phosphorylation in several kinases and kinase substrates, in quiescent GSCs. TG1 C1 cells for preparing cell lysates were incubated with DDPM (10  $\mu\text{M}$  in 1% DMSO) for 2 hours or treated with vehicle (1% DMSO). Cell lysates were prepared with RIPA lysis buffer system (Santa Cruz Biotechnology) (250  $\mu\text{L}$  of complete RIPA buffer supplemented with PMSF, sodium orthovanadate and protease inhibitor cocktail (according to the supplier's instructions) per  $1.0 \times 10^6$  cells). Total protein concentrations in extracts were determined with DC Protein Assay from Bio-Rad according to the microplate assay protocol of the manufacturer. Phosphokinase array membranes were then incubated with 200  $\mu\text{g}$  of protein extract in each condition overnight at  $4^\circ\text{C}$ . Following a washing step with washing buffer provided with the kit, membranes were incubated with provided secondary antibodies at room temperature for 2 hours and then in the presence of a solution containing streptavidine coupled to horseradish peroxidase (HRP) at room temperature for 30 min. Luminescent signals obtained after incubation with revealing solution, were detected with the Image Quant LAS 4000 imaging system (GE Healthcare Life Science). Spots were quantified with the ImageJ software.

### **Western blot analysis**

For total cell protein extract preparation, dissociated proliferating or quiescent TG1 and TG1 C1 GSCs treated with DDPM (10  $\mu\text{M}$  in 1% DMSO, 10, 30 and 120 min) or 1% DMSO or quiescent GSCs of both types treated with the inactive derivative of the compound (10  $\mu\text{M}$  in 1% DMSO, 10, 30 and 120 min) or 1% DMSO as well as dissociated TG1 cells overexpressing or not (empty vector) WT and mutant isoforms of WNK1, were collected and lysed in complete RIPA lysis buffer (Santa Cruz Biotechnology) and several passages through a 23G needle. Following

an incubation of 1 hour at 4°C, cell extracts were centrifuged for 15 min at 14000 rpm at 4°C. Cleared suspensions were quantified with the DC Protein Assay from Bio-Rad. Equivalent amounts of proteins (25-50 µg) were subsequently analyzed in 4-15% gradient Mini-PROTEAN TGX pre-cast gels from Bio-Rad and immunoblotting with appropriate antibodies listed in Supplementary Table S2. Specific antibody binding was detected by horseradish peroxidase-conjugated anti-rabbit or anti-mouse secondary antibodies. Proteins were visualized with the ECL Prime reagent (GE Healthcare Life Sciences) and the Image Quant LAS 4000 imaging system (GE Healthcare Life Science). Quantification of protein bands corrected to loading controls was done with the ImageJ software.

For extraction of membrane proteins, cells were collected and lysed in a lysis buffer prepared with 10 mM HEPES pH 7.4 (Thermo Fisher Scientific) and 2 mM EGTA (Sigma), completed with 1x protease inhibitors (Roche). Several passages through a 23G needle were performed to break the cells. The post nuclear supernatant was obtained after centrifugation (3000 rpm) for 10 minutes at 4 °C. Membrane protein extracts were recovered by centrifugation of the post nuclear supernatant for 90 minutes at 14000 rpm at 4°C, resuspended in PBS and quantified with DC protein Assay (Bio-Rad).

### **RNA extraction and RT-qPCR**

Total RNA was isolated from 5-10 x 10<sup>6</sup> proliferating or quiescent (9 days without medium renewal) TG1 and TG1 C1 GSCs using the TRI Reagent (Euromedex, France) according to the manufacturer's instructions. RNeasy mini kit columns (Qiagen) were used for further purification of RNA samples. NanoDrop ND-1000 (Labtech) was used for absorption spectra analysis and RNA purity assessment. Absorption ratios A260/A280 and A260/A230 were comprised between 1.8 and 2.1. RNA concentration was determined using the Qubit fluorometer and the Quant-it RNA Assay Kit (Invitrogen). RNA integrity was further evaluated with an Agilent 2100 Bioanalyzer and the RNA 6000 LabChip kit. Only RNA with a RNA Integrity Number (RIN) higher than 9 was processed (2100 expert software, Agilent Technologies). 1 µg of total RNA was reverse transcribed to single-stranded cDNA using the High Capacity cDNA Reverse Transcription kit (Applied Biosystems, Life Technologies). Real-time PCR analysis was performed with individual TaqMan gene expression assays in an ABI Prism 7000HT apparatus

(Applied Biosystems, Life Technologies) using standard experimental conditions designed by the manufacturer. NBCe 1/SLC4A4 assay ID: Hs00186798-m1. Results were normalized to the 18S rRNA expression levels determined in all conditions (assay ID: 4319413E). Results are shown as mean  $\pm$  SEM of two independent experiments performed in triplicates.

### **Statistical analysis**

Data were obtained from at least two independent experiments and are shown as mean ( $\pm$  SEM) or mean ( $\pm$  s.d.) as indicated in figure legends. P values were determined using unpaired two-tailed t-tests to compare two groups or one-way or two-way ANOVA to compare more than two groups. Indications are given in figure legends. The level of significance was set at  $p < 0.05$ . Statistical analyses were performed with the Prism 7.0 software (GraphPad).

## Abbreviations

GBM: glioblastoma; GPCR: G protein coupled receptor; GSCs: glioblastoma stem-like cells; IP3: inositol 1, 4, 5 triphosphate; IRBIT: inositol receptor binding protein released with inositol 1, 4, 5 triphosphate; NBC: Na<sup>+</sup>/HCO<sub>3</sub><sup>-</sup> co-transporter; NO: nitric oxide; OSR1: oxidative stress-responsive kinase 1; PDK1: phosphoinositide-dependent protein kinase 1; PIP2: phosphatidylinositol 4,5-bisphosphate; SGK1: serum and glucocorticoid-stimulated protein kinase-1; SPAK: STE20/SPS1-related proline/alanine-rich kinase; TMZ: temozolomide; WNK1: with no lysine (K) kinase 1.

## Author contributions

Conceived and designed the experiments: WC, JD, JH, MCK, MZ. Performed experiments: WC, LN, JD, LC, MZ. Analyzed the data: WC, MZ. Contributed reagents/materials/analysis/tools: SN, FB, EB, ER, PV, MPJ, HC. Wrote the paper: WC, MZ. Provided funding: MH.

## Acknowledgements

We thank R. Vauchelles for training and providing access to the confocal imaging platform "Plateforme d'Imagerie Quantitative (PIQ)" (Faculty of Pharmacy, Strasbourg-Illkirch, France) and N. Vitale (INCI, CNRS UPR3212, Strasbourg, France) for providing vectors for shRNA expression. We would also like to acknowledge C. Ebel for technical assistance on the flow cytometry platform of the IGBMC (Strasbourg-Illkirch, France).

## Conflicts of interest

The authors declare no conflict of interest.

## Funding

This work was supported by multiple grants from La Ligue Contre le Cancer (project (MZ) and PhD funding for WC) and has been performed within the LABEX ANR-10-LABX-0034\_Medalis. Additional funding was from Agence Nationale de la Recherche (ANR) (JH), Université de Strasbourg and Centre National de la Recherche Scientifique (CNRS).

## References

1. Ostrom QT, Gittleman H, Fulop J, Liu M, Blanda R, Kromer C, et al. CBTRUS Statistical Report: Primary Brain and Central Nervous System Tumors Diagnosed in the United States in 2008-2012. *Neuro-Oncol.* 2015;17: iv1-iv62. doi:10.1093/neuonc/nov189
2. Yang L-J, Zhou C-F, Lin Z-X. Temozolomide and Radiotherapy for Newly Diagnosed Glioblastoma Multiforme: A Systematic Review. *Cancer Invest.* 2014;32: 31–36. doi:10.3109/07357907.2013.861474
3. Chen W, Dong J, Haiech J, Kilhoffer M-C, Zeniou M. Cancer Stem Cell Quiescence and Plasticity as Major Challenges in Cancer Therapy. *Stem Cells Int.* 2016;2016. doi:10.1155/2016/1740936
4. O'Connor ML, Xiang D, Shigdar S, Macdonald J, Li Y, Wang T, et al. Cancer stem cells: A contentious hypothesis now moving forward. *Cancer Lett.* 2014;344: 180–187. doi:10.1016/j.canlet.2013.11.012
5. Chen J, Li Y, Yu T-S, McKay RM, Burns DK, Kernie SG, et al. A restricted cell population propagates glioblastoma growth after chemotherapy. *Nature.* 2012;488: 522–526. doi:10.1038/nature11287
6. Galli R, Binda E, Orfanelli U, Cipelletti B, Gritti A, Vitis SD, et al. Isolation and Characterization of Tumorigenic, Stem-like Neural Precursors from Human Glioblastoma. *Cancer Res.* 2004;64: 7011–7021. doi:10.1158/0008-5472.CAN-04-1364
7. Singh SK, Hawkins C, Clarke ID, Squire JA, Bayani J, Hide T, et al. Identification of human brain tumour initiating cells. *Nature.* 2004;432: 396–401. doi:10.1038/nature03128
8. Lee J, Kotliarova S, Kotliarov Y, Li A, Su Q, Donin NM, et al. Tumor stem cells derived from glioblastomas cultured in bFGF and EGF more closely mirror the phenotype and genotype of primary tumors than do serum-cultured cell lines. *Cancer Cell.* 2006;9: 391–403. doi:10.1016/j.ccr.2006.03.030
9. Patru C, Romao L, Varlet P, Coulombel L, Raponi E, Cadusseau J, et al. CD133, CD15/SSEA-1, CD34 or side populations do not resume tumor-initiating properties of long-term cultured cancer stem cells from human malignant glioblastoma. *BMC Cancer.* 2010;10: 66. doi:10.1186/1471-2407-10-66
10. Kreso A, Dick JE. Evolution of the Cancer Stem Cell Model. *Cell Stem Cell.*

2014;14: 275–291. doi:10.1016/j.stem.2014.02.006

11. Roesch A, Fukunaga-Kalabis M, Schmidt EC, Zabierowski SE, Brafford PA, Vultur A, et al. A temporarily distinct subpopulation of slow-cycling melanoma cells is required for continuous tumor growth. *Cell*. 2010;141: 583–594. doi:10.1016/j.cell.2010.04.020

12. Deleyrolle LP, Harding A, Cato K, Siebzehnruhl FA, Rahman M, Azari H, et al. Evidence for label-retaining tumour-initiating cells in human glioblastoma. *Brain*. 2011;134: 1331–1343. doi:10.1093/brain/awr081

13. Patel AP, Tirosh I, Trombetta JJ, Shalek AK, Gillespie SM, Wakimoto H, et al. Single-cell RNA-seq highlights intratumoral heterogeneity in primary glioblastoma. *Science*. 2014;344: 1396–1401. doi:10.1126/science.1254257

14. Ishii A, Kimura T, Sadahiro H, Kawano H, Takubo K, Suzuki M, et al. Histological Characterization of the Tumorigenic “Peri-Necrotic Niche” Harboring Quiescent Stem-Like Tumor Cells in Glioblastoma. *PLoS ONE*. 2016;11. doi:10.1371/journal.pone.0147366

15. Meacham CE, Morrison SJ. Tumour heterogeneity and cancer cell plasticity. *Nature*. 2013;501: 328–337. doi:10.1038/nature12624

16. Barami K. Relationship of neural stem cells with their vascular niche: Implications in the malignant progression of gliomas. *J Clin Neurosci*. 2008;15: 1193–1197. doi:10.1016/j.jocn.2008.01.002

17. Pisco AO, Huang S. Non-genetic cancer cell plasticity and therapy-induced stemness in tumour relapse: “What does not kill me strengthens me.” *Br J Cancer*. 2015;112: 1725–1732. doi:10.1038/bjc.2015.146

18. Molina ES, Pillat MM, Moura-Neto V, Lah TT, Ulrich H. Glioblastoma stem-like cells: approaches for isolation and characterization. *J Cancer Stem Cell Res*. 2014;1: 1. doi:10.14343/JCSCR.2014.2e1007

19. Li Z, Bao S, Wu Q, Wang H, Eyler C, Sathornsumetee S, et al. Hypoxia-Inducible Factors Regulate Tumorigenic Capacity of Glioma Stem Cells. *Cancer Cell*. 2009;15: 501–513. doi:10.1016/j.ccr.2009.03.018

20. Heddleston JM, Li Z, McLendon RE, Hjelmeland AB, Rich JN. The hypoxic microenvironment maintains glioblastoma stem cells and promotes reprogramming towards a cancer stem cell phenotype. *Cell Cycle*. 2009;8: 3274–3284. doi:10.4161/cc.8.20.9701

21. Rich JN. Cancer Stem Cells in Radiation Resistance. *Cancer Res*. 2007;67:

8980–8984. doi:10.1158/0008-5472.CAN-07-0895

22. Erasimus H, Gobin M, Niclou S, Van Dyck E. DNA repair mechanisms and their clinical impact in glioblastoma. *Mutat Res Mutat Res*. 2016;769: 19–35. doi:10.1016/j.mrrev.2016.05.005

23. Zeniou M, Fève M, Mameri S, Dong J, Salomé C, Chen W, et al. Chemical Library Screening and Structure-Function Relationship Studies Identify Bisacodyl as a Potent and Selective Cytotoxic Agent Towards Quiescent Human Glioblastoma Tumor Stem-Like Cells. *PLOS ONE*. 2015;10: e0134793. doi:10.1371/journal.pone.0134793

24. Dong J, Aulestia FJ, Assad Kahn S, Zeniou M, Dubois LG, El-Habr EA, et al. Bisacodyl and its cytotoxic activity on human glioblastoma stem-like cells. Implication of inositol 1,4,5-triphosphate receptor dependent calcium signaling. *Biochim Biophys Acta BBA - Mol Cell Res*. doi:10.1016/j.bbamcr.2017.01.010

25. McCormick JA, Ellison DH. The WNKs: Atypical Protein Kinases With Pleiotropic Actions. *Physiol Rev*. 2011;91: 177–219. doi:10.1152/physrev.00017.2010

26. Shekarabi M, Zhang J, Khanna AR, Ellison DH, Delpire E, Kahle KT. WNK Kinase Signaling in Ion Homeostasis and Human Disease. *Cell Metab*. 2017;25: 285–299. doi:10.1016/j.cmet.2017.01.007

27. Vitari AC, Deak M, Morrice NA, Alessi DR. The WNK1 and WNK4 protein kinases that are mutated in Gordon's hypertension syndrome phosphorylate and activate SPAK and OSR1 protein kinases. *Biochem J*. 2005;391: 17–24. doi:10.1042/BJ20051180

28. Xu B, Stippec S, Lazrak A, Huang C-L, Cobb MH. WNK1 Activates SGK1 by a Phosphatidylinositol 3-Kinase-dependent and Non-catalytic Mechanism. *J Biol Chem*. 2005;280: 34218–34223. doi:10.1074/jbc.M505735200

29. Algharabil J, Kintner DB, Wang Q, Begum G, Clark PA, Yang S-S, et al. Inhibition of  $\text{Na}^+ - \text{K}^+ - 2\text{Cl}^-$  Cotransporter isoform 1 Accelerates Temozolomide-mediated Apoptosis in Glioblastoma Cancer Cells. *Cell Physiol Biochem*. 2012;30: 33–48. doi:10.1159/000339047

30. Zhu W, Begum G, Pointer K, Clark PA, Yang S-S, Lin S-H, et al. WNK1-OSR1 kinase-mediated phospho-activation of  $\text{Na}^+ - \text{K}^+ - 2\text{Cl}^-$  cotransporter facilitates glioma migration. *Mol Cancer*. 2014;13: 31. doi:10.1186/1476-4598-13-31

31. Cheng C-J, Huang C-L. Activation of PI3-Kinase Stimulates Endocytosis of

ROMK via Akt1/SGK1-Dependent Phosphorylation of WNK1. *J Am Soc Nephrol*. 2011;22: 460–471. doi:10.1681/ASN.2010060681

32. Vitari AC, Deak M, Collins BJ, Morrice N, Prescott AR, Phelan A, et al. WNK1, the kinase mutated in an inherited high-blood-pressure syndrome, is a novel PKB (protein kinase B)/Akt substrate. *Biochem J*. 2004;378: 257–268. doi:10.1042/BJ20031692

33. Jiang ZY, Zhou QL, Holik J, Patel S, Leszyk J, Coleman K, et al. Identification of WNK1 as a Substrate of Akt/Protein Kinase B and a Negative Regulator of Insulin-stimulated Mitogenesis in 3T3-L1 Cells. *J Biol Chem*. 2005;280: 21622–21628. doi:10.1074/jbc.M414464200

34. Sarbassov DD, Guertin DA, Ali SM, Sabatini DM. Phosphorylation and Regulation of Akt/PKB by the Rictor-mTOR Complex. *Science*. 2005;307: 1098–1101. doi:10.1126/science.1106148

35. Lang F, Böhmer C, Palmada M, Seeböhm G, Strutz-Seeböhm N, Vallon V. (Patho)physiological Significance of the Serum- and Glucocorticoid-Inducible Kinase Isoforms. *Physiol Rev*. 2006;86: 1151–1178. doi:10.1152/physrev.00050.2005

36. García-Martínez JM, Alessi DR. mTOR complex 2 (mTORC2) controls hydrophobic motif phosphorylation and activation of serum- and glucocorticoid-induced protein kinase 1 (SGK1). *Biochem J*. 2008;416: 375–385. doi:10.1042/BJ20081668

37. de los Heros P, Alessi DR, Gourlay R, Campbell DG, Deak M, Macartney TJ, et al. The WNK-regulated SPAK/OSR1 kinases directly phosphorylate and inhibit the  $K^+ - Cl^-$  co-transporters. *Biochem J*. 2014;458: 559–573. doi:10.1042/BJ20131478

38. Parker MD, Boron WF. The divergence, actions, roles, and relatives of sodium-coupled bicarbonate transporters. *Physiol Rev*. 2013;93: 803–959. doi:10.1152/physrev.00023.2012

39. Yang D, Li Q, So I, Huang C-L, Ando H, Mizutani A, et al. IRBIT governs epithelial secretion in mice by antagonizing the WNK/SPAK kinase pathway. *J Clin Invest*. 2011;121: 956–965. doi:10.1172/JCI43475

40. Ch'En FF-T, Villafuerte FC, Swietach P, Cobden PM, Vaughan-Jones RD. S0859, an N-cyanosulphonamide inhibitor of sodium-bicarbonate cotransport in the heart. *Br J Pharmacol*. 2008;153: 972–982. doi:10.1038/sj.bjp.0707667



41. Kumar S, Flacke J-P, Kostin S, Appukuttan A, Reusch HP, Ladilov Y. SLC4A7 sodium bicarbonate co-transporter controls mitochondrial apoptosis in ischaemic coronary endothelial cells. *Cardiovasc Res.* 2011;89: 392–400. doi:10.1093/cvr/cvq330
42. Hong JH, Yang D, Shcheynikov N, Ohana E, Shin DM, Muallem S. Convergence of IRBIT, phosphatidylinositol (4,5) biphosphate, and WNK/SPAK kinases in regulation of the Na<sup>+</sup>-HCO<sub>3</sub><sup>-</sup> cotransporters family. *Proc Natl Acad Sci.* 2013;110: 4105–4110. doi:10.1073/pnas.1221410110
43. Yamada K, Park H-M, Rigel DF, DiPetrillo K, Whalen EJ, Anisowicz A, et al. Small-molecule WNK inhibition regulates cardiovascular and renal function. *Nat Chem Biol.* 2016;12: 896–898. doi:10.1038/nchembio.2168
44. Park S, Hong JH, Ohana E, Muallem S. The WNK/SPAK and IRBIT/PP1 Pathways in Epithelial Fluid and Electrolyte Transport. *Physiology.* 2012;27: 291–299. doi:10.1152/physiol.00028.2012
45. Tu S, Bugde A, Luby-Phelps K, Cobb MH. WNK1 is required for mitosis and abscission. *Proc Natl Acad Sci U S A.* 2011;108: 1385–1390. doi:10.1073/pnas.1018567108
46. Sengupta S, Tu S-W, Wedin K, Earnest S, Stippec S, Luby-Phelps K, et al. Interactions with WNK (With No Lysine) Family Members Regulate Oxidative Stress Response 1 and Ion Co-transporter Activity. *J Biol Chem.* 2012;287: 37868–37879. doi:10.1074/jbc.M112.398750
47. Ting Wu, Yun Dai. Tumor microenvironment and therapeutic response. *Cancer Lett.* 2016;
48. Ping Y-F, Zhang X, Bian X-W. Cancer stem cells and their vascular niche: Do they benefit from each other? *Cancer Lett.* 2016;380: 561–567. doi:10.1016/j.canlet.2015.05.010
49. Quail DF, Joyce JA. Microenvironmental regulation of tumor progression and metastasis. *Nat Med.* 2013;19: 1423–1437. doi:10.1038/nm.3394
50. Carmeliet P, Jain RK. Molecular mechanisms and clinical applications of angiogenesis. *Nature.* 2011;473: 298–307. doi:10.1038/nature10144
51. Gatenby RA, Gillies RJ. Why do cancers have high aerobic glycolysis? *Nat Rev Cancer.* 2004;4: 891–899. doi:10.1038/nrc1478
52. Parks SK, Cormerais Y, Marchiq I, Pouyssegur J. Hypoxia optimises tumour growth by controlling nutrient import and acidic metabolite export. *Mol Aspects Med.*

2016;47–48: 3–14. doi:10.1016/j.mam.2015.12.001

53. Pistollato F, Abbadi S, Rampazzo E, Persano L, Della Puppa A, Frasson C, et al. Intratumoral Hypoxic Gradient Drives Stem Cells Distribution and MGMT Expression in Glioblastoma. *STEM CELLS*. 2010;28: 851–862. doi:10.1002/stem.415

54. Das B, Tsuchida R, Malkin D, Koren G, Baruchel S, Yeger H. Hypoxia Enhances Tumor Stemness by Increasing the Invasive and Tumorigenic Side Population Fraction. *STEM CELLS*. 2008;26: 1818–1830. doi:10.1634/stemcells.2007-0724

55. Schreiner J, Nell G, Loeschke K. Effect of diphenolic laxatives on Na<sup>+</sup>-K<sup>+</sup>-activated ATPase and cyclic nucleotide content of rat colon mucosa in vivo. *Naunyn Schmiedeberg's Arch Pharmacol*. 1980;313: 249–255.

56. Rachmilewitz D, Karmeli F, Okon E. Effects of bisacodyl on cAMP and prostaglandin E<sub>2</sub> contents, (Na<sup>+</sup> + K<sup>+</sup>) ATPase, adenylyl cyclase, and phosphodiesterase activities of rat intestine. *Dig Dis Sci*. 1980;25: 602–608.

57. Beubler E, Schirgi-Degen A. Stimulation of enterocyte protein kinase C by laxatives in-vitro. *J Pharm Pharmacol*. 1993;45: 59–62.

58. Gaginella TS, Mascolo N, Izzo AA, Autore G, Capasso F. Nitric oxide as a mediator of bisacodyl and phenolphthalein laxative action: induction of nitric oxide synthase. *J Pharmacol Exp Ther*. 1994;270: 1239–1245.

59. Ikarashi N, Baba K, Ushiki T, Kon R, Mimura A, Toda T, et al. The laxative effect of bisacodyl is attributable to decreased aquaporin-3 expression in the colon induced by increased PGE<sub>2</sub> secretion from macrophages. *Am J Physiol - Gastrointest Liver Physiol*. 2011;301: G887–G895. doi:10.1152/ajpgi.00286.2011

60. Neri D, Supuran CT. Interfering with pH regulation in tumours as a therapeutic strategy. *Nat Rev Drug Discov*. 2011;10: 767–777. doi:10.1038/nrd3554

61. Parks SK, Pouyssegur J. The Na<sup>(+)</sup>/HCO<sub>3</sub><sup>(-)</sup> Co-Transporter SLC4A4 Plays a Role in Growth and Migration of Colon and Breast Cancer Cells. *J Cell Physiol*. 2015;230: 1954–1963. doi:10.1002/jcp.24930

62. Vaughan-Jones RD, Villafuerte FC, Swietach P, Yamamoto T, Rossini A, Spitzer KW. pH-Regulated Na<sup>+</sup> Influx into the Mammalian Ventricular Myocyte: The Relative Role of Na<sup>+</sup>-H<sup>+</sup> Exchange and Na<sup>+</sup>-HCO<sub>3</sub><sup>-</sup> Co-Transport. *J Cardiovasc Electrophysiol*. 2006;17: S134–S140. doi:10.1111/j.1540-8167.2006.00394.x

63. Lee BK, Jung Y-S. The Na<sup>+</sup>/H<sup>+</sup> exchanger-1 inhibitor cariporide prevents

glutamate-induced necrotic neuronal death by inhibiting mitochondrial  $\text{Ca}^{2+}$  overload. *J Neurosci Res.* 2012;90: 860–869. doi:10.1002/jnr.22818

64. Wei X, Shao B, He Z, Ye T, Luo M, Sang Y, et al. Cationic nanocarriers induce cell necrosis through impairment of  $\text{Na}^{+}/\text{K}^{+}$ -ATPase and cause subsequent inflammatory response. *Cell Res.* 2015;25: 237–253. doi:10.1038/cr.2015.9

65. An S-W, Cha S-K, Yoon J, Chang S, Ross EM, Huang C-L. WNK1 Promotes PIP2 Synthesis to Coordinate Growth Factor and GPCR-Gq Signaling. *Curr Biol.* 2011;21: 1979–1987. doi:10.1016/j.cub.2011.11.002

66. Moniz S, Veríssimo F, Matos P, Brazão R, Silva E, Kotevelets L, et al. Protein kinase WNK2 inhibits cell proliferation by negatively modulating the activation of MEK1/ERK1/2. *Oncogene.* 2007;26: 6071–6081. doi:10.1038/sj.onc.1210706

67. Solomon A, Bandhakavi S, Jabbar S, Shah R, Beitel GJ, Morimoto RI. *Caenorhabditis elegans* OSR-1 Regulates Behavioral and Physiological Responses to Hyperosmotic Environments. *Genetics.* 2004;167: 161–170. doi:10.1534/genetics.167.1.161

68. Oh E, Heise CJ, English JM, Cobb MH, Thurmond DC. WNK1 Is a Novel Regulator of Munc18c-Syntaxin 4 Complex Formation in Soluble NSF Attachment Protein Receptor (SNARE)-mediated Vesicle Exocytosis. *J Biol Chem.* 2007;282: 32613–32622. doi:10.1074/jbc.M706591200

69. Mendes AI, Matos P, Moniz S, Jordan P. Protein Kinase WNK1 Promotes Cell Surface Expression of Glucose Transporter GLUT1 by Regulating a Tre-2/USP6-BUB2-Cdc16 Domain Family Member 4 (TBC1D4)-Rab8A Complex. *J Biol Chem.* 2010;285: 39117–39126. doi:10.1074/jbc.M110.159418

## Legends

### Figure 1. DDPM modifies the phosphorylation status of WNK1 Thr60 in quiescent GSCs maintained in acidic pH culture conditions

**A.** Phospho-kinase Array membranes from R&D Systems were incubated with protein extracts from quiescent TG1 C1 GSCs treated with 10  $\mu$ M of DDPM (in 1% DMSO, green bars) or DMSO alone (C: grey bars) for 2 hours. The histogram represents the mean pixel intensity of the signal from triplicates within the same experiment ( $\pm$  s.d.), analyzed with the ImageJ software. The phosphorylation of WNK1-Thr60 was significantly decreased by DDPM (black arrow). Black rectangle illustrates modifications in the phosphorylation status of Akt Ser473 and Thr308 required for Akt activation. Activated Akt was shown to phosphorylate Thr60 in WNK1. **B.** The protein expression levels of WNK1 and phospho (p)-Thr60 WNK1 were determined by western blotting and appropriate antibodies in protein extracts from proliferating and quiescent TG1 and TG1 C1 GSCs. GAPDH expression was used as a loading control. Blots are representative out of at least two independent experiments. Quantification graphs with ImageJ (fold of normalized to GAPDH-relative mean expression of WNK1 (left) and p-Thr60-WNK1 (right) are shown ( $\pm$  SEM;  $n \geq 2$ )). WNK1 levels in these cell types were normalized to the level of the protein in proliferating TG1 GSCs. P-Thr60-WNK1 levels in quiescent TG1 and TG1 C1 CSCs were normalized to the levels observed in proliferating TG1 and TG1 C1 GSCs, respectively. Student t-test. \*  $p < 0.05$ , \*\*  $p < 0.005$ . **C.** Proliferating and quiescent TG1 GSCs were treated with DMSO (1%, C: Control) or with DDPM (10  $\mu$ M in 1% DMSO) for 10, 30 or 120 minutes (left and middle panel, respectively). Quiescent TG1 GSCs were treated with 1% DMSO (C) or with an inactive derivative of bisacodyl/DDPM (10  $\mu$ M in 1% DMSO) for 10, 30 or 120 minutes (right panel). Expression of WNK1 and p-Thr60-WNK1 was evaluated by western blotting using appropriate antibodies. GAPDH expression was used as a loading control. Blots are representative out of at least three independent experiments. Quantification graphs (fold of normalized to GAPDH-relative mean expression compared to control (C) conditions for each cell type and treatment conditions are shown under the blots for proliferating and quiescent TG1 GSCs treated with DDPM (left and middle panels, respectively) and for quiescent TG1 GSCs treated with the inactive derivative of the compound (right panel) ( $\pm$  SEM;  $n \geq 2$ ). Statistical analysis was performed by

pairwise comparison of results at each time point relatively to the levels of WNK1 and p-Thr60-WNK1 in control (C) conditions. Student t-test. \*  $p < 0.05$ , \*\*\*  $p < 0.0005$ ; \*\*\*\*  $p < 0.0001$ , ns: not significant.

**Figure 2. DDPM modifies the phosphorylation status of WNK1 partners Akt and SGK1 in GSCs**

**A, B.** Akt and p- Ser473-Akt (A upper left panel) and SGK1 and p-Thr256 SGK1 (B, upper left panel) protein levels were analyzed by western blotting, quantified with the ImageJ software, compared between proliferating and quiescent TG1 GSCs and represented as histograms. The loading control was GAPDH expression and results are representative of at least two independent experiments. Statistical analysis was performed by comparing expression levels in quiescent cells *versus* proliferating TG1 GSCs. Student t-test. \*  $p < 0.05$ , \*\*  $p < 0.05$ , \*\*\*  $p < 0.0005$ . Akt and p- Ser473-Akt (A) and SGK1 and p-Thr256 SGK1 (B) protein levels were also determined by western blotting as above in proliferating and quiescent TG1 GSCs treated with DMSO (1%, C: Control) or with DDPM (10  $\mu$ M in 1% DMSO) for 10, 30 or 120 minutes (A and B, middle left and middle right panels, respectively) or in quiescent TG1 GSCs treated with 1% DMSO (C) or with an inactive derivative of bisacodyl/DDPM (10  $\mu$ M in 1% DMSO) for 10, 30 or 120 minutes (A and B, right panels, respectively). The loading control was GAPDH expression and results are representative of at least two independent experiments. Pixel intensity quantification blots (normalized to GAPDH) expressed as fold expression compared to control (C) conditions are shown under the blots for proliferating and quiescent TG1 GSCs treated with DDPM (left and middle panels, respectively) and for quiescent TG1 GSCs treated with the inactive derivative of the compound (right panel) (+/- SEM;  $n \geq 2$ ). Statistical analysis was performed by pairwise comparison of results at each time point relatively to the levels of unphosphorylated and phosphorylated forms of Akt and SGK1 on selected residues in control (C) conditions. Student t-test. \*  $p < 0.05$ , \*\*  $p < 0.005$ , \*\*\*  $p < 0.0005$ , ns: not significant.

**Figure 3. DDPM modifies the catalytic activity of WNK1 and affects the phosphorylation status of WNK1 targets SPAK and OSR1 in proliferating and quiescent GSCs**

SPAK and OSR1 as well as phospho-Ser373-SPAK and phospho-Ser325-OSR1 protein levels were analyzed by western blotting, quantified with the ImageJ software and compared between proliferating and quiescent TG1 GSCs (upper left panel). The loading control was GAPDH expression and results are representative of at least two independent experiments. Statistical analysis was performed by comparing expression levels in quiescent cells *versus* proliferating TG1 GSCs. Student t-test. \*  $p < 0.05$ . Western blotting with appropriate antibodies was also used to determine the protein expression levels of WNK1 substrates SPAK and OSR1 as well as the levels of phospho-Ser373-SPAK and phospho-Ser325-OSR1, in proliferating and quiescent TG1 GSCs treated with DMSO (1%, C: Control) or with DDPM (10  $\mu$ M in 1% DMSO) for 10, 30, or 120 minutes (middle left and middle right panels), or in quiescent TG1 GSCs treated with DMSO (1%, C: Control) or an inactive derivative of the compound (10  $\mu$ M in 1% DMSO) for 10, 30 or 120 minutes (right panel). GAPDH expression was used as a loading control. Blots are representative out of at least three independent experiments. Quantification graphs (fold of normalized to GAPDH-relative mean expression compared to control (C) conditions for each cell type and treatment conditions) are shown under the blots for proliferating and quiescent TG1 GSCs treated with DDPM and for quiescent TG1 GSCs treated with the inactive derivative of the compound (+/- SEM;  $n \geq 2$ ). Statistical analysis was performed by pairwise comparison of results at each time point relatively to the levels of SPAK, OSR1 and p-SPAK/p-OSR1 in control (C) conditions. Student t-test. \*  $p < 0.05$ , \*\*  $p < 0.005$ ; ns: not significant. Blots and quantifications for OSR1 shown are from TG1 C1 GSCs.

**Figure 4 Inhibition of NBC  $\text{Na}^+/\text{HCO}_3^-$  co-transporters including NBCe1, a downstream target of the WNK1 signaling pathway, protects dissociated quiescent GSCs and GSC-derived macro-neurospheres from DDPM action**

**A.** Quiescent TG1 (left panel) and TG1 C1 (right panel) GSCs were pre-treated for 24 hours with increasing concentrations of the NBC-family  $\text{Na}^+/\text{HCO}_3^-$  co-transporter inhibitor S0859. Subsequently, cells were mock-treated (1% DMSO and S0859 from the pre-treatment) or incubated in the presence of DDPM (2 or 5  $\mu$ M for

TG1 GSCs; 1.5 and 2  $\mu$ M for TG1 C1 cells and S0859 from the pre-treatment) for 24 hours. Cell viability measurements were performed with the ATP-Glo cell survival-based assay. Results are expressed as a percentage of the viability of control TG1 or TG1 C1 GSCs incubated with 1% DMSO alone for 48 hours. Results are the mean of two independent experiments performed in triplicate ( $\pm$  SEM). Statistical analysis was performed with Two-way ANOVA and Tukey's multiple comparison test. \*  $p < 0.05$ , \*\*  $p < 0.005$ , \*\*\*  $p < 0.0005$ . **B.** At day 0, large TG1 GSC-derived neurospheres were treated with DMSO alone (1%; upper left and middle panels) or with the NBC inhibitor S0859 (100  $\mu$ M) in 1% DMSO (upper right panel) for 24 hours. DDPM (2  $\mu$ M) was subsequently added at day 1 to neurospheres (middle and right middle panels) and cells were incubated in the presence of the compound for another 24 hours. Scale bars: 200  $\mu$ m. The ATP-Glo assay was used to evaluate cell viability which was represented on the provided histogram as a percentage of the viability of the cells within the sphere treated in control conditions (1% DMSO, 48 hours). Results are from a distinct neurosphere for each condition tested in triplicate ( $\pm$  s.d.). Similar results were obtained in at least two independent additional experiments. Ordinary one-way ANOVA and Tukey's multiple comparison test. \*  $p < 0.05$ , \*\*\*  $p < 0.0005$ . **C.** The mRNA expression levels of NBCe1 were determined by RT-qPCR in proliferating and quiescent TG1 and TG1 C1 GSCs. 18S mRNA was used for normalization. Results were expressed as fold change ( $2^{\Delta\Delta Ct}$ ) considering proliferating TG1 GSCs as calibrator. Data are from two independent experiments, each performed in duplicate ( $\pm$  SEM). Ordinary one-way ANOVA and Dunnett's multiple comparisons test. \*  $p < 0.05$ , \*\*  $p < 0.005$ . **D.** Membrane compartment NBCe1 protein levels were evaluated in proliferating and quiescent TG1 and TG1 C1 GSCs with a commercially available antibody. Na<sup>+</sup>/K<sup>+</sup> ATPase levels in membrane protein extracts were used as loading controls. Relative membrane NBCe1 levels (corrected to Na<sup>+</sup>/K<sup>+</sup> ATPase) were represented as fold difference considering proliferating TG1 GSCs as a calibrator. Quantitative results are from 2 independent experiments ( $\pm$  SEM). Ordinary one-way ANOVA and Dunnett's multiple comparisons test. \*  $p < 0.05$ .

**Figure 5 Modulation of WNK1 signaling partners Akt, SGK1 and NBC Na<sup>+</sup>/HCO<sub>3</sub><sup>-</sup> co-transporters NBCE1/NBCN1 impacts DDPM cytotoxic activity in dissociated quiescent GSCs previously grown as neurospheres**

**A, B, C.** Quiescent TG1 GSCs were either mock-treated (1% DMSO) or incubated in the presence of DDPM at indicated concentrations and/or Akt inhibitor VIII (A), SGK1 inhibitor GSK 650394 (B) or a combination of both compounds (C) for 24 hours. Cell viability measurements were performed with the ATP-based CellTiter-Glo® cell viability assay. Results are expressed as a percentage of the viability of control TG1 GSCs incubated with 1% DMSO alone for 24 hours. Results are the mean of three (A, B) or two (C) independent experiments performed in triplicate (+/- SEM). Statistical analysis was performed with two-way ANOVA and Tukey's multiple comparisons test. \* p<0.05, \*\* p<0.005, \*\*\* p<0.0005; \*\*\*\* p<0.0001. **D, E.** Quiescent TG1 GSCs were incubated in 1% DMSO (controls) or pretreated for 24 hours with the indicated concentrations of the NBC inhibitor S0859 (in 1% DMSO) (D) or the Akt activator SC-79 (E). Indicated concentrations of DDPM alone (in 1% DMSO) (D, E) or DDPM combined to 10 µM of the VIII Akt inhibitor (D) were then added and treatment was pursued for 24 hours. Control cells were maintained in 1% DMSO. Cell viability assays, presentation of results and statistical analysis were performed as described in A, B and C. \* p<0.05, \*\* p<0.005, \*\*\* p<0.0005.

**Figure 6 Modulation of WNK1 levels and/or activity impacts GSC cell survival, aspect of GSC-derived macro-neurospheres and GSC clonal properties and growth**

**A.** Cell viability of proliferating and quiescent (7 days or 9 days without medium renewal) control (Empty vector) TG1 GSCs or TG1 GSCs stably overexpressing WT or mutant (T60A, T60D, T60E, K233M) forms of WNK1. Trypan blue staining was used. Results were expressed as the percentage of Trypan blue positive cells (dead cells) in each condition. Error bars represent the mean (+/- SEM) (n≥2). Ordinary two-way ANOVA and Tukey's multiple comparisons test. \* p<0.05, \*\*\* p<0.0005. **B.** Aspect of big 3D clonal neurospheres derived from single control (Empty vector) TG1 GSCs or TG1 GSCs stably overexpressing WT or mutant (T60A, T60D, T60E, K233M) forms of WNK1. Scale bars: 200 µm. **C.** Evaluation of the clonal properties of control (Empty vector) TG1 GSCs or TG1 GSCs stably overexpressing WT or mutant (T60A, T60D, T60E, K233M) forms of WNK1. The mean number of spheres



obtained at 2 weeks in culture was determined as a function of the initial number of cells in a well. Initial cell numbers seeded ranges from 1 to 50 cells/well. Only conditions for which statistically significant differences were recorded between cell types are represented (n=16 wells for each condition, +/-SEM). Ordinary two-way ANOVA and Tukey's multiple comparisons test. \* p<0.05, \*\* p<0.005, \*\*\* p<0.0005, \*\*\*\* p<0.000001. The graph representing all initial number of cells/well-conditions is shown in the supplementary data section (Supplementary Figure S9A). **D.** Growth rate measurements of 3D neurospheres derived from control (Empty vector) TG1 GSCs or TG1 GSCs stably overexpressing WT or mutant (T60A, T60D, T60E, K233M) forms of WNK1. Sphere volume ( $\mu\text{m}^3$ ) was evaluated with the ImageJ software at different time points (21, 24, 27, 30 and 34 days) following cell seeding. Results illustrated on the histogram are the mean (+/- SEM) from measurements at 34 days (n=12 spheres for each cell type). Ordinary two-way ANOVA and Tukey's multiple comparisons test. \* p<0.05, \*\*\* p<0.0005, \*\*\*\* p<0.0001. The graph representing all time points is provided in Supplementary Figure S9B.

**Figure 7 Modulation of WNK1 levels, Thr60 phosphorylation and catalytic activity impacts DDPM action on GSC-derived macro-neurospheres**

**A.** 3D macro-neurospheres were obtained from control TG1 GSCs (Empty vector) or TG1 GSCs stably overexpressing wild-type (WT) WNK1. 8 individual spheres of each type (and of similar size) were treated with 1% DMSO or DDPM (3  $\mu\text{M}$  in 1% DMSO) for 24 hours. Cell viability was evaluated following treatment with the 3D ATP-Glo assay and expressed (as a percentage) for each type of sphere with respect to DMSO alone-treated controls. Error bars represent the mean (+/- SEM) (n=8 spheres for each condition). Student t-test. \* p<0,05. Mann Whitney non-parametric two-tailed test: p=0.007. **B.** 3D neurospheres obtained as described in A (Empty vector as control and WT WNK1 overexpressing), were incubated in the presence of DMSO alone (1%) or pretreated with the indicated concentration of NBC inhibitor S0859 for 24 hours. DDPM alone (in 1% DMSO) or DDPM combined to 10  $\mu\text{M}$  of the VIII Akt inhibitor or 10  $\mu\text{M}$  of the SGK1 inhibitor (GSK 5650394) were then added and treatment was pursued for 24 hours. Control cells were maintained in 1% DMSO. Cell viability assays and data presentation was as in A. Two-way ANOVA, Empty vector versus WT WNK1: p=0.0038 (\*\*). **C.** Neurospheres derived from control (Empty vector) TG1 GSCs or TG1 GSCs stably overexpressing WT or

mutant (T60A, T60D, T60E, K233M) forms of WNK1 were treated with DMSO alone (1%) (control) or 1% DMSO in the presence of 2  $\mu$ M of DDPM for 24, 48 and 72 hours. Cell viability was evaluated following treatment with the 3D ATP-Glo assay and expressed (as a percentage) for each type of sphere with respect to DMSO alone-treated controls. Error bars represent the mean ( $\pm$  SEM) (n=3 spheres for each condition and each time point). Two-way ANOVA and Tukey's multiple comparisons test. \*  $p < 0.05$ , \*\*  $p < 0.005$ , \*\*\*  $p < 0.0005$ .

**Figure 8 Proposed model for signaling pathways underlying the cytotoxicity of bisacodyl/DDPM on GSCs and GSC-derived 3D macro-tumorspheres**

Bisacodyl/DDPM was shown to negatively regulate the phosphorylation status of WNK1 Thr60, which is potentially phosphorylated by kinases Akt and SGK1. The catalytic activity of WNK1 requiring phosphorylation of Ser382 is also transiently reduced by the compound. This would lead to reduced SPAK activity which in turn was shown to result in increased cell surface expression and activity of NBC  $\text{Na}^+/\text{HCO}_3^-$  co-transporters including NBCe1 and NBCn1. NBCe1 and NBCn1 are able to regulate intracellular pH homeostasis ( $\text{pH}_i$  alcalinization) through  $\text{HCO}_3^-$  influx. According to  $\text{Na}^+:\text{HCO}_3^-$  stoichiometry or gradient reversal that may occur even in slightly acidic pH conditions, NBCe1 can also operate net efflux of  $\text{HCO}_3^-$  with opposite effects on intracellular and extracellular ( $\text{pH}_e$ ) pH regulation. Stoichiometry of  $\text{Na}^+$  and  $\text{HCO}_3^-$  co-transport by NBC transporters is not indicated. Only the direction of co-transport is shown. Deregulation of  $\text{pH}_i/\text{pH}_e$  homeostasis outside of cell survival ranges may underlie the effect of the compound on GSCs (necrosis). Alternatively, bisacodyl/DDPM cytotoxicity may result from intracellular  $\text{Na}^+$  overload (co-transported with  $\text{HCO}_3^-$ ) which was shown to lead to abnormal intracellular calcium concentrations, mitochondrial damage and necrotic cell death. In agreement with these findings, Akt and SGK1 inhibitors reinforce the activity of bisacodyl/DDPM on quiescent GSCs. Conversely, Akt activation or NBC inhibition produce a protective effect. ?: direct protein targets of bisacodyl/DDPM in GSCs are currently unknown.

# Figure 2

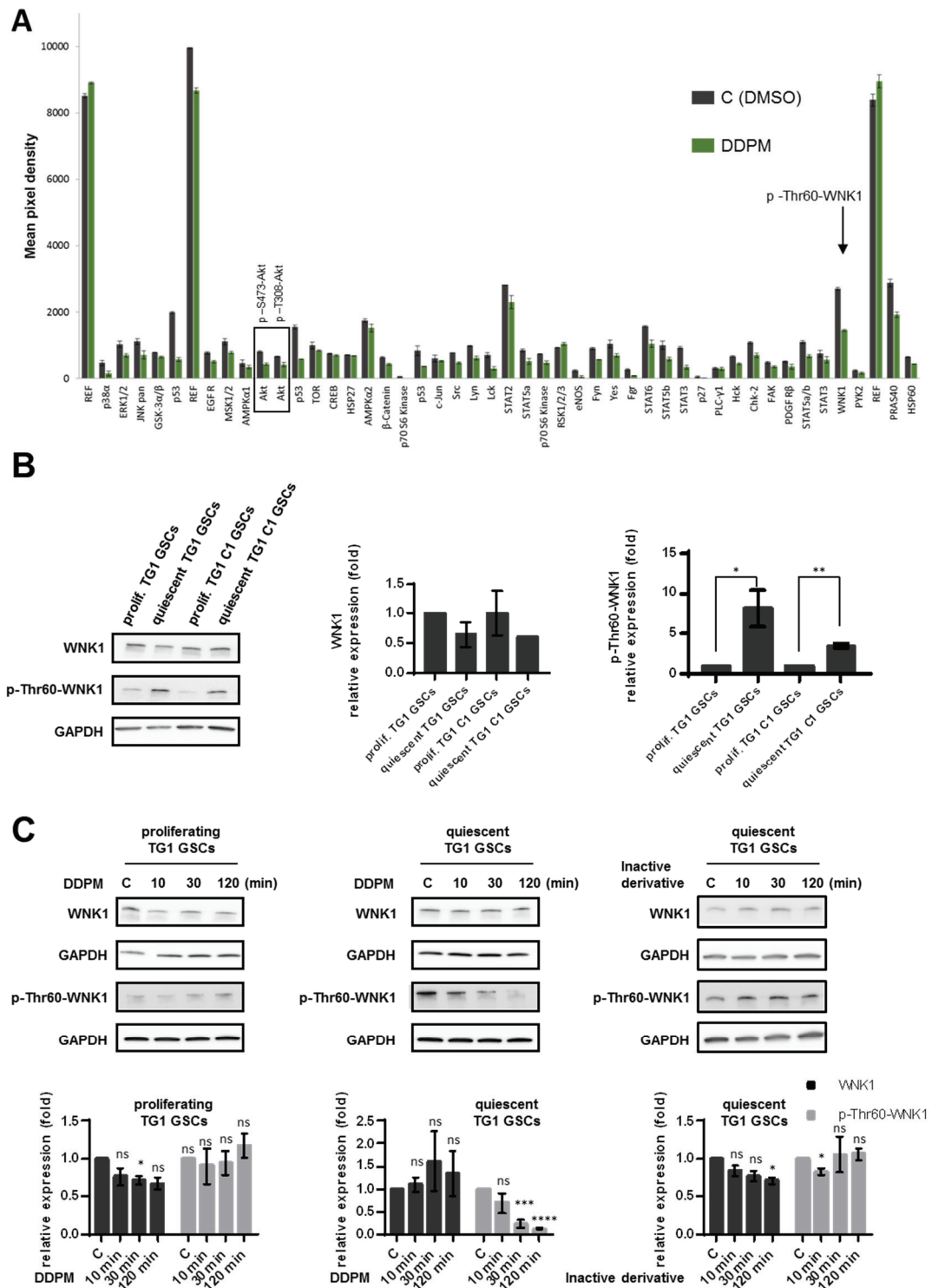
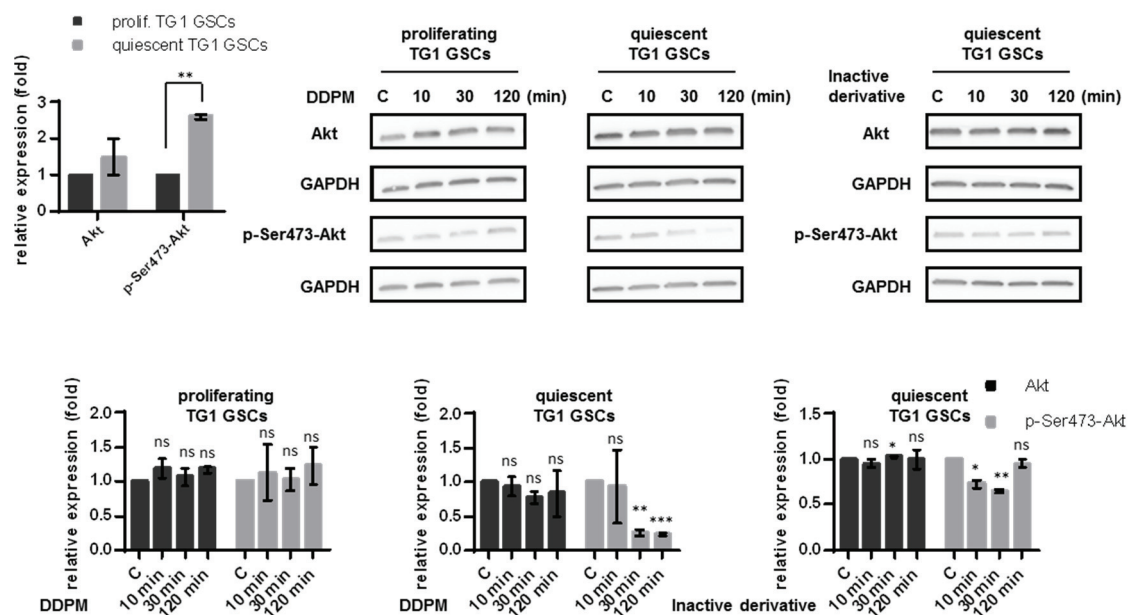


## Figure 2

A



B

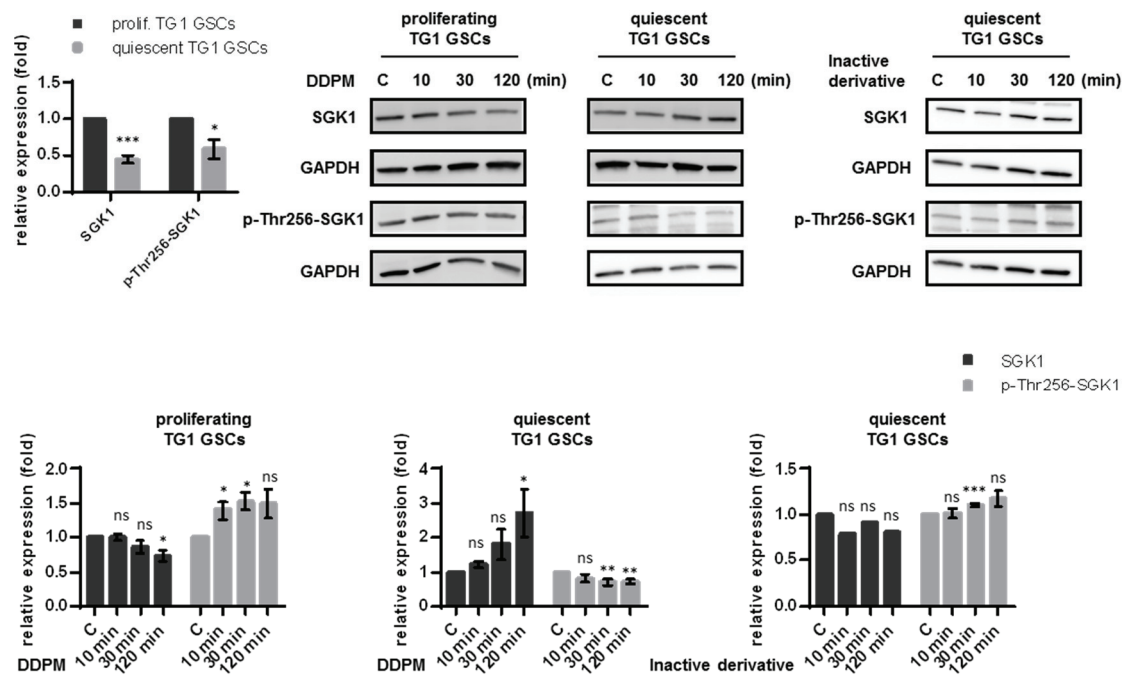
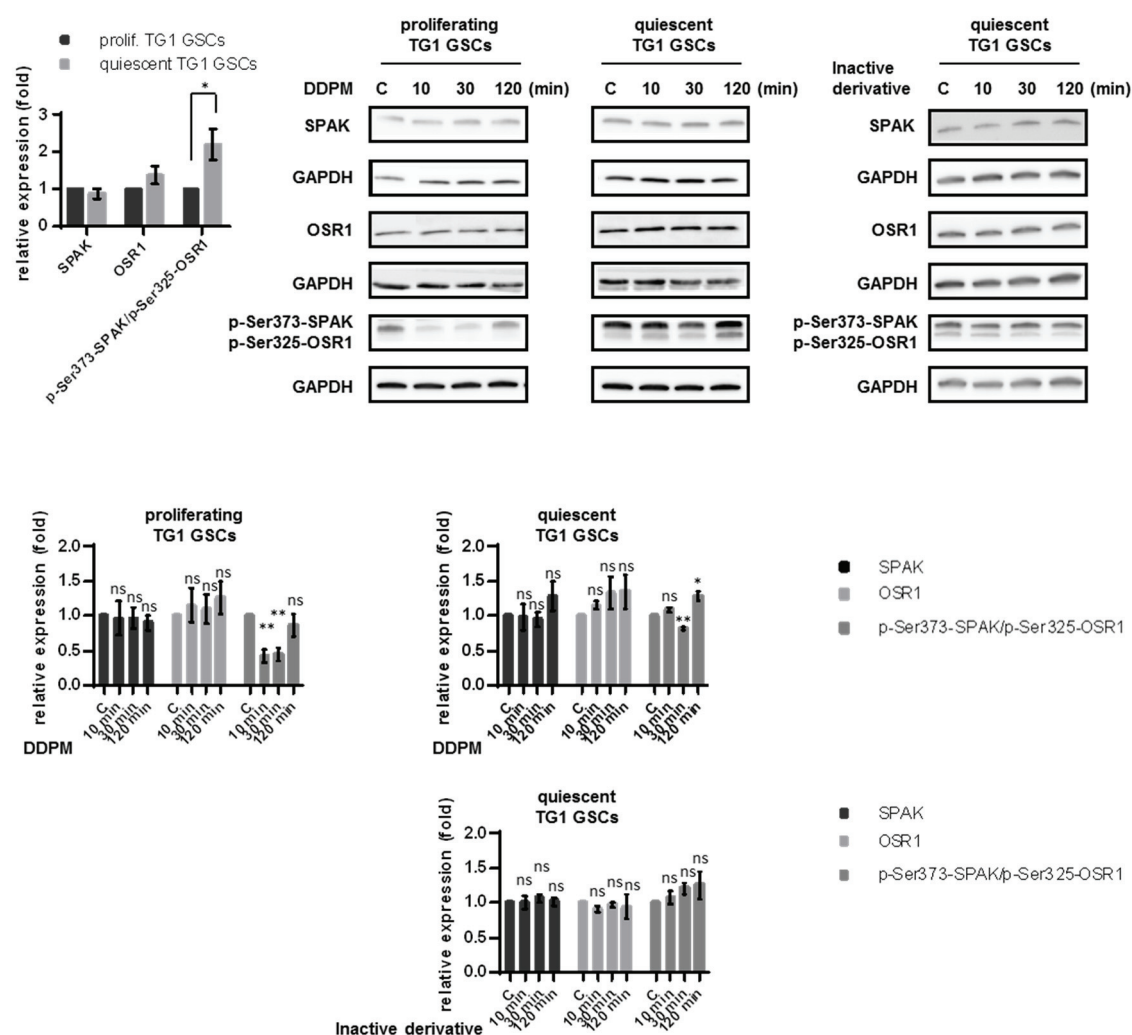
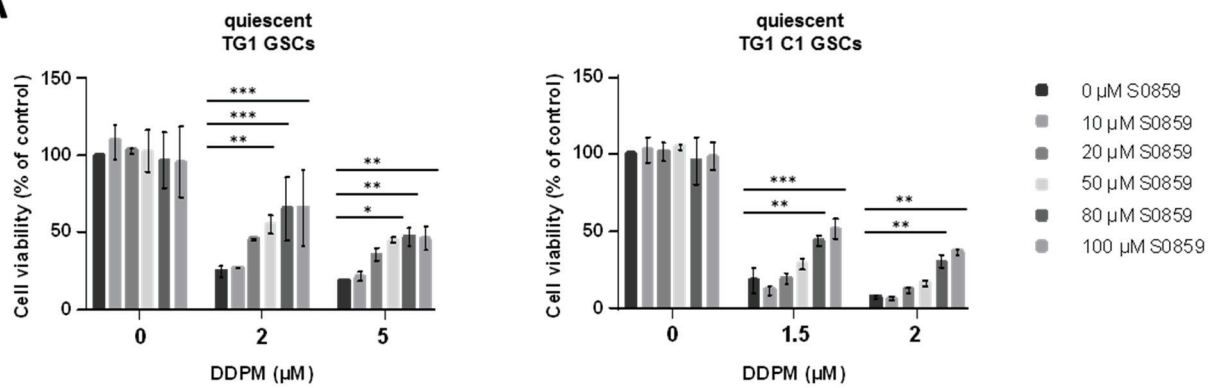


Figure 3

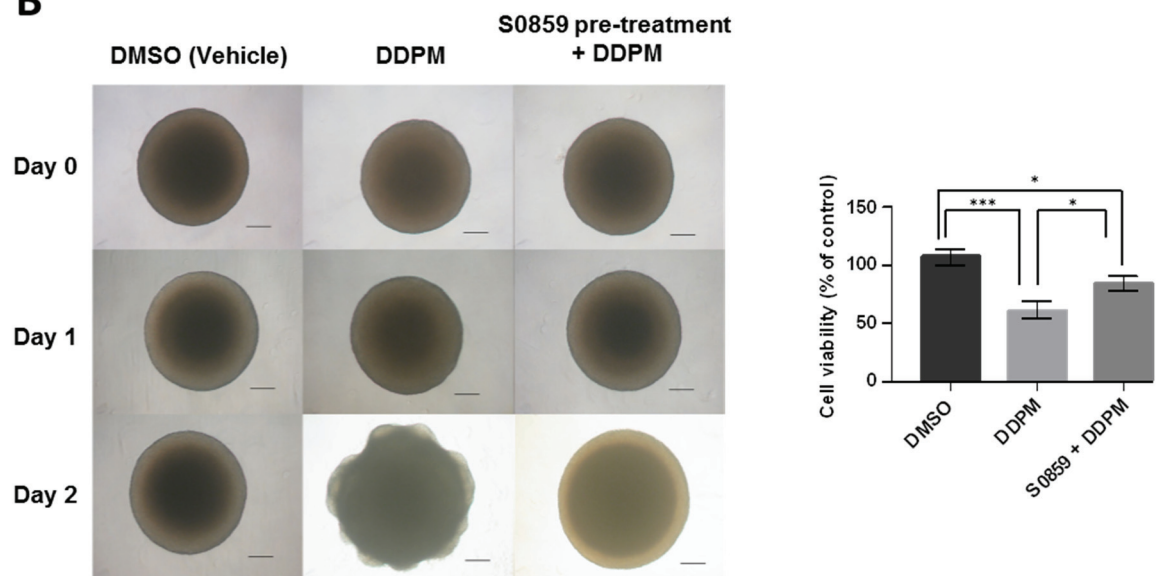


# Figure 4

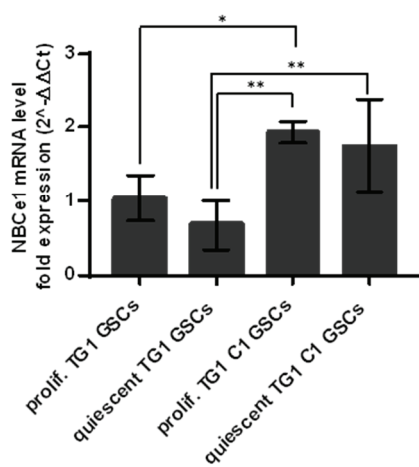
## A



## B



## C



## D

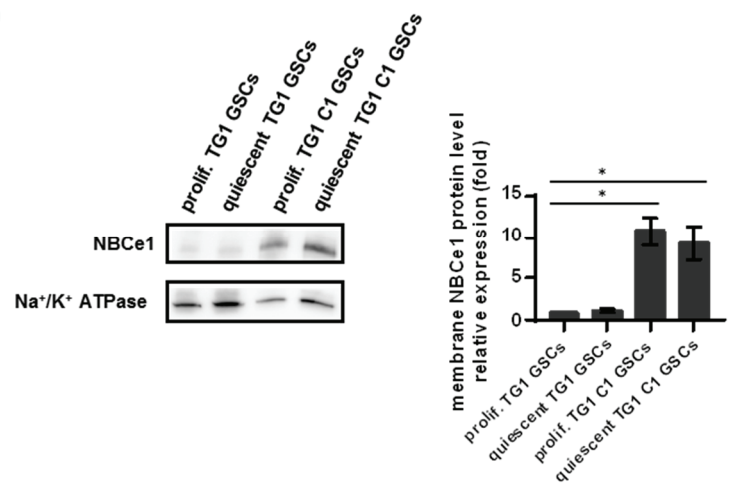
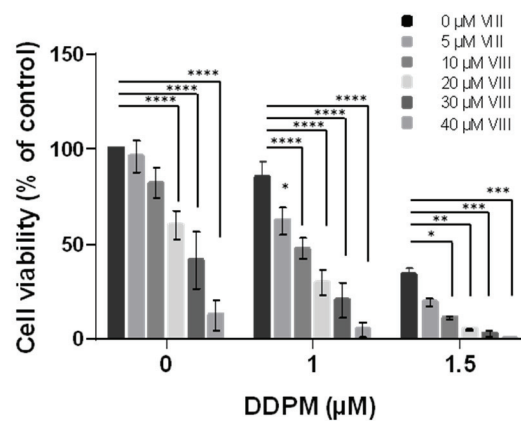
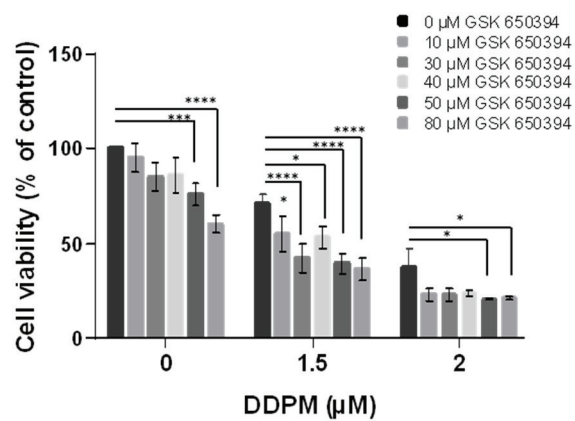


**Figure 5**

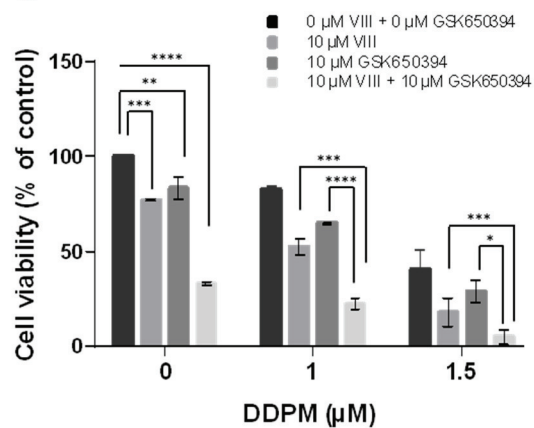
**A**



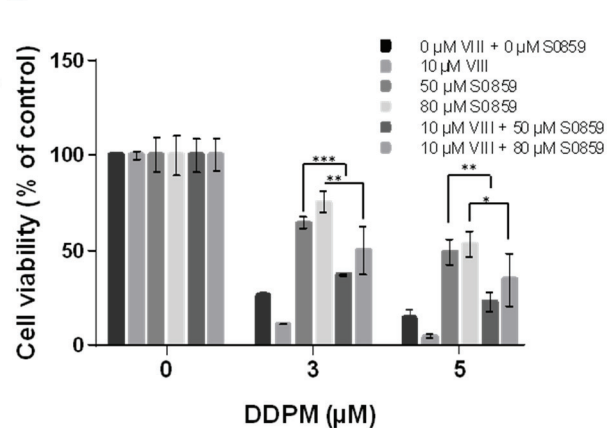
**B**



**C**



**D**



**E**

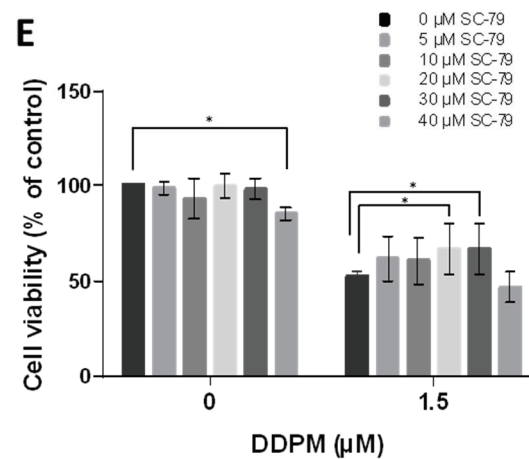


**Figure 6**

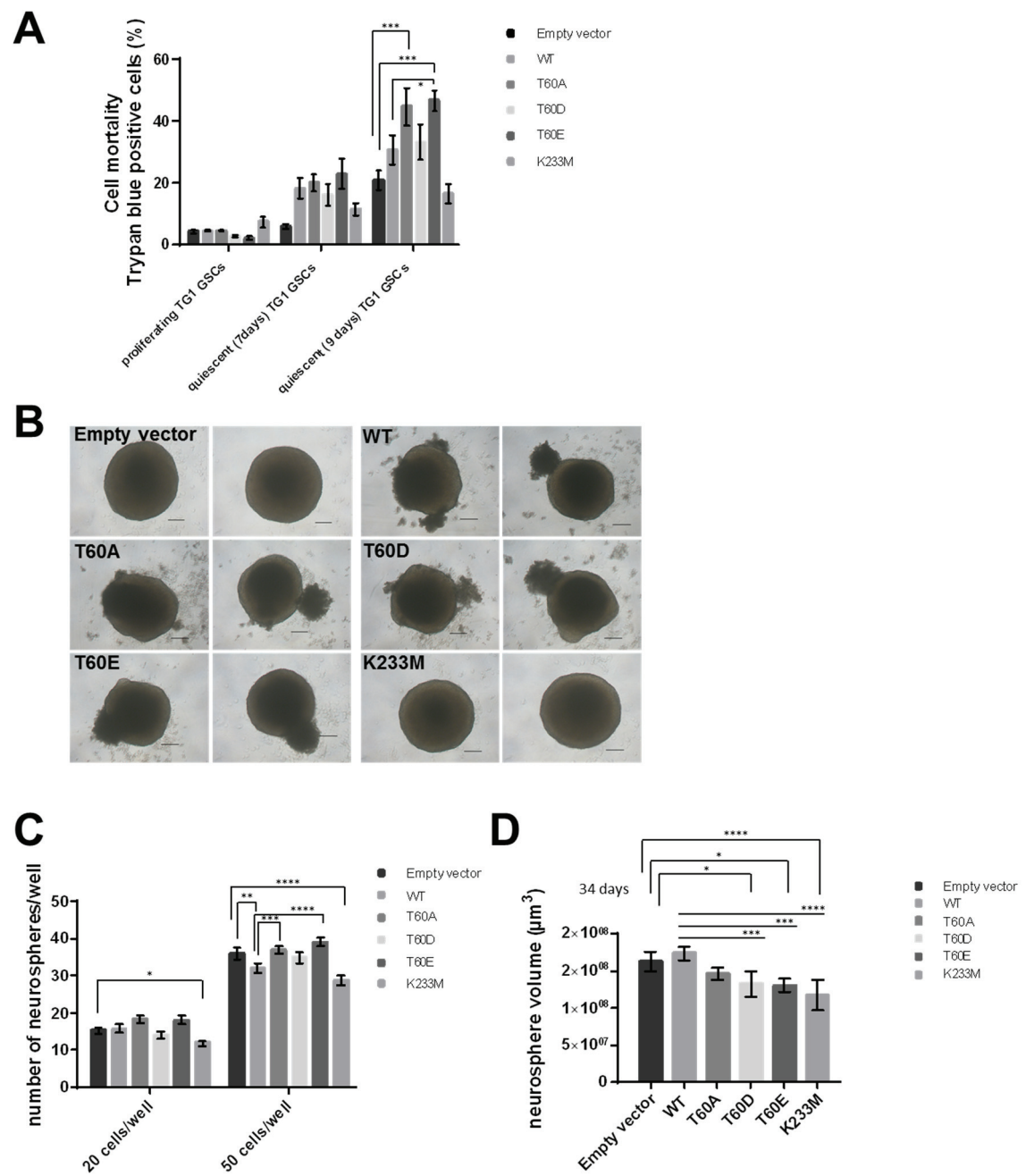
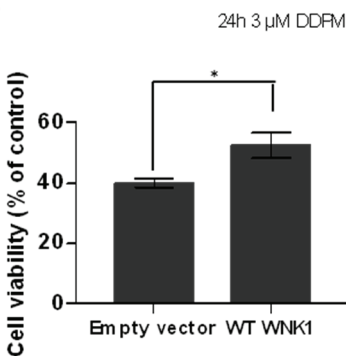


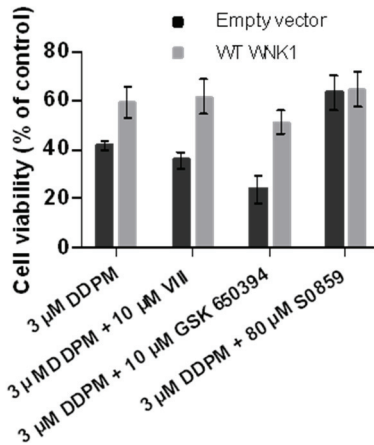


Figure 7

A



B



C

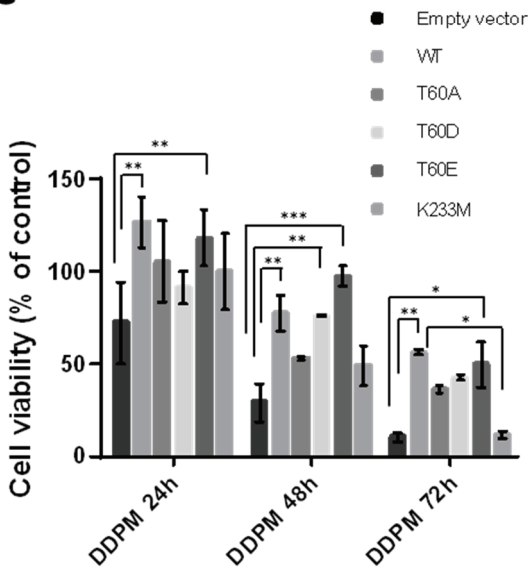
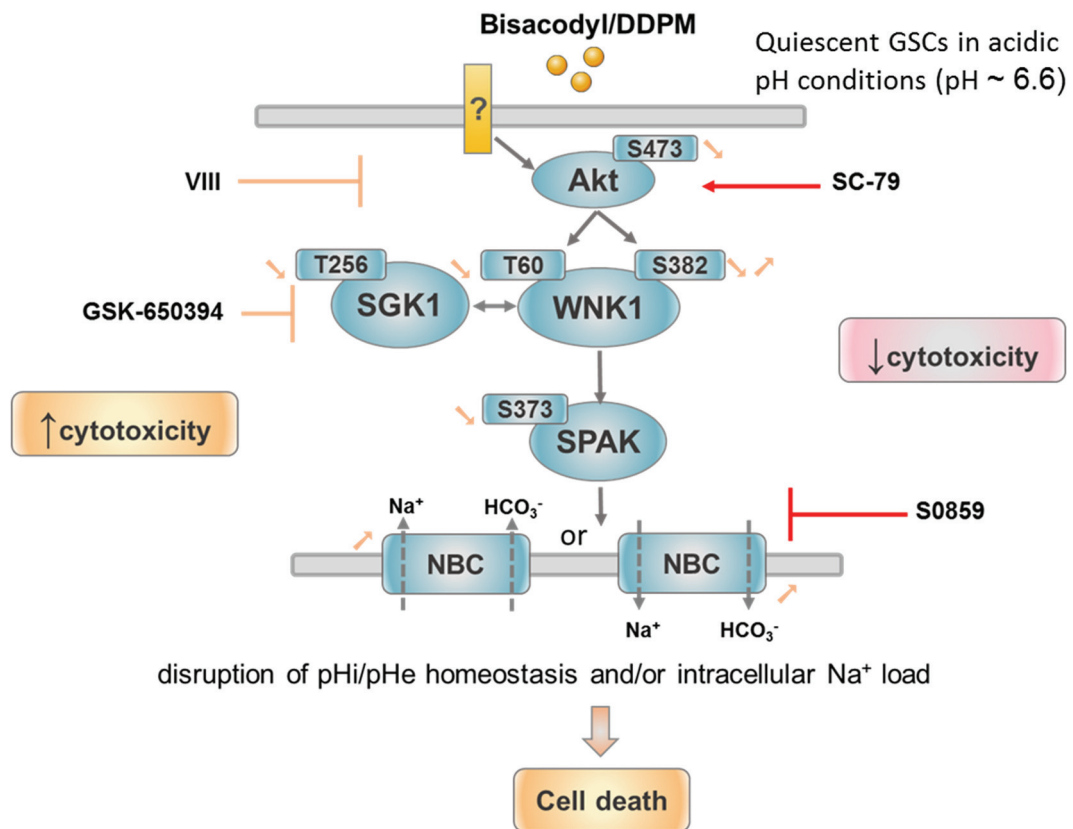


**Figure 8**



## Supplementary figure legends

### **Figure S1 Chemical structures and activity of bisacodyl, DDPM and inactive derivative used in the study, on GSCs**

**A.** Chemical structures of bisacodyl, its active derivative DDPM as well as of the inactive derivative used in the study. **B.** Dose-response curves of bisacodyl/DDPM (left panel) and of bisacodyl/DDPM-inactive derivative (right panel) on proliferating and quiescent TG1 GSCs. Cell viability was evaluated after 24 hours of treatment with the ATP-Glo cell viability assay. The fitted sigmoidal logistic dose-response curves to ATP-Glo cell survival assay readouts are shown. Results are mean ( $\pm$  s.d.) in biological triplicates from one experiment out of three independent experiments giving similar results. Bisacodyl/DDPM IC<sub>50</sub> value on quiescent TG1 GSCs is indicated on the graph.

### **Figure S2 DDPM induces modifications of the phosphorylation status of WNK1 and WNK1 partners Akt, SGK1 and SPAK/OSR1 in TG1 C1 GSCs**

**A, B, C, D.** The protein expression levels of WNK1 and phospho (p)-Thr60 WNK1 (A), Akt and p-Ser473-Akt (B), SGK1 and p-Thr256 SGK1 (C) and SPAK/OSR1 and p-Ser373-SPAK/p-Ser325-OSR1 (D) were determined by western blotting and appropriate antibodies in protein extracts from proliferating and quiescent TG1 C1 GSCs treated with DMSO (1%, C: Control) or with DDPM (10  $\mu$ M in 1% DMSO) for 10, 30 or 120 minutes. Quiescent TG1 C1 GSCs were also treated with 1% DMSO (C) or with an inactive derivative of bisacodyl/DDPM (10  $\mu$ M in 1% DMSO) for 10, 30 or 120 minutes. GAPDH expression was used as a loading control. Quantification graphs of corresponding blots (not shown) (fold of normalized to GAPDH-relative mean expression compared to control (C) conditions for each cell type and treatment conditions) are shown ( $\pm$  SEM;  $n \geq 2$ ). Statistical analysis was performed by pairwise comparison of results at each time point relatively to the levels of unphosphorylated and phosphorylated forms of WNK1, Akt, SGK1 and SPAK/OSR1 on selected residues in control (C) conditions. Student t-test. \*  $p < 0.05$ , \*\*  $p < 0.005$ , \*\*\*  $p < 0.0005$ , \*\*\*\*  $p < 0.0001$ ; ns: not significant. Some quantification results are missing (WNK1, p-Thr60 WNK1, SPAK, OSR1 and p-Ser373-SPAK/p-Ser325-

OSR1 in quiescent TG1 C1 GSCs treated with the inactive derivative of bisacodyl/DDPM). Results will be included in the final version of the manuscript.

**Figure S3 Inhibition of  $\text{Na}^+/\text{HCO}_3^-$  NBC co-transporter function partially protects quiescent GSCs from DDPM cytotoxic action**

**A, B.** Quiescent TG1 (A) or TG1 C1 (B) GSCs were pretreated with DMSO alone (1%) or increasing concentrations (10, 20, 50, 80 and 100  $\mu\text{M}$ ) of S0859 (24 hours of treatment). Increasing concentrations of DDPM were subsequently added. Cell viability was evaluated 24 hours later with the ATP-Glo cell viability assay. The fitted sigmoidal logistic dose-response curves to ATP-Glo cell survival assay readouts are shown. Results are mean ( $\pm$  s.d.) in biological triplicates from one experiment out of three independent experiments giving similar results. IC50 values are indicated below the graphs.

**Figure S4. The  $\text{Na}^+/\text{HCO}_3^-$  co-transporter NBCn1 shows higher expression in membrane extracts of proliferating and quiescent TG1 C1 GSCs compared to TG1 GSCs. The non-selective anion transport inhibitor DIDS is highly cytotoxic to quiescent GSCs and does not protect these cells from DDPM cytotoxicity**

**A.** Membrane compartment NBCn1 protein levels were evaluated in proliferating and quiescent TG1 and TG1 C1 GSCs with a commercially available antibody.  $\text{Na}^+/\text{K}^+$  ATPase levels in membrane protein extracts were used as loading controls. Relative membrane NBCn1 levels (corrected to  $\text{Na}^+/\text{K}^+$  ATPase) were represented as fold difference considering proliferating TG1 GSCs as a calibrator. Quantitative results are from 2 independent experiments ( $\pm$  SEM). Ordinary one-way ANOVA and Dunnett's multiple comparisons test. \*  $p < 0.05$ . **B.** Quiescent TG1 (left panel) and TG1 C1 (right panel) GSCs were pre-treated for 24 hours with increasing concentrations of the stilbene derivative DIDS inhibiting most  $\text{Na}^+$ -coupled  $\text{HCO}_3^-$  co-transporters but not NBCn1. Subsequently, cells were mock-treated (1% DMSO and DIDS from the pretreatment) or incubated in the presence of DDPM (10  $\mu\text{M}$  and DIDS from the pretreatment) for 24 hours. Cell viability measurements were performed with the ATP-Glo cell survival-based assay. Results are expressed as a percentage of the viability of control TG1 or TG1 C1 GSCs incubated with 1% DMSO

alone for 48 hours. Results are the mean of two independent experiments performed in triplicate (+/- SEM).

**Figure S5 Modulation of WNK1 signaling partners Akt, SGK1 and NBC Na<sup>+</sup>/HCO<sub>3</sub><sup>-</sup> co-transporters NBCe1/NBCn1 impacts DDPM cytotoxic activity in dissociated quiescent TG1 C1 GSCs previously grown as neurospheres**

**A, B, C.** Quiescent TG1 C1 GSCs were either mock-treated (1% DMSO) or incubated in the presence of DDPM at indicated concentrations and/or Akt inhibitor VIII (A), SGK1 inhibitor GSK 650394 (B) or a combination of both compounds (C) for 24 hours. Cell viability measurements were performed with the ATP-Glo cell survival based assay. Results are expressed as a percentage of the viability of control TG1 C1 GSCs incubated with 1% DMSO alone for 24 hours. Results are the mean of two independent experiments performed in triplicate (+/- SEM). Statistical analysis was performed with Two-way ANOVA and Tukey's multiple comparisons test. \* p<0.05, \*\* p<0.005, \*\*\* p<0.0005; \*\*\*\* p<0.0001. Quiescent TG1 C1 GSCs were incubated in 1% DMSO (controls) or pretreated for 24 hours with the indicated concentrations of the NBC inhibitor S0859 (in 1% DMSO) (D) or the Akt activator SC-79 (E). Indicated concentrations of DDPM alone (in 1% DMSO) (D, E) or DDPM combined to 10  $\mu$ M of the VIII Akt inhibitor (D) were then added and treatment was pursued for 24 hours. Control cells were maintained in 1% DMSO. Cell viability assays, presentation of results and statistical analysis were performed as described in A, B and C (n=2 in D, n=3 in E, mean+/- SEM). \* p<0.05, \*\* p<0.005, \*\*\* p<0.0005.

**Figure S6. RNAi-mediated inhibition of WNK1 expression does not affect quiescent GSC cell survival nor DDPM activity on these cells**

**A.** WNK1 expression levels were evaluated by western blotting in proliferating TG1 (upper panels) and TG1 C1 (lower panels) GSCs transfected with pEGFP-N2 RNAi (shRNA empty vector) or pEGFP-N2 RNAi expressing WNK1 or scramble shRNAs for 48 or 72 hours. Non-transfected TG1 and TG1 C1 GSCs were used as controls. GAPDH was the loading control in these experiments. **B.** FACS analysis following TO-PRO-3 staining of dead quiescent TG1 (left panel) or TG1 C1 (right panel) GSCs transfected with pEGFP-N2 RNAi (shRNA empty vector) or pEGFP-N2 RNAi expressing WNK1 or scramble shRNAs for 48 hours. Non-transfected TG1 and TG1 C1 GSCs were used as controls, respectively. **C.** Total cell and EGFP-expressing

cell mortality increase induced by a 24-hour treatment with DDPM (10  $\mu$ M) was evaluated by TO-PRO-3 staining and FACS analysis in quiescent TG1 (left panel) and TG1 C1 (right panel) GSCs transfected with pEGFP-N2 RNAi (shRNA empty vector) or pEGFP-N2 RNAi expressing WNK1 or scramble shRNAs for 48 hours.

**Figure S7 WT and mutant FLAG-WNK1 subcellular localization in proliferating and quiescent GSCs**

Proliferating and quiescent TG1 C1 GSCs were transiently transfected with the pCIneo-3FLAG Gateway vectors allowing overexpression of 3FLAG-tagged WT and mutant (T60A, T60D, T60E, K233) WNK1 isoforms. The presence and subcellular localization of overexpressed proteins (red) was determined by anti-FLAG primary antibody staining detected with an Alexa Fluor 568-conjugated secondary antibody and immunofluorescence analysis with a confocal microscope. Nuclei were stained with DAPI. Scale bars: 20  $\mu$ m.

**Figure S8 WT and mutant WNK1 proteins are overexpressed in stable cell lines derived from transfected TG1 GSCs**

**A.** WNK1 levels were evaluated by western blotting in protein extracts from proliferating TG1 GSCs stably transfected with pCIneo-3FLAG Gateway vectors in which cDNAs encoding WT and mutated (T60A, T60D, T60E, K233M) WNK1 proteins were cloned. GAPDH was used as a loading control. Empty lane corresponds to an additional sample which was removed from the gel. Quantification of pixel intensity (corrected to GAPDH) and expressed as fold expression relative to control cells stably transfected with the corresponding empty vector is shown. Results are expressed as mean ( $\pm$ -SEM) from two independent experiments.

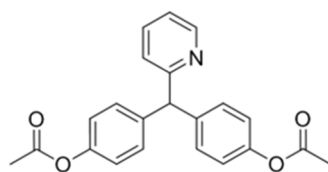
**Figure S9 Modulation of WNK1 levels and/or activity impacts TG1 GSCs' clonal properties and growth**

**A.** Evaluation of the clonal properties of control (Empty vector) TG1 GSCs or TG1 GSCs stably overexpressing WT or mutant (T60A, T60D, T60E, K233M) forms of WNK1. The mean number of spheres obtained after 2 weeks in culture was determined as a function of the initial number of cells in a well. Initial cell numbers seeded ranges from 1 to 50 cells/well (n=16 wells for each condition,  $\pm$ -s.d.). **B.**

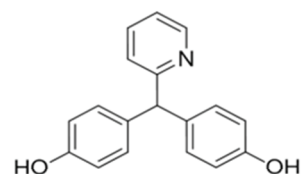
Growth rate measurements of 3D neurospheres derived from control (Empty vector) TG1 GSCs or TG1 GSCs stably overexpressing WT or mutant (T60A, T60D, T60E, K233M) forms of WNK1. Sphere volume ( $\mu\text{m}^3$ ) was evaluated with the ImageJ software at different time points (21, 24, 27, 30 and 34 days) following cell seeding (n=12 clonal spheres for each cell type +/- s.d.).

## Supplementary Figure S1

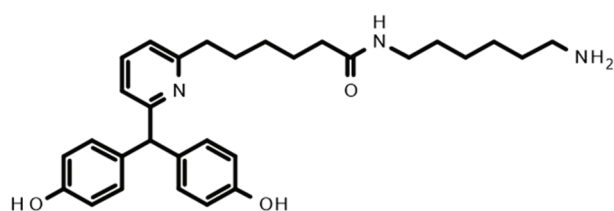
**A**



**Bisacodyl (laxative)**

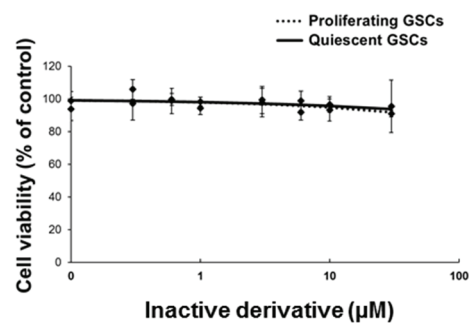
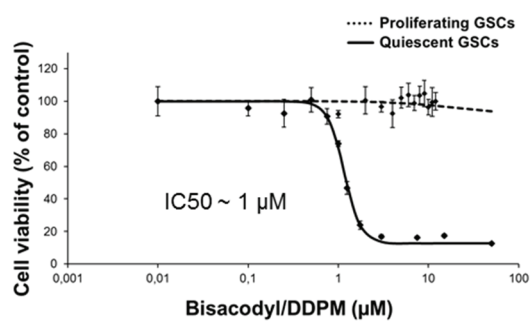


**DDPM**



**Inactive derivative**

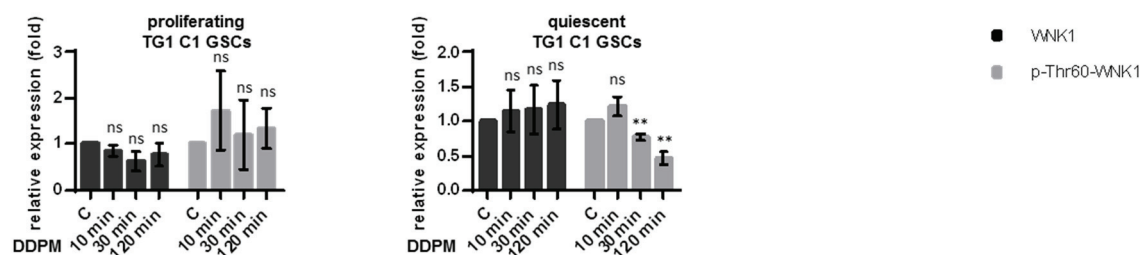
**B**



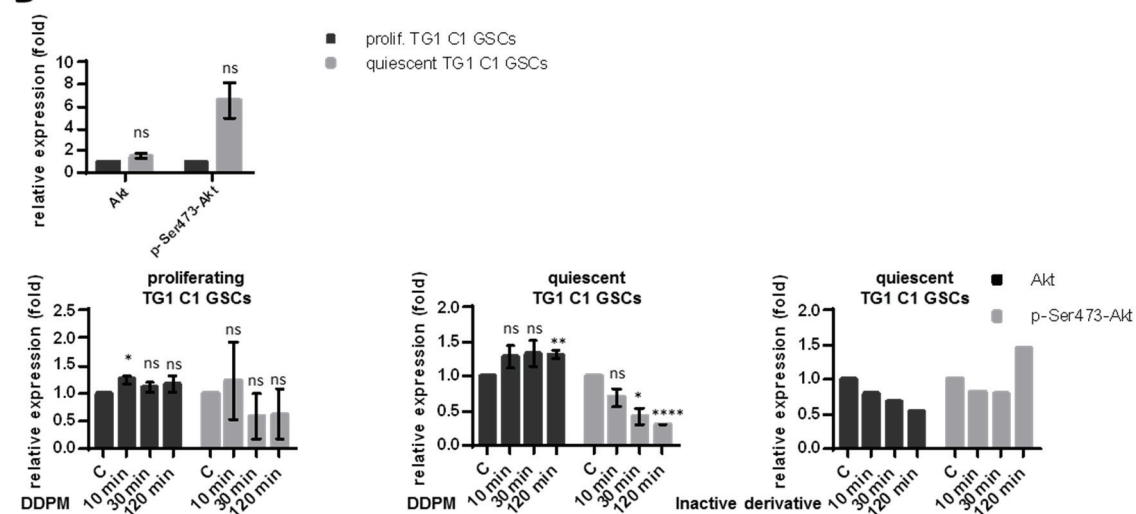


# Supplementary Figure S2

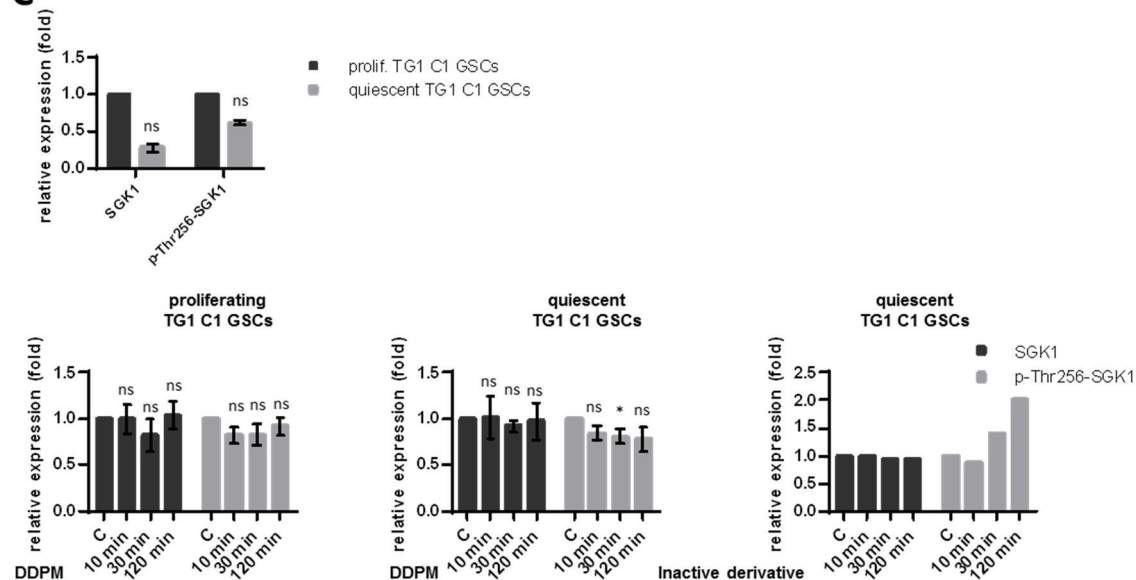
**A**



**B**

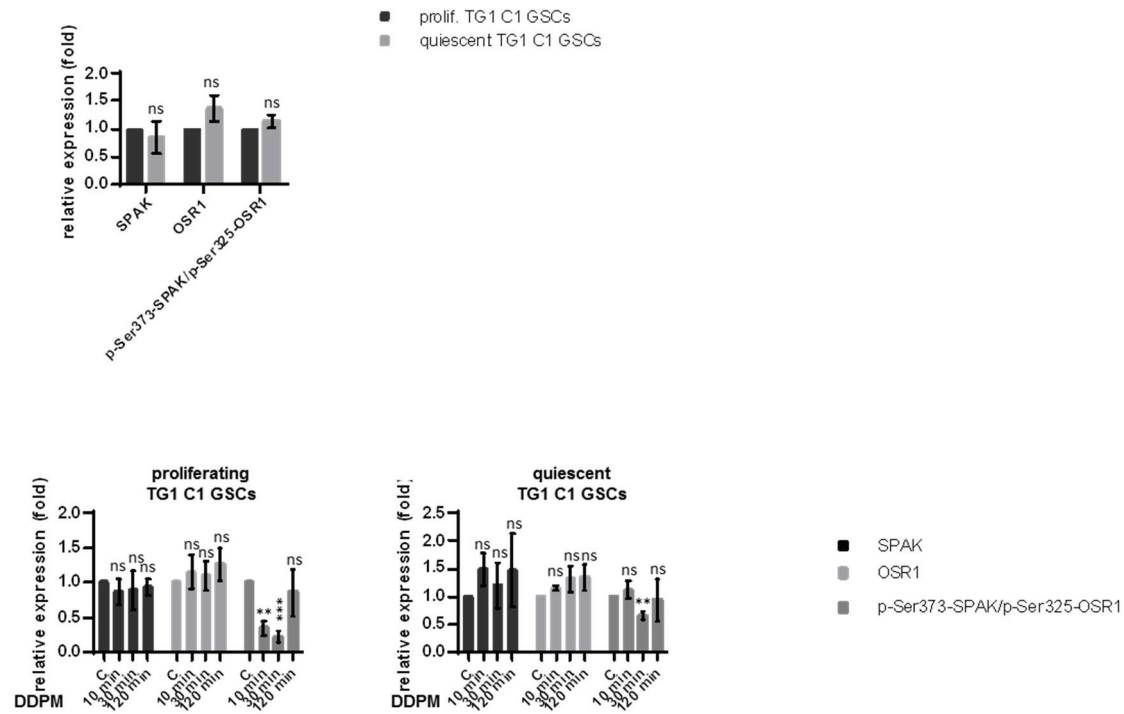


**C**

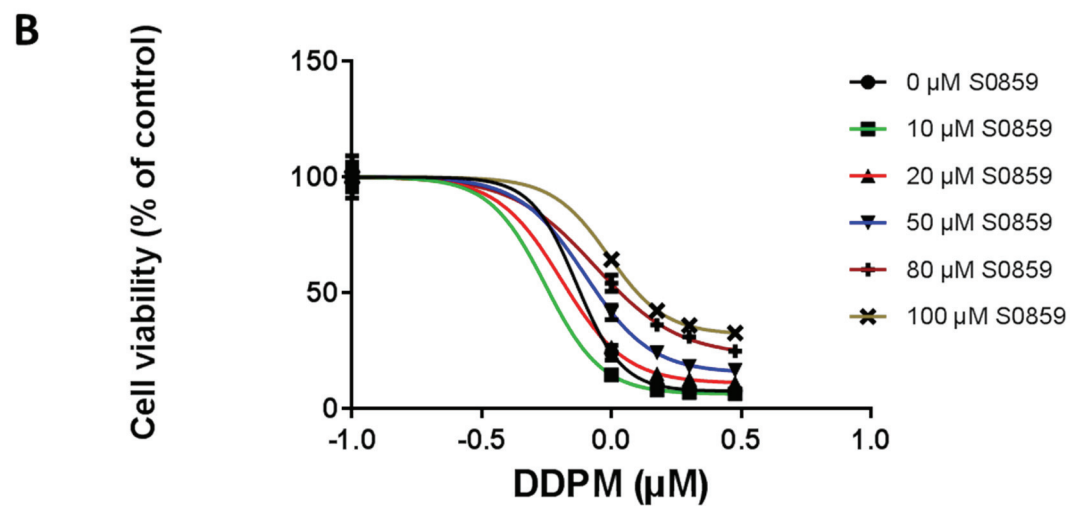
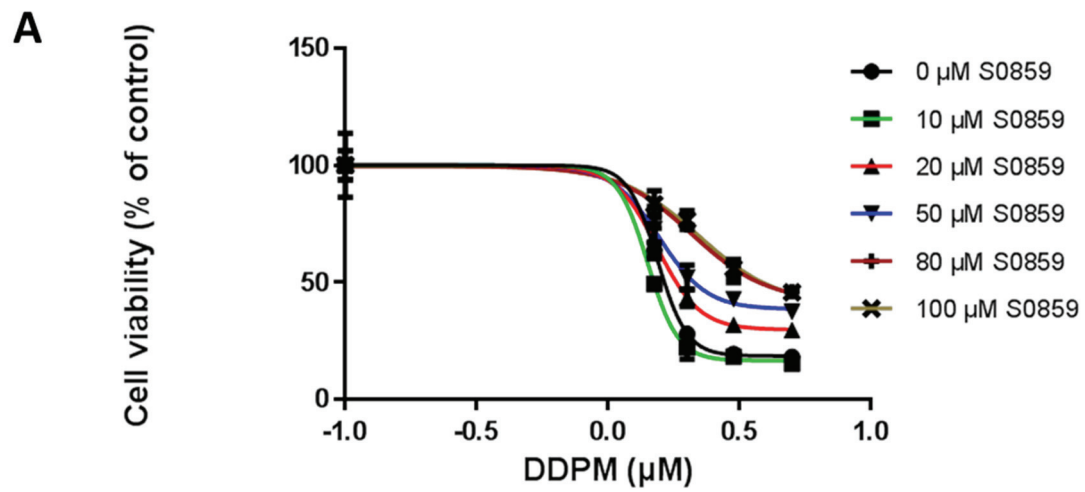


# Supplementary Figure S2

## D

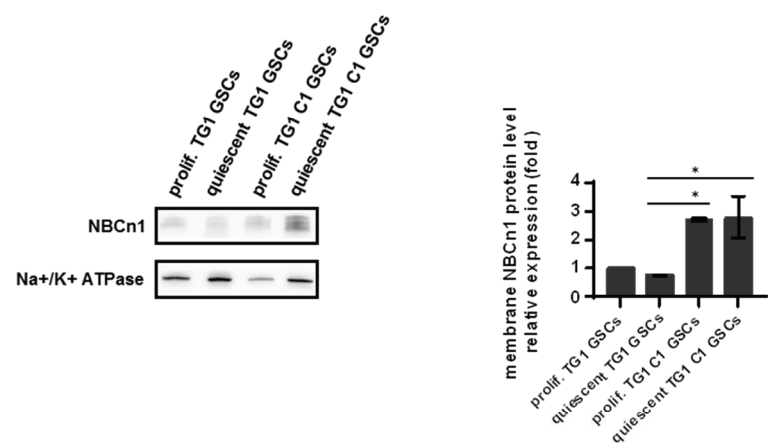


## Supplementary Figure S3

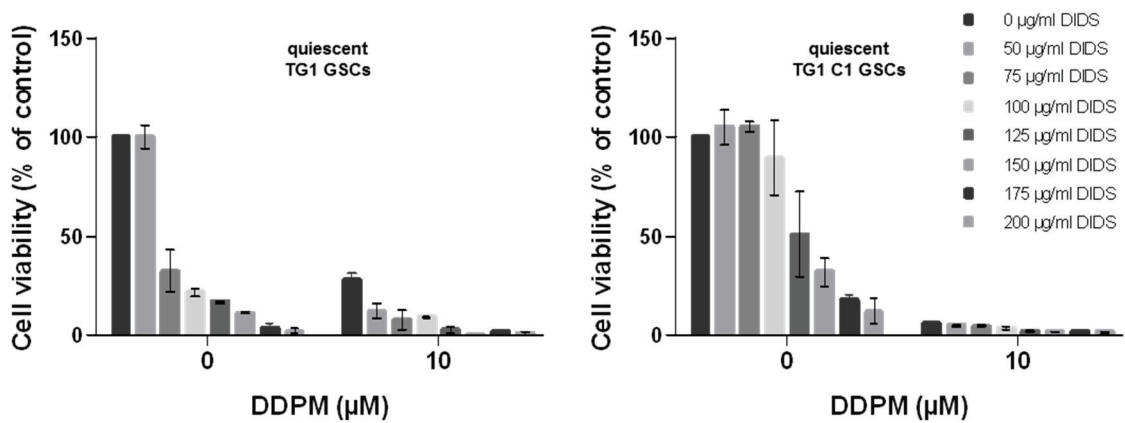


# Supplementary Figure S4

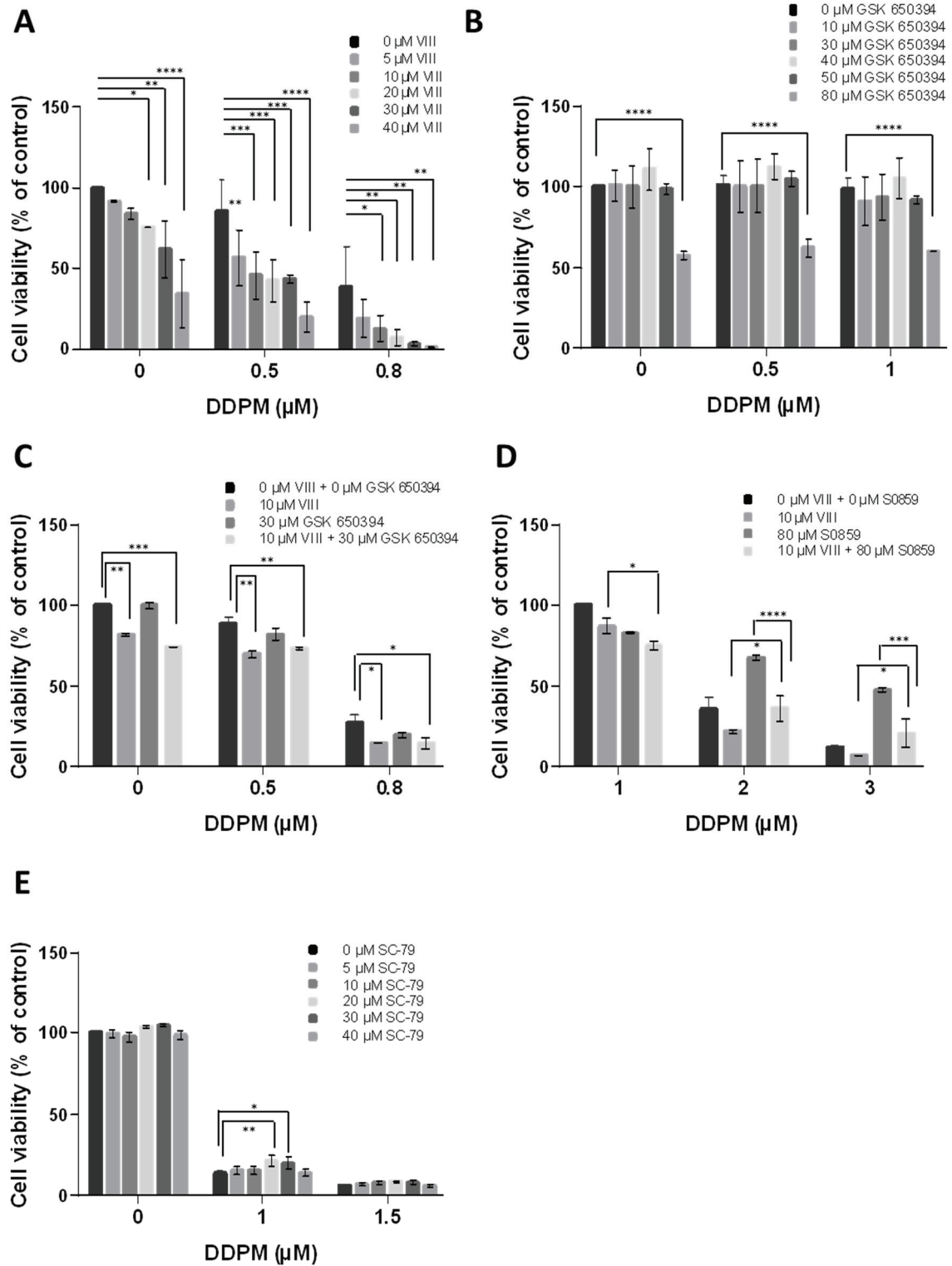
A



B

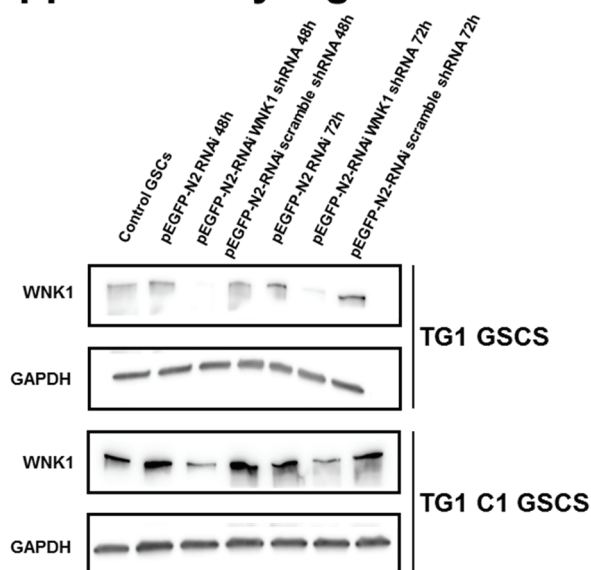


## Supplementary Figure S5

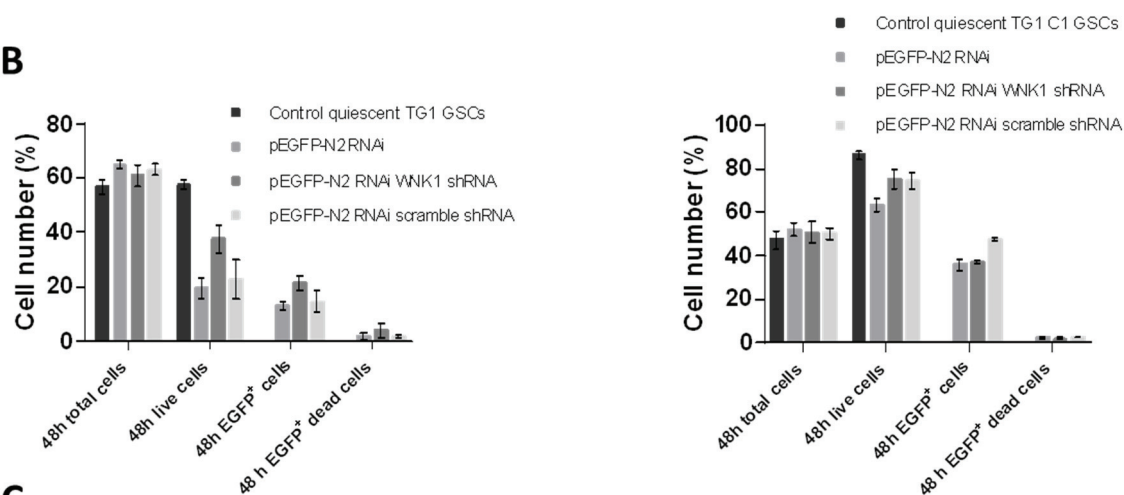


## Supplementary Figure S6

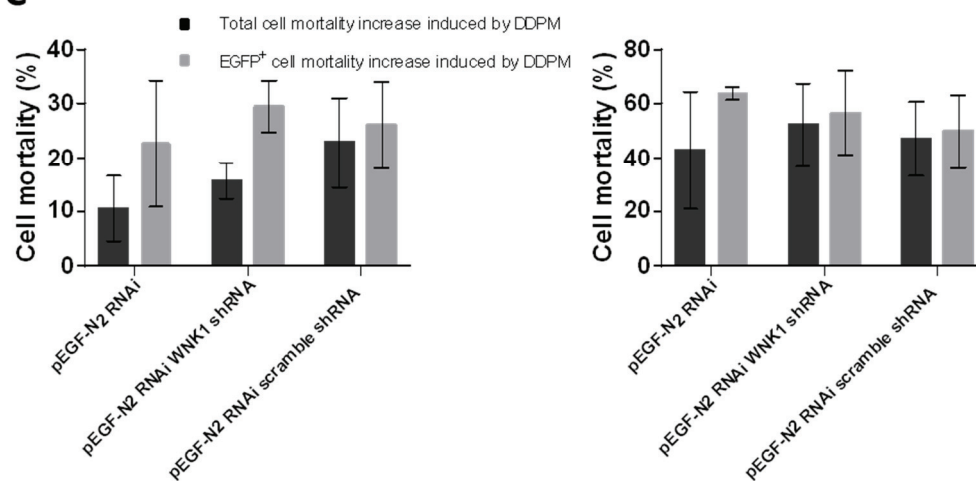
**A**



**B**



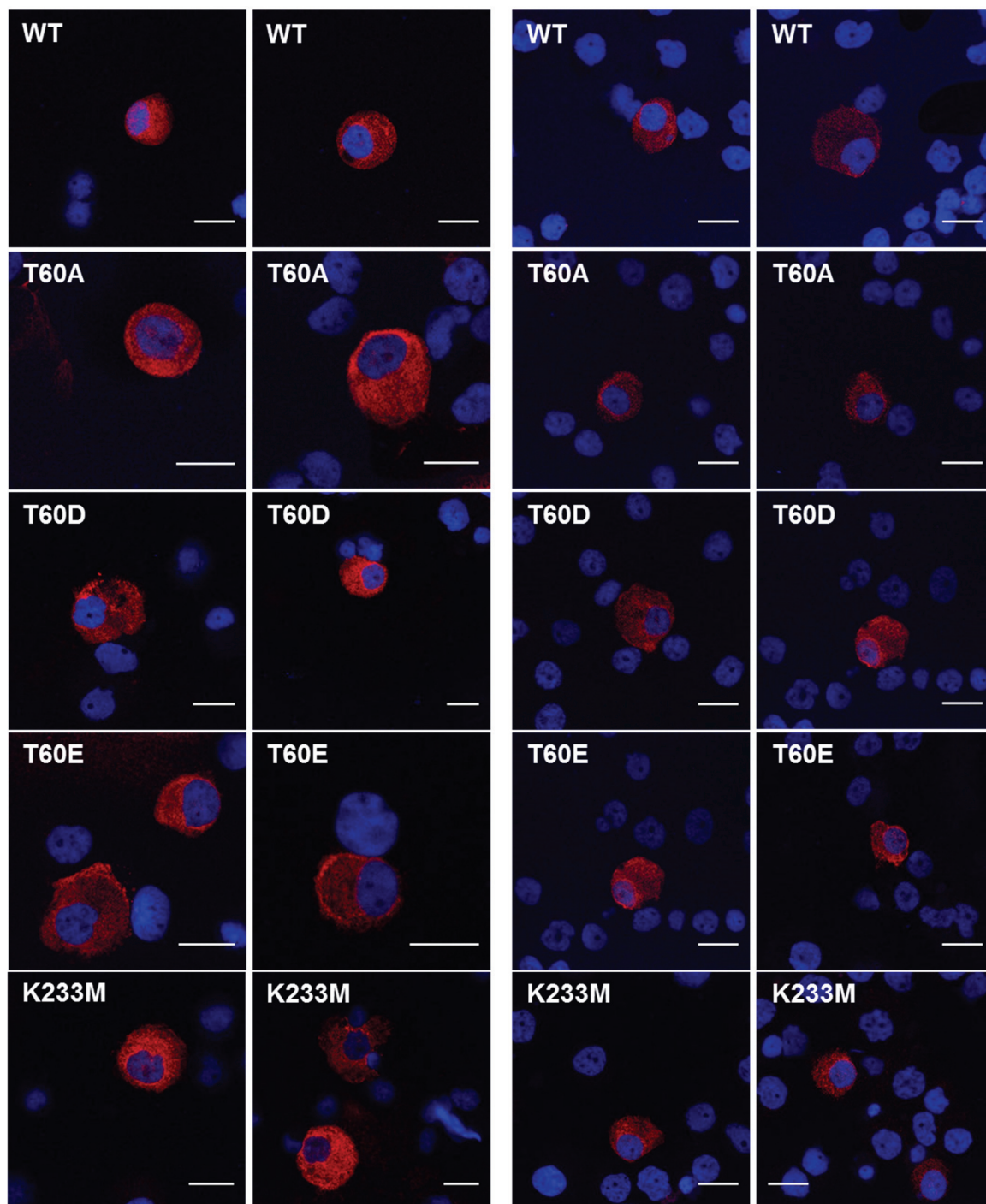
**C**



## Supplementary Figure S7

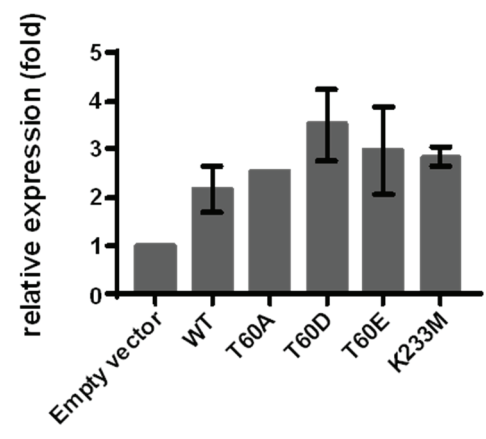
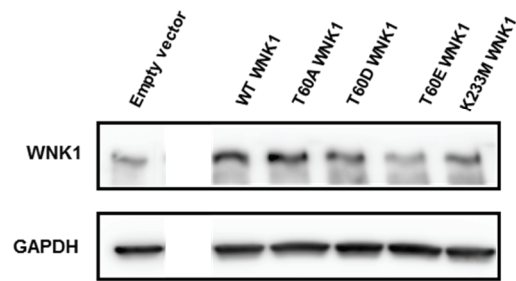
Proliferating  
TG1 C1 GSCs

Quiscent  
TG1 C1 GSCs





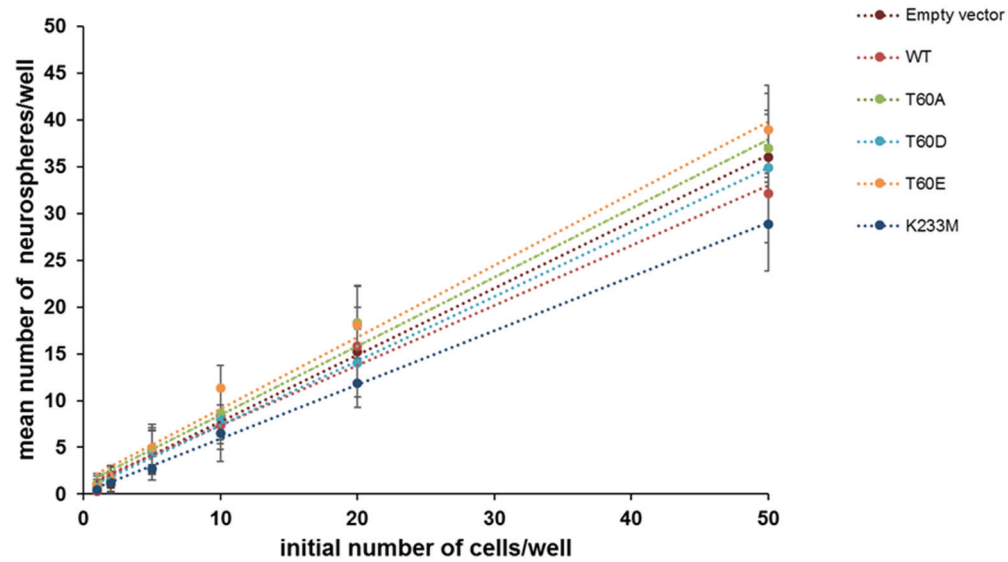
# Supplementary Figure S8



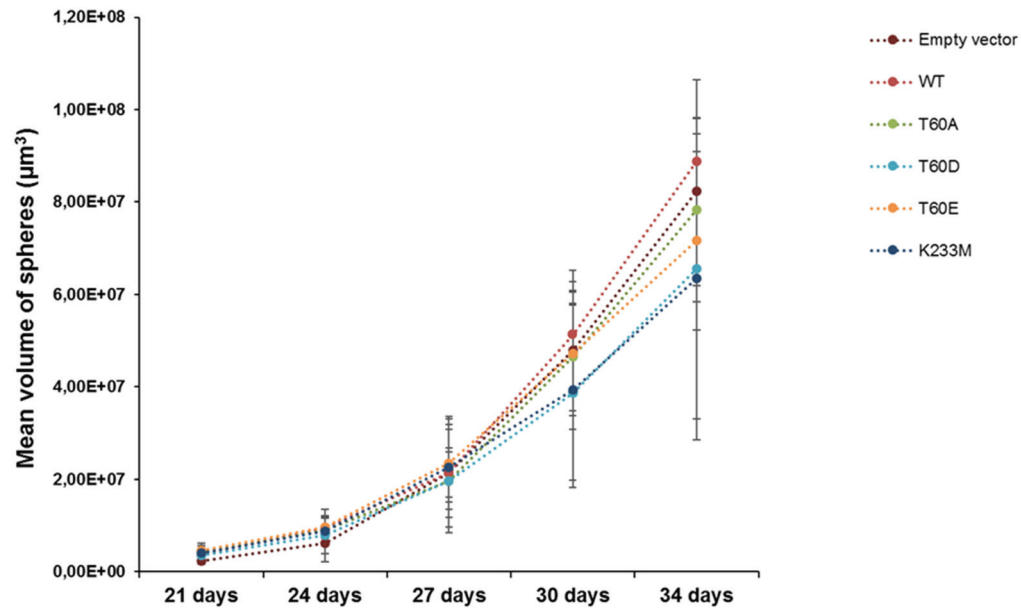


## Supplementary Figure S9

**A**



**B**



## Supplementary Materials and Methods

### Synthesis of bisacodyl/DDPM inactive derivative

The bisacodyl/DDPM inactive derivative (LPI3271) was synthesized starting from 6-bromo-2-pyridinecarboxaldehyde and phenol through the chemical strategy described by Zeniou et al. [1]. LPI3271 (N-(6-aminohexyl)-6-{6-[bis(4-hydroxyphenyl)methyl]pyridin-2-yl}hexanamide as a trifluoroacetate salt) : Anal. RP-HPLC purity > 98%. <sup>1</sup>H NMR (MeOD<sub>4</sub>): δ 1.38 (m, 6H), 1.50 (m, 2H), 1.65 (m, 4H), 1.75 (m, 2H), 2.19 (m, 2H), 2.91 (m, 2H), 3.05 (m, 2H), 3.15 (m, 2H), 5.86 (s, 1H), 6.80 (m, 4H), 6.93 (m, 4H), 7.38 (m, 1H), 7.78 (m, 1H), 8.38 (m, 1H); <sup>13</sup>C NMR (MeOD<sub>4</sub>): δ 26.54, 27.11, 27.46, 28.54, 29.65, 30.23, 30.35, 34.04, 36.79, 40.27, 40.85, 54.09, 116.99, 126.02, 126.37, 131.44, 131.57, 147.84, 158.36, 159.57, 160.39, 176.08. MS (ESI<sup>+</sup>): m/z [M + H]<sup>+</sup> calculated for C<sub>30</sub>H<sub>40</sub>N<sub>3</sub>O<sub>3</sub>, 490.3, found 490.2.

### WNK1 shRNA-mediated knockdown

Human WNK1 cDNA fragments encoding the 19-nucleotide siRNA sequence 5'-CAATGAGTCAGATATCGAA-3' derived from the target transcript and separated from its reverse 19-nucleotide complement by a short spacer or scramble siRNA sequence 5'-ACTACGAATGACGTATAGA-3' separated from its reverse 19-nucleotide complement by a short spacer, were cloned in the pEGFP-N2 RNAi vector kindly provided by Dr. N. Vitale (INCI, Strasbourg, France) downstream a H1-RNA promoter. Briefly, single-strand LIC sites (derived from the LIC cloning systems from Novagen) were added by asymmetrical PCR (Phusion Hot Start II High fidelity DNA polymerase from Thermo Fisher Scientific) on the pEGFP-N2 RNAi plasmid and by primer synthesis on siRNA encoding insert sequences (see Supplementary Table S1). Asymmetrical PCR products, containing double stranded LIC sites either at their 5' or at their 3' end, were treated with DpnI to eliminate circular template plasmids and denatured by heating and reannealed to obtain linearized double-stranded pEGFP-N2 RNAi vectors with 5' single stranded LIC sequences on both strands. Primers corresponding to siRNA sequences, spacers and complement were annealed to obtain inserts with overhanging 5' LIC sites. Vector and inserts were hybridized and introduced without prior *in vitro* ligation into competent *E.coli*

bacteria. Colonies obtained after *in vivo* ligation of the vector and inserts were screened by PCR to verify insert insertion. Recombinant vectors were prepared from positive colonies and sequenced in the siRNA encoding region. PCR and sequencing primer sequences are shown on Supplementary Table S1.

Empty pEGFP-N2 RNAi plasmids and WNK1 or scramble shRNA encoding vectors were introduced into cells by nucleofection with the Amaxa 4D-Nucleofector™ System (Lonza) and Primary Cell Nucleofector™ Solution P3. Transfection efficiency (EGFP<sup>+</sup> cells) was monitored using the IncuCyte® (ESSEN BioScience) live cell imaging system after transfection. Preliminary experiments were performed to determine the optimal transfection pulse for both proliferating and quiescent TG1 and TG1 C1 cells.

### **Protein extract preparation and western blotting**

Protein extract preparation from TG1 and TG1 C1 GSCs transfected with the pEGFP-N2 RNAi vector or with pEGFP-N2 RNAi WNK1 shRNA or scramble shRNA-expressing plasmids as well as western blotting conditions were as described in the Materials and Methods section of the main manuscript.

### **Flow Cytometry for cell viability determination**

TG1 and TG1 C1 GSCs transfected with the pEGFP-N2 RNAi vector or with pEGFP-N2 RNAi WNK1 shRNA or scramble shRNA-expressing plasmids were stained with TO-PRO®-3 (Thermo Fisher Scientific) and processed by FACS analysis to determine cell viability (FACSCalibur; BD Biosciences). Alternatively, transfected cells were recovered 48 hours post transfection and treated for 24 hours with DDPM (10  $\mu$ M in 1% DMSO) or DMSO alone (1%). FACS analysis following TO-PRO®-3 staining was performed at the end of treatment. Cytometric analyses were performed using the FlowJo software.

### **Immunocytochemistry and confocal microscopy**

Proliferating and quiescent (8 days without medium renewal) TG1 and TG1 C1 GSCs were transiently transfected with the pCIneo-3FLAG vectors encoding WT and mutant forms of WNK1 (T60A, T60D, T60E and K233M) as described in the Materials and Methods section in the main manuscript. 24 hours post-transfection, cells were collected, washed 3 times with PBS (phosphate-buffered saline) and

deposited on Superfrost microscope slides (CARL Roth) with the Cytospin™ Centrifuge (5 min 600 rpm). Then, cells were fixed in 4% paraformaldehyde (PFA) (Thermo Fisher Scientific) in PBS for 10 min at room temperature (RT). After washing with PBS, cells were permeabilized with 0.2% Triton X-100 in PBS for 10 min at RT, washed with PBS and non-specific sites were saturated during a 1-hour incubation in PBS containing 3% BSA (bovine serum albumin). Slides were then incubated with primary mouse anti-FLAG M2 antibody (1:250) from Sigma-Aldrich in PBS 1% BSA for 2 hours at RT. Washing with PBS was followed by an incubation with anti-mouse Alexa 568 antibody (Molecular Probes) (1:250 in PBS 1% BSA) for 45 min at RT, washing with PBS, DAPI staining of nuclei in PBS (1:500) for 20 min at RT and slide mounting in Fluoromount-G (SouthernBiotech). Images were captured with a Leica SPE confocal microscope equipped with an ORCA-ER chilled CCD camera (Hamamatsu) and the Openlab software (Improvision).

1. Zeniou M, Fève M, Mameri S, Dong J, Salomé C, Chen W, et al. Chemical Library Screening and Structure-Function Relationship Studies Identify Bisacodyl as a Potent and Selective Cytotoxic Agent Towards Quiescent Human Glioblastoma Tumor Stem-Like Cells. PLOS ONE. 2015;10: e0134793. doi:10.1371/journal.pone.0134793

## Supplementary Table S1. List of primers used in the study

DNA	Usage	Sequences
WNK1	PCR for Gateway cloning	Fwd 5'-GGGGACAAGTTTGTACAAAAAAGCAGGCTTCTGGCGGCCGCCAGAGAAG-3' Rev 5'-GGGGACCACTTTGTACAAAGAAAGCTGGGTCTTAAGTGGTCCGCAGTTGGAGCC-3'
WNK1	PCR for mutagenesis (T60A)	Fwd 5'-CAGGCGCCGCCGCCACGCTATGGACAAGGACAGC-3' Rev 5'-GCTGTCTTGTCCATAGCGTGGCGGCCGCCCTG-3'
WNK1	PCR for mutagenesis (T60D)	Fwd 5'-CAGGCGCCGCCGCCACGATATGGACAAGGACAGCC-3' Rev 5'-GGCTGTCTTGTCCATATCGTGGCGGCCGCCCTG-3'
WNK1	PCR for mutagenesis (T60E)	Fwd 5'-CAGGCGCCGCCGCCACGAGATGGACAAGGACAGCC-3' Rev 5'-GGCTGTCTTGTCCATCTCGTGGCGGCCGCCCTG-3'
WNK1	PCR for mutagenesis (K233M)	Fwd 5'-GAAATCGGCAGAGGCTCCTTTATGACGGTCTACAAAGGTCTGG-3' Rev 5'-CCAGACCTTTGTAGACCGTCATAAAGGAGCCTCTGCCGATTTC-3'
WNK1	sequencing	5'-GGGAGCAAAGAGGAGCCG-3'
WNK1	sequencing	5'-CTTGAGATGGCTACATCTG-3'
WNK1	sequencing	5'-CAGACAGTTTCATATGGTTC-3'
WNK1	sequencing	5'-CAGCTCCTACAACGACGAG-3'
WNK1	sequencing	5'-GGTGACAACCCCGAGGAG-3'
WNK1	sequencing	5'-GTAACCTCAGGTGGTCTC-3'
WNK1	sequencing	5'-CATTGTCTGAAGTAGATTC-3'
WNK1	sequencing	5'-GTCAGAAGATGCAAAGTCTG-3'
WNK1	sequencing	5'-CAGGGAGAAGACGACGAC-3'
WNK1	sequencing	5'-ATGGACTACAAAGACGATGACG-3'
pDONR 207	sequencing	pDONOR FP: GATC primer
pDONR 207	sequencing	pDONOR RP: GATC primer
pDONR 207	sequencing	CMV-F: GATC primer
WNK1	Primers for WNK1 shRNA encoding insert assembly	Fwd: 5'-GAGACCACAGATCCCCCAATGAGTCAGATATCGAATTCAGAGATTCGATATCTGACTCATTGTTTTTA-3' Rev: 5'-GGTATCGATAAGCTTAAAAACAATGAGTCAGATATCGAATCTCTTGAATTCGATATCTGACTCATTGGGG-3'
WNK1	Primers for scramble shRNA encoding insert	Fwd: 5'-GAGACCACAGATCCCCCACTACGAATGACGTATAGATTCAAGAGATCTATACGTCATTCGTAGTTTTTA-3' Rev: 5'-GGTATCGATAAGCTTAAAAAATACGAATGACGTATAGATCTCTTGAATCTATACGTCATTCGTAGTGGG-3'
pEGFP-N2 RNAi	PCR for pEGFP-N2 RNAi vector with LIC sites assembly	Fwd: 5'-GTCATGTTCTTCTGCGTTATC-3' Rev: 5'-GATCTGTGGTCTCATACAGAACTTATAAGATTCCCAAATCC-3'
pEGFP-N2 RNAi	PCR for pEGFP-N2 RNAi vector with LIC sites assembly	Fwd: 5'-AGCTTATCGATACCGTCATGTTCTTCTGCGTTATC-3' Rev: 5'-ATACAGAACTTATAAGATTCCCAAATCC-3'
WNK1	PCR for colony screening	Fwd: 5'-GAATTCGAACGCTGACGTCATC-3' Rev: 5'-GAACATGACGGTATCGATAAG-3'
WNK1	ShRNA vector sequencing	5'-GAATTCGAACGCTGACGTCATC-3'
WNK1	ShRNA vector sequencing	5'-GAACATGACGGTATCGATAAG-3'

**Supplementary Table S2. List of antibodies used in the study**

Name	Ref. Catalogue	Company	Dilution	Reference
Rabbit polyclonal anti-Akt	#9271	Cell signaling Technology	WB 1/1000	(1)
Rabbit polyclonal anti-phospho-Akt (Ser473)	#9272	Cell signaling Technology	WB 1/1000	(1)
Rabbit polyclonal anti-NBCe1/SLC4A4	#11867	Cell signaling Technology	WB 1/1000	(1)
Rabbit polyclonal anti-NBCn1/SLC4A7	Orb304589	Biorbyt	WB 1/1000	-
Rabbit polyclonal anti-OSR1	#3729	Cell signaling Technology	WB 1/1000	(2)
Rabbit polyclonal anti-SPAK	#2281	Cell signaling Technology	WB 1/800-1/1000	(2)
Rabbit polyclonal anti-phospho-SPAK (Ser373) / phospho-OSR1 (Ser325)	07-2273	EMD Millipore	WB 1/1000	(3)
Rabbit polyclonal anti-SGK1	NBP1-32635	Novus Biologicals	WB 1/1000	-
Rabbit polyclonal anti-phospho-SGK1 (Thr 256)	sc-16744	Santa Cruz Biotechnology	WB 1/800-1/1000	(4)
Rabbit polyclonal anti-WNK1	#4979	Cell signaling Technology	WB 1/500	(2)
Rabbit monoclonal anti-WNK1	AB174854	Abcam	WB 1/2000	-
Rabbit polyclonal anti-phospho-WNK1 (Thr60)	#4946	Cell signaling Technology	WB 1/500	(5)
Rabbit monoclonal anti-GAPDH (D16H11) XP®	#5174	Cell signaling Technology	WB 1/5000	(6)
Mouse monoclonal anti-Na <sup>+</sup> /K <sup>+</sup> ATPase	sc-71638	Santa Cruz Biotechnology	WB 1/1000	(7)
Goat anti-rabbit IgG, HRP-linked	#7074	Cell signaling Technology	WB 1/5000	(6)
Horse anti-mouse IgG, HRP-linked	#7076	Cell signaling Technology	WB 1/10000	(8)
Mouse monoclonal anti-FLAG® M2	F1804	Sigma-Aldrich	IF: 1:250	(9)
Goat anti-mouse Alexa Fluor 568 IgG	A11031	Molecular Probes	IF: 1:250	

1. Prasad V, Lorenz JN, Lasko VM, Nieman ML, Moamen A, J N, et al. Loss of the AE3 Cl<sup>-</sup>/HCO<sub>3</sub><sup>-</sup> exchanger in mice affects rate-dependent inotropy and stress-related AKT signaling in heart. *Front Physiol* [Internet]. 2013 [cited 2017 Mar 28];4. Available from: <http://journal.frontiersin.org/article/10.3389/fphys.2013.00399/abstract>
2. Tu S, Bugde A, Luby-Phelps K, Cobb MH. WNK1 is required for mitosis and abscission. *Proc Natl Acad Sci U S A*. 2011 Jan 25;108(4):1385–90.
3. Yang S-S, Huang C-L, Chen H-E, Tung C-S, Shih H-P, Liu Y-P. Effects of SPAK knockout on sensorimotor gating, novelty exploration, and brain area-dependent expressions of NKCC1 and KCC2 in a mouse model of schizophrenia. *Prog Neuropsychopharmacol Biol Psychiatry*. 2015 Aug 3;61:30–6.
4. Chen W, Chen Y, Xu B, Juang Y-C, Stippec S, Zhao Y, et al. Regulation of a Third Conserved Phosphorylation Site in SGK1. *J Biol Chem*. 2009 Feb 6;284(6):3453–60.
5. Nimmanon T, Ziliotto S, Morris S, Flanagan L, M. Taylor K. Phosphorylation of zinc channel ZIP7 drives MAPK, PI3K and mTOR growth and proliferation signalling. *Metallomics* [Internet]. 2017 [cited 2017 Mar 28]; Available from: <http://pubs.rsc.org/en/Content/ArticleLanding/2017/MT/C6MT00286B>
6. Xiao Y, Jiang Y, Song H, Liang T, Li Y, Yan D, et al. RNF7 knockdown inhibits prostate cancer tumorigenesis by inactivation of ERK1/2 pathway. *Sci Rep*. 2017 Mar 2;7:43683.
7. Lee SJ, Litan A, Li Z, Graves B, Lindsey S, Barwe SP, et al. Na,K-ATPase  $\beta$ 1-subunit is a target of sonic hedgehog signaling and enhances medulloblastoma tumorigenicity. *Mol Cancer* [Internet]. 2015 Aug 19 [cited 2017 Mar 28];14. Available from: <http://www.ncbi.nlm.nih.gov/pmc/articles/PMC4544806/>
8. Busnelli M, Manzini S, Hilvo M, Parolini C, Ganzetti GS, Dellera F, Ekroos K, Jänis M, Escalante-Alcalde D, Sirtori CR, Laaksonen R, Chiesa G (2017). Liver-specific deletion of the Plpp3 gene alters plasma lipid composition and worsens atherosclerosis in apoE(-/-) mice. *Sci Rep*, 7, pp. 44503.
9. Xue J, Zhou A, Tan C, Wu Y, Lee H-T, Li W, et al. Forkhead Box M1 Is Essential for Nuclear Localization of Glioma-associated Oncogene Homolog 1 in Glioblastoma Multiforme Cells by Promoting Importin-7 Expression. *J Biol Chem*. 2015 Jul 24;290(30):18662–70.

### **III. Discussion and conclusion**

#### **3.1. Glioblastoma: development of new therapeutic strategies in the presence of GSCs and of a complex tumor microenvironment**

Glioblastoma (GBM), with its invasiveness and the existence of glioblastoma stem-like cells (GSCs), two major impediment factors to efficient treatment, is the most aggressive form of brain tumor. The diffusive and invasive nature of GBMs makes total surgical resection impossible and contributes to chemotherapy and radiation resistance, and finally to tumor recurrence [249]. Many studies showed that a subpopulation of cancer cells, GSCs, which seem to play a pivotal role in tumor initiation and tumor bulk maintenance also contribute to therapy failure [250][251]. This population of cancer cells with specific properties in GBM can be identified with cell surface markers, functional markers and stem cell markers such as CD133 [116], CD44, SSEA-1 [128], ALDH [252] and A2B5 [129]. However, no single marker has been shown to be sufficient to identify and isolate GSCs. The specific role of GSCs not only relies on their self-renewal, *in vivo* tumor-initiation and multi-lineage differentiation abilities, but also on their specific microenvironment which is advantageous to preserve their characteristics, as hypoxia promotes stem cell maintenance and prevents differentiation [253]. Besides, recent evidence showed that GSCs can be reprogrammed by introducing the expression of specific combinations of transcription factors [155] and non-stem-like GBM cells can convert to GSCs after radiation or chemotherapy [254][255]. Environmental factors can also revert differentiated cancer cells into GSCs [5].

GBMs are complex tumors presenting necrotic cores surrounded by cellular pseudopalisades and microvascular hyperplasia (Figure 18). GBM cells with high expression levels of HIF1, VEGF and IL-8 are present in these regions, suggesting a hypoxic environment related to glycolysis, angiogenesis, cell proliferation, migration and invasion in GBM [256] [257]. As mentioned before, GSC cells residing in hypoxic microenvironments are protected from radiation and chemotherapy. Thus, GSCs are interesting targets for new therapies and experimental models assessing the ability of new compounds to eradicate GSCs within their microenvironment are required for the development of efficient GSC-targeting therapies.



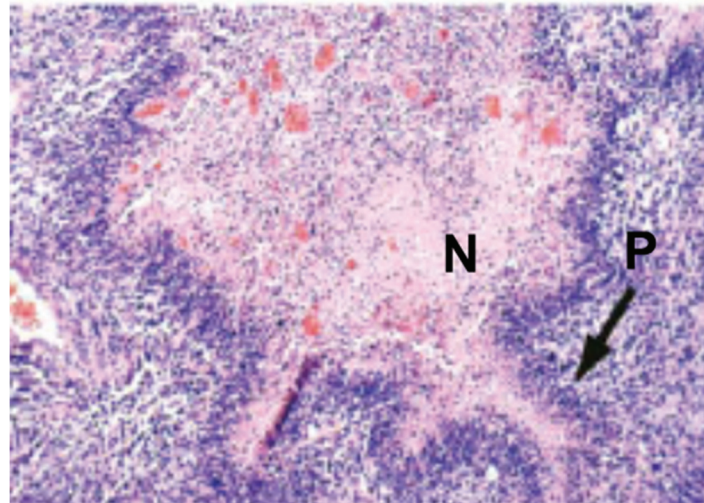


**Figure 18. Histopathological features of glioblastoma (GBM), from [256].** Section of a GBM tumor stained with hematoxyline/eosine. A cellular zone called pseudopalisade (P) surrounds a necrotic (N) region.

### **3.2 Experimental models for brain tumor studies**

#### **3.2.1 *In vitro* and *in vivo* experimental models**

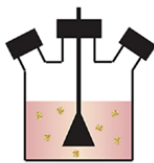
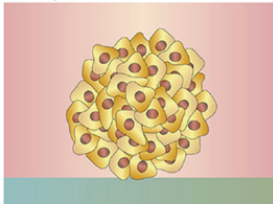
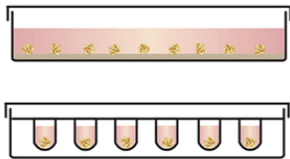
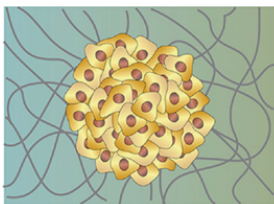
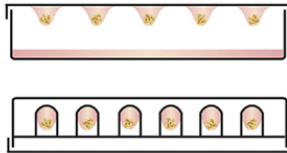
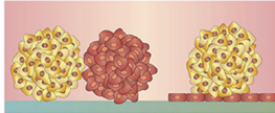





*In vivo* models have been widely used in cancer research for their ability to mimic, at least in part, the complexity of tumor development, progression, metastasis and therapy response in a living system. Mouse models are frequently used in cancer research. These include chemically induced models, human cancer cell xenografts in immune-compromised mice and genetically engineered mouse models. However, none of these models is representative of all aspects of cancer development in humans. In addition, such models are relatively expensive and time-consuming. Moreover, most *in vivo* studies of GBM are based on xenograft analysis deriving from single established cell lines which do not necessarily recapitulate the characteristic heterogeneity of the original tumor [258]. The poor predictive ability of mouse xenograft models as human cancer preclinical models is thus not surprising and causes a low rate of success in subsequent clinical trials [259] .

Attempts to obtain *in vivo* models that more closely resemble the human tumor have been made by generating engineered mouse models which can reproduce some tumoral histopathological features and more accurately recapitulate genetic events and subsequent molecular evolution of brain tumors.

Such models are considered as more effective preclinical screening methods for novel cancer therapeutics [260].

*In vitro* models, mainly represented by tumor-derived cell lines, also play an important role in cancer research including in the initial tests for drug screening because they provide strictly controllable experimental variables and are easy to use. Even though cell culture experiments are normally not capable of recapitulating both genetic and cellular heterogeneity of tumors and the complexity of the tumor-stroma interactions as *in vivo* models, advances in culture conditions, materials and microtechnologies are attempting to overcome some of these limitations [261]. Several *in vitro* models have been developed and used in brain tumor research, including monolayer cultures, spheroid formation and 3D (3 dimensional) confrontation/co-cultures [262]. Among them, monolayer cultures, the traditional way of maintaining GBM cells growing *in vitro* as adherent cultures in the presence of serum, have several limitations such as high expression levels of differentiation markers and tumorigenic but not invasive potential in xenograft models *in vivo* [263]. Furthermore, gene expression in adherent cell lines does not correlate to gene expression patterns observed in the original tumor [264]. On the other hand, tumor spheroids and 3D confrontation/co-cultures are able to recapitulate several cell-cell and cell-matrix interactions between tumor cells and the tumor microenvironment, and have been widely used for drug screening and development as well as for tumor proliferation, invasion, angiogenesis and immune response studies (co-culture/confrontation system). These approaches also reflect more accurately the original tumor gene expression profile compared to serum-containing adherent cultures [261][264].

To date, four general spheroid formation methods have been reported: suspension culture, liquid overlay technique on non-adherent surface, hanging drop and microfluidic methods (Figure 19) [265][266]. However, due to the big number of available *in vitro* models and their inherent differences in complexity and functionality, standard protocols are missing and it is thus difficult to compare results obtained in distinct experimental settings [265].

Spheroid Formation	Experimental Setup	Variables	Outputs
Suspension/Spinner Flasks 	Spheroids in Media 	Proliferation/ Migration/Invasion	Characterization of spheroid composition, growth and proliferation Protein and gene expression changes Migration and invasion assays
Liquid Overlay Technique Non-adherent Surfaces 	Spheroids in Matrix 	Drug Screening	Characterization of spheroid composition, growth and proliferation Protein and gene expression changes Survival assays Efficacy, distribution and accumulation of therapeutics
Hanging Drop Technique 	Coculture Spheroids 	Angiogenesis	Characterization of spheroid composition, growth and proliferation Protein and gene expression changes (i.e. angiogenic factors) Migration and invasion assays Angiogenesis assays
Microfluidic 	 <div style="display: flex; align-items: center;">  Cancer cell          Endothelial cell          Immune cell       </div>	Immune Cell Response	Characterization of spheroid composition Protein and gene expression changes Adhesion assays Infiltration of immune cells into spheroids Migration and extravasation assays

**Figure 19. Spheroid formation methods and their applications, from [265].** *In vitro* spheroid formation is achieved by several methods: suspension culture, liquid overlay technique on non-adherent surfaces, hanging drops and microfluidics. In suspension culture methods, agitation or increased cell medium viscosity promote spontaneous cell aggregation and spheroid formation. The liquid overlay method consists in culturing cells on non-adherent surfaces that favor spheroid formation. In the hanging drop method, cells are suspended in droplets of medium on culture lids. Finally, microfluidic devices may be used to generate spheroids in *in vitro* cultures. Applications of spheroids obtained by all these methods are indicated.

Despite their limitations, *in vivo* and *in vitro* tumor models have been and will continue to be important tools for cancer research. In addition, the use of patient-derived primary cancer cells combined to the remarkable efforts that have been made by The cancer Genome Atlas (TCGA) and the Cancer Cell Line Encyclopedia (CCLE) for providing genomic profile, gene expression, DNA copy number and mutation identification data is valuable to the development of more personalized treatment protocols for better patient treatment outcomes [8][267]. Combinations of

*in vitro* approaches with *in vivo* models that mimic in part histo-morphological, functional and microenvironmental features of human tumors in a living system, should lead to more rational and efficient therapeutic development.

### **3.2.2 The spheroid model in brain tumors**

Tumor spheroid cultures can be traced back to the 1970s and 1980s. Sutherland and colleagues used multi-cell spheroids as an experimental model to investigate the radiation survival of tumor cells in 1970 [268]. In this experimental model, they identified an outer zone of proliferating cells, an intermediate zone characterized by poor nutrient and oxygen supply and containing only few mitotic cells as well as a central necrotic zone [269]. Spheroid cell differentiation, proliferation or quiescent status and cell-cell contacts contributing to radiation resistance were also explored. The thickness of the viable cell rim surrounding the necrotic center was shown to vary between 100 to 200  $\mu\text{m}$ . This is similar to what is found in tumors *in vivo*. In addition, cellular heterogeneity was observed in spheroids due to  $\text{O}_2$  and growth factor deprivation as the spheroids' growth progressed. Radiation resistance was also linked to low  $\text{O}_2$  levels in spheroids. Moreover, a drug distribution gradient with the highest concentrations observed in outer layer cells was observed in several tumor spheroid systems [270]. As the tumor microenvironment is emerging as a critical player in tumor initiation and progression and therapy resistance, the spheroid culture system regained attention since, as discussed, it mimics several aspects of tumors *in vivo*.

### **3.2.3 Spheroid formation ability and cancer stem-like cells**

In 1992 Reynolds and Weiss showed that NSCs (neural stem cells) could be expanded as neurospheres *in vitro* in defined, serum-free media supplemented with growth factors [271]. Meanwhile, cancer stem-like cells were identified in many human cancers including in brain tumors [113]. Since brain tumor stem-like cells share many properties of NCSs, it was conceivable that this particular tumor cell subpopulation could also be expanded as neurospheres in *in vitro* experimental settings.

Cancer stem-like cell culture as free-floating spheres, also called tumorspheres, was first described in brain tumors by Singh and colleagues [115]. Numerous studies used this system of serum-free neuronal stem cell or DMEM (Dulbecco's modified Eagle's medium)/F12-based medium supplemented with various growth factors and nutrient mixtures to isolate spheroid-forming cells from patients. Such cells were able to self-renew and regenerate tumors in xenograft models with similar histopathological features as the ones observed in the original tumors [110][117][272]. GSCs used in our studies were isolated using similar experimental settings [119]. Methods for cancer stem-like cell isolation and expansion as spheres do not greatly differ from one cancer tissue of origin to another. Complementary cell sorting on the basis of putative cancer stem-like cell markers by fluorescent-activated cell sorting or magnetic-activated cell sorting can be performed to eliminate stromal cells and to enrich the CSC population [273]. Laks and coworkers then demonstrated a relationship between neurosphere formation, tumorigenic capacity and patient clinical outcome by using 32 glioma patient samples of which 15 were from GBM [274]. Another study conducted by Lee and colleagues showed that cells cultured in serum-free conditions in the form of spheroids exhibited self-renewal and differentiation capacities and had high genotypic similarity with their parental GBMs. When these cells were transferred into a serum-containing environment, they became adherent and lost their self-renewal ability and tumorigenic potential. These phenotypic modifications were accompanied by alterations in their gene expression profile in a passage-dependent manner [264]. More recently, an *in vitro* invasion GBM model was described in which GSC-containing spheroids were implanted into rat organotypic brain slices. Interestingly, the invasion pattern observed in this *in vitro* experimental setting was comparable to what was previously seen in *in vivo* GSC-xenograft mouse models [275].

Recent studies showed that GSCs can also be grown as adherent cultures on laminin-coated cell culture plates in the same serum-free medium as for neurosphere cultures. This monolayer adherent culture allows equal access to growth factors for all GSCs and does not induce differentiation (few cell differentiation markers) and apoptosis in these cells. Even though these GSC cell cultures were less heterogeneous than the corresponding neurosphere cultures,

they sustained the same tumorigenic ability when intracranially injected into immunocompromised mice [263]. Pollard and colleagues suggested that the adherent cancer stem-like cell cultures are a better system for high-throughput drug screens compared to suspension cultures. This application thus received a great deal of attention [276]. However, according to Reynolds and Vescovi, the validity of these conclusions is questionable since presented data are not always quantitative and lack reliable statistical analysis [277].

### **3.2.4 GSC *in vitro* models used in our study**

In our study, proliferating GSCs isolated from GBM patient samples are expanded as neurospheres *in vitro* in DMEM /F12-based medium supplemented with growth factors (bFGF and EGF) as described previously [119]. These cells exhibit long-term stability in culture and tumorigenic properties that support their capacity to establish a novel brain tumor from a few cells at least up to two years of consecutive passages [119]. As mentioned in the introduction section, *in vivo*, GSCs are also able to enter a slow-growing quiescent state, favored by hypoxic and acidic conditions of the tumor microenvironment, which increases their resistance to treatment [278]. We thus developed an *in vitro* model of quiescent GSCs. For quiescent GSC culture, cells were seeded in proliferating cell culture medium as single-cell suspensions and grown without medium renewal for 9 to 16 days. Under these culture conditions, which result in a progressive acidification of the cells' culture medium (pH of ~6.6 after 9 days in culture), most GSCs show low cell proliferation and low levels of DNA synthesis signifying they have entered into the G0 phase. Massive apoptosis is not observed. The quiescent state may be reversed by renewal of the culture medium. In addition, quiescent GSCs maintain the cell surface and stem-cell marker expression pattern and the same sphere-formation capacity and differentiation ability (when re-introduced in proliferating culture conditions) as proliferating GSCs.

In the lab, we have also set up conditions allowing to obtain clonal large-size (> 500  $\mu\text{m}$ ) GSC-derived tumorspheres. These spheroids recapitulate some critical characteristics of GBMs such as the presence of decreasing nutrient,  $\text{O}_2$ , and pH gradients for cells positioned close to the necrotic center [243][256]. To our

knowledge, such large spheres obtained from single GSCs have not been previously described in the literature.

### **3.3 Bisacodyl in GSCs**

#### **3.3.1 Bisacodyl**

Bisacodyl is a diphenyl methane derivative used as a stimulant laxative drug since 1952 and reclassified in 1996 as a category III laxative indicating that more safety and efficacy data are needed. More recently, bisacodyl has been introduced in clinical practice for bowel evacuation before radiological gastrointestinal procedures and for preoperative bowel preparation. Following administration, bisacodyl is hydrolyzed by intestinal and bacterial enzymes to DDPM, its deacetylated active metabolite which is responsible for its action. There are two major actions for bisacodyl's laxative effect: stimulation of myoelectrical activity and motility in the colon and stimulation of intestinal water secretion [279]. Bisacodyl was shown to act on epithelial cells, myenteric neurons and possibly smooth muscle cells by stimulating the iNOS (inducible nitric oxide synthase) which produces NO (nitric oxide). Released NO may act on epithelial cells to stimulate secretion and luminal fluid accumulation and relaxes smooth muscle [247]. In the colon, bisacodyl was reported to activate macrophages which caused secretion of inflammatory cytokines such as TNF- $\alpha$ , IL-1b and IL-6 (interleukin) that in turn increased the expression levels of COX2 (cyclooxygenase-2) acting as an autocrine factor in macrophages, as well as the secretion of PGE2 (prostaglandin E2) acting as a paracrine factor in intestinal epithelial cells by decreasing the expression levels of aquaporin-3. This results in a decrease of water absorption and a laxative effect [248]. Through oral administration, only 16% of bisacodyl is absorbed and the plasma levels of its active metabolite are not related to the laxative effect, suggesting that the systemic absorption of the compound is not required for its laxative action [280]. Some rare studies describe other effects of bisacodyl than its laxative effect on the human gastrointestinal tract [281][282].

### 3.3.2 Bisacodyl/DDPM cytotoxicity profile in GSCs

High-throughput screening (HTS) assays allow to test a large number of chemical substances for activity in diverse areas of biology, including anti-cancer drug screening. We have used both proliferating and quiescent GSCs to differentially screen the Prestwick chemical library, which is mainly composed of over 1000 FDA-approved drugs, seeking for compounds with cytotoxicity. After the primary screen and follow-up assays, the unique validated compound with a selective cytotoxicity towards quiescent GSCs without killing healthy non-cancerous cells, was bisacodyl. Further studies, confirmed that bisacodyl was transformed in its active metabolite DDPM which was responsible for the selective cytotoxicity of the compound towards quiescent GSCs [138]. Quiescent culture conditions lead to acidification of the cells' medium. Thus, when the compound is added, quiescent GSCs are in a slightly acidic medium (pH~6.6) compared to proliferating GSCs whose medium is set up to physiological pH (pH~7.4). A test in which proliferating cells were treated with bisacodyl/DDPM in slightly acidic medium conditions confirmed that acidification of the medium also sensitized proliferating GSCs to the compound [243]. Thus, acidification of the medium seems to be an important factor for bisacodyl's cytotoxicity although at similar extracellular pH conditions quiescent GSCs remained more sensitive to the compound compared to their proliferating counterparts [243].

Bisacodyl/DDPM was also shown to expand the necrotic core in large-size clonal tumorspheres derived from GSCs suggesting that the compound preferentially targets quiescent cells located at the inner hypoxic and acidic edge of the viable cell rim in these structures [243].

To determine whether bisacodyl/DDPM has *in vivo* anti-cancer activity, a xenograft mouse model obtained from GSC orthotopic implantation has been used. After intraperitoneal administration of bisacodyl, the presence of both bisacodyl and DDPM in mice brain confirmed the ability of these compounds to pass the blood brain barrier. Compared to the vehicle group, bisacodyl treated mice showed reduced tumor growth and a significant increase in survival rate [243].

The results we've got by now are mainly based on 2 types of GSCs, TG1 and TG1 C1 (OB1) cells, derived from adult GBM. Given the heterogeneity of GBM



lesions in patients, further studies should consider more types of GSCs. In addition, as reported in a study conducted by Piccirillo and coworkers, distinct CSC populations may co-exist within the same GBM sample and exhibit different growth properties and tumor-initiating capacities [283]. It would be thus interesting to consider the complexity of different GSC pools within the same tumor, for example, by investigating the cytotoxicity of bisacodyl/DDPM in co-cultures of different GSCs and in large-size tumorspheres derived from multiple GSC cell types.

Bisacodyl/DDPM could also be tested on GSCs isolated from pediatric GBMs. Indeed, although pediatric GBMs are not histopathologically very different from adult GBMs, they exhibit distinct pathogenetic mechanisms and molecular characteristics. In particular, pediatric GBMs, which mainly occur as *de novo* tumors, exhibit TP53 mutations but only rarely EGFR amplification and PTEN mutations [284][285][286]. However, approximately 80% of pediatric high-grade gliomas show overexpression of the activated/phosphorylated form of Akt (Ser 473) [287]. Other studies showed an association between RAS/Akt-activation and poor prognosis in pediatric GBM after analyzing 32 pediatric GBM samples [288]. Interestingly, our recent results suggest that combinations of bisacodyl/DDPM with an Akt inhibitor are more cytotoxic to GSCs compared to either inhibitor alone. It would be thus interesting to assess the antitumoral effect of bisacodyl combined to an Akt inhibitor in *in vivo* orthotopic models of both adult and pediatric GBMs.

### **3.3.3 Mechanisms and signaling pathways of bisacodyl in GSCs**

Calcium concentration plays an important role in cancer cell migration and tumor metastasis and multiple  $\text{Ca}^{2+}$  channels have been linked to cancer cell proliferation, migration and survival [289]. For example, the  $\text{Ca}^{2+}$ -permeable TRPC6 (transient receptor potential 6) channel was shown to promote a sustained elevation of intracellular  $\text{Ca}^{2+}$  which is critical for development of an aggressive phenotype in glioblastoma [290]. This protein was also shown to be involved in glioma cell cycle progression and inhibition of TRPC6 resulted in reduced growth of tumors in xenograft mouse models of the disease [291].  $\text{Ca}^{2+}$  signaling may also contribute to invasive properties of GBM cells *via* the activation of the CIC-3 channels and  $\text{Ca}^{2+}$ -activated  $\text{K}^+$  channels  $\text{KCa3.1}$ , which lead to cell volume regulation [292]. In GBM cells,  $\text{Ca}^{2+}$  release *via* the activation of inositol 1,4,5-trisphosphate receptor subtype 3

(IP3R3) was essential for cancer cell migration and invasion and the expression of IP3R3 was increased in GBM samples [293]. Interestingly, expression of type 1 1,4,5-trisphosphate receptor (IP3R1) is higher in quiescent GSCs grown at pH 6.5 and used in our study compared to proliferating GSCs grown at pH 7.4. Moreover, bisacodyl/DDPM was able to interfere and inhibit IP3R1-mediated  $\text{Ca}^{2+}$  mobilization in quiescent cells challenged with muscarinic and nicotinic agonists. Thus, by downregulating IP3R1-induced  $\text{Ca}^{2+}$  release, bisacodyl could indirectly cause quiescent GSC cell death [243].

As already discussed, bisacodyl/DDPM was initially selected for its selective cytotoxicity towards quiescent GSCs. Subsequent tests indicated that the compound is also active on proliferating GSCs provided the pH of their culture medium is set to acidic conditions. Thus, acidic microenvironments seem to play an important role in the response of GSCs to the compound. In tumor cells, increased glycolysis for energy production leads to high glucose consumption and enhanced acidification of the extracellular medium, which is frequently accompanied by various levels of hypoxia. Low extracellular pH, in the range of 5.6 to 6.8, is a hallmark of malignant cells [294]. High levels of acidity are also involved in cell growth arrest [295]. For example, acidosis associated hypoxia promotes the production of HIF1 which inhibits progression through the cell cycle by activating CDK inhibitors p21 and p27 [296]. Cell cycle arrest induced by acidic environments in proliferating GSCs may explain the sensitization of these cells to bisacodyl in acidic medium. Besides, acidosis triggers upregulation of several proteins, including MCTs, CAs, AEs, NBCs and NHEs [71]. These proteins participate in intracellular and extracellular pH ( $\text{pHi}$  and  $\text{pHe}$ ) regulation in tumor cells. Targeting one of these pH regulators could be a promising therapeutic strategy for the treatment of glioblastoma.

The WNK1 serine/threonine protein kinase is a known regulator of several ion channels and co-transporters, including  $\text{Na}^+/\text{HCO}_3^-$  co-transporters of the NBC family which play essential roles in intracellular pH regulation and whole body pH maintenance [202]. Analysis of the phospho-kinase profile in bisacodyl-treated quiescent GSCs revealed that bisacodyl/DDPM inhibit the phosphorylation of WNK1 Thr60 in an activity-dependent manner. Phosphorylation of this residue was proposed to be involved in scaffolding properties of WNK1 with other protein

partners. Interestingly, phosphorylation/activation levels of Akt and SGK1 protein kinases, for which WNK1 Thr60 might be a substrate, were also negatively affected by bisacodyl/DDPM. In addition, Akt and SGK inhibitors potentiated the effect of the compound on quiescent GSCs whereas an Akt activator partially protected the cells from bisacodyl/DDPM action. The catalytic activity of WNK1 was also modified by bisacodyl and was shown to contribute to the cytotoxic effect of the compound in quiescent GSCs. In other systems, WNK1 was shown to negatively regulate the cell surface expression and activity of the electrogenic  $\text{Na}^+/\text{HCO}_3^-$  co-transporter NBCe1. This process requires the N-terminal part of WNK1 (including Thr60) but not the catalytic activity of the enzyme. NBCn1, another member of the NBC family of co-transporters may be similarly regulated by WNK1. It is thus conceivable that bisacodyl, by interfering with the Thr60 phosphorylation status, may lead to abnormal activation of these NBC co-transporters resulting in necrotic cell death observed in quiescent GSCs treated with the compound. This hypothesis is supported by the fact that pretreatment of quiescent GSCs with an NBC inhibitor, partially protects cells from bisacodyl action. WNK1/SPAK-mediated NBC co-transporter surface expression/activity negative regulation is antagonized by IRBIT (inositol receptor binding protein released with inositol 1,4,5-triphosphate), an enzyme regulating both inositol 1,4,5-triphosphate receptors and ion co-transporters including NBCe1 [202][216]. At the resting state or when inositol 1, 4, 5 triphosphate (IP3) concentrations are low near IP3 receptors, IRBIT is bound to IP3 receptors and suppresses their activation. Increased levels of IP3 displace IRBIT and activate IP3R-mediated  $\text{Ca}^{2+}$  release from intracellular stores. Released IRBIT is able to bind to NBC co-transporters and enhance their activity both by increasing their cell surface levels and by directly modulating their activation status [297]. Interestingly, higher expression of IP3R1 was observed in quiescent GSCs in acidic conditions. Thus, in these cells, binding of IRBIT to IP3 receptors combined with high levels of WNK1 Thr60 phosphorylation may cooperate to maintain NBC co-transporter activity to levels allowing cell survival in these particular conditions. Abnormally high NBC activity, evoked by bisacodyl, may cause cell death through dysregulation of pH homeostasis in GSCs. In addition, NBC activation would also lead to high levels of  $\text{Na}^+$  uptake since this ion is co-transported with  $\text{HCO}_3^-$ . This could disturb  $\text{Na}^+$  electrochemical gradients which are important driving forces for  $\text{Na}^+$ -dependent transporters. Furthermore, elevated intracellular  $\text{Na}^+$  was shown to result in

intracellular  $\text{Ca}^{2+}$  overload leading to mitochondrial damage and necrotic cell death. Moreover,  $\text{Na}^+$  and  $\text{K}^+$  homeostasis are tightly related through  $\text{Na}^+/\text{K}^+$  ATPase and NKCC1 [298] suggesting that disturbance of  $\text{Na}^+$  homeostasis would also influence  $\text{K}^+$  homeostasis in GSCs. Finally, abnormal NBC activity may influence glycolytic pathways in GSCs. To adapt to hypoxia and acidic microenvironments, tumor cells shift their glucose metabolism from oxidative phosphorylation to glycolysis [70][72]. The first step of the glycolytic pathway is initiated by the uptake of glucose and the sequestration by hexokinase, which catalyzes the phosphorylation of glucose to glucose-6-phosphate. This reaction is pH dependent and needs strict control of  $\text{pH}_i$  as well as the activity of phosphofructokinase [72]. The evolutionarily conserved soluble adenylyl cyclase (sAC), functioning as a carbon dioxide, bicarbonate, and pH sensor in cells, was reported to be directly activated by bicarbonate ions, namely transported by NBCe1, and to be stimulated by  $\text{Ca}^{2+}$  [299][300][301]. Activation of this enzyme was shown to enhance glycolytic pathways [301].

In quiescent GSCs, pre-treatment with bisacodyl was shown to inhibit  $\text{Ca}^{2+}$  mobilization from intracellular stores mediated by acetylcholine or carbachol  $\text{IP}_3$  production and activation of  $\text{IP}_3$  receptors including  $\text{IP}_3\text{R1}$  [243]. Interestingly, Akt-mediated phosphorylation of WNK1 Thr60 was shown to promote  $\text{PIP}_2$  synthesis through phosphatidylinositol 4-kinase IIIa activation, thus sustaining  $\text{PLC-}\beta$  signaling,  $\text{IP}_3$  production and  $\text{IP}_3$  receptor activation mediated by Gq-coupled GPCRs (G protein coupled receptors) [235]. Inhibition of WNK1 Thr60 phosphorylation elicited by bisacodyl may thus underlie the negative effect of the compound on  $\text{Ca}^{2+}$  signaling in quiescent GSCs.

### **3.3.4 Direct protein targets of bisacodyl in GSCs**

Development of effective and safe therapeutic agents is the holy grail of medicine. For small-molecule drugs, a main challenge is the identification of their molecular targets and mechanisms of action underlying drug therapeutic effects. In addition, knowledge on potential off-target interactions allows to anticipate adverse side effects [302].

One of the aims of my thesis was to find out the direct protein target(s) of bisacodyl/DDPM in GSCs. Affinity chromatography is a useful technique that has

long been applied for elucidating direct protein binders of bioactive small molecules. Thus, we designed preliminary experiments of an affinity chromatography method to investigate the potential protein targets of bisacodyl/DDPM. For this, a derivative of bisacodyl/DDPM retaining activity was attached through a linker to CNBr-activated sepharose beads and incubated in the presence of total protein extracts from quiescent GSCs at pH 6.6 (condition in which the compound is active) or proliferating GSCs at pH 7.4 (condition in which the compound has no cytotoxicity) (Figure 20). Several washing steps were then followed by elution of retained proteins by denaturation and separation by gel electrophoresis. One of the limitations of the affinity chromatography approach arises from non-specific adsorption of background proteins to the support and linker [302]. To differentiate specific-binders from non-specific binders, inactivated sepharose beads were used to capture and identify background binding in quiescent GSCs at pH 6.6. In addition, functionalized beads were incubated with protein extracts from quiescent GSCs at pH 6.6 in the presence of free DDPM (competition).

Some of the eluted proteins were absent from control samples (inactivated sepharose beads and functionalized beads in the presence of competitor DDPM), suggesting they may represent proteins specifically bound to the compound derivative attached to the beads (Figure 20). However, intensities of these bands were very low requiring optimization of the process before subsequent identification by mass spectrometry. In the future, we will consider, first, to improve the bioactivity of bisacodyl/DDPM analogs which are coupled to the solid phase, then to refine negative controls to optimize specific-binding. Second, the quantity of protein extracts to use will be optimized to facilitate mass spectrometry processing.

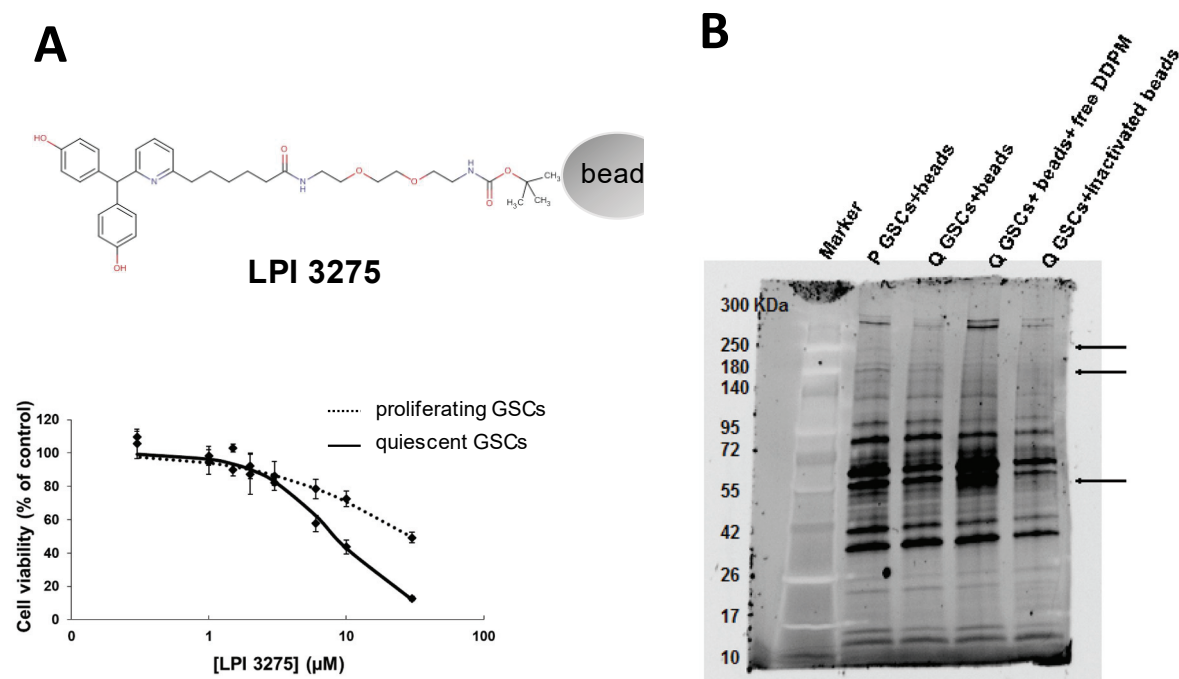


**Figure 20. Affinity chromatography for identifying direct protein target(s) of bisacodyl.** An active derivative of bisacodyl (LPI 3275) was coupled to sepharose beads through a linker. Chemical structure of LPI 3275 and dose-response curves of the compound on proliferating and quiescent GSCs are shown in A. Cell viability was measured with the ATP-Glo assay from Promega. A representative result obtained in affinity chromatography experiments is shown in B. Protein extracts from proliferating (P) and quiescent (Q) GSCs were incubated with functionalized beads (P GSCs + beads, Q GSCs + beads, respectively). Protein extracts from quiescent GSCs were also incubated with functionalized beads in the presence of free DDPM used as a competitor (Q GSCs + beads + free DDPM) as well as in the presence of inactivated non-functionalized beads (Q GSCs + inactivated beads) to identify non-specific binding. Several protein bands present only in the 'P GSCs + beads' and 'Q GSCs + beads' groups were identified (arrows) following washing of the beads and denaturation to detach retained proteins. Mass spectrometric identification of protein bands of interest requires optimization of the affinity chromatography experimental conditions.

### 3.3.5 Therapeutic interests of bisacodyl

Even though the direct targets of bisacodyl/DDPM are still unknown, its specific cytotoxic profile and *in vivo* anti-cancer activity, make it a potential anti-cancer molecule with great interest.

Indeed, most anticancer drugs are preferentially toxic to proliferating cells and exhibit poor penetration into solid tissues. Thus, cancer cells at the periphery of tumors close to blood vessels are more likely to be the targets of these anti-cancer drugs. As a consequence, repopulation of cancer cells after radiation or

chemotherapy has been observed for different types of solid cancers, causing therapy failure [303][304]. Many recent clinical trials were initiated to investigate whether modifying the schedule of chemotherapy to shorten the interval period between cycles may alter therapeutic response and clinical outcome. Such dose-dense chemotherapy accompanied with the use of colony-stimulating factors (CSFs) inducing proliferation in quiescent cells, including cancer stem-like cells, showed survival benefits in several studies, but exhibited high hematological toxicity risk for patients elder than 65 years [305]. Two other strategies were hence proposed as adjuvant therapies to enhance chemotherapy response by targeting quiescent cancer stem-like cells. They consist either in blocking the reawakening of quiescent cancer stem-like cells or in directly targeting and depleting cancer stem-like cells in the quiescent state [304]. For example, in human bladder cancer xenografts, blocking PGE2 (prostaglandin E2) signaling with PGE2-neutralizing antibodies or celecoxib, a cyclooxygenase-2 (COX-2) inhibitor, diminished paracrine effects of neighboring dying cells to recruit quiescent cancer stem-like cells that would then expand in response to chemotherapy [306]. In human gliomas, TMZ chemotherapy combined to gamma-secretase inhibitors (GSIs), which are Notch signaling pathway inhibitors, decreased tumor relapse and extended survival in xenograft models. Sphere-formation ability of cells after GSI-chemotherapy was also decreased suggesting that ability of repopulation was blocked by this adjuvant chemotherapy [307]. However, up to now, to our knowledge, with the exception of bisacodyl, no other compounds directly targeting quiescent GSCs in their microenvironment have been reported. In 2012, an international patent demand was filed for bisacodyl and analogues as anti-cancer drugs with activity on cancer stem-like cells (WO/2012/168885 A2; 13/12/2012).

### **3.4 Interests of WNK1 in GBM pathology and potential as a therapeutic target**

#### **3.4.1 WNK1 in GSCs**

In our experimental settings, high expression of Thr60-phosphorylated WNK1 was specifically found in quiescent GSCs in acidic conditions (pH ~6.6). In addition, we observed that acidic medium causes a prompt increase in the levels

phosphorylated WNK1 on Thr60 also in proliferating GSCs (results not presented in this thesis work) and that bisacodyl/DDPM, which cause necrotic cell death in GSCs under acidic conditions, alter the phosphorylation status of this residue in an activity-dependent manner. The catalytic activity of WNK1 also seems to be involved in the cytotoxic effect of the compound in GSCs. Moreover, modulation of Akt/SGK1/NBC signaling modifies the effect of the compound on GSCs and GSC-derived macro-tumorspheres and Thr60 and or/catalytically inactive mutants of WNK1 were shown to influence GSC cell survival, clonal and growth properties as well as GSC-derived macro-tumorsphere aspect. Altogether these data suggest that WNK1 and its signaling partners may contribute to GSC physiopathology, namely in acidic microenvironments.

In other systems, WNK1 is known to function both in kinase-dependent and independent manners through scaffolding [308]. Threonine 60 located in the N-terminal part of WNK1 was reported as a scaffolding site involved in interactions with other proteins including Akt, SPAK/OSR1, and SGK1 [205][211][212][308]. It would be thus interesting to investigate whether in GSCs, there are direct protein-protein interactions between these proteins and whether/how their interactions are affected by bisacodyl. In addition, immunoprecipitation techniques coupled to mass spectrometry could be used to identify other protein interactors of WNK1 (compared to WNK1 non phosphorylable/ phosphomimetic mutants on Thr60) in GSCs treated or not with bisacodyl. This could lead to the identification of novel potentially interesting therapeutic targets in GSCs.

### **3.4.2 Interests for WNK1 as a new protein kinase target**

The human genome encodes 518 protein kinases, which can be grouped into around 20 known families. Protein kinases participate to most signal transduction pathways and are involved in many cellular processes including cell metabolism, transcription and protein synthesis, cell cycle progression, cell motility, apoptosis and differentiation [309]. Mutations and dysregulation of protein kinases underlies many diseases including cancer.

Since 1978 when Collett and Erikson discovered the first oncogene product (src gene) as a protein kinase [310], protein kinases are intensively investigated as drug targets for cancer therapy because they have been found to be involved in



many essential processes of neoplasia, from tumor cell proliferation, invasion, angiogenesis and metastasis, to cell survival [311]. Most mutated genes implicated in oncogenesis encode protein kinases in an over-activating and dominant manner at the cellular level [312].

The development of selective protein kinase inhibitors to block the kinase activity of these proteins thus seems to be a promising approach for cancer therapy. According to their substrate recognition sites, kinases are divided into two major classes: tyrosine kinases and serine/threonine kinases. Receptor tyrosine kinases (RTKs), such as EGFR (HER1) and its homologs HER2, HER3, and HER4 are frequently over-activated in cancer cells. VEGFR and FGFR, which are involved in tumor vasculature development, are also considered as promising targets for anti-cancer agents [313][314]. CDKs (cyclin-dependent serine/threonine protein kinases), also have essential roles in cell proliferation and have got considerable attention in the development of inhibitors inducing cell cycle arrest or promoting differentiation and apoptosis [315]. Other small molecule inhibitors targeting other kinases, such as tyrosine kinases Bcr-Abl, protein kinase PKC, PI3K, and MAPK family proteins, have also been extensively investigated [316][317]. A number of protein kinase inhibitors have been approved by the FDA or are in a late-stage of clinical development to treat different cancers. These include tyrosine kinase inhibitor imatinib (Gleevec®, Novartis) for the treatment of leukemia and gastrointestinal stromal tumors and EGFR inhibitors erlotinib (Tarceva®, Genentech) and gefitinib (Iressa™, AstraZeneca) for non-small cell lung carcinoma therapy [318].

All protein kinases have the ability to catalyze the transfer of the terminal phosphate of ATP to substrates that contain a serine, threonine or tyrosine residue and they all share a conserved catalytic domain with an ATP-binding site. Most protein kinase inhibitors now in clinical development are targeting the ATP-binding site [311][314]. Considering the high degree of conservation in this site, it is difficult to find highly selective ATP-binding site inhibitors with favorable pharmaceutical properties to specifically target tumor cells [319].

WNK1 is a serine/threonine kinase with a kinase domain similar to the one found in MEK family members of MAPK cascades. Sequence analysis of the WNK1

kinase domain showed 30% identity to MEKK-like kinases but did not clearly categorize this domain in any kinase subgroup. Moreover, the conserved catalytic lysine (K250) in subdomain II, present in other protein kinases, is substituted by a cysteine in all WNK proteins. A lysine residue (K 233) in subdomain I executes the catalytic function [189]. This particular kinase domain structure and low homology with other kinases may be a window for developing kinase inhibitors for WNKs with higher selectivity and affinity. However, a high degree of identity is observed between catalytic domains of the 4 WNK family members, hindering the development of selective WNK1 catalytic activity inhibitors. Conversely, homology outside their catalytic domains is low except for three short WNK homology regions [194], suggesting that protein-protein interactions implicating Thr60 phosphorylation status in the N-terminal domain of WNK1 may distinguish WNK1 from other kinases. Therefore, developing small molecules that affect the docking of scaffold molecules to the N-terminal of WNK1 seems to be a promising strategy for WNK1 targeting. For the moment, only one pan WNK-kinase non-competitive allosteric inhibitor was reported in 2016 [320]. Inhibitors targeting other WNK1 functions are still lacking.

### **3.5 Drug repositioning**

Drug repositioning, also referred to as redirecting or repurposing, is a process of finding new uses for existing drugs outside the scope of the original medical indication [321]. Potential drug repositioning opportunities include but are not limited to: effectiveness in a distinct pathology following serendipitous drug testing, novel activity/target identification highlighting a potential use for other diseases, unexpected side effects found during clinical trials or setup of drug screening platforms to identify repositioning candidates [322].

Drug repositioning is an efficient strategy for its safety, cost and effort-saving advantage compared to the development of a brand-new drug (Figure 21) since most approved drugs already have established formulations and manufacturing methods and clinical and pharmacokinetic data which can be used to speed approval [322].

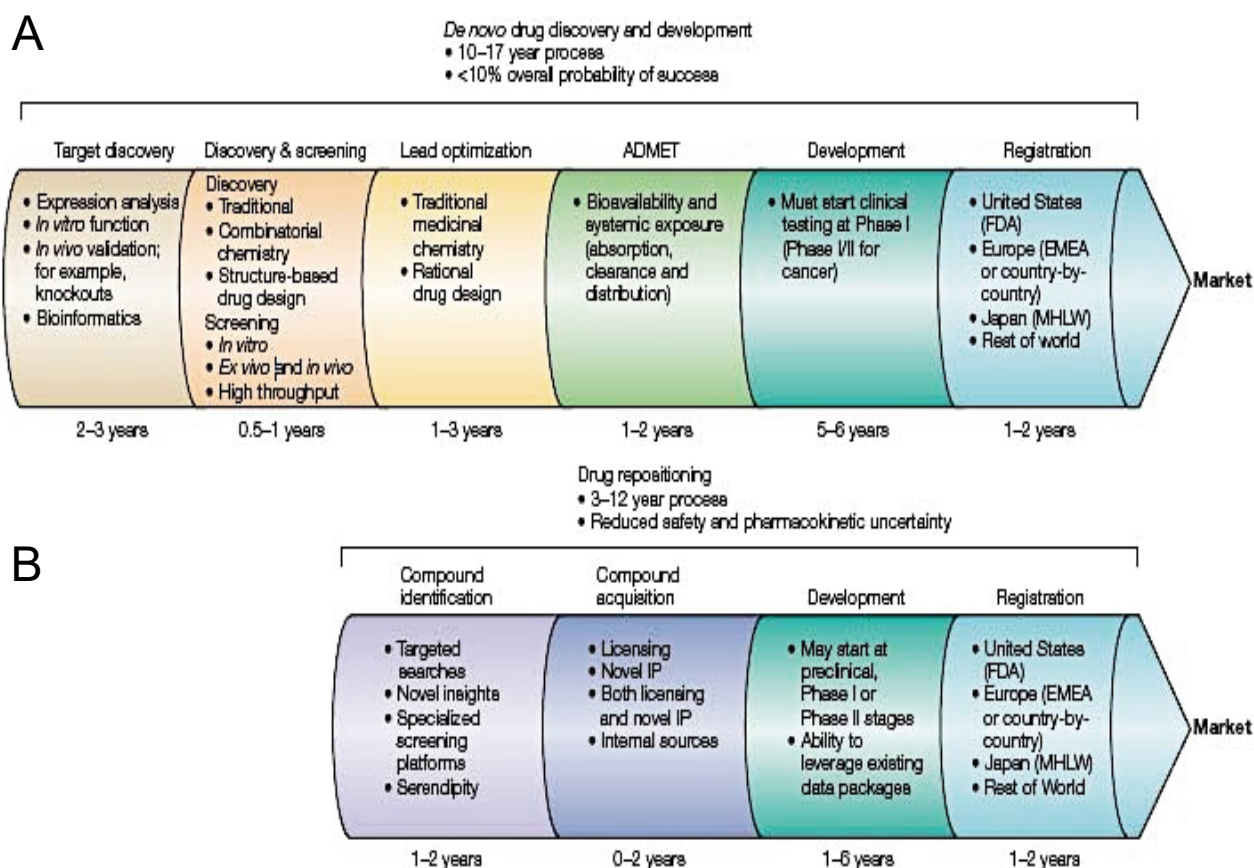


**Figure 21. Comparison of traditional *de novo* drug development versus drug repositioning, from [321].** **A.** Traditional *de novo* drug discovery and development pipeline takes 10 to 17 years to bring a new molecular entity to market, with a low probability of success. **B.** Drug repositioning reduced time, costs and risk through the drug development process due to previous research and development. ADMET, absorption, distribution, metabolism, excretion and toxicity; EMA, European Medicines Agency; FDA, Food and Drug Administration; IP, intellectual property; MHLW, Ministry of Health, Labour and Welfare.

Several drugs have been successfully repositioned to a new indication. The most prominent example is Celgene's Thalomid®, which is repositioned thalidomide, and its derivative Revlimid® (lenalidomide) [322]. Thalidomide was initially invented by Grünenthal and approved in 1957 in Germany and subsequently in other countries in Europe as an effective sedative and sleep-inducing agent. This compound was also found to be an effective anti-emetic drug during pregnancy. However, its use in this group of patients caused 500 to 12000 birth defects of newborns by the time it was withdrawn in 1961, reflecting the teratogenic effect of the drug that was unknown at the time of its approval due to limited animal studies. This error made thalidomide one of the most notorious failures in drug development

history [323]. Serendipitous experimental test for erythema nodosum leprosum (ENL), a painful inflammatory dermatological reaction of lepromatous leprosy, and the exclusion of pregnant women from the patient population, led to successful approval of thalidomide for ENL in 1998. Potential anti-cancer activity has been observed in hematological cancers and in various solid tumor cancers including mantle cell lymphoma, glioma, metastatic melanoma and pancreatic cancer [323][324][325]. The FDA approved thalidomide for multiple myeloma in 2003 and its current development in several indications is conducted by Celgene [323][326].

In conventional drug repositioning, a common first step is to screen libraries of already approved or off-patent drugs. Several companies provide small libraries consisting of 500-1000 compounds, including Enzi Life Sciences (Plymouth Meeting, PA, USA), Prestwick (Washington DC, USA) and Spectrum (Mircrosorce, Gaylordsville, CT, USA). The National Institute of Health's Chemical Genomics Center (NCGC) pharmaceutical collection has been also initiated in 2011 and contains over 2000 world-wide approved drugs in a screenable format [322]. Recycling the compounds that have failed clinical trials for lack of efficacy also represents a conventional model for repositioning. Another more effective model for drug repositioning consists in testing Phase I study approved compounds in several alternative indications to prioritize the most promising one thereby decreasing the risk for pharma companies [326].

Nevertheless, drug repositioning is still challenging for big pharma companies and this is reflected by the limited number of repositioning projects in recent years. First, drug repositioning remains expensive and risky and requires a lot of upfront investment. Second, patent protection of repositioned drugs can be particularly challenging. Concerning patent protection, intellectual property of the compound of interest may be held by another party or be off-patent (generic). In the former case, a deal is required to license or acquire intellectual property. For the latter case, the repositioner can rely on a novel method-of-use patent or simply a 'use' patent to protect new indications [321]. Even though the drug is patented for another indication, the generic version is marketed with only the off-patent indications on the label (skinny labeling). However, prescription of the generic version for the patented indication cannot be excluded [327]. Another limitation of drug repositioning resides in pricing of the drug for use in the new indication. With

the concept of differential pricing to support global equitable access to essential drugs, the principle is that prices should vary according to some measure of national wealth or affordability [328]. This differential pricing can be a limit to an increase of the cost of a generic off-patent drug to be used in another indication.

Bisacodyl repositioning as an anti-cancer drug is facing several of the limitations discussed in the previous section. For the treatment of glioblastoma, bisacodyl dosage and route of administration need to be modified. New studies are thus required to assess its toxicity and pharmacokinetic profile, thus precluding effective reduction of the risk, cost and time-to-market of the compound. Moreover, as GBM is a complex and heterogeneous disease, the high risk of lack of efficacy in later stages of development, due to disease complexity and heterogeneity, may give rise to great concerns for developers. Furthermore, bisacodyl is still on market for its indication as a stimulant laxative. Even if its new indication can create substantial value for patients, the off-patent indication may impede the commercialization of the repositioned drug. In addition, the differential pricing policy for alternative indications could hinder its repositioning. Pharma companies are not keen to reposition drugs from a low-price indication, such as stimulant laxative, to a more expensive one, such as oncology, despite the potential medical value for patients [326]. The low target price in some countries might be below the marginal cost of production. If this cannot be compensated by charging high prices in wealthy countries, no profit can be obtained for the developer. Besides, the market volumes for glioblastoma are small and may not be enough to reward developing costs. Thus, pharmaceutical companies may prefer to invest for developing drugs to treat common disorders or disorders preferentially found in high income countries [328][329].

Nevertheless, even if bisacodyl repositioning is not achieved, studies based on this compound highlighted new potentially interesting players contributing to GSC physiopathology including the WNK1 protein kinase and its signaling partners Akt, SGK1 and NBC  $\text{Na}^+/\text{HCO}_3^-$  co-transporters. Further exploration of signaling mechanisms and identification of additional cell partners of these proteins may lead to the identification of new therapeutic targets that may be exploited in the future for the development of new therapeutic strategies against GBM.

## List of references

1. Ostrom QT, Gittleman H, Fulop J, Liu M, Blanda R, Kromer C, et al. CBTRUS Statistical Report: Primary Brain and Central Nervous System Tumors Diagnosed in the United States in 2008-2012. *Neuro-Oncol.* 2015;17: iv1-iv62. doi:10.1093/neuonc/nov189
2. Louis DN, Perry A, Reifenberger G, Deimling A von, Figarella-Branger D, Cavenee WK, et al. The 2016 World Health Organization Classification of Tumors of the Central Nervous System: a summary. *Acta Neuropathol (Berl).* 2016;131: 803–820. doi:10.1007/s00401-016-1545-1
3. Jäkel S, Dimou L. Glial Cells and Their Function in the Adult Brain: A Journey through the History of Their Ablation. *Front Cell Neurosci.* 2017;11. doi:10.3389/fncel.2017.00024
4. Vigneswaran K, Neill S, Hadjipanayis CG. Beyond the World Health Organization grading of infiltrating gliomas: advances in the molecular genetics of glioma classification. *Ann Transl Med.* 2015;3. doi:10.21037/6335
5. Thakkar JP, Dolecek TA, Horbinski C, Ostrom QT, Lightner DD, Barnholtz-Sloan JS, et al. Epidemiologic and Molecular Prognostic Review of Glioblastoma. *Cancer Epidemiol Prev Biomark.* 2014;23: 1985–1996. doi:10.1158/1055-9965.EPI-14-0275
6. Jiang H, Cui Y, Wang J, Lin S, Jiang H, Cui Y, et al. Impact of epidemiological characteristics of supratentorial gliomas in adults brought about by the 2016 world health organization classification of tumors of the central nervous system. *Oncotarget.* 2016;5. doi:10.18632/oncotarget.13555
7. Adamson C, Kanu OO, Mehta AI, Di C, Lin N, Mattox AK, et al. Glioblastoma multiforme: a review of where we have been and where we are going. *Expert Opin Investig Drugs.* 2009;18: 1061–1083. doi:10.1517/13543780903052764
8. Parsons DW, Jones S, Zhang X, Lin JC-H, Leary RJ, Angenendt P, et al. An Integrated Genomic Analysis of Human Glioblastoma Multiforme. *Science.* 2008;321: 1807–1812. doi:10.1126/science.1164382
9. Ohgaki H, Kleihues P. The Definition of Primary and Secondary Glioblastoma. *Clin Cancer Res.* 2013;19: 764–772. doi:10.1158/1078-0432.CCR-12-3002
10. Hochberg F, Toniolo P, Cole P. Nonoccupational risk indicators of glioblastoma in adults. *J Neurooncol.* 1990;8: 55–60. doi:10.1007/BF00182087
11. Hemminki K, Li X. Familial Risks in Nervous System Tumors. *Cancer*

Epidemiol Prev Biomark. 2003;12: 1137–1142.

12. Weller M, Cloughesy T, Perry JR, Wick W. Standards of care for treatment of recurrent glioblastoma—are we there yet? *Neuro-Oncol*. 2012; nos273. doi:10.1093/neuonc/nos273

13. Reitman ZJ, Yan H. Isocitrate Dehydrogenase 1 and 2 Mutations in Cancer: Alterations at a Crossroads of Cellular Metabolism. *JNCI J Natl Cancer Inst*. 2010;102: 932–941. doi:10.1093/jnci/djq187

14. Kalkan R, Atli Eİ, Özdemir M, Çiftçi E, Aydın HE, Artan S, et al. IDH1 mutations is prognostic marker for primary glioblastoma multiforme but MGMT hypermethylation is not prognostic for primary glioblastoma multiforme. *Gene*. 2015;554: 81–86. doi:10.1016/j.gene.2014.10.027

15. Cohen A, Holmen S, Colman H. IDH1 and IDH2 Mutations in Gliomas. *Curr Neurol Neurosci Rep*. 2013;13: 345. doi:10.1007/s11910-013-0345-4

16. Nobusawa S, Watanabe T, Kleihues P, Ohgaki H. IDH1 Mutations as Molecular Signature and Predictive Factor of Secondary Glioblastomas. *Clin Cancer Res*. 2009;15: 6002–6007. doi:10.1158/1078-0432.CCR-09-0715

17. Toyota M, Ahuja N, Ohe-Toyota M, Herman JG, Baylin SB, Issa JP. CpG island methylator phenotype in colorectal cancer. *Proc Natl Acad Sci U S A*. 1999;96: 8681–8686.

18. Noshmehr H, Weisenberger DJ, Diefes K, Phillips HS, Pujara K, Berman BP, et al. Identification of a CpG Island Methylator Phenotype that Defines a Distinct Subgroup of Glioma. *Cancer Cell*. 2010;17: 510–522. doi:10.1016/j.ccr.2010.03.017

19. Nakamura M, Yonekawa Y, Kleihues P, Ohgaki H. Promoter hypermethylation of the RB1 gene in glioblastomas. *Lab Investig J Tech Methods Pathol*. 2001;81: 77–82.

20. Suzuki H, Yamamoto E, Maruyama R, Niinuma T, Kai M. Biological significance of the CpG island methylator phenotype. *Biochem Biophys Res Commun*. 2014;455: 35–42. doi:10.1016/j.bbrc.2014.07.007

21. Hegi ME, Diserens A-C, Gorlia T, Hamou M-F, de Tribolet N, Weller M, et al. MGMT Gene Silencing and Benefit from Temozolomide in Glioblastoma. *N Engl J Med*. 2005;352: 997–1003. doi:10.1056/NEJMoa043331

22. Erasimus H, Gobin M, Niclou S, Van Dyck E. DNA repair mechanisms and their clinical impact in glioblastoma. *Mutat Res Mutat Res*. 2016;769: 19–35. doi:10.1016/j.mrrev.2016.05.005

23. Köstler WJ, Yarden Y. Chapter 61 - The Epidermal Growth Factor Receptor

Family A2 - Bradshaw, Ralph A. In: Dennis EA, editor. Handbook of Cell Signaling (Second Edition). San Diego: Academic Press; 2010. pp. 435–441. Available: <http://www.sciencedirect.com/science/article/pii/B9780123741455000619>

24. Furnari FB, Cloughesy TF, Cavenee WK, Mischel PS. Heterogeneity of epidermal growth factor receptor signalling networks in glioblastoma. *Nat Rev Cancer*. 2015;15: 302–310. doi:10.1038/nrc3918
25. Zadeh G, Bhat KPL, Aldape K. EGFR and EGFRvIII in Glioblastoma: Partners in Crime. *Cancer Cell*. 2013;24: 403–404. doi:10.1016/j.ccr.2013.09.017
26. Gan HK, Kaye AH, Luwor RB. The EGFRvIII variant in glioblastoma multiforme. *J Clin Neurosci*. 2009;16: 748–754. doi:10.1016/j.jocn.2008.12.005
27. Fan Q-W, Cheng CK, Gustafson WC, Charron E, Zipper P, Wong RA, et al. EGFR Phosphorylates Tumor-Derived EGFRvIII Driving STAT3/5 and Progression in Glioblastoma. *Cancer Cell*. 2013;24: 438–449. doi:10.1016/j.ccr.2013.09.004
28. Inda M-M, Bonavia R, Mukasa A, Narita Y, Sah DWY, Vandenberg S, et al. Tumor heterogeneity is an active process maintained by a mutant EGFR-induced cytokine circuit in glioblastoma. *Genes Dev*. 2010;24: 1731–1745. doi:10.1101/gad.1890510
29. England B, Huang T, Karsy M. Current understanding of the role and targeting of tumor suppressor p53 in glioblastoma multiforme. *Tumour Biol J Int Soc Oncodevelopmental Biol Med*. 2013;34: 2063–2074. doi:10.1007/s13277-013-0871-3
30. Clynes D, Gibbons RJ. ATRX and the replication of structured DNA. *Curr Opin Genet Dev*. 2013;23: 289–294. doi:10.1016/j.gde.2013.01.005
31. Liu X-Y, Gerges N, Korshunov A, Sabha N, Khuong-Quang D-A, Fontebasso AM, et al. Frequent ATRX mutations and loss of expression in adult diffuse astrocytic tumors carrying IDH1/IDH2 and TP53 mutations. *Acta Neuropathol (Berl)*. 2012;124: 615–625. doi:10.1007/s00401-012-1031-3
32. Ceccarelli M, Barthel FP, Malta TM, Sabedot TS, Salama SR, Murray BA, et al. Molecular Profiling Reveals Biologically Discrete Subsets and Pathways of Progression in Diffuse Glioma. *Cell*. 2016;164: 550–563. doi:10.1016/j.cell.2015.12.028
33. Ramlee MK, Wang J, Toh WX, Li S. Transcription Regulation of the Human Telomerase Reverse Transcriptase (hTERT) Gene. *Genes*. 2016;7. doi:10.3390/genes7080050
34. Nonoguchi N, Ohta T, Oh J-E, Kim Y-H, Kleihues P, Ohgaki H. TERT promoter mutations in primary and secondary glioblastomas. *Acta Neuropathol (Berl)*. 2013;126: 931–937. doi:10.1007/s00401-013-1163-0



35. Mosrati MA, Malmström A, Lysiak M, Krysztofiak A, Hallbeck M, Milos P, et al. TERT promoter mutations and polymorphisms as prognostic factors in primary glioblastoma. *Oncotarget*. 2015;6: 16663–16673.
36. Gao K, Li G, Qu Y, Wang M, Cui B, Ji M, et al. TERT promoter mutations and long telomere length predict poor survival and radiotherapy resistance in gliomas. *Oncotarget*. 2015;7: 8712–8725. doi:10.18632/oncotarget.6007
37. Killela PJ, Reitman ZJ, Jiao Y, Bettegowda C, Agrawal N, Diaz LA, et al. TERT promoter mutations occur frequently in gliomas and a subset of tumors derived from cells with low rates of self-renewal. *Proc Natl Acad Sci U S A*. 2013;110: 6021–6026. doi:10.1073/pnas.1303607110
38. Brennan CW, Verhaak RGW, McKenna A, Campos B, Nounshmehr H, Salama SR, et al. The Somatic Genomic Landscape of Glioblastoma. *Cell*. 2013;155: 462–477. doi:10.1016/j.cell.2013.09.034
39. Clark KH, Villano JL, Nikiforova MN, Hamilton RL, Horbinski C. 1p/19q testing has no significance in the workup of glioblastomas. *Neuropathol Appl Neurobiol*. 2013;39: 706–717. doi:10.1111/nan.12031
40. Verhaak RGW, Hoadley KA, Purdom E, Wang V, Qi Y, Wilkerson MD, et al. Integrated Genomic Analysis Identifies Clinically Relevant Subtypes of Glioblastoma Characterized by Abnormalities in PDGFRA, IDH1, EGFR, and NF1. *Cancer Cell*. 2010;17: 98–110. doi:10.1016/j.ccr.2009.12.020
41. Turcan S, Rohle D, Goenka A, Walsh LA, Fang F, Yilmaz E, et al. IDH1 mutation is sufficient to establish the glioma hypermethylator phenotype. *Nature*. 2012;483: 479–483. doi:10.1038/nature10866
42. Comprehensive genomic characterization defines human glioblastoma genes and core pathways. *Nature*. 2008;455: 1061–1068. doi:10.1038/nature07385
43. Mao H, LeBrun DG, Yang J, Zhu VF, Li M. Deregulated Signaling Pathways in Glioblastoma Multiforme: Molecular Mechanisms and Therapeutic Targets. *Cancer Invest*. 2012;30: 48–56. doi:10.3109/07357907.2011.630050
44. Nakada M, Kita D, Watanabe T, Hayashi Y, Teng L, Pyko IV, et al. Aberrant Signaling Pathways in Glioma. *Cancers*. 2011;3: 3242–3278. doi:10.3390/cancers3033242
45. Nogueira L, Ruiz-Ontañón P, Vazquez-Barquero A, Moris F, Fernandez-Luna JL, Nogueira L, et al. The NFκB pathway: a therapeutic target in glioblastoma. *Oncotarget*. 2011;2: 646–653. doi:10.18632/oncotarget.322
46. Park S, Hatanpaa KJ, Xie Y, Mickey BE, Madden CJ, Raisanen JM, et al. The Receptor Interacting Protein 1 Inhibits p53 Induction through NF-κB Activation

and Confers a Worse Prognosis in Glioblastoma. *Cancer Res.* 2009;69: 2809–2816. doi:10.1158/0008-5472.CAN-08-4079

47. Bhat KPL, Balasubramaniyan V, Vaillant B, Ezhilarasan R, Hummelink K, Hollingsworth F, et al. Mesenchymal Differentiation Mediated by NF- $\kappa$ B Promotes Radiation Resistance in Glioblastoma. *Cancer Cell.* 2013;24: 331–346.

doi:10.1016/j.ccr.2013.08.001

48. Ping Y-F, Zhang X, Bian X-W. Cancer stem cells and their vascular niche: Do they benefit from each other? *Cancer Lett.* 2016;380: 561–567.

doi:10.1016/j.canlet.2015.05.010

49. Tanaka S, Louis DN, Curry WT, Batchelor TT, Dietrich J. Diagnostic and therapeutic avenues for glioblastoma: no longer a dead end? *Nat Rev Clin Oncol.* 2013;10: 14–26. doi:10.1038/nrclinonc.2012.204

50. Siegel RL, Miller KD, Jemal A. Cancer Statistics, 2017. *CA Cancer J Clin.* 2017;67: 7–30. doi:10.3322/caac.21387

51. Balkwill F, Mantovani A. Inflammation and cancer: back to Virchow? *The Lancet.* 2001;357: 539–545. doi:10.1016/S0140-6736(00)04046-0

52. Ting Wu, Yun Dai. Tumor microenvironment and therapeutic response. *Cancer Lett.* 2016;

53. Carmeliet P, Jain RK. Molecular mechanisms and clinical applications of angiogenesis. *Nature.* 2011;473: 298–307. doi:10.1038/nature10144

54. Hanahan D, Coussens LM. Accessories to the Crime: Functions of Cells Recruited to the Tumor Microenvironment. *Cancer Cell.* 2012;21: 309–322.

doi:10.1016/j.ccr.2012.02.022

55. Räsänen K, Vaheri A. Activation of fibroblasts in cancer stroma. *Exp Cell Res.* 2010;316: 2713–2722. doi:10.1016/j.yexcr.2010.04.032

56. Nieman KM, Kenny HA, Penicka CV, Ladanyi A, Buell-Gutbrod R, Zillhardt MR, et al. Adipocytes promote ovarian cancer metastasis and provide energy for rapid tumor growth. *Nat Med.* 2011;17: 1498–1503. doi:10.1038/nm.2492

57. Quail DF, Joyce JA. Microenvironmental regulation of tumor progression and metastasis. *Nat Med.* 2013;19: 1423–1437. doi:10.1038/nm.3394

58. Hui L, Chen Y. Tumor microenvironment: Sanctuary of the devil. *Cancer Lett.* 2015;368: 7–13. doi:10.1016/j.canlet.2015.07.039

59. Coniglio SJ, Eugenin E, Dobrenis K, Stanley ER, West BL, Symons MH, et al. Microglial Stimulation of Glioblastoma Invasion Involves Epidermal Growth Factor Receptor (EGFR) and Colony Stimulating Factor 1 Receptor (CSF-1R) Signaling. *Mol Med.* 2012;18: 519–527. doi:10.2119/molmed.2011.00217

60. Joyce JA, Pollard JW. Microenvironmental regulation of metastasis. *Nat Rev Cancer*. 2009;9: 239–252. doi:10.1038/nrc2618
61. Gabrusiewicz K, Liu D, Cortes-Santiago N, Hossain MB, Conrad CA, Aldape KD, et al. Anti-vascular endothelial growth factor therapy-induced glioma invasion is associated with accumulation of Tie2-expressing monocytes. *Oncotarget*. 2014;5: 2208–2220.
62. Özbek S, Balasubramanian PG, Chiquet-Ehrismann R, Tucker RP, Adams JC. The Evolution of Extracellular Matrix. *Mol Biol Cell*. 2010;21: 4300–4305. doi:10.1091/mbc.E10-03-0251
63. Naba A, Clauser KR, Hoersch S, Liu H, Carr SA, Hynes RO. The Matrisome: In Silico Definition and In Vivo Characterization by Proteomics of Normal and Tumor Extracellular Matrices. *Mol Cell Proteomics*. 2012;11: M111.014647. doi:10.1074/mcp.M111.014647
64. Popescu AM, Purcaru SO, Alexandru O, Dricu A. New perspectives in glioblastoma antiangiogenic therapy. *Contemp Oncol*. 2016;20: 109–118. doi:10.5114/wo.2015.56122
65. Fidoamore A, Cristiano L, Antonosante A, d&#x2019;Angelo M, Di Giacomo E, et al. Glioblastoma Stem Cells Microenvironment: The Paracrine Roles of the Niche in Drug and Radioresistance. *Stem Cells Int*. 2016;2016: e6809105. doi:10.1155/2016/6809105
66. Spence AM, Muzi M, Swanson KR, O'Sullivan F, Rockhill JK, Rajendran JG, et al. Regional Hypoxia in Glioblastoma Multiforme Quantified with [18F]Fluoromisonidazole Positron Emission Tomography before Radiotherapy: Correlation with Time to Progression and Survival. *Clin Cancer Res*. 2008;14: 2623–2630. doi:10.1158/1078-0432.CCR-07-4995
67. Seimiya H, Tanji M, Oh-hara T, Tomida A, Naasani I, Tsuruo T. Hypoxia Up-Regulates Telomerase Activity via Mitogen-Activated Protein Kinase Signaling in Human Solid Tumor Cells. *Biochem Biophys Res Commun*. 1999;260: 365–370. doi:10.1006/bbrc.1999.0910
68. Harris AL. Hypoxia — a key regulatory factor in tumour growth. *Nat Rev Cancer*. 2002;2: 38–47. doi:10.1038/nrc704
69. Zhao S, Lin Y, Xu W, Jiang W, Zha Z, Wang P, et al. Glioma-Derived Mutations in IDH1 Dominantly Inhibit IDH1 Catalytic Activity and Induce HIF-1 $\alpha$ . *Science*. 2009;324: 261–265. doi:10.1126/science.1170944
70. Warburg O. On the Origin of Cancer Cells. *Science*. 1956;123: 309–314. doi:10.1126/science.123.3191.309
71. Neri D, Supuran CT. Interfering with pH regulation in tumours as a

- therapeutic strategy. *Nat Rev Drug Discov*. 2011;10: 767–777. doi:10.1038/nrd3554
72. Chiche J, Brahimi-Horn MC, Pouysségur J. Tumour hypoxia induces a metabolic shift causing acidosis: a common feature in cancer. *J Cell Mol Med*. 2010;14: 771–794. doi:10.1111/j.1582-4934.2009.00994.x
73. Nigim F, Cavanaugh J, Patel AP, Curry WT, Esaki S, Kasper EM, et al. Targeting Hypoxia-Inducible Factor 1 $\alpha$  in a New Orthotopic Model of Glioblastoma Recapitulating the Hypoxic Tumor Microenvironment. *J Neuropathol Exp Neurol*. 2015;74: 710–722. doi:10.1097/NEN.0000000000000210
74. Stupp R, Hegi ME, Mason WP, van den Bent MJ, Taphoorn MJ, Janzer RC, et al. Effects of radiotherapy with concomitant and adjuvant temozolomide versus radiotherapy alone on survival in glioblastoma in a randomised phase III study: 5-year analysis of the EORTC-NCIC trial. *Lancet Oncol*. 2009;10: 459–466. doi:10.1016/S1470-2045(09)70025-7
75. Stupp R, Mason WP, van den Bent MJ, Weller M, Fisher B, Taphoorn MJB, et al. Radiotherapy plus Concomitant and Adjuvant Temozolomide for Glioblastoma. *N Engl J Med*. 2005;352: 987–996. doi:10.1056/NEJMoa043330
76. Mrugala MM. Advances and Challenges in the Treatment of Glioblastoma: A Clinician's Perspective. *Discov Med*. 2013;15: 221–230.
77. Mrugala MM. Advances and Challenges in the Treatment of Glioblastoma: A Clinician's Perspective. *Discov Med*. 2013;15: 221–230.
78. Vredenburgh JJ, Desjardins A, Herndon JE, Marcello J, Reardon DA, Quinn JA, et al. Bevacizumab Plus Irinotecan in Recurrent Glioblastoma Multiforme. *J Clin Oncol*. 2007;25: 4722–4729. doi:10.1200/JCO.2007.12.2440
79. Hainsworth JD, Ervin T, Friedman E, Priego V, Murphy PB, Clark BL, et al. Concurrent radiotherapy and temozolomide followed by temozolomide and sorafenib in the first-line treatment of patients with glioblastoma multiforme. *Cancer*. 2010;116: 3663–3669. doi:10.1002/cncr.25275
80. Chinot OL, Wick W, Mason W, Henriksson R, Saran F, Nishikawa R, et al. Bevacizumab plus radiotherapy-temozolomide for newly diagnosed glioblastoma. *N Engl J Med*. 2014;370: 709–722. doi:10.1056/NEJMoa1308345
81. Kovic B, Xie F. Economic Evaluation of Bevacizumab for the First-Line Treatment of Newly Diagnosed Glioblastoma Multiforme. *J Clin Oncol Off J Am Soc Clin Oncol*. 2015;33: 2296–2302. doi:10.1200/JCO.2014.59.7245
82. Nabors LB, Mikkelsen T, Hegi ME, Ye X, Batchelor T, Lesser G, et al. A safety run-in and randomized phase 2 study of cilengitide combined with chemoradiation for newly diagnosed glioblastoma (NABTT 0306). *Cancer*.

2012;118: 5601–5607. doi:10.1002/cncr.27585

83. Patel M, Siddiqui F, Jin J-Y, Mikkelsen T, Rosenblum M, Movsas B, et al. Salvage reirradiation for recurrent glioblastoma with radiosurgery: radiographic response and improved survival. *J Neurooncol.* 2009;92: 185. doi:10.1007/s11060-008-9752-9

84. Barbarite E, Sick JT, Berchmans E, Bregy A, Shah AH, Elsayyad N, et al. The role of brachytherapy in the treatment of glioblastoma multiforme. *Neurosurg Rev.* 2016; 1–17. doi:10.1007/s10143-016-0727-6

85. Gzell C, Back M, Wheeler H, Bailey D, Foote M. Radiotherapy in Glioblastoma: the Past, the Present and the Future. *Clin Oncol.* 2017;29: 15–25. doi:10.1016/j.clon.2016.09.015

86. Cho KH, Hall WA, Gerbi BJ, Higgins PD, McGuire WA, Clark HB. Single dose versus fractionated stereotactic radiotherapy for recurrent high-grade gliomas. *Int J Radiat Oncol.* 1999;45: 1133–1141. doi:10.1016/S0360-3016(99)00336-3

87. Vordermark D, Kölbl O, Ruprecht K, Vince GH, Bratengeier K, Flentje M. Hypofractionated stereotactic re-irradiation: treatment option in recurrent malignant glioma. *BMC Cancer.* 2005;5: 55. doi:10.1186/1471-2407-5-55

88. Weller M, Cloughesy T, Perry JR, Wick W. Standards of care for treatment of recurrent glioblastoma—are we there yet? *Neuro-Oncol.* 2012; nos273. doi:10.1093/neuonc/nos273

89. Kamran N, Calinescu A, Candolfi M, Chandran M, Mineharu Y, Asad AS, et al. Recent advances and future of immunotherapy for glioblastoma. *Expert Opin Biol Ther.* 2016;16: 1245–1264. doi:10.1080/14712598.2016.1212012

90. Zhou Q, Wang Y, Ma W. The progress of immunotherapy for glioblastoma. *Hum Vaccines Immunother.* 2015;11: 2654–2658. doi:10.1080/21645515.2015.1081727

91. Polivka J, Polivka J, Holubec L, Kubikova T, Priban V, Hes O, et al. Advances in Experimental Targeted Therapy and Immunotherapy for Patients with Glioblastoma Multiforme. *Anticancer Res.* 2017;37: 21–33.

92. Thomas AA, Ernstoff MS, Fadul CE. Immunotherapy for the Treatment of Glioblastoma. *Cancer J Sudbury Mass.* 2012;18: 59–68. doi:10.1097/PPO.0b013e3182431a73

93. Bloch O, Crane CA, Fuks Y, Kaur R, Aghi MK, Berger MS, et al. Heat-shock protein peptide complex–96 vaccination for recurrent glioblastoma: a phase II, single-arm trial. *Neuro-Oncol.* 2014;16: 274–279. doi:10.1093/neuonc/not203

94. Carter T, Shaw H, Cohn-Brown D, Chester K, Mulholland P. Ipilimumab and Bevacizumab in Glioblastoma. *Clin Oncol*. 2016;28: 622–626. doi:10.1016/j.clon.2016.04.042
95. Preusser M, Lim M, Hafler DA, Reardon DA, Sampson JH. Prospects of immune checkpoint modulators in the treatment of glioblastoma. *Nat Rev Neurol*. 2015;11: 504–514. doi:10.1038/nrneurol.2015.139
96. Szabo AT, Carpentier AF. Immunotherapy in human glioblastoma. *Rev Neurol (Paris)*. 2011;167: 668–672. doi:10.1016/j.neurol.2011.07.002
97. Stupp R, Taillibert S, Kanner AA, Kesari S, Steinberg DM, Toms SA, et al. Maintenance Therapy With Tumor-Treating Fields Plus Temozolomide vs Temozolomide Alone for Glioblastoma: A Randomized Clinical Trial. *JAMA*. 2015;314: 2535–2543. doi:10.1001/jama.2015.16669
98. Rich JN, Reardon DA, Peery T, Dowell JM, Quinn JA, Penne KL, et al. Phase II Trial of Gefitinib in Recurrent Glioblastoma. *J Clin Oncol*. 2004;22: 133–142. doi:10.1200/JCO.2004.08.110
99. Sathornsumetee S, Reardon DA, Desjardins A, Quinn JA, Vredenburgh JJ, Rich JN. Molecularly targeted therapy for malignant glioma. *Cancer*. 2007;110: 13–24. doi:10.1002/cncr.22741
100. Cloughesy TF, Wen PY, Robins HI, Chang SM, Groves MD, Fink KL, et al. Phase II Trial of Tipifarnib in Patients With Recurrent Malignant Glioma Either Receiving or Not Receiving Enzyme-Inducing Antiepileptic Drugs: A North American Brain Tumor Consortium Study. *J Clin Oncol*. 2006;24: 3651–3656. doi:10.1200/JCO.2006.06.2323
101. Yust-Katz S, Liu D, Yuan Y, Liu V, Kang S, Groves M, et al. Phase 1/1b Study of Lonafarnib and Temozolomide in Patients With Recurrent or Temozolomide Refractory Glioblastoma. *Cancer*. 2013;119: 2747–2753. doi:10.1002/cncr.28031
102. Galanis E, Buckner JC, Maurer MJ, Kreisberg JL, Ballman K, Boni J, et al. Phase II trial of temsirolimus (CCI-779) in recurrent glioblastoma multiforme: a North Central Cancer Treatment Group Study. *J Clin Oncol Off J Am Soc Clin Oncol*. 2005;23: 5294–5304. doi:10.1200/JCO.2005.23.622
103. Kreisl TN, Kotliarova S, Butman JA, Albert PS, Kim L, Musib L, et al. A phase I/II trial of enzastaurin in patients with recurrent high-grade gliomas. *Neuro-Oncol*. 2010;12: 181–189. doi:10.1093/neuonc/nop042
104. Bai R-Y, Staedtke V, Riggins GJ. Molecular targeting of glioblastoma: Drug discovery and therapies. *Trends Mol Med*. 2011;17: 301–312. doi:10.1016/j.molmed.2011.01.011

105. Caspani EM, Crossley PH, Redondo-Garcia C, Martinez S. Glioblastoma: A Pathogenic Crosstalk between Tumor Cells and Pericytes. *PLoS ONE*. 2014;9. doi:10.1371/journal.pone.0101402
106. Lu-Emerson C, Duda DG, Emblem KE, Taylor JW, Gerstner ER, Loeffler JS, et al. Lessons From Anti-Vascular Endothelial Growth Factor and Anti-Vascular Endothelial Growth Factor Receptor Trials in Patients With Glioblastoma. *J Clin Oncol*. 2015;33: 1197–1213. doi:10.1200/JCO.2014.55.9575
107. Gerstner ER, Chen P-J, Wen PY, Jain RK, Batchelor TT, Sorensen G. Infiltrative patterns of glioblastoma spread detected via diffusion MRI after treatment with cediranib. *Neuro-Oncol*. 2010;12: 466–472. doi:10.1093/neuonc/nop051
108. Kalpathy-Cramer J, Chandra V, Da X, Ou Y, Emblem KE, Muzikansky A, et al. Phase II study of tivozanib, an oral VEGFR inhibitor, in patients with recurrent glioblastoma. *J Neurooncol*. 2016; doi:10.1007/s11060-016-2332-5
109. Kreso A, Dick JE. Evolution of the Cancer Stem Cell Model. *Cell Stem Cell*. 2014;14: 275–291. doi:10.1016/j.stem.2014.02.006
110. Galli R, Binda E, Orfanelli U, Cipelletti B, Gritti A, Vitis SD, et al. Isolation and Characterization of Tumorigenic, Stem-like Neural Precursors from Human Glioblastoma. *Cancer Res*. 2004;64: 7011–7021. doi:10.1158/0008-5472.CAN-04-1364
111. Shackleton M, Quintana E, Fearon ER, Morrison SJ. Heterogeneity in Cancer: Cancer Stem Cells versus Clonal Evolution. *Cell*. 2009;138: 822–829. doi:10.1016/j.cell.2009.08.017
112. O'Connor ML, Xiang D, Shigdar S, Macdonald J, Li Y, Wang T, et al. Cancer stem cells: A contentious hypothesis now moving forward. *Cancer Lett*. 2014;344: 180–187. doi:10.1016/j.canlet.2013.11.012
113. Clarke MF, Dick JE, Dirks PB, Eaves CJ, Jamieson CHM, Jones DL, et al. Cancer Stem Cells—Perspectives on Current Status and Future Directions: AACR Workshop on Cancer Stem Cells. *Cancer Res*. 2006;66: 9339–9344. doi:10.1158/0008-5472.CAN-06-3126
114. Bonnet D, Dick JE. Human acute myeloid leukemia is organized as a hierarchy that originates from a primitive hematopoietic cell. *Nat Med*. 1997;3: 730–737. doi:10.1038/nm0797-730
115. Singh SK, Clarke ID, Terasaki M, Bonn VE, Hawkins C, Squire J, et al. Identification of a Cancer Stem Cell in Human Brain Tumors. *Cancer Res*. 2003;63: 5821–5828.
116. Singh SK, Hawkins C, Clarke ID, Squire JA, Bayani J, Hide T, et al.

- Identification of human brain tumour initiating cells. *Nature*. 2004;432: 396–401. doi:10.1038/nature03128
117. Yuan X, Curtin J, Xiong Y, Liu G, Waschmann-Hogiu S, Farkas DL, et al. Isolation of cancer stem cells from adult glioblastoma multiforme. *Oncogene*. 2004;23: 9392–9400. doi:10.1038/sj.onc.1208311
118. Hemmati HD, Nakano I, Lazareff JA, Masterman-Smith M, Geschwind DH, Bronner-Fraser M, et al. Cancerous stem cells can arise from pediatric brain tumors. *Proc Natl Acad Sci*. 2003;100: 15178–15183. doi:10.1073/pnas.2036535100
119. Patru C, Romao L, Varlet P, Coulombel L, Raponi E, Cadusseau J, et al. CD133, CD15/SSEA-1, CD34 or side populations do not resume tumor-initiating properties of long-term cultured cancer stem cells from human malignant glioblastoma. *BMC Cancer*. 2010;10: 66. doi:10.1186/1471-2407-10-66
120. Anxin Wang, Lisha Chen, Chunlin Li, Yimin Zhu. Heterogeneity in cancer stem cells. *Cancer Lett*. 2014;
121. Visvader JE, Lindeman GJ. Cancer Stem Cells: Current Status and Evolving Complexities. *Cell Stem Cell*. 2012;10: 717–728. doi:10.1016/j.stem.2012.05.007
122. Visvader JE, Lindeman GJ. Cancer stem cells in solid tumours: accumulating evidence and unresolved questions. *Nat Rev Cancer*. 2008;8: 755–768. doi:10.1038/nrc2499
123. Liu H, Lv L, Yang K. Chemotherapy targeting cancer stem cells. *Am J Cancer Res*. 2015;5: 880–893.
124. Hadjimichael C, Chanoumidou K, Papadopoulou N, Arampatzi P, Papamatheakis J, Kretsovali A. Common stemness regulators of embryonic and cancer stem cells. *World J Stem Cells*. 2015;7: 1150–1184. doi:10.4252/wjsc.v7.i9.1150
125. Liu A, Yu X, Liu S. Pluripotency transcription factors and cancer stem cells: small genes make a big difference. *Chin J Cancer*. 2013;32: 483–487. doi:10.5732/cjc.012.10282
126. Molina ES, Pillat MM, Moura-Neto V, Lah TT, Ulrich H. Glioblastoma stem-like cells: approaches for isolation and characterization. *J Cancer Stem Cell Res*. 2014;1: 1. doi:10.14343/JCSCR.2014.2e1007
127. Kalkan R. Glioblastoma Stem Cells as a New Therapeutic Target for Glioblastoma. *Clin Med Insights Oncol*. 2015;9: 95–103. doi:10.4137/CMO.S30271
128. Son MJ, Woolard K, Nam D-H, Lee J, Fine HA. SSEA-1 Is an Enrichment



- Marker for Tumor-Initiating Cells in Human Glioblastoma. *Cell Stem Cell*. 2009;4: 440–452. doi:10.1016/j.stem.2009.03.003
129. Ogden AT, Waziri AE, Lochhead RA, Fusco D, Lopez K, Ellis JA, et al. Identification of A2B5+CD133- tumor-initiating cells in adult human gliomas. *Neurosurgery*. 2008;62: 505-514-515. doi:10.1227/01.neu.0000316019.28421.95
130. Lathia JD, Gallagher J, Heddleston JM, Wang J, Eyler CE, MacSwords J, et al. Integrin Alpha 6 Regulates Glioblastoma Stem Cells. *Cell Stem Cell*. 2010;6: 421–432. doi:10.1016/j.stem.2010.02.018
131. Wang A, Qu L, Wang L. At the crossroads of cancer stem cells and targeted therapy resistance. *Cancer Lett*. 2017;385: 87–96. doi:10.1016/j.canlet.2016.10.039
132. Beier D, Hau P, Proescholdt M, Lohmeier A, Wischhusen J, Oefner PJ, et al. CD133+ and CD133- Glioblastoma-Derived Cancer Stem Cells Show Differential Growth Characteristics and Molecular Profiles. *Cancer Res*. 2007;67: 4010–4015. doi:10.1158/0008-5472.CAN-06-4180
133. Medema JP. Cancer stem cells: The challenges ahead. *Nat Cell Biol*. 2013;15: 338–344. doi:10.1038/ncb2717
134. Borah A, Raveendran S, Rochani A, Maekawa T, Kumar DS. Targeting self-renewal pathways in cancer stem cells: clinical implications for cancer therapy. *Oncogenesis*. 2015;4: e177. doi:10.1038/oncsis.2015.35
135. Huang Z, Wu T, Liu AY, Ouyang G. Differentiation and transdifferentiation potentials of cancer stem cells. *Oncotarget*. 2015;6: 39550–39563.
136. Wang R, Chadalavada K, Wilshire J, Kowalik U, Hovinga KE, Geber A, et al. Glioblastoma stem-like cells give rise to tumour endothelium. *Nature*. 2010;468: 829–833. doi:10.1038/nature09624
137. Ricci-Vitiani L, Pallini R, Biffoni M, Todaro M, Invernici G, Cenci T, et al. Tumour vascularization via endothelial differentiation of glioblastoma stem-like cells. *Nature*. 2010;468: 824–828. doi:10.1038/nature09557
138. Zeniou M, Fève M, Mameri S, Dong J, Salomé C, Chen W, et al. Chemical Library Screening and Structure-Function Relationship Studies Identify Bisacodyl as a Potent and Selective Cytotoxic Agent Towards Quiescent Human Glioblastoma Tumor Stem-Like Cells. *PLOS ONE*. 2015;10: e0134793. doi:10.1371/journal.pone.0134793
139. Hata AN, Engelman JA, Faber AC. The BCL-2 family: key mediators of the apoptotic response to targeted anti-cancer therapeutics. *Cancer Discov*. 2015;5: 475–487. doi:10.1158/2159-8290.CD-15-0011

140. Jin F, Zhao L, Zhao H-Y, Guo S-G, Feng J, Jiang X-B, et al. Comparison between cells and cancer stem-like cells isolated from glioblastoma and astrocytoma on expression of anti-apoptotic and multidrug resistance-associated protein genes. *Neuroscience*. 2008;154: 541–550. doi:10.1016/j.neuroscience.2008.03.054
141. Capper D, Gaiser T, Hartmann C, Habel A, Mueller W, Herold-Mende C, et al. Stem-cell-like glioma cells are resistant to TRAIL/Apo2L and exhibit down-regulation of caspase-8 by promoter methylation. *Acta Neuropathol (Berl)*. 2009;117: 445–456. doi:10.1007/s00401-009-0494-3
142. Boesch M, Wolf D, Sopper S. Optimized Stem Cell Detection Using the DyeCycle-Triggered Side Population Phenotype. *Stem Cells Int*. 2015;2016: e1652389. doi:10.1155/2016/1652389
143. DI C, ZHAO Y. Multiple drug resistance due to resistance to stem cells and stem cell treatment progress in cancer (Review). *Exp Ther Med*. 2015;9: 289–293. doi:10.3892/etm.2014.2141
144. Li L, Bhatia R. Stem Cell Quiescence. *Clin Cancer Res*. 2011;17: 4936–4941. doi:10.1158/1078-0432.CCR-10-1499
145. Sosa MS, Bragado P, Aguirre-Ghiso JA. Mechanisms of disseminated cancer cell dormancy: an awakening field. *Nat Rev Cancer*. 2014;14: 611–622. doi:10.1038/nrc3793
146. Saito Y, Uchida N, Tanaka S, Suzuki N, Tomizawa-Murasawa M, Sone A, et al. Induction of cell cycle entry eliminates human leukemia stem cells in a mouse model of AML. *Nat Biotechnol*. 2010;28. doi:10.1038/nbt.1607
147. Roesch A, Fukunaga-Kalabis M, Schmidt EC, Zabierowski SE, Brafford PA, Vultur A, et al. A temporarily distinct subpopulation of slow-cycling melanoma cells is required for continuous tumor growth. *Cell*. 2010;141: 583–594. doi:10.1016/j.cell.2010.04.020
148. Haraguchi N, Ishii H, Mimori K, Tanaka F, Ohkuma M, Kim HM, et al. CD13 is a therapeutic target in human liver cancer stem cells. *J Clin Invest*. 2010;120: 3326–3339. doi:10.1172/JCI42550
149. Martin-Padura I, Marighetti P, Agliano A, Colombo F, Larzabal L, Redrado M, et al. Residual dormant cancer stem-cell foci are responsible for tumor relapse after antiangiogenic metronomic therapy in hepatocellular carcinoma xenografts. *Lab Invest J Tech Methods Pathol*. 2012;92: 952–966. doi:10.1038/labinvest.2012.65
150. Chen W, Dong J, Haiech J, Kilhoffer M-C, Zeniou M. Cancer Stem Cell Quiescence and Plasticity as Major Challenges in Cancer Therapy. *Stem Cells Int*.

2016;2016. doi:10.1155/2016/1740936

151. Deleyrolle LP, Harding A, Cato K, Siebzehnrubl FA, Rahman M, Azari H, et al. Evidence for label-retaining tumour-initiating cells in human glioblastoma. *Brain*. 2011;134: 1331–1343. doi:10.1093/brain/awr081

152. Chen J, Li Y, Yu T-S, McKay RM, Burns DK, Kernie SG, et al. A restricted cell population propagates glioblastoma growth after chemotherapy. *Nature*. 2012;488: 522–526. doi:10.1038/nature11287

153. Patel AP, Tirosh I, Trombetta JJ, Shalek AK, Gillespie SM, Wakimoto H, et al. Single-cell RNA-seq highlights intratumoral heterogeneity in primary glioblastoma. *Science*. 2014;344: 1396–1401. doi:10.1126/science.1254257

154. Ishii A, Kimura T, Sadahiro H, Kawano H, Takubo K, Suzuki M, et al. Histological Characterization of the Tumorigenic “Peri-Necrotic Niche” Harboring Quiescent Stem-Like Tumor Cells in Glioblastoma. *PLoS ONE*. 2016;11. doi:10.1371/journal.pone.0147366

155. Suvà ML, Rheinbay E, Gillespie SM, Patel AP, Wakimoto H, Rabkin SD, et al. Reconstructing and Reprogramming the Tumor-Propagating Potential of Glioblastoma Stem-like Cells. *Cell*. 2014;157: 580–594. doi:10.1016/j.cell.2014.02.030

156. Quintana E, Shackleton M, Foster HR, Fullen DR, Sabel MS, Johnson TM, et al. Phenotypic Heterogeneity among Tumorigenic Melanoma Cells from Patients that Is Reversible and Not Hierarchically Organized. *Cancer Cell*. 2010;18: 510–523. doi:10.1016/j.ccr.2010.10.012

157. Mathieu J, Zhang Z, Zhou W, Wang AJ, Heddlestone JM, Pinna CMA, et al. HIF Induces Human Embryonic Stem Cell Markers in Cancer Cells. *Cancer Res*. 2011;71: 4640–4652. doi:10.1158/0008-5472.CAN-10-3320

158. Heddlestone JM, Li Z, McLendon RE, Hjelmeland AB, Rich JN. The hypoxic microenvironment maintains glioblastoma stem cells and promotes reprogramming towards a cancer stem cell phenotype. *Cell Cycle*. 2009;8: 3274–3284. doi:10.4161/cc.8.20.9701

159. Li Z, Bao S, Wu Q, Wang H, Eyler C, Sathornsumetee S, et al. Hypoxia-Inducible Factors Regulate Tumorigenic Capacity of Glioma Stem Cells. *Cancer Cell*. 2009;15: 501–513. doi:10.1016/j.ccr.2009.03.018

160. Helczynska K, Kronblad Å, Jögi A, Nilsson E, Beckman S, Landberg G, et al. Hypoxia Promotes a Dedifferentiated Phenotype in Ductal Breast Carcinoma in Situ. *Cancer Res*. 2003;63: 1441–1444.

161. Louie E, Nik S, Chen J, Schmidt M, Song B, Pacson C, et al. Identification of a stem-like cell population by exposing metastatic breast cancer cell lines to

repetitive cycles of hypoxia and reoxygenation. *Breast Cancer Res.* 2010;12: R94. doi:10.1186/bcr2773

162. Das B, Tsuchida R, Malkin D, Koren G, Baruchel S, Yeger H. Hypoxia Enhances Tumor Stemness by Increasing the Invasive and Tumorigenic Side Population Fraction. *STEM CELLS.* 2008;26: 1818–1830. doi:10.1634/stemcells.2007-0724

163. Platet N, Liu SY, Atifi ME, Oliver L, Vallette FM, Berger F, et al. Influence of oxygen tension on CD133 phenotype in human glioma cell cultures. *Cancer Lett.* 2007;258: 286–290. doi:10.1016/j.canlet.2007.09.012

164. Liu S, Kumar SM, Martin JS, Yang R, Xu X. Snail1 Mediates Hypoxia-Induced Melanoma Progression. *Am J Pathol.* 2011;179: 3020–3031. doi:10.1016/j.ajpath.2011.08.038

165. Hjelmeland AB, Wu Q, Heddlestone JM, Choudhary GS, MacSwords J, Lathia JD, et al. Acidic stress promotes a glioma stem cell phenotype. *Cell Death Differ.* 2011;18: 829–840. doi:10.1038/cdd.2010.150

166. Singh A, Settleman J. EMT, cancer stem cells and drug resistance: an emerging axis of evil in the war on cancer. *Oncogene.* 2010;29: 4741–4751. doi:10.1038/onc.2010.215

167. Thiery JP, Sleeman JP. Complex networks orchestrate epithelial–mesenchymal transitions. *Nat Rev Mol Cell Biol.* 2006;7: 131–142. doi:10.1038/nrm1835

168. Hoogen C van den, Horst G van der, Cheung H, Buijs JT, Lippitt JM, Guzmán-Ramírez N, et al. High Aldehyde Dehydrogenase Activity Identifies Tumor-Initiating and Metastasis-Initiating Cells in Human Prostate Cancer. *Cancer Res.* 2010;70: 5163–5173. doi:10.1158/0008-5472.CAN-09-3806

169. Hiraga T, Ito S, Nakamura H. Cancer Stem–like Cell Marker CD44 Promotes Bone Metastases by Enhancing Tumorigenicity, Cell Motility, and Hyaluronan Production. *Cancer Res.* 2013;73: 4112–4122. doi:10.1158/0008-5472.CAN-12-3801

170. Baccelli I, Schneeweiss A, Riethdorf S, Stenzinger A, Schillert A, Vogel V, et al. Identification of a population of blood circulating tumor cells from breast cancer patients that initiates metastasis in a xenograft assay. *Nat Biotechnol.* 2013;31: 539–544. doi:10.1038/nbt.2576

171. Wan L, Pantel K, Kang Y. Tumor metastasis: moving new biological insights into the clinic. *Nat Med.* 2013;19: 1450–1464. doi:10.1038/nm.3391

172. Malanchi I, Santamaria-Martínez A, Susanto E, Peng H, Lehr H-A, Delaloye J-F, et al. Interactions between cancer stem cells and their niche govern

- metastatic colonization. *Nature*. 2012;481: 85–89. doi:10.1038/nature10694
173. Sotiropoulou PA, Christodoulou MS, Silvani A, Herold-Mende C, Passarella D. Chemical approaches to targeting drug resistance in cancer stem cells. *Drug Discov Today*. 2014;19: 1547–1562. doi:10.1016/j.drudis.2014.05.002
174. Krause M, Dubrovskaya A, Linge A, Baumann M. Cancer stem cells: Radioresistance, prediction of radiotherapy outcome and specific targets for combined treatments. *Adv Drug Deliv Rev*. 2017;109: 63–73. doi:10.1016/j.addr.2016.02.002
175. Beier D, Röhrl S, Pillai DR, Schwarz S, Kunz-Schughart LA, Leukel P, et al. Temozolomide Preferentially Depletes Cancer Stem Cells in Glioblastoma. *Cancer Res*. 2008;68: 5706–5715. doi:10.1158/0008-5472.CAN-07-6878
176. Fouse SD, Nakamura JL, James CD, Chang S, Costello JF. Response of primary glioblastoma cells to therapy is patient specific and independent of cancer stem cell phenotype. *Neuro-Oncol*. 2014;16: 361–371. doi:10.1093/neuonc/not223
177. Okada M, Sato A, Shibuya K, Watanabe E, Seino S, Suzuki S, et al. JNK contributes to temozolomide resistance of stem-like glioblastoma cells via regulation of MGMT expression. *Int J Oncol*. 2014;44: 591–599.
178. Sato A, Sunayama J, Matsuda K, Seino S, Suzuki K, Watanabe E, et al. MEK-ERK Signaling Dictates DNA-Repair Gene MGMT Expression and Temozolomide Resistance of Stem-Like Glioblastoma Cells via the MDM2-p53 Axis. *STEM CELLS*. 2011;29: 1942–1951. doi:10.1002/stem.753
179. Johannessen T-CA, Prestegarden L, Grudic A, Hegi ME, Tysnes BB, Bjerkvig R. The DNA repair protein ALKBH2 mediates temozolomide resistance in human glioblastoma cells. *Neuro-Oncol*. 2013;15: 269–278. doi:10.1093/neuonc/nos301
180. Bao S, Wu Q, McLendon RE, Hao Y, Shi Q, Hjelmeland AB, et al. Glioma stem cells promote radioresistance by preferential activation of the DNA damage response. *Nature*. 2006;444: 756–760. doi:10.1038/nature05236
181. Bleau A-M, Hambardzumyan D, Ozawa T, Fomchenko EI, Huse JT, Brennan CW, et al. PTEN/PI3K/Akt Pathway Regulates the Side Population Phenotype and ABCG2 Activity in Glioma Tumor Stem-like Cells. *Cell Stem Cell*. 2009;4: 226–235. doi:10.1016/j.stem.2009.01.007
182. Campos B, Gal Z, Baader A, Schneider T, Sliwinski C, Gassel K, et al. Aberrant self-renewal and quiescence contribute to the aggressiveness of glioblastoma. *J Pathol*. 2014;234: 23–33. doi:10.1002/path.4366
183. Nowell PC. The clonal evolution of tumor cell populations. *Science*. 1976;194: 23–28. doi:10.1126/science.959840

184. Nguyen LV, Vanner R, Dirks P, Eaves CJ. Cancer stem cells: an evolving concept. *Nat Rev Cancer*. 2012;12: 133–143. doi:10.1038/nrc3184
185. Islam F, Qiao B, Smith RA, Gopalan V, Lam AK-Y. Cancer stem cell: Fundamental experimental pathological concepts and updates. *Exp Mol Pathol*. 2015;98: 184–191. doi:10.1016/j.yexmp.2015.02.002
186. Visvader JE. Cells of origin in cancer. *Nature*. 2011;469: 314–322. doi:10.1038/nature09781
187. Meacham CE, Morrison SJ. Tumour heterogeneity and cancer cell plasticity. *Nature*. 2013;501: 328–337. doi:10.1038/nature12624
188. Wellner U, Schubert J, Burk UC, Schmalhofer O, Zhu F, Sonntag A, et al. The EMT-activator ZEB1 promotes tumorigenicity by repressing stemness-inhibiting microRNAs. *Nat Cell Biol*. 2009;11: 1487–1495. doi:10.1038/ncb1998
189. Xu B, English JM, Wilsbacher JL, Stippec S, Goldsmith EJ, Cobb MH. WNK1, a Novel Mammalian Serine/Threonine Protein Kinase Lacking the Catalytic Lysine in Subdomain II. *J Biol Chem*. 2000;275: 16795–16801. doi:10.1074/jbc.275.22.16795
190. WNK kinases, a novel protein kinase subfamily in multi-cellular organisms. *Publ Online* 06 Sept 2001 Doi101038sjonc1204726. 2001;20. doi:10.1038/sj.onc.1204726
191. Wilson FH. Human Hypertension Caused by Mutations in WNK Kinases. *Science*. 2001;293: 1107–1112. doi:10.1126/science.1062844
192. McCormick JA, Ellison DH. The WNKs: Atypical Protein Kinases With Pleiotropic Actions. *Physiol Rev*. 2011;91: 177–219. doi:10.1152/physrev.00017.2010
193. Vidal-Petiot E, Cheval L, Faugoux J, Malard T, Doucet A, Jeunemaitre X, et al. A New Methodology for Quantification of Alternatively Spliced Exons Reveals a Highly Tissue-Specific Expression Pattern of WNK1 Isoforms. *PLoS ONE*. 2012;7: e37751. doi:10.1371/journal.pone.0037751
194. Moniz S, Jordan P. Emerging roles for WNK kinases in cancer. *Cell Mol Life Sci*. 2010;67: 1265–1276. doi:10.1007/s00018-010-0261-6
195. Lenertz LY, Lee B-H, Min X, Xu B, Wedin K, Earnest S, et al. Properties of WNK1 and Implications for Other Family Members. *J Biol Chem*. 2005;280: 26653–26658. doi:10.1074/jbc.M502598200
196. Vitari AC, Deak M, Collins BJ, Morrice N, Prescott AR, Phelan A, et al. WNK1, the kinase mutated in an inherited high-blood-pressure syndrome, is a novel PKB (protein kinase B)/Akt substrate. *Biochem J*. 2004;378: 257–268.

doi:10.1042/BJ20031692

197. Rozansky DJ, Cornwall T, Subramanya AR, Rogers S, Yang Y-F, David LL, et al. Aldosterone mediates activation of the thiazide-sensitive Na-Cl cotransporter through an SGK1 and WNK4 signaling pathway. *J Clin Invest*. 2009;119: 2601–2612. doi:10.1172/JCI38323

198. Tu S, Bugde A, Luby-Phelps K, Cobb MH. WNK1 is required for mitosis and abscission. *Proc Natl Acad Sci U S A*. 2011;108: 1385–1390. doi:10.1073/pnas.1018567108

199. Wang Z, Yang C-L, Ellison DH. Comparison of WNK4 and WNK1 kinase and inhibiting activities. *Biochem Biophys Res Commun*. 2004;317: 939–944. doi:10.1016/j.bbrc.2004.03.132

200. Hong C, Moorefield KS, Jun P, Aldape KD, Kharbanda S, Phillips HS, et al. Epigenome scans and cancer genome sequencing converge on WNK2, a kinase-independent suppressor of cell growth. *Proc Natl Acad Sci U S A*. 2007;104: 10974–10979. doi:10.1073/pnas.0700683104

201. Richardson C, Alessi DR. The regulation of salt transport and blood pressure by the WNK-SPAK/OSR1 signalling pathway. *J Cell Sci*. 2008;121: 3293–3304. doi:10.1242/jcs.029223

202. Park S, Hong JH, Ohana E, Muallem S. The WNK/SPAK and IRBIT/PP1 Pathways in Epithelial Fluid and Electrolyte Transport. *Physiology*. 2012;27: 291–299. doi:10.1152/physiol.00028.2012

203. Moniz S, Matos P, Jordan P. WNK2 modulates MEK1 activity through the Rho GTPase pathway. *Cell Signal*. 2008;20: 1762–1768. doi:10.1016/j.cellsig.2008.06.002

204. Richardson C, Rafiqi FH, Karlsson HKR, Moleleki N, Vandewalle A, Campbell DG, et al. Activation of the thiazide-sensitive Na<sup>+</sup>-Cl<sup>–</sup> cotransporter by the WNK-regulated kinases SPAK and OSR1. *J Cell Sci*. 2008;121: 675–684. doi:10.1242/jcs.025312

205. Vitari AC, Thastrup J, Rafiqi FH, Deak M, Morrice NA, Karlsson HKR, et al. Functional interactions of the SPAK/OSR1 kinases with their upstream activator WNK1 and downstream substrate NKCC1. *Biochem J*. 2006;397: 223–231. doi:10.1042/BJ20060220

206. Cheng C-J, Huang C-L. Activation of PI3-Kinase Stimulates Endocytosis of ROMK via Akt1/SGK1-Dependent Phosphorylation of WNK1. *J Am Soc Nephrol*. 2011;22: 460–471. doi:10.1681/ASN.2010060681

207. Ohta A, Schumacher F-R, Mehellou Y, Johnson C, Knebel A, Macartney TJ, et al. The CUL3–KLHL3 E3 ligase complex mutated in Gordon's hypertension

- syndrome interacts with and ubiquitylates WNK isoforms: disease-causing mutations in KLHL3 and WNK4 disrupt interaction. *Biochem J.* 2013;451: 111–122. doi:10.1042/BJ20121903
208. Zhou B, Wang D, Feng X, Zhang Y, Wang Y, Zhuang J, et al. WNK4 inhibits NCC protein expression through MAPK ERK1/2 signaling pathway. *Am J Physiol - Ren Physiol.* 2012;302: F533–F539. doi:10.1152/ajprenal.00032.2011
209. San-Cristobal P, Ponce-Coria J, Vázquez N, Bobadilla NA, Gamba G. WNK3 and WNK4 amino-terminal domain defines their effect on the renal Na<sup>+</sup>-Cl<sup>-</sup> cotransporter. *Am J Physiol - Ren Physiol.* 2008;295: F1199–F1206. doi:10.1152/ajprenal.90396.2008
210. Golbang AP, Cope G, Hamad A, Murthy M, Liu C-H, Cuthbert AW, et al. Regulation of the expression of the Na/Cl cotransporter by WNK4 and WNK1: evidence that accelerated dynamin-dependent endocytosis is not involved. *Am J Physiol - Ren Physiol.* 2006;291: F1369–F1376. doi:10.1152/ajprenal.00468.2005
211. Heise CJ, Xu B, Deaton SL, Cha S-K, Cheng C-J, Earnest S, et al. Serum and Glucocorticoid-induced Kinase (SGK) 1 and the Epithelial Sodium Channel Are Regulated by Multiple with No Lysine (WNK) Family Members. *J Biol Chem.* 2010;285: 25161–25167. doi:10.1074/jbc.M110.103432
212. Xu B, Stippec S, Chu P-Y, Lazrak A, Li X-J, Lee B-H, et al. WNK1 activates SGK1 to regulate the epithelial sodium channel. *Proc Natl Acad Sci U S A.* 2005;102: 10315–10320.
213. He G, Wang H-R, Huang S-K, Huang C-L. Intersectin links WNK kinases to endocytosis of ROMK1. *J Clin Invest.* 2007;117: 1078–1087. doi:10.1172/JCI30087
214. Cope G, Murthy M, Golbang AP, Hamad A, Liu C-H, Cuthbert AW, et al. WNK1 Affects Surface Expression of the ROMK Potassium Channel Independent of WNK4. *J Am Soc Nephrol.* 2006;17: 1867–1874. doi:10.1681/ASN.2005111224
215. Kahle KT, Rinehart J, Lifton RP. Phosphoregulation of the Na–K–2Cl and K–Cl cotransporters by the WNK kinases. *Biochim Biophys Acta BBA - Mol Basis Dis.* 2010;1802: 1150–1158. doi:10.1016/j.bbadis.2010.07.009
216. Yang D, Li Q, So I, Huang C-L, Ando H, Mizutani A, et al. IRBIT governs epithelial secretion in mice by antagonizing the WNK/SPAK kinase pathway. *J Clin Invest.* 2011;121: 956–965. doi:10.1172/JCI43475
217. Romero MF, Chen A-P, Parker MD, Boron WF. The SLC4 family of bicarbonate transporters. *Mol Aspects Med.* 2013;34: 159–182. doi:10.1016/j.mam.2012.10.008
218. Parker MD, Boron WF. The divergence, actions, roles, and relatives of



sodium-coupled bicarbonate transporters. *Physiol Rev.* 2013;93: 803–959.  
doi:10.1152/physrev.00023.2012

219. Electrogenic sodium-dependent bicarbonate secretion by glial cells of the leech central nervous system. *J Gen Physiol.* 1991;98: 637–655.

220. Hong JH, Yang D, Shcheynikov N, Ohana E, Shin DM, Muallem S. Convergence of IRBIT, phosphatidylinositol (4,5) bisphosphate, and WNK/SPAK kinases in regulation of the Na<sup>+</sup>-HCO<sub>3</sub><sup>-</sup> cotransporters family. *Proc Natl Acad Sci.* 2013;110: 4105–4110. doi:10.1073/pnas.1221410110

221. Dhillon AS, Hagan S, Rath O, Kolch W. MAP kinase signalling pathways in cancer. *Oncogene.* 2007;26: 3279–3290. doi:10.1038/sj.onc.1210421

222. Sun X, Gao L, Yu RK, Zeng G. Down-regulation of WNK1 protein kinase in neural progenitor cells suppresses cell proliferation and migration. *J Neurochem.* 2006;99: 1114–1121. doi:10.1111/j.1471-4159.2006.04159.x

223. Xu B, Stippec S, Lenertz L, Lee B-H, Zhang W, Lee Y-K, et al. WNK1 Activates ERK5 by an MEKK2/3-dependent Mechanism. *J Biol Chem.* 2004;279: 7826–7831. doi:10.1074/jbc.M313465200

224. Shaharabany M, Holtzman EJ, Mayan H, Hirschberg K, Seger R, Farfel Z. Distinct pathways for the involvement of WNK4 in the signaling of hypertonicity and EGF. *FEBS J.* 2008;275: 1631–1642. doi:10.1111/j.1742-4658.2008.06318.x

225. Moniz S, Veríssimo F, Matos P, Brazão R, Silva E, Kotevelets L, et al. Protein kinase WNK2 inhibits cell proliferation by negatively modulating the activation of MEK1/ERK1/2. *Oncogene.* 2007;26: 6071–6081.  
doi:10.1038/sj.onc.1210706

226. Jiang ZY, Zhou QL, Holik J, Patel S, Leszyk J, Coleman K, et al. Identification of WNK1 as a Substrate of Akt/Protein Kinase B and a Negative Regulator of Insulin-stimulated Mitogenesis in 3T3-L1 Cells. *J Biol Chem.* 2005;280: 21622–21628. doi:10.1074/jbc.M414464200

227. Hoorn EJ, Nelson JH, McCormick JA, Ellison DH. The WNK Kinase Network Regulating Sodium, Potassium, and Blood Pressure. *J Am Soc Nephrol JASN.* 2011;22: 605–614. doi:10.1681/ASN.2010080827

228. Chen S, Bhargava A, Mastroberardino L, Meijer OC, Wang J, Buse P, et al. Epithelial sodium channel regulated by aldosterone-induced protein sgk. *Proc Natl Acad Sci U S A.* 1999;96: 2514–2519.

229. Hong F, Larrea MD, Doughty C, Kwiatkowski DJ, Squillace R, Slingerland JM. mTOR-Raptor Binds and Activates SGK1 to Regulate p27 Phosphorylation. *Mol Cell.* 2008;30: 701–711. doi:10.1016/j.molcel.2008.04.027

230. Veríssimo F, Silva E, Morris JD, Pepperkok R, Jordan P. Protein kinase WNK3 increases cell survival in a caspase-3-dependent pathway. *Oncogene*. 2006;25: 4172–4182. doi:10.1038/sj.onc.1209449
231. Lee B-H, Min X, Heise CJ, Xu B, Chen S, Shu H, et al. WNK1 Phosphorylates Synaptotagmin 2 and Modulates Its Membrane Binding. *Mol Cell*. 2004;15: 741–751. doi:10.1016/j.molcel.2004.07.018
232. Oh E, Heise CJ, English JM, Cobb MH, Thurmond DC. WNK1 Is a Novel Regulator of Munc18c-Syntaxin 4 Complex Formation in Soluble NSF Attachment Protein Receptor (SNARE)-mediated Vesicle Exocytosis. *J Biol Chem*. 2007;282: 32613–32622. doi:10.1074/jbc.M706591200
233. Serysheva E, Berhane H, Grumolato L, Demir K, Balmer S, Bodak M, et al. Wnk kinases are positive regulators of canonical Wnt/ $\beta$ -catenin signalling. *EMBO Rep*. 2013;14: 718–725. doi:10.1038/embor.2013.88
234. Tang BL. (WNK)ing at death: With-no-lysine (Wnk) kinases in neuropathies and neuronal survival. *Brain Res Bull*. 2016;125: 92–98. doi:10.1016/j.brainresbull.2016.04.017
235. An S-W, Cha S-K, Yoon J, Chang S, Ross EM, Huang C-L. WNK1 Promotes PIP2 Synthesis to Coordinate Growth Factor and GPCR-Gq Signaling. *Curr Biol*. 2011;21: 1979–1987. doi:10.1016/j.cub.2011.11.002
236. Kankanamalage SG, Lee A-Y, Wichaidit C, Lorente-Rodriguez A, Shah AM, Stippec S, et al. Multistep regulation of autophagy by WNK1. *Proc Natl Acad Sci*. 2016;113: 14342–14347. doi:10.1073/pnas.1617649113
237. Mendes AI, Matos P, Moniz S, Jordan P. Protein Kinase WNK1 Promotes Cell Surface Expression of Glucose Transporter GLUT1 by Regulating a Tre-2/USP6-BUB2-Cdc16 Domain Family Member 4 (TBC1D4)-Rab8A Complex. *J Biol Chem*. 2010;285: 39117–39126. doi:10.1074/jbc.M110.159418
238. Br H, H S. Inhibition of the Sodium-Potassium-Chloride Cotransporter Isoform-1 reduces glioma invasion., Inhibition of the Sodium-Potassium-Chloride Cotransporter Isoform-1 Reduces Glioma Invasion. *Cancer Res*. 2010;70, 70: 5597, 5597–5606. doi:10.1158/0008-5472.CAN-09-4666
239. Haas BR, Cuddapah VA, Watkins S, Rohn KJ, Dy TE, Sontheimer H. With-No-Lysine Kinase 3 (WNK3) stimulates glioma invasion by regulating cell volume. *Am J Physiol - Cell Physiol*. 2011;301: C1150–C1160. doi:10.1152/ajpcell.00203.2011
240. Garzon-Muvdi T, Schiapparelli P, Rhys C ap, Guerrero-Cazares H, Smith C, Kim D-H, et al. Regulation of Brain Tumor Dispersal by NKCC1 Through a Novel Role in Focal Adhesion Regulation. *PLOS Biol*. 2012;10: e1001320.

doi:10.1371/journal.pbio.1001320

241. Algharabil J, Kintner DB, Wang Q, Begum G, Clark PA, Yang S-S, et al. Inhibition of  $\text{Na}^+ - \text{K}^+ - 2\text{Cl}^-$  Cotransporter isoform 1 Accelerates Temozolomide-mediated Apoptosis in Glioblastoma Cancer Cells. *Cell Physiol Biochem*. 2012;30: 33–48. doi:10.1159/000339047
242. Zhu W, Begum G, Pointer K, Clark PA, Yang S-S, Lin S-H, et al. WNK1-OSR1 kinase-mediated phospho-activation of  $\text{Na}^+ - \text{K}^+ - 2\text{Cl}^-$  cotransporter facilitates glioma migration. *Mol Cancer*. 2014;13: 31. doi:10.1186/1476-4598-13-31
243. Dong J, Aulestia FJ, Assad Kahn S, Zeniou M, Dubois LG, El-Habr EA, et al. Bisacodyl and its cytotoxic activity on human glioblastoma stem-like cells. Implication of inositol 1,4,5-triphosphate receptor dependent calcium signaling. *Biochim Biophys Acta BBA - Mol Cell Res*. doi:10.1016/j.bbamcr.2017.01.010
244. Schreiner J, Nell G, Loeschke K. Effect of diphenolic laxatives on  $\text{Na}^+ - \text{K}^+$ -activated ATPase and cyclic nucleotide content of rat colon mucosa in vivo. *Naunyn Schmiedebergs Arch Pharmacol*. 1980;313: 249–255.
245. Rachmilewitz D, Karmeli F, Okon E. Effects of bisacodyl on cAMP and prostaglandin E2 contents,  $(\text{Na} + \text{K})$  ATPase, adenylyl cyclase, and phosphodiesterase activities of rat intestine. *Dig Dis Sci*. 1980;25: 602–608.
246. Beubler E, Schirgi-Degen A. Stimulation of enterocyte protein kinase C by laxatives in-vitro. *J Pharm Pharmacol*. 1993;45: 59–62.
247. Gaginella TS, Mascolo N, Izzo AA, Autore G, Capasso F. Nitric oxide as a mediator of bisacodyl and phenolphthalein laxative action: induction of nitric oxide synthase. *J Pharmacol Exp Ther*. 1994;270: 1239–1245.
248. Ikarashi N, Baba K, Ushiki T, Kon R, Mimura A, Toda T, et al. The laxative effect of bisacodyl is attributable to decreased aquaporin-3 expression in the colon induced by increased PGE2 secretion from macrophages. *Am J Physiol - Gastrointest Liver Physiol*. 2011;301: G887–G895. doi:10.1152/ajpgi.00286.2011
249. Giese A, Bjerkvig R, Berens M e., Westphal M. Cost of Migration: Invasion of Malignant Gliomas and Implications for Treatment. *J Clin Oncol*. 2003;21: 1624–1636. doi:10.1200/JCO.2003.05.063
250. Rich JN. Cancer Stem Cells in Radiation Resistance. *Cancer Res*. 2007;67: 8980–8984. doi:10.1158/0008-5472.CAN-07-0895
251. Beier D, Schulz JB, Beier CP. Chemoresistance of glioblastoma cancer stem cells - much more complex than expected. *Mol Cancer*. 2011;10: 128. doi:10.1186/1476-4598-10-128

252. Choi SA, Lee JY, Phi JH, Wang K-C, Park C-K, Park S-H, et al. Identification of brain tumour initiating cells using the stem cell marker aldehyde dehydrogenase. *Eur J Cancer*. 2014;50: 137–149. doi:10.1016/j.ejca.2013.09.004
253. Keith B, Simon MC. Hypoxia-Inducible Factors, Stem Cells, and Cancer. *Cell*. 2007;129: 465–472. doi:10.1016/j.cell.2007.04.019
254. Auffinger B, Tobias AL, Han Y, Lee G, Guo D, Dey M, et al. Conversion of differentiated cancer cells into cancer stem-like cells in a glioblastoma model after primary chemotherapy. *Cell Death Differ*. 2014;21: 1119–1131. doi:10.1038/cdd.2014.31
255. Dahan P, Martinez Gala J, Delmas C, Monferran S, Malric L, Zentkowski D, et al. Ionizing radiations sustain glioblastoma cell dedifferentiation to a stem-like phenotype through survivin: possible involvement in radioresistance. *Cell Death Dis*. 2014;5: e1543. doi:10.1038/cddis.2014.509
256. Brat DJ, Castellano-Sanchez AA, Hunter SB, Pecot M, Cohen C, Hammond EH, et al. Pseudopalisades in Glioblastoma Are Hypoxic, Express Extracellular Matrix Proteases, and Are Formed by an Actively Migrating Cell Population. *Cancer Res*. 2004;64: 920–927. doi:10.1158/0008-5472.CAN-03-2073
257. Rong Y, Durden DL, Meir V, G E, Brat DJ. “Pseudopalisading” Necrosis in Glioblastoma: A Familiar Morphologic Feature That Links Vascular Pathology, Hypoxia, and Angiogenesis. *J Neuropathol Exp Neurol*. 2006;65: 529–539. doi:10.1097/00005072-200606000-00001
258. Clark MJ, Homer N, O'Connor BD, Chen Z, Eskin A, Lee H, et al. U87MG Decoded: The Genomic Sequence of a Cytogenetically Aberrant Human Cancer Cell Line. *PLOS Genet*. 2010;6: e1000832. doi:10.1371/journal.pgen.1000832
259. Johnson JI, Decker S, Zaharevitz D, Rubinstein LV, Venditti JM, Schepartz S, et al. Relationships between drug activity in NCI preclinical in vitro and in vivo models and early clinical trials. *Br J Cancer*. 2001;84: 1424–1431. doi:10.1054/bjoc.2001.1796
260. Huse JT, Holland EC. Genetically Engineered Mouse Models of Brain Cancer and the Promise of Preclinical Testing. *Brain Pathol*. 2009;19: 132–143. doi:10.1111/j.1750-3639.2008.00234.x
261. Hirschhaeuser F, Menne H, Dittfeld C, West J, Mueller-Klieser W, Kunz-Schughart LA. Multicellular tumor spheroids: An underestimated tool is catching up again. *J Biotechnol*. 2010;148: 3–15. doi:10.1016/j.jbiotec.2010.01.012
262. Corcoran A, Ridder LIFD, Duca DD, Kalala OJP, Lah T, Pilkington GJ, et al. Evolution of the brain tumour spheroid model: transcending current model limitations. *Acta Neurochir (Wien)*. 2003;145: 819–824. doi:10.1007/s00701-003-

263. Gilbert CA, Ross AH. Cancer Stem Cells: Cell Culture, Markers and Targets for New Therapies. *J Cell Biochem.* 2009;108: 1031–1038. doi:10.1002/jcb.22350
264. Lee J, Kotliarova S, Kotliarov Y, Li A, Su Q, Donin NM, et al. Tumor stem cells derived from glioblastomas cultured in bFGF and EGF more closely mirror the phenotype and genotype of primary tumors than do serum-cultured cell lines. *Cancer Cell.* 2006;9: 391–403. doi:10.1016/j.ccr.2006.03.030
265. Katt ME, Placone AL, Wong AD, Xu ZS, Searson PC. In Vitro Tumor Models: Advantages, Disadvantages, Variables, and Selecting the Right Platform. *Front Bioeng Biotechnol.* 2016;4. doi:10.3389/fbioe.2016.00012
266. Wu LY, Carlo DD, Lee LP. Microfluidic self-assembly of tumor spheroids for anticancer drug discovery. *Biomed Microdevices.* 2008;10: 197–202. doi:10.1007/s10544-007-9125-8
267. Barretina J, Caponigro G, Stransky N, Venkatesan K, Margolin AA, Kim S, et al. The Cancer Cell Line Encyclopedia enables predictive modelling of anticancer drug sensitivity. *Nature.* 2012;483: 603–607. doi:10.1038/nature11003
268. Sutherland RM, Inch WR, McCredie JA, Kruuv J. A Multi-component Radiation Survival Curve Using an in Vitro Tumour Model. *Int J Radiat Biol Relat Stud Phys Chem Med.* 1970;18: 491–495. doi:10.1080/09553007014551401
269. Sutherland RM, McCredie JA, Inch WR. Growth of Multicell Spheroids in Tissue Culture as a Model of Nodular Carcinomas. *JNCI J Natl Cancer Inst.* 1971;46: 113–120. doi:10.1093/jnci/46.1.113
270. Sutherland RM. Cell and environment interactions in tumor microregions: the multicell spheroid model. *Science.* 1988;240: 177–184. doi:10.1126/science.2451290
271. Reynolds BA, Weiss S. Generation of neurons and astrocytes from isolated cells of the adult mammalian central nervous system. *Science.* 1992;255: 1707–1710. doi:10.1126/science.1553558
272. Günther HS, Schmidt NO, Phillips HS, Kemming D, Kharbanda S, Soriano R, et al. Glioblastoma-derived stem cell-enriched cultures form distinct subgroups according to molecular and phenotypic criteria. *Oncogene.* 2007;27: 2897–2909. doi:10.1038/sj.onc.1210949
273. Weiswald L-B, Bellet D, Dangles-Marie V. Spherical Cancer Models in Tumor Biology. *Neoplasia N Y N.* 2015;17: 1–15. doi:10.1016/j.neo.2014.12.004
274. Laks DR, Masterman-Smith M, Visnyei K, Angenieux B, Orozco NM, Foran I, et al. Neurosphere Formation Is an Independent Predictor of Clinical Outcome in

- Malignant Glioma. *STEM CELLS*. 2009;27: 980–987. doi:10.1002/stem.15
275. Jensen SS, Meyer M, Petterson SA, Halle B, Rosager AM, Aaberg-Jessen C, et al. Establishment and Characterization of a Tumor Stem Cell-Based Glioblastoma Invasion Model. *PLOS ONE*. 2016;11: e0159746. doi:10.1371/journal.pone.0159746
276. Pollard SM, Yoshikawa K, Clarke ID, Danovi D, Stricker S, Russell R, et al. Glioma Stem Cell Lines Expanded in Adherent Culture Have Tumor-Specific Phenotypes and Are Suitable for Chemical and Genetic Screens. *Cell Stem Cell*. 2009;4: 568–580. doi:10.1016/j.stem.2009.03.014
277. Reynolds BA, Vescovi AL. Brain Cancer Stem Cells: Think Twice before Going Flat. *Cell Stem Cell*. 2009;5: 466–467. doi:10.1016/j.stem.2009.10.017
278. Wang S, Lin S-Y. Tumor dormancy: potential therapeutic target in tumor recurrence and metastasis prevention. *Exp Hematol Oncol*. 2013;2: 29. doi:10.1186/2162-3619-2-29
279. MANABE N, CREMONINI F, CAMILLERI M, SANDBORN WJ, BURTON DD. Effects of bisacodyl on ascending colon emptying and overall colonic transit in healthy volunteers. *Aliment Pharmacol Ther*. 2009;30: 930–936. doi:10.1111/j.1365-2036.2009.04118.x
280. W R, K B. [Pharmacokinetics and laxative effect of bisacodyl following administration of various dosage forms]. *Arzneimittelforschung*. 1988;38: 570–574.
281. J N, A K. Effects of sodium picosulfate, bisacodyl and sennoside in cultured human, rat and rabbit liver cells. *Arzneimittelforschung*. 1981;31: 1010–1013.
282. Toyoda K, Nishikawa A, Furukawa F, Kawanishi T, Hayashi Y, Takahashi M. Cell proliferation induced by laxatives and related compounds in the rat intestine. *Cancer Lett*. 1994;83: 43–49.
283. Piccirillo SGM, Combi R, Cajola L, Patrizi A, Redaelli S, Bentivegna A, et al. Distinct pools of cancer stem-like cells coexist within human glioblastomas and display different tumorigenicity and independent genomic evolution. *Oncogene*. 2009;28: 1807–1811. doi:10.1038/onc.2009.27
284. Braunstein S, Raleigh D, Bindra R, Mueller S, Haas-Kogan D. Pediatric high-grade glioma: current molecular landscape and therapeutic approaches. *J Neurooncol*. 2017; 1–9. doi:10.1007/s11060-017-2393-0
285. Pollack IF, Hamilton RL, James CD, Finkelstein SD, Burnham J, Yates AJ, et al. Rarity of PTEN deletions and EGFR amplification in malignant gliomas of childhood: results from the Children's Cancer Group 945 cohort. *J Neurosurg Pediatr*. 2006;105: 418–424. doi:10.3171/ped.2006.105.5.418

286. Gielen GH, Gessi M, Buttarelli FR, Baldi C, Hammes J, zur Muehlen A, et al. Genetic Analysis of Diffuse High-Grade Astrocytomas in Infancy Defines a Novel Molecular Entity. *Brain Pathol.* 2015;25: 409–417. doi:10.1111/bpa.12210
287. Pollack IF, Hamilton RL, Burger PC, Brat DJ, Rosenblum MK, Murdoch GH, et al. Akt activation is a common event in pediatric malignant gliomas and a potential adverse prognostic marker: a report from the Children's Oncology Group. *J Neurooncol.* 2010;99: 155–163. doi:10.1007/s11060-010-0297-3
288. Faury D, Nantel A, Dunn SE, Guiot M-C, Haque T, Hauser P, et al. Molecular Profiling Identifies Prognostic Subgroups of Pediatric Glioblastoma and Shows Increased YB-1 Expression in Tumors. *J Clin Oncol.* 2007;25: 1196–1208. doi:10.1200/JCO.2006.07.8626
289. Roderick HL, Cook SJ. Ca<sup>2+</sup> signalling checkpoints in cancer: remodelling Ca<sup>2+</sup> for cancer cell proliferation and survival. *Nat Rev Cancer.* 2008;8: 361–375. doi:10.1038/nrc2374
290. Chigurupati S, Venkataraman R, Barrera D, Naganathan A, Madan M, Paul L, et al. Receptor Channel TRPC6 Is a Key Mediator of Notch-Driven Glioblastoma Growth and Invasiveness. *Cancer Res.* 2010;70: 418–427. doi:10.1158/0008-5472.CAN-09-2654
291. Ding X, He Z, Zhou K, Cheng J, Yao H, Lu D, et al. Essential Role of TRPC6 Channels in G2/M Phase Transition and Development of Human Glioma. *JNCI J Natl Cancer Inst.* 2010;102: 1052–1068. doi:10.1093/jnci/djq217
292. Leclerc C, Haeich J, Aulestia FJ, Kilhoffer M-C, Miller AL, Néant I, et al. Calcium signaling orchestrates glioblastoma development: Facts and conjunctures. *Biochim Biophys Acta BBA - Mol Cell Res.* 2016;1863: 1447–1459. doi:10.1016/j.bbamcr.2016.01.018
293. Kang SS, Han K-S, Ku BM, Lee YK, Hong J, Shin HY, et al. Caffeine-Mediated Inhibition of Calcium Release Channel Inositol 1,4,5-Trisphosphate Receptor Subtype 3 Blocks Glioblastoma Invasion and Extends Survival. *Cancer Res.* 2010;70: 1173–1183. doi:10.1158/0008-5472.CAN-09-2886
294. Lindner D, Raghavan D. Intra-tumoural extra-cellular pH: a useful parameter of response to chemotherapy in syngeneic tumour lines. *Br J Cancer.* 2009;100: 1287–1291. doi:10.1038/sj.bjc.6605022
295. Casciari JJ, Sotirchos SV, Sutherland RM. Variations in tumor cell growth rates and metabolism with oxygen concentration, glucose concentration, and extracellular pH. *J Cell Physiol.* 1992;151: 386–394. doi:10.1002/jcp.1041510220
296. Goda N, Ryan HE, Khadivi B, McNulty W, Rickert RC, Johnson RS. Hypoxia-Inducible Factor 1 $\alpha$  Is Essential for Cell Cycle Arrest during Hypoxia. *Mol*

Cell Biol. 2003;23: 359–369. doi:10.1128/MCB.23.1.359-369.2003

297. Ando H, Kawaai K, Mikoshiba K. IRBIT: A regulator of ion channels and ion transporters. *Biochim Biophys Acta BBA - Mol Cell Res.* 2014;1843: 2195–2204. doi:10.1016/j.bbamcr.2014.01.031

298. Rose CR, Verkhratsky A. Principles of sodium homeostasis and sodium signalling in astroglia. *Glia.* 2016;64: 1611–1627. doi:10.1002/glia.22964

299. Zippin JH, Chen Y, Straub SG, Hess KC, Diaz A, Lee D, et al. CO<sub>2</sub>/HCO<sub>3</sub><sup>-</sup> and Calcium-regulated Soluble Adenylyl Cyclase as a Physiological ATP Sensor. *J Biol Chem.* 2013;288: 33283–33291. doi:10.1074/jbc.M113.510073

300. Chang J-C, Elferink O, PhD R. Role of the bicarbonate-responsive soluble adenylyl cyclase in pH sensing and metabolic regulation. *Front Physiol.* 2014;5. doi:10.3389/fphys.2014.00042

301. Choi HB, Gordon GRJ, Zhou N, Tai C, Rungta RL, Martinez J, et al. Metabolic Communication between Astrocytes and Neurons via Bicarbonate-Responsive Soluble Adenylyl Cyclase. *Neuron.* 2012;75: 1094–1104. doi:10.1016/j.neuron.2012.08.032

302. Sleno L, Emili A. Proteomic methods for drug target discovery. *Curr Opin Chem Biol.* 2008;12: 46–54. doi:10.1016/j.cbpa.2008.01.022

303. Kim JJ, Tannock IF. Repopulation of cancer cells during therapy: an important cause of treatment failure. *Nat Rev Cancer.* 2005;5: 516–525. doi:10.1038/nrc1650

304. Chan KS. Molecular Pathways: Targeting Cancer Stem Cells Awakened by Chemotherapy to Abrogate Tumor Repopulation. *Clin Cancer Res Off J Am Assoc Cancer Res.* 2016;22: 802–806. doi:10.1158/1078-0432.CCR-15-0183

305. Aapro MS, Bohlius J, Cameron DA, Lago LD, Donnelly JP, Kearney N, et al. 2010 update of EORTC guidelines for the use of granulocyte-colony stimulating factor to reduce the incidence of chemotherapy-induced febrile neutropenia in adult patients with lymphoproliferative disorders and solid tumours. *Eur J Cancer.* 2011;47: 8–32. doi:10.1016/j.ejca.2010.10.013

306. Kurtova AV, Xiao J, Mo Q, Pazhanisamy S, Krasnow R, Lerner SP, et al. Blocking PGE<sub>2</sub>-induced tumour repopulation abrogates bladder cancer chemoresistance. *Nature.* 2015;517: 209–213. doi:10.1038/nature14034

307. Gilbert CA, Daou M-C, Moser RP, Ross AH. Gamma-Secretase Inhibitors Enhance Temozolomide Treatment of Human Gliomas by Inhibiting Neurosphere Repopulation and Xenograft Recurrence. *Cancer Res.* 2010;70: 6870–6879. doi:10.1158/0008-5472.CAN-10-1378



308. Vitari AC, Deak M, Morrice NA, Alessi DR. The WNK1 and WNK4 protein kinases that are mutated in Gordon's hypertension syndrome phosphorylate and activate SPAK and OSR1 protein kinases. *Biochem J.* 2005;391: 17–24. doi:10.1042/BJ20051180
309. Manning G, Whyte DB, Martinez R, Hunter T, Sudarsanam S. The Protein Kinase Complement of the Human Genome. *Science.* 2002;298: 1912–1934. doi:10.1126/science.1075762
310. Collett MS, Erikson RL. Protein kinase activity associated with the avian sarcoma virus src gene product. *Proc Natl Acad Sci.* 1978;75: 2021–2024.
311. Dancey J, Sausville EA. Issues and progress with protein kinase inhibitors for cancer treatment. *Nat Rev Drug Discov.* 2003;2: 296–313. doi:10.1038/nrd1066
312. Futreal PA, Coin L, Marshall M, Down T, Hubbard T, Wooster R, et al. A census of human cancer genes. *Nat Rev Cancer.* 2004;4: 177–183. doi:10.1038/nrc1299
313. Noble MEM, Endicott JA, Johnson LN. Protein Kinase Inhibitors: Insights into Drug Design from Structure. *Science.* 2004;303: 1800–1805. doi:10.1126/science.1095920
314. Cohen P. Protein kinases — the major drug targets of the twenty-first century? *Nat Rev Drug Discov.* 2002;1: 309–315. doi:10.1038/nrd773
315. Small molecule modulators of cyclin-dependent kinases for cancer therapy. *Publ Online* 08 Febr 2001 Doi101038sjonc1204085. 2001;19. doi:10.1038/sj.onc.1204085
316. Zhang J, Yang PL, Gray NS. Targeting cancer with small molecule kinase inhibitors. *Nat Rev Cancer.* 2009;9: 28–39. doi:10.1038/nrc2559
317. Fabbro D, Ruetz S, Buchdunger E, Cowan-Jacob SW, Fendrich G, Liebetanz J, et al. Protein kinases as targets for anticancer agents: from inhibitors to useful drugs. *Pharmacol Ther.* 2002;93: 79–98. doi:10.1016/S0163-7258(02)00179-1
318. Eglen RM, Reisine T. The Current Status of Drug Discovery Against the Human Kinome. *ASSAY Drug Dev Technol.* 2009;7: 22–43. doi:10.1089/adt.2008.164
319. Davies SP, Reddy H, Caivano M, Cohen P. Specificity and mechanism of action of some commonly used protein kinase inhibitors. *Biochem J.* 2000;351: 95–105. doi:10.1042/bj3510095
320. Yamada K, Park H-M, Rigel DF, DiPetrillo K, Whalen EJ, Anisowicz A, et al.

Small-molecule WNK inhibition regulates cardiovascular and renal function. *Nat Chem Biol.* 2016;12: 896–898. doi:10.1038/nchembio.2168

321. Ashburn TT, Thor KB. Drug repositioning: identifying and developing new uses for existing drugs. *Nat Rev Drug Discov.* 2004;3: 673–683. doi:10.1038/nrd1468

322. P DP, S JA, B BM, S KN, A KA. Drug Repositioning: A Review. *Int J Pharma Res Rev.* 2015;4. Available: <https://www.omicsonline.org/scholarly-articles/drug-repositioning-a-review-61899.html>

323. Teo SK, Stirling DI, Zeldis JB. Thalidomide as a novel therapeutic agent: new uses for an old product. *Drug Discov Today.* 2005;10: 107–114. doi:10.1016/S1359-6446(04)03307-0

324. Baumann F, Bjeljac M, Kollias SS, Baumert BG, Brandner S, Rousson V, et al. Combined thalidomide and temozolomide treatment in patients with glioblastoma multiforme. *J Neurooncol.* 2004;67: 191–200.

325. Hwu W-J, Krown SE, Menell JH, Panageas KS, Merrell J, Lamb LA, et al. Phase II Study of Temozolomide Plus Thalidomide for the Treatment of Metastatic Melanoma. *J Clin Oncol.* 2003;21: 3351–3356. doi:10.1200/JCO.2003.02.061

326. Novac N. Challenges and opportunities of drug repositioning. *Trends Pharmacol Sci.* 2013;34: 267–272. doi:10.1016/j.tips.2013.03.004

327. Smith RB. Repositioned drugs: integrating intellectual property and regulatory strategies. *Drug Discov Today Ther Strateg.* 2011;8: 131–137. doi:10.1016/j.ddstr.2011.06.008

328. Lopert R, Lang DL, Hill SR, Henry DA. Differential pricing of drugs: a role for cost-effectiveness analysis? *The Lancet.* 2002;359: 2105–2107. doi:10.1016/S0140-6736(02)08911-0

329. Oprea TI, Mestres J. Drug Repurposing: Far Beyond New Targets for Old Drugs. *AAPS J.* 2012;14: 759–763. doi:10.1208/s12248-012-9390-1

## **IV. APPENDIX 1**

### **Review : Cancer Stem Cell Quiescence and Plasticity as Major Challenges in Cancer Therapy**

Wanyin Chen, Jihu Dong, Jacques Haiech, Marie-Claude Kilhoffer, and Maria Zeniou

Hindawi Publishing Corporation Stem Cells International Volume 2016, Article ID 1740936, 16 pages <http://dx.doi.org/10.1155/2016/1740936>

## Review Article

# Cancer Stem Cell Quiescence and Plasticity as Major Challenges in Cancer Therapy

Wanyin Chen, Jihu Dong, Jacques Haiech, Marie-Claude Kilhoffer, and Maria Zeniou

Laboratoire d'Innovation Thérapeutique, Université de Strasbourg/CNRS UMR7200,  
Laboratoire d'Excellence Medalis, Faculté de Pharmacie, 74 route du Rhin, 67401 Illkirch, France

Correspondence should be addressed to Maria Zeniou; zeniou@unistra.fr

Received 16 March 2016; Accepted 15 May 2016

Academic Editor: Javier Garcia-Castro

Copyright © 2016 Wanyin Chen et al. This is an open access article distributed under the Creative Commons Attribution License, which permits unrestricted use, distribution, and reproduction in any medium, provided the original work is properly cited.

Cells with stem-like properties, tumorigenic potential, and treatment-resistant phenotypes have been identified in many human malignancies. Based on the properties they share with nonneoplastic stem cells or their ability to initiate and propagate tumors *in vivo*, such cells were designated as cancer stem (stem-like) or tumor initiating/propagating cells. Owing to their implication in treatment resistance, cancer stem cells (CSCs) have been the subject of intense investigation in past years. Comprehension of CSCs' intrinsic properties and mechanisms they develop to survive and even enhance their aggressive phenotype within the hostile conditions of the tumor microenvironment has reoriented therapeutic strategies to fight cancer. This report provides selected examples of malignancies in which the presence of CSCs has been evidenced and briefly discusses methods to identify, isolate, and functionally characterize the CSC subpopulation of cancer cells. Relevant biological targets in CSCs, their link to treatment resistance, proposed targeting strategies, and limitations of these approaches are presented. Two major aspects of CSC physiopathology, namely, relative *in vivo* quiescence and plasticity in response to microenvironmental cues or treatment, are highlighted. Implications of these findings in the context of the development of new therapies are discussed.

## 1. Scope of This Review

Many if not most cancers are characterized by the presence of a subpopulation of tumor cells endowed with tumor initiation and propagation ability and a physiopathological state leading to great resistance to conventional therapies. Because it was initially presumed that such cells originated from malignant transformation of normal stem cells and in view of their tumorigenic potential, these cells were designated as cancer stem (or stem-like) cells or tumor initiating/propagating cells. In this review they will be referred to as cancer stem cells (CSCs).

Isolation and subsequent studies of CSCs from different types of tumors pointed to these cells as major components of conventional treatment failure. As a consequence, targeting CSCs is a promising perspective for the development of novel more effective anticancer therapeutic protocols. In this context, great efforts are made to identify and develop new anti-CSC therapies. However, the more we learn about CSCs,

the more it becomes obvious that targeting this particular cancer cell subpopulation will be challenging.

Cancer cells endowed with stem cell properties are maintained *in vivo* in a quiescent slow-growing state which preserves them from antiproliferating anticancer drugs. In addition, CSC function is elusive and may be enhanced or modified by environmental cues or treatment. Moreover, these modifications may occur in only a part of these cells leading to CSC heterogeneity within the same tumor. More importantly, normal or cancer cells without stem cell properties may be induced to treatment-resistant CSCs depending on signals from their microenvironment.

This review will describe CSCs' functional characteristics and some methods used for their identification. Relevant biological targets in CSCs will be presented with a focus on quiescence and plasticity, two major aspects of CSCs' physiopathology. Data presented aim to highlight future challenges in CSC targeting and elimination in order to eradicate tumors.

## 2. Malignancies with Hierarchical Organization and CSCs

Evidence for the presence of cancer cells with stem cell properties in human malignancies was provided by Bonnet and Dick in the late nineties. These authors described CD34<sup>+</sup>/CD38<sup>−</sup> cancer cells able to initiate acute myeloid leukemia in immunocompromised mice. They postulated that these cells originate from oncogenic transformation of hematopoietic stem cells since they presented similarities in cell surface marker expression, proliferation, self-renewal, and differentiation abilities [1]. This discovery is at the basis of the hierarchical or cancer stem cell (CSC) model postulating that tumors are hierarchically organized with CSCs at the apex of this hierarchy. CSCs would be unique among cancer cells through their ability to sustain *in vivo* long-term tumorigenic potential [2]. It is of note that the CSC model does not imply that CSCs arise from oncogenic transformation of normal stem cells since any cell in the hierarchy with proliferative ability could be at the origin of CSCs and thus of tumors [3, 4]. This hierarchical or CSC model was initially opposed to the clonal evolution theory suggesting that all undifferentiated cells within a tumor have equal tumorigenic potential provided by random additional mutations or epigenetic modifications [5]. Experimental data demonstrating that non-CSC populations may acquire CSC functionalities depending on the cell environmental context [6–8] supports the idea that the CSC and clonal evolution models present much more similarities than initially proposed.

Based on surface marker expression patterns, sphere formation ability, side population detection, and *in vivo* tumorigenic potential following serial transplantation [9], cancer stem cells have been subsequently isolated from numerous solid tumors, the first one being breast carcinoma [10, 11]. Additional solid tumors that adhere to the hierarchical or CSC model include, but are not limited to, brain [12–16], pancreatic [17, 18], colon [19–21], head and neck [22], hepatic [23], lung [24, 25], prostate [26], bladder [27], and ovarian malignancies [28, 29], as well as melanoma [30–32] and musculoskeletal sarcomas [33].

## 3. CSC Properties. What Defines a CSC?

Cell surface antigen expression profiles have been commonly used for enrichment of CSCs from tumors (Figure 1(a)). In acute myeloid leukemia, CSCs were shown to express CD34 (Cluster of Differentiation 34) and lack expression of CD38 [1, 34]. CD133 (prominin 1) expression was described and used for isolation of CSCs from various solid tumors including glioblastoma [15], prostate [26], colon [20, 21], lung [24], pancreatic [17], and ovarian cancers [35] and melanoma [36]. The CD44 adhesion molecule is another surface marker that has often been associated with CSC phenotypes. CSCs showing expressions of CD44 were described, for example, in breast [10], colorectal [19], pancreatic [18], and ovarian malignancies [29]. Several other surface markers have been used to define CSCs (reviewed in [37–39]). However, surface marker expression profiles may vary during tumor growth *in*

*vivo* and as a function of experimental conditions *in vitro*. In addition, these markers often lack specificity and heterogeneity in marker expression may exist between patients and even within the same tumor [39]. Combining different markers was proposed to improve reliability of this type of approach. Alternatively, new, functional markers, most of which are associated with the intrinsic stem properties of CSCs, have been used. Increased ALDH1 (aldehyde dehydrogenase 1) expression was, for example, used as a marker of CSCs from mammary tumors [11] as well as of CSCs from bladder, lung, colon, esophageal, and head and neck squamous cell carcinomas [38]. Although not restricted to CSCs, expression of components of signaling pathways associated with cell pluripotency was also used to characterize these cells. Proteins whose expression was linked to the stem-like phenotype of CSCs include the OCT-4 (octamer-binding transcription factor 4), SOX2, and NANOG transcription factors (Figure 1(a)) as well as components of the Wnt/ $\beta$ -catenin, Notch, and Hedgehog (Hh) signaling modules [40, 41]. Reverse transcription followed by real-time polymerase chain reaction (PCR) is an extremely sensitive method commonly used for CSC marker identification. In this approach, expression levels of the gene(s) of interest need to be normalized against endogenous control genes (housekeeping genes) whose expression should be robust and highly stable in the experimental conditions used. In a recent study, the stability of 15 commonly used housekeeping genes was evaluated in CSC spheroids from musculoskeletal sarcomas and carcinomas and from breast and renal malignancies as well as in the corresponding adherent native tumor cell lines [42]. Housekeeping genes encoding Tata-Binding Protein (TBP), Tyrosine 3-monooxygenase/tryptophan 5-monooxygenase activation protein zeta polypeptide (YWHAZ), peptidylprolyl isomerase A (PPIA), hydroxymethylbilane synthase (HMBS), or GAPDH (glyceraldehyde-3-phosphate dehydrogenase), were shown to be appropriate for comparative expression studies in cells used in this report. In addition, the authors suggested that more than one endogenous control gene should be used for normalization and that different, specific housekeeping genes should be considered for distinct CSCs and/or as a function of experimental conditions [42]. Recent data obtained in our laboratory with human glioblastoma CSCs and control cells further argue in favor of the necessity to validate appropriate housekeeping genes for each experimental setting [43, 44].

Since marker expression is definitely not sufficient to define a specific CSC subpopulation, it is now a consensus that phenotypic characterization must be accompanied by functional validation of CSCs [45, 46]. Thus, in addition to cell surface marker and stem cell marker expression profiling (Figure 1(a)) [9], various methods have been developed *in vitro* and *in vivo* to assess the stem cell properties of cells. Sphere formation assays following limiting dilution of cells are used for *in vitro* evaluation of cells' self-renewal and proliferation abilities (Figure 1(b)). Based on their increased efflux capacity of the Hoechst dye, mediated by overexpression of ATP-binding (ABC) cassette transporters, CSCs are designated as the side population (SP) cells (Figure 1(c)) [47–49]. Differentiation potential is demonstrated by the ability

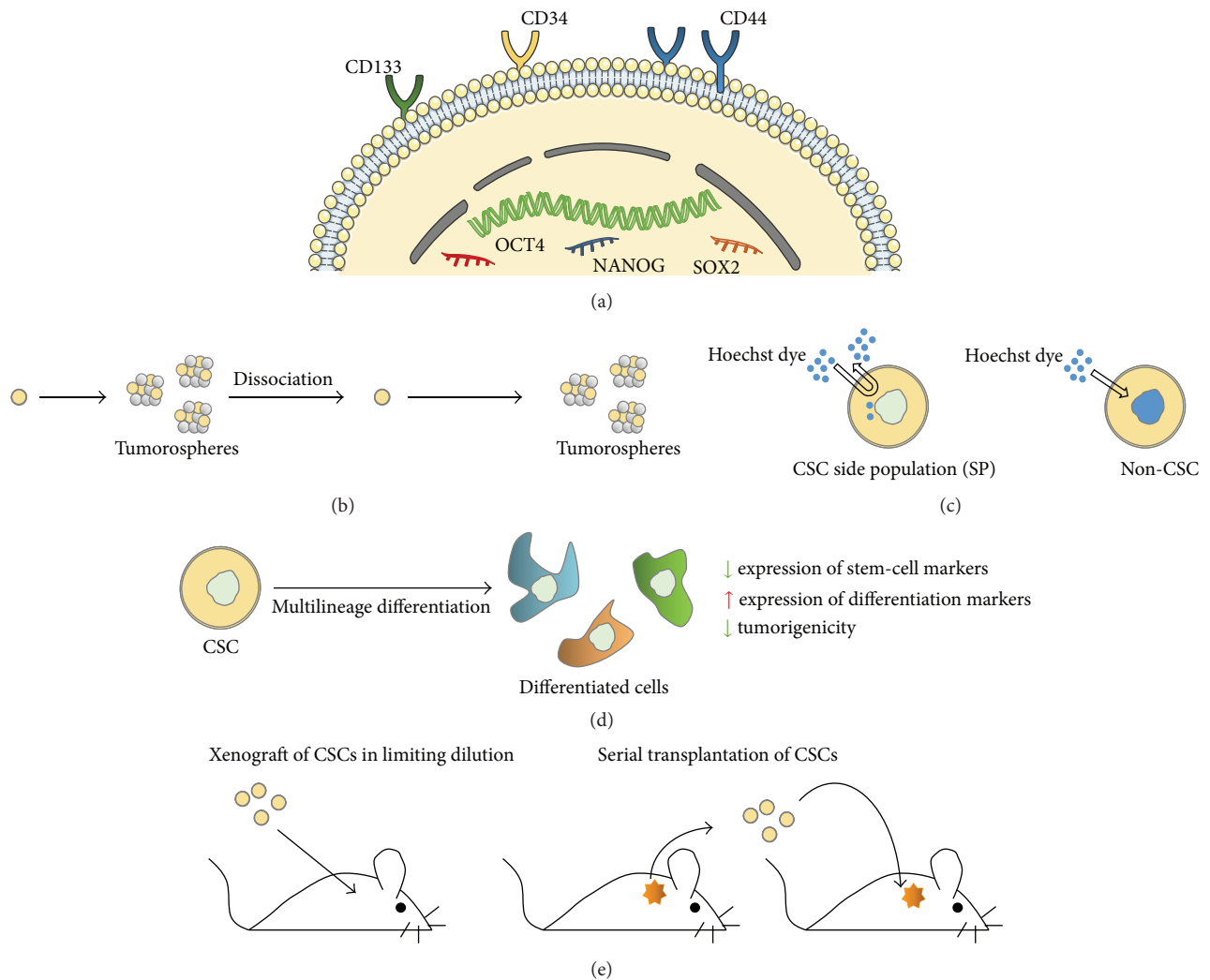


**FIGURE 1:** Cancer stem cell (CSC) properties and experimental methods for phenotypic and functional characterization of CSCs. (a) CSCs express cell surface antigens (CD133, CD34, and CD44) and signaling molecules (OCT4, NANOG, and SOX2) linked to a stem-like phenotype. CD: cluster of differentiation; OCT-4: octamer-binding transcription factor 4. (b) CSCs possess clonal properties and may be maintained *in vitro* for long intervals in serum-free medium. Under these conditions, they are able to form clonal tumorospheres. (c) CSCs present increased Hoechst efflux capacity compared to normal cells. Based on this property, they are designated as the side population (SP). (d) Multilineage differentiation (in the presence of serum) is another property of CSCs. Differentiation ability is verified by the decrease in the expression of stem cell markers accompanied by an increase in the expression of differentiation markers. Differentiated cells lose their tumorigenic potential. (e) CSCs at limiting dilutions are able to generate tumors after serial xenografting into immunocompromised mice. These tumors recapitulate the characteristics of the tumor from which CSCs were derived. Figure was constructed in part with objects from Servier Medical Art documents under license from Creative Commons Attribution 3.0 France (<http://creativecommons.org/licenses/by/3.0/fr/legalcode>).

of cells to undergo morphological changes when exposed to serum and by modifications in expression levels of stem cell and differentiation markers. In the differentiated state, cells lose their tumorigenic properties (Figure 1(d)). Finally, the gold standard for CSC validation is the *in vivo* ability of limiting dilutions of cells to recapitulate the heterogeneity and complexity of the initial tumor following serial orthotopic or ectopic transplantation in appropriate animal models (Figure 1(e)) [9, 38, 50]. Master and working cell banking of isolated CSCs, limited numbers of passages, and DNA fingerprinting are recommended to achieve nonderivation of CSCs from initial phenotypic and functional phenotypes

*in vitro*. Several CSC properties and associated validation methods are shown in Figure 1.

#### 4. Well Established Biological Targets in CSCs Related to Treatment Resistance

**4.1. Self-Renewal Signaling Molecules.** One of CSC's major features is their long-term self-renewal ability both *in vitro* and *in vivo*. Several pathways well known for their implication in embryonic development and differentiation and controlling stem cell self-renewal are preferentially activated in CSCs. These include the Wnt/ $\beta$ -catenin, Notch,



Hedgehog (Hh), and BMI1 pathways (Figure 2(a)) [51]. In addition, several studies suggest that EGF (epidermal growth factor), PI3K (phosphatidylinositol-3-phosphate kinase), MAPK (mitogen-activated protein kinase), and NF- $\kappa$ B- (nuclear factor kappa B-) mediated signaling is also involved in CSC self-renewal through cross-talk with the aforementioned pathways [52]. As a consequence, several strategies have been developed to target these pathways and a number of their inhibitors and/or regulators are under clinical investigation and some are already in clinical use [51, 53, 54]. However, various resistance mechanisms to these experimental drugs have been described. For example, resistance to inhibitors of Smoothened, a key molecule in the Hedgehog signaling pathway, has been attributed to activation of Smoothened downstream signaling partners by other signaling pathways [55]. Moreover, Smoothened mutations causing disruption of the inhibitor binding site were also described [56]. In addition to resistance mechanisms, some examples of absence of clinical efficacy have been reported [54, 57]. These concerned trials without previous patient stratification for mutations in the targeted pathways. Absence of efficacy was also attributed to the fact that the CSC phenotype is not only the result of dysregulation of a single pathway but also the outcome of cross-talk between multiple signals. Thus, targeting one single pathway may not be sufficient [54].

**4.2. Antiapoptotic Pathways.** Overexpression of antiapoptotic molecules is another feature of CSCs (Figure 2(b)). For example, overexpression of genes encoding BCL2 and BCL-XL, which act as negative regulators of mitochondrial membrane permeabilization and cytochrome C release [58], was reported in CSCs from high grade astrocytomas. In addition, higher levels of survivin, belonging to the IAP (inhibitors of apoptosis) family members and low mRNA levels of caspase 8 associated with TRAIL (tumor necrosis factor- (TNF-) related apoptosis-inducing ligand) resistance were described in other brain tumor-derived CSCs [59, 60]. Moreover, CSCs from glioblastoma, the most common and aggressive brain malignancy [61, 62], were less sensitive to BCL2 small molecule inhibitors compared to cancer cells without stem cell properties from the same tumor [63]. Interestingly, specific inhibition of antiapoptotic pathways was shown to reduce chemo- and radioresistance of glioblastoma CSCs and to specifically eliminate breast cancer stem cell activity [64, 65]. However, presumably because of the coexistence of multiple antiapoptotic mechanisms, clinical trials based on the use of death receptor agonists were not conclusive. Association of these compounds with other antiapoptotic molecules such as BCL2 antagonists may be more relevant for efficient tumor targeting and elimination [53].

**4.3. Resistance to DNA Damage and Proteins Involved in DNA Repair.** Lesions induced by radiotherapy and chemotherapy with DNA damaging agents need to be repaired by the DNA damage response (DDR) pathways to allow cancer cells' survival following treatment. DDR mechanisms include both arrest of cells at specific checkpoints of the cell cycle and recruitment of the DNA repair machinery leading to

elimination of lesions. Depending on the type of lesion, distinct sets of DNA repair proteins are involved [66].

In a pioneer study, Bao and coll. showed that CD133<sup>+</sup> glioblastoma CSCs contribute to radioresistance through preferential activation of the DNA damage checkpoint response (Figure 2(c)) involving the ataxia telangiectasia mutated (ATM) protein kinase and checkpoint kinase (Chk) 2 (Chk2). Interestingly, the radioresistance of these cells was reversed following specific inhibition of Chk1 and Chk2 [67]. Chk1 inhibitors were also able to sensitize pancreatic adenocarcinoma CSCs to gemcitabine, a cytidine analog used for the treatment of several malignancies including those of the pancreas [68].

In addition to activation of checkpoint responses, enhanced DNA repair mechanisms were reported for some types of CSCs (Figure 2(c)). Preferential activation of the DNA double strand break (DSB) repair response involving the polycomb group protein BMI1 and the ATM protein kinase was observed in cancerous neural stem cells [69]. BMI1 deficiency resulted in increased sensitivity to radiation in both glioblastoma and head and neck squamous cell cancer-derived CSCs [69, 70]. Preferential expression of other DNA repair-associated genes such as those encoding Methyl Guanine Methyl Transferase (MGMT) and BRCA1-related DNA repair proteins was reported in CSCs from glioblastoma and pancreatic tumors, respectively [71, 72]. Moreover, enhanced Non-Homologous End Joining (NHEJ) activity and a more-rapid DNA repair were reported in CSCs from mammary tumors [73].

Finally, CSCs' chemo- or radioresistance was also associated with lower levels of reactive oxygen species (ROS) either because of lower ROS production rates or because of the presence of more efficient ROS scavenging systems in these cells involving multiple signaling pathways [74]. Interfering with CSCs' intracellular redox balance is thus an interesting approach for CSC elimination (Figure 2(c)) [75, 76].

**4.4. Proteins Involved in Drug Efflux.** One of the characteristics of CSCs is their increased efflux capacity of the Hoechst dye defining them as the side population (SP) cells (Figure 1(c)) [47–49]. This property has been used and is still applied for isolation of CSCs from a variety of tumors [77–79]. Increased expression of proteins belonging to the ATP-binding (ABC) cassette transporter family is at the basis of this CSC property (Figure 2(d)) [80]. Among ABC transporters, P-glycoprotein (also known as multidrug resistance protein 1 (MDR1) or ABCB1), multidrug resistance associated proteins 1 and 2 (MRP1 or ABCC1 and MRP2 or ABCC2), and breast cancer resistance protein (BCRP or ABCG2) are main actors of the multidrug resistance (MDR) phenotype which was also associated with CSC physiopathology [80]. Overexpression of ABC family members was described in glioblastoma, lung cancer, osteosarcoma, prostate and ovarian cancer, and nasopharyngeal carcinoma [80]. Three generations of ABC transporter blockers have been used. A fourth one based on natural compounds is under development [81, 82]. Inhibitors of the third generation which are less toxic and more specific, namely, the ones targeting BCRP, are under investigation in clinical trials

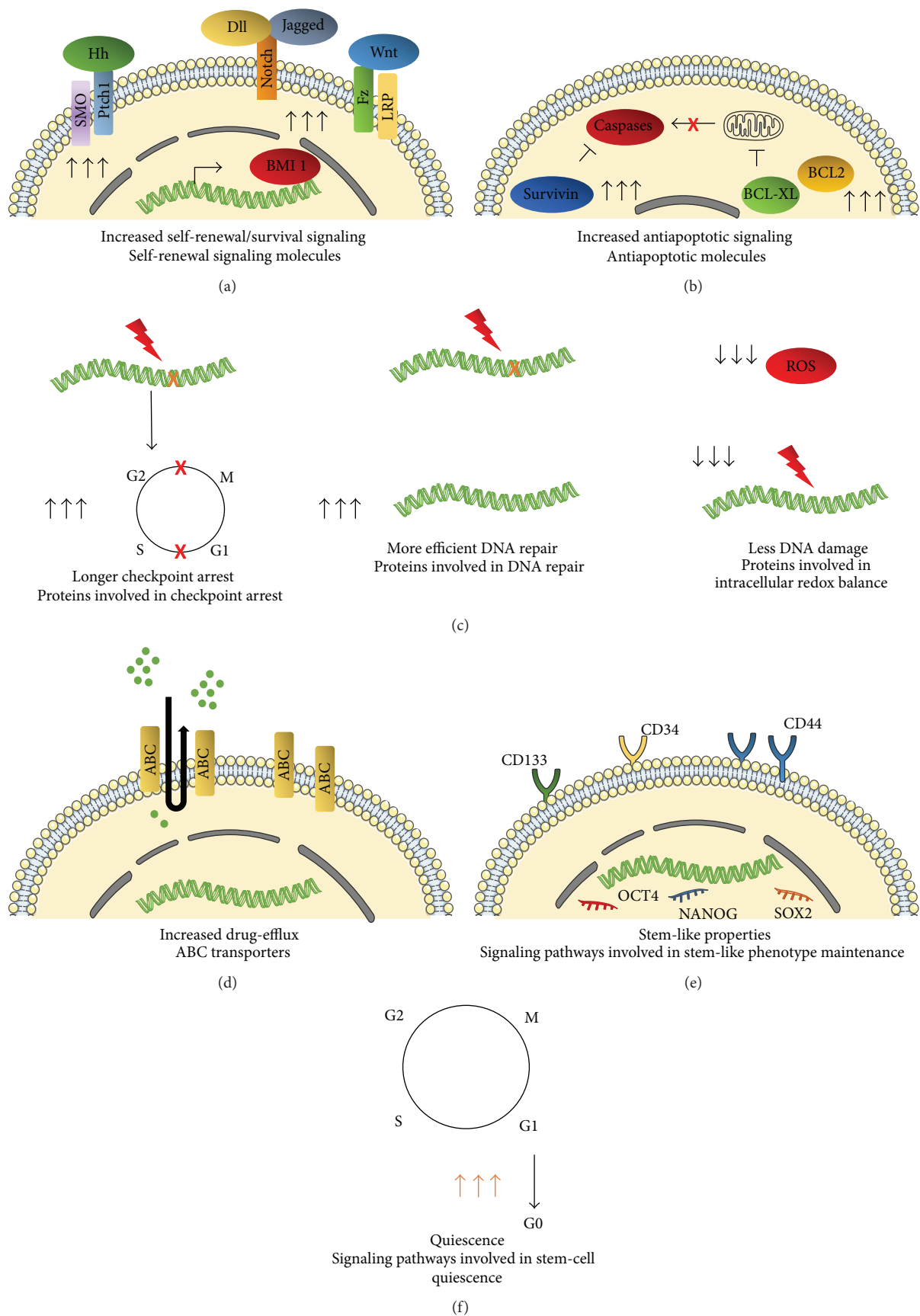


FIGURE 2: Continued.



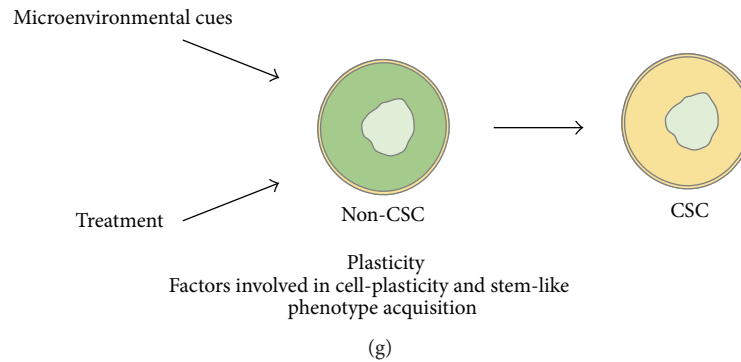


FIGURE 2: Mechanisms of CSCs' therapy resistance and relevant biological targets. ((a)-(b)) Increased self-renewal and prosurvival signaling have been reported for CSCs. Molecules involved in self-renewal/survival as well as antiapoptotic proteins overexpressed in CSCs are potentially interesting targets for therapies seeking CSC elimination. Hh: Hedgehog; SMO: Smoothened; Ptch1: Patched; Dll: Delta-like ligand; Wnt: wntless integration site; Fz: Frizzled; LRP: low-density lipoprotein receptor-related protein; BMI1: polycomb ring finger; BCL-XL: B-cell lymphoma extra-large; BCL2: B-cell lymphoma 2. (c) CSCs respond with higher efficacy to DNA damage *via* checkpoint arrest for longer time intervals and enhanced DNA repair. Moreover, reduced levels of ROS have been reported in CSCs leading to protection of the CSC genome from DNA damage. Proteins involved in checkpoint arrest, DNA repair, and intracellular redox balance are relevant biological targets in CSCs. (d) Increased expression/function of ABC transporters in CSCs underlies more efficient drug efflux from these cells. ABC transporters are thus interesting therapeutic targets in CSCs. (e) Tumor initiation and propagation properties of CSCs involve their stem-like phenotype. Signaling modules involved in the maintenance of this state are relevant targets for CSC elimination. CD: cluster of differentiation; OCT-4: octamer-binding transcription factor 4. (f) Quiescent CSCs have been evidenced in many human malignancies and are major determinants of CSCs' resistance to current treatments. Neutralization of the CSC quiescent phenotype is a promising approach for new anticancer protocols. (g) Induced CSC-like phenotypes may be obtained by the action of signals from the tumor microenvironment and/or as a result of therapy. Cell plasticity observed in human malignancies must be taken into account when developing new anticancer therapies. Figure was constructed in part with objects from Servier Medical Art documents under license from Creative Commons Attribution 3.0 France (<http://creativecommons.org/licenses/by/3.0/fr/legalcode>).

whereas others are already used in clinic, for example, in colon carcinoma [53, 80].

**4.5. Stem-Like Properties.** Tumorigenic properties of CSCs and treatment resistance are closely linked to their undifferentiated phenotype and stem-like characteristics (Figure 2(e)). It was thus proposed that inducing CSC differentiation would be an efficient way to increase therapy efficacy. Differentiation therapy with various agents including all-trans retinoic acid and vitamin D3 has been proposed in the context of hematopoietic malignancies [83]. SAHA (suberoylanilide hydroxamic acid), a histone deacetylase (HDAC) inhibitor, was used to induce differentiation of various cancer cell types including those of breast and endometrial carcinomas [83]. CSCs isolated from glioblastoma and treated *in vitro* with bone morphogenetic protein 4 (BMP4) expressed higher levels of differentiation markers and lost their ability to generate glioblastoma-like lesions in xenografted mouse brains. These effects were dependent on Smad signaling [84]. However, some glioblastoma CSCs were subsequently shown to resist BMP4-induced differentiation because of epigenetic silencing of BMP receptors in these cells [85]. In a recent communication, Balasubramaniyan et al. reported that glioblastoma CSCs retained their self-renewal and tumorigenic properties despite the induction of proneural differentiation factors by exposure to serum. Moreover, aberrant differentiation towards a mesenchymal phenotype was observed [86].

## 5. Emerging Biological Targets and Treatment Resistance of CSCs

**5.1. Cell Quiescence.** Cell quiescence may be defined as a reversible G0 phase from which cells may escape to reenter the cell cycle in response to physiological cell stimuli. It was suggested that cell quiescence is not just a passive state but rather a condition actively maintained and regulated by signaling pathways allowing rapid activation of quiescent cells and reentry in the cell cycle [87].

Signaling molecules participating in the regulation of stem cell quiescence include tumor suppressors p53 and RB (retinoblastoma protein), cyclin-dependent protein kinase inhibitors, namely, p21, p27, and p57, Notch-related pathways, and a number of miRNAs (micro-RNAs) [87]. Several transcription factors including FoxOs (Forkhead Box O) and NFI (Nuclear Factor 1) protein member NFIX have also been involved in gene expression regulation in quiescent cells [88, 89].

Specific strategies allowing long-term survival through adaptive responses to environmental stress were reported for quiescent CSCs. For example, FoxO transcription factors, *via* PI3K-Akt-dependent pathways and regulation of ROS levels, were shown to participate in such adaptive mechanisms. Adaptive metabolic responses and mechanisms favoring maintenance of genomic integrity were also reported for these cells [87, 90, 91].

In cancer biology, tumor dormancy designates a frequent clinical phenomenon in which disseminated tumor cells are maintained in a nonproliferating quiescent state for long time intervals. This phenomenon may occur at early stages of the disease or following therapeutic intervention. Awakening of these dormant cells leads to tumor progression and relapse which may occur after very long periods [91, 92].

In addition to disseminated dormant tumor cells, CSCs with quiescent phenotypes also exist within tumors as suggested by *in vitro* and *in vivo* data. In 2009, based on the label retention properties of cells, Dembinski and Krauss identified a subpopulation of slow cycling cells in pancreas adenocarcinoma cell lines. Partial overlap between this subpopulation and stem cell marker expression was observed for some cancer cells. Interestingly, these cells survived following chemotherapy and exhibited increased tumorigenic and invasive potentials [93]. A label retention strategy was also used to identify, purify, and establish transcriptional signatures of quiescent normal mammary stem cells from cultured mammospheres. Transcriptional signatures of these cells allowed prospective identification of slowly dividing CSCs in breast tumors and highlighted the heterogeneity of such malignancies with respect to their CSC content [94]. In liver cancer, the cell surface marker CD13 was identified as a functional hallmark of potentially dormant CSCs. CD13<sup>+</sup> cells retain dyes for long intervals, contain low levels of ROS, participate in chemoresistance, and present high tumorigenic potential in immunocompromised mice. In *in vivo* liver tumor models, combination of CD13 inhibition and 5 fluorouracil (5-FU) damaging cells in the S phase of the cell cycle led to tumor volume reduction in a more effective way compared to either treatment alone [95]. JARID1B which is a histone 3 demethylase involved in transcriptional repression of Notch ligands was identified as a marker of temporarily distinct slow cycling melanoma cells. Targeting the slow cycling phenotype of these cells through JARID1B knockdown inhibited continuous growth and metastatic progression of melanomas in animal models [96]. Relatively quiescent CSCs were also isolated from ovarian cancer patient specimens [97] as well as from the colo205 human colon adenocarcinoma cell line [98]. Label retaining glioblastoma CSCs generating tumors which present all the pathological features of the primary disease were first described by Deleyrolle et al. [99]. Endogenous glioblastoma CSCs, expressing a transgene that labels quiescent adult neural stem cells of the subventricular zone and staining negative for proliferation marker Ki-67 expression, were subsequently identified by Chen et al. in a genetically engineered mouse model of glioma. Following treatment with temozolomide (TMZ), one of the standards of care for glioblastoma together with surgery and radiotherapy, this cancer cell subpopulation was able to drive tumor regrowth through the production of highly dividing cells. Interestingly, ablation of this particular cancer cell subpopulation hindered tumor development [100]. In another study, Patel et al. used RNA seq-based single cell transcriptomic analysis to demonstrate that glioblastomas are highly heterogeneous tumors harboring variable proportions of cells expressing markers that have previously been associated with quiescence. These cells are also characterized by

the presence of a stemness signature which is attributed to glioblastoma CSCs [101]. Finally, HIF1 $\alpha$ - (hypoxia-inducible factor 1  $\alpha$ -) positive quiescent glioblastoma cells with stem properties were localized by immunocytochemical-based methods in perinecrotic niches in glioblastoma patient specimens. Suppressed phosphorylation of serine 2 in the CTD (C terminal domain) of RNA polymerase II, previously observed in various types of quiescent noncancerous stem cells, was used as an indicator of quiescence in their report [102].

The quiescent state of CSCs protects these cells from antiproliferating agents and is thus an important factor of CSC-related resistance to conventional therapy (Figure 2(f)). Three major strategies have been reported for targeting this particular slow cycling CSC subpopulation (Figure 3). The first one consists in forcing CSCs to reenter the cell cycle and was designated as the “locked-out” situation. This was suggested to be of benefit for cancer treatment since a majority of chemotherapeutic agents including mitotic inhibitors, antimetabolite drugs, and topoisomerase inhibitors may only exhibit cancer cell cytotoxicity on proliferating cells. For example, ablation of the F-box protein Fbxw7 leads to a decrease in ubiquitin-dependent degradation of c-Myc, Notch, and cyclin E and reentry in the cell cycle and increases the sensitivity of Phi + leukemia CSCs to imatinib [103]. Leukemia CSCs were also sensitized to cell cycle dependent chemotherapy after treatment with mitogens (GCSF) [104]. However, the “locked-out” approach might be risky in case all awakened cancer cells are not efficiently eliminated by available antiproliferating agents since this would lead to disease progression. Moreover, exit from dormancy of heterogeneous populations of cancer cells may increase the genetic and epigenetic complexity of the tumor and allow more efficient resistance to treatment [92]. To overcome these limitations, some authors have proposed alternative targeting strategies. One of them is the “locked-in” strategy in which pharmacological maintenance of CSCs in the G0 phase aims to prevent further tumor growth, relapse, and/or metastasis throughout the lifetime of a patient. Eradicating CSCs while they are dormant is another alternative to dormant cancer cell awakening.

Deeper understanding of signaling pathways and factors involved in cell quiescence is a prerequisite to the success of those latter strategies. For example, reduced PI3K-Akt signaling was associated with dormant phenotypes. In addition, inhibition of mitogenic signals was shown to trigger quiescence. Combining cell survival blockers, that is, ABT-737, a BCL2, and BCL-XL inhibitor to EGFR (Epidermal Growth Factor Receptor) inhibition by erlotinib, was able to lead to elimination of erlotinib-induced quiescent cells in non-small-cell lung cancer xenografts. Alternatively, the quiescent state may be actively induced by specific kinases including DYRK1B (dual specificity tyrosine phosphorylation-regulated kinase 1B). This kinase was shown to block proteins involved in the G0/G1/S transition. DYRK1A, a DYRK1B related kinase, can also induce quiescence together with coordinating survival *via* an antioxidant response. Inhibition of DYRK1A leads to cytotoxicity towards quiescent pancreatic cancer cells while preserving normal

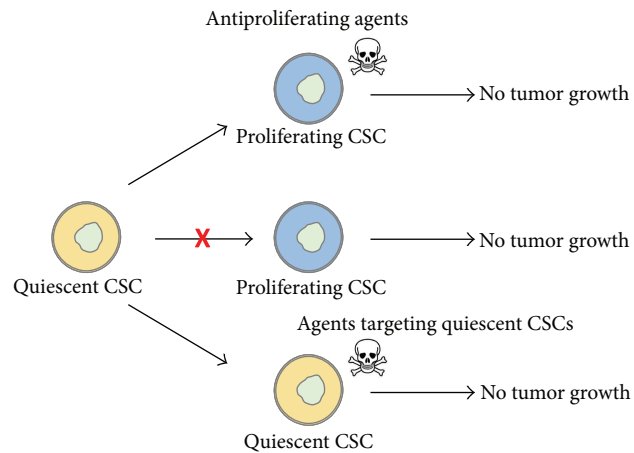


FIGURE 3: Strategies proposed for neutralization of the CSC quiescent phenotype involved in treatment resistance. Three strategies have been proposed to neutralize the quiescent CSC-state. Induction of CSC entry into the cell cycle would sensitize cells to antiproliferating agents. Blocking quiescent CSCs in G0 was proposed as an alternative for preventing new tumor growth. Targeting CSCs in the quiescent state was also proposed for the elimination of this particular CSC subpopulation. CSC: cancer stem cell. Figure was constructed in part with objects from Servier Medical Art documents under license from Creative Commons Attribution 3.0 France (<http://creativecommons.org/licenses/by/3.0/fr/legalcode>).

quiescent cells. The underlying mechanisms are not known [92]. The p38 MAPK (Mitogen-Activated Protein Kinase) along with TGF $\beta$  (Transforming Growth Factor beta)/BMP (Bone Morphogenetic Protein) signaling were also involved in the maintenance and/or induction of the quiescent state [105–107]. The DNA methylation inhibitor 5-azacytidine was shown to cause a decrease in expression of genes involved in exit from the G0 phase and entry in G1 in primary cells and in leukemia and breast cancer cell lines and upregulation of genes involved in a p38-related dormancy signature [105]. The same authors reported that combinations of 5-azacytidine and all-trans retinoic acid induce a stable quiescent state which may be maintained for a long period of time [92]. We have recently developed an *in vitro* model of reversibly quiescent glioblastoma CSCs based on the maintenance of patient derived CSCs without medium renewal for several days. These cells were shown to present decreased EdU (5-ethynyl-2'-deoxyuridine) incorporation rates and very low levels of Ki-67 expression. No significant increase in the expression of apoptotic markers was observed in these conditions. We additionally showed that quiescent glioblastoma CSCs showed similar expression of surface markers and comparable *in vitro* sphere forming and differentiation abilities, when returned to proliferation or differentiation-promoting culture conditions, as their proliferating counterparts. Moreover, *in vivo* engraftment capacity was maintained. Screening of the Prestwick Chemical library, mainly composed of FDA-approved drugs currently used in various therapeutic domains, on proliferating and quiescent glioblastoma CSCs, led to the identification of the stimulant laxative bisacodyl as a potent and specific inhibitor of quiescent glioblastoma CSC survival, with an IC<sub>50</sub> value around 1  $\mu$ M. Bisacodyl was ineffective on proliferating CSCs from the same patient, as well as on normal fetal neural stem cells and primary astrocytes [44]. To our knowledge, no other small molecules

with similar activity profiles have been reported so far. The molecular mechanisms underlying bisacodyl's activity on quiescent glioblastoma CSCs are currently under investigation in our laboratory.

**5.2. CSC Plasticity.** Initially, CSCs were considered as a static well-defined subpopulation of cancer cells with invariable functional characteristics distinguishing them from cells of the tumor mass. Nowadays, the CSC phenotype is considered as a transient state that any cell may acquire depending on cues provided by its microenvironment (Figure 2(g)) [108]. Epigenetic modifications are a major source of this kind of cell plasticity. Genomic alterations and selection of mutant cells may also participate in this phenomenon [109, 110].

Cell plasticity with acquisition of stem-like properties was described in several cancers. In melanoma, it was shown that many phenotypically distinct types of cancer cells with respect to surface marker expression were able to form tumors that recapitulate the characteristics of the original malignancy. This suggested that tumorigenic cells may undergo reversible phenotypical changes *in vivo* [111]. In addition, Roesch and colleges described a slow cycling melanoma CSC subpopulation whose existence within the tumor bulk was regulated over time as evidenced by marker expression modifications [96]. In another study, genetically engineered transformed mammary epithelial cells were shown to spontaneously generate cancer stem-like cells both *in vitro* and *in vivo* [6]. The same authors subsequently showed that switching of human basal breast cancer cells from a non-CSC to a CSC-state may be achieved through mesenchymal phenotype-inducing signals [7]. More recently, reprogramming of the tumor propagating potential of differentiated glioblastoma cells was achieved through expression of a set of transcription factors involved in neuronal development, namely, POU3F2, SOX2, SALL2, and OLIG2 [112].

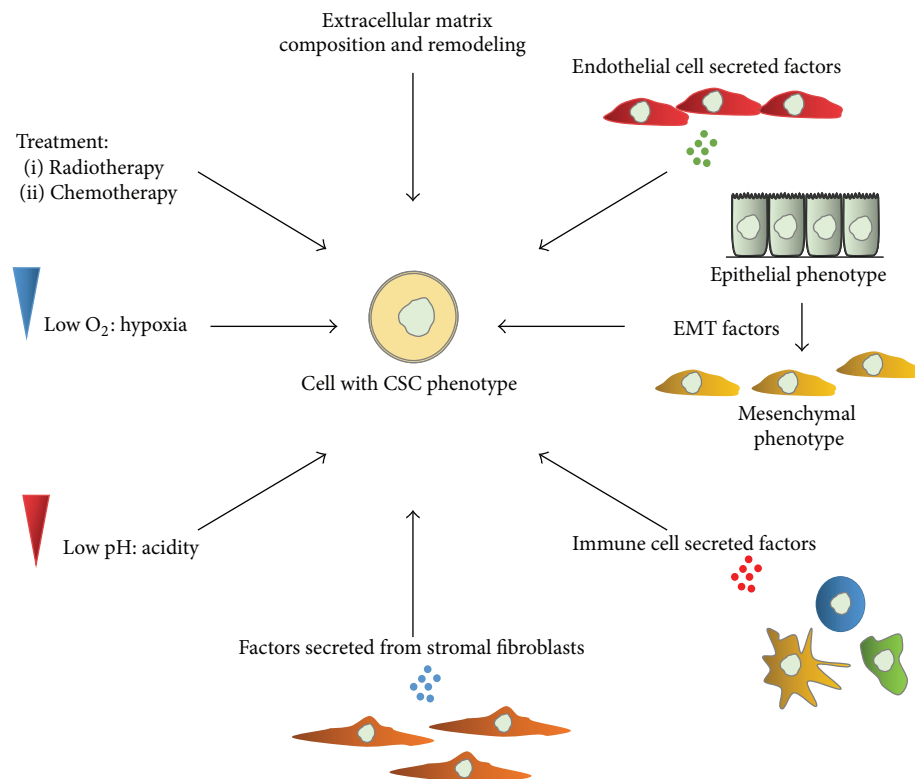


FIGURE 4: Mechanisms inducing CSC phenotypes. The CSC phenotype of cancer cells is influenced by cues related to the tumor microenvironment. These include remodeling of the extracellular matrix and signaling through factors secreted by endothelial, immune system cells and stromal fibroblasts. Signaling related to EMT (epithelial to mesenchymal transition) may also induce a CSC phenotype. Low oxygen (hypoxia) and acidic conditions nearby the CSC niche may induce and/or enhance the CSC phenotype of cells. Radiotherapy and chemotherapy have been shown to induce dedifferentiation of cancer cells and acquisition of a CSC phenotype. Figure was constructed in part with objects from Servier Medical Art documents under license from Creative Commons Attribution 3.0 France (<http://creativecommons.org/licenses/by/3.0/fr/legalcode>).

Induced CSCs were also obtained from colon cancer cells through introduction of three factors, OCT3/4, SOX2, and KLF4 [113].

Cancer cell plasticity with respect to the acquisition or loss of stem-like properties may be induced by either microenvironmental-/niche-derived signaling cues and/or as a result of antitumor therapeutic intervention (Figure 4). Tumors may be considered as organ-like structures in which cancer cell function is supported/regulated by matrix remodeling, blood vessel development, cancer associated fibroblast function, and recruitment of immune cells [114, 115]. Each of these factors may contribute to the functional properties of cancer cells and affect cell response to chemo- and radiotherapy by protecting cells from these agents [108]. It is important to note that vascular supply, access to growth factors, structural support, and interactions with immune cells vary within a single tumor. In other words, all cancer cells do not share the same microenvironmental conditions or the same niche [114]. Some authors suggested that within tumors, CSCs reside in particular niches whose function is to preserve their functional properties and plasticity and facilitate their metastatic potential [116]. In addition, it was proposed that CSC niches may be modified as a function of tumor stage or nature (initial or metastatic) [117].

Microenvironmental signals that can regulate cancer stem cell fate and metastatic potential include reorganizations of the extracellular matrix, autocrine and paracrine factors, low oxygen (hypoxia), and/or nutrient supply and signals derived from immune cells.

Extracellular matrix composition and remodeling have been associated with many aspects of cancer physiopathology as well as in the regulation of stem cell fate [118–120]. In a recent study, extracellular matrix small leucine-rich proteoglycans (SLRPs) decorin and lumican were shown to be expressed at higher levels in glioblastoma and neuroblastoma cancer cells induced *in vitro* to a more stem-like phenotype. Resulting cells forming neurospheres had a slow cycling phenotype and were more resistant to treatment [121].

A role of tumor microvascular endothelial cell-secreted factors on the induction of a stem cell phenotype in differentiated glioblastoma cells was also established. The authors showed that basic fibroblast growth factor (bFGF) secreted by endothelial cells induces increased stem cell marker expression and sphere forming ability of differentiated glioblastoma cells [122].

Epithelial to mesenchymal transition (EMT) is a process initially described in embryogenesis. During this process, differentiated polarized epithelial cells acquire a mesenchymal



phenotype and a more motile and invasive behavior [123, 124]. EMT is induced by environmental cues including TGF $\beta$  and receptor tyrosine kinase ligands and is accompanied by complex gene expression modifications [123]. In the context of cancer, EMT was initially described as a mechanism presumably providing cancer cells with invasive and metastatic properties. More recently, similarities between EMT-induced properties and CSC functional characteristics were highlighted and EMT following tumor microenvironmental cues was proposed to result in acquisition of CSC-like phenotypes by cancer cells [123, 125]. For example, it was shown that transformed human mammary epithelial cells acquire CSC properties after undergoing EMT [126, 127]. EMT in this case may be triggered by expression of particular transcription factors, cytokines including TGF $\beta$ , or following an immune response. In addition, in some cases, a stem-like phenotype has been reported for metastatic cancer cells which have presumably undergone EMT [123, 125]. Moreover, exposure of lung cancer cells to TGF $\beta$ 1 resulted in the switching of some cells to a stem-like phenotype [128].

Immune cells of the tumor microenvironment were also shown to secrete factors that are able to interfere with the stem cell properties of cancer cells. IL- (interleukin-) 22 secreted by T cells is able to modulate STAT3 signaling in cancer cells and expression of stem cell-associated genes like those encoding NANOG, SOX2, and POU5F1. This leads to increased tumorigenic potential of colorectal cancer cells [129]. Proinflammatory factors such as tumor necrosis factor alpha (TNF $\alpha$ ) and IL-6, secreted by immune cells in the tumor microenvironment, are able to modify the differentiation state of cancer cells through upregulation of the expression of mesenchymal phenotype-associated genes. This type of stem-like phenotype regulation was described for melanomas and breast and lung cancers. In colon cancer, NF- $\kappa$ B and Wnt activation was linked to dedifferentiation of cells lacking stem-like properties [108] whereas in breast cancer, T cells were shown to promote EMT and acquisition of CSC functions [130].

Interactions between other types of stromal cells and cancer cells were reported in various malignancies including pancreatic, breast, and colon cancer. In pancreatic cancer models, factors secreted from stellate cells (myofibroblasts) induce expression of stem-like or mesenchymal-like fate associated genes and favor CSC phenotypes [131, 132]. In colon cancer, hepatocyte growth factor secreted by myofibroblasts was shown to restore a CSC-like phenotype both *in vitro* and *in vivo* through regulation of the Wnt pathway [133, 134].

One of the hallmarks of solid tumors is the presence of hypoxic regions containing reduced oxygen levels (<2%). Hypoxic zones result from high oxygen demand of cancer cells and low oxygen supply due to irregularities in tumor vascularization or distance from supporting blood vessels [135]. Hypoxia-inducible factors (HIFs) are a family of transcription factors functioning as heterodimers in which one of several  $\alpha$  subunits (HIF1 $\alpha$ , HIF2 $\alpha$ , and HIF3 $\alpha$ ) is associated with a  $\beta$  subunit (HIF1 $\beta$ ). HIF proteins act as major sensors of low oxygen levels. Stabilization of HIF proteins leads to the regulation of the expression of numerous genes involved in

pH homeostasis, epigenetic regulation, extracellular matrix remodeling, proliferation, migration, survival, angiogenesis, and cell metabolism regulation by increasing glycolysis and decreasing mitochondrial function [136–138]. Hypoxic conditions were linked to promotion of stem-like properties as well as to EMT [138–140]. Increased expression of stem cell markers was observed in cancer cell lines from prostate, brain, kidney, cervix, lung, colon, liver, and breast tumors subjected to hypoxic conditions. These events were linked to HIF protein stabilization and function [141]. In addition, HIF proteins, and more particularly HIF2 $\alpha$ , were shown to regulate glioblastoma stem cell properties including sphere formation and tumorigenic potential [142, 143]. Several examples of hypoxia-induced promotion of a dedifferentiated phenotype were reported in breast carcinomas [144, 145]. Moreover, high numbers of tumorigenic cells were localized in hypoxic regions of neuroblastomas [146] and upregulation of CD133, a surface marker linked to CSCs, was reported in medulloblastoma cells under hypoxia [147].

Hypoxia was also linked to the induction of EMT via HIF-dependent or independent mechanisms [148–150]. Increased expression of EMT- and stem cell-related markers was observed in gastric cancer cells cultivated in hypoxic conditions. These cells had higher proliferation and migration rates and were more invasive. Increased ability to form colonies in soft agar was also reported for these cells [151]. In melanoma cells, hypoxic conditions lead to HIF-dependent Snail overexpression, decreased E-cadherin levels, and acquisition of melanoma CSC features [152].

One of the functional consequences of low oxygen availability in some regions of a tumor and HIF stabilization is the induction of glycolytic enzymes and a shift from oxidative phosphorylation to glycolysis for energy production. This leads to increased production of metabolic acids such as lactic acid and acidification of the cells' extracellular environment [153]. Acidic stress was also shown to promote CSC-like phenotypes. When CSCs from glioblastoma or CSC-depleted cultures of glioblastoma cells were exposed to low pH, an increase in the expression of CSC markers including OLIG2, OCT4, and NANOG was observed. In addition, cells acquired greater neurosphere formation capacity *in vitro* as well as increased tumorigenicity *in vivo* [154].

Cancer cell plasticity and generation of CSCs from non-CSC-like cancer cells have been frequently reported as a consequence of treatment. Ionizing radiation-reprogrammed breast cancer cells lacking stem cell properties into induced breast CSCs expressing the same markers as their nonirradiated counterparts and possessing increased mammosphere-formation ability and tumorigenic potential [155]. In head and neck squamous cell carcinomas, cisplatin was shown to promote survival and self-renewal of CSCs *in vitro* through increased expression of BMI1 [156]. Melanoma treatment with cisplatin and vemurafenib led to the enrichment of slow cycling cells which are able to sustain long-term tumor growth [157]. Colon cancer cells obtained following 5-FU (5-fluorouracil) treatment present mesenchymal stem-like properties, express stemness markers, and possess spherogenic potential [158]. Finally, several reports have linked chemotherapy to transition into a stem-like phenotype

associated with EMT. Some of these reports have been reviewed in [110, 125].

**5.3. CSC Metastatic Potential.** To form metastasis, primary tumor cells need to escape the physical barriers at the primary tumor site, enter the vascular system, infiltrate distant organs, survive, and proliferate at these secondary sites [159]. Because of all these bottlenecks, the metastatic process is rather inefficient and not all primary tumor cells possess metastatic potential. Metastatic potential of tumor cells is dependent both on their origin or their level of differentiation and on the occurrence of genetic and epigenetic changes linked to gene expression modifications that may act as cell fate determinants [160]. For example, in breast cancer, genes and signals involved in metastasis initiation and progression have been described. These include the *TWIST1* gene implicated in EMT, matrix metalloproteinase encoding genes involved in extracellular matrix degradation, genes playing a role in extravasation, in activation of prosurvival and self-renewal signaling pathways, and in initiation of tumor growth at the secondary site [161]. Some metastatic cues may act in a tissue-specific manner, thus directing primary tumor cell initiation of metastatic lesions to specific target organs. The ones driving organ-specific breast cancer metastasis have been reviewed in [161]. Because of their increased prosurvival and self-renewal ability and their tumor initiation properties, CSCs are attractive candidates as tumor cells participating in the metastatic process. Moreover, CSCs have been extensively linked to EMT [123, 125] and subsets of circulating tumor cells with metastatic initiation ability were shown to express high levels of stem cell markers [162–164]. Recently, human metastatic breast cancer cells were shown to possess a stem-like gene expression signature [165]. In addition, loss of differentiation-inducing factors or acquisition of stem cell signaling was related to the development of metastases [160] and CSCs were shown to participate in metastatic colonization by regulating components of their niche at secondary target organs [166]. Metastatic relapse is a major cause of cancer treatment failure. The lack of efficacy of current treatments against metastatic disease was attributed to the presence of genetic alterations in metastatic cells that differ from the ones that are present in primary tumor cells, to the clinical dormancy phenotype of metastatic cells before reamplification at the secondary site as well as to drug resistance induced by treatment. The involvement of treatment-resistant CSCs in this process is also contributing to this phenomenon [160].

## 6. Concluding Remarks

In the past years CSCs have been a topic of intense investigation. As a result, the literature referring to this particular cancer cell subpopulation is very rich and sometimes contradictory. Nowadays, researchers in the field agree that CSCs represent a population of cancer cells with specific properties which definitely distinguish them from cells of the tumor bulk. CSCs are thought to possess or to be able to acquire properties allowing them to resist conventional treatments with great efficacy. Several aspects underlying

CSCs' resistance to treatment have been discussed in this review. Because of their resistant phenotype, CSCs have a major implication in tumor relapse following treatment. This has been established for numerous types of malignancies. Thus, new therapies need to target both CSCs and more differentiated cancer cells to be efficient. Intense fundamental and clinical research is developing in this field.

The increasing amount of knowledge concerning signaling pathways and cell mechanisms used by CSCs to sustain their physiopathological functions and induce their resistance to treatment is put to profit for the identification of novel pertinent CSC-targeting strategies. Efforts to target CSCs are however complicated by the probable presence, *in vivo*, of CSCs with a slow-growing status. Such cells will greatly resist antiproliferating molecules disclosed through screening approaches on proliferating CSCs maintained and studied *in vitro*. In the future, development of experimental models of quiescent CSCs will be a prerequisite to understanding specific characteristics of these cells and identifying potentially successful strategies to specifically eliminate the slow-growing CSC subpopulation.

Another critical point is the elusive nature of CSCs. Within a tumor, cells may acquire, enhance, or lose CSC functionalities depending on their microenvironment and challenging by treatment. This implies that any cell within a tumor may become resistant to treatment and that heterogeneity in CSC content and nature may occur within the same tumor or between tumors in distinct patients. CSCs are thus moving targets and their elusive nature needs to be taken into account in future anticancer therapy developments. Combinations of treatments and continuous adaptability to patients' response may be part of the answer.

## Competing Interests

The authors declare that there is no conflict of interests regarding the publication of this paper.

## Acknowledgments

The authors thank “La Ligue contre le Cancer” for Ph.D. funding of Wanyin Chen as well as for additional financial support, the Strasbourg University, and the CNRS (Centre National de la Recherche Scientifique). Their projects are developed within the LABEX ANR-10-LABX-0034\_Medalis and received a financial support from French government managed by “Agence Nationale de la Recherche” under “Programme d'Investissement d'Avenir.”

## References

- [1] D. Bonnet and J. E. Dick, “Human acute myeloid leukemia is organized as a hierarchy that originates from a primitive hematopoietic cell,” *Nature Medicine*, vol. 3, no. 7, pp. 730–737, 1997.
- [2] M. Shackleton, E. Quintana, E. R. Fearon, and S. J. Morrison, “Heterogeneity in cancer: cancer stem cells versus clonal evolution,” *Cell*, vol. 138, no. 5, pp. 822–829, 2009.

- [3] F. Islam, B. Qiao, R. A. Smith, V. Gopalan, and A. K.-Y. Lam, "Cancer stem cell: fundamental experimental pathological concepts and updates," *Experimental and Molecular Pathology*, vol. 98, no. 2, pp. 184–191, 2015.
- [4] J. E. Visvader, "Cells of origin in cancer," *Nature*, vol. 469, no. 7330, pp. 314–322, 2011.
- [5] J. E. Visvader and G. J. Lindeman, "Cancer stem cells in solid tumours: accumulating evidence and unresolved questions," *Nature Reviews Cancer*, vol. 8, no. 10, pp. 755–768, 2008.
- [6] C. L. Chaffer, I. Brueckmann, C. Scheel et al., "Normal and neoplastic nonstem cells can spontaneously convert to a stem-like state," *Proceedings of the National Academy of Sciences of the United States of America*, vol. 108, no. 19, pp. 7950–7955, 2011.
- [7] C. L. Chaffer, N. D. Marjanovic, T. Lee et al., "XPoised chromatin at the ZEB1 promoter enables breast cancer cell plasticity and enhances tumorigenicity," *Cell*, vol. 154, no. 1, pp. X61–74, 2013.
- [8] D. Iliopoulos, H. A. Hirsch, G. Wang, and K. Struhl, "Inducible formation of breast cancer stem cells and their dynamic equilibrium with non-stem cancer cells via IL6 secretion," *Proceedings of the National Academy of Sciences of the United States of America*, vol. 108, no. 4, pp. 1397–1402, 2011.
- [9] L. Fulawka, P. Donizy, and A. Halon, "Cancer stem cells—the current status of an old concept: literature review and clinical approaches," *Biological Research*, vol. 47, no. 1, article 66, 2014.
- [10] M. Al-Hajj, M. S. Wicha, A. Benito-Hernandez, S. J. Morrison, and M. F. Clarke, "Prospective identification of tumorigenic breast cancer cells," *Proceedings of the National Academy of Sciences of the United States of America*, vol. 100, no. 7, pp. 3983–3988, 2003.
- [11] C. Ginestier, M. H. Hur, E. Charafe-Jauffret et al., "ALDH1 is a marker of normal and malignant human mammary stem cells and a predictor of poor clinical outcome," *Cell Stem Cell*, vol. 1, no. 5, pp. 555–567, 2007.
- [12] R. Galli, E. Binda, U. Orfanelli et al., "Isolation and characterization of tumorigenic, stem-like neural precursors from human glioblastoma," *Cancer Research*, vol. 64, no. 19, pp. 7011–7021, 2004.
- [13] H. D. Hemmati, I. Nakano, J. A. Lazareff et al., "Cancerous stem cells can arise from pediatric brain tumors," *Proceedings of the National Academy of Sciences of the United States of America*, vol. 100, no. 25, pp. 15178–15183, 2003.
- [14] S. K. Singh, I. D. Clarke, M. Terasaki et al., "Identification of a cancer stem cell in human brain tumors," *Cancer Research*, vol. 63, no. 18, pp. 5821–5828, 2003.
- [15] S. K. Singh, C. Hawkins, I. D. Clarke et al., "Identification of human brain tumour initiating cells," *Nature*, vol. 432, no. 7015, pp. 396–401, 2004.
- [16] X. Yuan, J. Curtin, Y. Xiong et al., "Isolation of cancer stem cells from adult glioblastoma multiforme," *Oncogene*, vol. 23, no. 58, pp. 9392–9400, 2004.
- [17] P. C. Hermann, S. L. Huber, T. Herrler et al., "Distinct populations of cancer stem cells determine tumor growth and metastatic activity in human pancreatic cancer," *Cell Stem Cell*, vol. 1, no. 3, pp. 313–323, 2007.
- [18] C. Li, D. G. Heidt, P. Dalerba et al., "Identification of pancreatic cancer stem cells," *Cancer Research*, vol. 67, no. 3, pp. 1030–1037, 2007.
- [19] P. Dalerba, S. J. Dylla, I.-K. Park et al., "Phenotypic characterization of human colorectal cancer stem cells," *Proceedings of the National Academy of Sciences of the United States of America*, vol. 104, no. 24, pp. 10158–10163, 2007.
- [20] C. A. O'Brien, A. Pollett, S. Gallinger, and J. E. Dick, "A human colon cancer cell capable of initiating tumour growth in immunodeficient mice," *Nature*, vol. 445, no. 7123, pp. 106–110, 2007.
- [21] L. Ricci-Vitiani, D. G. Lombardi, E. Pilozzi et al., "Identification and expansion of human colon-cancer-initiating cells," *Nature*, vol. 445, no. 7123, pp. 111–115, 2007.
- [22] M. E. Prince, R. Sivanandan, A. Kaczorowski et al., "Identification of a subpopulation of cells with cancer stem cell properties in head and neck squamous cell carcinoma," *Proceedings of the National Academy of Sciences of the United States of America*, vol. 104, no. 3, pp. 973–978, 2007.
- [23] Z. F. Yang, D. W. Ho, M. N. Ng et al., "Significance of CD90+ cancer stem cells in human liver cancer," *Cancer Cell*, vol. 13, no. 2, pp. 153–166, 2008.
- [24] A. Eramo, F. Lotti, G. Sette et al., "Identification and expansion of the tumorigenic lung cancer stem cell population," *Cell Death and Differentiation*, vol. 15, no. 3, pp. 504–514, 2008.
- [25] C. F. Bender Kim, E. L. Jackson, A. E. Woolfenden et al., "Identification of bronchioalveolar stem cells in normal lung and lung cancer," *Cell*, vol. 121, no. 6, pp. 823–835, 2005.
- [26] A. T. Collins, P. A. Berry, C. Hyde, M. J. Stower, and N. J. Maitland, "Prospective identification of tumorigenic prostate cancer stem cells," *Cancer Research*, vol. 65, no. 23, pp. 10946–10951, 2005.
- [27] K. S. Chan, I. Espinosa, M. Chao et al., "Identification, molecular characterization, clinical prognosis, and therapeutic targeting of human bladder tumor-initiating cells," *Proceedings of the National Academy of Sciences of the United States of America*, vol. 106, no. 33, pp. 14016–14021, 2009.
- [28] P. P. Szotek, R. Pieretti-Vanmarcke, P. T. Masiakos et al., "Ovarian cancer side population defines cells with stem cell-like characteristics and Mullerian Inhibiting Substance responsiveness," *Proceedings of the National Academy of Sciences of the United States of America*, vol. 103, no. 30, pp. 11154–11159, 2006.
- [29] S. Zhang, C. Balch, M. W. Chan et al., "Identification and characterization of ovarian cancer-initiating cells from primary human tumors," *Cancer Research*, vol. 68, no. 11, pp. 4311–4320, 2008.
- [30] D. Fang, T. K. Nguyen, K. Leishear et al., "A tumorigenic subpopulation with stem cell properties in melanomas," *Cancer Research*, vol. 65, no. 20, pp. 9328–9337, 2005.
- [31] E. Quintana, M. Shackleton, M. S. Sabel, D. R. Fullen, T. M. Johnson, and S. J. Morrison, "Efficient tumour formation by single human melanoma cells," *Nature*, vol. 456, no. 7222, pp. 593–598, 2008.
- [32] T. Schatton, G. F. Murphy, N. Y. Frank et al., "Identification of cells initiating human melanomas," *Nature*, vol. 451, no. 7176, pp. 345–349, 2008.
- [33] M. Salerno, S. Avnet, G. Bonucci et al., "Sphere-forming cell subsets with cancer stem cell properties in human musculoskeletal sarcomas," *International Journal of Oncology*, vol. 43, no. 1, pp. 95–102, 2013.
- [34] T. Lapidot, C. Sirard, J. Vormoor et al., "A cell initiating human acute myeloid leukaemia after transplantation into SCID mice," *Nature*, vol. 367, no. 6464, pp. 645–648, 1994.
- [35] T. Baba, P. A. Convery, N. Matsumura et al., "Epigenetic regulation of CD133 and tumorigenicity of CD133+ ovarian cancer cells," *Oncogene*, vol. 28, no. 2, pp. 209–218, 2009.
- [36] E. Monzani, F. Facchetti, E. Galmozzi et al., "Melanoma contains CD133 and ABCG2 positive cells with enhanced tumourigenic



- potential," *European Journal of Cancer*, vol. 43, no. 5, pp. 935–946, 2007.
- [37] B. Greve, R. Kelsch, K. Spaniol, H. T. Eich, and M. Götte, "Flow cytometry in cancer stem cell analysis and separation," *Cytometry Part A*, vol. 81, no. 4, pp. 284–293, 2012.
- [38] H. Liu, L. Lv, and K. Yang, "Chemotherapy targeting cancer stem cells," *American Journal of Cancer Research*, vol. 5, no. 3, pp. 880–893, 2015.
- [39] J. P. Medema, "Cancer stem cells: the challenges ahead," *Nature Cell Biology*, vol. 15, no. 4, pp. 338–344, 2013.
- [40] C. Hadjimichael, K. Chanoumidou, N. Papadopoulou, P. Arampatzis, J. Papamatheakis, and A. Kretsovali, "Common stemness regulators of embryonic and cancer stem cells," *World Journal of Stem Cells*, vol. 7, no. 9, pp. 1150–1184, 2015.
- [41] A. Liu, X. Yu, and S. Liu, "Pluripotency transcription factors and cancer stem cells: small genes make a big difference," *Chinese Journal of Cancer*, vol. 32, no. 9, pp. 483–487, 2013.
- [42] S. Lemma, S. Avnet, M. Salerno, T. Chano, N. Baldini, and J. S. Castresana, "Identification and validation of housekeeping genes for gene expression analysis of cancer stem cells," *PLoS ONE*, vol. 11, no. 2, Article ID e0149481, 2016.
- [43] M. Fève, J.-M. Saliou, M. Zeniou et al., "Comparative expression study of the endo-G protein coupled receptor (GPCR) repertoire in human glioblastoma cancer stem-like cells, U87-MG cells and non malignant cells of neural origin unveils new potential therapeutic targets," *PLoS ONE*, vol. 9, no. 3, Article ID e91519, 2014.
- [44] M. Zeniou, M. Fève, S. Mameri et al., "Chemical library screening and structure-function relationship studies identify bisacodyl as a potent and selective cytotoxic agent towards quiescent human glioblastoma tumor stem-like cells," *PLoS ONE*, vol. 10, no. 8, Article ID e0134793, 2015.
- [45] H. Clevers, "The cancer stem cell: premises, promises and challenges," *Nature Medicine*, vol. 17, no. 3, pp. 313–319, 2011.
- [46] A. B. Hjelmeland and J. N. Rich, "The quest for self-identity: not all cancer stem cells are the same," *Clinical Cancer Research*, vol. 18, no. 13, pp. 3495–3498, 2012.
- [47] M. Boesch, D. Wolf, and S. Sopper, "Optimized stem cell detection using the DyeCycle-triggered side population phenotype," *Stem Cells International*, vol. 2016, Article ID 1652389, 14 pages, 2016.
- [48] A. Golebiewska, N. H. C. Brons, R. Bjerkvig, and S. P. Niclou, "Critical appraisal of the side population assay in stem cell and cancer stem cell research," *Cell Stem Cell*, vol. 8, no. 2, pp. 136–147, 2011.
- [49] V. Richard, M. G. Nair, T. R. Santhosh Kumar, and M. R. Pillai, "Side population cells as prototype of chemoresistant, tumor-initiating cells," *BioMed Research International*, vol. 2013, Article ID 517237, 8 pages, 2013.
- [50] S. Bandhavkar, "Cancer stem cells: a metastasizing menace!," *Cancer Medicine*, vol. 5, no. 4, pp. 649–655, 2016.
- [51] A. Borah, S. Raveendran, A. Rochani, T. Maekawa, and D. S. Kumar, "Targeting self-renewal pathways in cancer stem cells: clinical implications for cancer therapy," *Oncogenesis*, vol. 4, no. 11, article e177, 2015.
- [52] M. Katoh, "Networking of WNT, FGF, Notch, BMP, and Hedgehog signaling pathways during carcinogenesis," *Stem Cell Reviews*, vol. 3, no. 1, pp. 30–38, 2007.
- [53] P. A. Sotiropoulou, M. S. Christodoulou, A. Silvani, C. Herold-Mende, and D. Passarella, "Chemical approaches to targeting drug resistance in cancer stem cells," *Drug Discovery Today*, vol. 19, no. 10, pp. 1547–1562, 2014.
- [54] N. Takebe, L. Miele, P. J. Harris et al., "Targeting Notch, Hedgehog, and Wnt pathways in cancer stem cells: clinical update," *Nature Reviews Clinical Oncology*, vol. 12, no. 8, pp. 445–464, 2015.
- [55] B. Ramaswamy, Y. Lu, K.-Y. Teng et al., "Hedgehog signaling is a novel therapeutic target in tamoxifen-resistant breast cancer aberrantly activated by PI3K/AKT pathway," *Cancer Research*, vol. 72, no. 19, pp. 5048–5059, 2012.
- [56] R. L. Yauch, G. J. P. Dijkgraaf, B. Aliche et al., "Smoothed mutation confers resistance to a hedgehog pathway inhibitor in medulloblastoma," *Science*, vol. 326, no. 5952, pp. 572–574, 2009.
- [57] A. E. Sloan, C. J. Nock, X. B. Ye et al., "Targeting glioma-initiating cells in GBM: ABTC-0904, a randomized phase 0/II study targeting the Sonic Hedgehog-signaling pathway," *Journal of Clinical Oncology*, vol. 32, abstract 2026, 2014, Proceedings of the 2014 ASCO Annual Meeting.
- [58] A. N. Hata, J. A. Engelman, and A. C. Faber, "The BCL2 family: key mediators of the apoptotic response to targeted anticancer therapeutics," *Cancer Discovery*, vol. 5, no. 5, pp. 475–487, 2015.
- [59] D. Capper, T. Gaiser, C. Hartmann et al., "Stem-cell-like glioma cells are resistant to TRAIL/Apo2L and exhibit down-regulation of caspase-8 by promoter methylation," *Acta Neuropathologica*, vol. 117, no. 4, pp. 445–456, 2009.
- [60] F. Jin, L. Zhao, H.-Y. Zhao et al., "Comparison between cells and cancer stem-like cells isolated from glioblastoma and astrocytoma on expression of anti-apoptotic and multidrug resistance-associated protein genes," *Neuroscience*, vol. 154, no. 2, pp. 541–550, 2008.
- [61] G. P. Dunn, M. L. Rinne, J. Wykosky et al., "Emerging insights into the molecular and cellular basis of glioblastoma," *Genes and Development*, vol. 26, no. 8, pp. 756–784, 2012.
- [62] F. B. Furnari, T. Fenton, R. M. Bachoo et al., "Malignant astrocytic glioma: genetics, biology, and paths to treatment," *Genes & Development*, vol. 21, no. 21, pp. 2683–2710, 2007.
- [63] K. E. Tagscherer, A. Fassl, B. Campos et al., "Apoptosis-based treatment of glioblastomas with ABT-737, a novel small molecule inhibitor of Bcl-2 family proteins," *Oncogene*, vol. 27, no. 52, pp. 6646–6656, 2008.
- [64] L. Piggott, N. Omidvar, S. Martí Pérez, R. French, M. Eberl, and R. W. Clarkson, "Suppression of apoptosis inhibitor c-FLIP selectively eliminates breast cancer stem cell activity in response to the anti-cancer agent, TRAIL," *Breast Cancer Research*, vol. 13, no. 5, article R88, 2011.
- [65] Y.-P. Yang, Y. Chien, G.-Y. Chiou et al., "Inhibition of cancer stem cell-like properties and reduced chemoradioresistance of glioblastoma using microRNA145 with cationic polyurethane-short branch PEI," *Biomaterials*, vol. 33, no. 5, pp. 1462–1476, 2012.
- [66] Q. E. Wang, "DNA damage responses in cancer stem cells: implications for cancer therapeutic strategies," *World Journal of Biological Chemistry*, vol. 6, no. 3, pp. 57–64, 2015.
- [67] S. Bao, Q. Wu, R. E. McLendon et al., "Glioma stem cells promote radioresistance by preferential activation of the DNA damage response," *Nature*, vol. 444, no. 7120, pp. 756–760, 2006.
- [68] V. A. Venkatesha, L. A. Parsels, J. D. Parsels et al., "Sensitization of pancreatic cancer stem cells to gemcitabine by Chk1 inhibition," *Neoplasia*, vol. 14, no. 6, pp. 519–525, 2012.
- [69] S. Facchino, M. Abdouh, W. Chatoo, and G. Bernier, "BM11 confers radioresistance to normal and cancerous neural stem cells through recruitment of the DNA damage response machinery," *Journal of Neuroscience*, vol. 30, no. 30, pp. 10096–10111, 2010.



- [70] Y.-C. Chen, C.-J. Chang, H.-S. Hsu et al., "Inhibition of tumorigenicity and enhancement of radiochemosensitivity in head and neck squamous cell cancer-derived ALDH1-positive cells by knockdown of Bmi-1," *Oral Oncology*, vol. 46, no. 3, pp. 158–165, 2010.
- [71] G. Liu, X. Yuan, Z. Zeng et al., "Analysis of gene expression and chemoresistance of CD133+ cancer stem cells in glioblastoma," *Molecular Cancer*, vol. 5, article 67, 2006.
- [72] L. A. Mathews, S. M. Cabarcas, E. M. Hurt, X. Zhang, E. M. Jaffee, and W. L. Farrar, "Increased expression of DNA repair genes in invasive human pancreatic cancer cells," *Pancreas*, vol. 40, no. 5, pp. 730–739, 2011.
- [73] C.-H. Chang, M. Zhang, K. Rajapakshe et al., "Mammary stem cells and tumor-initiating cells are more resistant to apoptosis and exhibit increased DNA repair activity in response to DNA damage," *Stem Cell Reports*, vol. 5, no. 3, pp. 378–391, 2015.
- [74] E. Singer, J. Judkins, N. Salomonis et al., "Reactive oxygen species-mediated therapeutic response and resistance in glioblastoma," *Cell Death and Disease*, vol. 6, no. 1, Article ID e1601, 2015.
- [75] L. Chang, P. Graham, J. Hao et al., "Cancer stem cells and signaling pathways in radioresistance," *Oncotarget*, vol. 7, no. 10, pp. 11002–11017, 2016.
- [76] S. Ding, C. Li, N. Cheng, X. Cui, X. Xu, and G. Zhou, "Redox regulation in cancer stem cells," *Oxidative Medicine and Cellular Longevity*, vol. 2015, Article ID 750798, 11 pages, 2015.
- [77] V. J. Bhagwandin, J. M. Bishop, W. E. Wright, and J. W. Shay, "The metastatic potential and chemoresistance of human pancreatic cancer stem cells," *PLoS ONE*, vol. 11, no. 2, Article ID e0148807, 2016.
- [78] T. Chiba, K. Kita, Y.-W. Zheng et al., "Side population purified from hepatocellular carcinoma cells harbors cancer stem cell-like properties," *Hepatology*, vol. 44, no. 1, pp. 240–251, 2006.
- [79] J. Liu, N. Chi, J. Y. Zhang, W. Zhu, Y. S. Bian, and H. G. Chen, "Isolation and characterization of cancer stem cells from medulloblastoma," *Genetics and Molecular Research*, vol. 14, no. 2, pp. 3355–3361, 2015.
- [80] C. Di and Y. Zhao, "Multiple drug resistance due to resistance to stem cells and stem cell treatment progress in cancer," *Experimental and Therapeutic Medicine*, vol. 9, no. 2, pp. 289–293, 2015.
- [81] D. L. Dragu, L. G. Necula, C. Bleotu, C. C. Diaconu, and M. Chivu-Economescu, "Therapies targeting cancer stem cells: current trends and future challenges," *World Journal of Stem Cells*, vol. 7, no. 9, pp. 1185–1201, 2015.
- [82] S. Karthikeyan and S. L. Hoti, "Development of fourth generation ABC inhibitors from natural products: a novel approach to overcome cancer multidrug resistance," *Anti-Cancer Agents in Medicinal Chemistry*, vol. 15, no. 5, pp. 605–615, 2015.
- [83] D. R. Pattabiraman and R. A. Weinberg, "Tackling the cancer stem cells—what challenges do they pose?" *Nature Reviews Drug Discovery*, vol. 13, no. 7, pp. 497–512, 2014.
- [84] S. G. M. Piccirillo, B. A. Reynolds, N. Zanetti et al., "Bone morphogenetic proteins inhibit the tumorigenic potential of human brain tumour-initiating cells," *Nature*, vol. 444, no. 7120, pp. 761–765, 2006.
- [85] J. Lee, M. J. Son, K. Woolard et al., "Epigenetic-mediated dysfunction of the bone morphogenetic protein pathway inhibits differentiation of glioblastoma-initiating cells," *Cancer Cell*, vol. 13, no. 1, pp. 69–80, 2008.
- [86] V. Balasubramaniyan, B. Vaillant, S. Wang et al., "Aberrant mesenchymal differentiation of glioma stem-like cells: implications for therapeutic targeting," *Oncotarget*, vol. 6, no. 31, pp. 31007–31017, 2015.
- [87] T. H. Cheung and T. A. Rando, "Molecular regulation of stem cell quiescence," *Nature Reviews Molecular Cell Biology*, vol. 14, no. 6, pp. 329–340, 2013.
- [88] B. Martynoga, J. L. Mateo, B. Zhou et al., "Epigenomic enhancer annotation reveals a key role for NFIX in neural stem cell quiescence," *Genes and Development*, vol. 27, no. 16, pp. 1769–1786, 2013.
- [89] J.-H. Paik, Z. Ding, R. Narurkar et al., "FoxOs cooperatively regulate diverse pathways governing neural stem cell homeostasis," *Cell Stem Cell*, vol. 5, no. 5, pp. 540–553, 2009.
- [90] J. R. Valcourt, J. M. S. Lemons, E. M. Haley, M. Kojima, O. O. Demuren, and H. A. Collier, "Staying alive: metabolic adaptations to quiescence," *Cell Cycle*, vol. 11, no. 9, pp. 1680–1696, 2012.
- [91] S. H. Wang and S. Lin, "Tumor dormancy: potential therapeutic target in tumor recurrence and metastasis prevention," *Experimental Hematology & Oncology*, vol. 2, no. 1, article 29, 2013.
- [92] M. S. Sosa, P. Bragado, and J. A. Aguirre-Ghiso, "Mechanisms of disseminated cancer cell dormancy: an awakening field," *Nature Reviews Cancer*, vol. 14, no. 9, pp. 611–622, 2014.
- [93] J. L. Dembinski and S. Krauss, "Characterization and functional analysis of a slow cycling stem cell-like subpopulation in pancreas adenocarcinoma," *Clinical and Experimental Metastasis*, vol. 26, no. 7, pp. 611–623, 2009.
- [94] S. Pece, D. Tosoni, S. Confalonieri et al., "Biological and molecular heterogeneity of breast cancers correlates with their cancer stem cell content," *Cell*, vol. 140, no. 1, pp. 62–73, 2010.
- [95] N. Haraguchi, H. Ishii, K. Mimori et al., "CD13 is a therapeutic target in human liver cancer stem cells," *The Journal of Clinical Investigation*, vol. 120, no. 9, pp. 3326–3339, 2010.
- [96] A. Roesch, M. Fukunaga-Kalabis, E. C. Schmidt et al., "A temporarily distinct subpopulation of slow-cycling melanoma cells is required for continuous tumor growth," *Cell*, vol. 141, no. 4, pp. 583–594, 2010.
- [97] M.-Q. Gao, Y.-P. Choi, S. Kang, J. H. Youn, and N.-H. Cho, "CD24<sup>+</sup> cells from hierarchically organized ovarian cancer are enriched in cancer stem cells," *Oncogene*, vol. 29, no. 18, pp. 2672–2680, 2010.
- [98] Z. Vincent, K. Urakami, K. Maruyama, K. Yamaguchi, and M. Kusuha, "CD133-positive cancer stem cells from Colo205 human colon adenocarcinoma cell line show resistance to chemotherapy and display a specific metabolomic profile," *Genes & Cancer*, vol. 5, no. 7-8, pp. 250–260, 2014.
- [99] L. P. Deleyrolle, A. Harding, K. Cato et al., "Evidence for label-retaining tumour-initiating cells in human glioblastoma," *Brain*, vol. 134, no. 5, pp. 1331–1343, 2011.
- [100] J. Chen, Y. Li, T.-S. Yu et al., "A restricted cell population propagates glioblastoma growth after chemotherapy," *Nature*, vol. 488, no. 7412, pp. 522–526, 2012.
- [101] A. P. Patel, I. Tirosh, J. J. Trombetta et al., "Single-cell RNA-seq highlights intratumoral heterogeneity in primary glioblastoma," *Science*, vol. 344, no. 6190, pp. 1396–1401, 2014.
- [102] A. Ishii, T. Kimura, H. Sadahiro et al., "Histological characterization of the tumorigenic 'Peri-Necrotic Niche' harboring quiescent stem-like tumor cells in glioblastoma," *PLoS ONE*, vol. 11, no. 1, Article ID e0147366, 2016.

- [103] S. Takeishi, A. Matsumoto, I. Onoyama, K. Naka, A. Hirao, and K. I. Nakayama, "Ablation of Fbxw7 eliminates leukemia-initiating cells by preventing quiescence," *Cancer Cell*, vol. 23, no. 3, pp. 347–361, 2013.
- [104] Y. Saito, N. Uchida, S. Tanaka et al., "Induction of cell cycle entry eliminates human leukemia stem cells in a mouse model of AML," *Nature Biotechnology*, vol. 28, no. 3, pp. 275–280, 2010.
- [105] A. P. Adam, A. George, D. Schewe et al., "Computational identification of a p38 SAPK-regulated transcription factor network required for tumor cell quiescence," *Cancer Research*, vol. 69, no. 14, pp. 5664–5672, 2009.
- [106] P. Bragado, Y. Estrada, F. Parikh et al., "TGF- $\beta$ 2 dictates disseminated tumour cell fate in target organs through TGF- $\beta$ -RIII and p38 $\alpha/\beta$  signalling," *Nature Cell Biology*, vol. 15, no. 11, pp. 1351–1361, 2013.
- [107] A. Kobayashi, H. Okuda, F. Xing et al., "Bone morphogenetic protein 7 in dormancy and metastasis of prostate cancer stem-like cells in bone," *The Journal of Experimental Medicine*, vol. 208, no. 13, pp. 2641–2655, 2011.
- [108] M. C. Cabrera, R. E. Hollingsworth, and E. M. Hurt, "Cancer stem cell plasticity and tumor hierarchy," *World Journal of Stem Cells*, vol. 7, no. 1, pp. 27–36, 2015.
- [109] A. Avgustinova and S. A. Benitah, "The epigenetics of tumour initiation: cancer stem cells and their chromatin," *Current Opinion in Genetics & Development*, vol. 36, pp. 8–15, 2016.
- [110] A. O. Pisco and S. Huang, "Non-genetic cancer cell plasticity and therapy-induced stemness in tumour relapse: 'what does not kill me strengthens me,'" *British Journal of Cancer*, vol. 112, no. 11, pp. 1725–1732, 2015.
- [111] E. Quintana, M. Shackleton, H. R. Foster et al., "Phenotypic heterogeneity among tumorigenic melanoma cells from patients that is reversible and not hierarchically organized," *Cancer Cell*, vol. 18, no. 5, pp. 510–523, 2010.
- [112] M. L. Suvà, E. Rheinbay, S. M. Gillespie et al., "Reconstructing and reprogramming the tumor-propagating potential of glioblastoma stem-like cells," *Cell*, vol. 157, no. 3, pp. 580–594, 2014.
- [113] N. Oshima, Y. Yamada, S. Nagayama et al., "Induction of cancer stem cell properties in colon cancer cells by defined factors," *PLoS ONE*, vol. 9, no. 7, Article ID e101735, 2014.
- [114] M. R. Junttila and F. J. de Sauvage, "Influence of tumour micro-environment heterogeneity on therapeutic response," *Nature*, vol. 501, no. 7467, pp. 346–354, 2013.
- [115] L. Lacina, J. Plzak, O. Kodet et al., "Cancer microenvironment: what can we learn from the stem cell niche," *International Journal of Molecular Sciences*, vol. 16, no. 10, pp. 24094–24110, 2015.
- [116] V. Plaks, N. Kong, and Z. Werb, "The cancer stem cell niche: how essential is the niche in regulating stemness of tumor cells?" *Cell Stem Cell*, vol. 16, no. 3, pp. 225–238, 2015.
- [117] M. A. LaBarge, "The difficulty of targeting cancer stem cell niches," *Clinical Cancer Research*, vol. 16, no. 12, pp. 3121–3129, 2010.
- [118] H. C. Chong, C. K. Tan, R.-L. Huang, and N. S. Tan, "Matricellular proteins: a sticky affair with cancers," *Journal of Oncology*, vol. 2012, Article ID 351089, 17 pages, 2012.
- [119] P. Lu, V. M. Weaver, and Z. Werb, "The extracellular matrix: a dynamic niche in cancer progression," *The Journal of Cell Biology*, vol. 196, no. 4, pp. 395–406, 2012.
- [120] F. M. Watt and W. T. S. Huck, "Role of the extracellular matrix in regulating stem cell fate," *Nature Reviews Molecular Cell Biology*, vol. 14, no. 8, pp. 467–473, 2013.
- [121] C. Farace, J. A. Oliver, C. Melguizo et al., "Microenvironmental modulation of decorin and lumican in temozolomide-resistant glioblastoma and neuroblastoma cancer stem-like cells," *PLoS ONE*, vol. 10, no. 7, Article ID e0134111, 2015.
- [122] E. Fessler, T. Borovski, and J. P. Medema, "Endothelial cells induce cancer stem cell features in differentiated glioblastoma cells via bFGF," *Molecular Cancer*, vol. 14, article 157, 2015.
- [123] A. Singh and J. Settleman, "EMT, cancer stem cells and drug resistance: an emerging axis of evil in the war on cancer," *Oncogene*, vol. 29, no. 34, pp. 4741–4751, 2010.
- [124] J. P. Thiery and J. P. Sleeman, "Complex networks orchestrate epithelial-mesenchymal transitions," *Nature Reviews Molecular Cell Biology*, vol. 7, no. 2, pp. 131–142, 2006.
- [125] M. R. Doherty, J. M. Smigiel, D. J. Junk, and M. W. Jackson, "Cancer stem cell plasticity drives therapeutic resistance," *Cancers (Basel)*, vol. 8, no. 1, p. 8, 2016.
- [126] S. A. Mani, W. Guo, M.-J. Liao et al., "The epithelial-mesenchymal transition generates cells with properties of stem cells," *Cell*, vol. 133, no. 4, pp. 704–715, 2008.
- [127] A. Mitra, L. Mishra, and S. Li, "EMT, CTCs and CSCs in tumor relapse and drug-resistance," *Oncotarget*, vol. 6, no. 13, pp. 10697–10711, 2015.
- [128] F. Andriani, G. Bertolini, F. Facchinetti et al., "Conversion to stem-cell state in response to microenvironmental cues is regulated by balance between epithelial and mesenchymal features in lung cancer cells," *Molecular Oncology*, vol. 10, no. 2, pp. 253–271, 2016.
- [129] I. Kryczek, Y. Lin, N. Nagarsheth et al., "IL-22<sup>+</sup> CD4<sup>+</sup> T cells promote colorectal cancer stemness via STAT3 transcription factor activation and induction of the methyltransferase DOT1L," *Immunity*, vol. 40, no. 5, pp. 772–784, 2014.
- [130] M. Santisteban, J. M. Reiman, M. K. Asiedu et al., "Immune-induced epithelial to mesenchymal transition in vivo generates breast cancer stem cells," *Cancer Research*, vol. 69, no. 7, pp. 2887–2895, 2009.
- [131] S. Hamada, A. Masamune, T. Takikawa et al., "Pancreatic stellate cells enhance stem cell-like phenotypes in pancreatic cancer cells," *Biochemical and Biophysical Research Communications*, vol. 421, no. 2, pp. 349–354, 2012.
- [132] E. Lonardo, J. Frias-Aldeguer, P. C. Hermann, and C. Heeschen, "Pancreatic stellate cells form a niche for cancer stem cells and promote their self-renewal and invasiveness," *Cell Cycle*, vol. 11, no. 7, pp. 1282–1290, 2012.
- [133] J. Evans, A. Essex, H. Xin, N. Amitai, L. Brinton, and E. Griner, "Registered report: Wnt activity defines colon cancer stem cells and is regulated by the microenvironment," *eLife*, vol. 4, Article ID e07301, 2015.
- [134] L. Vermeulen, F. De Sousa E Melo, M. van der Heijden et al., "Wnt activity defines colon cancer stem cells and is regulated by the microenvironment," *Nature Cell Biology*, vol. 12, no. 5, pp. 468–476, 2010.
- [135] J. A. Bertout, S. A. Patel, and M. C. Simon, "The impact of O<sub>2</sub> availability on human cancer," *Nature Reviews Cancer*, vol. 8, no. 12, pp. 967–975, 2008.
- [136] N. C. Denko, "Hypoxia, HIF1 and glucose metabolism in the solid tumour," *Nature Reviews Cancer*, vol. 8, no. 9, pp. 705–713, 2008.
- [137] E. Paolicchi, F. Gemignani, M. Krstić-Demonacos, S. Dedhar, L. Mutti, and S. Landi, "Targeting hypoxic response for cancer therapy," *Oncotarget*, vol. 7, no. 12, pp. 13464–13478, 2016.

- [138] B. Philip, K. Ito, R. Moreno-Sánchez, and S. J. Ralph, "HIF expression and the role of hypoxic microenvironments within primary tumours as protective sites driving cancer stem cell renewal and metastatic progression," *Carcinogenesis*, vol. 34, no. 8, pp. 1699–1707, 2013.
- [139] J. M. Heddlestone, Z. Li, J. D. Lathia, S. Bao, A. B. Hjelmeland, and J. N. Rich, "Hypoxia inducible factors in cancer stem cells," *British Journal of Cancer*, vol. 102, no. 5, pp. 789–795, 2010.
- [140] Y. Kim, Q. Lin, P. M. Glazer, and Z. Yun, "Hypoxic tumor microenvironment and cancer cell differentiation," *Current Molecular Medicine*, vol. 9, no. 4, pp. 425–434, 2009.
- [141] J. Mathieu, Z. Zhang, W. Zhou et al., "HIF induces human embryonic stem cell markers in cancer cells," *Cancer Research*, vol. 71, no. 13, pp. 4640–4652, 2011.
- [142] J. M. Heddlestone, Z. Li, R. E. McLendon, A. B. Hjelmeland, and J. N. Rich, "The hypoxic microenvironment maintains glioblastoma stem cells and promotes reprogramming towards a cancer stem cell phenotype," *Cell Cycle*, vol. 8, no. 20, pp. 3274–3284, 2009.
- [143] Z. Li, S. Bao, Q. Wu et al., "Hypoxia-inducible factors regulate tumorigenic capacity of glioma stem cells," *Cancer Cell*, vol. 15, no. 6, pp. 501–513, 2009.
- [144] K. Helczynska, Å. Kronblad, A. Jögi et al., "Hypoxia promotes a dedifferentiated phenotype in ductal breast carcinoma in situ," *Cancer Research*, vol. 63, no. 7, pp. 1441–1444, 2003.
- [145] E. Louie, S. Nik, J.-S. Chen et al., "Identification of a stem-like cell population by exposing metastatic breast cancer cell lines to repetitive cycles of hypoxia and reoxygenation," *Breast Cancer Research*, vol. 12, no. 6, article R94, 2010.
- [146] B. Das, R. Tsuchida, D. Malkin, G. Koren, S. Baruchel, and H. Yeger, "Hypoxia enhances tumor stemness by increasing the invasive and tumorigenic side population fraction," *STEM CELLS*, vol. 26, no. 7, pp. 1818–1830, 2008.
- [147] N. Platet, S. Y. Liu, M. E. Atifi et al., "Influence of oxygen tension on CD133 phenotype in human glioma cell cultures," *Cancer Letters*, vol. 258, no. 2, pp. 286–290, 2007.
- [148] R. P. Hill, D. T. Marie-Egyptienne, and D. W. Hedley, "Cancer stem cells, hypoxia and metastasis," *Seminars in Radiation Oncology*, vol. 19, no. 2, pp. 106–111, 2009.
- [149] T. van den Beucken, E. Koch, K. Chu et al., "Hypoxia promotes stem cell phenotypes and poor prognosis through epigenetic regulation of DICER," *Nature Communications*, vol. 5, article 5203, 2014.
- [150] Y. J. Yang, H. J. Na, M. J. Suh et al., "Hypoxia induces epithelial-mesenchymal transition in follicular thyroid cancer: involvement of regulation of twist by hypoxia inducible factor-1 $\alpha$ ," *Yonsei Medical Journal*, vol. 56, no. 6, pp. 1503–1514, 2015.
- [151] J. Guo, B. Wang, Z. Fu, J. Wei, and W. Lu, "Hypoxic microenvironment induces EMT and upgrades stem-like properties of gastric cancer cells," *Technology in Cancer Research & Treatment*, vol. 15, no. 1, pp. 60–68, 2016.
- [152] S. Liu, S. M. Kumar, J. S. Martin, R. Yang, and X. Xu, "Snail mediates hypoxia-induced melanoma progression," *The American Journal of Pathology*, vol. 179, no. 6, pp. 3020–3031, 2011.
- [153] J. Chiche, M. C. Brahimi-Horn, and J. Pouyssegur, "Tumour hypoxia induces a metabolic shift causing acidosis: a common feature in cancer," *Journal of Cellular and Molecular Medicine*, vol. 14, no. 4, pp. 771–794, 2010.
- [154] A. B. Hjelmeland, Q. Wu, J. M. Heddlestone et al., "Acidic stress promotes a glioma stem cell phenotype," *Cell Death and Differentiation*, vol. 18, no. 5, pp. 829–840, 2011.
- [155] C. Lagadec, E. Vlashi, L. Della Donna, C. Dekmezian, and F. Pajonk, "Radiation-induced reprogramming of breast cancer cells," *STEM CELLS*, vol. 30, no. 5, pp. 833–844, 2012.
- [156] C. Nör, Z. C. Zhang, K. A. Warner et al., "Cisplatin induces Bmi-1 and enhances the stem cell fraction in head and neck cancer," *Neoplasia*, vol. 16, no. 2, pp. 137–146, 2014.
- [157] A. Roesch, A. Vultur, I. Bogeski et al., "Overcoming intrinsic multidrug resistance in melanoma by blocking the mitochondrial respiratory chain of slow-cycling JARID1B(high) cells," *Cancer Cell*, vol. 23, no. 6, pp. 811–825, 2013.
- [158] C. Denise, P. Paoli, M. Calvani et al., "5-Fluorouracil resistant colon cancer cells are addicted to OXPHOS to survive and enhance stem-like traits," *Oncotarget*, vol. 6, no. 39, pp. 41706–41721, 2015.
- [159] S. Vanharanta and J. Massagué, "Origins of metastatic traits," *Cancer Cell*, vol. 24, no. 4, pp. 410–421, 2013.
- [160] L. Wan, K. Pantel, and Y. Kang, "Tumor metastasis: moving new biological insights into the clinic," *Nature Medicine*, vol. 19, no. 11, pp. 1450–1464, 2013.
- [161] S. Kimbung, N. Loman, and I. Hedenfalk, "Clinical and molecular complexity of breast cancer metastases," *Seminars in Cancer Biology*, vol. 35, pp. 85–95, 2015.
- [162] I. Baccelli, A. Schneeweiss, S. Riethdorf et al., "Identification of a population of blood circulating tumor cells from breast cancer patients that initiates metastasis in a xenograft assay," *Nature Biotechnology*, vol. 31, no. 6, pp. 539–544, 2013.
- [163] T. Hiraga, S. Ito, and H. Nakamura, "Cancer stem-like cell marker CD44 promotes bone metastases by enhancing tumorigenicity, cell motility, and hyaluronan production," *Cancer Research*, vol. 73, no. 13, pp. 4112–4122, 2013.
- [164] C. van den Hoogen, G. van der Horst, H. Cheung et al., "High aldehyde dehydrogenase activity identifies tumor-initiating and metastasis-initiating cells in human prostate cancer," *Cancer Research*, vol. 70, no. 12, pp. 5163–5173, 2010.
- [165] D. A. Lawson, N. R. Bhakta, K. Kessenbrock et al., "Single-cell analysis reveals a stem-cell program in human metastatic breast cancer cells," *Nature*, vol. 526, no. 7571, pp. 131–135, 2015.
- [166] I. Malanchi, A. Santamaria-Martínez, E. Susanto et al., "Interactions between cancer stem cells and their niche govern metastatic colonization," *Nature*, vol. 481, no. 7379, pp. 85–91, 2012.

## Reprofilage d'une petite molécule chimique à activité thérapeutique et cellules souches cancéreuses. Etude et compréhension du mécanisme d'action du bisacodyl sur les cellules souches cancéreuses isolées de glioblastome

### Résumé

Les glioblastomes (GBM) sont les formes les plus agressives de tumeurs gliales avec une survie médiane des patients traités n'excédant pas 2 ans. Ce mauvais pronostic est dû, entre autres, à l'hétérogénéité de ces tumeurs avec la présence de cellules souches cancéreuses (CSCs) en prolifération ou quiescentes, particulièrement résistantes aux traitements conventionnels. Cibler ces cellules au sein du microenvironnement tumoral hypoxique et acide fait donc partie des thérapies d'avenir des GBMs.

Le laxatif bisacodyl a été identifié par criblage de la chimiothèque Prestwick comme un composé induisant la mort par nécrose des CSCs de glioblastome (GSCs en prolifération et en quiescence), uniquement dans des conditions de faible acidité retrouvées également au sein des tumeurs. Une activité antitumorale *in vivo* a également été démontrée pour ce composé.

Cette thèse présente l'identification du mode d'action du bisacodyl dans les GSCs. Celui-ci implique la serine/thréonine kinase WNK1 et ses partenaires, les kinases Akt et SGK1 et des co-transporteurs  $\text{Na}^+/\text{HCO}_3^-$  NBC. Nos résultats ont également révélé un rôle de WNK1 dans la physiopathologie des GSCs.

Mots clés : Glioblastome, cellules souches cancéreuses, tumorosphères, acidité tumorale, quiescence, bisacodyl, WNK1, Akt, SGK1, co-transporteurs  $\text{Na}^+/\text{HCO}_3^-$  NBC.

### Résumé en anglais

Glioblastoma (GBM), the most aggressive glial tumor, is currently incurable with a very short-term patient survival (< 2 years). The heterogeneity of GBM and the presence of highly resistant proliferating and quiescent cancer stem-like cells (CSCs), is largely responsible for poor prognosis in this disease. Thus, new approaches targeting glioblastoma CSCs (GSCs), within the acidic/hypoxic tumor microenvironment, are promising strategies for treating GBM.

The laxative bisacodyl was identified in a high throughput screening of the Prestwick chemical library as a compound inducing necrotic cell death in proliferating and quiescent GSCs only in acidic microenvironments similar to those found in tumors. Bisacodyl was further shown to induce tumor shrinking and to increase survival in *in vivo* GBM models.

In this thesis work we identify bisacodyl's mechanism of action in GSCs. This mechanism involves the serine/threonine kinase WNK1 and its signaling partners including protein kinases Akt and SGK1 and NBC  $\text{Na}^+/\text{HCO}_3^-$  cotransporters. Our data also highlight a previously unknown role of WNK1 in GSC physiopathology.

Keywords: Glioblastoma, cancer stem-like cells, tumorospheres, intratumoral acidity, quiescence, bisacodyl, WNK1, Akt, SGK1, NBC  $\text{Na}^+/\text{HCO}_3^-$  cotransporters.